

XXXIV European Congress on Molecular Spectroscopy - **EUCMOS 2018**

E
U C
M O
S

Coimbra – Portugal

19 – 24 August 2018

SCIENTIFIC PROGRAMME

ABSTRACTS

LIST OF AUTHORS

Book of Abstracts of the XXXIV European Congress on Molecular Spectroscopy

EUCMOS 2018

Coimbra, Portugal

August 19-24, 2018

Edited by:

Rui Fausto

Elisa M. Brás

Licínia L. G. Justino

Bernardo A. Nogueira

Department of Chemistry

University of Coimbra

R. Larga, s/n

P-3004-535 Coimbra (Portugal)

Printed and bound:

João Duarte, Unipessoal, Lda – OGAMI

Copies:

250

Legal Deposit:

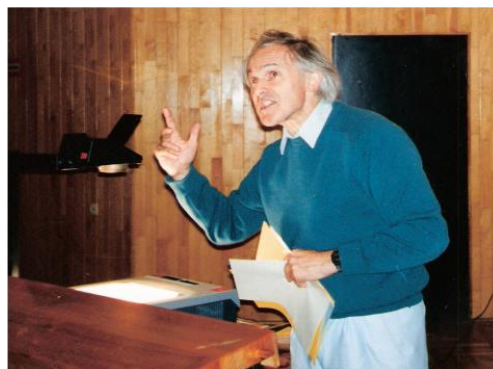
443831/18

ISBN 978-989-20-8611-8



Welcome

After 18 years, the **European Congress on Molecular Spectroscopy** (EUCMOS) returns to Portugal. The previous edition of EUCMOS held in Coimbra took place in the year 2000. I am sure that all those who had the opportunity to attend that meeting, still keep it in their memory as an extraordinary conference. At that time, the opening lecture was delivered by the Nobel Prize winner Professor Sir **Harold Walter Kroto**, whom we all miss so dearly. Harold Kroto passed away in April 20th 2016, and I would like to dedicate this congress to his memory. Besides being an outstanding scientist who dedicated his life to spectroscopy and education in science, Harry was also a good friend, whose acute and fine humor and modesty were marks of his personality.



EUCMOS 2018 appears as a new opportunity for scientists working in the field of molecular spectroscopy and related subjects to meet for a week and share their works in an environment that has been prepared to stimulate the exchange of ideas and help to find new paths to address the most important contemporary scientific challenges in this domain. It is very gratifying to know that leading scientists in the field of molecular spectroscopy have accepted our invitation and will share with us their knowledge.

Coimbra is a very beautiful and peaceful town situated on the Mondego River, approximately 185 km Northeast of Lisboa and 98 km Southeast of Porto. The city served as the capital of Portugal from 1139 to 1385 and was the birthplace of six monarchs from the Portuguese 1st Dynasty. Noted for its cultural traditions and artistic treasures, Coimbra was long the intellectual capital of Portugal and remains one of its most important cities. The life of the city depends primarily on its University, which was founded in 1290 and it is one of the oldest universities in Europe. Like an acropolis, the white buildings of the University of Coimbra now dominate the hilltop overlooking the north bank of Mondego. However, the University of Coimbra has been able to conciliate the past with both the present and future and it is also a "modern" university, very well equipped with up-to-date technology in the various fields of knowledge, and where science and technology are considered to play an essential role. The Science and Technology Faculty has actually more than 8000 students and

more than 300 senior professors that dedicate to the most relevant branches of fundamental and applied science, being the largest and the most prominent faculty of the University. The Chemistry and the Physics Departments are certainly among the most important research centres in these fields of research in Portugal, and both have since long ago attained the respect of the international scientific community.

I am sure that the outcome of EUCMOS 2018 will be an important contribution to the progress of Chemistry and Physics, in particular of molecular spectroscopy, and that this meeting will confirm the excellence of the EUCMOS series, now ready to celebrate its 67th anniversary, since the first event in Basel in 1951. It is a pleasure for me now, as chairman of EUCMOS 2018, and also as President of the International Steering Committee of EUCMOS, to extend a warm invitation to you to attend the congress and wish you a very nice stay in Coimbra.



A handwritten signature in black ink, which appears to read 'Rui Fausto'. The signature is fluid and cursive, with a long horizontal stroke extending to the right.

Rui Fausto, Ph.D.

Chairman of EUCMOS XXXIV

**THE ORGANIZING COMMITTEES OF EUCMOS 2018 GRATEFULLY
ACKNOWLEDGE SUPPORT FROM**

Faculdade de Ciências e Tecnologia da Universidade de Coimbra (FCTUC)

Departamento de Química - FCTUC

Fundação para a Ciência e a Tecnologia (FCT)

Entidade Regional de Turismo do Centro de Portugal

Sociedade Portuguesa de Química

Universidade de Coimbra

ORGANIZING COMMITTEES

INTERNATIONAL COMMITTEE

President:

R. Fausto (*Coimbra, Portugal*)

Vice-Presidents:

M. Schmitt (*Düsseldorf, Germany*)

H. Ratajczak (*Wroclaw, Poland*)

Members:

A. J. Barnes (*Salford, UK*)

J. R. Durig (*Kansas City, MO, USA*)

H. Hamaguchi (*Hsinchu, Taiwan*)

J. Laane (*College Station, USA*)

I. Palinko (*Szeged, Hungary*)

G. Zerbi (*Milan, Italy*)

J. Bellanato (*Madrid, Spain*)

T. A. Ford (*Durban, South Africa*)

H. M. Heise (*Iserlohn, Germany*)

H. H. Mantsch (*Ottawa, Canada*)

S. Turrell (*Vileneuve d'Ascq, France*)

ORGANIZING COMMITTEE

R. Fausto (*FCTUC, Coimbra*)

B. A. Nogueira (*CQC, Coimbra*)

E. M. Brás (*CQC, Coimbra /CCMAR, Faro*)

A. R. Cardoso (*FCTUC, Coimbra*)

S. Góbi (*CQC, Coimbra*)

G. O. Ildiz (*CQC Coimbra /IKU, Istanbul*)

A. Ismael (*CCMAR, Faro*)

A. J. L. Jesus (*FFUC, Coimbra*)

L. L. G. Justino (*CQC, Coimbra*)

N. Kuş (*CQC, Coimbra /Techn. U., Eskişehir*)

S. Lopes (*CQC, Coimbra*)

T. Nikitin (*CQC, Coimbra*)

C. M. Nunes (*CQC, Coimbra*)

S. M. V. Pinto (*CQC/Coimbra /SNS, Pisa*)

I. Reva (*FCTUC, Coimbra*)

J. Roque (*CQC, Coimbra*)

A. P. Simão (*FCTUC, Coimbra*)

M. I. L. Soares (*CQC, Coimbra*)

A. Tabanez (*FCTUC, Coimbra*)

O. Ünsalan (*CQC, Coimbra /Ege U., Izmir*)

M. S. C. Henriques (*CFisUC, Coimbra*)

SCIENTIFIC PROGRAMME COMMITTEE

President:

R. Fausto (*Coimbra, Portugal*)

Members:

L. G. Arnaut (*Coimbra, Portugal*)

A. J. Barnes (*Salford, UK*)

M. L. S. Cristiano (*Faro, Portugal*)

T. A. Ford (*Durban, South Africa*)

J. Gaspar Martinho (*Lisbon, Portugal*)

H. M. Heise (*Iserlohn, Germany*)

J. Laane (*College Station, USA*)

A. Lowenschuss (*Jerusalem, Israel*)

M. Oshtrakh (*Ekaterinburg, Russia*)

J. A. Paixão (*Coimbra, Portugal*)

H. Ratajczak (*Wroclaw, Poland*)

J. Santos (*Coimbra, Portugal*)

M. Schmitt (*Düsseldorf, Germany*)

T. Trindade (*Aveiro, Portugal*)

S. Turrell (*Vileneuve d'Ascq, France*)

The Organizing Committees of EUCMOS 2018
Thank very much the lecturers and
Participants in general for their valuable
Contribution to the scientific programme

WE GRATEFULLY ACKNOWLEDGE SUPPORT FROM OUR SPONSORS



Navigate your way

The new UV-1900 UV-VIS-NIR spectrophotometer provides the industry's fastest scan function for data acquisition. It is capable of high-accuracy quantitative analysis and the detection of low-concentration components. The new LabSolutions UV-Vis control software is equipped with functions for data pass/fail judgment.

High performance measurements
featuring high resolution and sensitivity based on the patented LO-RAY-LIGH technology

The industry's fastest scan level
providing measurement within three seconds and following even the fastest chemical reaction

Excellent operability for fast complete analysis
through easy-to-use color touch panel with large and intuitive icons

Compliant with advanced regulations
such as Pharmacopeia of various countries, GLP/GMP, FDA 21 CFR Part 11 and more



www.shimadzu.eu/navigate-your-way

SPECTROMETERS

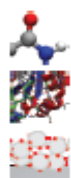
WITH BUILT-IN PULSE SHAPERS

2D IR

- + Rapid-scan acquisition
- + Scatter removal
- + Flexible design

2D Visible

- + High repetition rates
- + Easy to align



MOLECULAR STRUCTURE & DYNAMICS



PROTEIN STRUCTURE & DYNAMICS



MATERIALS SCIENCE



Transient Absorption

- + Add nanosecond delay capabilities to either 2D spectrometer
- + One spectrometer, many experiments!



FEMTOSECOND DYNAMICS



REAL-TIME KINETICS



MOLECULAR INTERACTIONS

PULSE SHAPERS

MID-IR, VISIBLE, NEAR-IR

fast&flexible

100 kHz repetition rates
user-adjustable bandwidth / resolution
advanced control software, designed for 2D spectroscopy

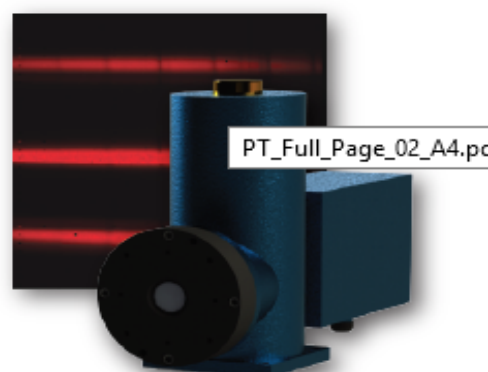


MID-IR DETECTORS NEXT-GEN MCT ARRAYS

128 x 128 MCT (16k pixels!)
Low-noise, High-resolution
More pixels = More possibilities

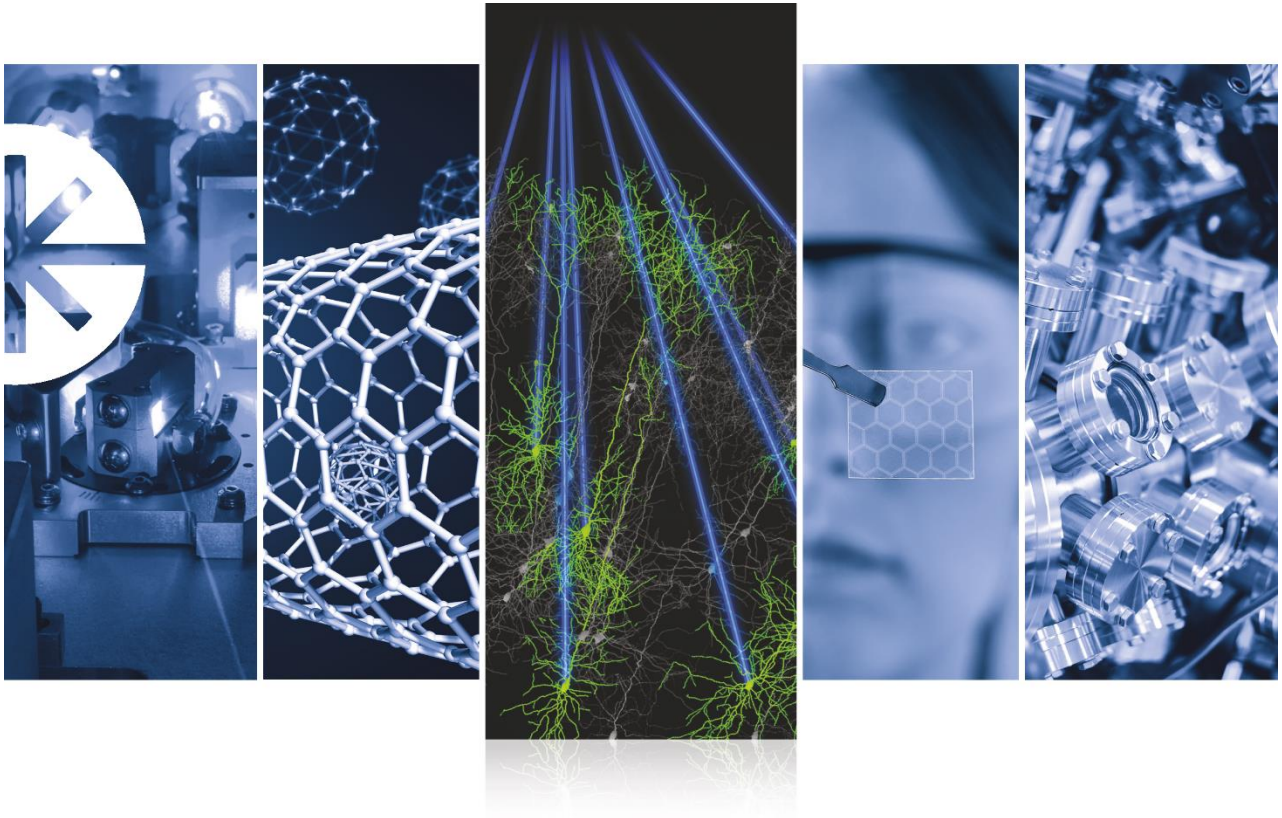
2D IR & Mid-IR Transient Absorption

- + Detection of multiple signals: Probe & Reference, Parallel & Perpendicular, or even Parallel, Perpendicular & Reference all at once!
- + Microscopy (FT-IR, Pump-Probe, 2D IR)
- + Direct imaging of beam = easy alignment



PT_Full_Page_02_A4.pc

phasetechspectroscopy.com



LEADING & INNOVATING TO ACCELERATE YOUR RESEARCH

Whether unlocking the mysteries of matter or mapping brain function, Coherent has the lasers to advance your research. With our unique HALT/HASS reliability protocol, we deliver unmatched laser performance for maximum productivity and improved data quality.

Attosecond Experiments to **Neuroscience**, **Gravitational Wave Studies** to **Spectroscopy**—
Discover More—coherent.com/industrial-revolution



thermo
scientific

Authorised Distributor

UNICAM

Sistemas Analíticos, Lda.



MILESTONE

HELPING
CHEMISTS

Microwave Digestion – Mercury

Cromatografia

HPLC - uPLC

HPLC - MSMS

GC - GCMS

IÓNICA

Espectrometria

ICP - ICPMS

UV-VIS

FTIR-RAMAN

ABS. ATÓMICA

www.thermounicam.pt



Spectra-Physics Solstice Ace Unsurpassed Operating Stability, and Flexible Configurations

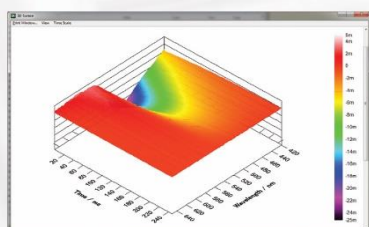
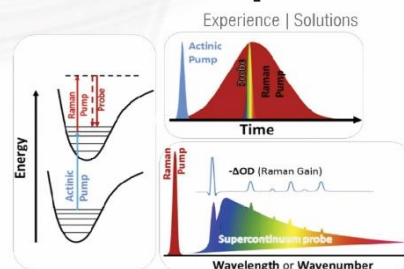
The Spectra-Physics® Solstice® Ace was the first femtosecond ultrafast amplifier designed, built and tested to meet rigorous industrial standards, and is capable of **reliable operation over a $\pm 5^\circ\text{C}$ temperature range**.

Using Spectra-Physics' patented Ace regenerative amplifier cavity, the Solstice Ace is available at **repetition rates configurable between 1 kHz and 10 kHz** (delivering >7 W at 1 kHz, >8 W at 5 kHz and >7 W at 10 kHz) **with pulse width configurations ranging from <35 fs to <120 fs**. For every configuration of Solstice Ace, the beam quality is exceptional ($M^2 < 1.25$) making it perfect for **OPA pumping** and a wide range of **non-linear spectroscopy applications**.

Newport FSRs

Newport's **Femtosecond Stimulated Raman Spectrometer (FSRS)** is the first commercially available turn-key FSRs spectrometer. FSRs is a nonlinear optical spectroscopy that has the advantage of time-resolved vibrational spectroscopy, allowing for additional tools useful for interpreting and assigning molecular dynamics and detection of "dark" molecular states.

- Flexibly designed femtosecond pump-probe spectrometer
- Broad pump-probe delay range and high pump-probe delay resolution
- Flexible imaging spectrograph supports automated switching of spectral range (detector) and resolution



Ultrafast Systems EOS Fire

EOS Fire is a unique (Patent No.: US 7,817,270 B2) broadband pump-probe sub-nanosecond **Transient Absorption Spectrometer** designed to work with a wide variety of pulsed lasers. A complete turn-key system, EOS Fire measures transients with **sub-ns time resolution** and a **virtually unlimited time window**.

EOS Fire offers a broad **probe spectral probe**, with options from 350 nm up to 2400 nm, and spectral resolution optimized for transient absorption.



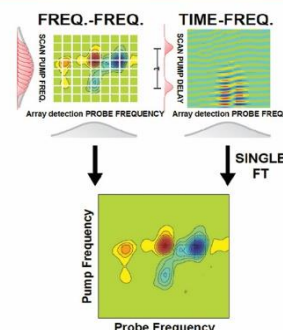
PhaseTech Spectroscopy 2SQuick IR

The 2DQuick IR combines the control of a mid-IR pulse shaper with the speed of an array detector for the most powerful 2D IR spectrometer ever.

With rapid-scan pulse shaping, the 2DQuick can scan time delays on a shot-by-shot basis. This means that a full 2D IR spectrum can be measured in less than a second. Multiple spectra can then be averaged as needed for the desired signal-to-noise.

- Observe real-time changes in proteins or other samples
- Spectra in < 1 second! - Publication-quality spectra in minutes

PHASETECH
spectroscopy shaping science



M. G. BRANDÃO - PORTUGAL
RUA DE SERRALVES, 599
4150-708 PORTO - PORTUGAL

TEL (+351) 226 167 370
FAX (+351) 226 167 379

mtb@mtbBRANDAO.COM
WWW.MTBBRANDAO.COM



EUCMOS 2018 SCIENTIFIC PROGRAMME

TIMETABLE

PROGRAMME TIMETABLE						
Time	19 th (Sunday)	20 th (Monday)	21 st (Tuesday)	22 nd (Wednesday)	23 rd (Thursday)	24 th (Friday)
8:30		Opening Ceremony				
9:00		SURFACES AND INTERFACES	REACTION INTERMEDIATES	ASTROPHYSICS AND COMPUTATIONAL	BIOSPECTROSCOPY	BIOMEDICAL APPLICATIONS
10:00		PL - 1: Mischä Bonn (D)	PL - 3: Robert J. McMahon (USA)	PL - 5: Harold Linartz (NL)	PL - 7: Janina Diekmann (D)	PL - 8: Klaus Gerwert (D)
10:30		KL-1: André Peremans (B)	KL-4: Martin Suhm (D)	KL-18: Andrzej Sobolewski (PL)	KL -23: Marco van de Weert (DN)	KL-25: Nancy Pleshko (USA)
		Coffee Break	Coffee Break	Coffee Break	Coffee Break	Coffee Break
11:00		KL-2: Tito Trindade (PT)	LOW TEMPERATURE - DYNAMICS // REACTIVE SPECIES // GAS PHASE - INTRAMOLECULAR INTERACTIONS	MATERIALS // COMPUTATIONAL // BIOMEDICAL APPLICATIONS	KL-24: Markus Arndt (AT)	KL-26: Hugh Byrne (IR)
			KL-5: Nigel Young (UK) // KL-8: Mike Ashfold (UK) // KL-11: Jan Lundell (FIN)	KL-19: Micahel Oshtrakh (RUS) // KL-20: Frederic Merkt (CH) // KL-21: Anders Engdahl (SW)		
11:20		OC1: Andrzej Kudelski (PL)	KL-6: Igor Reva (PT) // KL-9: Cláudio Nunes (PT) // KL-12: Elangannan Arunan (IND)	OC24: Irina V. Alenkina (RUS) // OC29: Franco Egidi (I) // OC34: Katarzyna Marzec (PL)	OC44: Alberto Mezzetti (F)	KL-27: Herbert Michael Heise (D)
11:40		OC2: Veronika Sutrová (CZ)	KL-7: Nicolay Kotov (CZ) // KL-10: Anna Gudmundsdottir (USA) // KL-13 José Luís Alonso (SP)	OC25: Jorge Costa Pereira (PT) // OC30: Bernardo de Souza (BRA) // OC35: Martynas Velicka (LIT)	OC45: Valery Andrushchenko (CZ)	KL-28: Luís Arnaut (PT)
12:00		OC3: Daria Ruth Galimberti (F)	OC13: Joanna Hetmanczyk (PL) // OC16: Julien Guthmuller (PL) // OC19: Sérgio R. Domingos (D)	OC26: Bence Kutus (H) // OC31: Malgorzata Biczysko // OC36: Czesława Paluszkievicz (PL)	OC46: Tatsuya Mori (J)	KL-29: Henry H. Mantsch (CAN)
12:20		OC4: Paula C. Pinheiro (PT)	OC14: Ivan Giba (RUS) // OC17: Kess Marks (SW) // OC20: Thomas E. Wall (UK)	OC27: Seoncheol Cha (D) // OC32: Elena Yu. Tupikina (RUS) // OC37: Maciej Roman (PL)	OC47: Jakub Kaminsky (CZ)	EUCMOS XXXV Presentation
12:40		OC5: Petr Praus (CZ)	OC15: Eva Scholtzová (SK) // OC18: Lucia K. Noda (BRA) // OC21: Gyorgy Tarczay (HUN)	OC28: Svetlana S. Khokhlova (RUS) // OC33: Marco Mendolicchio (I) // OC38: Ewelina Szafraniec (PL)	OC48: Maria Lurdes Cristiano (PT)	Closing Ceremony
13:00		Lunch	Lunch	Lunch	Lunch	Lunch

PROGRAMME TIMETABLE						
Time	19 th (Sunday)	20 th (Monday)	21 st (Tuesday)	22 nd (Wednesday)	23 rd (Thursday)	24 th (Friday)
		MATERIALS AND ANALYTICAL	HIGH-RESOLUTION SYMPOSIUM	NEW METHODS // ENERGY // MIXTURES		
15:00		PL- 2: Wybren Jan Buma (NL)	PL- 4: Luca Evangelisti (I)	PL - 6: Eberhard Riedle (D)		
16:00		OC6: Monika Plass (CH)	KL-14: Otto Dopfer (D) // KL-16: Michael Schmitt (D)	KL-22: Mustafa Culha (TR) // OC39: Mirosław A. Czarnecki (PL)		
16:20		OC7: Sven P. K. Koehler (UK)	KL-15: Leonardo Alvarez-Valtierra (MX) // KL-17: Elena R. Alonso (SP)	OC40: Omar A. El Seoud (BRA) // OC42: Ivan Nemec (HUN)		
16:40		OC8: Terao Wakana (J)	OC22: Mirko Lindic (D) // OC23: América Torres-Boy (MX)	OC41: Helena Nogueira (PT) // OC43: Simona Rada (ROM)		
17:00		Coffee Break	Coffee Break	Coffee Break		
17:30		KL-3: José Gaspar Martinho (PT)				
18:00	Registration	OC9: Sylvia Turrel (F)				
18:20		OC10: Yasmine Schulenburg (D)	Poster Session I	Poster Session II		
18:40		OC11: Dhanya Puthenmadom (B)				
19:00	Welcome party	OC12: Lucia Bonoldi (I)				
20:00						
21:00					Gala Dinner	

MONDAY, 20th AUGUST

Novel Molecular Terahertz Spectroscopies

Mischa Bonn

*Max Planck Institute for Polymer Research, Department of Molecular Spectroscopy
Ackermannweg 10, 55128 Mainz, Germany
bonn@MPIP-Mainz.MPG.de*

Terahertz spectroscopy, spanning the range from 0-20 THz, or equivalently, 0-660 cm^{-1} , has been widely and very successfully used in the study of charge carrier dynamics in semiconductors [1]. There have been decidedly fewer successful studies reporting molecular spectroscopy in this interesting fingerprint region, where optical phonons and low-frequency vibrational modes are active. At room temperature, substantial thermal excitation of these low-frequency modes typically occurs, determining the structural dynamics in a variety of systems. Here, I describe our recently developed new types of terahertz spectroscopies to obtain important insights in both phonon dynamics in solid-state materials [2] and coupling between high-frequency modes and low-frequency modes in water [3] and other systems.

References

1. R. Ulbricht, E. Hendry, J. Shan, T. F. Heinz, M. Bonn, *Rev. Mod. Phys.* 83 (2011) 543.
2. H. Kim, J. Hunger, E. Cánovas, M. Karakus, Z. Mics, M. Grechko, D. Turchinovich, S. H. Parekh, M. Bonn, *Nat. Commun.* (2017) DOI: 10.1038/s41467-017-00807-x.
3. M. Grechko, T. Hasegawa, F. D'Angelo, H. Ito, D. Turchinovich, Y. Nagata, M. Bonn, *Nat. Commun.* (2018) DOI: 10.1038/s41467-018-03303-y.

Non Linear Optics at Interfaces: Sensitive Probing of Biomolecular Recognition by Sum Frequency Generation and the Quest of Super Resolution Infrared Microscopy of Biological Tissues

N. Hedaoui^a, C. Bouchened^b and André Peremans^c

^a *Centre de Développement des Technologies Avancée (CDTA), Cité 20 août 1956 Baba Hassen, Alger.*

^b *Université des Sciences et de la Technologie Houari Boumediene (USTHB), BP 32 El Alia, Bab Ezzouar 16111, Alger.*

^c *Université de Namur (UNAMUR), PMR, 61 rue de Bruxelles, Namur, Belgique
andre.peremans@unamur.be*

Since the pioneering work of Guyot-Sionnest in 1987, vibrational spectroscopies exploiting the non-linear optical processes have opened new opportunities for the analysis of biological systems, as well as, for bypassing the spatial resolution limit imposed by diffraction in infrared microscopy.

Indeed, biological molecules are complex and their infrared spectroscopy signature barely modified upon the structural change resulting from bio-recognition interactions. However, the selection rules of sum-frequency generation (SFG) makes this technique particularly sensitive to these structural modifications, and adapted for the determination of the biological films configuration as we demonstrated for: avidin-biocytin, penicillin derivative molecule, and biomimetic lipid systems.

Chemical cartography of biological tissues is traditionally realized by anchoring fluorescent chromophores on specific chemical functions. In 1994, Hell demonstrated the possibility of bypassing the spatial resolution limit, due to diffraction, in fluorescent microscopy using the stimulated-emission-depletion (STED) process. We recently demonstrated that the intrinsic non-linear optical properties of vibrational transitions also enable to perform super-resolution infrared microscopy on semiconductor and polymer materials, opening the prospect of label-free super resolution vibrational microscopy.

Developing the Surface Chemistry of Hybrid Nanomaterials for SERS

Tito Trindade

Department of Chemistry – CICECO, University of Aveiro, 3810-193 Aveiro, Portugal
tito@ua.pt

The application of conventional Raman spectroscopy for trace detection of compounds of environmental and biological interest has been hampered by their low intense Raman signals. This is consequence of the small Raman scattering cross-section, which usually implies that the sample under analysis should be present in reasonable amounts. Surface enhanced Raman scattering (SERS) is a surface method that has been exploited in several areas with great impact in the development of new analytical platforms for chemical detection of vestigial amounts of certain organic compounds. The SERS effect originates enhanced Raman signals for molecules present in the vicinity of certain metal surfaces, typically of gold and silver [1,2]. Among the several factors that affect such Raman signal enhancement, the chemical nature and morphological features of employed SERS substrates are of paramount relevance. As such, great efforts have been made in order to fabricate highly sensitive SERS substrates with controlled features at the nanoscale level [3,4].

This lecture will provide an overview of our research on several nanomaterials that have been investigated aiming at the fabrication of SERS substrates [4]. In particular, hybrid nanostructures that result from more than one type of material will be described, together with surface modification strategies that intend to improve their applicability as SERS substrates for analytical detection. Examples of such nanomaterials include metal (Ag, Au) loaded polymer nanocomposites and multiphasic inorganic nanostructures of colloidal nature. Although the emphasis has been on materials development rather than the implementation of analytical protocols, several types of analytes have already been tested in SERS detection by using these nanomaterials. Here we will consider the SERS detection of organic compounds that raise serious concerns due to their adverse effects as water pollutants. Finally, the challenges that this approach faces in real applications will be addressed together with important recent developments that might mitigate some of these limitations, such as instrumentation development associated to surface chemistry methods.

References

1. R. Aroca, *Surface-Enhanced Vibrational Spectroscopy*, 1st ed., Wiley, Chichester, 2006.
2. S.-Y. Ding, E.-M. You, Z.-Q. Tian and M. Moskovits, *Chem. Soc. Rev.* 46 (2017) 4042.
3. S. L. Kleinman, R. R. Frontiera, A.-I. Henry, J. A. Dieringer and R. P. Van Duyne, *Phys. Chem. Chem. Phys.* 15 (2013) 21.
4. S. Fateixa, H. I. S. Nogueira and T. Trindade, *Phys. Chem. Chem. Phys.*, 17 (2015) 21046.

Acknowledgements: This work was developed within the scope of the project CICECO- Aveiro Institute of Materials, POCI-01-0145-FEDER-007679 (FCT Ref. UID /CTM /50011/2013), financed by national funds through the FCT/ MEC and when appropriate co-financed by Fundo Europeu de Desenvolvimento Regional (FEDER) under the PT2020 Partnership Agreement.

Plasmonic Nanoparticles with Many Sharp Apexes and Edges as Efficient Nanoresonators for Shell-Isolated Nanoparticle-Enhanced Raman Spectroscopy

Andrzej Kudelski

*Faculty of Chemistry, University of Warsaw, ul. Pasteura 1, 02-093 Warsaw, Poland
akudel@chem.uw.edu.pl*

One method allowing for investigations of various interfaces, even so-called buried interfaces (*e.g.*, surfaces of solid samples in a high pressure gas or liquid) is the deposition of plasmonic nanostructures on the analysed surfaces and subsequent recording of the Raman spectra. Plasmonic structures act as electromagnetic nanoresonators leading to a local enhancement of the intensity of the electric field of the incident radiation, which leads to an increase in the efficiency of Raman scattering for molecules in close proximity to such nanoresonators. Because many biological molecules can change their structure during interaction with metal surfaces, plasmonic nanostructures are sometimes covered with very thin layers of chemically inert oxides, which prevent direct interaction between the sample being analysed and the metal surface. The Raman analysis of surfaces using surface-protected plasmonic nanoparticles is called shell-isolated nanoparticle-enhanced Raman spectroscopy (SHINERS) [1]. In this contribution, the examples of using of plasmonic nanoparticles with many sharp apexes and edges, such as: bipyramidal-Au@SiO₂, decahedral-Ag@SiO₂, cubic-Ag@SiO₂, and silica-covered star-shaped Au-Ag nanoparticles as SHINERS nanoresonators will be presented (see Figure 1). Since the highest field enhancement is usually generated on sharp edges and apexes of plasmonic nanostructures, the Raman enhancement factor induced by such anisotropic nanoparticles is significantly (even above one order of magnitude) larger than the enhancement factor generated by respective standard semi-spherical nanostructures. Synthesized SHINERS nanoresonators were used for measurements of some thiolate monolayers formed on a platinum surface and for detecting the pesticides thiram and methyl parathion deposited on surfaces of various fruits and vegetables. For example, the limit of detection of thiram deposited on a tomato skin was estimated as 1.2 ng cm⁻².

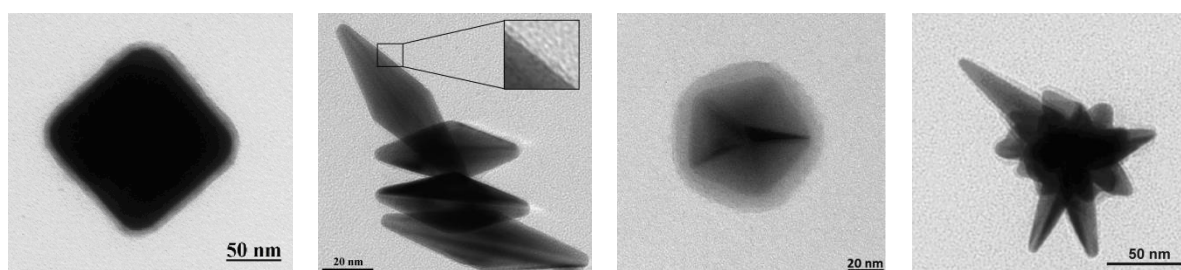


Figure 1 – TEM images of various SHINERS nanoresonators.

References

1. J. F. Li, Y. F. Huang, Y. Ding, Z. L. Yang, S. B. Li, X. S. Zhou, F. R. Fan, W. Zhang, Z. Y. Zhou, D. Y. Wu, B. Ren, Z. L. Wang, and Z. Q. Tian, *Nature*, 464 (2010) 392.

Acknowledgements: The author thanks the Faculty of Chemistry, University of Warsaw.

Ag Nanosponge Aggregate with Incorporated Hydrophobic Adsorbates as a Sample for Effective SER(R)S Spectral Detection

Veronika Sutrová^{a,b}, I. Šloufová^a, E. Pavlova^b and B. Vlčková^a

^a Dept. of Physical and Macromolecular Chemistry, Charles University, Hlavova 2030, 128 43, Prague 2, CZ

^b Institute of Macromolecular Chemistry, ASCR, v.v.i., Heyrovsky Sq. 2, 162 06 Prague 6, CZ
sutrovav@natur.cuni.cz

Surface-enhanced Raman scattering (SERS) and Surface-enhanced resonance Raman scattering (SERRS) spectroscopies are well-known spectro-analytical methods, which utilize enhancement of Raman scattering of molecules by plasmonic metal nanostructures. Effective localization of molecules into “hot spots” (i.e. strong, nanoscale localized optical fields generated in plasmonic metal nanostructures, such as nanoparticle (NP) assemblies, by an external optical excitation) provides large enhancement of their Raman signal. Presence of “hot spots” has been predicted and proved experimentally in fractal aggregates [1,2] and in dimers of Ag NPs [3,4]. Recently, we obtained strong indices about the presence of “hot spots” in 3D Ag nanosponge aggregates containing hydrophilic adsorbates [5].

In this contribution, we report preparation and SERS spectral testing of 3D Ag nanosponge aggregates, which were assembled in a two-phase system containing a Ag-NPs hydrosol modified by adsorbed Cl^- and a dichloromethane solution of the selected hydrophobic adsorbates, namely fullerenene (C_{60}) and 5,10,15,20-tetraphenyl-21H,23H-porphine (TPP). Ag-NPs hydrosol was prepared by reduction of AgNO_3 by $\text{NH}_2\text{OH}\cdot\text{HCl}$ [6]. For SE(R)RS spectral measurements, 3D Ag nanosponge aggregates with incorporated testing adsorbate and chloride anions were prepared and let to dry. SERS and SERRS spectra were measured at four excitation wavelengths, namely 445, 532, 633 and 780 nm. The concentration values of the limits of SE(R)RS spectral detection of TPP were determined as follows: 1×10^{-13} M at 445 nm excitation (SERRS), and 1×10^{-8} M at 532 nm, 1×10^{-8} M at 633 nm and 1×10^{-7} M at 780 nm (SERS). Furthermore, the following concentration values of the limits of SERS spectral detection were determined for C_{60} : 1×10^{-6} M at 445 nm, 1×10^{-7} M at 532 nm, 1×10^{-5} M at 633 nm and 1×10^{-6} M at 780 nm. A comparison of the limits of the SE(R)RS spectral detection of TPP with those of C_{60} shows that the former are significantly lower than the latter ones. This can be caused by several factors, such as a less effective incorporation of C_{60} into the internal structure of Ag nanosponge aggregate than that of TPP. We have also tested the systems, in which the Ag nanosponge aggregate was overlayed by a solution of the testing adsorbate. In that case, the limits of SE(R)RS spectral detection are, for both adsorbates, by two orders of magnitude higher than in case of their incorporation into the internal structure of Ag nanosponge aggregates. Incorporation of the adsorbates into the aggregates structure thus represent a substantially more effective way of their SERRS and/or SERS spectral detection.

References

1. M. I. Stockman, V. M. Shalaev, M. Moskovits, R. Botet and T. F. George, *Phys. Rev. B*, 46 (1992) 2821.
2. P. Zhang, T. L. Haslett, C. Douketis and M. Moskovits, *Phys. Rev. B*, 57 (1998) 15513.
3. H. Xu, J. Aizpurua, M. Käll and P. Apell, *Phys. Rev. E*, 62 (2000) 4318.
4. B. Vlčková, M. Moskovits, I. Pavel, K. Šišková, M. Sládková and M. Šlouf, *Chem. Phys. Lett.*, 455 (2008) 131.
5. V. Sutrová, I. Šloufová, M. Nevorlová and B. Vlčková, *J. Raman. Spectrosc.*, 46 (2015) 559.
6. N. Leopold and B. Lendl, *J. Phys. Chem. B*, 107 (2003) 5273.

Acknowledgements: The authors thank to grants 892217 (GAUK), 17-05007S (GACR), TE01020118 (TACR) and POLYMAT LO1507 (MSMT, NPU I).

Molecular Organization at Charged Solid-Water Interfaces: vSFG $\chi(2)(\omega)$ signal, $\chi(3)(\omega)$ Contribution and How to Use Them for Revealing Interfacial Structures

Daria Ruth Galimberti, Simone Pezzotti and Marie-Pierre Gaigeot

LAMBE UMR8587, Université d'Evry val d'Essonne, Blvd F. Mitterrand, Bat Maupertuis, 91025 Evry,
France Université Paris-Saclay, France
dariaruth.galimberti@univ-evry.fr

The understanding of the molecular organization at mineral-water interfaces is a mandatory first step on the path to the rationalization of physico-chemical phenomena taking place at these interfaces and governing for example the transport of organic molecules and pollutants in soils, heterogeneous catalysis for e.g. photovoltaics and batteries, drugs encapsulation and relishing... Non-linear vSFG (vibrational Sum Frequency Generation) spectroscopy is one of the most powerful techniques to get an understanding of the water structural organization at interfaces, since SFG signal is zero for centrosymmetric media such as bulk water. However, due to the complexity of the involved interfacial phenomena and the interplay of multiple contributions, the interpretation of these spectra based on the experiments alone is not so trivial.

For charged interfaces, the molecular interpretation of SFG spectral signatures becomes even more complex: the signatures arising from the first water layer in contact with the solid surface are convoluted with the signatures of water located farther away from the surface. The deconvolution of these signatures is mandatory to correctly interpret vSFG spectra of charged interfaces, as shown by Shen *et al.* [1] recently. In collaboration with Shen's group, using DFTMD simulations, we have developed [2,3] an unambiguous and universal structural definition for the two spatial interfacial regions denoted as BIL (Binding Interfacial Layer) and DL (Diffuse Layer) in ref.1, using water structural properties only. In particular, our deconvolution scheme allows demonstrate that the DL spectrum arises from the non-linear third order contribution of bulk liquid water, therefore with a universal molecular origin at any charged interface. We furthermore show how our deconvolution scheme provides direct knowledge of the isoelectric point at any aqueous surface and characterization of the formation of an Electric Double Layer (EDL) when aqueous ionic solutions are considered [2,3].

References

1. Y.-C. Wen, S. Zha, X. Liu, S. Yang, P. Guo, G. Shi, H. Fang, Y. R. Shen and C. Tian, *Phys. Rev. Lett.*, 116 (2016).
2. S. Pezzotti, D. R. Galimberti, Y. R. Shen and M.-P. Gaigeot, *Phys. Chem. Chem. Phys.*, 20 (2018) 5190.
3. S. Pezzotti, D. R. Galimberti, M.-P. Gaigeot and Y. R. Shen, *Submitted to J. Phys. Chem. C*.

Magneto-Plasmonic Nanoparticles for Separation and SERS Detection of Antibiotics

Paula C. Pinheiro, Sara Fateixa and Tito Trindade

Department of Chemistry, CICECO-Aveiro Institute of Materials, University of Aveiro,
3810-193 Aveiro, Portugal
pcpinheiro@ua.pt

Vestigial antibiotics dissolved in water sources have been regarded with increasing concern due to potential risks to human health and ecological negative impact. In particular, the occurrence of these pharmaceuticals in aquatic ecosystems might contribute to the increasing resistance of some pathogenic microorganisms to conventional antibiotics [1]. Common methods for detection of antibiotic vestiges are generally time-consuming, cost intensive and involve complex laboratorial procedures. In this context, surface-enhanced Raman scattering (SERS) emerges as an interesting method to explore because it affords high sensitivity, spectroscopic fingerprints, easy sample preparation, and non-destructive analyses. Our interest in this field, prompted us to develop several types of nanostructured platforms for SERS detection of bioanalytes dissolved in water, including molecules of antibiotics [2-4].

Here, we report the preparation of multifunctional hybrid nanostructures that combine magnetic (Fe_3O_4) and plasmonic (Ag, Au) colloidal nanoparticles. The ability of such magneto-plasmonic nanocomposites for SERS detection of antibiotics (e.g. penicillin G) dissolved in aqueous solutions was evaluated in a range of operational conditions. Taking advantage of the magnetic properties of the nanocomposites, these materials can be used to concentrate the target analyte on the substrate and as such to contribute for a more effective SERS detection. Additionally, adsorption studies were carried out for assessing the performance of such substrates. The results will be discussed on a perspective of using these materials as analytical platforms for laboratorial monitoring and also in local sampling points located in remote regions.



Figure 1 – Schematic representation of a magneto-plasmonic nanostructure.

References

1. C. Xi, Y. Zhang and C. F. Marrs, *Appl. Environ. Microbiol.*, 75 (2009) 5714.
2. S. Fateixa, H. I. S. Nogueira and T. Trindade, *Phys. Chem. Chem. Phys.*, 17 (2015) 21046.
3. P. C. Pinheiro, S. Fateixa, H. I. S. Nogueira and T. Trindade, *J. Raman Spectrosc.*, 46 (2015) 30.
4. P. C. Pinheiro, S. Fateixa, H. I. S. Nogueira and T. Trindade, *Magnetochemistry*, 46 (2017) 32.

Acknowledgements: P. C. Pinheiro thanks Fundação para a Ciência e Tecnologia (FCT) for the grant SFRH/BD/96731/2013. S. Fateixa thanks FCT for the Grant SFRH/BPD/93547/2013. This work was financed by national funding from FCT (Fundação para a Ciência e a Tecnologia) by FEDER through program COMPETE and by national funding through FCT in the frame of project CICECO - FCOMP-01-0124-FEDER- 037271 (Ref. FCT Pest-C/CTM/LA0011/2013).

Metal-Enhanced Fluorescence of Riboflavin Deposited on Spacer-Modified Ag Substrate: Spectral Intensity and Lifetime Study

Petr Praus^a, Eva Kočiřová^a, Martin Šubr^a, Franck Sureau^b, Ondřej Kylián^c,
Anna Kuzminova^b, Marek Procházka^a and Josef Štěpánek^a

^a Charles University, Faculty of Mathematics and Physics, Ke Karlovu 5, 12116 Prague, Czech Republic

^b Laboratoire Jean Perrin, case courrier 114, 4 Place Jussieu, 75005 Paris, Université P. et M. Curie, France

^c Charles University, Faculty of Mathematics and Physics, Department of Macromolecular Physics V,
Holeřovičkách 2, 18000 Prague
praus@karlov.mff.cuni.cz

Metal-enhanced fluorescence (MEF) is a case if the excited fluorophore strongly interacts with surface plasmons of nanostructural metal surface leading to increases in fluorescence intensity and decreases in lifetime. This phenomenon strongly depends on the fluorophore molecule distance from the metal surface [1].

Confocal microspectrofluorimeter adapted for time-resolved intracellular fluorescence measurements by using a phase-modulation principle with homodyne data acquisition was employed to obtain fluorescence emission spectra and to determine fluorescence lifetimes. Experimental setup is appropriately arranged for the lifetime determination in measured spectrum as well [2,3]. MEF spectra of riboflavin (vitamin B₂), which is a biologically important molecule, were obtained from solution deposited on silver nanoislands [4] covered by a polytetrafluoroethylene (PTFE) spacer of thickness from 0 to 20 nm. We have focused on the fluorescence intensity enhancement factor and the lifetime shortening in dependence on the PTFE spacer thickness (see Fig. 1).

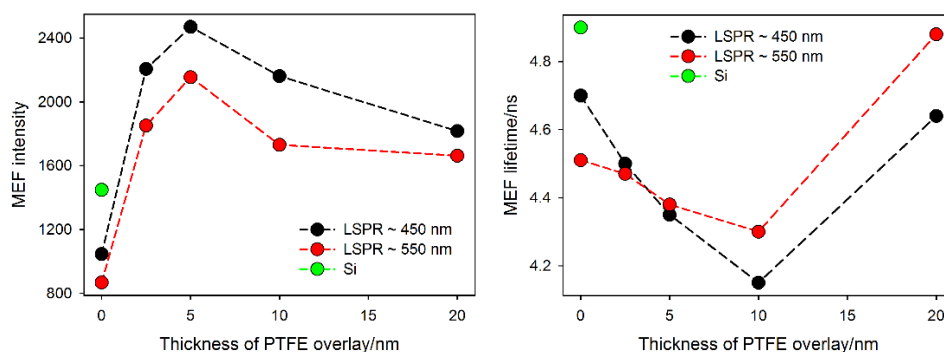


Figure 1 – Left: Surface-enhanced fluorescence (SEF) intensity spectra of riboflavin in a water solution dropped on Ag nanoislands covered by a PTFE spacer of various thickness. Right: Riboflavin lifetimes measured at a water solution/spacer interface. Concentration of the riboflavin stock solution was 10^{-5} M; comparison to the droplet on a Si wafer is made.

References

1. K. Ray and J. R. Lakowicz, *J. Phys. Chem. C*, 117 (2013) 15790.
2. E. Kočiřová, P. Praus, J. Bok, S. Bonneau and F. Sureau, *J. Fluoresc.*, 25 (2015) 1245.
3. P. Praus *et al.*, *Curr. Org. Chem.*, 11 (2007) 515.
4. M. Šubr, M. Petr, O. Kylián, J. Kratochvíl and M. Procházka, *J. Mat. Chem. C*, 3 (2015) 11478.

Acknowledgements: The funding from the Czech Science Foundation grant P205/12/G118 is gratefully acknowledged

Tailoring Photoactive Materials: Light on the Dark Side of the Force

Wybren Jan Buma

*Van 't Hoff Institute for Molecular Sciences, University of Amsterdam,
Science Park 904, 1098 XH Amsterdam, The Netherlands
w.j.buma@uva.nl*

Absorption of light brings molecules into an activated state. From this state radiative processes can occur, but much more interesting are the nonradiative, dark processes in which the photon energy is transformed into other forms such as mechanical and chemical energy. We aim to control these light-to-activity pathways as they allow us to use photon energy to drive targeted applications such as energy conversion, photocatalysis, photon-driven molecular nanotechnology, as well as optogenetics and photopharmacology.

Key to tailoring photoactivity are studies of the potential energy surfaces of electronically excited states. This is not trivial because photoactivity is generally associated with (ultra)fast conversions of energy. Using eye-catchers from molecular nanotechnology, health care, and various areas where photochromic compounds are employed, we have shown in recent years how 'slow' spectroscopies can map the excited-state potential energy surfaces and reveal the dynamics that occur on these surfaces. This is exciting as there is a huge amount of photoresponsive systems that so far have been deemed inaccessible because of their short excited-state lifetimes. There is thus still much to be learnt on the dark side of the forces that act upon molecules after light absorption.

Thermal Degradation Behaviour of Elastomers

Monika Plass^a, Ahmar Hasnain^a and Varun Thakur^b

^a *Dow Europe GmbH, Core R&D Analytical Sciences*

^b *Elastomer & Electrical Telecommunication Bachtobelstr. 3, 8810 Horgen, Switzerland*
mplass@dow.com

The thermal behaviour of EPDM elastomers has been studied under oxidative as well as inert conditions using thermal gravimetric analysis hyphenated with FTIR spectroscopy.

The coupling of these two analytical techniques allows to study the gas molecules evolved at inert and oxidative conditions and thus is a great tool for the investigation of degradation effects complementary to TGA/MS analysis.

In the presentation we will be discussing the challenges of the TGA/FTIR spectroscopy as routine method for pure polymer and polymer formulation analysis and compare with other techniques usually applied for the investigation of thermal stability analysis.

On the example of ethylene-propylene-diene copolymers (EPDM) with different comonomer composition the degradation mechanism will be presented. The evolved species will be characterized by FTIR and mass spectrometry. In particular, the effect of ethylene and diene content on the thermal stability of the polymer will be shown.

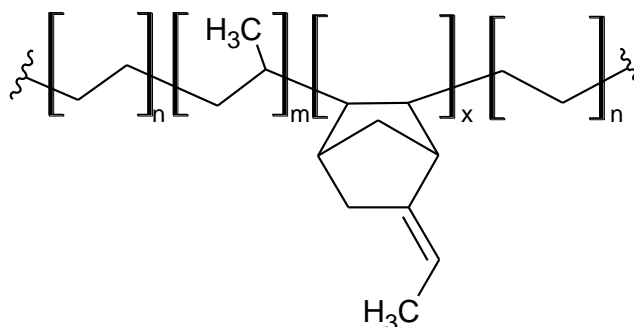


Figure 1 – Structure of EPDM

Characterisation, Coverage, and Orientation of Functionalised Graphene using Sum-Frequency Generation Spectroscopy

Sven P. K. Koehler, Huda AlSalem and Chloe Holroyd

Manchester Metropolitan University, Chester Street, Manchester, M1 5GD, UK

Photon Science Institute, University of Manchester, Oxford Road, Manchester, M13 9PL, UK

s.koehler@mmu.ac.uk

Graphene has received much attention due to its remarkable (opto-)electronic properties. However, graphene does not possess a band gap, which limits its implementation in many proposed applications. Hence more attention has recently been paid to modified graphene and graphene derivatives. Graphene is most commonly characterised by Raman spectroscopy, but this has a number of drawbacks when investigating functionalised graphene. We have hence employed vibrational sum-frequency generation (SFG) spectroscopy to directly identify functional groups bound to graphene based on their vibrational signatures.

In the work reported here, we studied 1) polymer impurities on graphene [1], 2) phenyl-decorated graphene [2], and 3) hydrogenated graphene [3]. The SFG spectra below show the aromatic C-H stretches of the phenyl rings on graphene, and the C-H stretches of hydrogenated graphene. While comparison with a self-assembled monolayer of phenyl thiols allows us to extract surface coverages for the phenyl-decorated graphene ($\sim 2.0 \times 10^{14} \text{ cm}^{-2}$, or $\sim 5\%$ of carbon atoms of graphene), we can extract information about the binding motifs of hydrogen to graphene by comparison with density functional theory calculations.

We have also established that the de-coherence times of the vibrationally excited aromatic C-H bonds on phenyl-graphene and on phenyl-self-assembled monolayers are below 1 ps [4], and hence independent of the presence of the graphene substrate.

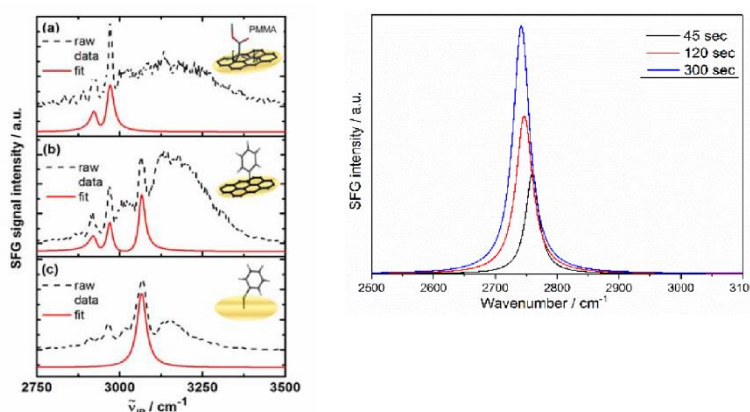


Figure 1 – (Left) Raw (black dotted) and fitted (solid red) SFG spectra of (a) PMMA on pristine graphene, (b) phenyl-functionalised graphene, and (c) a phenyl-self-assembled monolayer. (Right) Fitted C-H stretches of hydrogenated graphene after different Birch reduction times.

References

1. C. Holroyd, A. B. Horn, C. Casiraghi and S. P. K. Koehler, *Carbon*, 117 (2017) 473.
2. H. AlSalem, A. B. Horn and S. P. K. Koehler, *Phys. Chem. Chem. Phys.*, 20 (2018) 8962.
3. H. AlSalem, X. Just, I. Larossa and S. P. K. Koehler, *submitted* (2018).
4. H. AlSalem and S. P. K. Koehler, *in preparation*.

Detection of Boson Peak and Fracton of Sodium Carboxymethyl Starch by Terahertz Time-domain Spectroscopy

Terao Wakana^a, Tatsuya Mori^a, Karolina Kaczmarek^b, Beata Grabowska^b, Yasuhiro Fujii^c, Akitoshi Koreeda^c, Jae-Hyeon Ko^d and Seiji Kojima^a

^a Division of Materials Science, University of Tsukuba, 1-1-1 Tennodai, Tsukuba, Ibaraki 305-8573, Japan

^b AGH – University of Science and Technology, Faculty of Foundry Engineering, Reymonta 23, 30 059 Krakow, Poland

^c Department of Physical Sciences, Ritsumeikan University, 1-1-1 Noji-higashi, Kusatsu, Shiga 525-8577, Japan

^d Department of Physics, Hallym University, 1 Hallymdaehakgil, Chuncheon, Gangwondo 24252, Korea
mori@ims.tsukuba.ac.jp (Tatsuya Mori)

For glass forming materials, universal excitation called boson peak is observed in the terahertz region [1]. We have recently pointed out how this BP appears in the infrared spectrum [2,3], although this fact was familiar to past researchers [4]. On the other hand, in polymer glass, there is fractal dynamics, so-called fracton, which is expected to appear above boson peak frequency as a result of self-similarity of monomer molecules and anomalous diffusion process [5]. The fracton dynamics has been discussed experimentally by using low-frequency Raman scattering [6].

Starch is a natural polymer formed by polymerization of a number of α -glucose molecules by glycosidic linkage and includes straight-chain amylose and amylopectin having a branched structure. It is known that the content of both amylose and amylopectin is changed depending on the plant from which it is derived, and the crystallinity is lowered when the amylose content is high [7]. Furthermore, the microwave-treated carboxymethyl starch (CMS-Na) used in this study is amorphous with almost zero degree of crystallinity and it is suitable as a basic research substance of polymer glass [8].

In this study, we attempt to detect universal boson peak behavior in glassy materials and fracton expected to universally appear in polymer glass, using terahertz time-domain spectroscopy and low-frequency Raman scattering, for CMS-Na.

References

1. T. Nakayama, *Rep. Prog. Phys.*, 65, (2002) 1195.
2. M. Kabeya, T. Mori, Y. Fujii, A. Koreeda, B. W. Lee, J. H. Ko and S. Kojima, *Phys. Rev. B*, 94 (2016) 224204.
3. W. Terao, T. Mori, Y. Fujii, A. Koreeda, M. Kabeya and S. Kojima, *Spectrochim. Acta A*, 192 (2018) 446.
4. T. Ohsaka and S. Oshikawa, *Phys. Rev. B*, 57, (1998) 4995.
5. S. Alexander and R. Orbach, *J. Phys. (Paris)*, 43 (1982) L625.
6. S. Saikan, T. Kishida, Y. Kanematsu, H. Aota, A. Harada and M. Kamachi, *Chem. Phys. Lett.*, 166 (1990) 358.
7. N. W. H. Cheetham and L. Tao, *Carbohydr. Polym.*, 36 (1998) 277.
8. K. Kaczmarek, B. Grabowska, T. Spychaj, M. Zdanowicz, M. Sitarz, A. Bobrowski and S. Cukrowicz, *Spectrochim. Acta A*, in press.

Acknowledgements: This work was partially supported by JSPS KAKENHI Grants No. 17K14318, the Nippon Sheet Glass Foundation for Materials Science and Engineering, and the Asahi Glass Foundation.

Biphotonic Materials for Bioimaging

José M. G. Martinho, Inês F. A. Mariz and Ermelinda Maças

Centro de Química Estrutural and IN- Institute of nanoscience and Nanotechnology, Instituto Superior Técnico,
Av. Rovisco Pais 1, 1049 Lisboa, Portugal
jgmartinho@tecnico.ulisboa.pt

Two-photon optical microscopy have attracted much attention for 3D-imaging in biological media owing to the deep tissue penetration of the excitation light, reduced out-of-focus photobleaching, up-converted emission and well separated emission from the scattered excitation light.

Fluorescent probes with high two-photon absorption (TPA) cross-section, fluorescence quantum yield and photostability are needed to reach the potential of the technique. In this communication the photophysical properties of a family of quinolinizinium dyes [1] polymers and hybrid polymer nanoparticles based on the 1,3,5-triazine unit [2] and N-doped carbon dots [3] are presented.

The carbon dots are particularly suitable as TPA fluorophores for bioimaging due to their high photostability, water solubility, biocompatibility and versatile surface chemistry despite their modest TPA cross-section (200-1000 GM) and fluorescence quantum yield. The dispersion of carbon dots is heterogeneous with carbon dot sizes of the order of 5 nm (diameter) and excitation wavelength dependent emission with two main bands with maximum at 440 nm (blue) and 520 nm (green) by one-photon excitation (OPExc). Interestingly, by two-photon excitation (TPExc) only the green emission was observed shown in Fig. 1. This results in the selective excitation of the green emitting site by TPA.

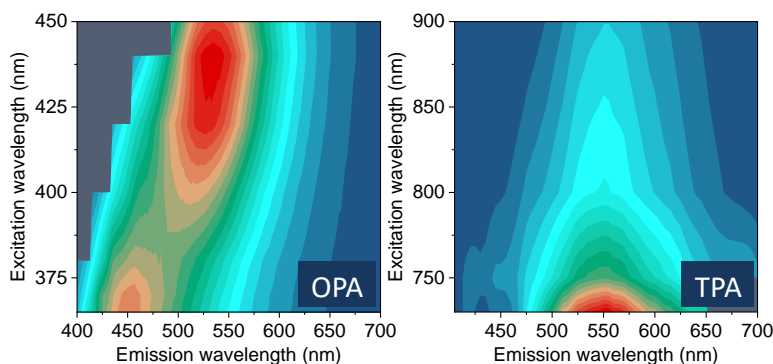


Figure 1 – Excitation-wavelength dependence of the emission spectra of carbon dots by one-photon (OPA) and two-photon absorption (TPA).

References

1. G. Marcelo, S. Pinto, T. Cañeque, I. F. A. Mariz, A. M. Cuadro, J. J. Vaquero, J. M. G. Martinho and E. M. S. Maças, *J. Phys. Chem. A*, 119 (2015) 2351.
2. I. F. A. Mariz, E. M. S. Maças, J. M. G. Martinho, L. Zou, P. Zhou, X. Chen and J. Qin., *J. Mater. Chem. B* 1 (2013) 2109.
3. C. M. Santos, F. A. Mariz, S. N. Pinto, G. Gonçalves, I. Bdikin, P. A. A. P. Marques, M. G. Neves, J. M. G. Martinho and E. Maças, *Nanoscale* 00 (2018) 000.

Acknowledgements: The authors thanks FCT for: UID/NAN/50024/2013, SFRH/BPD/75782/2011, IF/00759/2013 and PD/BD/127805/2016).

The What, How and Where in Art and Archaeology: Use of Raman Spectroscopy for the Study of Ceramics, Glasses and Porcelains

S. Turrell^a, O. Robbe-Cristini^b, M. Moreau^a, A. Didier^c and B. Richard^d

^a LASIR (CNRS, UMR 8516), Université Lille, 59650 Villeneuve d'Ascq, France

^b PhLAM (CNRS, UMR 8523), Université Lille, 59650 Villeneuve d'Ascq, France

^c Equipe Archéologie de l'Asie Central (CNRS, UMR 7041) Nanterre, France

^d UFR Sciences, URCA, Université de Reims, 51687 Reims, France

sylvia.turrell@univ-lille1.fr

Art conservators have long been armed with analytical techniques to explore the chemical make-up of paints and dyes, glasses and ceramics. But often the questions for researchers at the arts/science interface concern, not just the chemical content of the material or object, but also technologies possibly used for the fabrication or for the surface decoration. Often questions concerning the identification of corrosion products or the determination of contaminants, or the evolution of chemical mechanisms involved can aid in the identification of the provenance and authenticity of an object, as well as details related to production or storage. But all of these problems involve structural information of complex artefacts and thus require a multi-technique approach to perform adequate characterization of original and altered compounds.

In this context, Raman spectroscopy has shown to be an extremely powerful addition to the panel of techniques for the non-destructive or minimally destructive characterization of such materials.

In this presentation, three case studies will be presented in order to demonstrate the broad domains in which Raman spectroscopy can contribute to the unravelling of problems related to glasses and porcelains. The examples, covering the determination of raw materials, of fabrication processes and of firing techniques, will be: the comparison of characteristics and evolutions of painting techniques (raw materials, fabrics and painting processes) of potters in two regions of bronze-age Pakistan; the laboratory determination of firing temperatures of ancient Deruta potteries; the verification and comparison of techniques used in four different factories for the 20th century fabrication of faïences and porcelains.



Figure 1 – Kachi-Bolan potteries, 3000 BCE, Pakistan



Figure 2 – Cup tessons, 20th cent., Fismes, France

References

1. P. Colomban, I. Robert, C. Roche, G. Sagon, *et al.*, *Revue d'Archéométrie* (2004) 28.
2. A. Dinsdale and E. Horwood, *Pottery Science – Materials, Process and Products*, (1986).
3. D. Didier, A. Bouquillon, Y. Coquinot, A-S Le Ho, *et al.*, *South Asian Archaeologie*, (in print).

Analysis of the Historical Collection of Dyes at the Hochschule Niederrhein Using Infrared Spectroscopy

Yasmine Schulenburg^a, Jochen S. Gutmann^b and Jürgen Schram^a

^a Hochschule Niederrhein, University of Applied Sciences: Faculty of Chemistry - Instrumental Analysis,
Frankenring 20, D-47798 Krefeld, Germany

^b University of Duisburg-Essen: Faculty of Chemistry - Physical Chemistry, Universitätsstraße 5,
D-45141 Essen, Germany

yasmine.schulenburg@hs-niederrhein.de

Main subject and basis of the analysis is the Historical Collection of Dyes at the Hochschule Niederrhein, University of Applied Sciences which is the biggest and oldest collection of this type. It was continuously established by the precursor institutions of the Hochschule Niederrhein since the 1860s and comprises about 10,600 containers with colourants as well as books with colour samples corresponding to the particular era of production. It represents nearly all dyes invented by the German chemical industry until middle of the 20th century and thus, broadly documents the development of both this industry and the synthetic dyes.

As this development is very interesting for the field of natural sciences, comprehending it is part of a project named “Weltbunt” (meaning “Coloured World”). The project intends to investigate the correlations between the inventions in the chemical industry and the changes in fashion and everyday life. The instrumental-analytic part of the project focuses on the history of the chemical industry by analysing the dye powders. The method used is FTIR (Fourier transform infrared spectroscopy), precisely an IR spectrophotometer linked to a corresponding IR microscope.

The research starts with the choice of the most suitable sample preparation and the exact measuring method to provide comparability of the spectra in the course of the project. For the sample preparation, either a KBr pellet can be made from the dye or the powder itself can be measured. Concerning the method, three alternatives are available: measuring in transmission mode or in absorption mode, in this case either by using an ATR (attenuated total reflection) unit or the IR microscope mentioned above. Combination yields in five different options from which the optimal approach needs to be selected i.a. by comparing the resulting spectra with a modern spectral database.

After having decided the ideal procedure, it will be of special interest to look at dyes with identical names, but from different producers. Furthermore, to differentiate between products from one manufacturer with up to now mostly unexplained affixes like “Anthracyanin FL” and “Anthracyanin 3 GL” will be another idea to pursue. The project also aims for findings about the trading of patents which probably already took place in the time before World War I which could be proved *e.g.* by comparing the spectra of dyes which have been marketed under different trade names but are chemically identical. Thereby, information about the raw material deployed, the synthesis processes and possible contamination can be gathered, too. With the data measured a spectral database of historical dyes shall be established during the project to bridge the gap between the pure dyes, their colouring reaction products which can be found in the sample books including the corresponding formulations and the coloured textiles as final product.

Acknowledgements: The authors thank the German Federal Ministry of Education and Research for financially supporting the project.

Fourier Transform-Infrared Microscopic Investigation of Cysteic Acid in Virgin and Damaged Hair

Dhanya Puthenmadom and Charlene Fournier

Dow Corning Corporation, Rue Jules Bordet, Parc Industriel - Zone C, B-7180 Seneffe, Belgium

dhanya.puthenmadom@dow.com

Damage caused by chemical, mechanical, physical and environmental factors are a subject of major concern in the society. Daily hair care routines such as brushing, heat drying, setting hairstyle with a heating device, chemical treatment and coloring process causes damage to the hair. Of all treatments, bleaching is the most damaging, raising the outer cuticle and breaking the hair disulfide bonds. Undesirable changes are induced in the morphological, chemical, and physical properties of hair by such damage. People notice these changes from the hair texture and physical appearance of hair. Damaged hair is dry, brittle, inelastic and more prone to breakage and split ends. It is also more porous and swollen and therefore more vulnerable to other chemical and non-chemical processes. In the present study, Fourier transform infrared (FT-IR) microscopic technique was used to analyze hair subjected to different types of chemical and physical treatments. The goal of the study was to understand the extent of damage as well as chemical and structural changes associated with them. Damage is caused when the disulphide linkage in the amino acid cystine is broken down to cysteic acid. Higher amounts of cysteic acid indicates higher degree of damage. The analysis clearly showed the presence of cysteic acid in both virgin and treated hair. The presence of lower amounts of cysteic acid in virgin hair could be most likely due to environmental factors such as exposure to UV radiation from sunlight. An increase in cysteic acid content while going from virgin to color to heat treated to bleached hair indicates bleaching as the most damaging treatment. This study demonstrates FT-IR microscope as an important technique to detect functional groups responsible for damage and to provide insight into the chemical distribution of these functional groups on the surface of hair.

References

1. J. Strassburger and M. M. Breuer, *J. Soc. Cosmet. Chem.*, 36 (1985) 61.
2. C.R. Robbins, *Springer-Verlag Berlin Heidelberg*, 5th edition (2012) 105.

Thermal Maturity of Organic Matter from Fossil Fuel Fields by Raman Spectroscopy: Spectral Parameters and Chemometric Data Treatment

L. Bonoldi^a, D. Barbieri^b, L. Di Paolo^b, F. Frigerio^a, D. Grigo^c and A. Savoini^d

^a Phys. Chem. Dep., eni spa, v. F. Maritano 26, 20097 S. Donato Milanese, Italy

^b Geology and Geochem. Laboratories, via F. Maritano 26, 20097 S. Donato Milanese, Italy

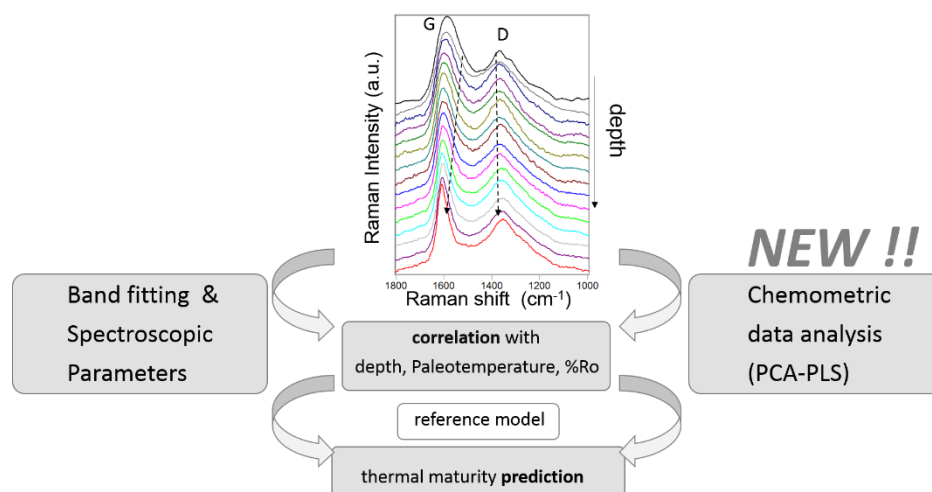
^c Exploration & Production Division, eni spa, Via Emilia 1, 20097 S. Donato Milanese, Italy

^d Phys. Chem. Dep., eni spa, Via Fauser 4, 28100 Novara, Italy

lucia.bonoldi@eni.com

Sedimentary organic matter (OM) evolves following temperature and pressure over burial history. During the exploration for fossil energy sources, the degree of evolution (thermal maturity) of OM has to be accurately determined and recently spectroscopic analysis are more and more widely applied [1], especially Raman [2]. However, its utility may be limited by some subjectivity in band fitting or spectroscopic parameters selection [3].

Here the maturity of the OM samples from two drilling wells is evaluated from the Raman spectra analysed by both the more traditional extraction of spectral parameters (band distances and area ratios) and by Principal Component Analysis-Partial Least Square regression (PCA-PLS). Being multivariate and automated, the chemometric method presents the advantage of being intrinsically unaffected by arbitrariness: the whole spectrum is analysed in a systematic way to extract the ranges of maximum variance in correlation to maturity. Traditional and chemometric method results agree satisfactorily, with good prediction of the maximum temperatures of ageing during burial time, as obtained from the thermodynamical modelling of geological data (Scheme 1). The influence of the sample geographical origin and kerogen type (marine, lacustrine or terrestrial origin) on Raman spectra is discussed.



Scheme 1. Workflow of Organic Matter Maturity prediction by Raman Spectroscopy and PCA-PLS methods.

References

1. L. Bonoldi, L. Di Paolo and C. Flego, *J. Vibr. Spectrosc.* 87 (2016) 14.
2. S. Potgieter-Vermaak, N. Maledi, N. Wagner, J. H. P. Van Heerden, R. Van Grieken and J. H. Potgieter, *J. Raman Spectrosc.* 42 (2011) 123.
3. J. S. Lupoi, L. P. Fritz, T. M. Parris, P. C. Hackley, L. Solotky, C. F. Eble and S. Schlaegle, *Front. Energy Res.*, 5, n8 (2017).

Acknowledgements: The authors thank E. Previde Massara and R. Galimberti for useful discussions.

TUESDAY, 21st AUGUST

Rotational Spectroscopy, Molecular Structure Determination, and Radioastronomy

Robert J. McMahon^a, Brent K. Amberger^a, Brian J. Esselman^a, Zachary N. Heim^a, Joshua D. Shutter^a, Maria A. Zdanovskaia^a, John F. Stanton^b, Zbigniew Kisiel^c and R. Claude Woods^a

^a Department of Chemistry, University of Wisconsin, 1101 University Avenue, Madison, WI 53706 USA

^b Department of Chemistry, University of Florida, P.O. Box 117200, Gainesville, FL 32611 USA

^c Institute of Physics, Polish Academy of Sciences, 02-668 Warszawa, Poland

robert.mcmahon@wisc.edu

The recent detection of benzonitrile in interstellar space represents a significant milestone in astrochemistry [1]. The detection of a simple derivative of benzene by radioastronomy has been a long-sought goal of many, including us. Our interests in astrochemistry have drawn us into the field of high-resolution rotational spectroscopy because this technique is the basis by which molecules are identified in space using radioastronomy. I will describe our studies of the millimeter-wave rotational spectra of several polar aromatic compounds, including pyridazine, pyrimidine, and benzonitrile, with the goal of providing high-quality laboratory data to facilitate observational astronomy.

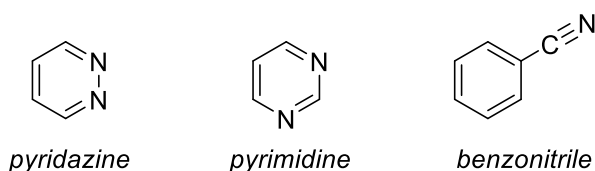


Figure 1

Recent studies represent a striking demonstration of the power of modern experimental and theoretical methods for the prediction, analysis, and interpretation of spectroscopic and structural data [2]. In simple but non-trivial systems, modern electronic structure methods are able to predict structural parameters (bond lengths, bond angles) to within the accuracy of high-precision experimental measurement. This outcome validates both the accuracy of the *ab initio* method and the claimed uncertainties of the theoretical/experimental structure determination. The significance of these findings derives from the demonstrated ability to predict molecular structural parameters with very high accuracy. The availability of accurate structural parameters will transform the ability of molecular spectroscopists to interpret the complex rotational spectra of molecules. This ability, in turn, will enable a new era in the analysis of radio-astronomical data and the understanding of the chemistry of interstellar space.

References

1. B. A. McGuire, A. M. Burkhardt, S. Kalenskii, C. N. Shingledecker, A. J. Remijan, E. Herbst and M. C. McCarthy, *Science*, 359 (2018) 202.
2. B. K. Amberger, B. J. Esselman, J. F. Stanton, R. C. Woods and R. J. McMahon, *J. Chem. Phys.*, 143 (2015) 104310.

Acknowledgements: The authors gratefully acknowledge funding from the U.S. National Science Foundation (NSF-1664912) and our respective institutions for support of this project.

Vibrational Spectroscopy at the Service of Quantum Chemistry

Martin A. Suhm

*Institut für Physikalische Chemie, Georg-August-Universität Göttingen, Tammannstr. 6,
37077 Göttingen, Germany
msuhm@gwdg.de*

The relationship between spectroscopy and quantum chemistry can adopt puzzle solving (\leftarrow) or benchmarking (\rightarrow) character. In benchmarking mode, the experimental side should make every effort to facilitate theoretical prediction, by reducing unnecessary complexity, removing thermal excitation and solvent embedding, addressing fundamental properties, etc. [1]. Furthermore, it is essential to secure the experimental findings by studying homologous series and by applying multi-messenger approaches [2].

The theoretical description of intermolecular interactions is comparatively mature. To push and challenge the best available computational methods in this field, experiment can go beyond small and harmonic systems, such that the nuclear dynamics treatment becomes non-standard and electronic structure treatments are not easily converged. After all, there may be effects such as many-body dispersion or chirality recognition which only emerge beyond a certain system size. On the other hand, it should be avoided that electronic structure theory can blame nuclear dynamics for failure and vice versa. Strategies to disentangle these two ingredients for a successful comparison of theory and experiment are also needed to avoid fortuitous and misleading error cancellation.

The talk will focus on two non-covalent interaction topics which we currently use to benchmark quantum chemistry in the field of intermolecular interactions – intermolecular energy balances [3] and subtle solvation shifts of OH stretching fundamentals [4]. Our experimental tool is linear vibrational spectroscopy in supersonic jet expansions [5].

References

1. R. A. Mata and M. A. Suhm, *Angew. Chem. Int. Ed.* 56 (2017) 11011; H. C. Gottschalk *et al.*, *J. Chem. Phys.* 148 (2018) 014301.
2. D. Bernhard, F. Dietrich, M. Fatima, C. Perez, A. Poblitzki, G. Jansen, M. A. Suhm, M. Schnell, M. Gerhards, *Phys. Chem. Chem. Phys.*, 19 (2017) 18076.
3. A. Poblitzki, H. C. Gottschalk, M. A. Suhm, *J. Phys. Chem. Lett.*, 8 (2017) 5656.
4. S. Oswald, M. A. Suhm, *Angew. Chem. Int. Ed.*, 56 (2017) 12672.
5. M. A. Suhm, F. Kollipost, *Phys. Chem. Chem. Phys.*, 15 (2013) 10702.

Acknowledgements: The author thanks the DFG for funding and his group members and cooperation partners for their valuable contributions, as reflected in part in the references.

Matrix Isolation Studies of Transition Metal and Main Group Fluorides

Nigel A. Young, Ahmed K. Sakr, and Howard V. Snelling

Chemistry, School of Mathematics and Physical Sciences, The University of Hull, Hull, HU6 7RX, UK

Physics, School of Mathematics and Physical Sciences, The University of Hull, Hull, HU6 7RX, UK

n.a.young@hull.ac.uk

Our work involves the synthesis and characterisation of reactive species using matrix isolation techniques at cryogenic temperatures. In particular, we have been exploiting the “one atom at a time” approach to synthesis using the reaction between thermally evaporated metal atoms and fluorine molecules and atoms in argon matrices at 10 K [1]. In this talk, recent examples using this approach involving nickel and molybdenum fluorides will be presented, as well as some Lewis acid-base chemistry of SiF₄.

References

1. A. V. Wilson, T. Nguyen, F. Brosi, X. Wang, L. Andrews, S. Riedel, A.J. Bridgeman and N.A. Young, *Inorg. Chem.*, 55 (2016) 1108.

Acknowledgements: The authors thank the University of Hull for funding.

Calculations of Spectra and Kinetics in the Context of Matrix Isolation

Igor Reva

CQC, Department of Chemistry, University of Coimbra, 3004-535 Coimbra, Portugal
reva@qui.uc.pt

Nowadays, a chemist who does calculations is often primarily an experimentalist, which also reflects the background of the author. In the present communication we shall briefly describe the method of matrix isolation as a tool providing much valuable experimental spectroscopic information and opens doorway to studies of structure and reactivity of organic molecules.

Over the past decades our capability to carry out quantum chemical calculations increased tremendously. At present, accurate calculations of geometries, relative energies, vibrational spectra, and other chemically relevant properties have become routine for molecules up to several tens of atoms, especially when using density functional theory (DFT) methods for closed-shell molecules. Exploration of the diversity of behavior of matrix-isolated compounds with interactive presentation of experimental and computational spectra within a journal article became almost a *sine qua non* for laboratory-based research. The few illustrative examples chosen here reflect the research interests of the author and will overview some publications with the emphasis on the respective computational parts. It will be shown that infrared spectra of matrix-isolated molecules can be reliably reproduced using computed vibrational spectra [1,2] and rationalized in terms of computed relative energies and torsional barriers [3-5]. For specific cases of molecules with flat potential energy surfaces [6] or with hypervalent atoms [7], the required calculations will be addressed. For studies of reactive intermediates, the importance of calculations on open-shell structures will be highlighted [8-10]. Further, evidence will be provided that matrix-isolated molecules need not be considered as preserved in aspic. They can be changed by external light (lamp, laser, or even a light source of the infrared spectrometer), or may decay spontaneously (by tunneling) [9-13]. The kinetic equations and models used for computation of tunneling rate constants will be discussed. Finally, anharmonic calculations of vibrational overtones (including their IR intensities), as aid in running of matrix-isolation spectroscopic experiments, will be presented [11-13].

References

1. S. Breda, I. D. Reva, L. Lapinski, M. J. Nowak and R. Fausto, *J. Mol. Struct.*, 786 (2006) 193.
2. A. Olbert-Majkut, I. D. Reva and R. Fausto, *Chem. Phys. Lett.*, 456 (2008) 127.
3. I. D. Reva, S. G. Stepanian, L. Adamowicz and R. Fausto, *Chem. Phys. Lett.*, 374 (2003) 631.
4. L. Lapinski, I. Reva, M. J. Nowak and R. Fausto, *Phys. Chem. Chem. Phys. (PCCP)*, 13 (2011) 9676.
5. I. Reva, A. J. Lopes Jesus, M. T. Rosado, R. Fausto, M. E. Eusébio and J. S. Redinha, *PCCP*, 8 (2006) 5339.
6. L. Duarte, R. Fausto and I. Reva, *Phys. Chem. Chem. Phys.*, 16 (2014) 16919.
7. L. Duarte, I. Reva, M. L. S. Cristiano and R. Fausto, *J. Org. Chem.* 78 (2013) 3271.
8. C. M. Nunes, I. Reva, T. M. Pinho e Melo, R. Fausto, T. Šolomek and T. Bally, *JACS*, 133 (2011) 18911.
9. C. M. Nunes, S. N. Knezz, I. Reva, R. Fausto, R. J. McMahon, *J. Am. Chem. Soc.*, 138 (2016) 15287.
10. C. M. Nunes, I. Reva, S. Kozuch, R. J. McMahon, R. Fausto, *J. Am. Chem. Soc.*, 139 (2017) 17649.
11. I. Reva, M. J. Nowak, L. Lapinski and R. Fausto, *J. Chem. Phys.*, 136 (2012) 064511.
12. I. Reva, C. M. Nunes, M. Biczysko, R. Fausto, *J. Phys. Chem. A*, 119 (2015) 2614.
13. A. J. Lopes Jesus, I. Reva, C. Araujo-Andrade and R. Fausto, *J. Am. Chem. Soc. (JACS)*, 137 (2015) 14240.

Acknowledgements: The author thanks all research colleagues from Coimbra, Faro, Fribourg, Helsinki, Kharkov, Madison, Pisa, Beer-Sheva, Warsaw, Wrocław, and Zacatecas, on whose hard work the above examples are based. The Portuguese “*Fundação para a Ciência e a Tecnologia*” (FCT) is acknowledged for the “*Investigador FCT*” grant.

Investigation of Phase-Behavior of an Ionic Liquid at Sub-Zero Temperatures in the Presence of Additives

Nikolay Kotov, A. Šturcová, V. Raus, A. Zhigunov and J. Dybal

*Institute of Macromolecular Chemistry, Czech Academy of Sciences,
Heyrovsky Sq. 2, 162 06, Prague, Czech Republic
kotov@imc.cas.cz*

Ionic liquids (ILs) are salts composed of cations and anions, which often have very low to negligible vapour pressure, which allows their use as substitutes for volatile organic solvents. As the number of ion combinations in neat ILs is *ca.* 10^6 , it allows researchers to apply a chosen combination of a cation and an anion that is suitable for the desired aim, which is why ILs are also called “designer solvents” [1]. 1-butyl-3-methylimidazolium chloride (bmimCl) is a typical representative of imidazolium-based ILs, which has been studied intensively due to its ability to effectively dissolve cellulose [2]. The butyl chain of this IL was shown to adopt two conformations upon crystallization: anti–anti (AA) and gauche–anti (GA), to which the bands at 730, 625 cm^{-1} and 701, 603, 500 cm^{-1} in Raman spectra of neat bmimCl were assigned, respectively [3,4]. Although both conformers exist simultaneously in amorphous bmimCl, when it crystallizes, either AA or GA conformation of the bmim⁺ cation prevails, which is related to orthorhombic or monoclinic crystal lattice of the IL [3].

Since imidazolium-based ionic liquids are highly hygroscopic they must be handled under moisture-free conditions otherwise IL–water interactions must be taken into account. Unfortunately, even careful drying of all components cannot be perfect. Therefore, traces of water remain in the system and the effect of this water content has to be understood. Many groups have already studied water-IL interactions at different concentrations, both computationally and by various experimental methods and concluded that added water can take several roles depending on its concentration. However, the concentration ranges in which added water acts differently are still assessed only very vaguely [5]. In the present work, neat bmimCl as well as mixtures based on this IL were studied by vibrational spectroscopic methods in conjunction with other techniques at laboratory and sub-zero temperatures. Various phenomena, such as crystal polymorphism and phase-separation were observed in the studied samples. They were dependent on contribution of capillary forces and the temperature history of the samples. Such information provides an insight into the process of crystallization of bmimCl as well as into its interactions with co-solvents and is also highly significant for use of ILs as solvent media, *e.g.* in polymer dissolution, blending and separations.

References

1. N. V. Plechkova and K. R. Seddon, *Chem. Soc. Rev.*, 37 (2008) 123.
2. R. P. Swatloski, *et al.*, *J. Am. Chem. Soc.*, 124 (2002) 4974.
3. H.-O. Hamaguchi and R. Ozawa, *Adv. Chem. Phys.*, 131 (2005) 85.
4. R. W. Berg, *et al.*, *J. Phys. Chem. B*, 109 (2005) 19018.
5. R. Hayes, G. G. Warr and R. Atkin, *Chem. Rev.*, 115 (2015) 6357.

Acknowledgements: The authors thank the Czech Science Foundation (Grant No. 17-03810S) for financial support.

Phase Transition, Structure and Reorientational Dynamics of H₂O Ligands and ReO₄⁻ Anions in [Ba(H₂O)₄](ReO₄)₂

Joanna Hetmańczyk^a, Łukasz Hetmańczyk^a and Katarzyna Gąssowska^a

^a Faculty of Chemistry, Jagiellonian University, Gronostajowa 2, 30-387, Kraków, Poland

joanna.hetmanczyk@uj.edu.pl

At room temperature tetraaquabarium perrhenate crystallizes in a monoclinic crystal system, within the space group P2₁/n, with four molecules in the unit cell. The following unit cell constants: $a = 7.3703(5) \text{ \AA}$, $b = 12.4550(9) \text{ \AA}$, $c = 12.1611(9) \text{ \AA}$, $\beta = 90.040(2)^\circ$ were determined by us.

The polymorphism of the mentioned above compound was investigated by means of differential scanning calorimetry (DSC). One reversible phase transition has been found at: $T_c^h = 275 \text{ K}$ (on heating) and $T_c^c = 247 \text{ K}$ (on cooling). The thermal hysteresis of the phase transition temperature T_c equal to ca. 28 K and the heat flow anomaly sharpness suggest that the detected phase transition is a first-order type.

Using three complementary spectroscopy methods (IINS, IR and RS) all characteristic frequencies of the vibrations of H₂O and ReO₄⁻ were detected. The proton-weighted phonon density functions $G(v)$ calculated in one phonon harmonic approximation from the time-of-flight INS spectra in 5 K show some separate peaks characteristic for ordered phase. The density functional perturbation theory plane wave calculations of the normal modes within the periodic boundary conditions (CASTEP code [1,2]) were performed. We have obtained good agreement between calculated and experimental data (IR, RS and IINS spectra).

The dynamic of H₂O ligands and ReO₄⁻ anions, in the high-temperature and low temperature phases, was examined by band shape analyzes of the selected band in the infrared and Raman scattering spectra [3]. The temperature dependence of the bandwidth associated with $\delta(\text{H}_2\text{O})$ mode, suggest that the ligands reorient fast (correlation time in the picosecond range) in both high and low temperature phases. The estimated mean value of activation energy for the reorientation of H₂O ligands is: $E_a(\text{I/II}) = 13.9 \text{ kJ}\cdot\text{mol}^{-1}$.

The estimated mean activation energy values for the reorientation of ReO₄⁻ anions is $E_a(\text{II}) = 3.1 \text{ kJ}\cdot\text{mol}^{-1}$ for the low temperature phase. In case of FT-IR and RS data we observed splitting as well as narrowing of same bands connected with H₂O and ReO₄⁻ vibrations in the vicinity of phase transition.

The molecular dynamics of H₂O ligands in [Ba(H₂O)₄](ReO₄)₂ were also investigated by inelastic/quasielastic incoherent neutron scattering (IINS/QENS) on NERA [4] time of flight spectrometer. The quasielastic peak registered in the high temperature phase (at 295 K) shows broadening, which is most probably connected with instantaneous stochastic jumps of protons in water molecules around the two-fold axis. The reorientational correlation time $\tau_R(\text{H}_2\text{O})$ is of an order of 10^{-11} s .

References

1. S. J. Clark, M. D. Segall, C. J. Pickard, P. J. Hasnip, M. J. Probert, K. Refson and M. C. Payne, *Z. Kristallogr.*, 220 (2005) 567.
2. K. Refson, S. J. Clark and P. R. Tulip, *Phys. Rev. B*, 73 (2006) 155114.
3. C. Carabatos-Nédelec and P. Becker, *J. Raman Spectrosc.*, 28 (1997) 663.
4. I. Natkaniec, D. Chudoba, Ł. Hetmańczyk, V. Yu. Kazimirov, J. Krawczyk, I. L. Sashin and S. Zalewski, *J. Phys.: Conference Series.*, 554 (2014) 012002.

Spectral Diagnostics of Hydrogen Bonds by ^{31}P NMR Chemical Shifts

I. S. Giba, V. V. Mulloyarova and P. M. Tolstoy

St. Petersburg State University, Universitetskiy pr., 26, St. Petersburg, Russia, 198504

johnsgiba@gmail.com

Phosphorus-containing acids have POH and P=O groups and, thus, are able to participate in the formation of hydrogen bonds as a donor and as a proton acceptor [1]. Despite the fact that intermolecular complexes involving phosphorus-containing acids are often mentioned in the literature, information on the determination of the geometry of hydrogen bonds from ^{31}P NMR spectra is fragmentary [2].

This work is devoted to the study of intermolecular complexes with hydrogen bond formed by phosphinic acids $\text{RR}'\text{POOH}$ as proton donors and nitrogen-containing bases as proton acceptors. The complexes dissolved in a deuterated freonic mixture $\text{CDF}_3/\text{CDF}_2\text{Cl}$ were studied by low-temperature ^1H and ^{31}P NMR spectroscopy, and also by quantum-chemical calculations at the B3LYP/6-311++G(d,p) level of theory.

The aim of the work was to interpret ^1H and ^{31}P NMR chemical shifts in terms of interatomic distances within the OHN hydrogen bond. The other goal was to study the additional factors influencing ^{31}P NMR chemical shifts of POOH group (see Figure 1).

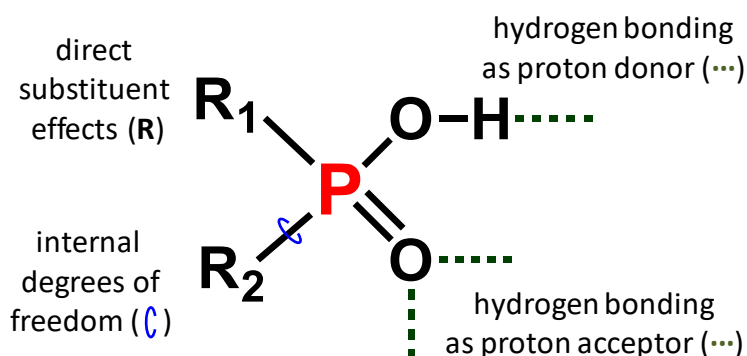


Figure 1 – Factors of ^{31}P NMR chemical shift sensitivity for phosphinic acids.

We show that ^{31}P NMR chemical shift is determined not only by the position of the bridging proton in the OHN hydrogen bond, but also by additional interactions such as CHO hydrogen bond formed between the ortho-proton of the substituted pyridine and the P=O group, as well as the type of acid substituents and their internal degrees of freedom.

References

1. V. V. Mulloyarova, I. S. Giba, M. A. Kostin, G. S. Denisov, I. G. Shenderovich and P. M. Tolstoy, *Phys. Chem. Chem. Phys.*, 20 (2018) 4901.
2. I. G. Shenderovich, *J. Phys. Chem. C*, 117 (2013) 26689.

Acknowledgements. This work was supported by RSF grant 18-13-00050. We thank Mikhail Vovk and Artem Grevtsev (Center for Magnetic Resonance. Research park of St. Petersburg State University) for their help in conducting the NMR experiments.

Beidellite Intercalates and their Characterization by Means of DFT Method

Eva Scholtzová^a, Luboš Jankovič^a, Peter Škorňa^a and Daniel Tunega^b

^a *Institute of Inorganic Chemistry of Slovak Academy of Sciences, Dúbravská cesta 9,
Bratislava 84536, Slovakia*

^b *Institute for Soil Research, University of Natural Resources and Life Sciences, Peter-Jordan-Strasse 82,
A-1190 Vienna, Austria,
eva.scholtzova@savba.sk*

Organoclays are hybrid materials prepared by intercalation from clay minerals and organic cations, mostly of alkylammonium type. They are a subject of a great interest because they can have specific properties suitable for new technological applications, e.g. in a preparation of polymer-clay nanocomposites, as active sorbents, drug release retardation from biocomposite hydrogels, storage of radioactive waste, reinforcement of anti-microbial paper packaging improving its tensile strength, etc. In a recent time, closer attention is also paid to phosphonium-based organic cations that can be used to prepare organoclays with improved properties and higher stability than those prepared with the conventional alkylammonium cations [1,2].

In the present work we investigate structural properties and stability of beidellite (Bd) clay mineral intercalated with tetraethyl- (4P2), tetrabutyl- (4P4), tetrahexyl- (4P6), and tetraoctylphosphonium (4P8) cations by means of first principle methods based on functional theory (DFT). The work is a part of the systematic study of the effect of 4PX cations (X= 2, 4, 6 and 8) on physicochemical properties of the alkylphosphonium-beidellite organoclays. Beidellite is layered aluminosilicate clay with predominant Si/Al substitutions in tetrahedral sheets (differing from montmorillonite, in which substitutions are mainly in octahedral sheet). The different type of the substitutions affects a charge distribution in clay layers. In beidellite, the charges are better localized at the Si/Al sites in comparison to montmorillonite and it is expected that it can improve the stability of the beidellite-based organoclays [3]. Preliminary results showed a good agreement of the predicted d_{001} basal spacing (~ 14.5 Å) for the structures of the 4PX-Bd samples (X= 1-4) with the experimentally determined values of the prepared organoclay samples (~ 14.2 Å). Further, the planned *ab initio* molecular dynamics (AIMD) calculations will help in a detailed analysis of the experimental FTIR spectra of the 4PX-Bd organoclays.

References

1. E. Scholtzová, J. Madejová, L. Jankovič, D. Tunega, *Clays clay Miner.*, 64 (2016) 399.
2. E. Scholtzová, *proceed. BIT's 5th Annual Conference of AnalytiX-2017, Fukuoka, Japan*, (2017) 117.
3. E. Scholtzová, D. Tunega, *Scientific Research Abstracts, 16th ICC, Granada, Spain*, (2017) 689.

Acknowledgement: The authors (ES; LJ, PS) are grateful for the financial support by the Slovak Grant Agency VEGA (Grant 2/0141/17) and Slovak Research and Development Agency (APVV-15-0741 and APVV-15-0347). DT thanks the Austrian Grant Agency (FWF), project No. I3263-N34.

Exploring Photoinduced Bond Fissions in the Gas and Solution Phase

M. N. R. Ashfold

School of Chemistry, University of Bristol, Bristol, U.K. BS8 1TS
Mike.ashfold@bristol.ac.uk

Azoles, phenols, *etc.* are common chromophores in the nucleobases and the aromatic amino-acids that dominate the near UV absorption spectra of many biological molecules. $\pi^* \leftarrow \pi$ excitations are responsible for the strong UV absorptions, but such molecules also possess excited states formed from $\sigma^* \leftarrow \pi$ electron promotions. The $\pi\sigma^*$ states generally have much smaller absorption cross-sections, but can have profound photophysical importance. This presentation will (i) summarise photofragment translational spectroscopy (PTS) experiments and complementary *ab initio* calculations used to explore $\pi\sigma^*$ -state mediated bond fission processes following UV excitation of heteroaromatic molecules in the gas phase, (ii) describe ultrafast pump-probe experiments designed to explore the extent to which analogous processes occur in solution, (iii) show how such solution phase studies offer a means of exploring $\pi\sigma^*$ -state mediated ring-opening of heterocycles like thiophenes and pyrones and (iv) outline recent efforts to explore the dynamics of photoinduced ring-opening processes in the gas phase.

References

1. M. N. R. Ashfold, D. Murdock and T. A. A. Oliver, *Annu. Rev. Phys. Chem.*, 68 (2017) 63.
2. M. N. R. Ashfold, M. Bain, C.S. Hansen, *et al.*, *J. Phys. Chem. Letts.*, 8 (2017) 3440.

Acknowledgements: This programme of work is supported by EPSRC Programme Grant EP/L005913.

Spectroscopic Observation of Quantum Tunneling: Discoveries on the Potential Energy Surfaces of Phenylnitrenes

Cláudio M. Nunes^a, Igor Reva^a, Robert J. McMahon^b and Rui Fausto^a

^a CQC, Department of Chemistry, University of Coimbra, 3004-535 Coimbra, Portugal

^b Department of Chemistry, University of Wisconsin-Madison, Madison, WI 53706-1322, United States
cmnunes@qui.uc.pt

Quantum tunneling is a fascinating phenomenon that has important implications in organic, catalytic, biological and interstellar chemistry. Not only tunneling can have a profound influence on the chemical reaction rates, but it can also control the selectivity of chemical reactions. Recent results in this area are starting to reveal that tunneling is, in fact, more relevant to chemistry and biochemistry than previously recognized.

The most impressive experimental evidence of quantum tunneling in chemical reactions is obtained using cryogenic temperatures. Indeed, under conditions of negligible thermal energy, the occurrence of any chemical reaction is, most probably, due to tunneling. If such transformation spans from seconds to tens of hours, then it can be directly observed and monitored using stationary spectroscopic methods (such as IR, UV-Vis, EPR, etc).

Here, we will present direct spectroscopic observation of tunneling reactions on the potential energy surface of phenylnitrenes (Scheme 1). For instance, we discovered that triplet 2-formylphenylnitrene ³**2**, generated by photolysis of azide **1** in cryogenic matrices at 10 K, rearranges by hydrogen-atom tunneling to iminoketene **3** [1]. Moreover, benzazirine **4**, generated by irradiation of 2-formylphenylnitrene ³**2**, undergoes ring expansion by heavy-atom tunneling to cyclic ketenimine **5** [2]. Experimental and theoretical results providing support for the occurrence of different tunneling reactions will be discussed.

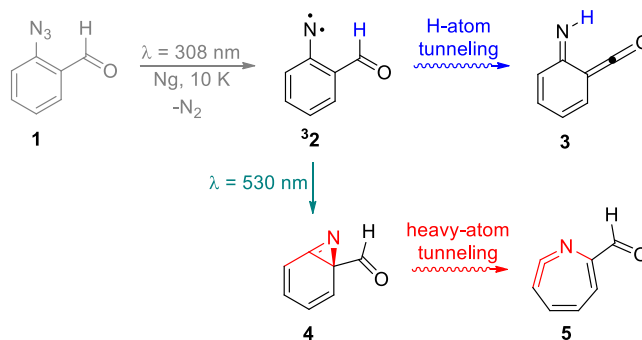


Figure 1 – Tunneling reactions under cryogenic conditions discovered on the potential energy surface of 2-formyl phenylnitrene by direct spectroscopic observation.

References

1. C. M. Nunes, S. N. Knezz, I. Reva, R. Fausto and R. J. McMahon. *J. Am. Chem. Soc.*, 138 (2016) 15287.
2. C. M. Nunes, I. Reva, S. Kozuch, R. J. McMahon and R. Fausto, *J. Am. Chem. Soc.* 139 (2017) 17649.

Acknowledgements: The Coimbra Chemistry Centre (CQC) is supported by FCT, through the project UI0313/QUI/2013, also co-funded by FEDER/COMPETE 2020-EU. C.M.N. and I.R. acknowledge FCT for Postdoctoral Grant No. SFRH/BPD/86021/2012 and “Investigador FCT” grant, respectively.

Using Transient Spectroscopy to Understand Photosalient Behavior of Vinyl Azides Crystals

Anna Gudmundsdottir
University of Cincinnati, OH, USA
annag@uc.edu

The quest for sustainable chemistry is reinforcing interest in solid-state photochemistry as a sustainable tool for synthetical applications because organic crystals can be used to carry out photoreactions without solvents and most photoreactions can be initiated by sunlight or photocatalysts [1]. In particular, solid-state photoreactions are generally more regio- and stereoselective than their solution counterparts, because the rigid packing of molecules in the crystal lattice prevents significant rotation and diffusion [2]. In contrast, recent findings highlight that organic crystals can also be flexible and compression can make them bend, curl, hop, or twist when exposed to light or external pressure [3]. Thus, photosalient crystals can convert light into mechanical energy, and they have a potential role in the fabrication of mechanically tunable components for actuation, energy harvesting, flexible electronics, and switchable reflectors. In addition, such crystals can be used as sensors and probes.

We have shown that photolysis of diene azide derivatives results in formation of triplet nitrenes and N₂ gas. The release of N₂ molecules from the crystal lattice is distinctive for each azide derivative. For example, some crystals tolerate a build-up of large N₂ bubbles within the crystals before cracking, whereas others shatter fiercely upon exposure to light. The behavior of azide crystals and their solid-state reaction mechanisms will be discussed and correlated to the azide crystal packing arrangements.

References

1. (a) K. L. Skubi, T. R. Blum and T. P. Yoon, *Chem. Rev.*, 116 (2016) 10035; (b) D. Staveness, I. Bosque and C. R. J. Stephenson, *Acc. of Chem. Res.*, 49 (2016) 2295; (c) D. M. Schultz and T. P. Yoon, *Science*, 343 (2014) 6174.
2. V. Ramamurthy and K. Venkatesan, *Chem. Rev.*, 87 (1987) 433.
3. P. Naumov, S. Chizhik, M. K. Panda, N. K. Nath and E. Boldyreva, *Chem. Rev.*, 115 (2015) 12440.

Theoretical Investigation of Herzberg-Teller Effects in Resonance Raman Spectra

Julien Guthmuller

Faculty of Applied Physics and Mathematics, Gdańsk University of Technology, Narutowicza 11/12,
80-233 Gdańsk, Poland
julien.guthmuller@pg.edu.pl

Vibrational resonance Raman (RR) spectroscopy is a useful tool to provide information on structures and properties of molecular excited states [1]. Therefore, an accurate simulation of absorption and RR spectra, by quantum chemistry methods, can help in the interpretation of experimental data as well as in the design of new compounds for specific applications e.g. in dye-sensitized solar cells or as photocatalysts [2,3]. Moreover, the calculation of RR intensities and their comparison with experimental data offers an opportunity to assess the ability of standard quantum chemistry methods to predict excited state properties [4,5].

In this contribution, simplified sum-over-state expressions are presented to calculate RR intensities [6], which allow inclusion of Franck-Condon (FC) and Herzberg-Teller (HT) effects. The molecular properties are calculated with density functional theory and the different methods are applied to the molecules of *trans*-porphycene [7] and to a Ruthenium-Palladium supramolecular photocatalyst [3]. For both systems, HT effects are shown to have a significant impact on the RR intensities (Fig. 1) and it is concluded that such contributions should be included in the simulation of RR spectra.

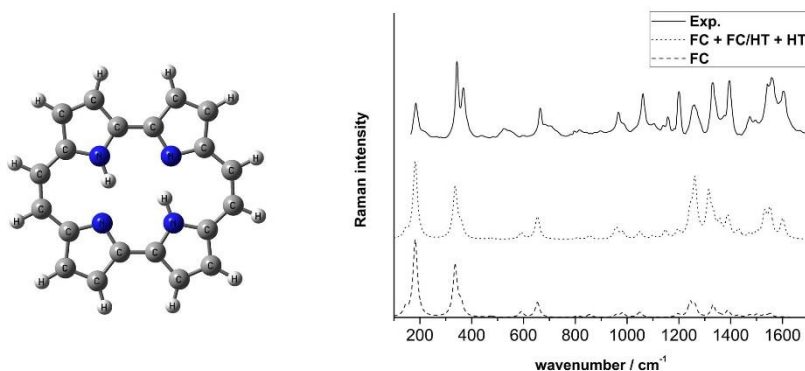


Figure 1 – RR spectra of *trans*-porphycene.

References

1. M. Wächtler, J. Guthmuller, L. González and B. Dietzek, *Coord. Chem. Rev.*, 256 (2012) 1479.
2. S. Kupfer, J. Guthmuller, M. Wächtler, S. Losse, S. Rau, B. Dietzek, J. Popp and L. González, *Phys. Chem. Chem. Phys.*, 13 (2011) 15580.
3. J. Guthmuller and L. González, *Phys. Chem. Chem. Phys.*, 12 (2010) 14812.
4. J. Guthmuller, *J. Chem. Theory Comput.*, 7 (2011) 1082.
5. M. Staniszevska, S. Kupfer, M. Łabuda and J. Guthmuller, *J. Chem. Theory Comput.* 13 (2017) 1263.
6. J. Guthmuller, *J. Chem. Phys.*, 144 (2016) 064106.
7. J. Guthmuller, *J. Chem. Phys.*, 148 (2018) 124107.

Acknowledgements: The author is grateful to the Narodowe Centrum Nauki (Project No. 2014/14/M/ST4/00083) for financial support. The calculations have been performed at the Universitätsrechenzentrum of the Friedrich-Schiller University of Jena and at the Wrocław Centre for Networking and Supercomputing (grant No. 384).

Sum Frequency Generation Spectroscopy Studies of Temperature Dependent Naphthalene Dehydrogenation on Nickel (111)

K. M. Marks^a, M. Ghadami Yazdi^b, P. H. Moud^c, W. Piskorz^d, A. Kotarba^d, T. Hansson^a,
K. Engvall,^c M. Göthelid^b and H. Öström^a

^a Department of Physics, Fysikum, Stockholm University, 106 91 Stockholm, Sweden

^b Material Physics, SCI, KTH Royal Institute of Technology, 16440 Kista, Sweden

^c Department of Chemical Engineering, KTH Royal Institute of Technology, 10044 Stockholm, Sweden

^d Faculty of Chemistry, Jagiellonian University in Kraków, Ingardena 3, 30-060 Kraków, Poland
kess.marks@fysik.su.se

Naphthalene and other higher hydrocarbons are molecules typically present in the product of biomass gasification. These molecules are considered a hindrance and need to be removed in order to use the gas product as an energy source. An elegant way to do this is by catalytically converting these molecules to syngas molecules such as CO and H₂. [1] Nickel based catalysts are used commonly for the conversion of hydrocarbons and are considered a possible catalyst for biomass gasification [2].

We combine sum frequency generation (SFG) spectroscopy with other techniques such as X-ray photoelectron spectroscopy (XPS), scanning tunneling microscopy (STM) and temperature programmed desorption (TPD) to study the mechanisms of adsorption and temperature driven dehydrogenation of naphthalene on a nickel(111) single crystal surface.

The naphthalene molecule in the monolayer adsorbs flat on the surface at room temperature and below as we have confirmed with STM before [3]. At sufficiently cold temperatures a multilayer is formed on top of the monolayer, where the molecules sit in an upright geometry, as has been observed for benzene on nickel(111) [4].

Upon heating, the naphthalene decomposes and at about 380 K the production of hydrogen molecules due to dehydrogenation of the naphthalene begins. Based on our measurements we believe that at first two hydrogen atoms on one side of the naphthalene molecule break off which allows the molecule to adopt a tilted geometry. This interpretation is mainly supported by our SFG measurements, where a resonant signal appears around 3060 cm⁻¹ at 380 K which closely resembles the multilayer resonance we see at much colder temperatures. However, since the multilayer desorbs already at 200 K, it is likely that we are observing the monolayer molecules adopting an upright position. The naphthalene continues to dehydrogenate until 680 K where there is no more hydrogen production recorded with TPD and the SFG resonances are gone as well. Changes in the left-over carbon species on the surface are recorded up to 885 K using XPS, identifying both carbidic and graphitic carbon.

References

1. K. Engvall *et al.*, *Top. Catal.*, 54 (2011) 949.
2. J. Rostrup-Nielsen and L. J. Christiansen, *Concepts in Syngas manufacture*. 2011, Singapore, United States: World Scientific Publishing Company.
3. M. Ghadami Yazdi, *et al.*, *J. Phys. Chem. C*, 121 (2017) 22199.
4. H. P. Steinrück, *et al.*, *Surf. Sci.*, 218 (1989) 293.

Assignment of the Electronic Transition of Phenothiazine Radical Cation in the Visible Region – A Resonance Raman Spectroscopy and Theoretical Calculation Investigation

Lucia Kiyomi Noda and Norberto Sanches Gonçalves

Rua Prof. Artur Riedel, 275 – Jd. Eldorado – CEP 09972-270 – Diadema – SP, Brazil
lucia.noda@unifesp.br

Phenothiazine (PTZ) derivatives represent an important class of molecules [1], being studied in a number of fields of chemical and pharmaceutical research, primarily because of the biological activity of these substances and because of its application in solar energy transformation [2]. The interesting chemical and biological properties of PTZs are considered to relate to their relative stable radical cations, whose formation and reactivity have been extensively studied [3]. The most intense electronic transition of PTZ radical cation in the visible region is located at *ca.* 500 nm. Hester *et al.* had performed a resonance Raman investigation of PTZ radical cation in aqueous solution in the contour of this band and observed enhancement of several Raman bands, but the most enhanced one was found at 476 cm^{-1} , tentatively assigned to a C-N-C deformation mode [4].

In the present work we had performed a theoretical calculation of the structure, the vibrational frequencies and the electronic spectrum of the PTZ radical cation, with DFT-B3LYP/6-31G(d,p) and TD-DFT. In the ground state PTZ radical cation is planar, in contrast to the folded structure of the PTZ molecule. The Raman band at 476 cm^{-1} was assigned to a C-S-C bending mode. The reason for the preferential enhancement of the C-S-C vibrational mode was investigated using TD-DFT, in order to obtain the molecular orbitals involved in the electronic transition at *ca.* 500 nm. The molecular orbitals involved in the electronic transition are depicted below, together with the phenothiazine structure:

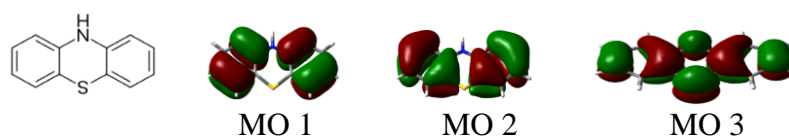


Figure 1 – Phenothiazine structure and molecular orbitals involved in the electronic transition.

The TD-DFT calculations show that the electronic transition at *ca.* 500 nm is from MO 1 and MO 2, both double occupied molecular orbitals, localized at the aromatic rings and goes toward MO 3, a single occupied molecular orbital. As can be seen, MO 3 has contributions of S and N atomic orbitals, but with predominance of S atomic orbitals, which are absent in MO 1 and MO 2. The predominance of S atomic orbitals in MO 3 explain the preferential resonance Raman enhancement of a C-S-C vibrational mode. The particular enhancement of C-S-C deformation mode is explained considering that in the excited state, originated from this electronic transition, the PTZ radical cation undergoes folding around the N-S axes, with decreasing C-S-C angle, as revealed by TDDFT results.

References

1. A. Jaszczyszyn *et al.*, *Pharmacol. Rep.* 64 (2012) 16.
2. W. J. Albery, A. W. Foulds, K. J. Hall, A. R. Hillman, R. G. Edgell and A. F. Orchard, *Nature* 282 (1979) 793.
3. N. J. Turro, I. V. Khudyakov and H. van Willigen, *J. Am. Chem. Soc.* 117 (1995) 12273.
4. R. Hester and K. P. J. Williams, *J. Chem. Soc., Perkin Trans. 2* (1981) 852.

Vibrational Excitation Induced Chemistry

Jan Lundell

Department of Chemistry, University of Jyväskylä, P.O. Box 35, 40014 Jyväskylä, Finland
jan.c.lundell@jyu.fi

Recently it has become evident that low-temperature matrix isolation technique combined with narrow-band light sources is a powerful tool to study properties and reactivity of chemical entities [1]. This approach has been very successful to provide the first unequivocal production and IR assignment of the higher energy form of formic acid, *i.e.* *cis*-HCOOH [2]. Encouraged by the success stories with small carboxylic acids [3], it has been demonstrated that selective light-induced conformational changes can be induced besides molecules also in hydrogen-bonded complexes [4,5]. This has led to a plethora of studies where higher-energy and less favourable chemical species can be easily made and studied.

In the last decade the selective light-induced chemistry has been extended beyond fundamental and first overtone vibrational excitations, *i.e.* applying visible light photons instead of IR photons to obtain vibrationally locally hot species [6]. Such experiments allow to study processes connected with molecules and complexes where high excess of energy is present [7-12]. Again, the low-temperature matrix isolation technique helps to distinguish various isomerization and decomposition processes and products, and enable to gain insight of the chemistry involved in the studied chemical entities.

In this talk, selective light-induced process studies in low-temperature matrices is reviewed, and possibilities for further studies and applications are discussed.

References

1. L. Khriachtchev (Ed.) *Physics and Chemistry in Low Temperatures*, PAN Stanford Publishing, USA, 2011.
2. M. Pettersson, J. Lundell, L. Khriachtchev and M. Räsänen, *J. Am. Chem. Soc.*, 119 (1997) 11715.
3. E. M. S. Macoas, L. Khriachtchev, M. Pettersson, J. Lundell, R. Fausto and M. Räsänen, *J. Mol. Struct.*, 34 (2004) 73.
4. K. Marushkevich, L. Khriachtchev, J. Lundell, A. Domanskaya and M. Räsänen, *J. Phys. Chem. A*, 114 (2010) 3495.
5. K. Marushkevich, L. Khriachtchev, M. Räsänen, M. Melavuori and J. Lundell, *J. Phys. Chem. A*, 116 (2012) 2101.
6. A. Olbert-Majkut, J. Ahokas, J. Lundell and M. Pettersson, *J. Chem. Phys.*, 129 (2008) 041101.
7. A. Olbert-Majkut, J. Ahokas, J. Lundell and M. Pettersson, *J. Raman Spectrosc.*, 42 (2011) 1670.
8. A. Olbert-Majkut, J. Ahokas, M. Pettersson and J. Lundell, *Biomed. Spectrosc. Imaging*, 2 (2013) 339.
9. A. Olbert-Majkut, J. Ahokas, M. Pettersson and J. Lundell, *J. Phys. Chem. A*, 117 (2013) 1492.
10. A. Olbert-Majkut, M. Wierzejewska and J. Lundell, *Chem. Phys. Lett*, 616-617 (2014) 91.
11. A. Olbert-Majkut, J. Lundell and M. Wierzejewska, *J. Phys. Chem. A*, 118 (2014) 350.
12. J. Ahokas, I. Kosendiak, J. Krupa, J. Lundell and M. Wierzejewska, *J. Mol. Struct.*, 1163 (2018) 294.

Spectroscopic Microwave Spectroscopic Investigations on Large Amplitude Motions: Intermolecular Bonding in Ar-(H₂O)₂, (H₂S)₂ and CH₃CN-CO₂

E. Arunan, Arijit Das and Sharon Priya Gnanasekar

Department of Inorganic and Physical Chemistry, Indian Institute of Science, Bangalore, India 560012

arunan@iisc.ac.in

Microwave spectroscopy of weakly bound complexes formed in a molecular beam has helped enormously in fundamental understanding of intermolecular interaction/bonding. However, starting with the first direct observation of a ‘hydrogen bond’ in HF dimer by Klemperer, microwave spectroscopists had to deal with large amplitude motions in these weakly bound complexes [1]. The HF dimer exhibited donor-acceptor interchange tunnelling that would break the ‘hydrogen bond’ raising a question about whether HF dimer is ‘hydrogen bonded’. Goswami and Arunan proposed a criterion for hydrogen bond in such situations suggesting that there be at least one bound level below the barrier for any large amplitude motion which can break the ‘intermolecular bond’ [2]. In this talk, we will discuss recent results from our laboratory on three weakly bound complexes namely Ar-(H₂O)₂, (H₂S)₂ and CH₃CN-CO₂.

For Ar-(H₂O)₂, we have assigned A₁ and B₁ states recently which are shifted by more than 4 GHz from the E₁ state which is unaffected by tunnelling. Due to the symmetry rules, transitions from A₁ state appears below the E₁ state and B₁ state appears above the E₁ state and these could not be assigned earlier [3]. For (H₂S)₂, only K=0 lines were observed until recently and the implied structure would be that of two spheres i.e H₂S is spherical [4]. We have recently measured the K=1 transitions which are essential in proving that the dimer is hydrogen bonded [5]. The energy level splitting in H₂S dimer do not seem to correlate with those of (H₂O)₂. While in these two cases, the tunnelling motions could break the intermolecular bond, the third case of CH₃CN-CO₂ has free internal rotation of the methyl rotor. This does not affect the intermolecular ‘carbon bond’⁶ between N of CH₃CN and C of CO₂ in a T-shaped geometry. Symmetry restrictions from this free rotor forbid the m=0, K=1 states and so only K=0 transitions have been assigned. Moreover, rotational transitions from a ‘π stacked structure’ have been found as well. This talk will summarize the recent results on these three complexes.

References

1. T. R. Dyke, B. J. Howard, and W. Klemperer, *J. Chem. Phys.* **56** (1972) 2442.
2. M. Goswami, E. Arunan. *Phys. Chem. Chem. Phys.* **11** (2009) 8974.
3. E. Arunan, T. Emilsson, and H. S. Gutowsky, *J. Chem. Phys.* **116** (2002)
4. a. F. J. Lovas, R. D. Suenram, L. H. Coudert, *43rd Int. Symp. on Molecular Spectroscopy* (1988).
b. P. K. Mandal, *Ph.D. Thesis, Indian Institute of Science* (2005).
5. A. Das, P. K. Mandal, F. J. Lovas, C. Medcraft, N. Walker and E. Arunan *Manuscript to be submitted*.
6. D. Mani and E. Arunan, *Phys. Chem. Chem. Phys.* **15** (2013) 14377.

Laboratory Millimeter and Submillimeter Wave Studies of Interstellar Molecules

J. L. Alonso, L. Kolesnikova, E. R. Alonso, I. Leon and S. Mata

*Grupo de Espectroscopía Molecular (GEM). Unidad Asociada CSIC,
Laboratorios de Espectroscopía y Bioespectroscopía. Edificio Quifima,
Universidad de Valladolid. 47005 Valladolid, Spain
jlalonso@qf.uva.es*

Up to date, over 190 molecules have been unambiguously identified in the interstellar medium due to the ongoing astronomical observations complemented with elaborated laboratory studies. Many of these molecules are organic containing abundant interstellar elements H, C, N, and O and are found especially in the hot cores, i.e. in the regions of prolific star formation with temperatures higher than 100 K through the interpretation of molecular line surveys at millimeter and submillimeter wavelengths. The identification of specific species requires direct comparison of the particular frequencies observed in interstellar space with spectroscopic measurements of known species in a laboratory experiment. The vast amount of data generated by the ALMA motivates laboratory spectroscopists to record and analyze rotational spectra of potential interstellar molecules and to fulfill the first requirement for an unequivocal identification of new molecules in space, i.e. the availability of transition frequencies with high accuracy from microwave to sub-millimeter wave range. A general procedure is being used at Valladolid [1-3] combining different time and/or frequency domain spectroscopic tools of varying importance for providing the precise set of spectroscopic constants that could be used to search for this species in the ISM. This is illustrated in the present contribution through its application to several significant examples [4-7].

References

1. L. Kolesniková, E. R. Alonso, S. Mata and J. L. Alonso, *ApJ. Suppl. Series*, 229 (2017) 26.
2. E. R. Alonso, L. Kolesnikova and J. L. Alonso, *J. Chem. Phys.*, 147 (2017) 124312.
3. E. R. Alonso, L. Kolesniková, Z. Kisiel, E. B. Jaworska, I. León, J. C. Guillemin and J. L. Alonso, *ApJ* (2018).
4. L. Kolesniková, J. L. Alonso, C. Bermúdez, E. R. Alonso, B. Tercero, J. Cernicharo and J.C. Guillemin, *A&A*, 591(2016) A75.
5. E. R. Alonso, L. Kolesniková, I. Peña, S. T. Shipman, B. Tercero, J. Cernicharo and J. L. Alonso, *J. Mol. Spectrosc.*, 316 (2015), 84.
6. E. R. Alonso, L. Kolesniková, B. Tercero, C. Cabezas, J. L. Alonso, J. Cernicharo and J.-C. Guillemin, *ApJ*, 832 (2016) 42.
7. L. Kolesnikova, E. R. Alonso, S. Mata, J. Cernicharo and J. L. Alonso, *ApJ. Suppl. Series*, 233 (2017) 24.

Acknowledgements: The authors thank the financial fundings from Ministerio de Ciencia e Innovacion (Consolider-Ingenio 2010 CSD2009-00038 program "ASTROMOL", CTQ2013-40717-P and CTQ2016-76393-P), Junta de Castilla y Leon (Grants VA175U13 and VA077U16) and European Research Council under the European Union's Seventh Framework Programme (FP/2007-2013) / ERC-2013- SyG, Grant Agreement n. 610256 NANOCOSMOS.

Sensing Chirality with Rotational Spectroscopy: from Enantiomer Differentiation to Molecular Recognition

Sérgio R. Domingos, Cristóbal Pérez and Melanie Schnell

*Deutsches Elektronen-Synchrotron (DESY), Notkestr. 85, 22607 Hamburg, Germany,
Max Planck Institute for the Structure and Dynamics of Matter, Luruper Chaussee 149, 22761 Hamburg,
Germany, Christian-Albrechts-Universität zu Kiel, Institut für Physikalische Chemie,
24118 Kiel, Germany
sergio.domingos@desy.de*

The rules that govern aggregation at the molecular level are loosely established. Molecular recognition is mediated *via* a delicate balance between the prevailing intermolecular interactions at play, hydrogen bonding and dispersion interactions. Using high resolution broadband rotational spectroscopy and supersonic jets, an emerging trend is set to unravel these basic yet key non-covalent interactions using a bottom-up approach. The highly resolved rotational spectrum of a supersonically-cooled molecular beam provides an unrivalled molecular fingerprint that we use to solve conformational heterogeneities [1] and also the chirality [2] of increasingly larger and more complex molecular systems. Ongoing studies including chiral dimer topologies, non-planar polycyclic aromatic hydrocarbons and molecular rotary motors [3] will be presented. A preview of a new proof-of-concept experiment for quantum-state-specific enantiomeric enrichment using tailored microwave fields will be showcased and discussed [4].

References

1. S. R. Domingos, C. Pérez, C. Medraft, P. Pinacho and M. Schnell, *Phys. Chem. Chem. Phys.*, 18 (2016) 16682.
2. S. R. Domingos, C. Pérez and M. Schnell, *Annu. Rev. Phys. Chem.*, 69 (2018) 499.
3. S. R. Domingos, A. Cnossen, W. J. Buma, W. R. Browne, B. L. Feringa and M. Schnell, *Angew. Chem. Int. Ed.*, 56 (2017) 11209.
4. C. Pérez, A. L. Steber, S. R. Domingos, A. Krin, D. Schmitz and M. Schnell., *Angew. Chem. Int. Ed.*, 56 (2017) 12512.

Acknowledgements: The authors thank the Alexander von Humboldt Foundation for Postdoctoral Fellowship for S.R.D. and C.P. This work was supported by the excellence cluster “The Hamburg Centre for Ultrafast Imaging - Structure, Dynamics and Control of Matter at the Atomic Scale” of the Deutsche Forschungsgemeinschaft.

Mid-IR Detection and Spectroscopy of Polyatomic Molecules inside a Cryogenic Buffer Gas Cell

T. E. Wall^a, J. M. Bieniewska^a, B. Darquié^b, T. J. Sears^c, B. E. Sauer^a and M. R. Tarbutt^a

^a Centre for Cold Matter, Blackett Laboratory, Imperial College London, Prince Consort Road, London, SW7 2AZ, UK

^b Laboratoire de Physique des Lasers, CNRS, Université Paris 13, Sorbonne Paris Cité, 93430, Villetaneuse, France

^c Department of Chemistry, Stony Brook University, Stony Brook, NY 11790-3400, USA
t.wall@imperial.ac.uk

We are building a cryogenic buffer gas source of cold polyatomic molecules, which will be used in experiments testing fundamental physics. The source consists of a copper cell mounted on the 4 K stage of a cryo-cooler, through which cryogenically cooled 4 K helium is flowed at a rate of around 2 sccm. We inject a vapour of polyatomic molecules into the cell through a room temperature tube. Collisions with the He cools the molecules to the same temperature as the cell.

During the development of this source we are using 1,3,5-trioxane, a solid with a high vapour pressure at room temperature. We probe the buffer gas cooling by performing wavelength modulation (WM) spectroscopy inside the cell. We drive vibration-rotation transitions close to Q-branch origin of the ν_5 vibrational fundamental band, using 10.2 μm radiation from a quantum cascade laser.

I will present WM spectroscopy data, including recent sub-Doppler spectra that exhibit large Lamb dips, from which we can infer information about collision rates inside the cell. I will discuss our plans for the sensitive detection of a beam of cold, polyatomic molecules using cavity-enhanced absorption spectroscopy.

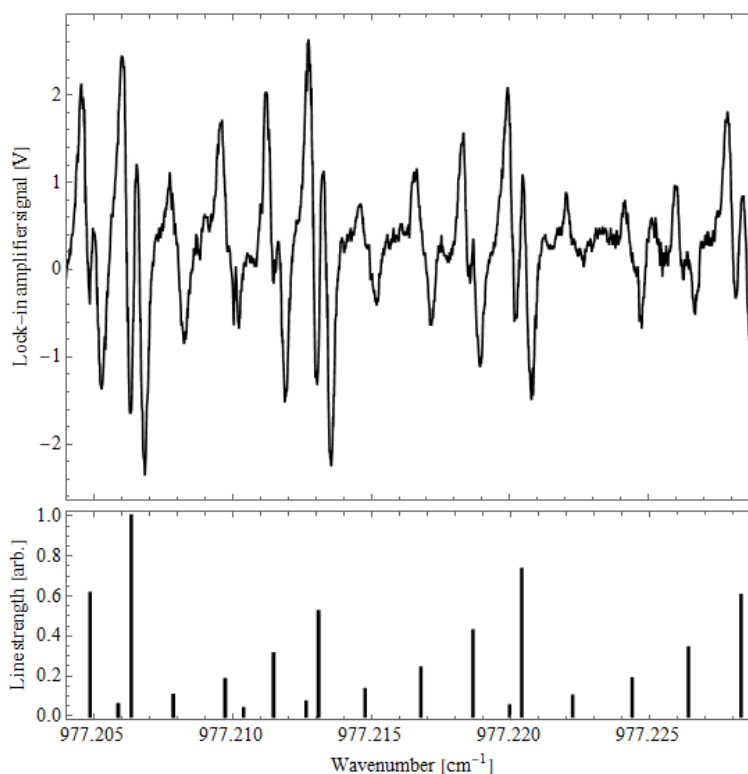


Figure 1 – Upper: WM spectrum of cryogenically cooled trioxane. Lower: calculated stick spectrum.

The The Role of Matrix Isolation Spectroscopy in Conformational Studies of Small and Medium Sized Biomolecules

György Tarczay

*Laboratory of Molecular Spectroscopy, Institute of Chemistry, Eötvös University,
PO Box 32, H-1518, Budapest 112, Hungary
tarczay@caesar.elte.hu*

IR spectroscopy is one of the most frequently used experimental methods for exploring the conformational landscape of small and medium-sized biomolecules. While NMR spectroscopy very often provides time-averaged structures for these molecular systems, the IR spectrum is a composition of the spectra of individual conformers. Most conveniently, IR spectroscopic investigations on peptides are carried out in solutions using Fourier-transform IR spectrometers. Although this method is simple and well-tried, it has serious limitations. Since the spectral bands of solvated peptides are usually broad, this method allows the observation of the few most abundant conformers only. Another limitation is that similar conformers cannot be easily distinguished because the theoretical prediction of vibrational spectra, especially in the solution phase, has larger uncertainty than the difference in the experimental spectra of these conformers.

In order to avoid the above-mentioned problems and obtain better resolution, one can study the spectra of the free molecules in the gas phase. Among the gas-phase methods, jet-cooled microwave (MW) and laser spectroscopic (*e.g.*, resonance-enhanced multiphoton ionization (REMPI)) methods are found to be the most powerful techniques for conformational studies of neutral peptides. Another possibility for improving the resolution is recording the IR spectra of molecules isolated in low-temperature noble gas matrices. When matrix-isolation IR (MI-IR) spectroscopy is combined with selective NIR laser irradiation, similarly to double resonance methods, spectra of individual conformers can be detected. Both gas-phase and the MI-IR methods have the further advantage that for spectral analysis quantum chemical computations can be carried out *in vacuo*, without using more time demanding and less accurate computations that account for the solvent effects.

In the case of chiral molecules, such as most peptides, vibrational circular dichroism (VCD) spectroscopy can support the analysis of IR spectra. This is because the sign and the intensity of VCD bands are very sensitive not only to the configuration but also to the conformation. The simultaneous application of MI-IR and MI-VCD spectroscopy has turned out to be an extremely useful method in the structural studies of flexible chiral molecules.

In my talk I will show examples how the combination of the above-mentioned methods and some others can be applied to explore the conformational potential energy surface of biomolecules. I will summarize the advantages and the limitations of our methods. Finally, I will mention some further ideas that we plan to test in the future in order to extend the applicability of these techniques towards more complicated molecular systems.

Investigation of Non-Covalent Interactions by Microwave Spectroscopy

Luca Evangelisti

Department of Chemistry “G. Ciamician” - University of Bologna, via Selmi 2, Bologna 40123, Italy
luca.evangelisti6@unibo.it

Several questions are usually addressed: which is the preferred binding site, which type of interactions are established, whether any conformational change takes place in the monomers upon complexation. Another important question is what are the driving forces of the interactions and how they can be influenced. The nature and driving forces of intermolecular interactions in non-covalently bound molecular complexes can be studied to a very high degree of accuracy by pulsed-jet microwave spectroscopy [1]. From the detailed structural and dynamical data that can be obtained, the site and geometry of the interaction and information on the binding energy can be inferred without ambiguity.

So, answers to these questions allow insight into the molecular interaction process at the molecular level, bridging the gap between gas-phase and bulk properties.

Some chosen examples of published [2] and unpublished results of complexes of medium-size organic molecules with different partners formed in a supersonic expansion and characterized by rotational spectroscopy will be discussed. The partner molecules are held together by hydrogen bonds, weak hydrogen bonds and lone-pair- π -hole interactions.

It will be shown how non-covalent interactions compete to shape the conformational space of the complexes and which are the structural changes caused in the monomers upon complexation. It will be also shown how these interactions can be drastically changed through substitution (in particular substitution halogen atoms) of atoms or functional group, in this way achieving an effective tuning of the interactions themselves.

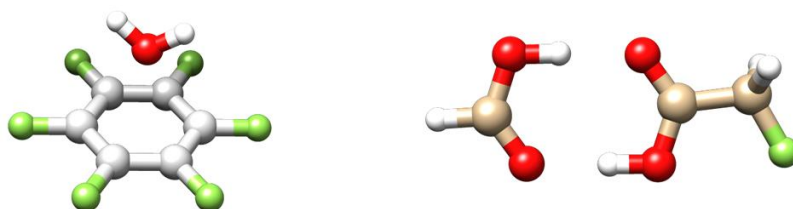


Figure 1 – Examples of molecular complexes studied by microwave spectroscopy.

References

1. M. Becucci and S. Melandri, *Chem. Rev.*, 116 (2016) 5014.
2. L. Evangelisti, K. Brendel, H. Meider, W. Caminati and S. Melandri, *Angew. Chem. Int. Ed.*, 56 (2017) 13699.

Acknowledgements: The author thanks Marie Curie Fellowship PIOF-GA-2012-328405.

Geometric and Electronic Structure of Flavins

Otto Dopfer

Institut für Optik und Atomare Physik, TU Berlin, Hardenbergstr. 36, D-10623 Berlin, Germany
dopfer@physik.tu-berlin.de

In addition to DNA/RNA and amino acids (proteins), flavins are an important class of biomolecules. Flavins (Fl) are derived from the 7,8-dimethyl-10-alkylisoalloxazine chromophore, and differ by their substituent R at the N10 position. The most important examples of the flavin family are lumichrome (LC, R=H), lumiflavin (LF, R=CH₃), riboflavin (RF, vitamin B₂, R=ribityl), flavin mononucleotide (FMN, co-enzyme), and flavin adenosine dinucleotide (FAD, flavo-protein). Their diverse photochemical properties arising from the LC chromophore make them of fundamental importance for many biological systems and phenomena. Their relevance was acknowledged by the Nobel Prize in Chemistry awarded to Paul Karrer in 1937 for his work on flavins and vitamins. Flavins absorb in a wide spectral range from the optical to the UV region, and their optical and photochemical properties vary sensitively with their oxidation, protonation, metalation, and solvation state. Despite their importance, prior to our work, flavins have not been characterized in the gas phase to determine their intrinsic properties. To this end, we systematically characterized the geometric structure of protonated and metalated flavins (X⁺Fl with X=H, Li-Cs, Cu-Au) by IRMPD spectroscopy at room temperature in a FT-ICR mass spectrometer coupled to the IR free electron laser FELIX [1-3]. Comparison of the IRMPD spectra recorded in the fingerprint range with DFT calculations allows for establishing the preferred protonation and metalation sites, the interaction strength, and the type of bonding (electrostatic, covalent). In a second step, we utilized a recently commissioned cryogenic ion trap spectrometer (BerlinTrap) [4] to record first optical spectra of H⁺Fl and M⁺Fl at low temperature (T=20 K) to probe their complex electronic structure arising from the rich manifold of excited states with $\pi\pi^*$ and $n\pi^*$ character [4,5]. The analysis of these high-resolution vibronic spectra is accomplished by TD-DFT calculations coupled to Franck-Condon simulations, providing detailed insight into the excited state properties (e.g., structure, vibrations, lifetime, spectral shifts upon protonation and metalation, energy and nature of electronic state, metal binding energy). The results confirm that protonation and metalation have indeed a drastic impact on the photochemical properties of these simple flavins.

References

1. J. Langer, A. Günther, S. Seidenbecher, G. Berden, J. Oomens and O. Dopfer, *Chem. Phys. Chem.*, 15 (2014) 2550.
2. A. Günther, P. Nieto, G. Berden, J. Oomens and O. Dopfer, *Phys. Chem. Chem. Phys.*, 16 (2014) 14161.
3. P. Nieto, A. Günther, G. Berden, J. Oomens and O. Dopfer, *J. Phys. Chem. A*, 120 (2016) 8297.
4. A. Günther, P. Nieto, D. Müller, A. Sheldrick, D. Gerlich and O. Dopfer, *J. Mol. Spectrosc.*, 332 (2017) 8.
5. A. Sheldrick, D. Müller, A. Günther, P. Nieto and O. Dopfer, *Phys. Chem. Chem. Phys.*, 20 (2018) 7407.

Acknowledgements: The authors thank Deutsche Forschungsgemeinschaft (DFG, project DO 729/6) for financial support.

Towards High Resolution Phosphorescence Spectroscopy

Leonardo Álvarez-Valtierra and Michael Schmitt

División de Ciencias e Ingenierías, Universidad de Guanajuato-campus León. Loma del Bosque 103 Col. Lomas del Campestre, 37150 León Gto. Mexico

Physikalische Chemie I, Heinrich-Heine-Universität, 40204 Düsseldorf, Germany

So far, several groups around the world have studied and reported very interesting molecular systems in the topics of either vibrationally resolved or rotationally resolved spectroscopy in a supersonic beam. Different spectral results have been reported such as benzene derivatives [1], indole derivatives [2], polycyclic aromatic molecules [3], etc. mainly focusing on *Fluorescence* measurements in the gas phase. The technique has been exploited for the discrimination of different conformers in the jet [4], tunneling effects from vibrational motions [3], internal rotation of attached groups to the chromophore [5], formation of clusters in the jet [6], to mention just a few.

However, in terms of *Phosphorescence* spectroscopy, some ketones; such as p-benzoquinone [7], xanthone [8], and anthraquinone [9] have been studied so far at “low” resolution, either in the gas or the condensed phase. Also, some other studies have been performed on different molecular systems, such as pyrazine [10], dibenzofuran [11], and dibenzothiophene [12], where it has been revealed the existence of Intersystem Crossing dynamics upon electronic excitation of them.

In the talk, it will be discussed, how we plan to develop a technique able to get the high resolution phosphorescence spectra and the corresponding spectral analyses of these molecular systems in the gas phase.

References.

1. J. W. Ribblett, W. E. Sinclair, D. R. Borst, J. T. Yi, and D. W. Pratt, *J. Phys. Chem.*, 110A (2006) 1478.
2. C. Kang, J. T. Yi, and D. W. Pratt, *Chem. Phys. Lett.*, 423 (2006) 7.
3. L. Alvarez-Valtierra and D. W. Pratt, *J. Chem. Phys.*, 126 (2007) 224308.
4. M. Schneider, M. Wilke, M. Hebestreit, J. A. Ruiz-Santoyo, L. Alvarez-Valtierra, J. T. Yi, W. Leo Meerts, D. W. Pratt and M. Schmitt, *Phys. Chem. Chem. Phys.* 19 (2017) 21364.
5. J. A. Ruiz-Santoyo, J. Wilke, M. Wilke, J. T. Yi, D. W. Pratt, M. Schmitt, and L. Alvarez-Valtierra, *J. Chem. Phys.* 144 (2016) 044303.
6. L. Alvarez-Valtierra, D. F. Plusquellic, and D. W. Pratt, *J. Phys. Chem.* 115A (2011) 9557.
7. I. Suzuka, M. Sanekata, M. Ito, and N. Ohta, *Laser Chem.* 14 (1994) 143.
8. E. A. Gastilovich, V. G. Klimenko, R. N. Nurmukhametov and S. A. Serov, *Chem. Phys.* 292 (2003) 81.
9. T. Narisawa, M. Sano and Y. J. I'haya, *Chem. Lett.* XX (1975) 1289.
10. K. W. Holtzclaw, L. H. Spangler, and D. W. Pratt, *Chem. Phys. Lett.* 161 (1989) 347.
11. J. T. Yi, L. Alvarez-Valtierra, and D. W. Pratt, *J. Chem. Phys.* 124 (2006) 244302.
12. L. Alvarez-Valtierra, J. T. Yi, and D. W. Pratt, *J. Phys. Chem.* 113A (2009) 2261.

Acknowledgements: The authors thank the financial support granted by the bilateral project DFG-CONACYT 277871, to perform and develop such experiments.

Dipole Moments of Anisole in Ground and Excited State via Condensed Phase Thermochromic Spectroscopy and Gas Phase HRLIF Spectroscopy

Mirko Lindic, Michael Schneider, Marie-Luise Hebestreit and Michael Schmitt
Heinrich-Heine-Universität, Physikalische Chemie 1, Universitätsstraße 1, 40225 Düsseldorf, Germany
Mirko.Lindic@hhu.de

The dipole moment of anisole in ground and first excited singlet states was investigated and compared for the gas and the condensed phase. The dipole moments in solution have been determined using the method of thermochromic shifts of the fluorescence emission and absorption spectra. To test the validity of the method the simple model molecule anisole was measured with temperature dependent UV/Vis-absorption and fluorescence spectroscopy. Contrary to previous studies, the solvent cavity volume was determined experimentally via concentration dependent density measurements. To create exact values for comparison with those from the condensed phase high resolution laser induced fluorescence Stark spectra have been measured in order to reliably determine the excited state dipole moments for a direct comparison. A critical survey about the method will be given.

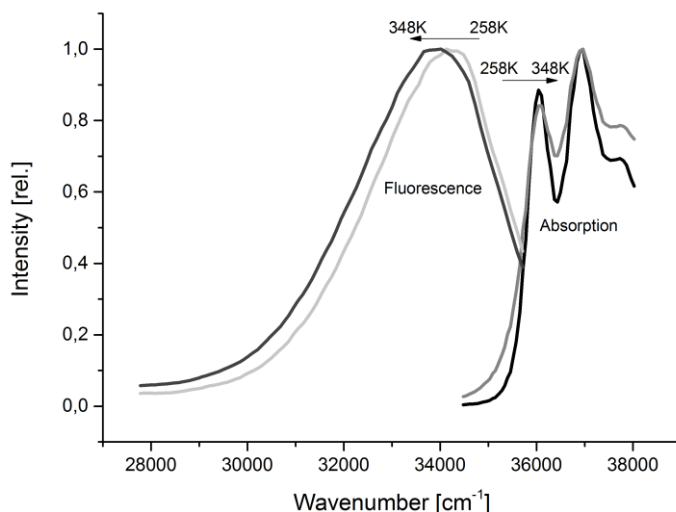


Figure 1

Excited State Dipole Moments from High Resolution Spectroscopy

Michael Schmitt

Heinrich-Heine-Universität, Institut für Physikalische Chemie I, Düsseldorf, Germany

Rotationally resolved electronic Stark spectroscopy is a versatile tool for the accurate determination of rotational constants (*i.e.*, the geometries) of molecules in both electronic states, connected by the electronic transition, centrifugal distortion constants (*i.e.* the force field of the molecule), barriers to hindered internal motions, transition dipole moments (*i.e.* the electronic nature of the excited state), and the permanent dipole moments of both states connected by the electronic transition. The latter provide an easy access to the electronic nature of the state under investigation, because they differ in size and in direction for different electronic states. The most reliable values for dipole moments of ground and electronically excited states are obtained from gas phase electronic Stark experiments, since the dependence of the frequency shift of individual rovibronic lines from the electric field strength yields immediately the dipole moment in ground and excited state. Moreover, not only the absolute value of the total dipole moment can be determined, but also the unsigned Cartesian components of the dipole moment in both electronic states.

The use of genetic algorithms (GA) and evolutionary strategies (ES), which we advanced in the last years, greatly improved the possibility to fit and simulate also very congested and overlapping spectra. We extended the existing experiment in order to measure electronic Stark spectra using different geometrical set-ups with different selection rules. The resulting spectra with parallel and perpendicular selection rules at different electric field strengths are fitted at the same time using evolutionary strategies, improving the accuracy by about one order of magnitude. In this presentation, we will critically discuss the limits for the method, as well as the future aspects, which keep alive this fascinating facet of molecular spectroscopy.

A variation of the thermochromic effect will be presented, which is able to yield dipole moment changes upon electronic excitation of molecules in solution that are largely independent of the solvent used to close the gap between gas phase dipole moment changes and those obtained in solutions.

The Gas Phase Study of Artificial Sweeteners: Structure-Sweetness Connection

E. R. Alonso, L. Kolesníková, I. León, S. Mata and J. L. Alonso

Grupo de Espectroscopia Molecular (GEM), Unidad Asociada CSIC. Laboratorios de Espectroscopia y Bioespectroscopia, Edificio Quifima, Universidad de Valladolid, 47005 Valladolid, Spain
elenarita.alonso@uva.es

Since early last century, abundant research has addressed the link between sweetness and the structure of sweeteners. None of these theories has been able to offer a unified explanation regarding the sweetness-structure relation until Shallenberger and Acree's proposal [1,2]. They observed that the sweetness depends on the strength of two H-bonds by which the sweetener is bound to the sweet receptor. They established that one of the two electronegative atoms might act as a proton donor (AH) in the hydrogen bond interaction and the other as acceptor (B). These two groups form what is called the *glucophore*, which refers to the part of the sweetener that interacts with the sweet receptor. Gas phase studies of diverse artificial sweeteners, concretely saccharine and several sugar alcohols (sorbitol, dulcitol, mannitol, erythritol, etc.) have been carried out by means of broadband [3] and narrow-band [4] microwave spectroscopy techniques in combination with a laser ablation technique for vaporize the sample. The structural characterization in isolation conditions of these molecules gives us valuable information to contrast with the postulated theories about the sweet taste, deepening in the origin of the sweet properties of certain molecules.

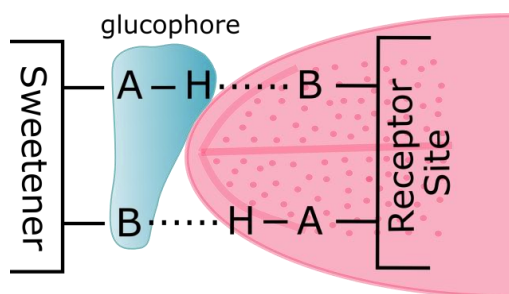


Figure 1 – Glucophore structure and its interaction with the receptor site

References

1. R. S. Shallenberger and T. E. Acree, *Nature*, 216 (1967) 480.
2. R. S. Shallenberger, T. E. Acree and C. Y. Lee, *Nature*, 221 (1969) 555.
3. G. G. Brown, B. C. Dian, K. O. Douglass, S. M. Geyer, S. T. Shipman and B. H. Pate, *Rev. Sci. Instrum.*, (2008) 79.
4. J. L. Alonso and J. C. López. "Microwave Spectroscopy of Biomolecular Building Blocks": Topics in Current Chemistry, Springer, Heidelberg, 364 (2015) 335.

Acknowledgements: The authors thank the financial fundings from Ministerio de Ciencia e Innovacion (Consolider-Ingenio 2010 CSD2009-00038 program "ASTROMOL", CTQ2013-40717-P and CTQ2016-76393-P), Junta de Castilla y Leon (Grants VA175U13 and VA077U16) and European Research Council under the European Union's Seventh Framework Programme (FP/2007-2013) / ERC-2013- SyG, Grant Agreement n. 610256 NANOCOSMOS, are gratefully acknowledged. E. R. A. thanks Ministerio de Ciencia e Innovacion for FPI grant (BES-2014-067776).

Analysis of the Rotationally Resolved Electronic spectra of 3CI and its Water Cluster through Genetic Algorithms

Michael Schneider^a, América Torres-Boy^b, Marie Hebestreit^a, Leonardo Álvarez-Valtierra^b
and Michael Schmitt^a

^a Heinrich-Heine-Universität, Institut für Physikalische Chemie I, D-40225 Düsseldorf, Germany

^b Division de Ciencias e Ingenierías, Universidad de Guanajuato, León, Guanajuato 37150, Mexico
torresba2014@licifug.ugto.mx

In this work, we study the transition $S_1 \leftarrow S_0$ of the 3-cyanoindole (3CI) and some of its Van der Waals clusters with water, $3CI-(H_2O)_n$ ($n = 1$ and 2), through the experimental technique of high resolution (rotational) electronic spectroscopy in the gas phase (HRLIF).

Computational calculations were used as the first approximation of the rotational constants values for ground and first excited state, in order to fit the experimental spectrum obtained. These calculations were made following the DFT method using a consistent correlation numerical basis (cc-pVTZ).

The technique of spectral analysis based on Genetic Algorithms is an excellent computational tool to solve the experimental rotational spectra, which allows a fully automated adjustment, considerably reducing the computational fitting time assigning the rovibronic lines.

The data obtained from the spectra indicate the existence of a single conformer of $3CI-(H_2O)_1$ [1] and two conformers [2] of $3CI-(H_2O)_2$ each, in the molecular jet, respectively. Assignments to different transitions in the spectra of the clusters were made based on a Franck-Condon analysis of the electronic spectrum at vibrational resolution. The understanding of reorganization processes in a molecular level is key in the determination of dipolar moments in condensed phase.

The structural information of the molecule and its clusters are widely discussed from the information extracted from the experimental spectra.

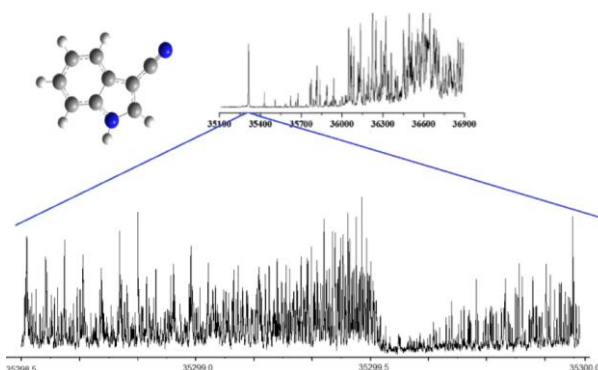


Figure 1 – Comparison between UVHB spectrum reported by Min *et al.* [2] and HRLIF spectrum obtained for 3CI.

References

1. L. Meerts and M. Schmitt, *Int Rev Phys Chem.*, 3 (2007) 25.
2. A. Min, A. Ahn, C. J. Moon, J. H. Lee, M. Y. Choi and S. K. Kim, *Chem. Phys. Lett.*, 20 (2014) 614.

Acknowledgements: Computational support provided by “Lilo Science” computational cluster at the Radboud University, Nijmegen (The Netherlands) is greatly appreciated.

WEDNESDAY, 22nd AUGUST

Solid State Spectroscopy in Support of Interstellar Chemistry

Harold Linnartz

Laboratory for Astrophysics, Leiden Observatory, PO Box 9513, NL2300 RA Leiden, The Netherlands
linnartz@strw.leidenuniv.nl

Spectroscopy is *the* tool to unravel the chemistry of the heavens. High resolution gas phase studies have resulted in the identification of more than 200 different molecules in space. More recently, also frozen molecules, typically molecular ices situated on cold dust grains have been investigated. Astronomical observations show that ices in space consist mainly of water with large contributions from CO, CO₂, CH₃OH, NH₃ and other species. This has resulted in a new research field – solid state astrochemistry – in which the formation of many of the observed gas phase species can be linked to surface processes.

This talk will summarize our spectroscopic knowledge of ice in space, information that is very valuable, particularly as the James Webb Space Telescope will allow new and detailed views on the Icy Universe. The talk also will show how spectroscopy can be used to monitor molecule formation in the solid state under interstellar conditions. A special focus will be on the formation of water and so called COMs, complex organic molecules that are considered the building blocks of life. In Figure 1 a reaction scheme based on radical surface diffusion is shown that relates the hydrogenation of CO-ice to the formation of larger species already detected in space, such as glycolaldehyde and ethylene glycol, and possibly larger molecules, like glyceraldehyde and glycerol.

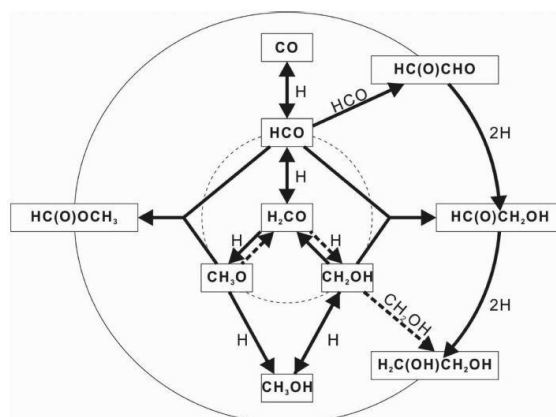


Figure 1. Non-energetic solid state formation scheme of glycol aldehyde and ethyleneglycol upon CO hydrogenation as expected for dark cloud condition (taken from [1]). See also [2-4].

References

1. K.-J. Chuang, G. Fedoseev, S. Ioppolo, E. F. van Dishoeck and H. Linnartz, *MNRAS*, 455 (2016) 1702.
2. G. Fedoseev, K.-J. Chuang, S. Ioppolo, D. Qasim, E. F. van Dishoeck and H. Linnartz, *ApJ*, 842 (2017) A52.
3. H. Linnartz, G. Fedoseev and S. Ioppolo, *Int. Rev. Phys. Chem.* 34 (2015) 205.
4. G. Fedoseev, T. Lamberts, S. Ioppolo, H. M. Cuppen and H. Linnartz, *MNRAS*, 448 (2015) 1288.

www.laboratory-astrophysics.eu

Burning Water with Sunlight: insights from Computational Chemistry

Andrzej L. Sobolewski

Institute of Physics, Polish Academy of Sciences, Al. Lotnikow 32/46, 02-668 Warsaw, Poland
sobola@ifpan.edu.pl

Polymeric or partially crystalline materials consisting of *s*-triazine or heptazine (tri-*s*-triazine) units connected by imide groups or nitrogen atoms and collectively referred to as graphitic carbon nitrides (g-C₃N₄) have received enormous attention since the discovery of their photocatalytic activity for hydrogen evolution with visible light [1]. The mechanism of the photoinduced water-splitting reaction catalyzed by g-C₃N₄ is generally discussed in terms of the band structure of the amorphous or crystalline materials and the mobility of photoinduced electrons and holes which are supposed to eventually drive the reduction of protons and the oxidation of water, respectively. However, the fundamental mechanistic principles of the photoinduced reaction and the catalytic cycle are currently not well understood.

In this contribution, I provide first-principles computational evidence that water splitting with heptazine-based materials [2], as well as with other azines [3,4] and TiO-porphyrines [5,6] is a molecular photochemical process taking place in hydrogen-bonded chromophore-water complexes. The water splitting occurs homolytically via an electronically driven nonadiabatic proton-transfer reaction from water to chromophore, resulting in ground-state hydrogenated molecular radicals and OH radicals. The excess hydrogen atom of the hypervalent molecular radical can be photodetached by a second photon, which regenerates the catalyst, or the long-lived hydrogenated radicals can recombine to yield H₂ in a dark reaction when a suitable catalyzer (colloidal platinum) is present. The OH radicals produced in the reaction can be recombined to H₂O₂ with suitable catalyzers (carbon or metal-oxide nano dots).

References

1. X. Wang, K. Maeda, A. Thomas, K. Takanabe, G. Xin, J. M. Carlsson, K. Domen and M. Antonietti, *Nature Mater.*, 8 (2009) 76.
2. J. Ehrmaier, T. N. V. Karsili, A. L. Sobolewski and W. Domcke, *J. Phys. Chem. A*, 121 (2017) 4754.
3. X. Liu, A. L. Sobolewski, R. Borrelli and W. Domcke, *Phys. Chem. Chem. Phys.*, 15 (2013) 5957.
4. X. Liu, T. N. V. Karsili, A. L. Sobolewski and W. Domcke, *Chem. Phys.*, 464 (2016) 78.
5. O. Morawski, K. Izdebska, E. Karpiuk, A. Suchocki, Y. Zhydachevskii and A. L. Sobolewski, *Phys. Chem. Chem. Phys.*, 16 (2014) 15256.
6. O. Morawski, K. Izdebska, E. Karpiuk, A. Suchocki, Y. Zhydachevskii and A. L. Sobolewski, *J. Phys. Chem. C*, 119 (2015) 1408.

Ordinary Chondrites: What Can We Learn Using Mössbauer Spectroscopy?

A. A. Maksimova and M. I. Oshtrakh

*Department of Experimental Physics, Institute of Physics and Technology, Ural Federal University,
Ekaterinburg, 620002, Russian Federation
oshtrakh@gmail.com*

Study of extraterrestrial matter is very important due to a number of reasons, such as (i) analysis of Solar system evolution, (ii) investigation of the extreme conditions on minerals formation, (iii) analysis of thermal history of matter, (iv) investigation of structural and chemical variations of extraterrestrial minerals in space, etc. The main space messengers reached Earth are various meteorites which can be classified in several groups related to their origin and chemical composition. There are iron, stony-iron, and stony meteorites. All meteorites contain iron-bearing minerals. Therefore, ^{57}Fe Mössbauer spectroscopy is a useful tool for the study of extraterrestrial materials with very complex composition. In the present work, we will consider investigations of various ordinary chondrites which are a part of stony meteorites (undifferentiated meteorites in the modern classification [1]) and can be considered as Solar system peers. Ordinary chondrites consist of various iron-bearing minerals such as olivine ($\text{Fe, Mg}_2\text{SiO}_4$), orthopyroxene (Fe, MgSiO_3), clinopyroxene (Fe, Ca, MgSiO_3), troilite FeS , α -, α_2 - and γ -phases of Fe-Ni-Co alloy, chromite FeCr_2O_4 , etc., as well as their weathering products. All ordinary chondrites were divided into three groups H, L and LL related to the total iron content and metallic iron alloy content: H (high total iron), L (low total iron) and LL (low total iron and low metallic iron). In spite of a complex composition of ordinary chondrites with different phases in magnetic and paramagnetic states as well as ferrous and ferric compounds, ^{57}Fe Mössbauer spectroscopy was successfully applied for their investigation more than 55 years (the first review on the study of stony meteorites was published in 1964 [2]). Development of Mössbauer spectroscopy with a high velocity resolution increased possibilities of technique in a better quality investigation of meteorites and new results obtaining [3, 4]. Using Mössbauer spectroscopy it was possible to identify the main iron-bearing minerals of ordinary chondrites and their relative composition, the processes of their weathering with estimation of their terrestrial age, the distribution of Fe^{2+} and Mg^{2+} cations in silicate minerals, an analysis of the thermal history of silicates, systematics of ordinary chondrites from H, L and LL groups using Mössbauer parameters. These results are considered in comparison with some other complimentary techniques such as optical and scanning electron microscopy, X-ray diffraction, etc.

References

1. M. K. Weisberg, T. J. McCoy and A.N. Krot, in: *Meteorites and the Early Solar System II*, The University of Arizona Press, Tucson, 2006, pp. 19–52.
2. E. L. Sprenkel-Segel and S. S. Hanna, *Geochim. Cosmochim. Acta*, 28 (1964) 1913.
3. M. I. Oshtrakh, V. I. Grokhovsky, E. V. Petrova, M. Yu. Larionov, M. V. Goryunov and V. A. Semionkin, *J. Mol. Struct.*, 1044 (2013) 268.
4. A. A. Maksimova, M. I. Oshtrakh, V. I. Grokhovsky, E. V. Petrova and V. A. Semionkin, *Hyperfine Interact.*, 237 (2016) 134.

Acknowledgements: This work was supported by the Ministry of Education and Science of the Russian Federation (the Project # 3.1959.2017/4.6) and Act 211 of the Government of the Russian Federation, contract № 02.A03.21.0006.

Characterization of the Iron Core in Ferrifol[®], a Pharmaceutical Analogue of Ferritin, Using Mössbauer Spectroscopy and Magnetization Measurement

I. V. Alenkina^a, I. Felner^b, E. Kuzmann^c and M. I. Oshtrakh^a

^a Department of Experimental Physics, Institute of Physics and Technology, Ural Federal University, Ekaterinburg, 620002, Russian Federation

^b Racah Institute of Physics, The Hebrew University, Jerusalem, 91904 Israel

^c Laboratory of Nuclear Chemistry, Institute of Chemistry, Eötvös Loránd University, Budapest, Hungary
alenkina-ira@mail.ru

Ferritin molecules are responsible for iron storage in various living systems with a further iron release for organism's needs. Ferritin consists of a spherical multi-protein shell with nano-sized iron core inside the protein hollow. The iron core is in the form of ferrihydrite ($5\text{Fe}_2\text{O}_3 \times 9\text{H}_2\text{O}$) with inorganic phosphates. Ferritin analogues such as iron-polysaccharide complexes appeared to be good medicaments for treatment of iron deficiency anemia. Ferrifol[®] (CTS Chemical Industries Ltd., Israel) is one out of various commercial pharmaceutical products which are manufactured for this purpose. The structure of Ferrifol[®] molecule represents a polymaltose shell surrounding nano-sized iron core being in the form of akaganéite ($\beta\text{-FeOOH}$). We report here the characterization of the iron core in Ferrifol[®] by Mössbauer spectroscopy and magnetization studies.

Mössbauer measurements were performed using: (i) a Mössbauer spectrometer with a high velocity resolution (registration in 4096 channels) in the temperature range from 295 to 90 K and (ii) a Mössbauer spectrometer with a lower velocity resolution (registration of two mirror spectra in 512 channels before folding) in the temperature range from 60 to 20 K. Magnetization measurements were performed using a Quantum Design superconducting quantum interference device (SQUID) magnetometer in the temperature range 300–4 K.

Mössbauer spectroscopy demonstrated that the iron core was in the paramagnetic state down to 60 K. A slow decrease of magnetic relaxation represented by magnetically split components (sextets) appears in the spectra at 40 and 20 K. At the temperature range 295–90 K the Mössbauer spectra of Ferrifol[®] demonstrated non-Lorentzian two-peak spectra which were better fitted using a superposition of 5 different quadrupole doublets with similar isomer shifts. An unusual line broadening was also observed in this temperature range. Magnetization measurements showed that the blocking temperature is at ~33 K and the Ferrifol[®] iron core is mainly in the paramagnetic state. These results are in agreement with previous data obtained for ferritin and some other iron-polymaltose analogues [1,2]. The observed complex character of the Mössbauer spectra of Ferrifol[®] and the temperature dependent variations of Mössbauer parameters were interpreted as a result of the different ^{57}Fe local micro-environments in the corresponding iron core layers/regions and their low temperature structural re-arrangements.

References

1. I. V. Alenkina, M. I. Oshtrakh, Z. Klencsár, E. Kuzmann, A. V. Chukin and V. A. Semionkin. *Spectrochim. Acta, Part A: Molec. and Biomolec. Spectrosc.*, 130 (2014) 24.
2. M. I. Oshtrakh, I. V. Alenkina, Z. Klencsár, E. Kuzmann and V. A. Semionkin. *Spectrochim. Acta, Part A: Molec. and Biomolec. Spectrosc.*, 172 (2017) 14.

Acknowledgements: This work was supported by the Ministry of Education and Science of the Russian Federation (the Project # 3.1959.2017/4.6) and Act 211 of the Government of the Russian Federation, contract № 02.A03.21.0006.

Excitation-Emission Fluorescence Analysis: Resolving Relevant Underlying Contributions

Jorge Costa Pereira^a, Alberto A. C. C. Pais^a, Hugh D. Burrows^a,
Júlio César R. Azevedo^b and Heloise G. Knapik^c

^a CQC, Department of Chemistry, University of Coimbra, P-3004 535 Coimbra, Portugal

^b Department of Chemistry and Biology, Federal University of Technology - Parana, Rua Deputado Heitor de Alencar Furtado, 4900, 81280-340, Curitiba-PR, Brazil

^c Department of Hydraulic and Sanitation, Federal University of Parana, Centro Politecnico, Bl. 5, Av. Cel Francisco H. dos Santos, 81531-990, Curitiba-PR, Brazil
Jcpereira@qui.uc.pt

Light provides one of most important ways to obtain insight on matter – from single molecules to ourselves, the surroundings and evenly deep space. Spectroscopy is thus a very important and convenient analytical field for exploring and developing our knowledge about the universe, its composition and respective energetic states.

Spectroscopy benefits from various characteristics that allow its use in Qualification and Quantification. Environmental Quality control is a specially challenging task because each sample consists of a complex ensemble of several materials (typically organic), embedded in a specific inorganic matrix, each compound with specific spectroscopic characteristics. In terms of analytical approaches, standard analytical procedures typically require different separation steps and subsequent quantification of each analyte of interest [1].

Using various multivariate analytical methodologies we have developed the direct sample characterization of complex aquatic bodies, accessing different contributions of dissolved organic matter contributions in these aqueous environmental samples [2,3]. The first task is to determine the number of independent contributions. With this information we have obtained selective signal resolution in terms of sources (specific spectra) and contributions (related to the system composition).

In this work we demonstrate the use of Excitation-Emission Fluorescence spectroscopy in the characterization of aquatic samples. This approach has allowed us to a) identify the number of underlying contributions, b) estimate respective signal sources and c) respective contributions in terms of system composition [2,3].

The same strategy is now being applied to the non-invasive analysis of ¹H-NMR signals for oncologic diagnosis based on biological fluids [4,5].

References

1. A. H. I. Rodrigo, A. O. L. O. Marcante, J. Costa Pereira and J. C. R. Azevedo, *Clean-Soil, Air, Water*, 45 (2017) 1700334.
2. F. Almeida Brehm, J. C. R. Azevedo, J. Costa Pereira and H. D. Burrows, *Env. Monit. and Assess.*, 187 (2015) 703.
3. J. Costa Pereira, J. C. R. Azevedo, H. G. Knapik and H. D. Burrows, *Spect. Acta A: Mol. and Biomolec. Spect.*, 165 (2016) 69.
4. J. Costa Pereira, I. Jarak and R. A. Carvalho, *Magn. Reson. Chem.*, 55 (2017) 936.
5. J. Costa Pereira, I. Jarak and R. A. Carvalho, *Appl. Magn. Reson.*, (2018). <https://doi.org/10.1007/s00723-018-1010-5>.

Acknowledgements: The authors thank to the Coimbra Chemistry Centre (CQC), supported by FCT, through the project UI0313/QUI/2013, also co-funded by FEDER/COMPETE 2020-UE.

The Hydrolysis of Mg^{2+} Ions in the Presence of Gluconate

Bence Kutus,^a Csilla Dudás,^a Eszter Orbán,^a Ákos Buckó,^b

István Pálinkó,^c Pál Sipos^a and Gábor Peintler^b

^a Department of Inorganic and Analytical Chemistry, University of Szeged, 7 Dóm tér, H-6720 Szeged, Hungary

^b Department of Physical Chemistry and Material Science, University of Szeged, 1 Rerrich B. tér,
H-6720 Szeged, Hungary

^c Department of Organic Chemistry, University of Szeged, 8 Dóm tér, H-6720 Szeged, Hungary
kutusb@chem.u-szeged.hu

In the concrete-based radioactive waste repositories established in underground salt mines, concentrated MgCl_2 - or NaCl -containing solutions are assumed to be formed by the incidental intrusion of water [1]. D-gluconate (Gluc^-), used as an additive for the formulation of cementitious materials [2], is considered as a potential ligand for the mobilization of actinide ions [3]. The complexation reaction between Gluc^- and radionuclides may be affected by the equilibria taking place between Mg^{2+} and Gluc^- ions, thus, quantitative description of the $\text{Mg}^{2+}/\text{Gluc}^-$ system is of particular interest.

During this work, a potentiometric as well as ^1H and ^{13}C NMR spectroscopic studies were undertaken to reveal the speciation between Mg^{2+} and Gluc^- ions. The experiments were performed at 25 °C, 4 M ionic strength and in the pH range of 2–12. In addition to the MgGluc^+ species known from literature [4], the formation of the MgGlucOH^0 and $\text{MgGluc}(\text{OH})_2^-$ complexes was observed. ^1H and ^{13}C NMR spectra indicated that the protons were displaced from the metal-coordinated water molecules rather than the hydroxy functions of gluconate. In this respect, the $\text{Mg}(\text{II})$ gluconate complexes differ markedly from the $\text{Ca}(\text{II})$ gluconate ones [5], for which pronounced ^1H NMR peak broadening was detected as a result of metal-promoted ligand deprotonation.

Unexpectedly, the titration data implied the presence of a trinuclear magnesium(II) complex with the formula of $\text{Mg}_3\text{Gluc}_2(\text{OH})_4$. Additionally, its formation was corroborated by the variations of the ^1H and ^{13}C NMR chemical shifts observed on the pH-dependent spectra. More importantly, this species appears to be the ligand-stabilized form of $\text{Mg}_3(\text{OH})_4^{2+}$, which was invoked in previous solubility studies; however, it is still considered as an uncertain complex due to experimental difficulties associated with its detection [6].

Concerning the waste repositories, our calculations suggest that the formation of these deprotonated complexes does not affect considerably the solubility of $\text{Mg}(\text{OH})_2$ under the concentrations prevailing in pore waters.

References

1. C. Bube, V. Metz, E. Bohnert, K. Garbev, D. Schild and B. Kienzler, *Phys. Chem. Earth*, 64 (2013) 87.
2. S. Ramachandran, P. Fontanille, A. Pandey and C. Larroche, *Food. Technol. Biotechnol.*, 44 (2006) 185.
3. X. Gaona, V. Montoya, E. Colàs, M. Grivé and L. Duro, *J. Contam. Hydrol.*, 102 (2008) 217.
4. R. K. Cannan and A. Kibrick, *J. Am. Chem. Soc.*, 60 (1938) 2314.
5. A. Pallagi, É. G. Bajnóczi, S. E. Canton, T. Bolin, G. Peintler, B. Kutus, Z. Kele, I. Pálinkó and P. Sipos, *Environ. Sci. Technol.*, 48 (2014) 6604.
6. P. L. Brown and C. Ekberg: *Hydrolysis of Metal Ions*. Wiley-VCH, Weinheim, Germany (2016) 193.

Acknowledgements: The authors thank the financial support provided by the New National Excellence Program (Project No. UNKP-17-3-IV-SZTE-9) and the National Research, Development and Innovation Office (Project No. NKFIH K 124265).

Correlation of Hydrogen-Bonding and Catalytic Activity for Diol-based Asymmetric Organocatalysts

Seoncheol Cha, Manfred Wagner and Johannes Hunger

Max-Planck Institute for Polymer Research, Ackermannweg 10, 55128, Mainz, Germany
cha@mpip-mainz.mpg.de

1-naphthyl substituted $\alpha,\alpha,\alpha,\alpha$ -tetraaryl-1,3-dioxolane-4,5-dimethanol (1nTADDOL, Fig. 1) is one of the most efficient diol-based asymmetric organo-catalysts and has been proven to provide excellent stereoselectivity for a wide range of chemical conversions, including e.g. the hetero-Diels-Alder reaction [1]. The hydrogen-bonding structure and dynamics of 1nTADDOL and its reactive intermediates formed with substrate molecules, which is at the heart of the catalytic activation due to 1nTADDOL, have however remained experimentally unverified at the molecular level.

In this contribution, we present an investigation of the intramolecular structure of 1nTADDOL and its intermolecular interaction with substrate molecules to understand the origin of the stereoselectivity using a combination of IR, NMR and IR pump-probe spectroscopy. The presence of hydrogen-bonded OH groups (OH stretching vibration at $\sim 3370\text{ cm}^{-1}$) and free OH groups (~ 3520 and 3670 cm^{-1}) of 1nTADDOL in the infrared spectra can be explained by the formation of intramolecular hydrogen bonds (Fig. 2). Interestingly, the free OH vibrational mode is split into two different bands indicating the existence of distinctively different free OH groups in 1nTADDOL. IR and NMR spectra of 1nTADDOL in different solvents show that the intramolecular hydrogen-bonding structure markedly depends on the solvent. IR pump-probe spectroscopy experiments suggest that a model substrate molecule (benzaldehyde) exclusively affects the vibrational relaxation of the red-shifted free OH, rather than the blue shifted free OH-group (Fig. 3). This observation points at substrate induced changes of vibrational coupling, which can be explained from a specific interaction with the reactive intermediates. Thus, our results indicate the formation of a structurally unique reactive intermediate, which is likely related to the high enantioselectivity of 1nTADDOL catalysis.

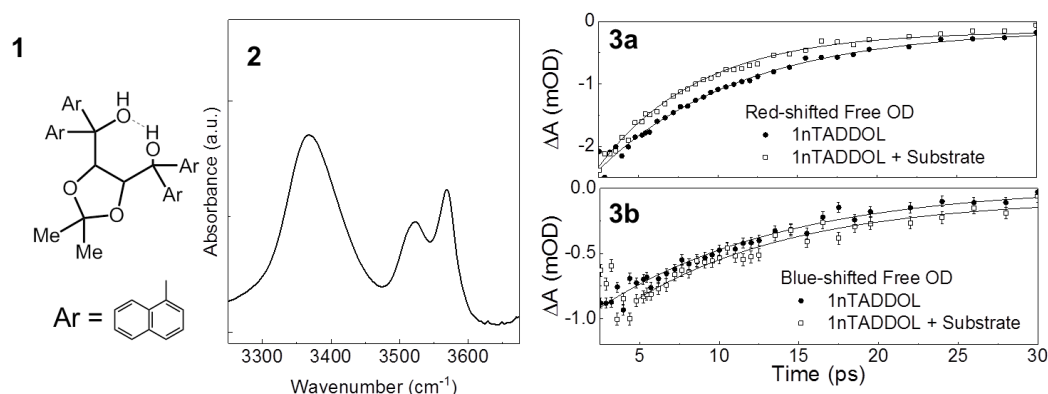


Figure 1 – (1) Molecular structure of TADDOL. (2) IR absorption spectrum of 1nTADDOL in toluene. (3) Transient absorption traces for the OD stretching vibration of 1nTADDOL- d_2 with and without substrate for red- and blue-shifted free OD groups.

References

1. Y. Huang, A. K. Unni, A. N. Thadani and V. H. Rawal, *Nature*, 424 (2003) 424.

Fluorescence Quenching of Xanthone and Xanthione Derivatives in Protic and Aprotic Solvents

Svetlana S. Khokhlova^a, Anatoly I. Ivanov^a, Roman G. Fedunov^a, Stanislav L. Bondarev^b, Sergey A. Tikhomirov^b, Tamara F. Raichenok^b and Oleg V. Bugarov^b, Vyacheslav K. Ol'khovik^c and Nikolai A. Galinovskii^c

^a Volgograd State University, 400062 Volgograd, Russian Federation

^b B. I. Stepanov Institute of Physics, National Academy of Sciences of Belarus, Prospect Nezavisimosti 68, Minsk BY-220072, Republic of Belarus

^c Institute of Chemistry of New Materials, National Academy of Sciences of Belarus, Fr. Skaryna Street 36, Minsk BY-220141, Republic of Belarus
svetlana.khokhlova@volsu.ru

New compounds 1,3-dimethoxy xanthione [1], 2,7-diamino xanthione and 2,7-diamino xanthone [2] have been synthesized and their absorption and transient spectra have been measured in various solvents. Quantum chemical calculations with semiempirical, DFT and TD-DFT methods provided an important information about electronic structure of diamino and methoxy derivatives of xanthone and xanthione. The theoretical electronic absorption spectra of 2,7-diamino xanthone (Fig. 1), as well as for the rest of compounds, are in good agreement with experimental spectra.

Theoretical fitting of transient absorption spectra of the compounds has been conducted with modern and very precise method developed in [3]. The method gives good qualitative and quantitative coincidence with the experimental results.

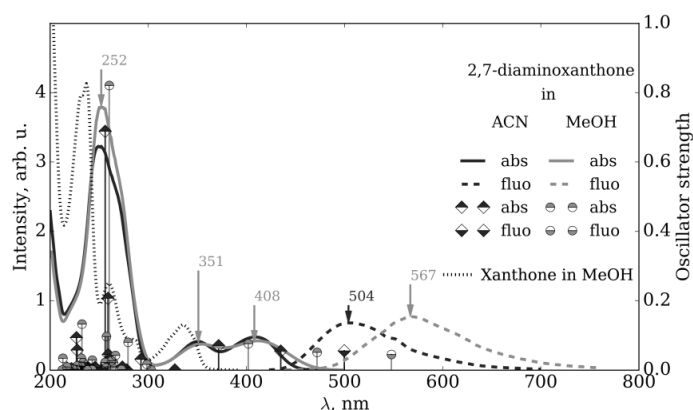


Figure 1 – Absorption (abs) and fluorescence (fluo) of 2,7 - diaminoxanthone in methanol (MeOH) and acetonitrile (ACN) obtained experimentally (lines) and calculated theoretically (symbols). Experimental absorption spectra of xanthone in MeOH is shown by dotted line.

References

1. R. G. Fedunov, M. V. Rogozina, S. S. Khokhlova, A. I. Ivanov, S. A. Tikhomirov, S. L. Bondarev, T. F. Raichenok, O. V. Bugarov, V. K. Ol'khovik and D. A. Vasilevskii, *Chem. Phys.*, 494 (2017) 1.
2. S. L. Bondarev, S. A. Tikhomirov, T. F. Raichenok, O. V. Bugarov, R. G. Fedunov, S. S. Khokhlova, A. I. Ivanov V. K. Ol'khovik and N. A. Galinovskii, *J. Lumin.*, 198 (2018) 226.
3. R. G. Fedunov and A. I. Ivanov, *J. Russ. Laser Res.* 33 (2012) 152.

Acknowledgements: The study was supported by a grant from the Russian Science Foundation (Grant No. 16-13-10122).

Precision Spectroscopy in Cold Samples of Few-Electron Molecules

Maximilian Beyer, Nicolas Hölsch, Luca Semeria, Paul Jansen, Frédéric Merkt

Physical Chemistry Laboratory, ETH Zurich, CH 8093 Zurich, Switzerland

merkt@phys.chem.ethz.ch

Few-electron molecules represent attractive systems for precision spectroscopy because their properties can be calculated with extraordinary accuracy by *ab initio* quantum-chemical methods [1,2]. Comparing experimental and theoretical results thus offers the opportunity to assess the limitations of *ab initio* calculations, ultimately and ideally at the level where their accuracy is limited by either the uncertainties of the fundamental constants or so far unrecognized physical effects. We present the results of precision measurements in cold samples of hydrogen (H_2) and metastable He_2 molecules. The cold-molecule samples are prepared in supersonic beams using pulsed cryogenic valves and, in the case of metastable He_2 , a multistage Zeeman decelerator.

In the case of the metastable $a^3\Sigma_u^+$ state of He_2 , we exploit multistage Zeeman deceleration to prepare slow beams of cold and fully magnetized molecules in selected spin-rotational components [3]. We use the long transit times of these molecules through microwave and laser fields to carry out highly precise measurements of (i) fine-structure intervals in the metastable a state, (ii) the frequencies of transitions to high Rydberg states of He_2 , and (iii) the spin-rovibrational energy level structure of the $X^+ 2\Sigma_u^+$ ground state He_2^+ by Rydberg-series extrapolation [4].

In the case of H_2 , we measure transitions from selected rovibrational levels of the $GK^1\Sigma_g^+$ state to high Rydberg states belonging to p and f series converging on different rovibrational levels of $X^+ 2\Sigma_g^+$ ground state of H_2^+ . The transition frequencies are determined with a relative precision ($\Delta\nu/\nu$) of $2\cdot 10^{-10}$ [5]. Extrapolation of these series by multichannel quantum defect theory enables us to determine the spin-rovibrational intervals of H_2^+ at unprecedented accuracy. The relevance of these results in the context of measurements of fundamental constants and elementary-particle properties will be discussed.

References

1. V. I. Korobov, L. Hilico and J.-P. Karr, *Phys. Rev. Lett.*, 118 (2017) 233001.
2. M. Puchalski, J. Komasa and K. Pachucki, *Phys. Rev. A*, 95 (2017) 052506.
3. P. Jansen, L. Semeria, L. Esteban Hofer, S. Scheidegger, J. A. Agner, H. Schmutz and F. Merkt, *Phys. Rev. Lett.*, 115 (2015) 133202.
4. P. Jansen, L. Semeria and F. Merkt, *Phys. Rev. Lett.*, 120 (2018) 043001.
5. M. Beyer, N. Hölsch, J. A. Agner, J. Deiglmayr, H. Schmutz and F. Merkt, *Phys. Rev. A*, 97 (2018) 012501; 039903(E).

Acknowledgements: This work is supported financially by the Swiss National Science Foundation (Project No. 200020-172620) and the European Research Council (ERC) under the European Union's Horizon 2020 research and innovation programme (Advanced Grant 743121).

New Avenues for Computational Chiral Spectroscopy

Franco Egidi, Marco Fusè, Julien Bloino and Vincenzo Barone

Scuola Normale Superiore, Piazza dei Cavalieri 7, Pisa, Italy

franco.egidi@sns.it

Chiral spectroscopies are powerful techniques that allow the determination of the absolute configuration of a chiral sample, as well as provide additional detail and more specific insight into the sample's properties when compared to non-chiral measurements. From circular birefringence to vibrational circular dichroism, there is a wide array of available techniques depending on the property of interest. In almost all cases, in order to assign the absolute configuration of a sample from an experimental measurement, a theoretical calculation is required to determine the sign of the property associated with each enantiomer [1]. For this reason, several methods have been developed in the past to accurately reproduce the chiral response of molecular systems. Recently, we have expanded upon the available theoretical and computational techniques to simulate the emission of circularly polarized radiation of a system in a triplet state, a phenomenon known as circularly polarized phosphorescence (CPP) [2,3], and applied it to both organic and inorganic systems, of the type that has found applications in electroluminescent devices such as OLEDs, sensors, and probes. In addition, to provide a more profound insight into the chiral response, we revisited vibrational circular dichroism (VCD) [4] a well-known spectroscopy that exposes the chiral vibrational signature of a system. Thanks to recent developments both regarding the treatment of anharmonic effects [5] and in graphical visualization tools, we have expanded upon a visualization technique that can be used to truly expose the origin of the vibrational chiral response of a system by plotting the movement of the electrons during the vibration [6]. These efforts will be able to offer new and more accurate tools for the study of chiral systems through spectroscopy.

References

1. J. Autschbach, *Chirality* 21 (2009) E116.
2. F. Egidi, M. Fusè, A. Baiardi, J. Bloino, X. Li and V. Barone, *Chirality*, (submitted).
3. G. Baryshnikov, B. Minaev and H. Ågren, *Chem. Rev.* 117 (2007) 6500.
4. G. Magyarfalvi, G. Tarczay and E. Vass, *WIREs Comput. Mol. Sci.* 1 (2011) 403.
5. L. A. Nafie, *J. Phys. Chem. A* 101 (1997) 7826.
6. J. Bloino and V. Barone, *J. Chem. Phys. A* 136 (2012) 124108.

Predicting Excited State Dynamics from Scratch – a Path Integral Approach Implemented on ORCA

Bernardo de Souza^a, Robert Iszak^b and Frank Neese^b

^a Universidade Federal de Santa Catarina, Departamento de Química, 88040-900, Brazil

^b Max-Planck-Institut für Kohlenforschung, Kaiser-Wilhelm-Platz 1, D-45470, Mülheim an der Ruhr, Germany
bernardo.souza@ufsc.br

The recent growth of interest on molecular photochemistry and photophysics promoted by the development of applications such as organic solar cells, OLEDs and photoredox chemistry led many researches to develop new interesting methods to calculate vertical transition energies, oscillator strengths and other static properties. However, as the processes involved are so fast, one has to go beyond the static picture and include the dynamic aspects of those systems to completely describe them. With that in mind, we developed new theoretical models to predict dynamic properties of excited states completely from *ab initio* using the analytical solution for the path integral to the nuclear movement [1]. These models were implemented very efficiently on the free software ORCA, where different methods to compute excited state static properties such as TD-DFT, CASSCF, (ST)EOM, ROCIS are already available. Our first paper¹ considers only the processes of absorption and fluorescence, but we already have developed and implemented the theory to compute phosphorescence rates and spectrum, resonant Raman spectrum and intersystem crossing rates, being thus able to predict quantum yields at 77K for some organic molecules. With the complete theoretical spectrum, we can go as far as predicting the actual color of emission for any given molecule, such as presented on the Figure 1 below.

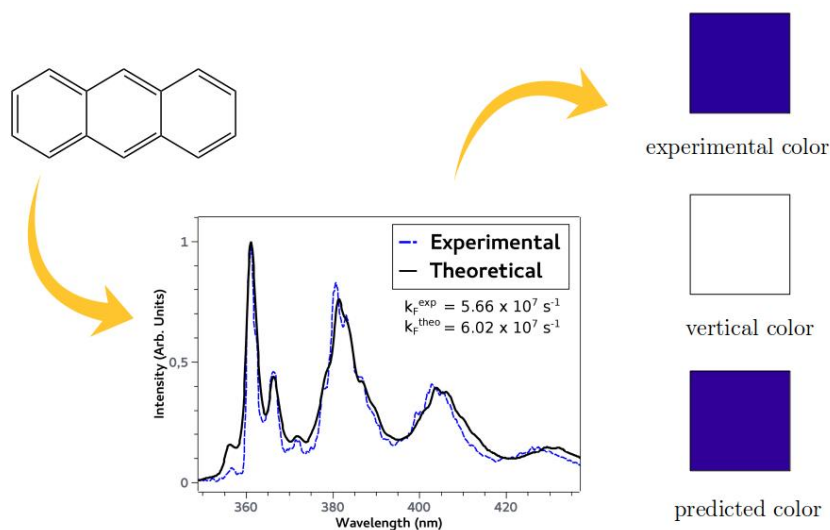


Figure 1 – Calculated (solid black) and experimental (dashed blue) fluorescence spectra of anthracene, in gas phase at 433 K using WB97X/DEF2-TZVP and ORCA_ESD.

References

1. B. de Souza, F. Neese and R. Izsák, *J. Chem. Phys.*, 148 (2018) 034104.

Acknowledgements: The authors thank CAPES, the Humboldt Foundation and the Max Planck Society for support and funding.

Simulation of Fully Anharmonic Vibrational Spectra of Biomolecular Building Blocks

Malgorzata Biczysko, Zhongming Jiang and Hongli Zhang
Shanghai University, 99 Shangda Rd, 200444 Shanghai, China
biczysko@shu.edu.cn

Advanced spectroscopic experiments are widely applied for understanding the biomolecules structure-function relationships, allowing a direct detection of different 3D-conformational schemes via microwave (MW) measurements or indirect analysis through 'fingerprint' vibrational features in infrared (IR), Raman, Resonance Raman, UV-vis or fluorescence spectra, including also their chiral counterparts. However, the conformational flexibility and great variety of possible interactions results that these experimental spectroscopic studies are extremely difficult to interpret. In this talk I will present the status and perspectives of the ongoing project aiming to bridge the gap between sophisticated experimental techniques and often over-simplified analysis, focusing specifically on protein and DNA building blocks. In this context, inclusion of anharmonic effects on rotational constants, thermodynamic properties, and on both line positions and intensities of vibrational (IR, Raman, VCD, ROA...) spectra is paving a way toward significantly improved level of accuracy and understanding of state-of-the-art contemporary spectroscopic results.

In this framework, computational protocol is developed through a multistep strategy, starting from isolated molecules, oligomers and weakly-bonded complexes/clusters. Extension to larger and more complex systems relies on reduced dimensionality approaches and effective schemes to select transitions of interest. Such procedures will be discussed focusing on the challenges represented by an accurate description of 3D-conformational structure of flexible systems and vibrational modes involved in the inter- or intra-molecular hydrogen bonds.

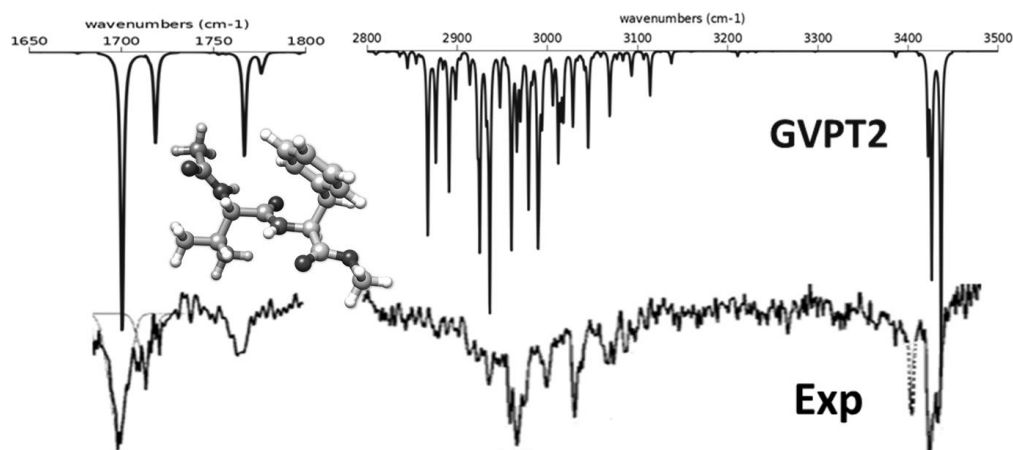


Figure 1 – Experimental and fully anharmonic (GVPT2) IR spectrum of Ac-Val-Phe-OMe dipeptide

References

1. M. Biczysko, Z. Jiang and J. Bloino, *Phys. Chem. Chem. Phys.*, submitted.
2. Z. Jiang, M. Biczysko and N. W. Moriarty, *Proteins*, 86 (2018) 273.
3. M. Biczysko, J. Bloino and C. Puzzarini, *Wires Comp. Mol. Sci.*, 8 (2018) e1349.
4. J. Bloino, A. Baiardi and M. Biczysko *Int. J. Quant. Chem.*, 116 (2016) 1543.
5. T. Fornaro, M. Biczysko, J. Bloino and V. Barone, *Phys. Chem. Chem. Phys.*, 18 (2016) 8479.
6. T. Fornaro, I. Carnimeo and M. Biczysko, *J. Phys. Chem. A*, 119 (2015) 5313.

3D Outer Electronic Shell Visualization by Laplacian of a Helium Chemical Shift

Elena Yu. Tupikina^a, Peter M. Tolstoy^b and Gleb S. Denisov^a

^a Department of Physics, Saint Petersburg State University, St. Petersburg 198504, Russian Federation

^b Center for Magnetic Resonance, Saint Petersburg State University, St. Petersburg 198504, Russian Federation
elenatupikina@gmail.com

The outer electronic shell visualization is an important problem for physical chemistry, since its features determine the ability of a molecule to be involved in non-covalent interaction. There was a number of attempts to find a parameter that could be sensitive to such features of outer electronic shell as the direction of lone pairs localization. For example, such parameters as molecular electrostatic potential (MESP) [1], and electron localization function (ELF) [2] were proposed for these purposes.

Our idea is to use ³He atom as a probe particle. Previously we have shown that the laplacian of helium chemical shift, $\nabla^2\delta_{\text{He}}$, is sensitive to lone pair localization regions [3]. Its sensitivity to lone pairs is preserved at distances as large as 2.0–2.5 Å from the center of nucleus (in comparison with the distance to MESP minima, located at 1.0–1.5 Å or maxima of ELF, which are as close as 1.0 Å to the nucleus).

In this work we extend the set of investigated objects to fluorine containing CH-acids with different hybridization of carbon atom – FCCH, C₂HF₃, F₃CH. We scan outer electronic shell of investigated molecules by ³He atom, then calculate NMR chemical shift for each scan point δ_{He} and finally calculate laplacian of helium chemical shift $\nabla^2\delta_{\text{He}}$. 3D surfaces of $\nabla^2\delta_{\text{He}}$ can clearly demonstrate the direction of fluorine atoms lone pairs localization.

References

1. T. Clark, M. Hennemann and J. S. Murray, *J. Mol. Model.*, 13 (2007) 291.
2. A. D. Becke and K. E. Edgecombe, *J. Chem. Phys.*, 92 (1990) 5397.
3. E. Yu. Tupikina, A. A. Efimova, G. S. Denisov and P. M. Tolstoy, *J. Phys. Chem. A*, 121 (2017) 9654.

Acknowledgements: This work is supported by Russian Foundation for Basic Research (RFBR) grant № 17-03-00497.

The MSR Route to Accurate Equilibrium Molecular Structures through the Semi-Experimental Approach

Marco Mendolicchio, Nicola Tasinato, Daniele Licari and Vincenzo Barone
Scuola Normale Superiore, Piazza dei Cavalieri 7, I-56126 Pisa, Italy
marco.mendolicchio@sns.it

The knowledge of the equilibrium structure of isolated molecular systems of chemical and biological interest is fundamental to get a deep understanding of several chemical-physical processes, in the framework of the so-called structure-property relationship. Moreover, accurate equilibrium geometries represent invaluable benchmarks for testing different computational methods rooted into quantum or classical mechanics. While the amount of experimental data is ever increasing, but these are often influenced by vibrational and/or environmental effects. In fact, the molecular structures obtained through isotopic substitution are vibrationally averaged properties, but vibrational effects are usually not explicitly considered during the inversion of the spectroscopic data, making the resulting structures dependent on the isotopic species investigated. In order to overcome these issues, the determination of the equilibrium structure, defined as the geometry related to the minimum of the Born-Oppenheimer (B-O) potential energy surface (PES), appears as the most appealing alternative. This kind of structure is more challenging to be inferred at the experimental level, but its determination allows the inclusion of vibrational effects and, within the B-O approximation, it is independent of isotopic substitutions. Furthermore, the corresponding structural parameters can be directly compared with theoretical results. In this contribution, we present the recently developed MSR (Molecular Structure Refinement) software [1,2] specifically designed for the calculation of equilibrium structures by means of the so-called semi-experimental approach [3,4]. In addition to being equipped with a flexible choice of the optimization algorithm and a detailed error analysis, the MSR program has been provided of an efficient protocol for defining automatically the minimum set of non-redundant internal coordinates employable in the fit. This strategy is based on the extraction of all A_1 coordinates from a set of symmetry internal coordinates, in a completely black-box implementation. The MSR program has been also equipped with the possibility of including predicate observations [5] in the fit, i.e. augmenting the set of input data (e.g. rotational constants) through suitable estimates of the structural parameters. Finally, the user-friendliness of MSR is enhanced by an intuitive graphical user interface from which all it can be fully controlled and where results are displayed at the end of the structural refinement. In this contribution, the underlying theory and the implementation are presented in some detail, and the main features of the code are illustrated through the determination of the equilibrium structure of molecules of biochemical and astrochemical interest.

References

1. M. Mendolicchio, E. Penocchio, D. Licari, N. Tasinato and V. Barone, *J. Chem. Theory Comput.*, 13 (2017) 3060.
2. E. Penocchio, M. Mendolicchio, N. Tasinato and V. Barone, *Can. J. Chem.*, 94 (2016) 12.
3. P. Pulay, W. Meyer and J. Boggs, *J. Chem. Phys.*, 68 (1978) 5077.
4. J. Demaison, *Mol. Phys.*, 105 (2007) 3109.
5. L. Bartell, D. Romanesko, T. Wong, G. Sims and L. Sutton, *Chemical Society Specialist Periodical Report No. 20: Molecular Structure by Diffraction Methods*, 3 (1975) 72.

Pre-Plaque Conformational Changes in Alzheimer's Disease-Linked A β and APP

O. Klementieva,^a K. Willén,^a I. Martinsson,^a B. Israelsson,^a A. Engdahl,^b J. Cladera,^c P. Uvdal^{b,d} and G. K. Gouras^a

^a Experimental Dementia Research Unit, Department of Experimental Medical Science, Lund University, 22184 Lund, Sweden

^b Max IV laboratory, Lund University, P O Box 118, 22100 Lund Sweden

^c Department of Biochemistry and Molecular Biology, Universitat Autònoma de Barcelona, 08193 Bellaterra, Spain

^d Chemical Physics, Chemical CenterLund University, 22100 Lund, Sweden

Reducing levels of the aggregation-prone A β peptide that accumulates in the brain with Alzheimer's disease (AD) has been a major target of experimental therapies. An alternative approach may be to stabilize the physiological conformation of A β . To date, the physiological state of A β in brain remains unclear, since the available methods used to process brain tissue for determination of A β aggregate conformation can in themselves alter the structure and/or composition of the aggregates. Here, using synchrotron-based Fourier transform infrared micro-spectroscopy, non-denaturing gel electrophoresis and conformational specific antibodies we show that the physiological conformations of A β and amyloid precursor protein (APP) in brain of transgenic mouse models of AD are altered before formation of amyloid plaques. Furthermore, focal A β aggregates in brain that precede amyloid plaque formation localize to synaptic terminals. These changes in the states of A β and APP that occur prior to plaque formation may provide novel targets for AD therapy. A β is a class of aggregation-prone proteins, which may misfold into stable, β -sheet rich fibrils. A β is linked to the development of synaptic pathology in Alzheimer's disease (AD). However, a main question in the AD field is how A β contributes to AD neuropathology? Up to now there is little evidence for protein structural changes in diseased neuron. Our aim is to study the distribution of β -sheet structures in AD transgenic neurons in order to uncover sub-cellular mechanism(s) by which amyloid β -sheet structures are involved in AD pathology.

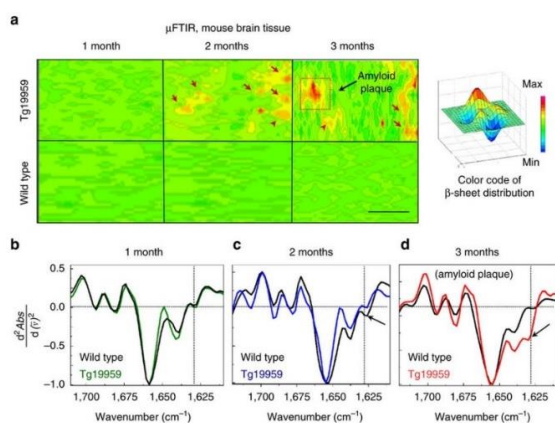


Figure 1 – (a) FTIR maps were integrated for the β -sheet spectral region at 1,635–1,620 cm⁻¹ to visualize absorption intensities for the β -sheet content in brain sections of Tg19959 (upper panels) and wild type (lower panels) mice at 1, 2 and 3 months, respectively. β -sheet content is shown in red (arrows). Scale bar, 50 μ m. (b) Averaged and normalized 2nd derivatives of the Amide I absorption band; β -sheet structures in 1-month Tg19959 mice are similar to those in wild-type mice. (c) Averaged and normalized 2nd derivatives of FTIR spectra taken from areas with increased β -sheet content in the corresponding μ FTIR maps in a. d) Same as in c, but for 3 month-old Tg19959.

References

1. O. Klementieva, K. Willén, I. Martinsson, B. Israelsson, A. Engdahl, J. Cladera, P. Uvdal, and G. K. Gouras, *Nat. Commun.*, 8 (2017) 14725.

Raman, FT-IR, AFM and Complementary Techniques in Studies of the Biochemical, Mechanical and Functional Alterations in Red Blood Cells

Katarzyna M. Marzec^{a,b}, Jakub Dybas^{a,c}, Aneta Błat^{a,c}, Mateusz Mardyla^{a,d}, Katarzyna Bulat^a,
Malgorzata Baranska^{a,b} and Stefan Chłopicki^{a,e}

^a Jagiellonian Centre for Experimental Therapeutics (JCET), Jagiellonian University, 30-348, Kraków, Poland

^b Center for Medical Genomics (OMICRON), Jagiellonian University, Kopernika 7C, 31-034 Krakow, Poland

^c Faculty of Chemistry, Jagiellonian University, Krakow, Poland

^d Faculty of Motor Rehabilitation, Univ. School of Physical Education, Jana Pawła 78, 31-571 Krakow, Poland

^e Chair of Pharmacology, Jagiellonian University Medical College, Krakow, Poland

katarzyna.marzec@jcet.eu

Confocal Raman spectroscopy (CRS) uses the advantages of immersion confocal microscopy as well as provides information about the biochemical changes of the sample on the molecular level. Fourier transform infrared (FT-IR) spectroscopy has additional advantage of not only detection but also easy quantification of many biochemical changes. It was already shown that both, IR and RS have huge diagnostic potential [1,2] also in red blood cells (RBCs) studies [3-5]. If specific molecular change of RBCs has specific marker bands the diagnosis could take even up to several seconds what gives additional possibility of the *in vitro/ex vivo* changes monitoring. Moreover, those techniques allow for an analysis of the molecular changes in a single RBC in small quantity of blood without previous staining or fixation. Atomic force microscopy (AFM) can additionally provide a mechanical fingerprint of single-cell pathological changes [6] also for RBCs [7] what makes this a promising technique in cell alteration diagnosis. Here we presented the application of RS, FT-IR and AFM supported by complementary techniques for detection of biochemical and functional changes (RS, IR) as well as mechanical properties (AFM) of human as well as murine RBCs (obtained from both, healthy control as well as pathologically changed). RBCs were analyzed from the point of hemoglobin structure, alterations of the lipids and proteins inside RBC membrane and mechanical properties such as stiffness, topography and adhesion. We have presented that a set of specific RS/FT-IR/AFM information may allow for detection of some RBCs alterations in the first place, even on the single cell level. Presented results will be focused on the *in vitro* studies of human RBCs as well as application of vibrational spectroscopy for detection, differentiation and visualisation of different hemoglobin forms, as well as pathologically or chemically induced RBCs alterations [3-7].

References

1. K. Kochan, K. Chrabaszcz, B. Szczur, E. Maslak, J. Dybas and K. M. Marzec, *Analyst* 141 (2016) 5329.
2. K. M. Marzec, T. P. Wrobel, A. Rygula, E. Maslak, A. Jasztal, A. Fedorowicz, S. Chłopicki and M. Baranska, *J. Biophotonics*, 7 (2014) 744.
3. K. M. Marzec, D. Perez-Guaita, M. de Veij, D. McNaughton, M. Baranska, M. W. A. Dixon, L. Tilley and B. R. Wood, *Chem. Phys. Chem.*, 15 (2014) 3963.
4. D. Perez-Guaita, K. Kochan, M. Batty, C. Doerig, J. Garcia-Bustos, S. Espinoza, D. McNaughton, P. Heraud and B. R. Wood, *Anal. Chem.*, 90 (2018) 3140.
5. K. M. Marzec, J. Dybas, S. Chłopicki and M. Baranska, *J. Phys. Chem. B*, 120 (2016) 12249.
6. J. Tang, C. Jiang, X. Xiao, Z. Fang, L. Li, L. Han, A. Mei, Y. Feng, Y. Guo, H. Li and W. Jiang, *Clin. Chim. Acta*, 444 (2015) 264.
7. K. M. Marzec, A. Rygula, B. R. Wood, S. Chłopicki and M. Baranska, *J. Raman Spectrosc.* 46 (2015) 76.

Acknowledgements: Financial support of the Polish National Science Centre (UMO-2016/23/B/ST4/00795) is greatly acknowledged.

ATR-FTIR Spectroscopy: Towards *In vivo* Detection of Cancerous Tissue Areas

Martynas Velicka^a, Milda Pucetaite^a, Vidita Urboniene^a, Rimante Bandzeviciute^a, Justinas Ceponkus^a, Feliksas Jankevicius^{b,c}, Valdas Sablinskas^a and Gerald Steiner^d

^a Vilnius University, Institute of Chemical Physics, Sauletekio av. 3, Vilnius, LT-10257, Lithuania

^b Vilnius University, Faculty of Medicine, Santariskiu str. 2, Vilnius, LT-08661, Lithuania

^c National Cancer Institute, Santariškių str. 1, Vilnius, LT-08660, Lithuania

^d Dresden University of Technology, Faculty of Medicine Carl Gustav Carus, Fetscherstr. 13, Dresden, 01307, Germany
martynas.velicka@ff.vu.lt

Successful resection of cancerous tissue is highly dependent on the correct identification of the definite border between cancerous and healthy tissues. For a surgeon this, however, is not always an easy task to do by the naked eye. In such cases additional histopathological diagnosis of the inspected tissues is needed. Alas, the method is time-consuming and provide results which are in fact not always conclusive or reliable.

Pilot spectroscopic studies of kidney tissue touch imprint smears were conducted previously [1]. It was shown that chemometric analysis of the collected ATR-FTIR spectra is effective for distinguishing cancerous and normal tissues. The most prominent spectral markers of cancerous tissue are located in the wavenumber region between 950 cm⁻¹ and 1200 cm⁻¹. These marker bands were assigned to the vibrations of glycogen molecules which are accumulated by the cancerous cells to sustain their accelerated metabolic rate. In the end, the application of the method used in the pilot studies is somewhat limited due to the need to relocate the tissue under inspection from the operating table to the vicinity of the FTIR spectrometer. Furthermore, the procedure to form a tissue smear on the ATR crystal of a FTIR spectrometer requires time and equipment.

Here we present the results of *in situ* analysis of the suspected kidney and brain tissues using a new design of a portable spectroscopic tool [2]. The portable spectrometer is coupled with an ATR fiberprobe which allows the rapid and easy sampling due to the changeable ATR tips. The higher signal-to-noise ratio is attained with liquid nitrogen cooled MCT detector used in the setup instead of the conventional DTGS of portable FTIR spectrometer. MCT enables to compensate the signal-to-noise loss due to the losses in the optical fiber. Thus a high accuracy spectral analysis can be performed employing the unique software dedicated for distinguishing the cancerous and normal tissues areas. Results of this study are promising and the improved setup brings us one step closer towards the *in vivo* detection of cancerous tissues during the surgery.

References

1. V. Urboniene, M. Pucetaite, F. Jankevicius, A. Zelvyis, V. Sablinskas and G. Steiner, *J. Biomed. Opt.*, 19 (2014) 1.
2. V. Sablinskas, M. Velicka, M. Pucetaite, V. Urboniene, J. Ceponkus, R. Bandzeviciute, F. Jankevicius, T. Sakharova, O. Bibikova and G. Steiner, *Proc. of SPIE Imaging, Manipulation, and Analysis of Biomolecules, Cells, and Tissues XVI*, 10497 (2018) 1.

Acknowledgements: This research was funded by a grant (MIP-020/2015) from the Research Council of Lithuania.

Vibrational Studies of Salivary Glands Tissues

Czesława Paluszkiewicz^a, Wojciech M. Kwiatek^a, Mariangela Cestelli Guidi^b,
Natalia Piergies^a, Ewa Pięta^a, Monika Woźniak^a, Maciej Misiólek^c and Wojciech Ścierski^c

^a Institute of Nuclear Physics, Polish Academy of Science, 31-342 Krakow, Poland

^b Laboratori Nazionali di Frascati/INFN, Via E. Fermi 40, 00-044 Frascati, Italy

^c Medical University of Silesia, Department of Otorhinolaryngology, 41-800 Zabrze, Poland
czeslaw.paluszkiewicz@ifj.edu.pl

The most common recognized neoplasms of the parotid gland are pleomorphic adenoma (mixed tumor) and adenolymphoma (Warthin tumor). The metastasis is not often observed in the salivary gland neoplasms. However, tumors developing in the head and neck even if they are not malignant form can lead to transformations in pathogenic promote the development of malignant tumors [1]. In this study, we present the vibrational spectroscopy investigations of salivary glands tissues from patients with diagnosed cancer disease within the parotid gland. Spectroscopic methods such as infrared absorption spectroscopy with Fourier transformation (FTIR), including microspectroscopy, and Raman spectroscopy (RS) have a number of medical applications [2-3]. Figure 1 shows FTIR spectra of pleomorphic adenoma tissue collected from two different areas. The observed spectral patterns indicate significant changes in the spectral regions of $1000 - 1100 \text{ cm}^{-1}$ and $1700 - 1730 \text{ cm}^{-1}$ which are associated with the investigated area. The observed differentiation within the same tissue sample corresponds to the histopathological assessment. The obtained data were compared with the spectra recorded for saliva samples from those patients. Such analysis may deliver spectroscopic markers, which will be essential in preliminary diagnosis.

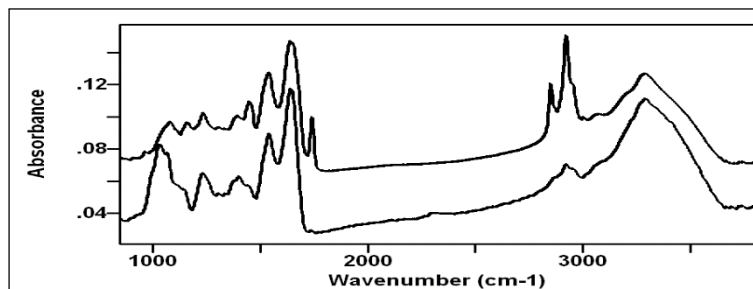


Figure 1 – FTIR spectra of salivary glands tissue from two different areas of the sample.

References

1. C. Kian Chai, I. Ping Tang and N. Prepageran, *Int. J. Otolaryn. Head Neck Surg.*, 2 (2013) 156.
2. H. Abramczyk H and B. Brożek-Pluska, *Anal. Chim. Acta*, 909 (2016) 91.
3. C. Paluszkiewicz, N. Piergies, A. Sozańska, P. Chaniecki, M. Rękas, J. Miszczyk, M. Gajda and W. Kwiatek *Spectrochim. Acta A Mol. and Biomol. Spectrosc.*, 188 (2018) 332.

Acknowledgements: The research leading to this result has been supported by the project CALIPSO plus under the Grant Agreement 730872 from the EU Framework Programme for Research and Innovation HORIZON 2020. The research was partially carried out using equipment purchased in the frame of the project co-funded by the Małopolska Regional Operational Program Measure 5.1. Krakow Metropolitan Area as an important hub of the European Research Area for 2007-2013, project No. MRPO.05.01.00-12-013/15.

Raman Spectroscopy of Urine Extracellular Vesicles in Diabetic Patients

Maciej Roman^a, Agnieszka Kaminska^b, Czesława Paluszkievicz^a and Ewa Stepien^b

^a Institute of Nuclear Physics Polish Academy of Sciences, PL-31342 Krakow, Poland

^b Department of Medical Physics, Marian Smoluchowski Institute of Physics, PL-30348 Krakow, Poland
Maciej.Roman@ifj.edu.pl

Extracellular vesicles (EVs) are nano-sized membranous vesicles present in urine and other body fluids. They play a crucial role in many biological processes including: angiogenesis, thrombosis or intercellular communication. Due to the presence in almost all body fluids, EVs are considered as potential biomarkers of diseases. Rich source of EVs in human body is urine, where EVs are released by glomerular epithelial cells. Urine is of great interest for diagnostic application due to easy and non-invasive way of collection. Urinary EVs (UEVs) contain different biomolecules such as proteins, nucleic acids (DNA, mRNAs, microRNAs, small RNAs) and lipids. Furthermore, it is well known that both number and content of UEVs can reflect the state of damage of the kidney.

Many optical and non-optical techniques have been used so far to characterize EVs, including high-resolution imaging with electron microscopy, nanoparticle tracking analysis (NTA), dynamic light scattering (DLS), tunable resistive pulse sensing (TRPS), flow cytometry, atomic force microscopy and many others. However, all above-mentioned methods have some limitations, so modern and efficient techniques are required to investigate physical and chemical properties of EVs. Raman spectroscopy is a non-destructive, label-free method, based on inelastic scattering, which can provide information about chemical composition of EVs. Thus, Raman spectroscopy seems to be a promising tool for clinical applications.

In our study we would like to demonstrate the potential diagnostic usefulness of Raman spectroscopy technique for chemical characterization of UEVs isolated from diabetic patients and healthy subjects as well as endothelial derived EVs isolated from *in vitro* cell culture model. Since Raman spectra of EVs are complex, detailed analysis of all chemical differences between the studied samples required application of advanced chemometric methods such as Cluster Analysis (CA) and Partial Least Squares regression (PLS regression). Our results show unequivocally that Raman spectroscopy can be applied to distinguish diabetic and healthy subjects as well as endothelial EVs isolated from hyperglycemic cell culture medium.

References

1. A. Combes, A. C. Simon, G. E. Grau, D. Arnoux, L. Camoin, F. F. Sabatier, M. Mutin, M. Sanmarco, J. Sampol and F. Dignat-George, *J. Clin. Invest.*, 104 (1999) 93.
2. M. Salih, R. Zietse and E. J. Hoorn, *Am. J. Physiol. Renal Physiol.*, 306 (2014) 1251.
3. K. Barreiro and H. Holthofer, *Cell Tissue Res.*, 369 (2017) 217.
4. V. Sunkara, H. K. Woo and Y. K. Cho, *Analyst*, 141 (2016) 371.
5. I. Tatischeff, E. Larquet, J. M. Falcon-Perez, P. Y. Turpin and S. G. Kruglik, *J. Extracell. Vesicles*, 1 (2012) 19179.

Acknowledgements: The research was partially performed at the Institute of Nuclear Physics Polish Academy of Sciences using equipment purchased in the frame of the project co-funded by the Małopolska Regional Operational Programme Measure 5.1 Krakow Metropolitan Area as an important hub of the European Research Area for 2007- 2013, project No. MRPO.05.01.00-12-013/15. The study was also supported by the Polish National Centre (NCN) the grant OPUS 4 for Ewa Stepien (2012/07B/NZ5/02510).

Raman Imaging Study of Lipid Droplets in Liver Sinusoidal Endothelial Cells upon Non-Alcoholic Fatty Liver Disease Progression

Ewelina Szafraniec^a, Edyta Kus^b, Stefan Chlopicki^c and Malgorzata Baranska^{a,b}

^a Jagiellonian University, Faculty of Chemistry, Gronostajowa 2, 30-397 Krakow, Poland

^b Jagiellonian Centre for Experimental Therapeutics (JCET), Bobrzynskiego 14, 30-348 Krakow, Poland

^c Jagiellonian University Medical College, Chair of Pharmacology, Grzegorzeczka 16, 31-531 Krakow, Poland
baranska@chemia.uj.edu.pl

Liver sinusoidal endothelial cells (LSECs) are highly specialized endothelial cells representing the permeable barrier between blood and hepatocytes in liver sinusoids. LSECs are involved in the transport of nutrients, lipids and lipoproteins, they also have the highest endocytosis capacity of human cells [1]. Development of Non-Alcoholic Fatty Liver Disease (NAFLD) involves pathogenic mechanisms of LSECs, hepatocytes and other liver cells. While, the pathogenesis of NAFLD is not fully understood yet, the accumulating evidence highlights the pivotal role of LSECs in development of NAFLD and its progression to NASH and fibrosis [1,2]. Since the culturing of LSECs is not possible, as they lose their characteristic phenotype, the cell isolation procedure was applied in this study. Additionally, the use of an animal model of NAFLD induced by High Fat Diet (HFD) provides a possibility to study the progression of the disease. Application of Raman imaging technique enables to link the chemical and spatial information and therefore study chemical changes in chosen subcellular structures. Here we use Raman imaging to investigate cell-specific changes in the biochemical phenotype of primary LSECs at early (at 2nd week) and late (15th and 20th weeks) stage of NAFLD. Combining Raman imaging with chemometrical analysis enables to determine the spectroscopical profile of LSEC. Although not significant, we detected changes that occurred in nuclear DNA, level of proteins in cytoplasm and increase of degree of unsaturation of lipids accumulated in lipid droplets. The later finding is puzzling, as the function of lipid droplets in endothelial cells is still investigated [3].

References

1. J. Poisson, S. Lemoine, C. Boulanger, F. Durand, R. Moreau, D. Valla and P. E. Rautou, *J. Hepatol.*, 66 (2017) 212.
2. M. Miyao, H. Kotani, T. Ishida, C. Kawai, S. Manabe, H. Abiru and K. Tamaki, *Lab Invest.* 95 (2015) 1130.
3. A. Kuo, M. Y. Lee and W. C. Sessa, *Circ Res.* 120 (2017) 1289.

Acknowledgements: The authors thank the National Science Centre (NCN) for financial support in the framework of grant and UMO-2016/22/M/ST4/00150 and UMO-2015/16/W/NZ4/00070.

From Lasers to High Power LEDs, from Photochemistry to Photocatalysis

Eberhard Riedle

BMO, LMU München, Oettingenstrasse 67, 80538 Munich, Germany

Riedle@Physik.uni-muenchen.de

Over the last decades, ultrafast technology and spectroscopy have advanced greatly. Fully tuneable pulses with a duration below 30 fs are now available. For probing of the temporal evolution of a molecular sample excited by such a pump pulse white light fs pulses are the method of choice. In this way a time resolved spectroscopy with probing from 250 nm to well into the NIR has become available [1,2]. By utilizing a referencing scheme, a sensitivity in the range of 10 μ OD – very close to the shot noise limit - can be reached [3].

For complex chemical processes involving multiple steps and diffusive encounters, the scan range of the fs experiment is not sufficient. While it has been thought that the excitation pulses are the crucial issue, it has now become clear that it is the continuum probing. Therefore, a ns OPO system is substituted for the fs pump and electronically synchronized to the continuum. In this way the full range from early femtoseconds to milliseconds can be covered [2].

Such a comprehensive excitation and detection scheme has for the first time allowed to quantitatively analyse all 4 steps of a molecular motor [4]. Not only the decay rates typically reported in time resolved spectroscopy were determined, but also the efficiencies of all steps. This is possible by spectral deconvolution and comparison with the ground state bleach.

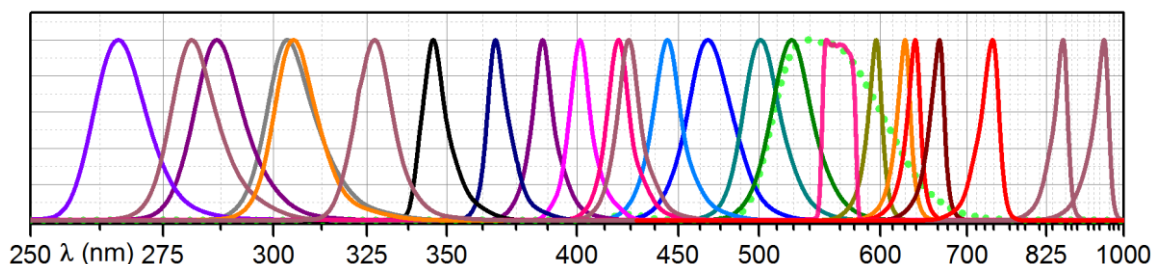


Figure 1 – Range of available high power LEDs for quantitative measurements.

For direct comparison we can measure the reaction quantum yields with 5 % accuracy by photometric measurement of the absorbed light from a high power LED that is imaged into the sample in a precise fashion. UV/vis spectroscopy and GC or NMR are used to quantify the action due to the illumination. LEDs ranging continuously from 265 to 1000 nm are available. The power at the samples scales from tens of mW in the deep UV to hundreds of mW in the visible. For blue, green and red illumination this even goes up into the 10 W range. Such high powers are most helpful for the quantitative investigation of photocatalytic processes.

References

1. U. Megerle, I. Pugliesi, C. Schrieffer, C. F. Sailer and E. Riedle, *Appl. Phys. B*, 96 (2009) 215.
2. E. Riedle, M. Bradler, M. Wenninger, C. F. Sailer and I. Pugliesi, *Faraday Disc.*, 163 (2013) 139.
3. M. Bradler and E. Riedle, *J. Opt. Soc. Am. B*, 31 (2014) 1465.
4. R. Wilcken, M. Schildhauer, F. Rott, L. Huber, M. Guentner, S. Thumser, K. Hoffmann, S. Oesterling, R. de Vivie-Riedle, E. Riedle and H. Dube, *J. Am. Chem. Soc.*, 140 (2018) 5311.

Acknowledgements: The author thanks the many students that contributed to the technical and scientific developments. Financial support through SFB749 und GRK1646 is gratefully acknowledged.

Surface-Enhanced Raman Scattering: A Potential Technique to Study Living Single Cells

Mustafa Çulha^a, Gamze Kuku^a, Mine Altunbek^a, Deniz Yasar Oztas^a and Melike Saricam^a

^a Department of Genetics and Bioengineering, Yeditepe University, Istanbul 34755, Turkey

mculha2@gmail.com or mculha@yeditepe.edu.tr

The study of single eukaryotic cells is an ongoing research effort with a potential impact on biology, biotechnology and medicine. In almost all molecular biology experiments, a population of cells other than single cell is studied. The heterogeneity in a cell population causes an average result and the biomolecular information originating from single cell molecularly different from others is lost. With the recent advances in cell sorting technology, it is now single cell analysis is more pronounced. The study of single cells can revolutionize the understanding of the fundamentals of many diseases, developmental biology, cell signaling, stem cell, and drug discovery studies. Therefore, a number of cell sorting and analysis techniques including Mass Spectroscopy and Electrophoresis are proposed for the goal [1, 2]. Due to its complex and dynamic structure, the study of living cells at single cell level is not an easy task and a technique should possess certain criteria to meet the requirements such as high spatial and temporal resolutions and being able to analyze a cell while it is alive. Surface-enhanced Raman scattering (SERS) is a highly sensitive vibrational spectroscopic technique and it can serve as an excellent tool to study living single cells by satisfying more of these criteria than any other currently available technique. As a part of our effort to utilize the technique in biology, biotechnology and medicine, we continue to investigate the potential of the technique to use in single cell analysis. We previously showed that SERS could be used to study real-time dynamics of molecular processes taking place in living cells, especially upon external stimulation, in a contactless, noninvasive, and nondestructive way [3]. In this presentation, the experimental conditions to obtain meaningful SERS spectra with a high reproducibility from living single cells and the origin of the obtained spectra by putting an emphasis on the cellular uptake of SERS active substrates, AuNPs, are outlined [4]. The observed spectral changes on the cellular spectra upon exposing the cells to external stimuli are discussed. The results indicate that the spectral changes can be related to cellular processes taking place in a living cell depending on the environmental stress conditions, which can be used to understand the cellular molecular dynamics under several conditions.

References

1. E. J. Lanni, S. S. Rubakhin and J. V. Sweedler, *J. Proteomics*, 75 (2012) 75 5036.
2. Jennifer L. Zabzdyr and Sheri J. Lillard, *Anal. Chem.*, 73 (2001) 5771.
3. G. Kuku, M. Altunbek, and M. Çulha *Anal. Chem.* 89 (2017) 11160.
4. G. Kuku, M. Saricam, F. Akhatova, A. Danilushkina, R. F. Fakhrullin, and M. Çulha, *Anal. Chem.* 88 (2016) 9813.

Acknowledgements: The authors acknowledge the financial support from The Scientific and Technological Research Council of Turkey (TUBITAK, Project no: 113Z554) and Yeditepe University.

Microheterogeneity in Binary Mixtures: Spectroscopic and Chemometric Studies

Mirosław A. Czarnecki, Paweł Tomza, Władysław Wrzeszcz, Sylwester Mazurek
and Roman Szostak

*Faculty of Chemistry, University of Wrocław, F. Joliot-Curie 14, 50-383 Wrocław, Poland
mirosław.czarnecki@chem.uni.wroc.pl*

The presence of heterogeneity at a molecular level (microheterogeneity) in binary mixtures leads to deviations from the behaviour of the ideal mixture. The molecular origin of this phenomenon is not fully elucidated as yet. The appearance of microheterogeneity was clearly observed in binary mixtures of water with aliphatic alcohols. Therefore, a lot of experimental and theoretical works were devoted to studies of these mixtures. In contrast, examinations of microheterogeneity in non-aqueous mixtures are less extensive. Here, we present results of spectroscopic (ATR-IR and NIR) and chemometric (PCA, MCR-ALS, 2DCOS) studies of binary mixtures of (a) aliphatic alcohols with aliphatic alcohols [1,2], (b) aliphatic alcohols with alkanes [3], (c) alkanes with alkanes [4] and (d) alkanes with aromatic hydrocarbons [4]. Our results reveal that the molecular structure of all studied mixtures is similar. The mixtures are composed of the homoclusters of both components and the mixed clusters (heteroclusters). It is of note that the homoclusters present in the mixtures are similar to those appearing in bulk components. The relative population of different species depends on overall mixture composition. The highest population of the heteroclusters occurs at mixture composition near to equimolar. At this composition is observed the largest deviation from the ideal mixture. However, the degree of deviation of the mixture from the ideal mixture is strongly correlated with the molecular structure of both components of the mixture.

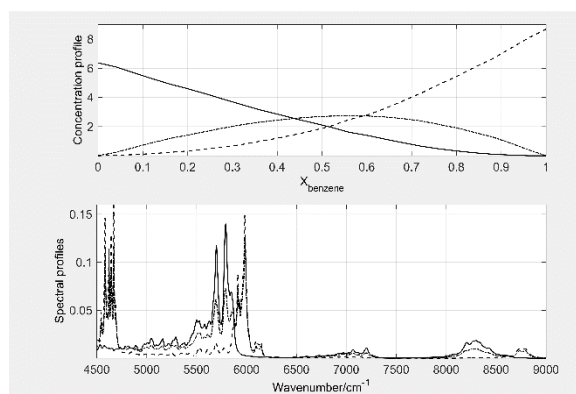


Figure 1 – Concentration (top) and spectral (bottom) profiles of cyclohexane/benzene mixture obtained from MCR-ALS. Solid, dashed and dash-dot lines represent the homoclusters of cyclohexane, benzene and the heteroclusters, respectively.

References

1. W. Wrzeszcz, P. Tomza, M. Kwaśniewicz, S. Mazurek, R. Szostak and M. A. Czarnecki, *RSC Adv.*, 6 (2016) 37195.
2. W. Wrzeszcz, S. Mazurek, R. Szostak, P. Tomza and M. A. Czarnecki, *Spectrochim. Acta A-Mol. Biomol. Spectrosc.*, 188 (2018) 349.
3. W. Wrzeszcz, P. Tomza, M. Kwaśniewicz, S. Mazurek, M. A. Czarnecki, *RSC Adv.*, 6 (2016) 94294.
4. In preparation.

Acknowledgements: The authors thank NCN (Poland) for Grant no. 2013/11/B/ST4/00501.

Perichromism: A Successful Approach for Probing Molecular Interactions in Different Media

Omar A. El Seoud

*Institute of Chemistry, the University of São Paulo, Rua Prof. Lineu Prestes 748,
05508-000 São Paulo, SP, Brazil
elseoud.usp@gmail.com*

Probing the interactions in different media (liquids, solids, gases) that affect, *e.g.*, rates and equilibria of chemical reactions is essential for applying green chemistry principles. For reactions in liquid phase, the solvent participates *inter alia* in heat-, mass and proton transfers; this participation affects the yields of competing reactions. Adsorption on solid surfaces of, *e.g.*, thin films and nanoparticles is governed by substrate-surface interactions. Consequently, we need to understand, hence quantify and exploit substance-medium interactions. The latter are complex; hence cannot be rationalized in terms of a single mechanism, or quantified by a single medium descriptor, *e.g.*, solvent dielectric constant. A successful approach to probe these interactions is to use perichromic probes. These are substances whose spectra, absorption or emission, are particularly sensitive to some property of the medium, including Lewis acidity and basicity, dipolarity and polarizability. The medium effect is then quantified, usually by a linear combination of these descriptors. The use of this approach will be presented by showing results relevant to solvation [1], adsorption on solid surfaces [2], dissolution of asphaltenes [3] and analysis of biofuels and their blends with petroleum-based fuel [4].

References

1. O. A. El Seoud, *Pure Appl. Chem*, 81 (2009) 697.
2. L. C. Fidale, T. Heinze and O. A. El Seoud, *Carbohydr. Polym.*, 93 (2013) 129.
3. L. P. Novaki, R. Lira, M. M. N. Kwon, M. C. K. de Oliveira, F. A. Meireles, G. Gonzalez and O. A. El Seoud, *Energy & Fuels* 32 (2018) 3281.
4. P. D. Galgano, C. Loffredo, B. M. Sato, C. Reichardt and O. A. El Seoud, *Educ. Res. Pract.*, (2012) 147.

Acknowledgements: I thank the financial support of CNPq (307022/2014-5) and FAPESP (2014/22136-4).

Raman Imaging in SERS Studies of Silver Loaded Textiles

Helena Nogueira, Sara Fateixa and Tito Trindade

University of Aveiro, CICECO and Chemistry Department, 3810-193 Aveiro, Portugal
helenanogueira@ua.pt

Surface-enhanced Raman scattering (SERS) has been recently used with acute relevance in many areas. Although the SERS effect was discovered during the 70s, this spectroscopic method is benefiting from the unprecedented progress observed in the last few decades in instrumentation and materials development specific to nanoscale science. Indeed, the design of SERS active nanomaterials is a key aspect in further exploitation of SERS in diverse areas, including medicine, environmental monitoring and trace chemical analysis [1].

The current developments of techniques such as Raman imaging, through high resolution Raman mapping with short measurement times, have brought a new look on composites and its applications. Such an image can show either the chemical heterogeneity or a specific response as SERS activity [2] or a labeling process (Figure 1). In this communication, our latest results in the development of SERS active substrates will be presented together with its evaluation using Raman imaging. Illustrative examples of SERS applications will be provided along with perspectives of development in chemical detection applied to real contexts. For example, SERS and Raman imaging were used with advantage in the monitoring of textile fiber dyeing [2]. Our results demonstrate that by using Raman imaging associated to the presence of Ag nanoparticles it is possible to distinguish the local distribution of the organic dye (methylene blue) on the textile surface. Composites of linen fibres and Ag nanoparticles were prepared by distinct methods and used as SERS substrates. Raman imaging allowed to explore the Ag distribution on the textile surface and to its interior, together with the study of the dye adsorption molecular species. Textile fibres containing Ag nanoparticles have been widely explored for antimicrobial fabrics. This investigation allows to foresee the use of this technique in terms of quality control of Ag containing fabrics.

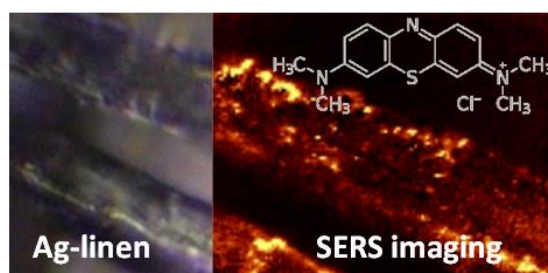


Figure 1 – Optical photograph (left) and Raman image (right) of a silver containing textile fibre dyed with methylene blue (chemical structure shown).

References

1. S. Fateixa, H. I. S. Nogueira and T. Trindade, *Phys. Chem. Chem. Phys.*, 17 (2015) 21046.
2. S. Fateixa, M. Wilhelm, H. I. S. Nogueira and T. Trindade, *J. Raman Spectrosc.*, 47 (2016) 1239.

Acknowledgements: This work was developed within the scope of the project CICECO-Aveiro Institute of Materials, POCI-01-0145-FEDER-007679 (FCT Ref. UID /CTM /50011/2013), financed by national funds through the FCT/MEC and when appropriate co-financed by FEDER under the PT2020 Partnership Agreement. S. Fateixa thanks FCT for the Grant SFRH/BPD/ 93547/2013.

Raman Vibrational Spectroscopic Study of NLO Molecular Crystals Based on Aminopyrimidinium Salts

Ivan Němec, Irena Matulková, Róbert Gyepes, Matouš Kloda and Ivana Císařová
Charles University, Faculty of Science, Department of Inorganic Chemistry, Hlavova 8, Prague 2,
CZ 128 40, Czech Republic
ivan.nemec@natur.cuni.cz

The class of hydrogen-bonded molecular crystals can be considered as a successful result of crystal engineering of novel materials for nonlinear optics (NLO). These materials are based on properly arranged organic molecules (carriers of NLO properties) interacting with selected inorganic or organic anions. The energy of formed hydrogen bonds counteracts the natural tendencies of the organic ions to form centrosymmetric pairs. In addition, the formed hydrogen-bonded structures frequently gain advantageous chemical and physical properties.

The resulting NLO properties have several technical applications ranging from harmonic generations to stimulated light scattering. A very recent application of hydrogen-bonded salts of organic molecules (e.g. guanylurea hydrogen phosphite¹) is based on stimulated Raman scattering (SRS). This $\chi^{(3)}$ NLO phenomenon is used for the development of compact and efficient frequency converters of the one-micron laser emission based on neodymium or ytterbium lasants.²

This contribution deals with characterization of molecular crystals based on inorganic and organic salts of aminopyrimidines by the combination of experimental (i.e. vibrational spectroscopy, XRD and calorimetry) and theoretical (solid state quantum-chemical calculations) methods. Especially temperature-dependent vibrational spectroscopic methods are very useful tool for monitoring and explanation of phase transformations, which might crucially influence the most of their physical properties (including the optical ones). The several examples of aminopyrimidinium salts of inorganic oxyacids and dicarboxylic acid will be discussed in detail.

References

1. A. A. Kaminskii, P. Becker, H. Ree, O. Lux, A. Kaltenbach, H. J. Eichler, A. Shirakawa, H. Yoneda, I. Němec, M. Fridrichová and L. Bohatý, *Physica Status Solidi B* 250(2013) 1837.
2. A. A. Kaminskii, *Laser and Photonics Reviews* 1 (2007) 93.

Acknowledgements: Financial support from the CUCAM project (project No. CZ.02.1.01/0.0/0.0/15_003/0000417) is gratefully acknowledged.

The Optimization of the Recycled Lead with Manganese Dioxide Contents for Applications in Automobile Batteries

Simona Rada^{a,b}, Marius Rada^b, Denisa Cuibus^a, Horatiu Vermesan^a and Eugen Culea^a

^a Department of Physics & Chemistry, Technical University of Cluj-Napoca, 400020, Romania

^b National Institute for Research & Development of Isotopic and Molecular Technologies,
Cluj-Napoca, 400293, Romania
radasimona@yahoo.com

Nowadays, hundreds of millions of lead-acid batteries are produced worldwide, which makes the lead-acid battery the most successful power source of all time. The raw material for their production is practically unlimited and about 95% of the battery material can be recycled. Lead is the most important raw material of lead acid batteries and it is the most reused material.

In the car battery, the positive electrode active material is made of lead dioxide (PbO₂), the negative electrode of spongy metallic lead (Pb) and as electrolyte a 38% H₂SO₄ solution is used. In this paper, we present the synthesis, characterization and electrochemical performances of materials obtained by the recycling of the anodic and cathodic electrodes of spent lead acid battery and the incorporation of MnO₂ contents. Samples were obtained by an eco-innovative technology concerning both economic aspects (reduction of production costs, improving of energy efficiency) as well as environmental ones (the environmental friendly character) [1].

The effect of MnO₂ concentration on Pb-PbO₂ host network [2] was investigated by X-ray diffraction (XRD) analysis, InfraRed (IR), UltraViolet-Visible (UV-Vis), Photoluminescence (PL) and Electron Paramagnetic Resonance (EPR) spectroscopy. Electrochemical performances of samples used as working electrode were demonstrated by measurements of Cyclic Voltammetry (VC).

References

1. S. Rada, M. L. Unguresan, L. Bolundut, M. Rada, H. Vermesan, M. Pica and E. Culea, *J. Electroanal. Chem.* 780 (2016) 187.
2. S. Rada, D. Cuibus, H. Vermesan, M. Rada and E. Culea, *Electrochim. Acta* 268 (2018) 332.

Acknowledgements: This research was supported by the PED Projects with the No. 82PED/2017.

THURSDAY, 23rd AUGUST

Photo-Addition of Psoralen to DNA Traced by Time Resolved Spectroscopy

Janina Diekmann^a, Christian Torres Ziegenbein^a, Julia Gontcharov^b,
Wolfgang Zinth^b and Peter Gilch^a

^a *Institut für Physikalische Chemie, HHU Düsseldorf, Universitätsstr. 1, 40225 Düsseldorf, Germany*

^b *Lehrstuhl für BioMolekulare Optik, LMU München, Oettingenstr. 67, 80538 München, Germany*
gilch@hhu.de

Psoralens are natural compounds with pharmaceutical applications [1]. In a UV-dependent therapy (PUVA) they are employed to treat skin diseases like psoriasis and vitiligo. The pharmaceutical action of psoralens can be related to their interaction with DNA [2]. Psoralens intercalate into DNA and upon photo-excitation they can bind to thymine bases (see Figure 1). These photo-adducts prevent DNA from replicating and may result in apoptosis of diseased cells. The photo-adduct bears a cyclobutane moiety. The same moiety appears in intrinsic photolesions of DNA. Pyrimidine bases, in particular thymine, can form cyclobutane pyrimidine dimers (CPD) upon UV-excitation [3]. The CPD formation proceeds in less than a picosecond. The primarily excited singlet state is the precursor of the CPD. Heretofore, no experimental results on the formation kinetics of the psoralen-DNA-adduct were available.

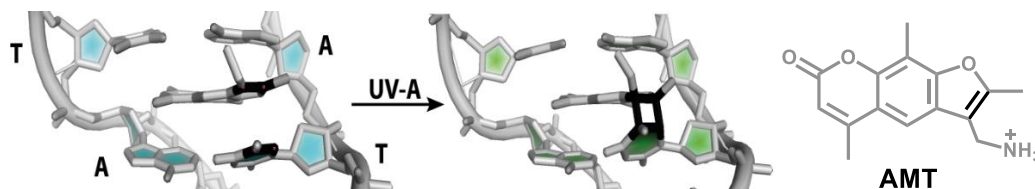


Figure 1 – Psoralen derivatives like AMT intercalate into DNA. Upon irradiation with UV-A-light they bind covalently to DNA forming a cyclobutane ring.

Experiments on the psoralen derivative AMT (see Figure 1) and duplex DNA containing all bases revealed a photo-induced electron transfer competing with the photo-addition [4]. The base guanine hereby acts as an electron donor. Thus, in the spectroscopic studies on the photo-addition A,T-only DNA was used to prevent this electron transfer (see Figure 1). Intercalated AMT was excited by laser pulses centered at 355 nm. The spectroscopic response was probed in the UV/Vis and mid-IR range. The singlet lifetime of intercalated AMT (1 ns) is hardly affected by intercalation into A,T-only DNA. Along with the singlet decay the population of the AMT triplet state rises. By means of UV/Vis and in particular IR detection the triplet state is shown to be the precursor of the photo-adduct. The addition proceeds with characteristic times of 1-6 and ~50 μ s. This behaviour is in stark contrast with CPD formation proceeding on the sub-picosecond time scale from a singlet precursor. The origin of this difference will be discussed in relation with results from quantum chemistry [5].

References

1. T. C. Ling, T. H. Clayton, J. Crawley, L. S. Exton, V. Goulden, S. Ibbotson, K. McKenna, M. F. Mohd Mustapa, L. E. Rhodes, R. Sarkany and R. S. Dawe, *Brit. J. Dermatol.* 174 (2016) 24.
2. N. Kitamura, S. Kohtani and R. Nakagaki, *J. Photochem. Photobiol. C-Photochem. Rev.* 6 (2005) 168.
3. W. J. Schreier, P. Gilch and W. Zinth, *Annu. Rev. Phys. Chem.* 66 (2015) 497.
4. S. Fröbel, L. Levi, S.M. Ulamec and P. Gilch, *ChemPhysChem* 17 (2016) 1377.
5. X. B. Huang and R. B. Zhang, *Photochem. Photobiol.* 89 (2013) 891.

Acknowledgements: The authors thank the Deutsche Forschungsgemeinschaft (grant GI 349/6-1) and the Jürgen Manchot Stiftung for financial support.

The Trials and Tribulations of Becoming a Spectroscopy Specialist

Marco van de Weert

Department of Pharmacy, Faculty of Health and Medical Sciences, University of Copenhagen;
Universitetsparken 2, 2100 Copenhagen, Denmark
Marco.vandeweert@sund.ku.dk

Scientists have a wide range of spectroscopic methods available to study molecular structure and behavior. Proper interpretation of the results requires the scientist to be aware of the pitfalls of the methodology. This expertise is generally obtained through years of experience working with the techniques. However, it is not always easy to make the step from user to expert, as expert assistance may not be directly available, textbooks may be too basic for the research question being studied, and methods sections in scientific papers may be too succinct. The trials and tribulations of becoming an expert spectroscopist become even larger when also the peer review process fails, and fundamental errors enter the scientific literature.

Such an occasion will be illustrated using the example of spectroscopic approaches to characterize ligand-binding to proteins. Although there are many excellent papers available, I and co-workers have documented how many hundreds of fundamentally incorrect papers have recently entered the scientific literature [1-3]. Flaws include, but are not limited to, ignoring the well-known inner-filter effect in fluorescence, reporting protein amide backbone fluorescence when there is none, performing FRET calculations when lifetime measurements show there is none, and incorrect execution and analysis of UV-VIS spectra. Many of these papers have appeared in specialty journals, which means that novices in the field may be fooled into believing these papers contain the state-of-the-art. The presentation will end with a number of suggestions to alleviate this situation and help train new scientists in proper use of spectroscopic methods.

References

1. M. van de Weert and L. Stella, *J. Mol. Struct.*, 998 (2011) 144.
2. L. Stella, M. van de Weert, H. D. Burrows and R. Fausto, *J. Mol. Struct.*, 1077 (2014) 1.
3. A. Bortolotti, Y. H. Wong, S. S. Korsholm, N. H. B. Bahring, S. Bobone, S. Tayyab, M. van de Weert and L. Stella, *RSC Adv.*, 6 (2016) 112870.

New Avenues for Matter-Wave Assisted Spectroscopy

Markus Arndt

University of Vienna, Faculty of Physics, Quantum Nanophysics, Boltzmannngasse 5, A-1090 Wien, Austria
markus.arndt@univie.ac.at

Recent advances in the realization of matter-wave interferometry with complex molecules [1,2] have opened new avenues to study their electronic and optical properties in molecular beams. The molecular matter-wave interferogram represents a free-flying nanostructure of the probability density to find a molecule. It represents a nanometric ruler in free space that is measurably shifted when the molecules interact with external perturbations. This setup is highly sensitive to external fields [3] and can even reveal the absorption of on average less than a single photon per molecule. I will discuss recent experiments [4] and new ideas [5,6] how to exploit quantum-interference assisted metrology to learn about the optical absorption of complex molecules, even in a setting where the molecule has not seen the spectroscopic radiation in a classical sense [7].

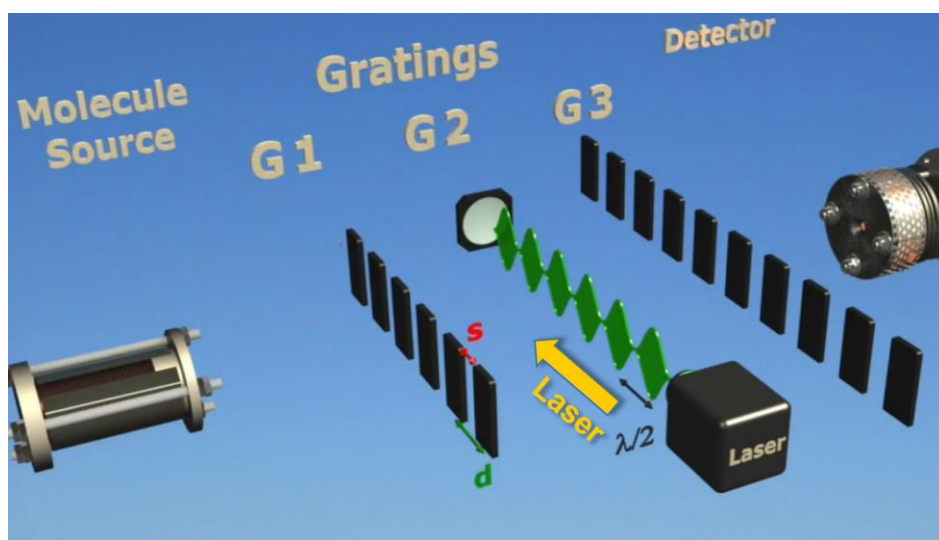


Figure 1 – A three-grating matter-wave interferometer allows imprinting a nanostructure onto a molecular beam in free flight. The displacement of the molecular interference pattern can serve as a sensitive tool for spectroscopy [4].

References

1. M. Arndt and K. Hornberger, *Nat. Phys.*, 10 (2014) 271.
2. M. Arndt, *Phys. Today*, 67 (2014) 30.
3. L. Mairhofer, S. Eibenberger, J. P. Cotter, M. Romirer, A. Shayeghi and M. Arndt, *Angew. Chem. Int. Ed.*, 56 (2017) 10947.
4. S. Eibenberger, X. Cheng, J. P. Cotter, and M. Arndt, *Phys. Rev. Lett.*, 112 (2014) 250402.
5. J. Rodewald, P. Haslinger, N. Dörre, B. A. Stickler, A. Shayeghi, K. Hornberger and M. Arndt, *Appl. Phys. B*, 123 (2016).
6. C. Brand, B. A. Stickler, C. Knobloch, A. Shayeghi, K. Hornberger and M. Arndt, *arXiv:1710.01035*, (2017).
7. J. P. Cotter, S. Eibenberger, L. Mairhofer, X. Cheng, P. Asenbaum, M. Arndt, K. Walter, S. Nimmrichter, and K. Hornberger, *Nat. Commun.*, 6 (2015) 7336.

Acknowledgements: This research has been funded by the European Research Council within project 320694

Photoprotective Mechanisms in Photosynthesis Studied by Time-Resolved FTIR Difference Spectroscopy

A. Mezzetti^a, M. Alexandre^a, B. Robert^b, C. Buchel^c and D. Kirilovsky^a

^a Sorbonne Université, LRS UMR 7197, 4 Pl Jussieu, 75005 Paris, France

^b I2BC, UMR 9198, CEA-Saclay, Univ. Paris-Saclay, 91191 Gif-sur-Yvette, France

^c Institute Molecular Bioscience, University Frankfurt, Germany

alberto.mezzetti@libero.it

Time-resolved FTIR difference spectroscopy (TR-FTIR-DS) is a powerful technique in the investigation of biochemical reactions, providing time-resolved details at the atomic level on the reaction mechanisms (H^+ transfer, e^- transfer, chemical modification of molecules, ...) [1]. We have studied photoprotection mechanisms in by TR-FTIR-DS, not only on isolated proteins, but also *in vivo*.

In a first study the photoactivation mechanism of the Orange Carotenoid Protein (OCP), a water soluble protein found in cyanobacteria implicated in photoprotection was studied. Whereas previous TR-FTIR-DS studies from our groups showed the molecular details of the conformational changes associated to the photoactivation of the protein [2], recent results on wild-type and mutants OCPs show that an intermediate state in the OCP photocycle can be trapped at low temperature, and – by using specific mutants - can be characterized by TR-FTIR-DS [3].

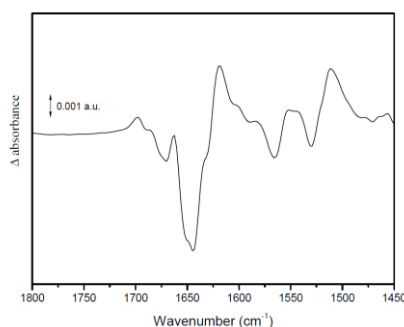


Figure. 1 – FTIR difference spectrum after continuous illumination of wild-type OCP. In the 1680-1620 cm^{-1} region bleaching of α helix signal can be observed.

In a second study, we studied the photoprotective mechanism of diatoms *in vivo*. In this case in was possible, on a second time scale, to follow by TR-FTIR-DS the response of the microorganism to strong light, implying a xanthophyll cycle. We could follow different chemical events (chemical epoxydation/de-epoxydation of carotenoids; plastoquinone pool reduction; localized pH changes; energy dissipation mechanisms; reorganization of the membrane structure) and calculate the kinetics for each of these processes [4].

The results will be discussed in the framework of the present knowledge of photoprotection mechanisms in cyanobacteria and diatoms, as well as in the framework of present and future capabilities of the TR-FTIR-DS technique.

References

1. A. Mezzetti, W. Leibl *Photosynth. Res.*, 131 (2017) 121.
2. A. Wilson, M. Gwizdala, A. Mezzetti, M. Alexandre, C. A. Kerfeld, D. Kirilovsky, *Plant Cell*, 24 (2012) 1972.
3. A. Mezzetti, A. Thurotte, M. Alexandre, D. Kirilovsky, in preparation.
4. A. Mezzetti, M. Alexandre, C. Buchel, B. Robert, in preparation.

VCD Spectroscopy of Nucleic Acid Supramolecular Structures

Valery Andrushchenko

*Institute of Organic Chemistry and Biochemistry, Academy of Sciences, Flemingovo nam. 2,
Prague, 16610, Czech Republic
andrushchenko@uochb.cas.cz*

Vibrational spectroscopy is a versatile, widely available and highly informative tool, which has been successfully used for conformational and structural studies of various molecules, including biomolecules. In addition to classical methods, namely infrared (IR) and Raman spectroscopy, recent development of the chiroptical vibrational techniques, such as vibrational circular dichroism (VCD) and Raman optical activity (ROA) significantly broadened the applicability of the vibrational spectroscopy and enhanced the obtained structural information. VCD spectroscopy is particularly useful for studies of supramolecular assemblies of biomolecules due to enhanced signal originating from their higher-order arrangement. Supramolecular structures often represent a problem for other chiral methods, such as electronic circular dichroism (ECD) and ROA because of strong light scattering, which, however, affects VCD to lesser extent.

We will demonstrate how enhanced VCD signal allows to detect and characterize condensed DNA, guanine quadruplexes and ordered dGMP structures templated by Eu^{3+} ions.

Acknowledgements: The author thanks Czech Science Foundation (grant 16-04902S) for the support.

Detection of Fractal Dynamics of Protein by Terahertz Spectroscopy

Tatsuya Mori^a, Yasuhiro Fujii^b, Jiang Yue^a, Leona Motoji^a, Wakana Terao^a, Suguru Kitani^c, Akitoshi Koreeda^b, Kentaro Shiraki^a, Yohei Yamamoto^a and Seiji Kojima^a

^a Division of Materials Science, University of Tsukuba, 1-1-1 Tennodai, Tsukuba, Ibaraki 305-8573, Japan

^b Department of Physical Sciences, Ritsumeikan University, 1-1-1 Noji-higashi, Kusatsu, Shiga 525-8577, Japan

^c Materials and Structures Laboratory, Tokyo Institute of Technology, 4259 Nagatsuta-cho, Midori-ku, Yokohama 226-8503, Japan
mori@ims.tsukuba.ac.jp

Glassy materials universally show the boson peak, which is one of the unsolved problems on glass physics, in the terahertz region [1-3]. On the other hand, in polymer glass and proteins having self-similarity of monomer molecules, it is expected that fractal dynamics appears above boson peak frequency [4,5].

Until now, the fractal dynamics often has been discussed by using low-frequency Raman scattering [5], and recent terahertz spectroscopic studies have not mentioned about detection of such excitation. In this study, we propose how to detect fractal dynamics by terahertz spectroscopy using protein as an example.

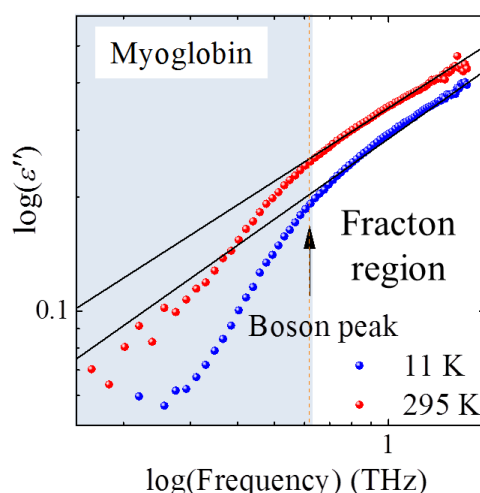


Figure 1 – $\log \varepsilon''$ vs \log frequency for the imaginary part of complex dielectric constants of myoglobin.

References

1. T. Nakayama, *Rep. Prog. Phys.* **65**, 1195 (2002).
2. M. Kabeya, T. Mori, Y. Fujii, A. Koreeda, B.W. Lee, J.H. Ko and S. Kojima, *Phys. Rev. B*, **94**, (2016) 224204.
3. W. Terao, T. Mori, Y. Fujii, A. Koreeda, M. Kabeya and S. Kojima, *Spectrochim. Acta A*, **192** (2018) 446.
4. S. Alexander and R. Orbach, *J. Phys. (Paris)* **43**, L625 (1982).
5. S. Saikan, T. Kishida, Y. Kanematsu, H. Aota, A. Harada and M. Kamachi, *Chem. Phys. Lett.*, **166** (1990) 358.

Acknowledgements: This work was partially supported by JSPS KAKENHI Grants No. 17K14318, the Nippon Sheet Glass Foundation for Materials Science and Engineering, and the Asahi Glass Foundation.

Structure and Interactions of Saccharides Studied by Vibrational Optical Activity Methods

Jakub Kaminsky^a, Lubos Plamitzer^a, Radek Pohl^a, Vladimir Kopecky^b
and Hector Martinez-Seara Monne^a

^aIOCB ASC CR, Flemingovo nam. 2, 166 10 Prague, Czech Republic

^bCharles University, Ke Karlovu 5, 121 16 Prague, Czech Republic

jakub.kaminsky@uochb.cas.cz

The global economy is predicted to become increasingly carbohydrates-based over the next decade. While the growing impact of carbohydrates on energy, food security and healthcare are already clear, the future development of new carbohydrate-based therapeutics, materials and energy sources will depend heavily on our building a better understanding at the molecular level of the structure-function relationships of carbohydrates. As traditional structural methods are often difficult to apply to carbohydrates, new approaches are urgently required. The main topic of the talk is to present a new spectroscopic approach to studying carbohydrate structures at the molecular level. We have developed widely applicable yet structurally sensitive approach based on chiral variants of vibrational spectroscopies for studying carbohydrates that exploit diverse interactions of carbohydrates with circularly polarized light (Figure 1; e.g. [1]). These spectroscopic techniques are able to reveal previously unknown details on all aspects of complex carbohydrate structure and organization, from the hydration of small sugars to the inter/intramolecular interactions of oligo- or polysaccharides and glycoproteins that govern their physiological functions and use as healthcare products e.g. hyaluronan.

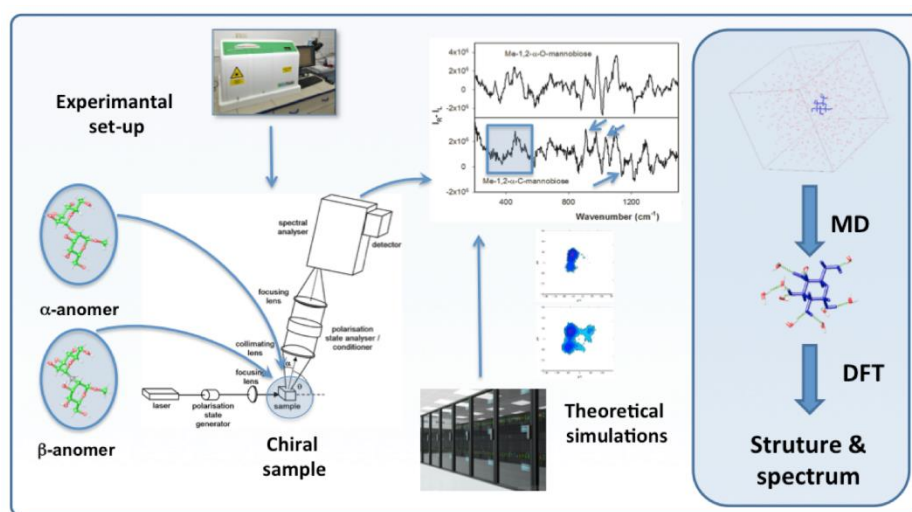


Figure 1 – General approach for studying carbohydrate structures based on Raman/ROA spectroscopic analysis.

References

1. A. Melcrová, J. Kessler, P. Bouř and J. Kaminský, *Phys. Chem. Chem. Phys.*, 18 (2016) 2130.

Acknowledgements: The grant of the Czech Science Foundation (16-00270S) is gratefully acknowledged.

Saccharinate-based Ligands: Structure, Reactivity and Properties

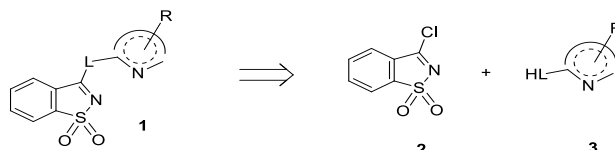
Amin L. Ismael^a, Lília L. Cabral^a, Elisa Brás^b, Rui Fausto^b and Maria L. S. Cristiano^a

^a CCMAR and Dep. of Chemistry and Pharmacy, University of Algarve, 8005-139 Faro, Portugal

^b CQC, Department of Chemistry, University of Coimbra, 3004-535, Coimbra, Portugal

mcristi@ualg.pt

Saccharin (3-oxo-1,2-benzisothiazole 1,1-dioxide) and saccharinates have important applications in coordination chemistry, as ligands [1]. However, conjugates that combine the saccharyl system with other heterocycles have been scarcely explored hitherto, in spite of their expectable capabilities as bridging ligands. We have designed and prepared a representative library of saccharinate-based ligands **1** from tailored building blocks (**2**, **3**) [2], in view of exploring their potential as chelants. The monomeric structure and photochemistry of selected conjugates was investigated, using matrix isolation coupled to FTIR spectroscopy and molecular orbital calculations. Then their chelating properties towards divalent cations of transition metals were scrutinised, revealing properties that may support relevant applications of the ligands and corresponding complexes [3]. The journey from molecular design to the proposal of applications will be described, emphasizing the relevance of detailed structural studies for the optimisation of properties.



3 = unsaturated 5 membered rings:
Thiodiazole/Triazoles/Tetrazoles

R=H, alkyl, phenyl
L=NH, S

References

1. D. W. Cho, S. W. Oh, D. U. Kim, H. J. Park, J. Y. Xue, U. C. Yoon, P. S. Mariano, *Bull. Korean Chem. Soc.*, 31 (2010) 2453.
2. L. Frija, R. Fausto, R. Loureiro, M. L. S. Cristiano, *J. Mol. Catal. A-Chemical*, 305 (2009) 142; A. Ismael, A. Borba, L. Duarte, B. M. Giuliano, A. Gómez-Zavaglia, M. L. S. Cristiano, *J. Mol. Struct.*, 1025 (2012) 105.
3. A. Ismael, A. Borba, M. S. C. Henriques, J. A. Paixão, R. Fausto, M. L. S. Cristiano, *J. Org. Chem.*, 80 (2015) 392; A. Ismael, M. S. C. Henriques, C. Marques, M. J. Rodrigues, L. Barreira, J. A. Paixão, R. Fausto, M. L. S. Cristiano, *RSC Adv.*, 6 (2016) 71628; L. Cabral, E. M. Brás, M. S. C. Henriques, C. Marques, L. Frija, L. Barreira, J. A. Paixão, R. Fausto, M. L. S. Cristiano, *Eur. J. Chem.*, 24 (2018) 3251.

Acknowledgements: We acknowledge Fundação para a Ciência e a Tecnologia (FCT)-Portugal and COMPETE (projects UID/Multi/04326/2013, UI0313/QUI/2013, PTDC/QEQ-QFI/3284/2014, PTDC/MAR-BIO/4132/2014). The Coimbra Chemistry Centre (CQC) is supported by FCT, through the project UI0313/QUI/2013, also co-funded by FEDER/COMPETE 2020-EU.

FRIDAY, 24th AUGUST

Label-Free Tissue Classification by QCL based IR-Imaging

Klaus Gerwert

Department of Biophysics
Ruhr-University Bochum, Germany
gerwert@bph.rub.de, www.bph.rub.de

Infrared imaging in combination with bioinformatics is an emerging tool for label-free, non-invasive annotation of tissue. For the entities colon, bladder, and lung, classifiers are established to annotate cancerous tissue in an automated workflow with sensitivity and specificity of over 95% [1]. Recently, deep learning methods are applied to improve the classifier performance. However, the therapeutic decision of the clinician requires a differential diagnosis of the cancer. Therefore, in the next step a predictive differential diagnostics is established. We were able to differentiate between subtypes in lung [2], colon [3] and recently bladder cancer to predict, how aggressive the cancer will develop.

An important milestone was than the combination with–omics technologies providing in addition to spatial also molecular resolution. The label-free classified tissue is cut out by laser microdissection and analyzed by proteomics. This is successfully applied to the lung infiltrating mesothelioma subtypes cancer [4] validation approach identifying the biomarker panel used in pathology. Recently, we identified in a discovery approach a novel biomarker, which differentiate between a very aggressive form of bladder cancer and inflammation only, which is difficult to distinguish by pathology today. For the aggressive form the bladder has to be resected.

A major break-through is obtained now by a QCL-based microscope. The IR images show the same quality as the FTIR-images before. Especially disturbing coherence effects are largely reduced. Most advantageous is the short measuring-time. This is now drastically reduced down to few minutes for typical pathological thin section. It is now fully comparable to fresh frozen pathology and has no interobserver variability. The QCL based approach opens now new avenues for clinical applications of tissue classification by IR-imaging.

References

1. A. Kallenbach-Thieltges , F. Großerüschkamp, A. Mosig, M. Diem, A. Tannapfel, K. Gerwert, *J. Biophotonics*, 6 (2013) 88.
2. F. Großerüschkamp F., A. Kallenbach-Thieltges, T. Behrens, T. Brüning, M. Altmayer, G. Stamatis, D. Theegarten, K. Gerwert, *Analyst*, 140 (2015) 2114.
3. C. Kuepper, F. Großerueschkamp, A. Kallenbach-Thieltges, A. Mosig, A. Tannapfel and K. Gerwert, *Faraday Discussion*, 187 (2016) 105.
4. F. Großerueschkamp, T. Bracht, H. C. Diehl, C. Kuepper, M. Ahrens, A. Kallenbach-Thieltges, A. Mosig, M. Eisenacher, K. Marcus, T. Behrens, T. Brüning, D. Theegarten, B. Sitek and K. Gerwert, *Scientific Reports*, 7 (2017) 44829.

Non-Destructive Applications of Infrared Spectroscopy for Assessment of Tissue Pathology and Regeneration

Nancy Pleshko

Dept. of Bioengineering, Temple University, Philadelphia, PA 19122 USA

npleshko@temple.edu

Tissue engineering approaches are being developed to overcome the limitations of current repair methods, which are due in large part to the challenges of regenerating native diseased tissues. Current gold standard techniques to assess the composition and integrity of engineered and repairing tissues, including histology, biochemical evaluation, and mechanical testing, are destructive, which limits real time monitoring of tissue development. This is an important area to address, as engineered tissues developed in similar environments can exhibit very different matrix and biomechanical properties [1]. Accordingly, non-destructive techniques to assess engineered tissues during development such that appropriate compositional endpoints can be defined are desirable [2]. Fourier transform infrared (FTIR) spectroscopy in the mid and near-infrared range are intrinsically label free, can be non-destructive, and provide specific information on the chemical composition of tissues. Here, we describe the use of spectroscopic techniques for non-destructive assessment and imaging of tissue repair and regeneration, and discuss the potential for clinical translation.

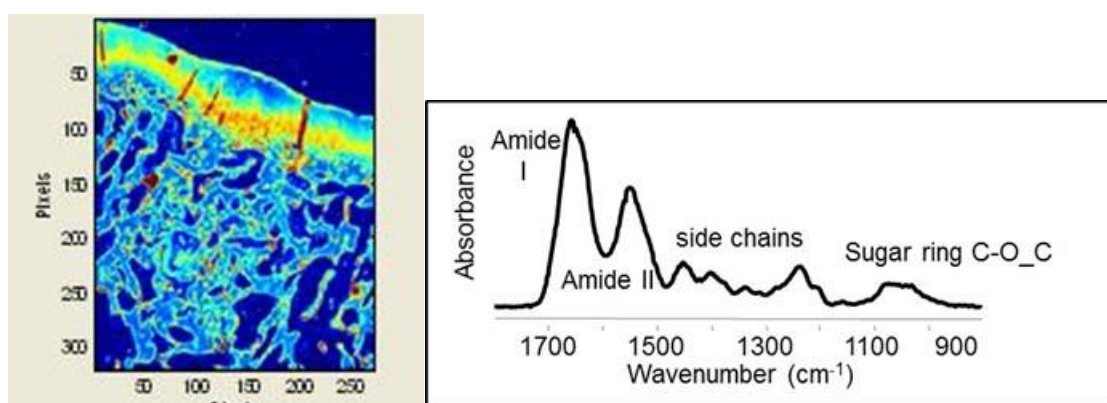


Figure 1 – A. FTIR imaging of a histological section of repairing cartilage defect and subchondral bone (left). The contrast is based on inherent molecular vibrations of sugar rings in glycosylated proteins. Infrared absorbances in cartilage arise from collagen amide and side chain absorbances, and proteoglycans (glycosylated proteins (right)).

References

1. F. Yousefi, M. Kim, Y. S. Nahri, R. L. Mauck and N. Pleshko. *Tissue Eng. Part A*. 24 (2017) 106.
2. W. Querido, J. M. Falcon, S. Kandel and N. Pleshko, *Analyst*, 142 (2017) 4005

Acknowledgements: Contributions from members of the Tissue Imaging and Spectroscopy Lab at Temple University are greatly appreciated!

Advancing Raman Microspectroscopy for Cellular and Subcellular Analysis: Towards *In vitro* High Content Spectralomic Analysis

Hugh J. Byrne^a, Franck Bonnier^b, Alan Casey^c, Marcus Maher^a, Jennifer McIntyre^a, Esen Efeoglu^{a,c} and Zeineb Farhane^{a,c}

^a FOCAS Research Institute, Dublin Institute of Technology, Kevin Street, Dublin 8, Ireland

^b Université François-Rabelais de Tours, Faculty of Pharmacy, EA 6295 Nanomédicaments et Nanosondes, 31 avenue Monge, 37200 Tours, France

^c School of Physics and Optometric & Clinical Sciences, Dublin Institute of Technology, Kevin Street, Dublin 8, Ireland
hugh.byrne@dit.ie

In the confocal mode, Raman microspectroscopy can profile the biochemical content of biological cells at a subcellular level, and any changes to it by exogenous agents, such as therapeutic drugs or toxicants. As an exploration of the potential of the technique as a high content, label free analysis technique for cellular and subcellular analysis, this work monitors the spectroscopic signatures associated with the uptake and response pathways of commercial chemotherapeutic agents and polymeric nanoparticles by human lung cells, probing the limitations of the technique in terms of reproducibility and specificity of spectral signatures of subcellular events and pathways. The subtle spectroscopic changes associated with the cellular perturbations are elucidated using a range of multivariate data mining techniques, and the challenge of identifying consistent reproducible label free spectral markers is addressed. It is demonstrated that the signatures are reproducible and characteristic of the cellular event, and can be used, for example, to identify the mode of action of the agent as well as the subsequent cell death pathway, and even mechanisms of cellular resistance. Data mining approaches are discussed and a spectralomics approach is proposed.

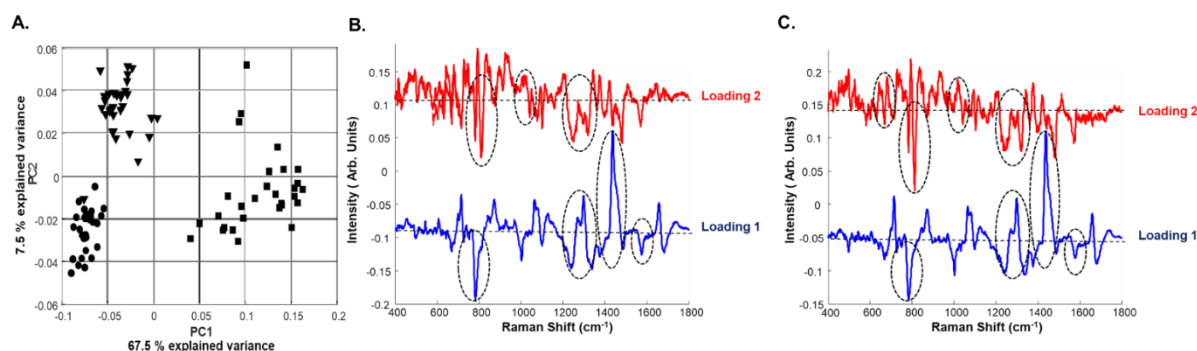


Figure 1 – Principle Components Analysis of nucleolus, nucleus and cytoplasm in immersion conditions A. Calu-1 cell line: Cytoplasm ■Nucleus ▼Nucleolus ● B. Calu-1 differentiating PC loadings C. A549 differentiating PC loadings [1]

References

1. Z. Farhane, F. Bonnier, A. Casey, A. Maguire, L. O'Neill and H. J. Byrne, *Analyst*, 140 (2015) 5908.

Acknowledgements: This work was funded by Science Foundation Ireland (11/PI/1108).

Infrared Spectroscopy for Clinical Chemistry and Medical Diagnostics - Techniques and Chemometrics for a Successful Marriage of Two Fields

H. Michael Heise

*South-Westphalia University of Applied Sciences, Interdisciplinary Center for Life Sciences,
58644 Iserlohn, Germany
heise.h@fh-swf.de*

Mid-infrared spectroscopy has now been used within clinical chemistry for many decades, while in the beginning the analysis of urinary and gall stones in combination with the KBr-pellet technique had been the first established application. Spectral libraries were used for compound identification. Later also microscopy was added for elucidation of the disease history. For medical diagnostics based on multiple analytes, whole blood and derived body fluids such as plasma, serum and dialysates, as well as urine, have been analysed by us reagent-free. Here, statistical calibration models such as PCR (principal component regression) or PLS (partial least squares) were very successful in the majority of cases, for which appropriate outlier diagnostics were also calculated. Spectral variable selection was also optimised for robust calibration modeling, with a small number of variables similar to multiple linear regression models. Our suggested approach looked at the structure of the PLS regression vector and the pairwise selection of respective minima and maxima, weighted accordingly to the magnitude of the extreme value variables and with largest ones first selected. We also tested the impact of pharmaceuticals at concentrations in blood as reached with prescribed doses. The goal is a laboratory analyser for clinical chemistry. In this context, dry-film preparations robotically prepared on multi-well titer plates (MTP) were analysed in transmission aiming at high-throughput applications. The field of disease pattern recognition has been widened and worked out for urinary bladder cancer detection using pattern recognition and classification methods such as linear discriminant analysis or random forests [1].

Another important application is continuous patient monitoring under intensive care conditions. For this glucose, besides lactate and others, is one of the most important parameters [2,3]. We use the combination of microdialysis and infrared spectroscopy, where we have PLS and classical least squares (CLS) calibration implemented. The chemical complexity of dialysates is less than for whole blood, plasma or serum, as large molecules such as proteins or cellular components can be removed. In combination with chemical markers for dialysis recovery, we are able to predict whole blood concentrations accurately over several days without the need for changing the dialysis equipment. The use of extended cavity quantum cascade lasers (EC-QCLs) [4] for replacing conventional FTIR-spectrometers creates further challenges concerning the available spectral range for multi-analyte monitoring, which will be discussed in detail.

References

1. J. Ollesch, M. Heinze, H.M. Heise, T. Behrens, T. Brüning and K. Gerwert, *J. Biophotonics*, 7 (2014) 210.
2. T. Vahlsing, S. Delbeck, J. Budde, D. Ihrig, S. Leonhardt and H.M. Heise, *Proc. SPIE*, 10072 (2017) 100720D.
3. H. M. Heise, L. Cocchieri, T. Vahlsing, D. Ihrig and J. Elm, *Proc. SPIE*, 10072 (2017) 100720E.
4. M. Grafen, S. Delbeck, H. Busch, H.M. Heise and A. Ostendorf, *Proc. SPIE*, 10501 (2018) 105010A.

Acknowledgements: The author thanks especially Dr. J. Ollesch, formerly at PURE, Department of Biophysics, Ruhr-University Bochum (Germany) for the fine collaboration in the past.

Spectroscopic Determinants in Photodynamic Therapy

Luis G. Arnaut

Chemistry Department, University of Coimbra, 3004-535 Coimbra, Portugal

lgarnaut@ci.uc.pt

Photodynamic therapy (PDT) is clinically approved to treat solid tumors. It is based on the combination of light with a drug absorbing that light (i. e., a photosensitizer) and molecular oxygen, to generate reactive oxygen species (ROS: singlet oxygen, superoxide ion, hydrogen peroxide, hydroxyl radical) that are cytotoxic [1]. The photodynamic efficacy of a photosensitizer depends on its ability to strongly absorb light in the near infrared, where human tissues are more transparent, and use that light to generate ROS. Additionally, the efficacy of a photosensitizer is related to its subcellular localization, because ROS are short-lived species that diffuse very little before reacting with biological molecules.

Bacteriochlorins (Figure 1) offer new hope for the development of efficient PDT treatments because they have strong near-infrared absorptions and efficiently generate ROS. Structural changes in bacteriochlorins allow for the control of their photostability, of the nature of the ROS generated and of their subcellular localization, as well as for the control of other parameters relevant to therapy, such as biodistribution and pharmacokinetics [2-5]. This work unveils relations between the molecular structure and spectroscopy of bacteriochlorins and their efficacy in PDT, and offers a view from the design of bacteriochlorins based on such relations to their introduction in the clinic.

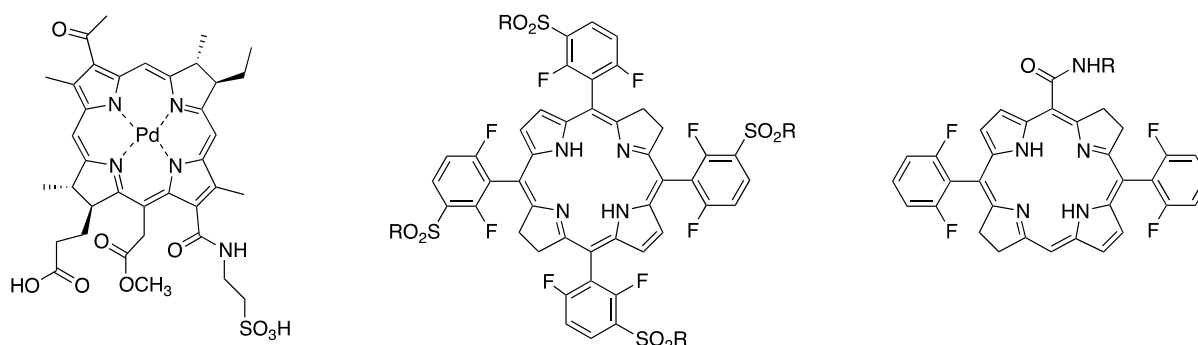


Figure 1 – Bacteriochlorins used as photosensitizers in PDT.

References

1. J. M. Dabrowski and L. G. Arnaut, *Photochem. Photobio. Sci.*, 14 (2015) 1765.
2. L. G. Arnaut *et al.*, *Chem. Eur. J.*, 20 (2014) 5346.
3. L. B. Rocha *et al.*, *Eur. J. Cancer*, 51 (2015) 1822.
4. A. F. S. Luz *et al.*, *Lasers Surg. Med.*, 50 (2018) *in press*.
5. L. C. Gomes-da-Silva *et al.*, *EMBOJ*, 37 (2018) *in press*.

Acknowledgements: The author thanks the Portuguese Science Foundation (007630UID/QUI/00313/2013, PTDC/QEQ-MED/3521/2014, Roteiro/0152/2013/022124) for financial support.

Spectroscopy in the 21st Century: The Future of Molecular Spectroscopy

Henry Horst Mantsch

Professor Emeritus, National Research Council, Ottawa, Canada

henry.mantsch@rogers.com

Occasionally one is faced with the question: “Is there a future for molecular spectroscopy and for the various meetings dedicated to it like EUCMOS”. My answer is an unqualified “Yes”. Molecular spectroscopy is a relatively young discipline which came into its own only in the middle of the last century, spurred by the influential work of Gerhard Herzberg whose trilogy “Molecular Spectra and Molecular Structure” is frequently referred to as the “Bible” of molecular spectroscopy. Since then a number of key scientific, technological and conceptual discoveries have catapulted molecular spectroscopy to where it is today. Significant leaps forward include the arrival of the laser, the exploitation of Fourier transform and resonance methods, the introduction of time and space resolved spectroscopies or the advent of surface-, metal- and tip-enhanced spectroscopies, to mention only a few.

As we consult the notorious crystal ball for predicting the future of molecular spectroscopy we need to distinguish between (i) the near or immediate future and (ii) the far or remote future. The former might encompass a further miniaturization of the instrumentation and the adaptation of new advances achieved in other fields of human endeavour; certainly molecular spectroscopy will become even more interdisciplinary as it penetrates all areas of human activity. However, in order to foresee or foretell the far future of molecular spectroscopy one must take a huge leap in faith. Are there limitations to our knowledge, boundaries beyond which we shall be unable to go? The history of science is full of developments in which such boundaries have been broken. Accordingly, I intend to go out on a limb and invoke some of the emerging new forces such as the recently detected gravitational waves or the still enigmatic dark energy. The intent of my presentation is to stir up the pot and encourage “out-of-the-box” reasoning.

POSTERS – TUESDAY, 21st AUGUST

Computational

Excited State Energy Mechanism and Luminescent Properties of Eu(III) Complex with Phenanthroline - Theoretical and Experimental Study

Ivelina Georgieva^a, Natasha Trendafilova^a, Tsvetan Zahariev^a, Nina Danchova^b and Stoyan Gutzov^b

^a Institute of General and Inorganic Chemistry, Bulgarian Academy of Sciences, Acad. G. Bonchev Str. 11, 1113 Sofia, Bulgaria

^b Department of Physical Chemistry, Faculty of Chemistry and Pharmacy, University of Sofia, J. Bourchier 1, 1164 Sofia, Bulgaria
ntrend@svr.igic.bas.bg

The excited state properties of $\text{Eu}(\text{phen})_2(\text{NO}_3)_3$ complex (phen=1,10-phenanthroline) were studied using ground state DFT and excited state TD-DFT calculations in combination with Sparkle/RM1, Judd-Ofelt and Malta's approximations. The study included calculations of the vertical excitation energies, relaxation/optimization of the first singlet and triplet excited states (S_1 , T_1), examination of their character, prediction of the excited state energy transitions and competitive radiative processes. Deeper understanding of the photoluminescence process for Eu(III) complex was achieved by calculations of ligand-to-Eu(III) intramolecular energy transfer and back-transfer rates as well as of the quantum efficiency and quantum yield of the Eu(III) emission applying the Luminescent Package LUMPAC. The validation of the combined approach used for description of the antenna *phen* chromophore and its complex with europium(III) was based on comparison with the experimental absorption and emission spectra of *phen*, $\text{Eu}(\text{phen})_2(\text{NO}_3)_3$ and $\text{Gd}(\text{phen})_2(\text{NO}_3)_3$. The most probable channel of the energy transfer involves transition between the lowest energy triplet state (T_1) of *phen* ligand and the 5D_0 level of Eu(III). The predicted luminescent quantum yield is of 32 %.

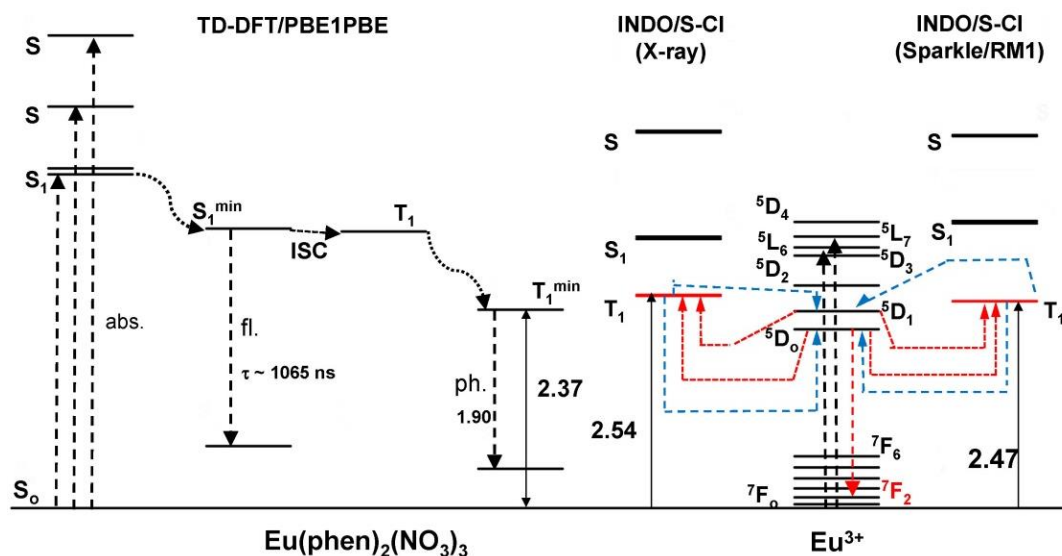


Figure 1 – Excitation, emission, transition energies (in eV) and luminescent properties of $\text{Eu}(\text{phen})_2(\text{NO}_3)_3$.

Acknowledgements: The authors thank the Bulgarian Science Fund, Grant DH09/9/2016 for the financial support. The calculations were performed at the computer cluster of the Bulgarian academy of Sciences “MADARA”.

Synthesis, Photophysical Properties and DFT Quantum Chemical Calculations of Novel Azo Diketopyrrolopyrrole Dyes

Anton Georgiev^a, Jozef Krajčovič^b, Ani Stoilova^a, Deyan Dimov^c, Ivaylo Zhivkov^{b,c} and Martin Weiter^b

^a Department of Organic Chemistry, Department of Physics, 8 St. Kliment Ohridski Blvd, University of Chemical Technology and Metallurgy, 1756 Sofia, Bulgaria

^b Materials Research Centre, Fac. of Chemistry, Purkyňova 118, Brno Univ. of Techn., Brno, Czech Republic

^c Department of Optical Materials, 109 "Acad. G. Bonchev" Blvd., Institute of Optical Materials and Technologies, Bulgarian Academy of Science, 1113 Sofia, Bulgaria
antonchem@abv.bg

Diketopyrrolopyrrole (DPP) and azo dyes are widely used in photonic technology due to their photosensitivity. Here, we present the synthesis of three novel azo diketopyrrolopyrrole (Azo-DPP) dyes in order to investigate their spectral and photophysical properties. The molecular geometry was optimized by DFT/B3LYP hybrid functional combined with the standard 6-31+G(d,p) basis set for *trans* (*E*) and *cis* (*Z*) isomers. The thermodynamic parameters such as total electronic energy $E(\text{RB3LYP})$, enthalpy H_{298} , free Gibbs energy G_{298} and dipole moment μ were computed for *trans* (*E*) and *cis* (*Z*) isomers in order to estimate the $\Delta E_{\text{trans} \rightarrow \text{cis}}$, $\Delta \mu_{\text{trans} \rightarrow \text{cis}}$, $\Delta H_{\text{trans} \rightarrow \text{cis}}$, $\Delta G_{\text{trans} \rightarrow \text{cis}}$ and $\Delta S_{\text{trans} \rightarrow \text{cis}}$ values. The introduction of electron withdrawing (EW) or electron donating (ED) substituents on phenylazo fragments was to obtain unsymmetrical electron ("push-pull") distribution on the molecular backbone of Azo DPP dyes (Fig. 1).

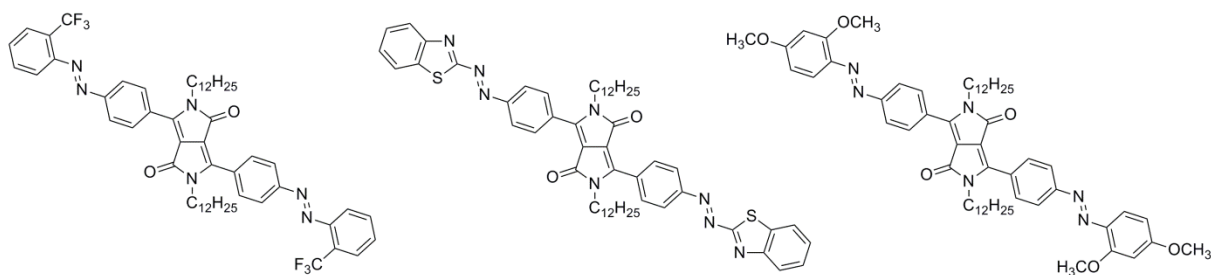


Figure 1 – Structure of the Azo-DPP dyes with different EW and ED groups.

The dynamic photoisomerization experiments have been performed in DMF solution with UV-irradiation $\lambda = 355$ nm (for *E*→*Z* conversion) and white light 400-800 nm (for *Z*→*E* conversion) in the spectral region 300 - 800 nm at equal concentrations and times of illumination in order to investigate the of *trans*→*cis*→*trans* isomerization kinetics of the dyes. The fluorescence spectra were also done to estimate absorption and emission properties of *trans* (*E*) and *cis* (*Z*) isomers.

References

1. M. Grzybowski and D. T. Gryko, *Adv. Opt. Mater.*, 3 (2015) 280.
2. H. M. Dhammika Bandara and S. C. Burdette, *Chem. Soc. Rev.*, 41 (2012) 1809.

Acknowledgements: This work was financially supported by the Bulgarian National Scientific Fund Project ДН 18/5 of the Ministry of Education and Science.

Quantum Chemical Characterization of the Infrared Spectra of *E*- and *Z*-Ethanamine and its Isotopes

Sandra M. V. Pinto, Nicola Tasinato and Vincenzo Barone
Scuola Normale Superiore, Piazza dei Cavalieri 7, I-56126 Pisa, Italy
sandra.vieirapinto@sns.it

Ethanamine is a molecule of interest in the field of prebiotic chemistry, because of its plausible role in the formation of alanine (one of the twenty amino acids in the genetic code) [1-3]. It can be found with abundance in the hot cores of interstellar medium clouds, such as the Sagittarius B2 cloud (Sgr B2) [1], where both isomers (*E* and *Z*) have been identified.

The infrared (IR) spectra is a fingerprint of a molecule and plays an essential role on retrieving the chemical composition of planetary spheres. Thus, the thorough knowledge of the spectroscopic properties of astrochemical species like ethanamine is a fundamental prerequisite for the fruitful interpretation of astronomical observational data retrieved by either ground-based observatories and spectrometers on board satellites or airborne. Recently, an accurate characterization of the molecular structure of *E*- and *Z*-ethanamine as well as of its spectroscopic properties have been carried out for what concerns the IR and rotational spectra of the main isotopic species [4]. In the present contribution, we extended the work investigating, by means of the state-of-art of computational methods, fundamental IR transitions, overtones and combination bands of both *E* and *Z* isomers of ethanamine (CH_3CHNH) and deuterated ethanamine (CD_3CDND). The predicted IR spectra are used to re-investigate the experimental data recorded in argon matrix by Stolkin *et al.* [5]. Finally, we are also investigating the IR spectra of two other isotopic species ($\text{CH}_3\text{CH}^{15}\text{NH}$ and $\text{CH}_3^{13}\text{CHNH}$), however the available spectra were recorded in low-resolution gas-phase IR, where only the strongest fundamental bands were observed [6].



Figure 1 – Structure of *E*-ethanamine (left-side) and *Z*-ethanamine (right-side).

References

1. R. A. Loomis, *et al.*, *Astrophys. J. Lett.*, 765 (2013) L9.
2. D. E. Woon, *Astrophys. J. Lett.*, 571 (2002) L177.
3. J. E. Elsila, *et al.*, *Astrophys. J.*, 660 (2007) 911.
4. A. Melli, *et al.*, *Astrophys. J.*, 855 (2018) 123.
5. I. Stolkin *et al.* *Chem. Phys.*, 21 (1977) 327.
6. K. Hashigushi, *et al.*, *J. Mol. Spectrosc.*, 105 (1984) 81.

Acknowledgements: The authors thank the SMARTLAB@SNS for computer resources. The work has been financially supported by MIUR (PRIN 2015 project “STARS in the CAOS” - Grant Number 2015F59J3R) and Scuola Normale Superiore (COSMO project - Grant Number GR16_B_TASINATO).

Conformational Studies of 3-Cyclopropylaminomethylene-pentane-2,4-dione Using Vibrational and NMR Spectra, and *Ab initio* Calculations

Anton Gatiaľ^a, Peter Herich^a, Viktor Milata^b and Michal Šoral^c

^a Department of Physical Chemistry, ^b Department of Organic Chemistry, ^c Central Laboratories, Faculty of Chemical and Food Technology, Slovak University of Technology, Radlinského 9, SK-81237 Bratislava, Slovakia
anton.gatial@stuba.sk

The aim of this work is the conformational study and interpretation of vibrational and NMR spectra of the title compound $\text{H}_5\text{C}_3\text{-NH-CH=C(COCH}_3)_2$ (CPAMP). It belongs to the so-called push-pull olefines which are often used as starting reactants or intermediates in many organic syntheses. The high polar character of push-pull ethylenes and the electronic interactions between substituents are responsible for their non-linear optical properties. The electron donor cyclopropylamino group in the investigated compound has a special influence on its conformational equilibria due to the possibility to create an intramolecular hydrogen bond.

CPAMP can theoretically exist in eight *EZa*, *EZs*, *EEa*, *EEs*, *ZEa*, *ZEs*, *ZZa* and *ZZs* conformations where the first and second letters express the orientation of the carbonyl oxygen to the C=C bond for *trans* and *cis* acetyl group, respectively, and the conformational possibility due to the *anti* and *syn* orientation of the cyclopropylamino group to the C=C bond is denoted by the third letter. This work contains theoretical calculations and X-ray, vibrational and NMR study as well. X-ray study revealed *EZa* conformer in solid state. In the IR and Raman spectra in very polar solvents only one conformer is present but in less polar solvents the second one is observed. MP2 and DFT calculations in different basis sets predict for CPAMP the conformer with *EZ* orientation of both acetyl groups as the most stable one followed by the *ZZ* one (Table 1) and with *anti* orientation of cyclopropylamino group. It has been shown that the conformers with *E* orientations of both acetyl groups are not the stable ones. These observations are explained by the influence of environment polarity on the conformational equilibrium and are discussed with respect to the SCRF solvent effect calculations using PCM model.

Table 1 – MP2/cc-pVTZ and B3LYP/cc-pVTZ calculated *ab initio* relative energies ΔE and dipole moments μ of CPAMP conformers in vacuum (n – not found)

CPAMP (MP2)	<i>EZa</i>	<i>EZs</i>	<i>EEa</i>	<i>EEs</i>	<i>ZEa</i>	<i>ZEs</i>	<i>ZZa</i>	<i>ZZs</i>
ΔE (kJ/mol)	0.00	35.87	n	n	36.53	40.04	10.03	40.64
μ (D)	5.19	5.43			5.92	4.97	1.94	2.87
CPAMP (B3LYP)	<i>EZa</i>	<i>EZs</i>	<i>EEa</i>	<i>EEs</i>	<i>ZEa</i>	<i>ZEs</i>	<i>ZZa</i>	<i>ZZs</i>
ΔE (kJ/mol)	0.00	46.90	69.42 ^x	n	35.38	53.59	8.20	50.11
μ (D)	5.46	5.71	7.89 ^x		6.34	5.37	1.91	2.91

^xvalues obtainable only using cc-pVDZ basis set

Acknowledgement: This work has been supported by Ministry of Education, Science, Research and Sport of the Slovak Republic within the Research and Development Operational Programme for the project "University Science Park of STU Bratislava – phase II.", ITMS 313021D243 and by High Performance Computing center at Slovak University of Technology in Bratislava (SIVVP project No. 26230120002), both co-funded by the European Regional Development Funds.

The support from the Slovak Research and Development Agency (projects APVV-15-0079) and the Scientific Grant Agency of the Ministry of Education of Slovak Republic (projects VEGA No. 1/0598/16) is appreciated as well.

Density Functional Theory Approaching on Structural Analysis of New Tetramer Barbiturate Molecule

İlkan Kavlak and Güneş Süheyla Kürkcüoğlu

Physics Department, Eskişehir Osmangazi University, Eskişehir, TR-26480, Turkey

gkurkcuo@ogu.edu.tr

Poly(vinyl chloride) (PVC) has a poor heat stability. The degradation is thermostatically occurred by dehydrochlorination in the polymer chains so that inorganic or organic thermal stabilizers are commonly used for protect the polymer from heat degradation [1]. Barbiturate is also known plastic additives which is nontoxic organic, thermally stable materials of high melting point. Especially, barbiturate can act as H-donor through their enolic hydrogen groups, which can intervene with the radical species derived from the thermal degradation of PVC [1]. In this study, the new tetramer single crystal structure of barbiturate has been synthesized. Then, its structure was analyzed by elemental analysis, single crystal X-ray diffraction, PXRD pattern and vibrational spectroscopic (FT-IR and Raman) techniques (Figures 1 and 2). Additionally, the geometries of monomer and dimer forms of barbiturate ligand, and the geometry of the synthesized new single crystal structure of barbiturate were optimized by density functional theory (DFT-B3LYP) methods with LANL2DZ basis set. Furthermore, the optimized geometric parameters, normal mode frequencies and corresponding vibrational assignments of the molecules have been determined via same method and basis set. Moreover, reliable vibrational assignments have been made on the basis of potential energy distribution (PED). Regression equations have been obtained in order to show the good agreement between the experimental and theoretical vibration modes. These equations are obtained as $y = 0.9954x + 7.8131$ R^2 ; $R^2 = 0.9995$. The results were shown that a good agreement was observed between obtained theoretical and experimental data.

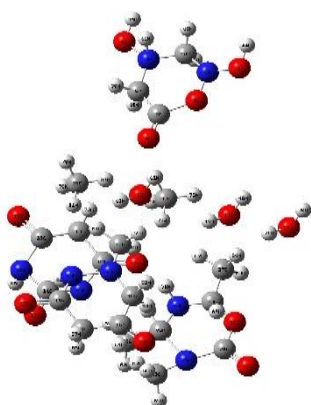


Figure 1 – The molecular structure of the new tetramer barbiturate molecule.

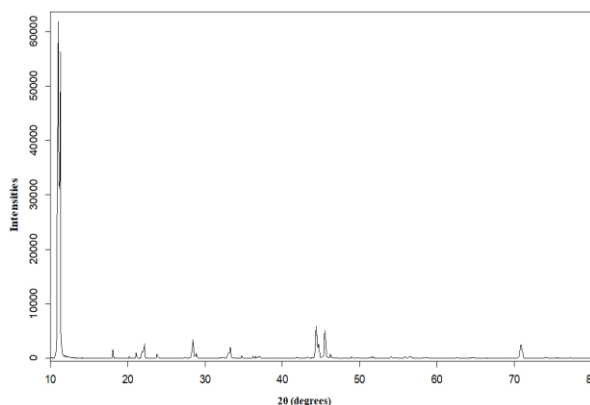


Figure 2 – PXRD pattern of the molecule.

References

1. N. A. Mohamed, A. A. Yassin, K. D. Khalil and M. W. Sabaa, *Polym. Degrad. Stab.*, 70 (2000) 5.

Acknowledgements: This work was supported by the Research Fund of Eskişehir Osmangazi University (Project No. 2017-1588).

Structural, Spectroscopic and Energetic Properties of Creatinine Conformers by Quantum-chemical Calculations

Alice Balbi^a, Nicola Tasinato^a, Lorenzo Spada^{a,b}, Cristina Puzzarini^b and Vincenzo Barone^a

^a Scuola Normale Superiore, Piazza dei Cavalieri 7, I-56126, Pisa, Italy

^b Dipartimento di Chimica "Giacomo Ciamician", Università di Bologna, Via Selmi 2, I-40126, Bologna, Italy
alice.balbi@sns.it

The conformational landscape of naturally occurring biomolecules is of particular interest because it determines their functional specificity in view of the structure – property relationship [1]. In this respect, investigations under isolation conditions are of foremost chemical significance, because they allow avoiding the competition between intra- and inter-molecular interactions in tuning the overall conformational behaviour. Under this point of view, *rotational spectroscopy is an excellent tool for retrieving the structure of molecules in the gas phase. However, in many cases and especially for biomolecules, the support of quantum-chemical (QC) calculations is fundamental for guiding experiment and interpreting the acquired spectra.* In fact, by comparing the rotational spectra recorded experimentally with theoretical results, it is possible to make an initial assignment of the rotational transitions in terms of rotational quantum numbers. Furthermore, a complex conformational mixture often characterizes the spectra of biochemical molecules: in such cases, QC calculations represent the most effective way to investigate the conformational landscape ruling the observed spectroscopic behaviour.

Creatinine is a breakdown product of creatine phosphate in muscles and high levels of this molecule in blood are usually associated to severe liver diseases. In this work, QC calculations are performed in order to identify the relevant stationary points on the potential energy surface (PES) of creatinine, i.e., the minima and the corresponding connecting transition states, and to determine their structural and energetic properties. For the minima, spectroscopic parameters relevant to rotational spectroscopy are determined. Structural and spectroscopic data are evaluated by using density functional theory (DFT). In particular, the B3LYP and B2PLYP functionals augmented by the DFT-D3 [2] dispersion corrections are employed in conjunction with the SNSD [3] and m-aug-cc-pVTZ-dH [4,5] basis sets. Accurate electronic energies are then computed using a composite scheme based on the CCSD(T) method and taking into account extrapolation to the complete basis set limit and core-valence effects.

References

1. B. Chandramouli, S. Del Galdo, G. Mancini, N. Tasinato and V. Barone, *Biopolymers*, (2018) doi.org/10.1002/bip.23109.
2. S. Grimme, J. Anthony, S. Ehrlich and H. Krieg, *J. Chem. Phys.*, 132 (2010) 154104.
3. I. Carnimeo, C. Puzzarini, N. Tasinato, P. Stoppa, A. Pietropolli Charmet, M. Biczysko, C. Cappelli and V. Barone, *J. Chem. Phys.*, 139 (2013) 074310.
4. E. Papajak, H. R. Leverentz, J. Zheng and D. G. Truhlar, *J. Chem. Theory Comput.*, 5 (2009) 1197.
5. L. Spada, N. Tasinato, F. Vazart, V. Barone, W. Caminati and C. Puzzarini, *Chem. Eur. J.*, 23 (2017) 4876.

Acknowledgements: The authors thank the SMART@SNS Laboratory (<http://dreams.sns.it>) for providing high-performance computer facilities and Scuola Normale Superiore (SNS) for financial support. L.S. thanks SNS for his post-doctoral position.

Theoretical Investigation of the Electron Transfer Dynamics in a Hydrogen-Evolving Ru-Pd Molecular Photocatalyst

M. Staniszevska^a, S. Kupfer^b and J. Guthmüller^a

^a Faculty of Applied Physics and Mathematics, Gdańsk University of Technology, Narutowicza 11/12, 80233, Gdańsk, Poland

^b Institute for Physical Chemistry, Friedrich-Schiller University Jena, Helmholtzweg 4, 07743, Jena, Germany
mstaniszevska@mif.pg.gda.pl

Time dependent density functional theory calculations and the Marcus theory of electron transfer (ET) were applied on the molecular photocatalyst [1] [(tbbpy)₂Ru(tpphz)PdCl₂]²⁺ in order to elucidate the light-induced relaxation pathways populated upon excitation in the visible region. The dependency of the catalytic efficiency on the excitation wavelength [2] leads to the question of how the nature of the initially populated excited states affects the subsequent ET processes and ultimately the generation of hydrogen. This contribution investigates the situation of a direct excitation into a metal (Ru) to ligand charge transfer (MLCT) singlet state localized on the tpphz part of the complex. The computational results show that after the initial excitation, MLCT triplet states are energetically accessible, but that an ET toward the catalytic center (PdCl₂) from these states is a slow process, with estimated time constants above 1 ns. Instead, the calculations predict that low-lying Pd-centered states - describing an energy transfer toward the catalytic center - are efficiently populated. Thus, it is postulated that these states lead to the dissociation of a Cl⁻ ion and are consequently responsible for the experimentally observed degradation of the catalytic center [3,4]. Following dissociation, it is shown that the ET rates from the MLCT states to the charge separated states are significantly increased (i.e. 10⁵-10⁶ times larger). This demonstrates that alteration of the catalytic center is required to generate efficient charge separation.

References

1. S. Rau, B. Schäfer, D. Gleich, E. Anders, M. Rudolph, M. Friedrich, H. Görls, W. Henry and J. G. Vos, *Angew. Chem. Int. Ed.*, 45 (2006) 6215.
2. S. Tschierlei, M. Karnahl, M. Presselt, B. Dietzek, J. Guthmüller, L. González, M. Schmitt, S. Rau and J. Popp, *Angew. Chem. Int. Ed.*, 49 (2010) 3981.
3. M. G. Pfeffer, T. Kowacs, M. Wachtler, J. Guthmüller, B. Dietzek and J. G. Vos, *Angew. Chem. Int. Ed.*, 54 (2015) 6627.
4. M. G. Pfeffer, B. Schafer, G. Smolentsev, J. Uhlig, E. Nazarenko, J. Guthmüller, C. Kuhnt, M. Wächtler, B. Dietzek, V. Sundstrom and S. Rau, *Angew. Chem. Int. Ed.*, 54 (2015) 5044.

Acknowledgements: The authors are grateful to the Narodowe Centrum Nauki (Project No. 2014/14/M/ST4/00083) for financial support. The calculations have been performed at the Universitätsrechenzentrum of the Friedrich-Schiller University of Jena and at the Wrocław Center for Networking and Supercomputing (grant no. 384). Furthermore, we are grateful for the support of the COST Action CM1202 Perspect-H₂O.

Structure and NMR Properties of Acetic Acid/Cyclohexane Binary Solutions Studied Using Molecular Dynamics/Quantum Mechanics Approaches

Dovilė Lengvinaitė and Kęstutis Aidas

Institute of Chemical Physics, Vilnius University, Sauletekis ave. 3, LT-10257 Vilnius, Lithuania
dovile.lengvinaite@vu.ff.lt

Acetic acid is one of the simplest organic acids with considerable importance in chemistry. Molecular association in liquid acetic acid has been a subject of extensive investigations using diffraction techniques, spectroscopic measurements and computational methods. Neutron diffraction data suggest that cyclic dimer clusters yield a good description of the liquid structure on the molecular level. In contrast, molecular dynamics simulations show that acetic acid molecules prefer to form chain-like structures linked via hydrogen-bonding (HB). Similar results have been deduced using large-angle X-ray scattering. Raman spectroscopy and ab-initio calculations also lead to the conclusion that acetic acid molecules form a chain structure [1].

The ^1H NMR measurements of acetic acid and cyclohexane binary solutions showed a very interesting non-monotonic evolution of the chemical shift of the acidic proton with the changing concentration of the components [2]. This evolution clearly reflects the peculiarities of the association of acetic acid in these systems, which until now have not been thoroughly studied. The formation of acetic acid dimers or higher order associates and the change in the *cis-trans* conformational equilibrium are only some of the processes at the molecular level that could influence the measured NMR spectral parameters.

In order to explain these NMR results, we performed MD simulations of acetic/acid cyclohexane binary solutions. Three molecular systems were considered: pure acetic acid involving only the *trans* conformers, acetic acid monomer and cyclic dimer dissolved in cyclohexane. MD simulations were performed using OPLS-AA and GAFF force fields by utilizing Molsim program. Analysis of the radial distribution functions of the liquid acetic acid does not allow for unambiguous identification of the predominant molecular associates in the liquid state. We have thus performed careful geometrical analysis of the recorded trajectories which shows that cyclic dimers and trimers as well as chain-like structures are all formed in the liquid acetic acid. We have quantified the percentage of all these aggregates.

We also have performed calculations of the ^1H NMR chemical shift of the acidic proton by using the combined quantum mechanics/molecular mechanics (QM/MM) method. Our results reproduce experimental data very well and allow explaining the experimentally observed evolution of the chemical shift of the acidic proton with the changing concentration of the binary solution. The peak in the chemical shift is observed when cyclic dimers of the acetic acid are predominant in the binary solution. However, in pure acetic acid other types of aggregates are also formed leading to the increased shielding of the acidic proton by around 0.5 ppm. These experimental results are very well reproduced by our QM/MM calculations.

References

1. S. Fathi, S. Bouazizi, S. Trabelsi, *et.al.*, *J. Mol. Liq.*, 69 (2014) 196.
2. L. L. Kimtys and V. J. Balevicius, *J. Molec. Liq.*, 151 (1979) 15.

Acknowledgements: The authors thank to the High Performance Computing Center “HPC Sauletekis” in Vilnius University Faculty of Physics.

A Theoretical Study on Molecular Structures and Vibrational Spectra of Cyanide Complexes with 1,2-Dimethylimidazole: $[M(dmi)_2Ni(\mu-CN)_4]_n$ (M = Cu, Zn or Cd)

Biray Kınık, İlkan Kavlak and Güneş Süheyla Kürkçüoğlu
Physics Department, Eskişehir Osmangazi University, Eskişehir, TR-26480, Turkey
gkurkcuo@ogu.edu.tr

The cyanide-bridged complexes with 1,2-dimethylimidazole, $[M(dmi)_2Ni(\mu-CN)_4]_n$ (dmi = dimethylimidazole; M(II) = Cu, Zn or Cd), was experimentally investigated by FT-IR, Raman spectroscopy and X-ray single crystal diffraction analysis in our previous study [1]. In this study, the molecular geometry and vibrational frequencies of the complexes in the ground state have been calculated by using DFT-B3LYP and DFT-B3PW91 with LANL2DZ basis set. A good correlation was found via comparison of the experimental and theoretical vibrational frequencies of the complexes. The complexes have been studied in the 4000-250 cm^{-1} region and assignments of all the observed bands were made. The analysis of the FT-IR and Raman spectra indicates that there are some structure-spectra correlations.

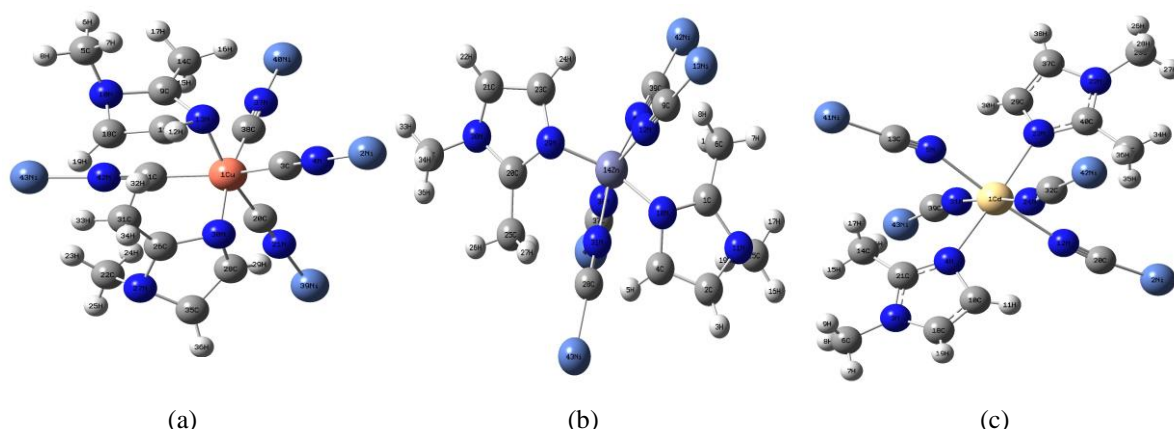


Figure 1 – Optimized molecular geometry of $[M(dmi)_2Ni(\mu-CN)_4]_n$ (M = Cu(II) (a), Zn (II) (b), Cd(II) (c)).

References

1. G. S. Kürkçüoğlu, E. Sayın and O. Şahin, *J. Mol. Struct.*, 1101 (2015) 82.

Acknowledgements: This work was supported by the Research Fund of Eskişehir Osmangazi University (Project Number. 2015-830).

A Theoretical Study on the Molecular Structure and Vibrational Spectra of Homonuclear Cyanide Complex of $[\text{Ni}(\text{etim})_4\text{Ni}(\mu\text{-CN})_2(\text{CN})_2]_n$

Güneş Süheyla Kürkçüoğlu and İlkan Kavlak

Physics Department, Eskişehir Osmangazi University, Eskişehir, TR-26480, Turkey

gkurkcuo@ogu.edu.tr

The homonuclear cyanide-complex of the type: $[\text{Ni}(\text{etim})_4\text{Ni}(\mu\text{-CN})_2(\text{CN})_2]_n$ was experimentally investigated by FT-IR, Raman spectroscopy and X-ray single crystal diffraction analysis in our previous study [1,2]. In this study, the molecular geometry and vibrational frequencies of the complex in the ground state have been calculated by using DFT-B3LYP and DFT-B3PW91 with LANL2DZ basis set. A good correlation was found via comparison of the experimental and theoretical vibrational frequencies of the complex. The analysis of the FT-IR and Raman spectra indicates that there are some structure spectra correlations.

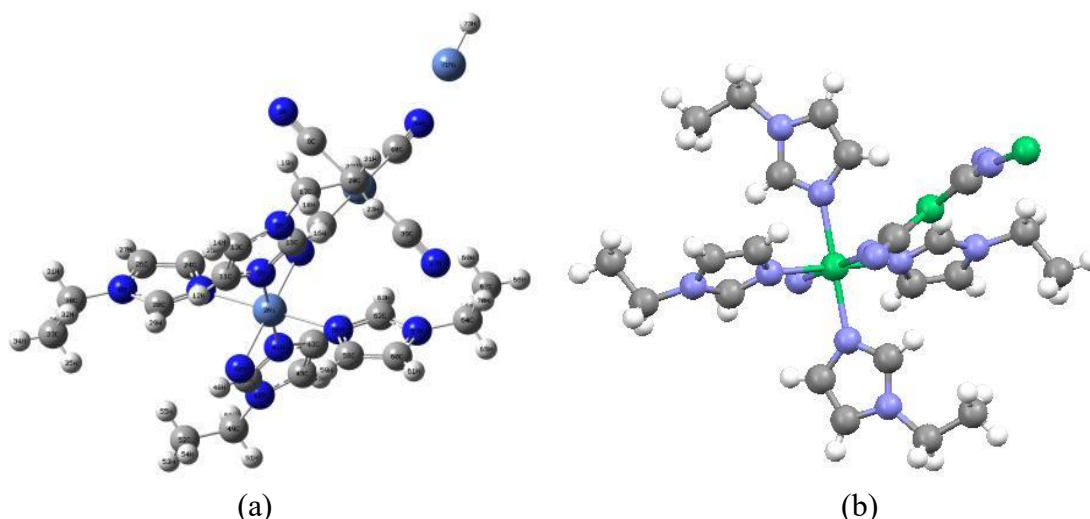


Figure 1 – Molecular model and optimized structure (a) and experimental schema (b) of the complex.

References

1. A. F. Çetinkaya, G. S. Kürkçüoğlu, O. Z. Yeşilel, T. Hökelek and Y. Süzen, *J. Mol. Struct.*, 1048 (2013) 252.
2. G. S. Kürkçüoğlu, F. Çetinkaya Kiraz and E. Sayın, *Spectrochim. Acta A Mol. Biomol. Spectrosc.*, 149 (2015) 8.

Acknowledgements: This work was supported by the Research Fund of Eskişehir Osmangazi University (Project Number. 2015-830).

Coordinative Bonding Perturbation of some First Series Transition Metal Ions by the Glycine Ligand

P. F. Tseki

*Department of Chemical & Physical Sciences Walter Sisulu University NMD Campus Mthata 5117, South Africa
ptseki@wsu.ac.za*

The coordinative bonding interaction involving glycine ligand with three randomly, selected transition metals ions titanium, chromium and nickel is analysed using standard perturbation principles. The experimental measurements are achieved by accurately determining the spectral shifts or magnitudes of perturbations extracted from the corresponding uv-visible spectra of the solution complexes. The observed spectral shifts are interpreted as perturbations on the appropriate excited electronic state of the transition metal ion while the immediate excited but unperturbed states and the ground state facilitate the redistribution of the perturbation energy within the transition metal ion electronic energy states. A plot of the observed spectral shifts or magnitudes of perturbations against the computed intensities of perturbation (IP), where $IP = \{ \frac{1}{2} \sum_i (m_i e_i^2) \}^{-1}$ (with m_i and e_i denoting the molality of the interacting species in solution and their corresponding g or j Jorgensen parameters, respectively) allows for the determination of a polynomial functional representing the perturbation profile of the octahedral transition metal ion by successive glycine ligands. A break up of the functional into its perturbation tuning parameter components λ^n where n is the order of perturbation correction on the energy of the bare transition metal ion, gives the relative magnitudes of the components of the perturbation tuning parameters *lambda*, and therefore insight into the detailed mechanism of the transition metals electronic energy redistribution to accommodate coordinative bonding interaction with a glycine ligand. DFT calculated glycine ligand perturbations on the transition metal ion are conducted and compared with experimental data with somewhat encouraging results.

$$\nu_n = \nu_n^{(0)} + \lambda \nu_n^{(1)} + \lambda^2 \nu_n^{(2)} + \dots,$$

where ν_n is the observed d-d electronic transition frequency, $\nu_n^{(0)}$ is the transition frequency in the absence of any ligand perturbation and $\lambda \nu_n^{(1)}$, $\lambda^2 \nu_n^{(2)}$ + are the first and second order terms in the perturbation expression.

References

1. I. R. Levine 2009. Quantum Chemistry: Pearson Prentice Hall, pp. 248-254.
2. D. J. Griffiths 2005. Introduction to Quantum Mechanics: Pearson Prentice Hall, 2nd ed. pp. 249-256.
3. M. W. Hanna 1981. Quantum Chemistry: The Benjamin/Cummings, 3rd ed. pp 69-77.
4. F. A. Cotton, G. Wilkinson, P. L. Gaus 1995. Basic Inorganic Chemistry: John Wiley, 3rd ed. pp 519-536.

Acknowledgements: The author thanks Walter Sisulu University for financial support.

Computational Insight into the PNP-Lariat Ether Complexes with Some Alkali and Alkaline Earth Metal Cations

Ines Despotović

Ruđer Bošković Institute, Bijenička cesta 54, 10000 Zagreb, Croatia

Ines.Despotovic@irb.hr

Supramolecular host-guest chemistry has attracted the growing attention of numerous researches over the past decades. The lariat ethers, the crown ethers having a side arm attached to the macrocyclic system, were found to display very interesting cation-binding properties [1]. In this work a complexation of some alkali and doubly-charged alkaline earth metal cations with PNP-lariat ethers $[N_3P_3R_4O(CH_2CH_2O)_4]$ ($R=H$ (**1**), NMe_2 (**2**), $NC(NMe_2)_2$ (**3**)) in the gas phase has been studied by the DFT B3LYP/6-311+G(3df,2p)//B3LYP/6-31+G(d,p) quantum chemical method. The obtained computational results indicate that these ligand structures act as efficient and very selective scavengers of Li^+ , Na^+ , K^+ , Be^{2+} , Mg^{2+} and Ca^{2+} cations, exhibiting gas phase cation affinities in a wide range of $64.2 - 496.1 \text{ kcal mol}^{-1}$. The cation affinity of the hosts has been found to be significantly amplified by attaching the electron-donating group to the P_3N_3 ring. The Bader's topological analysis of the electron density distribution function has been performed for the studied complexes with the aim to gain more insight into their bonding properties. It was found that the coordination bonds of the s-block metal centers with the N/O atoms in the studied complexes possess the predominantly ionic character, except those of Be^{2+} metal cations with the N atoms that corespond to the intermediate type of interactions. The charge donation from the PNP-lariat ether to the metal cation was established from the orbital population analysis. The amount of charge transferred from the host to the metal cation has found to be particularly significant in the complexes with alkaline earth metal cations. The structural features of considered PNP-lariat ethers complexes

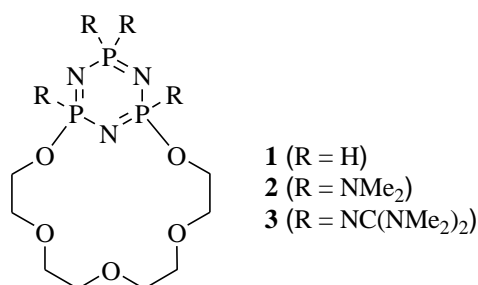


Figure 1 – Structural formula of macrocyclic systems **1** – **3**.

are provided and will be discussed. The calculated IR and UV-VIS absorption spectra of the selected complexes will be presented.

References

1. G. W. Gokel, *Chem. Soc. Rev.*, 21 (1992) 39.
2. I. Despotović, manuscript in preparation.

Acknowledgements: The author thank to Zagreb University Computing Centre (SRCE) for generously granting computational resources on the ISABELLA cluster (isabella.srce.hr) and the CRO-NGI infrastructure (www.cro-ngi.hr).

Notes

**Low Temperature
Astrochemistry/Astrophysics
High-Resolution
Time-Resolved**

Formic Acid Dimers in a Nitrogen Matrix¹

Susy Lopes^a, Rui Fausto^a and Leonid Khriachtchev^{b*}

^a CQC, Department of Chemistry, University of Coimbra, Rua Larga, P-3004-535 Coimbra, Portugal

^b Department of Chemistry, University of Helsinki, P.O. Box 55, FI-00014 Helsinki, Finland
susylopes@ci.uc.pt

Formic acid (HCOOH) dimers are studied by infrared spectroscopy in a nitrogen matrix and *ab initio* calculations. The lifetime of the high-energy *cis*-FA in a nitrogen matrix is very long (~11 h) compared with other noble-gas matrices [1]. Due to this stabilization, a large proportion of the *cis* conformer can be produced by vibrational excitation of the lower-energy (*trans*) conformer. Three *trans-trans*, four *trans-cis*, and three *cis-cis* dimers are found in the experiments. The *cis-cis* dimers of formic acid are reported for the first time. Several conformational processes are obtained using selective excitation by infrared light, some of them also for the first time. In particular, we report on the formation of *cis-cis* dimers upon vibrational excitation of *trans-cis* dimers. Tunneling decays of several dimers have been detected in the dark. The tunneling decay of *cis-cis* dimers of formic acid as well as the stabilization of *cis* units in *cis-cis* dimers are also observed for the first time.

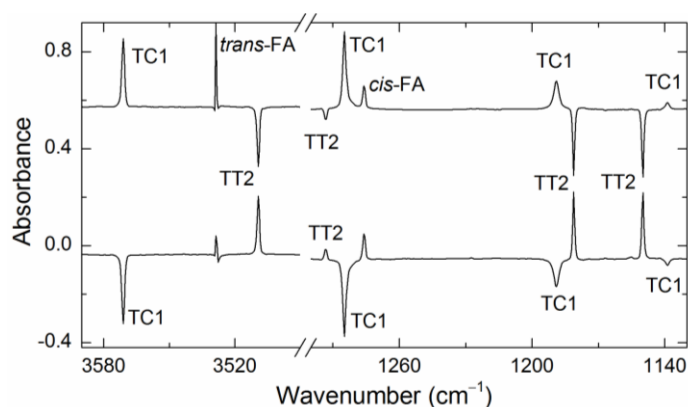


Figure 1 – Light-induced interconversion between the *trans-trans* dimer TT2 and the *trans-cis* dimer TC1 in a nitrogen matrix. The difference spectra show the results of excitation at 6848.8 cm⁻¹ (upper spectrum) and 6969.8 cm⁻¹ (lower spectrum) corresponding to the first overtones of the OH stretching fundamentals at 3509.2 cm⁻¹ (TT2) and 3571.1 cm⁻¹ (TC1), respectively. The spectra were measured at 8.9 K.

References

1. S. Lopes, R. Fausto and L. Khriachtchev, *J. Chem. Phys.*, 148 (2018) 034301.

* In memory of Dr. Leonid Khriachtchev.

Acknowledgements: The authors acknowledge the financial support from the Portuguese “Fundação para a Ciência e a Tecnologia” (FCT) (Post-doctoral Grant ref. SFRH/BPD/77276/2011 and Project PTDC/QEQ-QFI/3284/2014 – POCI-01-0145-FEDER-016617) and from the Academy of Finland through the Project KUMURA (No. 1277993). The Coimbra Chemistry Centre (CQC) is also supported by FCT (Project UI0313/QUI/2013) and COMPETE-UE. We also thank the CSC–IT Center for Scientific Computing Ltd. (Espoo, Finland) for allocation of computer time.

Raman Spectroscopy of Matrix Isolated Complex between Glycolic Acid and Nitrogen: High Overtone Induced Isomerization

Jussi Ahokas^a, Iwona Kosendiak^b, Justyna Krupa^b, Maria Wierzejewska^b and Jan Lundell^c

^a Department of Chemistry and NanoScience Center, P.O. Box 35, 40014 University of Jyväskylä, Finland

^b Faculty of Chemistry, University of Wrocław, Joliot-Curie 14, 50-383, Wrocław, Poland

^c Department of Chemistry, P.O. Box 35, 40014 University of Jyväskylä, Finland

jussi.m.e.ahokas@jyu.fi

Matrix isolation technique combined with Raman spectroscopy provide a suitable method to investigate high overtone induced isomerization and chemistry on the ground electronic states of the molecules [1,2]. The high overtone excitations of the matrix isolated molecules can be generated by the direct absorption of visible light. The photon energy at 532 nm (18797 cm^{-1}) is sufficient to excite fifth overtone manifold of the O-H stretching mode of carboxylic acids. Glycolic acid is the smallest α -hydroxycarboxylic acid containing two OH groups and it is capable to form inter- and intramolecular hydrogen bonds. The near-infrared induced isomerization of glycolic acid has been carefully studied in low temperature matrices [3]. The different near-infrared induced isomerization processes has been found in argon and nitrogen matrices, thus the interaction between glycolic acid and its neighbouring species plays a significant role in the photo-induced isomerization.

In the present investigation, we have studied the high overtone induced isomerization of the complex between glycolic acid and nitrogen in argon matrix. The isomerization kinetics of the complexes will be compared with the isomerization kinetics of glycolic acid and the results will be presented. The Raman spectrum of the complexes between the different glycolic acid conformers and nitrogen will also be presented.

References

1. A. Olbert-Majkut, J. Ahokas, J. Lundell and M. Pettersson, *J. Chem. Phys.*, 129 (2008) 041101.
2. A. Olbert-Majkut, J. Ahokas, M. Pettersson and J. Lundell, *J. Phys. Chem. A*, 117 (2013) 1492.
3. A. Halasa, L. Lapinski, I. Reva, H. Rostkowska, R. Fausto and M. J. Nowak, *J. Phys. Chem. A*, 118 (2014) 5626.

Study of Acetylsalicylic Acid by the Means of Matrix Isolation

Rasa Platakyte and Justinas Ceponkus

Institute of Chemical Physics, Vilnius University, Saulėtekio al. 3, Vilnius 10257, Lithuania

rasa.platakyte@gmail.com

Acetylsalicylic acid (ASA, more commonly known as aspirin) is a non-steroidal anti-inflammatory drug which has been widely used for over 100 years. The molecule itself is an aromatic compound with carboxy and ester groups at the *ortho* positions. Matrix isolation experiments have been previously performed with salicylic acid (SA) but not with ASA [1]. As the vapor pressure of ASA is too low to make the mixture at room temperature it was heated to between 60 °C and 110 °C, searching for the optimal temperature since thermal decomposition occurs by elimination of acetic acid and evaporation of both SA and ASA [2].

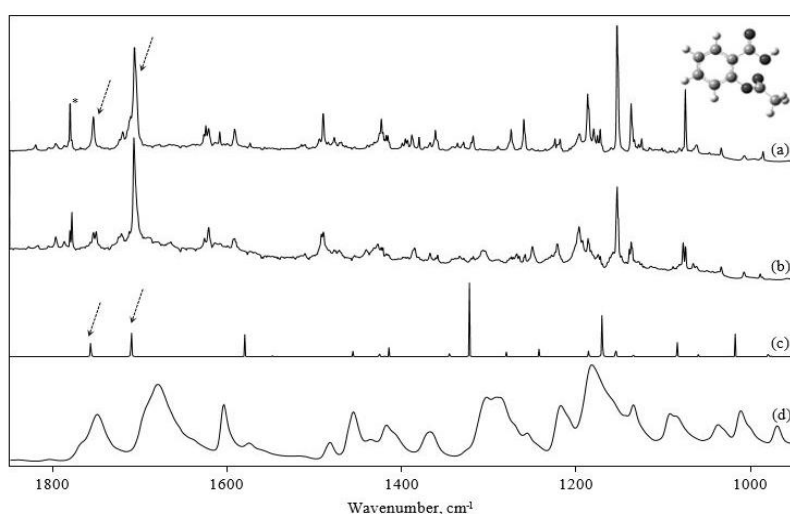


Figure 1. (a) ASA in argon matrix after deposition and (b) heated to 40K, (c) calculated spectrum (B3LYP/6311++G(3df,3pd)), (d) ATR spectrum, *acetic acid ν C=O band.

The best results seem to be obtained by heating the sample to 70 °C (figure 1) even if we still have some amount of acetic acid. The clearest region for the comparison of two molecules is between 1800 cm^{-1} and 1650 cm^{-1} where we can observe C=O stretching vibrations. Acetic acid has a band at 1778 cm^{-1} for its one and only C=O group while ASA has two at 1752 cm^{-1} and 1705 cm^{-1} . The difference corresponds well to the theoretically calculated values of C=O stretching vibrations (1828 cm^{-1} in ester group and 1780 cm^{-1} in carboxy group). Upon heating the deposited sample to 40 K, we can observe splitting of certain bands which does not disappear after cooling the sample back to 10 K. This effect could possibly be due to molecular complex formation with water or conformational changes.

References

1. M. Miyagawa, N. Akai and M. Nakata, *Chem. Phys. Letters*, 602 (2014) 52.
2. Y. Asakura Ribeiro, A. C. F. Caires, N. Boralle and M. Ionashiro, *Termochim. Acta*, 279 (1996) 177.

Acknowledgments: Computations were performed on resources at the High Performance Computing Center “HPC Saulėtekis” in Vilnius University Faculty of Physics.

Photochemistry of Matrix-Isolated 3-(Tetrazol-5-yl)aniline

Magdalena Pagacz-Kostrzewa, Magdalena Sałdyka and Maria Wierzejewska

Faculty of Chemistry, University of Wrocław, Joliot-Curie 14, 50-383 Wrocław, Poland

magdalena.pagacz-kostrzewa@chem.uni.wroc.pl

Tetrazole derivatives have drawn attention of chemists due to their diverse practical applications as environmentally friendly energetic materials and valuable ligands in coordination chemistry forming new topologies and exhibiting interesting properties such as spin-crossover phenomena. However, the most spectacular are applications of tetrazoles in medicine and pharmacy. Many of the medicinal applications of tetrazole derivatives originate from the properties of the tetrazolic acid fragment CN_4H . It has similar acidity to the carboxylic group, is almost allosteric with it, but is metabolically more stable. Hence, the COOH groups are often replaced by the CN_4H fragments in biologically active molecules and the tetrazole ring is found in drugs or potent medicines with diverse pharmacological activity.

From the fundamental point of view, tetrazole derivatives have been found to be challenging molecules due to their interesting structures (tautomers/conformers) and usually rich photochemistry that strongly depend on the specific substituents attached to the ring [1-3].

In this contribution, the molecular structure and photochemistry of 3-(tetrazol-5-yl)aniline (TA) were studied in argon and nitrogen matrices by infrared spectroscopy and B3LYP/6-311++G(2d,2p) calculations. TA exists in two tautomeric forms: *1H* and *2H*. The infrared spectra of TA/Ar and TA/ N_2 show that only *2H*-tautomer is present in low temperature matrices. Phototransformations of the monomeric TA isolated low-temperature matrices were induced by narrow-band UV radiation from the OPO laser system. The monochromatic radiation of the 335 nm wavelength led to the decomposition of the studied compound. The obtained results indicate that the tetrazole ring cleavage and nitrogen elimination take place in the matrices leading to the N-(3-aminophenyl)carbodiimide and (3-aminophenyl)cyanamide formation.

References

1. M. Pagacz-Kostrzewa, J. Krupa and M. Wierzejewska, *J. Phys. Chem. A*, 118 (2014) 2072.
2. M. Pagacz-Kostrzewa, J. Krupa and M. Wierzejewska, *J. Photochem. Photobiol. A*, 277 (2014) 37.
3. M. Pagacz-Kostrzewa, I. D. Reva, R. Bronisz, B. M. Giuliano, R. Fausto and M. Wierzejewska, *J. Phys. Chem. A*, 115 (2011) 5693.

Acknowledgements: The research was supported by the National Science Centre Project No. 2014/13/D/ST4/01741. A grant of computer time from the Wrocław Center for Networking and Supercomputing is gratefully acknowledged.

Photochemistry of Acetohydroxamic Acid in Solid Argon. FTIR and Theoretical Studies

Magdalena Sałdyka

Faculty of Chemistry, University of Wrocław, Joliot-Curie 14, 50-383 Wrocław, Poland
magdalena.saldyka@chem.uni.wroc.pl

Hydroxamic acids (RCONHOH) exhibit a wide spectrum of biological activities that stimulated progress in the chemistry of this class of compounds. They are known to be involved in iron transport phenomena, and are active as antibiotics, antitumor and antifungal agents, and specific enzyme inhibitors [1]. Extensive work has been carried out on the formation of hydroxamic acids, their reactions and structure in the ground state. However, the photochemical properties of hydroxamic acids are still not well recognized. The knowledge of the excited-state behaviour of hydroxamic acids is very important as many of these compounds, on exposure to sunlight, may be transformed to intermediates and photoproducts that are more toxic than parent compounds. According to the literature, photoirradiation of this class of compounds may lead to the initial photolytic scission of the N-O bond or to the acylaminoxyl radical generation [2]. The literature reports on the structural properties of acetohydroxamic acid (AHA) inform that the stability of different conformers of AHA is strongly dependent on the environment. The studies on the tautomeric and structural properties of acetohydroxamic acid showed that AHA trapped from the gas phase into solid argon exists in the matrix predominantly as the 1Z keto isomer with intramolecular hydrogen bond. The 1E keto form is also present in equilibrium with the 1Z keto one, however its population is low with respect to the 1Z keto isomer [3]. The importance of the AHA molecule for pharmaceutical applications triggers questions about the influence of UV-VIS irradiation on the structure and photochemical properties of AHA. The performed irradiation of acetohydroxamic acid isolated in argon matrices with full output of a Xe arc lamp or to 225 nm OPO radiation promotes the isomerization, 1Z \rightarrow 1E, and AHA photodissociation reactions [4]. Four pairs of coproducts are experimentally found in the photolysis, they form the complexes: CH₃OH \cdots HNCO (1), H₂O \cdots CH₃NCO (2), H₂O \cdots CH₃CNO (3) and CO \cdots CH₃NHOH (4). The structures of the complexes were optimized at the MP2 computational level with the aug-cc-pVTZ basis set. Three local minima were predicted for the complex (1), two for the complexes (2) and (3) and four local minima were found for the complex (4). The comparison of the theoretical spectra with the experimental ones allowed to determine the structures of the complexes formed in the matrix. The mechanisms of the reaction channels leading to formation of the four co-products are proposed. It is concluded that the first step in formation of the (1), (2) and (3) complexes is the scission of the N-O bond, whereas the creation of the complex (4) is due to the cleavage of the C-N bond.

References

1. S. P. Gupta (Ed.), *Hydroxamic acids: A unique family of chemicals with multiple biological activities*, Springer-Verlag, Berlin Heidelberg (2013).
2. E. Lipczyńska-Kochany, *Chem. Rev.*, 91 (1991) 477.
3. M. Sałdyka and Z. Mielke, *Vibrational Spectroscopy*, 45 (2007) 46.
4. M. Sałdyka and Z. Mielke, *J. Phys. Chem. A*, 122 (2018) 60.

UV-Induced Conformational Isomerization Study of Matrix-Isolated 2-Amino-5-Chlorobenzoic Acid

Sandra M. V. Pinto^{a,b}, Nihal Kuş^{b,c} and Rui Fausto^b

^a *Scuola Normale Superiore, Piazza dei Cavalieri 7, I-56126 Pisa, Italy*

^b *CQC, Department of Chemistry, University of Coimbra, P3004-535 Coimbra, Portugal*

^c *Department of Physics, Eskişehir Technical University, 26470 Eskişehir, Turkey*
sandra.vieirapinto@sns.it

In this work, 2-amino-5-chlorobenzoic acid (ACIBA) was studied by matrix isolation spectroscopy in argon matrix at 15 K. The molecule has four different conformers, differing by internal rotation about the C–C and C–O bonds. The lowest energy form (O=C–C–C dihedral angle of 0°) was experimentally observed in the IR spectra of the as-deposited ACIBA matrices. UV irradiation at $\lambda > 234$ nm of the matrix-isolated compound was found to lead to conversion of this conformer into the other conformers and also to decarboxylation of the compound, with production of CO₂ and 2-amino-5-chlorobenzene (ACIB), whose vibrational signatures could be identified in the spectra of the photolysed matrix.

The analysis of the experimental data on matrix isolated ACIBA was supported by extensive quantum chemical calculations.

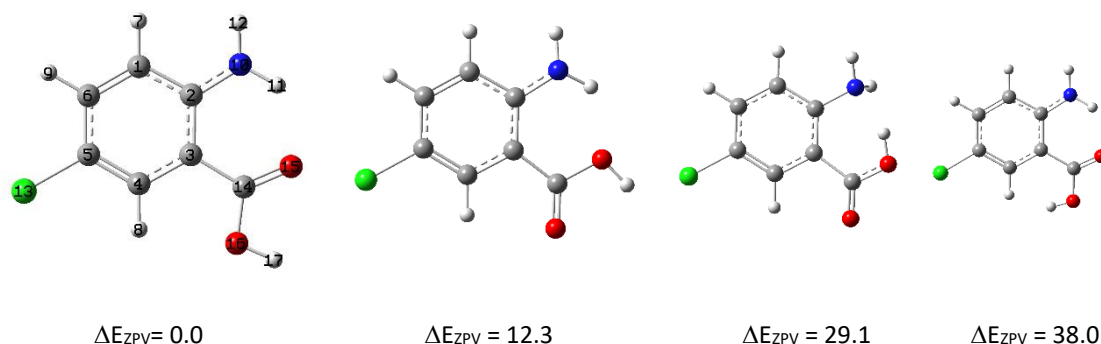


Figure 1 – Conformers of ACIBA. Conformer I corresponds to the lowest energy form. (Relative energies are given in kJ mol⁻¹).

Acknowledgements: These studies were supported by Anadolu University Commission of Scientific Research Project under Grant no. 1705F407. The Coimbra Chemistry Centre (CQC) is supported by FCT, through the project UI0313/QUI/2013, also co-funded by FEDER/COMPETE 2020-EU.

Structural and Spectroscopic Properties of Weak Complexes of Atmospheric Relevance

Justyna Krupa and Maria Wierzejewska

University of Wrocław, Faculty of Chemistry, 14 F. Joliot-Curie str., 50-383 Wrocław, Poland

justyna.krupa@chem.uni.wroc.pl

Weak interactions are important for understanding properties of matter including gas phase, liquid and solid state [1,2]. Many physical and chemical processes are governed by non-covalent interactions characterized by binding energy typically less than 80 kJ mol^{-1} . Molecular complexes are considered to contribute into gas-phase chemistry of interstellar media and planetary atmospheres [3,4]. Isothiocyanic acid (HNCS) and isocyanic acid (HNCO) are well known as interstellar molecules and were detected in the rich molecular cloud Sagittarius B2 (Sgr B2) [5,6].

In this contribution, we present results of theoretical and experimental studies of complexes formed by HNCS [7] and HNCO with sulfur dioxide. As the main experimental method matrix isolation (MI) combined with the infrared spectroscopy (FTIR) was used. MI-FTIR is an established technique for studying weak molecular complexes providing valuable spectroscopic and structural information. Data obtained for the complex isolated in low temperature inert matrix are the best available approach to the complex in the gas phase. The experimental studies are supported by theoretical calculations at the MP2 and B3LYPD3 levels with the 6-311++G(3df,3pd) basis set.

Five different structures of the 1:1 stoichiometry were optimized for both HNCS \cdots SO₂ and HNCO \cdots SO₂ systems. Three of them involve a weak N-H \cdots O hydrogen bond whereas two other geometries are stabilized by van der Waals interactions of various types. The HNCS/SO₂/Ar and HNCO/SO₂/Ar spectra analysis evidences that at least one of the three hydrogen bonded structures is present in freshly deposited matrices. Changes observed in the spectra upon annealing of the matrices are discussed as well.

References

1. Y. Cheng, Y. Qi, Y. Tang, Ch. Zheng, Y. Wan, W. Huang and R. Chen, *J. Phys. Chem. Lett.*, 7 (2016) 3609.
2. M. T. Rodgers and P. B. Armentrout, *Chem. Rev.*, 116 (2016) 5642.
3. A. A. Vigasin and Z. Slanina (Eds.), *Molecular Complexes in Earth's, Planetary, Cometary, and Interstellar Atmospheres*, World Scientific Publishing Co. Pte. Ltd., Singapore, 1998.
4. V. Vaida, *J. Chem. Phys.*, 135 (2011) 020901.
5. L. E. Snyder and D. Buhl, *Astrophys. J.*, 177 (1972) 619.
6. M. A. Frerking, R. A. Linke and P. Thaddeus, *Astrophys. J.*, 234 (1979) L143.
7. J. Krupa and M. Wierzejewska, *Spectrochim. Acta A*, 183 (2017) 144.

Acknowledgements: The research was supported by the National Science Centre Project No. 2013/11/B/ST4/00500. A grant of computer time from the Wrocław Center for Networking and Supercomputing is gratefully acknowledged.

FTIR, DFT and MP2 Studies on Glycolic Acid Nitrogen Complexes

Iwona Kosendiak^a, Jussi Ahokas^b, Justyna Krupa^a, Jan Lundell^b and Maria Wierzejewska^a

^a Faculty of Chemistry, F. Joliot-Curie 14, 50-383 Wrocław, University of Wrocław, Poland

^b University of Jyväskylä, Department of Chemistry, FI-40014 Jyväskylä, Finland

iwona.kosendiak@chem.uni.wroc.pl

Glycolic acid (hydroxyacetic acid, GA) is the primary representant of the α -hydroxy carboxylic acids. GA monomeric structures and their occurrence in the gas phase have been already described by means of quantum mechanical calculations and matrix isolation technique coupled with infrared spectroscopy. Three most stable conformers (SSC, GAC and AAT) were identified in argon matrix after deposition [1-3].

In this contribution the molecular structure of GA complexes with nitrogen have been studied in low temperature argon matrices by means of FTIR spectroscopy and theoretically at the MP2/6-311++G(2d,2p) and DFT B3LYP/6-311++G(2d,2p) levels. The calculations carried out for the nitrogen complexes of SSC, GAC, AAT monomers revealed presence of 9 and 11 stable structures for GA:N₂ 1:1 and 1:2 ratio, respectively. In all these minima N₂ is joined to monomers by the O-H \cdots N or C-H \cdots N hydrogen bonds. Analysis of the obtained spectra and wavenumber shifts of GA modes compared to the theoretical predictions allowed to conclude which of these structures were present in argon matrices.

References

1. I. Reva, S. Jarmelo, L. Łapiński and R. Fausto, *J. Phys. Chem. A*, 108 (2004) 6982.
2. I. Reva, S. Jarmelo, L. Łapiński and R. Fausto, *Chem. Phys. Lett.*, 389 (2004) 68.
3. D. K. Havey, K. J. Feierabend, K. Takahashi, R. T. Skodje and V. Vaida, *J. Phys. Chem. A*, 110 (2006) 6439.

Acknowledgements: The research was supported by the National Science Centre Project No. 2013/11/B/ST4/00500. A grant of computer time from the Wrocław Center for Networking and Supercomputing is gratefully acknowledged. The work was supported by Academy of Finland research project “Vibrational excitation induced chemistry” (Proj.No 286844).

IR Spectroscopy of Acetic Acid Dimers in Helium Nanodroplets

Julia A. Davies^a, Magnus W. D. Hanson-Heine^b, Nicholas A. Besley^b, Shengfu Yang^a
and Andrew M. Ellis^a

^a Department of Chemistry, University of Leicester, University Road, Leicester, LE1 7RH, UK

^b School of Chemistry, University of Nottingham, University Park, Nottingham, NG7 2RD, UK
jad63@le.ac.uk

Dimers of carboxylic acids are classic examples of hydrogen bonded structures. The well-known cyclic dimer of *trans* acetic acid (AA), which contains two strong O–H···O=C bonds, is the lowest energy structure and is prevalent in the gas phase. However, in the crystalline state, one strong O–H···O=C and one weak C–H···O=C bond form between adjacent AA molecules resulting in the formation of catemer chains, which link together to form extended structures [1]. We aim to gain an insight into the pairing of hydrogen bonds within catemer chains by preparing the dimeric repeating unit in liquid helium nanodroplets at ~0.37 K, which we subsequently probe using IR depletion spectroscopy [2].

Figure 1 shows an IR depletion spectrum that was measured by monitoring the change in ion signal detected by a mass spectrometer as the IR wavelength was scanned. The spectrum is dominated by three IR features at 3292, 3429 and 3578 cm⁻¹ and these are assigned to bound and free OH stretching modes in two metastable dimers of *trans* AA. The structures of these dimers are presented in Fig. 1 and were calculated at the MP2/6-311(2+,2+)G(2d,2p) level of theory. The most abundant dimer, which is shown on the left, has the same hydrogen bonding motif as the catemer, whilst the dimer on the right looks remarkably similar apart from the location of the carboxyl hydrogen on the second AA molecule.

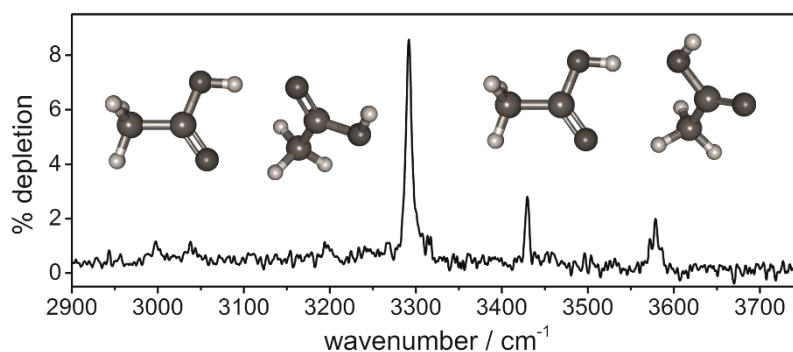


Figure 1 – Experimental IR spectrum for *trans* acetic acid dimers formed inside helium nanodroplets along with calculated structures for the two assigned metastable dimers.

The mechanism by which the two metastable dimers are formed inside helium nanodroplets will be presented, along with quantitative information on the pairs of hydrogen bonding interactions of fundamental importance to the crystalline structure of AA.

References

1. C. Rovira and J. J. Novoa, *J. Phys. Chem. B*, 105 (2001) 1710.
2. M. I. Sulaiman, S. Yang and A. M. Ellis, *J. Phys. Chem. A* 121 (2017) 771.

Acknowledgements: The authors wish to thank the Leverhulme Trust for providing financial support (grant number RPG-2016-308) for this work.

Chemistry Triggered by Infrared Vibrational Excitation – A Case Study of Thiourea

Sándor Góbi, Cláudio M. Nunes, Igor Reva and Rui Fausto
CQC, Department of Chemistry, University of Coimbra, 3004-535, Coimbra, Portugal
sgobi@qui.uc.pt

Proton transfer processes in thiourea isolated in an argon matrix at low temperature are already well studied. Irradiating UV light ($\lambda < 300$ nm) induces an intramolecular proton-transfer reaction. The initial isomer of thiourea (**I**, thione tautomeric form) converts into its thiol tautomer with both *anti* (*a-II*) and *syn* (*s-II*) conformations. Keeping this sample at 10 K and in darkness the reverse reaction (proton tunneling) takes place, leading to the conversion of *a-II* into the precursor **I**. [1,2] Moreover, according to quantum chemical computations, the NIR irradiation of *a-II* should lead to vibrationally activated tunneling to **I** or induce an over-the-barrier transformation to *s-II*. Therefore, after the generation of *a-II*, the matrix was irradiated at frequencies corresponding to the overtones and combination bands of this isomer in order to confirm the theoretical results and to observe the formation of **I** and *s-II*.

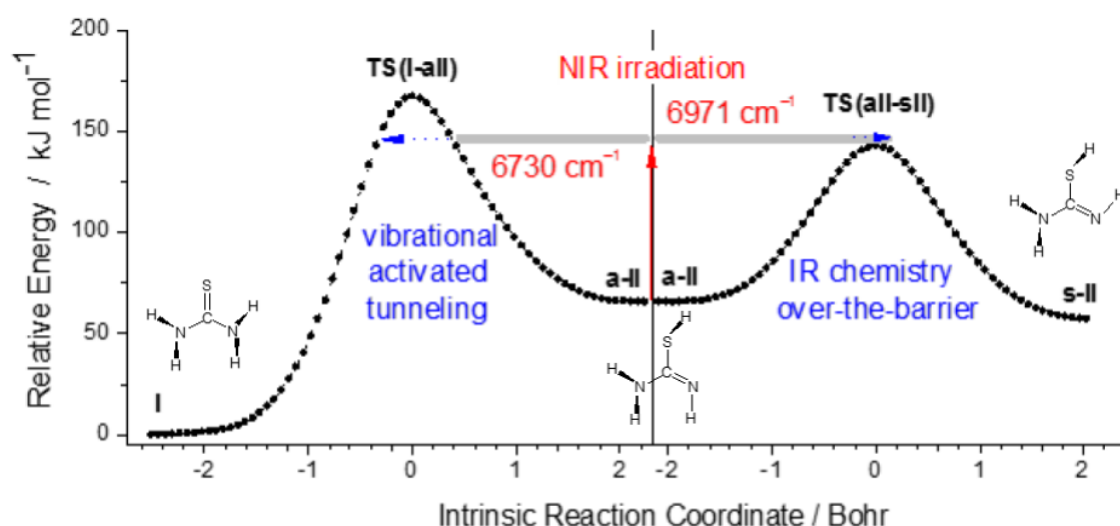


Figure 1 – Potential energy surface for the conversion of *anti-II* into **I** and *syn-II*.

References

1. H. Rostkowska, L. Lapinski, A. Khvorostov and M. J. Nowak, *J. Phys. Chem. A*, 107 (2003) 6373.
2. H. Rostkowska, L. Lapinski and M. J. Nowak, *Phys. Chem. Chem. Phys.*, 20 (2018) 13994.

Acknowledgements: The authors thank the projects PTDC/QEQ-QFI/3284/2014, POCI-01-0145-FEDER-016617, and POCI-01-0145-FEDER-028973 funded by FCT (Lisbon) and COMPETE 2020-EU. The CQC is supported by FCT (Project UI0313/QUI/2013), also co-funded by FEDER/COMPETE 2020-EU. Funding is also acknowledged from the Project “LaserLab – Portugal – Roadmap for the Portuguese Scientific Infrastructures of Strategic Interest” (Project 22124, co-funded by the EU-COMPETE) through the “Programa Operacional Regional do Centro” (CENTRO2020).

Jet-Cooled Laser Induced Fluorescence and Dispersed Fluorescence of $\text{CH}_x\text{F}_{3-x}\text{CH}_2\text{O}$ ($x=1, 2, 3$) Radicals

György Tarczay, Benedek Koncz, Gábor Bazsó and Kristóf Hegedűs
Institute of Chemistry, Eötvös University, PO Box 32, H-1518, Budapest 112, Hungary
tarczay@caesar.elte.hu

Hydrofluorocarbons (HFCs) are commonly used as refrigerants, solvents, propellants, and for etching in semiconductor industry. Their industrial production largely increased in the late 1980s, because the Montreal Protocol has phased out the production of chlorofluorocarbons (CFCs) that largely contributed to the depletion of Earth's ozone layer. Although HFCs do not have ozone depletion potential (ODP), it has turned out that these compounds can largely contribute to the global warming. For example, the compounds of monofluoro ethane (R161), 1,1-difluoro ethane (R152a), and 1,1,1-trifluoro ethane (R143a) have zero ODP, while their global warming potentials (GWP, as compared to CO_2) are 12, 124, and 4470 [1]. In addition, each of these compounds is relatively stable in the atmosphere, especially 1,1,1-trifluoro ethane, that has an atmospheric lifetime of 40–52 years [1,2]. Realizing this problem, more than 150 nations have agreed in 2016 to cut back their HCF use from 2019. Even if their production would drastically decrease in the next few years, due to their long atmospheric lifetime, CFCs will pollute the atmosphere for decades.

As hydrocarbons, HFCs decompose in the atmosphere by reacting with hydroxyl radical (OH). In the first step of this reaction a fluorohydrocarbon radical is formed (1), which in subsequent reactions with O_2 and then with NO yields fluorinated alkylperoxy (2), and fluorinated alkoxy radicals (3) [3]. Therefore, to understand the details of these atmospheric reactions and to monitor these species in the gas phase, first the structure and the spectra of these species have to be studied and analyzed. The purpose of the present work was to spectroscopically characterize β -monofluoro- (MFEO), β,β -difluoro (DFEO), and β,β,β -trifluoro ethoxy (TFEO) radical by moderate resolution LIF and DF spectroscopy. We also analyze the tendencies in structural and spectroscopic properties as the function of fluorine atom, which can help to understand the reactivity and therefore the atmospheric lifetime of these species.

References

1. P. Forster, V. Ramaswamy, P. Artaxo, T. Berntsen, R. Betts, D. W. Fahey, J. Haywood, J. Lean, D. C. Lowe, G. Myhre, J. Nganga, R. Prinn, G. Raga, M. Schulz and R. Van Dorland (2007). "Chapter 2: Changes in Atmospheric Constituents and in Radiative Forcing". In S. Solomon, H. L. Miller, M. Tignor, K. B. Averyt, M. Marquis, Z. Chen, M. Manning and D. Qin, *Climate Change 2007: The Physical Science Basis. Contribution of Working Group I to the Fourth Assessment Report of the Intergovernmental Panel on Climate Change*. Cambridge, United Kingdom and New York, NY, USA: Cambridge University Press.
2. R. G. Derwent, A. Volz-Thomas and M. J. Prather, World Meteorological Organization Global Ozone Research Project, Report No. 20, *Sci. Asses. Stratosph. Ozone 2* (1989) 124.
3. O. J. Nielsen, E. Gamborg, J. Sehested, T. J. Wallington and M. D. Hurley, *J. Chem. Phys.* 98 (1994) 9518.

Acknowledgements: The work was supported by the Hungarian Scientific Research Fund (OTKA K108649).

Matrix Isolation Studies of Nickel Fluorides

Ahmed K. Sakr, Howard V. Snelling and Nigel A. Young

Departments of Chemistry and Physics, The University of Hull, Hull, HU6 7RX, UK

A.A.Sakr@2015.hull.ac.uk

Nickel is commonly found in its +2 oxidation state, but higher oxidation state compounds are known. In the case of the fluorides, NiF₂ is well known in the solid and vapour phase, NiF₃ in the solid state is mixed valence (Ni²⁺[Ni⁴⁺F₆]), and NiF₄ is unstable above –65 °C. This study focuses on the molecular properties of the nickel fluorides species. It is looking at vapour phase species using matrix isolation techniques to stabilise the NiF_n species formed. The studied compounds were made by reacting metal atoms of Ni with different concentration of F₂/Ar in the gas phase and condensation at *ca.* 10 K. Nickel metal atoms are thermally generated by heating a filament of pure nickel. The characterisation is conducted by UV-Vis and IR spectroscopy [1]. Photolysis and annealing of the matrix were carried out. Although NiF₂ is well studied in rare gas matrices [2-5], there are no reports of molecular matrix isolated NiF, NiF₃ or NiF₄.

Computational calculations using B3LYP/6-311+G(d) and B3LYP/def2tzvpp within G09W have been used to help assign the spectral features and determine the molecular geometry of each of NiF, NiF₂, and probably NiF₄ molecules formed.

References

1. A. J. Bridgeman, G. Cavigliasso, N. Harris and N. A. Young, *Chem. Phys. Lett.*, 351 (2002) 319.
2. J. W. Hastie, R. H. Hauge and J. L. Margrave, *J. Chem. Soc. D.*, 24 (1969) 1452.
3. J. W. Hastie, R. H. Hauge and J. L. Margrave, *High Temp. Sci.*, 1 (1969) 76.
4. D. A. Van Leirsburg and C.W. DeKock, *J. Phys. Chem.*, 78 (1974) 134.
5. V. N. Bukharina, A. Y. Gerasimov, Y. B. Predtechenskii and V. G. Shklyarik, *Opt. Spektrosk.*, 65 (1988) 876.

Acknowledgements: I would like to thank the University of Hull for funding my PhD, as well as my supervisors for all of their support.

Rotationally Resolved Electronic Spectrum of N-MethylCarbazole in the Gas Phase: A Study of Methyl Group Internal Rotation

José Arturo Ruiz-Santoyo^a, Sergio Augusto Romero-Servín^a, John T. Yi^b,
Josué Adin Minguela-Gallardo^a and Leonardo Álvarez-Valtierra^a

^a Division of Sciences and Engineering, Campus León, University of Guanajuato 37150, Mexico

^b Department of Chemistry, Winston-Salem State University, Winston-Salem, North Carolina 27110, USA
leoav@fisica.ugto.mx

Rotationally resolved fluorescence excitation spectrum of the origin band in the $S_1 \leftarrow S_0$ transition of N-MethylCarbazole has been recorded in the collision-free environment of a molecular beam, using High Resolution Laser Induced Fluorescence (HRLIF) technique.

N-MethylCarbazole is a fascinating molecule. It is a planar molecule and its symmetry leads to study of an internal potential of six-fold symmetry. While the barriers to such rotation are often small, methyl groups can have profound effects on intramolecular dynamics. So, due the very low barrier, the potential barrier can be treated as a perturbation. Our interest is on learning about the effect due to the bond among nitrogen atom and the torsional barrier height of the $-CH_3$ group in N-MethylCarbazole molecule, in both S_0 and S_1 states.

Inertial parameters determined from the spectral analysis performed on this molecular system such as rotational constants and the potential energy curves of the internal rotation of the methyl group, in both electronic states, will be discussed in this talk.

The change of the barrier height by electronic excitation in N-MethylCarbazole, where the nitrogen is present, will be compared with other toluene derivatives in terms of the internal rotational motion of the attached $-CH_3$ group where the bond is given with a carbone atom.

References

1. W. A. Majewski, J. F. Pfanstiel, D. F. Plusquellic, and D. W. Pratt, in *Laser Techniques in Chemistry*, edited by T. R. Rizzo and A. B. Myers (John Wiley & Sons, New York, 1995), p. 101.
2. David R. Borst and David W. Pratt. *J. Chem. Phys.*, 113 (2000) 3658.
3. J. A. Ruiz-Santoyo, J. Wilke, M. Wilke, J. T. Yi, D. W. Pratt, M. Schmitt and L. Álvarez-Valtierra. *J. Chem. Phys.* 144 (2016) 044303.
4. K. Okuyama, N. Mikami and M. Ito, *J. Phys. Chem.*, 89 (1985) 5617.

Acknowledgements: The authors thank to “DFG-Conacyt research grant 277871 for the financial support to develop this work”. Also, the authors are very grateful to the research group of High Resolution Molecular Spectroscopy of Universität Düsseldorf and its leader, Professor Dr. Michael Schmitt.

Rotationally Resolved Electronic Stark Spectroscopy of 3-Cyanoindole and the 3-Cyanoindole-Water Complex

Michael Schneider, Marie-Luise Hebestreit, Christian Henrichs and Michael Schmitt
Heinrich-Heine-Universität, 40225 Düsseldorf, Germany
m.schneider@hhu.de

The electronic origin of 3-cyanoindole has been investigated using high resolution laser induced fluorescence spectroscopy (HRLIF) to analyse its electronic nature. By means of evolutionary algorithms, molecular parameters like the rotational constants in the electronic ground and first excited state and the orientation of the transition dipole moment were determined. To investigate the permanent dipole moments in the ground and first excited state a homogeneous static electric field was applied, which lifts the M degeneracy by the Stark effect and results in band splittings and shifts.

To understand how solvation influences the electronic nature of the excited state, the binary 3-cyanoindole water cluster was investigated. The different molecular parameters were used to assign the band to optimized CC2-pVTZ structures by comparing the experimental and calculated *ab initio* values.

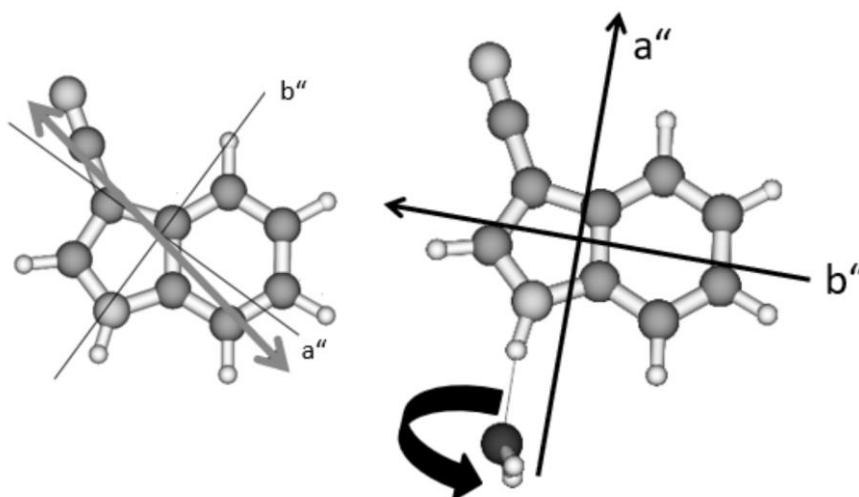


Figure 1 – 3-Cyanoindole and its water cluster within their main inertial axes.

Observation of 1,2-, 1,3- and 1,4-Dimethoxybenzenes *via* High Resolution Laser Induced Fluorescence Stark Spectroscopy

Marie-Luise Hebestreit, Michael Schneider, Christian Henrichs and Michael Schmitt
Heinrich-Heine-Universität, Physikalische Chemie I, Universitätsstraße 1, 40225 Düsseldorf, Germany
Marie-Luise.Hebestreit@hhu.de

The different rotamers of 1,2-, 1,3- and 1,4-dimethoxybenzene were investigated using high resolution laser induced fluorescence spectroscopy. The molecular parameters, obtained from fit using an evolutionary strategies were compared to the results of *ab initio* calculations and used for structural assignment. To investigate the permanent dipole moments in the ground and first electronically excited singlet state, a homogeneous field was applied, which lifts the M degeneracy by the Stark effect. The resulting experimental permanent dipole moments were compared to predicted dipole moments via vectorial addition of the anisole dipoles and to the results of *ab initio* calculations.

Finally, the conformational space of 1,3-dimethoxybenzene is discussed in particular.

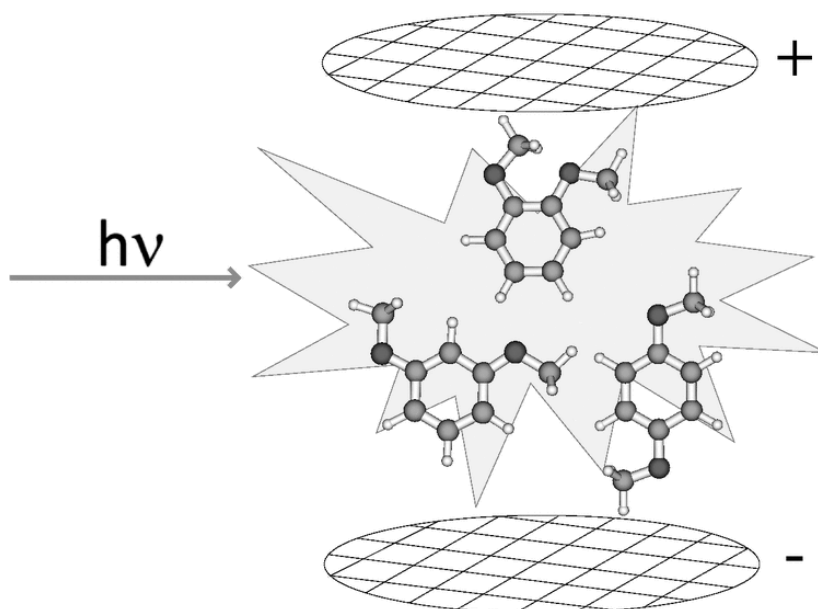


Figure 1 – Graphical Abstract observation of 1,2-, 1,3- and 1,4-dimethoxybenzenes *via* high resolution laser induced fluorescence Stark spectroscopy.

References

1. M. Schneider, M. Wilke, M.-L. Hebestreit, J. A. Ruiz-Santoyo, L. Álvarez-Valtierra, J. T. Yi, W. L. Meerts, D. W. Pratt and M. Schmitt, *Phys. Chem. Chem. Phys.*, 19 (2017) 21364.
2. M. Schneider, M. Wilke, M.-L. Hebestreit, C. Henrichs, W. L. Meerts and M. Schmitt, *ChemPhysChem.*, 19 (2018) 307.

Electronic Spectra of 1,2 Dimethoxybenzene

Christian Henrichs, Marie-Luise Hebestreit, Michael Schneider and Michael Schmitt
Heinrich-Heine-Universität Düsseldorf, Physikalische Chemie 1, Universitätsstrasse 1, Germany
christian.henrichs@uni-duesseldorf.de

The structural changes of 1,2 dimethoxybenzene upon excitation to the lowest electronically excited singlet state are interesting, since its two rotamers behave differently upon electronic excitation. We investigated these structural changes of 1,2 dimethoxybenzene using a combination of high resolution laser induced fluorescence spectroscopy (HRLIF) and vibronically resolved fluorescence emission spectroscopy. The HRLIF spectra yield the rotational constants of the ground and in the first excited state, which are not sufficient for a complete structural determination. The problem of fitting structural changes of 3N-6 geometry parameters to a set of only 3 rotational constants can be resolved using additional information from complementary experiments. With the aid of Franck-Condon (FC) analyses using a normal mode analysis based on the CC2/cc-pVTZ optimized structures we were able to fit the relevant parameters both to the FC intensities as well as to the rotational constants.

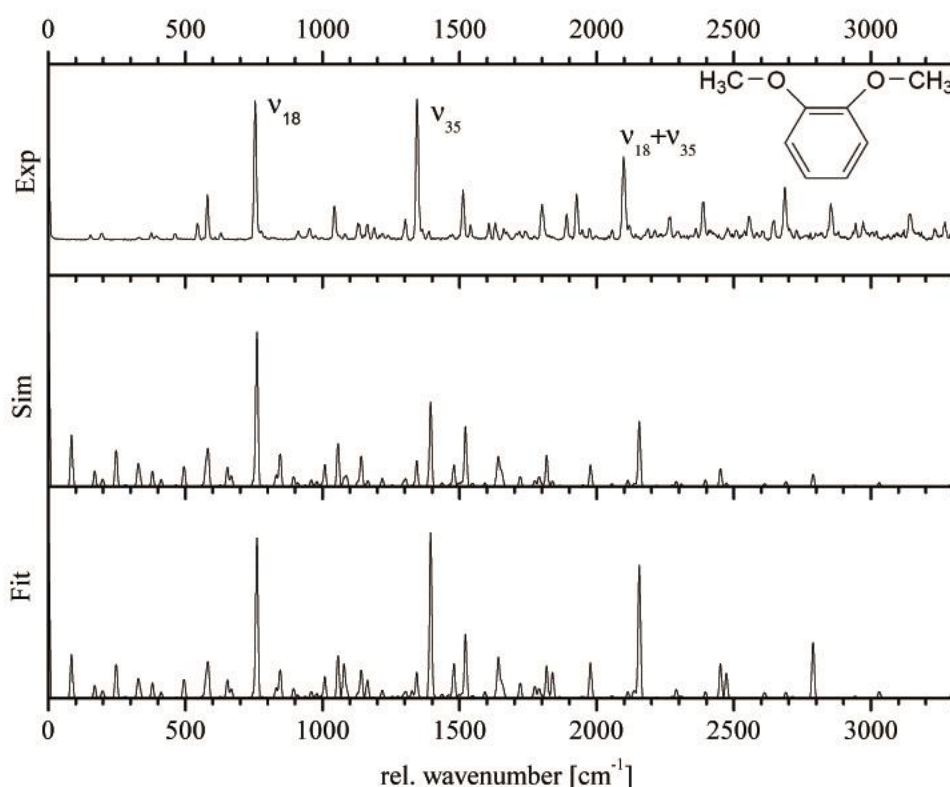


Figure 1 – Dispersed fluorescence spectrum of the electronic origin (1st trace: Experimental spectrum, 2nd trace: Simulated spectrum, 3rd trace: Fit spectrum).

Photophysics of 2-[4-(Dimethylamino)benzylidene]malononitrile in Ionic Liquids Probed by Time Resolved Infrared Spectroscopy

Rômulo A. Ando^a, Lisa N. Q. Nguyen^a and Terry L. Gustafson^b

^aLaboratório de Espectroscopia Molecular, Instituto de Química, Departamento de Química Fundamental, Universidade de São Paulo, 05508-000, São Paulo, Brazil

^bDepartment of Chemistry and Biochemistry - The Ohio State University - 2104 Newman & Wolf from Laboratory, 43210, Columbus, OH, USA
raando@iq.usp.br

Benzylidene malononitriles are commonly used as molecular spectroscopic probes to investigate solvent properties [1]. The molecule 2-[4-(dimethylamino)benzylidene] malononitrile (DMN – Figure 1) is an archetypal “push-pull” chromophore presenting a huge change of dipole moment within the $S_0 \rightarrow S_1$ electronic transition. Fluorescence investigations in different media indicate that the relaxation from S_1 state may involve the internal rotation by three distinct nonradiative deactivation channels (represented by the curved arrows in Figure 1) [2]. Although the reaction mechanism is still controversial, the reaction rate is demonstrated to be solvent dependent, and can be used to measure the solvent friction [2]. In this work we used time-resolved infrared spectroscopy (TRIR) to investigate the photophysics of DMN in a series of conventional solvents and ionic liquids in order to have a deep understanding of the DMN reaction mechanism and how its rate depends on solvent properties. Figure 1 shows preliminary TRIR spectra of DMN in acetone and in the ionic liquid 1-butyl-3-methylimidazolium bis(trifluoromethylsulfonyl)imide, $[C_4C_1][NTf_2]$, illustrating the distinct time evolution behavior of the bands assigned to the $\nu(CN)$ stretching of the charge transfer state and the respective rotational isomer.

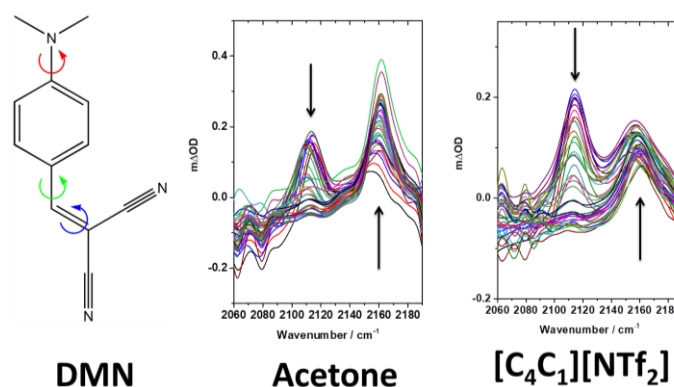


Figure 1 – Structure of DMN and TRIR spectra in different solvents obtained from 0 to 3000 ps. The arrows indicate the concomitant decreasing and increasing of the bands with time.

References

1. A. M. Kelley, *Int. J. Quantum Chem.*, 104 (2005) 602.
2. H. Jin, M. Liang, S. Arzhantsev, X. Li and M. Maroncelli, *J. Phys. Chem. B*, 114 (2010) 7565.

Acknowledgements: The authors thank FAPESP 2015/24818-8 for the financial support and Barbara Dunlap for the assistance in the TRIR experiments.

Time Resolved Spectroscopic Temperature Measurement Techniques During CW-Laser Matter Interaction of Glass–Fiber-Reinforced-Polymers (GFRP)

Hartmut Borchert, Vadim Allheily, Lionel Merlat, Jens Kokot and Rüdiger Schmitt
*French-German Research Institute of Saint-Louis, 5 rue du Général Cassagnou, BP 70034,
 68301 Saint-Louis, France
 hartmut.borchert@isl.eu*

Composite materials (GFRP) have shown a significant increase in their use for aerospace and military applications in recent years. Concurrent maturation of the technology in near Infrared High Energy Lasers has proven to be promising for use in directed energy weaponry. The binding matrix of many common aerospace composite materials are made of polymeric materials. The thermodynamics of GFRP as well as the thermo-mechanical behavior of such heterogeneous materials submitted to a typical laser weapon irradiation need therefore to be further explored to understand precisely the deterioration process induced by the illumination.

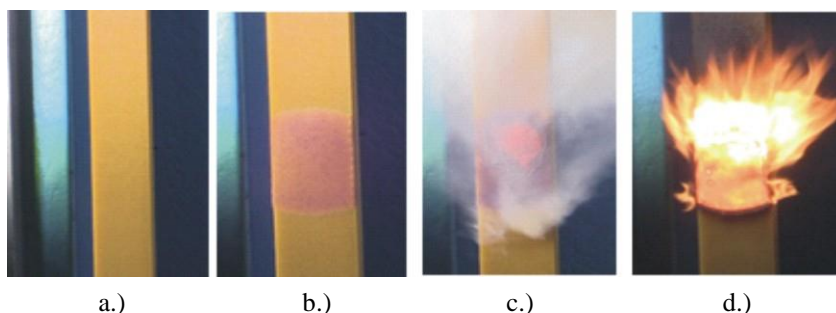


Figure 1 – Glass-Epoxy, Hexcel-7581-M21, P=2500W, t = 5 s.

In Fig. 1 front views at different time delays clearly evidence the complicated nature of smoky plume and flame combustion creation during the irradiation process [1]. During the energy deposition rise of the continuous laser wave, the GFRP target heats up due to absorption in the outer epoxy layer (Fig. 1.b). Further increase of the energy reveals a smoky plume optically thin directly above the surface of the GFRP-target (Fig. 1.c and 1.d). Time resolved emission spectroscopy was used to investigate the chemical decomposition and surface temperature in the low and high temperature regime during the laser matter interaction process [2]. The spectral emission in the visible range is dominated by continuum emission which provides the distribution temperature in time based on Planck's law. In the low temperature regime (infrared wavelength bands from 2 μm up to 14 μm) a four channel infrared detector system was designed to retrieve the distribution temperature. The experimental, time resolved signal from four different infrared detectors at center wavelengths of 3,348 μm , 4,49 μm , 7,41 μm and 10,57 μm are used to reconstruct the Planck-function by a fitting routine with the temperature as parameter. The calibration of the system was made with a conventional Black-body source PY5. The obtained temperature distribution in time was then compared to measurements with a conventional pyrometer. With the concept of this four channel detector we overcome the difficulties of acquisition speed and single band nature of conventional pyrometers.

References

1. C. Th. Alkemade, *Fundamentals of analytical flame spectroscopy*, Hilger Bristol, 1972.
2. V. Allheily, L. Merlat, F. Lacroix, A. Eichhorn and G. L'Hostos, *Phys. Procedia*, 83 (2016) 1044.

Ultrafast Transient Absorption Spectroscopy: Probing the Excited State Dynamics of Charge Transfer Reactions in Ionic Deep Eutectic Solvents

Anuradha Das, Egmont J. Rohwer and Thomas Feurer

¹*Institute of Applied Physics, University of Bern, Sidlerstrasse 5, CH-3012 Bern, Switzerland
anuradha.das@iap.unibe.ch*

Ultrafast excited state dynamics of 4-(N, N' dimethylamino) benzonitrile [DMABN] has been investigated in a deep eutectic solvent (DES) consisting of (0.75 Acetamide + 0.25 Potassium thiocyanate) using transient absorption spectroscopy on the femtosecond-picosecond timescale (Fig. 1a). Subsequently measured reaction times of the photoexcited intramolecular charge transfer molecule (DMABN) in the DES have been compared with reaction times obtained from conventional solvents like n-hexane and acetonitrile (Fig. 1b). A strong dynamic solvent control over reaction time is noticed in DES. From steady state fluorescence, a dual emission from the locally excited (LE) and intramolecular charge transfer (CT) states of the molecule has been observed in DES, similar to polar solvents. The distribution of dual emission (LE/ CT) as well as the reaction time changes considerably in the studied temperature range. The observed change at higher temperature is an effect of faster rotation of the N(Me₂)-CH bond of DMABN [1,2]. The LE/CT ratio and position change with excitation wavelength, which is due to the presence of microheterogeneous domains in DES.

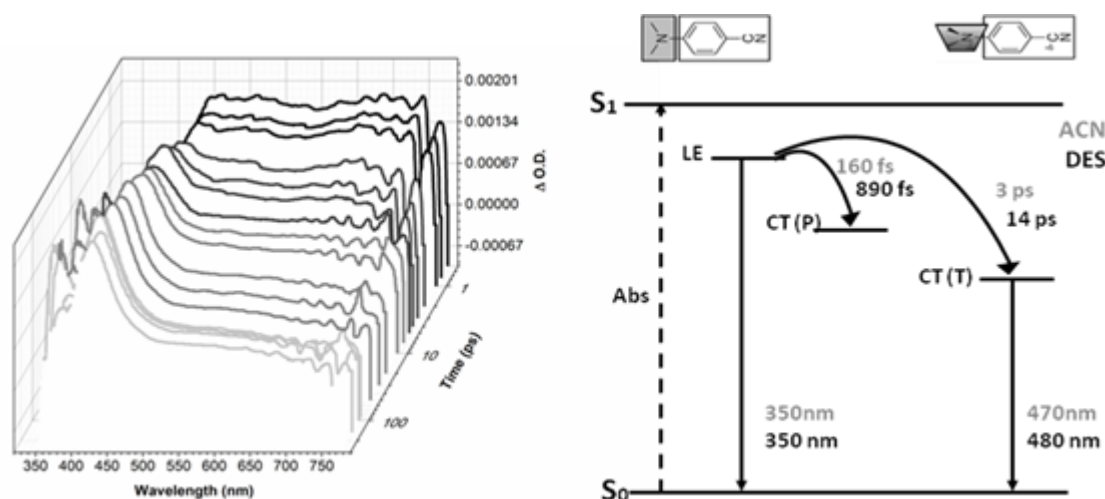


Figure 1 – (a) Representative selection of transient absorption (TA) spectra at different time delays
(b) Schematic of intramolecular charge transfer pathways of DMABN in acetonitrile (ACN) and in deep eutectic solvent.

References

1. S. I. Druzhinin, N. P. Ernsting, S. A. Kovalenko, L. P. Lustres, T. A. Senyushkina and K. A. Zachariasse, *J. Phys. Chem. A*, 110 (2006) 2955.
2. T. Fujiwara, M. Z. Zgierski and E. C. Lim, *Phys. Chem. Chem. Phys.*, 13 (2011) 6779.

Acknowledgements: The authors thank Swiss NSF and NCCR-MUST for the funding.

Photoinduced Relaxation Dynamics of Ferricyanide Ion Dissolved in Ionic Liquid Studied by Ultrafast XUV Photoelectron Spectroscopy

Nataliia Kuzkova^{a,b}, Christoph Merschjann^{a,b} and Igor Yu. Kiyan^a

^a*Institute of Methods for Material Development, Helmholtz-Zentrum Berlin, Albert-Einstein-Straße 15, 12489 Berlin, Germany*

^b*Department of Physics, Freie Universität Berlin, Arnimallee 14, 14195 Berlin, Germany*
nataliia.kuzkova@helmholtz-berlin.de

Revealing the electron dynamics in the light-harvesting systems after photoexcitation is the key to understanding and to optimization of their function in catalytic and photovoltaic applications. Here, femtosecond time-resolved XUV photoelectron spectroscopy (PES) was applied to monitor the relaxation dynamics following optical ligand-to-metal charge transfer excitation of ferricyanide ion, $[\text{Fe}(\text{CN})_6]^{3-}$, dissolved in ionic liquid (IL). The 1-ethyl-3-methylimidazolium dicyanamide ([emim][DCA]) was used as the solvent. By measuring transient photoemission signal of the primary and subsequently populated electronic states, we could follow the electron dynamics with a sub-100 fs time resolution and identify the relaxation pathway on the absolute scale of electron binding energies.

This work is especially aimed at studying how the solvent affects the photoinduced electron dynamics of the transition-metal coordination complex. Due to the distinct properties of ILs, such as high viscosity, favourable solvation behavior, and high thermal stability, they represent a novel class of solvents which can be implemented under high-vacuum conditions required for PES.

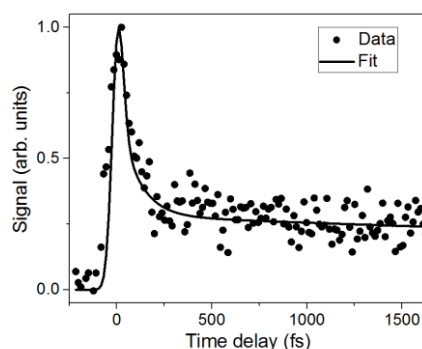


Figure 1 – Transient photoemission signal of the $[\text{Fe}(\text{CN})_6]^{3-}$ dissolved in IL as a function of time integrated over a range of kinetic energies encompassing the excited state dynamics. The solid curve represents fit results to a model that assumes a sequence of two intersystem crossings.

Although the study of the relaxation dynamics in $[\text{Fe}(\text{CN})_6]^{3-}$ was performed previously in various solvents [1-3], the relaxation mechanism has received controversial interpretations. In this study, we confirm the ultrafast biexponential decay of the excited electron population (Figure 1), which is associated with a sequence of intersystem crossings in the molecular compound [2]. However, the relaxation rates in IL are found to be different.

References

1. W. Zhang, M. Ji, Z. Sun and K.J. Gaffney, *J. Am. Chem. Soc.*, **134**, 5 (2012) 2581.
2. N. Engel, S. I. Bokarev, A. Moguilevski, A. A. Raheem *et al.*, *Phys. Chem. Chem. Phys.*, **19** (2017) 14248.
3. J. Ojeda, C. A. Arrell, L. Longetti, M. Chergui and J. Helbing, *Phys. Chem. Chem. Phys.*, **19** (2017) 17052.

Intermolecular Energy Balances Based on Acetophenone

Julia Stachowiak, Charlotte Zimmermann, Hannes C. Gottschalk and Martin A. Suhm

Institut für Physikalische Chemie, Georg-August-Universität Göttingen, Tammannstr. 6,

37077 Göttingen, Germany

msuhm@gwdg.de

Unsymmetrically substituted ketones like acetophenone offer two non-equivalent C=O lone electron pairs to hydrogen bond donors. Their relative attractivity depends on the sterical demand of the donor and its secondary interactions with the substituents of the ketone acceptor. The donor can switch easily between the sites, such that any preference for one or the other site in vacuum can be probed down to fairly low temperatures (<100 K) despite using non-equilibrium supersonic jet expansions. Because the local hydrogen bond environment is quite similar on both sides, any zero point vibrational energy corrections should largely cancel. We use this intermolecular energy balance design to test how well different electronic structure methods are able to predict the relative energy of the two docking isomers, down to a sub-kJ/mol level. It is essential to construct a broad experimental data base with systematic chemical variations for rigorous comparison with theory. Otherwise, fortuitous error cancellation may hide deficiencies in the investigated electronic structure approaches.

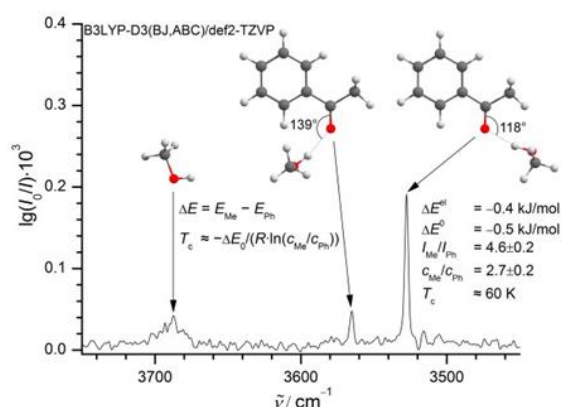


Figure 1 – OH-stretching infrared spectrum of the 1:1 acetophenone-methanol complex illustrating the intermolecular balance situation with a clear docking preference for the aliphatic side despite a sub-kJ/mol energy preference [1].

Here, we present our first steps towards an extensive acetophenone-based docking balance database [1]. Regioselective fluorination, deuteration and alkylation are employed to drive the balance from one side to the other, always checking whether theoretical predictions follow experiment in a systematic way. The tool to probe the docking ratios is FTIR spectroscopy in supersonic slit jet expansions, mostly probing the OH stretching fundamentals [2].

References

1. A. Poblitzki, H. C. Gottschalk, M. A. Suhm, *J. Phys. Chem. Lett.* 8 (2017) 5656–5665.
2. M.A. Suhm, F. Kollipost, *Phys. Chem. Chem. Phys.* 15 (2013) 10702–10721.

Acknowledgements: We thank the German research foundation (DFG) for support within the priority program SPP 1807 on London dispersion interactions and Göttingen University for start-up funding in the framework of the research training group RTG 2455 (www.uni-goettingen.de/en/587836.html) on benchmark experiments for numerical quantum chemistry, which offers several PhD positions in 2019.

Contest of Molecular Noses: Chirality Recognition between α -Pinene and Alcohols

Caroline Stelbrink, Robert Medel, and Martin A. Suhm

*Institut für Physikalische Chemie, Georg-August-Universität Göttingen, Tammannstr. 6,
37077 Göttingen, Germany
msuhm@gwdg.de*

α -Pinene is a chiral bicyclic monoterpene abundant in nature whose enantiomeric forms can be distinguished by odour receptors of many animals, e.g. honey bees, seals or humans [1]. The molecular mechanisms responsible for such subtle olfactory recognition are still poorly understood. Simple models for olfactory receptors are chiral alcohols which can form hydrogen bonds with functional groups of the odourant. α -Pinene is an especially suitable test case for a contest of chiral alcohols as molecular noses because of its rigid conformation and the accessibility of only one side of its π -bond due to steric hindrance. This limits the conformational space of possible diastereomeric clusters so that straightforward spectral information is obtained which can readily be compared with theoretical predictions. Chirality recognition [2] can be used as a benchmark for the description of intermolecular forces by theoretical methods because one constituent is merely mirror-inverted so that other deficits of the methods should largely cancel.

Here, we present a contest of four alcohols for the recognition of α -pinene's chirality and a comparison with theory at B3LYP-D3(BJ)/def2-TZVP level. As a probe for hydrogen bonded clusters the OH stretching fundamentals were measured by FTIR spectroscopy in supersonic slit jet expansions [3].

Unlike the biological noses, where all of the five tested animals succeed [1], only two out of four among our molecular noses are able to distinguish between α -pinene's enantiomers.

References

1. A. Rizvanovic, Olfactory discrimination performance and long-term odor memory in Asian elephants (*Elephas maximus*), *Master Thesis* (2012), Linköping University.
Available at: <http://urn.kb.se/resolve?urn=urn:nbn:se:liu:diva-78026>
2. A. Zehnacker and M. A. Suhm, *Angew. Chem. Int. Ed.* 47 (2008) 6970.
3. M. A. Suhm and F. Kollipost, *Phys. Chem. Chem. Phys.*, 15 (2013) 10702.

Acknowledgements: We thank the German research foundation (DFG) for support within the priority program SPP 1807 on London dispersion interactions and Göttingen University for start-up funding in the framework of the research training group RTG 2455 (www.uni-goettingen.de/en/587836.html) on benchmark experiments for numerical quantum chemistry, which offers several PhD positions in 2019.

Photochemistry of a Matrix Isolated Dispiro-1,2,4- Trioxolane: Criegee Intermediate Formation and Ring Expansion

E. M. Brás^{a,c}, L. I. L. Cabral^{a,b}, R. Fausto^c and M. L. S. Cristiano^{a,b}

^aCenter of Marine Sciences, CCMar, University of Algarve, P-8005-039 Faro, Portugal

^bDepartment of Chemistry and Pharmacy, FCT, University of Algarve, P-8005-039 Faro, Portugal

^cCQC, Department of Chemistry, University of Coimbra, P-3004-535 Coimbra, Portugal
ecbras@ualg.pt

Artemisinin and derivatives (1, Figure 1a) are used as antimalarials, with artemisinin-based combinations (known as ACT's) providing effective therapeutic tools against *P. falciparum* malaria [1,2]. Previous works in artemisinin based drugs established the peroxide bond as the pharmacophore [2], suggesting that the antiparasitic action is subsequent to reductive cleavage of the peroxide bond, catalyzed by Fe (II) or by heme released during parasite hemoglobin digestion [2]. This irreversible reaction may generate carbon-centered free radicals, or carbocations, that react with parasite biomolecular targets [2].

It was demonstrated that selected trioxolanes show peroxide-dependent activity, *in vitro* and *in vivo*, against sensitive and multidrug-resistant *P. falciparum* parasites (including strains resistant to ACT's), emphasizing the potential of trioxolanes in antimalarial chemotherapy [3,4]. However, available information on their structure and photoreactivity is scarce.

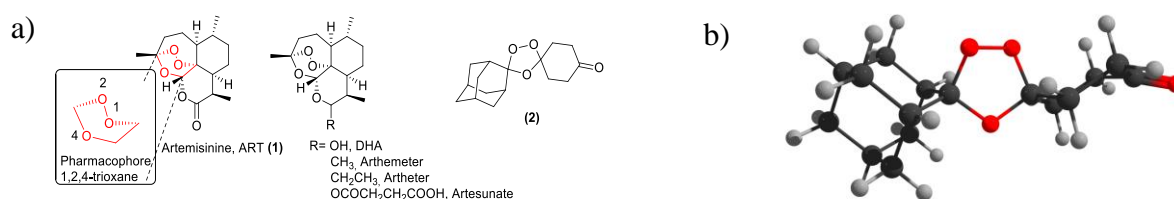


Figure 1 - Structures of endoperoxides with antiparasitic activity. a) Artemisinin-derived drugs; b) Calculated structure of dispiro-1,2,4-trioxolane 2.

We report the photochemical behavior of a matrix-isolated dispiro-1,2,4-trioxolane (2). Broadband UV irradiation of the compound isolated in a cryogenic argon matrix led to cleavage of the O–O bond, followed by a radical-mediated rearrangement with formation of a Criegee-type intermediate [2,5], in line with the postulated mechanism of action for trioxolanes [2].

References

1. D. L. Klayman, *Science*, 228 (1985) 1049.
2. Y. Tang, Y. Dong, X. Wang, K. Sriraghavan and K.J. Wood, *J. Org. Chem.*, 70 (2005) 5103.
3. F. Arie, B. Witkowski, C. Amaratunga, J. Beghain, A.-C. Langlois, N. Khim *et al.*, *Nature*, 505 (2014) 55.
4. L. Lobo, L. I. L. Cabral, M. I. Sena, B. Guerreiro, A. S. Rodrigues, V. F. Andrade-Neto, M. L. S. Cristiano and F. Nogueira, *Malaria J.*, 17 (2018) 145.
5. L. Khachatryan, Y. Haas and J. Pola, *J. Chem. Soc., Perkin Trans 2*, (1997) 1147.

Acknowledgements: We acknowledge financial support from “Fundação para a Ciência e a Tecnologia” (FCT) and FEDER/COMPETE 2020-EU through projects: PTDC/MAR-BIO/4132/2014 and UID/Multi/04326/2013 (CCMAR); PTDC/QEQ-QFI/3284/2014 – POCI-01-0145-FEDER-016617 and UI0313/QUI/2013 (CQC). E.M.B. and L.I.L.C. acknowledge FCT and CCMAR for grants within project PTDC/MAR-BIO/4132/2014.

Matrix Isolation Study of Fumaric and Maleic Acids in Solid Nitrogen

Timur Nikitin, Susy Lopes, and Rui Fausto

CQC, Department of Chemistry, University of Coimbra, 3004-535 Coimbra, Portugal
timur.nikitin@uc.pt

Maleic and fumaric acids, the simplest aliphatic dicarboxylic acids with a C=C double bond, are multifunctional chemical intermediates that find applications in many fields of industrial chemistry.

Monomers of maleic and fumaric acids were isolated in a nitrogen matrix and characterized by infrared absorption spectroscopy. Narrowband near-infrared irradiation (NIR) of the first OH overtone efficiently promotes the formation of higher energy conformers, which were identified based on calculations. Upon ultraviolet irradiation, conversion of fumaric acid into maleic acid is observed. The results of this study carried out in nitrogen matrix are compared with those from a similar study performed in argon matrix published previously [1].

To aid the interpretation of the experimental spectra, vibrational spectra, as well as relative energies of maleic and fumaric acids, were calculated using Density Functional Theory (DFT/B3LYP) level of approximation with anharmonic corrections. Calculations show that the most stable conformers are planar for both acids (H–C=C–H dihedral equal to 0° for maleic acid and H–C=C–H dihedral equal to 180° for fumaric acid). New conformers have been discovered in addition to those already reported [1].

References

1. E.M.S. Maçôas, R. Fausto, J. Lundell, M. Pettersson, L. Khriachtchev, and M. Räsänen, *J. Phys. Chem. A*, 105 (2001) 3922.

Acknowledgements: T. N. is grateful to FCT for financial support through the project PTDC/QEQ-QFI/3284/2014. S.L. acknowledges FCT for Post-doctoral Grant ref. SFRH/BPD/77276/2011. The Coimbra Chemistry Centre is supported by the FCT through the project UI0313/QUI/2013 co-funded by COMPETE-UE.

Conformational Control of an Aldehyde Fragment by Selective Vibrational Excitation of Interchangeable Remote Antennas

A. J. Lopes Jesus,^{a,b} Cláudio M. Nunes,^a Igor Reva,^a and Rui Fausto^a

^a CQC, Department of Chemistry, University of Coimbra, 3004-535, Coimbra, Portugal.

^b CQC, Faculty of Pharmacy, University of Coimbra, 3004-295, Coimbra, Portugal.

ajorge@ff.uc.pt

In this work, we applied interchangeable vibrational antennas to achieve conformational control over the remote heavy aldehyde fragment. The molecular framework used for this purpose was 2-formyl-2*H*-azirine bearing either an OH or NH₂ group acting as a vibrational antenna. The target molecules (**3** and **4** in Figure 1) were photogenerated in low-temperature (15 K) argon matrixes from 3-hydroxy- or 3-amino-isoxazole (**1** and **2** in Figure 1) by using UV-light [1].

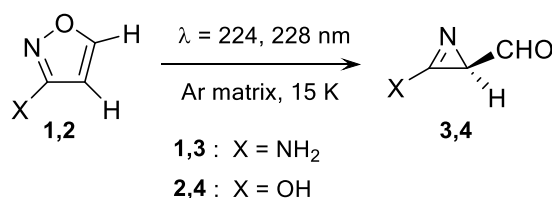


Figure 1 – Generation of 2-formyl-2*H*-azirines (**3**, **4**) by UV-irradiation of isoxazoles (**1**, **2**).

Each substituted 2-formyl-2*H*-azirine may adopt two conformers (**A** and **B**), differing by the orientation of the aldehyde group with respect to the 2*H*-azirine ring. These conformers could be interconverted by selective excitations using near-IR (NIR) laser light tuned at the wavenumbers corresponding to the first overtones of the OH group (2*v*), or NH₂ (antisymmetric, 2*v_a*, and symmetric, 2*v_s*) stretching vibrations, and to the combination mode of the two fundamental NH₂ stretching modes (*v_a* + *v_s*), see Figure 2.

All the reactants and photoproducts, including conformers **A** and **B** of the photoproducts, were identified by collecting experimental infrared spectra in mid-IR and NIR domains. The assignments were aided by carrying out harmonic and also anharmonic infrared spectra, including anharmonic frequencies and anharmonic IR intensities of transitions of up to two quanta.

As far as we know, this is the first experimental evidence of conformational change of an aldehyde group induced by vibrational excitation with monochromatic NIR light, in the electronic ground state. Remarkably, this process was found to occur upon excitation of any of the four resonant frequencies of the two vibrational antennas accessible in our experiments.

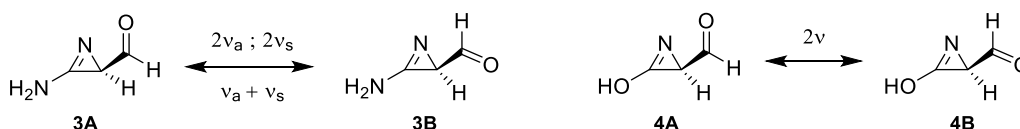


Figure 2 –NIR-induced interconversions between the conformers **A** and **B** of the two 2-formyl-2*H*-azirines.

References

1. A. J. Lopes Jesus Cláudio M. Nunes Rui Fausto and Igor Reva, *Chem. Commun.*, 54 (2018) 4778.

Regularities in the Manifestation of Resonance Dipole-Dipole Interaction in the Spectra of Low-Temperature Condensed Molecular Systems

T. S. Kataeva, O. S. Golubkova, D. N. Shchepkin and T. D. Kolomiitsova

Department of Physics, Saint Petersburg State University, 7/9 Universitetskaya Nab.,

199034 Saint Petersburg, Russian Federation

st016902@student.spbu.ru

The resonance dipole-dipole (RDD) interaction manifests itself in IR spectra of the condensed molecular systems, molecules of which have strong in absorption bands ($A > 100$ km/mole). In this case, the molecule has relatively large dipole moment derivative ($\sim 0.3 - 0.5$ D), and contours of these bands mainly are formed by the RDD interaction [1].

In this work, we were studied strong in absorption bands of several molecular systems (C_2F_6 , CF_4) in condensed phases within RDD interaction framework. From this point of view the bands contours were examined in thin films RAIR spectra, extinction and Raman spectra.

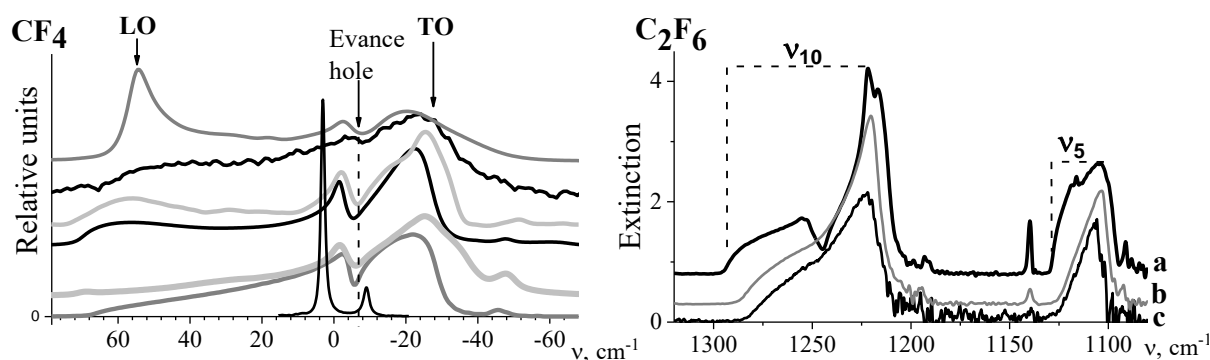


Figure 1 – The ν_3 and $\nu_1+\nu_3$ band contours formed by the RDD interaction of the liquid and crystalline CF_4 in IR, Raman and extinction spectra (left). The ν_{10} and ν_5 band contours formed by the RDD interaction in the extinction spectra of α -crystalline (a), β -crystalline (b), and liquid (c) C_2F_6 (right).

The RDD interaction is manifested itself as the inhomogeneous broadening of the strong bands and the appearance of the LO-TO splitting. This pattern is observed in various spectra of liquid and crystalline CF_4 in the case of a strong fundamental ν_3 band and a combinational $\nu_1+\nu_3$ band. The main regularities of the manifestation of the RDD interaction in the extinction spectra of liquid and crystalline C_2F_6 were reviewed and analyzed using the example of strong fundamental ν_5 and ν_{10} bands.

References

1. A. P. Burtsev, V. N. Bocharov., T. D. Kolomiitsova and D. N. Shchepkin, *Opt. and Spectr.*, 100 (2006) 415.

Acknowledgements: This work was supported by the Russian Foundation for Basic Research; project no 17-03-00590 A. The experiment was performed at the center for Geo-Environment Research and Modeling (GEOMODEL) of Research park of St. Petersburg State University.

Notes

Molecular Structure and Properties [Organic Compounds]

Theoretical and Experimental Studies on Sulindac

E. Chelmecka^a, W. E. Śmiszek-Lindert^b, M. Kadela-Tomanek^c and M. Miliński^d

^a Department of Statistics, School of Pharmacy with the Division of Laboratory Medicine in Sosnowiec, Medical University of Silesia, Katowice, Poland, 30 Ostrogórska Street, 41-200 Sosnowiec, Poland

^b Department of Pharmacognosy and Phytochemistry, SPLMS, SUM, Jagiellońska 4, 41-200 Sosnowiec, Poland

^c Department of Organic Chemistry, SPLMS, SUM, Jagiellońska 4, 41-200 Sosnowiec, Poland

^d Department of Pharmaceutical Chemistry, SPLMS, SUM, Jagiellońska 4, 41-200 Sosnowiec, Poland
echelmecka@sum.edu.pl

Nonsteroidal anti-inflammatory drugs (NSAIDs) are a class of drugs widely used to alleviate the symptoms associated with conditions in which an inflammatory component is present, e.g. osteoarthritis and rheumatoid arthritis, as well as several instances of somatic pain. Sulindac is a prodrug with a sulfoxide moiety that requires *in vivo* reduction to sulindac sulfide, the pharmacologically active metabolite. Because sulindac has a chiral sulfur center, it can exist as either the R- or S-epimer. Earlier *in vivo* studies on the metabolism of sulindac, containing a mixture of both epimers, showed that sulindac could be reduced to sulindac sulfide and oxidized to sulindac sulfone [1].

For sulindac the geometry was optimized performing density functional theory (DFT) calculations at B3LYP level with the Gaussian 09 software package. To confirm theoretical results, the NMR, IR and Raman measurements were carried out. The experimental ¹H, ¹³C shifts and IR and Raman spectra are compared with calculated spectroscopic characteristic. For analysis of the intermolecular interactions in the crystal lattice of sulindac the Hirshfeld Surface method has been used. This tool is based on the calculation of the promolecular electron density both crystal and in gas phase, and provides a convenient means of quantifying the interactions within the crystal structures, revealing significant similarities and differences between related structures by individuate the packing motifs. To obtain the fingerprint plots the CrystalExplorer program has been used.

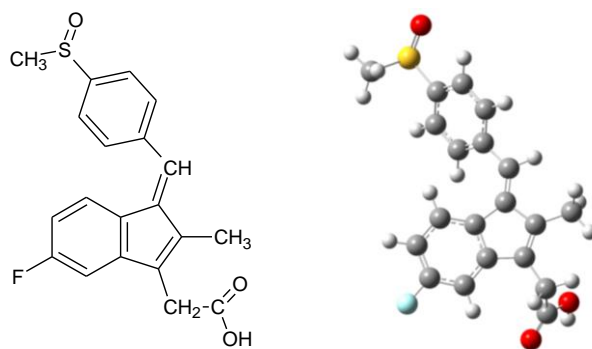


Figure 1 – The chemical structure of sulindac molecule

References

1. D. Brunell, D. Sagher, S. Kesaraju, N. Brot and H. Weissbach, *Drug Metab. Dispos.*, 39 (2011) 1014.

Acknowledgements: Calculations have been carried out using resources provided by Wrocław Centre for Networking and Supercomputing (<http://wcss.pl>), grant No. 95. This work was founded by the grant KNW-1-053/N/7/Z of the Medical University of Silesia in Katowice.

Determination of Dipole Moments in the Electronically Excited State of Quinoxaline *via* Thermochromic Methods

Matthias Zajonz, Mirco Lindic, Marie-Luise Hebestreit and Michael Schmitt

Heinrich-Heine-Universität, Physikalische Chemie I, Universitätsstraße 1, 40225 Düsseldorf, Germany

Matthias.Zajonz@hhu.de

Since the concept of dipole moments was established by Peter Debye over 100 years ago the most common way of determination in solution are solvatochromic methods [1,2]. The problem by using solvatochromic methods is variation of different solvents which changes many variables like the affinity for hydrogen bonds, the permittivity, the cavity volume, etc [3]. To avoid the variation of too many variables and for the determination of dipole moments in the electronically excited state from quinoxaline thermochromic methods according to Bilot and Kawski [3] were used. The advantages of thermochromic methods lies in keeping the solvent same and making necessary diversification for obtaining data by changing temperature and the related change of the permittivity as the refractive index. For that a temperature stabilized vacuum chamber was constructed and ethyl acetate as solvent was chosen because of the possible temperature range for the measurements and the good solubility of quinoxaline in that solvent. Additionally, the equation for the calculations of the dipole moments was improved by exchanging the Onsager radius against the cavity volume according to the improvements of Demissie [4]. Finally, the dipole moments from the thermochromic methods were compared with the results of *ab initio* calculation.

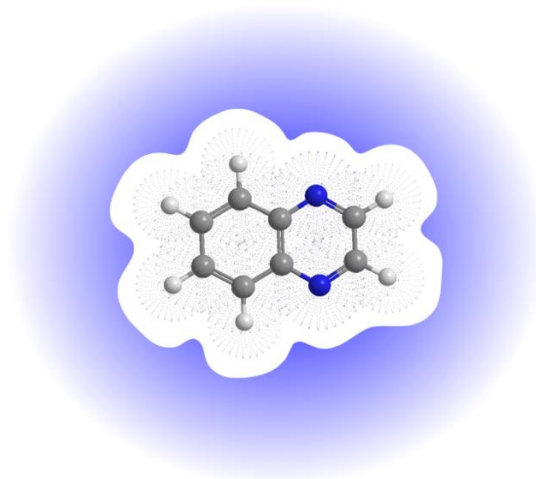


Figure 1 – Graphical Abstract of quinoxaline in solution

References

1. P. Debye, *Phys. Z.*, 13 (1912) 97.
2. P. Suppan and N. Ghoneim, *Solvatochromism*, Royal Society of Chemistry, Cambridge, 1997.
3. L. Bilot and A. Kawski, *Z. Naturforsch.*, 17A (1962) 621.
4. E. G. Demissie, E. T. Mengesha and G. W. Woyessa, *J. Photochem. Photobiol. A*, 337 (2016) 184.

The Study of Vibrational Spectroscopies for 5-Bromo-2-oxindole (5Br2O) Dimer

A. Eşme^a, H. Caliskan^b and S. G. Sagdinc^b

^aKocaeli University, Faculty of Education, Department of Mathematics and Science Education, 41380, Umuttepe, Kocaeli, Turkey

^bDepartment of Physics, Science and Art Faculty, Kocaeli University, 41380, Umuttepe, Kocaeli, Turkey
seda.sagdinc@gmail.com

Oxindoles exhibit widely range of biological effects which include the antiviral, antifungal, antibacterial, antiproliferative, anticancer, anti-inflammatory, antihypertensive and the anticonvulsant activities [1]. These characteristics make oxindoles and its derivatives attractive to many research groups as resources for chemical and pharmacological studies. The FT-IR (4000–400 cm⁻¹) and FT-Raman (3500–0 cm⁻¹) spectra of 5-bromo-2-oxindole dimer (5Br2O) have been measured and analyzed. The assignment of bands observed vibrational spectra have been made by comparison of its theoretical vibrational frequencies obtained using the B3LYP method with 6-311++G(d,p) basis set. The detailed vibrational assignments were performed with the DFT calculation, and the potential energy distribution (PED) of 5Br2O was obtained by the Vibrational Energy Distribution Analysis 4 (VEDA4) program. The scaled frequencies resulted in good agreement with the observed spectral patterns.

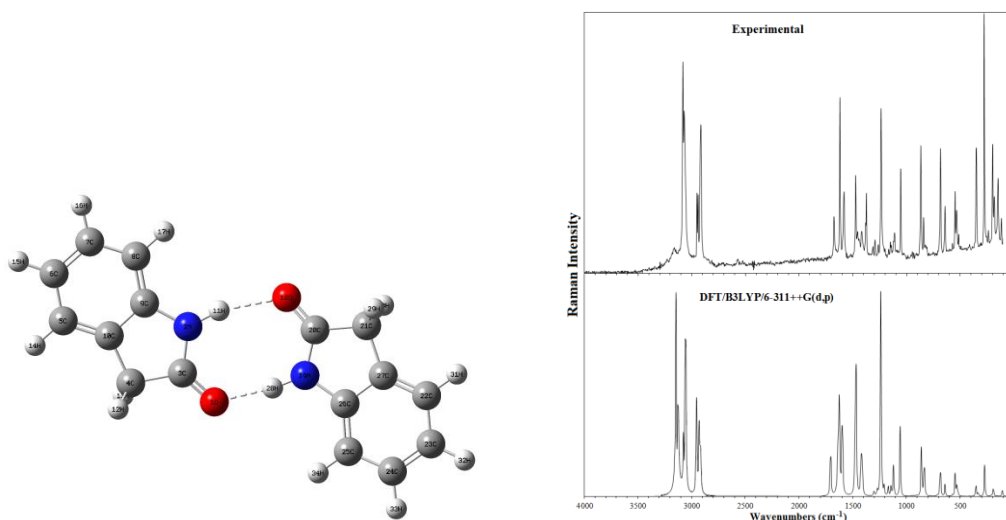


Figure 1 – The optimized structure and the Raman spectra of 5-bromo-2-oxindole.

References

1. S. S. S. Rudrangi, V. K. Bontha, V. R. Manda and S. Bethi, *Asian J. Research Chem.*, 4 (2011) 335.

Acknowledgements: The author would like to thank Kocaeli University Research Fund for its financial support (Grant No. 2017/008).

Spectroscopic (FT–IR, FT–Raman, UV–Vis) Analysis on Monomeric and Dimeric Structures of 4–Pyridazinecarboxylic Acid by HF and DFT Methods

A. Eşme^a and S. G. Sagdinc^b

^a Kocaeli University, Faculty of Education, Department of Mathematics and Science Education, 41380, Umuttepe, Kocaeli, Turkey

^b Department of Physics, Science and Art Faculty, Kocaeli University, 41380, Umuttepe, Kocaeli, Turkey
seda.sagdinc@gmail.com

Pyridazines containing two nitrogen atoms at 1,2 position in its ring structure are known as an important type of heterocyclic derivatives. Pyridazine derivatives have been reported to possess a wide range of biological activities; these include antiviral including anti-HIV activities and anticancer [1] and antimicrobial [2] activities. In this study, the optimized molecular structure, energies, UV–Vis, vibrational studies (FT–Raman and FT–IR) for 4–pyridazinecarboxylic acid (4PCA) were performed using the ab initio Hartree–Fock (HF) and density functional theory (DFT/B3LYP) methods with the 6–311++G(d,p) basis set. The detailed vibrational assignments for monomeric and dimeric structures of 4PCA were performed with the HF and DFT calculations, and the potential energy distribution (PED) was obtained by the Vibrational Energy Distribution Analysis 4 (VEDA4) program. The dimeric structure of 4PCA with the DFT/B3LYP/6–311++G(d,p) level caused by the shifts of O–H and C=O bands in the vibrational spectra of 4PCA were also studied.

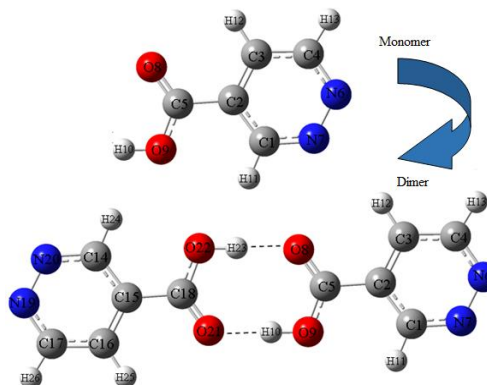


Figure 1 – The optimized molecular structures of monomeric and dimeric forms of 4PCA obtained from the DFT/B3LYP/6–311++G(d,p) level.

References

1. (a) M. Rodriguez-Ciria, A. M. Sanz, M. J. R. Yunta, F. Gomez-Contreras, P. Navarro, I. Fernandez, M. Pardo and C. Cano, *Bioorg. Med. Chem.* 11 (2003) 2143; (b) L. C. Bloomer, L. L. Wotring and L. B. Townsend, *Cancer Res.*, 25 (1982) 813.
2. (a) R. M. Butnariu, M. D. Caprosu, V. Bejan, I. I. Mangalagiu, M. Ungureanu, A. Poiata, C. Tuchilus and M. Florescu, *Heterocycl. Chem.*, 44 (2007) 1149; (b) M. Caprosu, R. Butnariu and I. I. Mangalagiu, *Heterocycles* 65 (2005) 1871; (c) M. Ungureanu, I. Mangalagiu, G. Grosu and M. Petrovanu, *Ann. Pharm. Fr.*, 55 (1997) 69.

Acknowledgements: The authors would like to thank Kocaeli University Research Fund for its financial support (Grant No. 2017/015HD).

Structural and Vibrational Investigation on Alkaloid Scopolamine Hydrobromine by Using their FTIR and FT-Raman Spectra

S. A. Brandán^a, R. A. Rudyk^a, M. A. Checa^a and C. A. N. Catalán^b

^a Cátedra de Química General, Instituto de Química Inorgánica, Facultad de Bioquímica, Química y Farmacia, Universidad Nacional de Tucumán, Ayacucho 471, (4000) San Miguel de Tucumán, Tucumán, Argentina

^b INQUINOA-CONICET, Instituto de Química Orgánica, Facultad de Bioquímica, Química y Farmacia, Universidad Nacional de Tucumán, Ayacucho 471, T4000INI San Miguel de Tucumán, Argentina
brandansa@yahoo.com.ar

The structures of two R and S enantiomeric series of alkaloid scopolamine as free base, cationic and hydrobromide forms have been theoretically studied in gas and aqueous solution phases by using hybrid B3LYP/6-31G* calculations. The theoretical R structures for those three forms can be seen in Figure 1. The most stable structures for the free base and hydrobromine forms in the two media are the R2 ones while for the cationic species the S2 forms are the most stable in the same media.

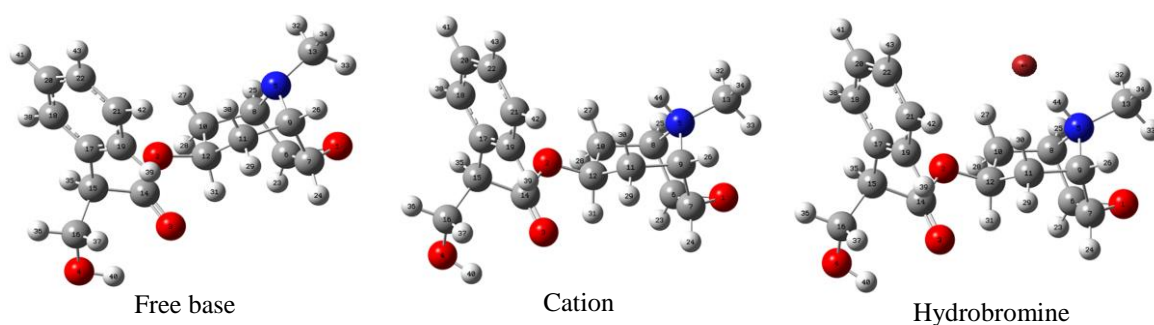


Figure 1 - Theoretical structures of alkaloid scopolamine as free base, cationic and hydrobromine species

On the other hand, the force fields for the most stable structures of the three different forms of scopolamine were computed by using the scaled quantum mechanical force field (SQMFF) methodology [1], their normal internal coordinates and the experimental infrared and Raman spectra of scopolamine hydrobromide in the solid state. Later, the complete vibrational assignments were performed by using their force fields and the Molvib program [2]. The normal internal coordinates used for these species were similar to those reported for other alkaloids [3-5]. The force constants were calculated for the three species and compared among them and with other reported for known alkaloids [3-5].

References

1. G. Rauhut and P. Pulay, *J. Phys. Chem.*, 99 (1995) 3093.
2. T. Sundius, *Vib. Spectrosc.*, 29 (2002) 89.
3. R. A. Rudyk and S. A. Brandán, *Indian J. Res.*, 6 (2017) 616.
4. S. A. Brandán, *Indian J. Applied Res.*, 7 (2017) 511.
5. D. Romani, S. A. Brandán, *Indian J. Res.*, 6 (2017) 587.

Acknowledgements: The authors thank to CIUNT, CONICET and Prof. T. Sundius for their permission to use Molvib.

A Theoretical and Experimental Investigation of Vibrational Spectra and Electronic Transitions on 2-Pyridineethanol and 2-Pyridinemethanol

Özge Bağlayan^a, İlkan Kavlak^b, Mustafa Şenyel^a and Güneş Süheyla Kürkçüoğlu^b

^a Physics Department, Eskişehir Technical University, Eskişehir, TR-26470, Turkey

^b Physics Department, Eskişehir Osmangazi University, Eskişehir, TR-26480, Turkey
gkurkcuo@ogu.edu.tr

The vibrational spectra of 2-pyridineethanol (hepy) and 2-pyridinemethanol (hmpy) were theoretically and experimentally analyzed in the region 4000-250 cm⁻¹. The work done by Kürkçüoğlu *et al.* has been expanded in this study [1]. The optimized geometric parameters, normal mode frequencies and corresponding vibrational assignments of the molecules have been examined by means of the density functional theory (DFT) and Hartree-Fock (HF) methods via the 6-311++G(d,p) basis set. Furthermore, reliable vibrational assignments have been made on the basis of potential energy distribution (PED). Theoretical and experimental vibrational wavenumbers were compared and the best agreement with these data were obtained. Additionally, transition energies of the molecules were investigated in 5 different solvents which are methanol, ethanol, dimethylsulfoxide, tetrahydrofuran and toluene. The maximum point of UV spectra of hepy were observed for methanol, ethanol, DMSO, THF, and toluene solution as 253 nm, 283 nm, 277 nm, 246 nm, 249 nm, respectively. These maximum points were calculated as 283 nm for methanol, ethanol and DMSO, 249 nm for DMSO, 251 nm for THF, 243 nm for toluene atmosphere. Transition energies of the both molecules were theoretically determined in the same wavelengths. However, these energy levels were observed as 257 nm for methanol, 273 nm for ethanol, 251 nm for DMSO, 245 nm for THF and 242 nm for toluene solution. The obtained results were shown that observed and calculated wavelengths were shifted by polarizability of the solvents (Figure 1). All these transitions were determined singlet symmetry and described as HOMO-LUMO transitions (Figure 2).

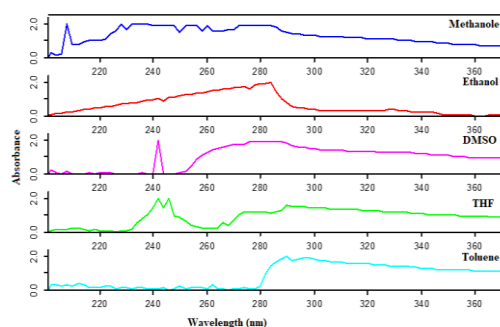


Figure 1 – A demonstration of the solvent effect on UV spectra of the 2-pyridinemethanol.

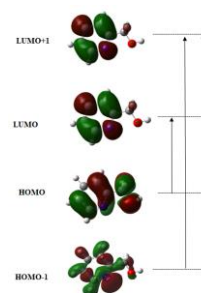


Figure 2 – HOMO-LUMO transitions of 2-pyridineethanol.

References

1. G. S. Kürkçüoğlu, E. Sayın, K. Gör, T. Arslan and O. Büyükgüngör, *Vib. Spectrosc.*, 71 (2014) 105.

Acknowledgements: This work was supported by the Research Fund of Anadolu University (Project Number. 1503F103)

Thermal *Trans-Cis* Isomerization of Cloro-Azobenzene System

Fanny C. Alvarez Escalada^a, Valentina Rey^b and Ana E. Ledesma^a

^a Departamento de Química, Facultad de Ciencias Exactas y Tecnologías, Universidad Nacional de Santiago del Estero-CONICET, Av. Belgrano (S) N° 1912, 4200, Santiago del Estero, Argentina

^b Instituto de Bionanotecnología del NOA (INBIONATEC)- Universidad Nacional de Santiago del Estero, Argentina

Azobenzenes are molecules that contain two aromatic rings linked by an N=N bond. They can be present in two stereoisomeric forms: *trans* and *cis*. The *trans* → *Cis* isomerization in aqueous solution could be induced by light illumination with appropriate wavelength in the UV range or changes in the temperature or pH values.

In this work, the thermal *trans* → *Cis* isomerization of 3,3',4,4'-tetrachloroazobenzene (TCAB) was studied in the 18-60 °C temperature range using different warm-up time and pH values in order to evaluate their behaviour in that conditions. We analysed the system by UV-visible and infrared spectroscopies. TCAB is a contaminant not commercially manufactured, it is a metabolite formed from the degradation of chloranilide herbicides, like propanil and remains deposited in the soil. For this reason, we evaluate the effects of the temperature and pH of media as probable degradation process. An ethanolic solution of TCAB (1 mg/4 ml) was prepared and kept in the dark. An aliquot (50 µL) was transferred into a 1 cm light path quartz cuvette containing 2000 µL of water and used to further analyses. When the temperatures increase, the thermal *trans-cis* isomerization occurs and is carried out by the appearance of two isosbestic points at 258 and 381 nm. The UV-Vis spectra of the *trans-cis* conversion of TCAB in Water at 40°C (as example) is showed in Fig. 1. The aggregate products were also observed in the visible region. The infrared spectra showed the structural changes induced by changes in the temperature. The isomerization is highly dependent of the pH independent the used temperature. We observed a predominance of the *cis* isomer at high temperature and basic and acid conditions.

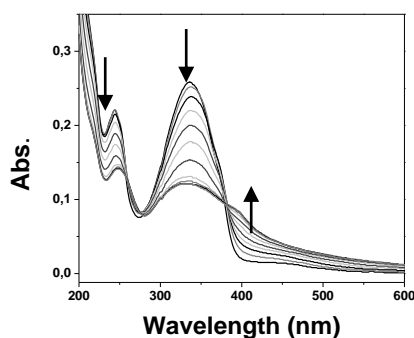


Figure 1. UV-Vis spectra for the thermal *trans-cis* isomerization of TCAB in water at 40°C

References

1. M. V. Castillo, J. L. Pergomet, G. A. Carnavale, L. Davies, J. Zinczuk and S. A. Brandan, *Spectrochim. Acta Part A*, 134 (2015) 577.
2. G. Angelini, C. Campestre, L. Scotti and C. Gasbarri, *Molecules*, 22 (2017) 1273.
3. H. Xiao, J. Kuckelkorn, L. K. Nüser, T. Floehr, M. P. Henning, M. R. Nickoll, A. Schäffer and H. Hollert, *Sci. Total Environ.*, 551-552 (2016) 304.

Acknowledgements: The authors thank Dra. Silvia A. Brandan and their coworkers for the TCAB compound.

Photoreduction Study of Benzophenone in Condensed Phase

Jorge Josue Campos-Amador, Sergio Romero-Servin, Rigoberto Castro-Beltrán and
Leonardo Álvarez-Valtierra

*Division of Sciences and Engineering, University of Guanajuato. 103 Loma del Bosque, Lomas del Campestre,
León, Gto, ZIP Code 37150, Mexico*
leoav@fisica.ugto.mx (Álvarez-Valtierra)

Optimization, intensification, reduction of production costs, and sustainable processes are some of the most important activities involved in industry's issues which are increasing and becoming more and more important in recent years [1]. Around the world, depending on the zone and its needs, different kinds or varieties of processes are being carried out; some of them need high temperatures (around 200-300 °C), releasing great amounts of greenhouse gases to the atmosphere; others are using different types of catalysts, for example platinum, gold, potassium permanganate, enzymes, etc., which over time start losing their effects over the reaction rate. At the present time, decreasing those parameters, such as production time, energy and production costs, operating temperature, and others, represents improvement, in which profits will be higher and higher day to day; otherwise, the result would be the opposite, losing money [2].

In this work, we have used UV radiation to control chemical reactions [3]. In particular, we have focused on the photoreduction of benzophenone in isopropyl alcohol [4]. In the past, we have tried this chemical reaction using the sun light over several days. However, we have tried a new "faster" method by vibronically exciting the reaction coordinate involved in such transformation. This latest method has shown evidence of photocatalysis (a faster synthesis of crystals of Benzopinacol, the product). Moreover, this experiment is being carried out at 18.5 ± 0.5 °C, and using a UV lamp operating at 254 nm, with a FWHM of about 2 nm, without the presence of additional lines. Finally, in this work we will show a comparison of the activation energy of each experiment (the sun light vs the UV lamp at 254 nm), and its kinetics parameters, proposing a tentative overall order of reaction.

References

1. T. Van Gerven and A. Stankiewicz, *Ind. Eng. Chem. Res.*, 48 (2009) 2465.
2. G. J. Harmsen, *Chemical Engineering and Processing: Process Intensification*, 46 (2007) 774.
3. R. N. Zare, *Science*, 279 (1998) 1875.
4. N. Filipescu and F. L. Minn, *J. Am. Chem. Soc.*, 90 (1968) 1544.

Combined Effect of Hydrogen Bonding Interactions and Freezing of Rotameric Equilibrium on the Enhancement of Photostability

Barbara Golec^a, Krzysztof Nawara^b, Alexandr Gorski^a, Randolph P. Thummel^c,
Jerzy Herbich^a and Jacek Waluk^{a, b}

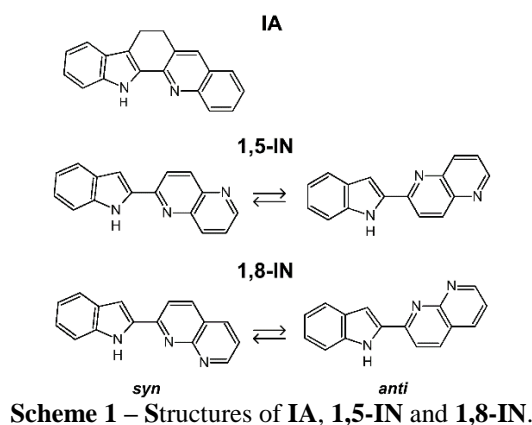
^a Institute of Physical Chemistry, Polish Academy of Sciences, Kasprzaka 44/52, 01-224 Warsaw, Poland

^b Faculty of Mathematics and Natural Sciences, College of Science, Cardinal Stefan Wyszyński University, Długa 5, 01-815 Warsaw, Poland

^c Department of Chemistry, University of Houston, Houston, Texas 77204-5003, USA
bgolec@ichf.edu.pl

The problem of making the organic chromophores more photostable against UV light is one of the basic and important tasks of science. Here we demonstrate that the photostability of 12,13-dihydro-5*H*-indolo[3,2-*c*]acridine (**IA**, Scheme 1) of a rigid bifunctional indole derivative with proton donor/acceptor functionalities can be enhanced by interaction with a protic partner [1]. The formation of hydrogen bonds with alcohols leads to a significant decrease of the triplet formation efficiency and an increase of photostability of the chromophore. The photodegradation yield of **IA** was found to be about 200 times lower in methanol and 1-propanol than in *n*-hexane. This molecule, which can exist exclusively in the *syn* form, is about 4 times more photostable in alcohols than similar, but non-rigid molecules such as 2-(1'*H*-indol-2'-yl)-[1,5]naphthyridine, **1,5-IN**, and 2-(1'*H*-indol-2'-yl)-[1,8]naphthyridine, **1,8-IN** (Scheme 1) which can exist in both *syn* and *anti* forms [2]. This additional photostability enhancement is due to elimination of a slower channel of excited state deactivation in alcohol complexes, $S_0 \leftarrow S_1$ internal conversion. The dominant, faster channel of S_1 depopulation, observed in cyclic 1:1 hydrogen bonded complexes, is the excited state double proton transfer, manifested by the presence of low energy tautomeric fluorescence.

We hope that the present findings can help in the design of more photostable systems.



References

1. B. Golec, K. Nawara, A. Gorski, R. P. Thummel, J. Herbich and J. Waluk, *Phys. Chem. Chem. Phys.* (2018) DOI: 10.1039/c8cp00726h.
2. B. Golec, M. Kijak, V. Vetokhina, A. Gorski, R. P. Thummel, J. Herbich and J. Waluk, *J. Phys. Chem. B*, 119 (2015) 7283.

Acknowledgements: This work was supported by the Polish National Science Centre grant 2016/22/A/ST4/00029. The computations were conducted with the support of PL-Grid Infrastructure.

Photorelaxation Processes in Dipyridylpolyenes

Yukihiro Shimoi and Yoriko Sonoda

National Institute of Advanced Industrial Science and Technology, Tsukuba, 305-8568, Japan
y.shimoi@aist.go.jp

Diphenylpolyenes and other polyenes substituted by aromatic groups exhibit various photophysical properties [1]. In this presentation, we pick up dipyridylpolyenes among this class of compounds and investigate their photorelaxation processes using density functional theory (DFT) calculations to explain observed fluorescence properties in these compounds.

We observed weak fluorescence of 1,2-di(4-pyridyl)ethylene (DPE, Fig. 1 (a)) with emission maximum depending on solvent polarity: $\lambda_{\text{max}} = 368$ nm in hexane and 403 nm in acetonitrile. This is in contrast to its absorption maximum almost independent of solvent.

Figure 1 shows the energy diagram of DPE obtained by time-dependent DFT calculations of the TD-B3LYP/6-311G(d,p) level. The lowest photoaccessible state from the ground state (S_0) is the S_3 state with the nature of $\pi-\pi^*$ transition. The lowest excited singlet state (S_1) and its almost degenerate S_2 state are characterized as $n-\pi^*$ transitions. The S_1 state relaxes the molecular geometry with increasing a CNC bond angle in one of the pyridyl groups. The geometry at the ground state is centrosymmetric. Meanwhile, the photorelaxed geometry at the S_1 state breaks this symmetry and induces a finite permanent dipole moment even though the molecule keeps planer conformation. Thus, this photorelaxation process is a possible mechanism to explain the observed fluorescence properties by means of Lippert-Mataga theory and is alternative to twisted intermolecular charge transfer (TICT) mechanism. We will also discuss the DPE analogues with longer polyene lengths.

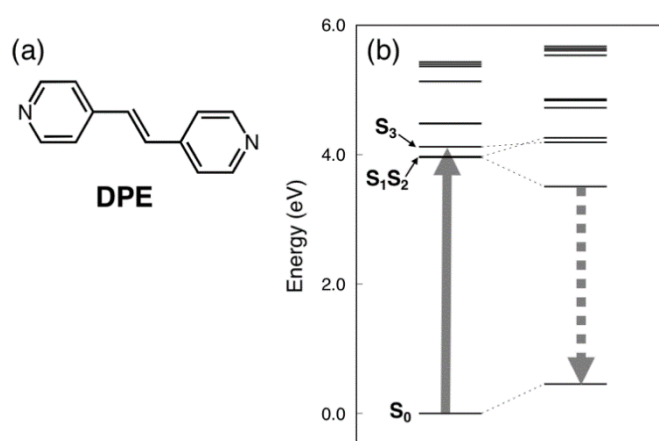


Figure 1 – (a) Molecular structure of 1,2-di(4-pyridyl)ethylene (DPE). (b) Energy diagrams of DPE at the ground state (left) and at the relaxed S_1 state obtained by calculations of the TD-B3LYP/6-311G(d,p) level.

References

1. Y. Sonoda *et al.*, *J. Phys. Chem. A*, 117 (2013) 566; Y. Sonoda *et al.*, *Cryst. Growth Des.*, 16 (2016) 4060 and references therein.

Synthesis and Conformational Study of Alcohols Derived from 3-Methyl-3-azabicyclo[3.3.1]nonane

I. Iriepa^a and J. Bellanato^b

^a Dpto. Química Orgánica y Química Inorgánica, Ctra. Madrid-Barcelona Km 33.6, 28871, Alcalá de Henares, Madrid, Universidad de Alcalá, Spain

^b Instituto de Estructura de la Materia, C.S.I.C., Serrano, 121, 28006 Madrid, Spain
isabel.irieta@uah.es

Following our research program related to the synthesis and structural study of potential pharmacologically interesting compounds, we have synthesized some alcohols derived from 3-methyl-3-azabicyclo[3.3.1]nonane.

The tertiary alcohols (**2-11**) (Fig. 1) were obtained by addition of arylmagnesium bromide or aryllithium to the previously synthesized ketone **1** (3-methyl-3-azabicyclo[3.3.1]nonan-9-one). The nucleophilic attack to the ketone occurred from both faces of the carbonyl group. As a consequence of these attacks a mixture of both α and β epimers have been obtained.

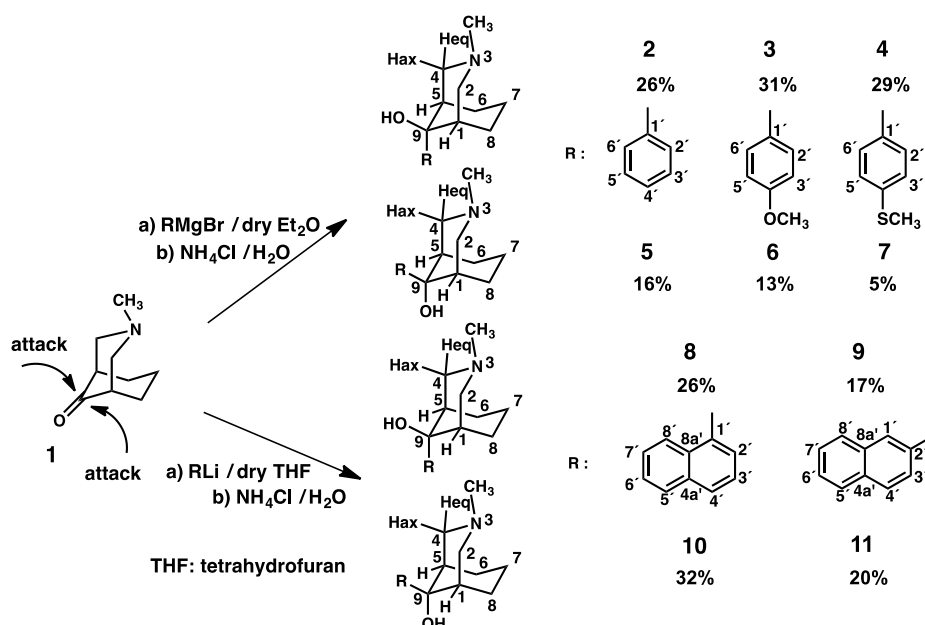


Figure 1

A study by ^1H and ^{13}C NMR has been done to determine the preferred conformations in solution and the configuration of C9. The assignments of proton and carbon resonances have been made on the basis of our data for related systems, double resonance experiments (DR) for compounds **2, 5, 8-11**, gHSQC (Heteronuclear Single Quantum Coherence) and TOCSY (Total Correlation Spectroscopy) experiments for compounds **8-11**.

The configuration at C9 can be inferred on the basis of upfield shifting γ -gauche effect exerted by the hydroxyl group on the C2(4) atoms for the α -epimers, and on the C6(8) atoms for the β -epimers.

Both α (**2-4, 8, 9**) and β alcohols (**5-7, 10, 11**) adopt in CDCl_3 solution a chair-chair conformation with the $N\text{-CH}_3$ group in equatorial position. These conclusions are supported by the values for $W_{1/2}$ of H1(5) (12 Hz), the $N\text{-CH}_3$ ^{13}C chemical shift of about 45 ppm and the $\Delta\delta$ [H7ax-H7eq] ~ 1.1 ppm (attributed to the field exerted by the lone pair on H7ax).

Identification and Structural Characterization of Novel Synthetic Cathinones

Elżbieta Bednarek, Agata Błażewicz, Jerzy Sitkowski, Lech Kozerski

National Medicines Institute, Chełmska 30/34, 00-725 Warsaw, Poland

e.bednarek@nil.gov.pl

Synthetic cathinones are very popular on the recreational drug market and have emerged as the second largest group of psychoactive substances after synthetic cannabinoids in Europe, according to the European Monitoring Centre for Drugs and Drug Addiction (EMCDDA).

As many as 118 synthetic cathinones have been notified until 2017 via the European Union Early Warning System (EU-EWS) of EMCDDA and novel derivatives still appear on the market, mainly due to their legal status.

The National Medicines Institute, which is the Official medicines Control Laboratory (OMCL) in Poland and a member of the European OMCL Network, has analyzed more than six thousand samples of designer drugs from the Polish market containing new psychoactive substances (NPSs) between 2008 and 2017. As it was stated in our previous paper [1], the majority of over 150 compounds found in these samples were synthetic cathinones.

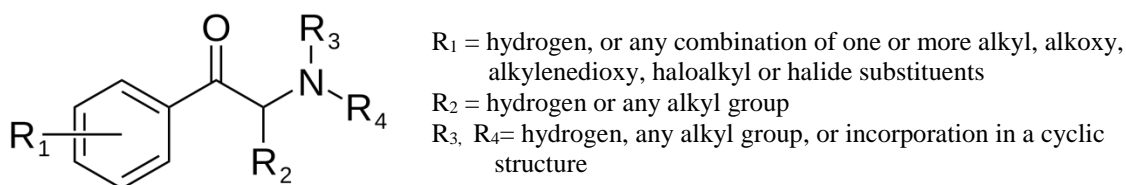


Figure 1 - General chemical structure of substituted cathinones

The aim of this study was to use NMR spectroscopy for the structure identification of novel substituted cathinones: propylcathinone, 2,4-dimethylmethcathinone, 2,4-dimethylethcathinone, 2,4-dimethyl- α -pyrrolidinopropio-phenone, 4-bromo- α -pyrrolidinopropiophenone and 2,4-dimethylisocathinone.

The signals in the ^1H and ^{13}C NMR spectra of studied compounds were assigned to the proton and carbon atoms in the appropriate structural fragments using general knowledge of chemical shifts dispersion. The assignment of proton resonances were confirmed with the aid of the proton-proton coupling pattern and the $^1\text{H}\{^1\text{H}\}$ COSY experiment whereas the assignment of carbon resonances were confirmed on the basis the $^1\text{H}\{^{13}\text{C}\}$ HSQC and $^1\text{H}\{^{13}\text{C}\}$ HMBC experiments.

The information obtained from two-dimensional NMR experiments allowed us to confirm the proton and carbon connecting scheme in studied compounds, and finally, taking into account molecular formulas determined on the basis of QTOF-MS to prove their structures.

References

1. A. Błażewicz, E. Bednarek, J. Sitkowski, M. Popławska, K. Stypułkowska, W. Bocian, L. Kozerski, *Forensic Toxicol* 35 (2017) 317.

Acknowledgements: This study was supported by grant from the National Science Centre Poland-UMO-2013/09/B/ST4/00106.

Molecular Complex of Guanidinium Trichloroacetate. Resumption X-ray and Theoretical DFT Studies

Marek Drozd and Marek Daszkiewicz

Division of Structure Research, Institute of Low Temperature and Structure Research, Polish Academy of Sciences, Okólna 2 str., 50-422 Wrocław, Poland
m.drozd@int.pan.wroc.pl

Many compounds with guanidinium cation are known in literature. Some of these chemical complexes exhibit various types of structural phase transitions, some of them being ferroelectric substances. Some compounds without macroscopic symmetry center, which based on guanidine molecule, are used as second harmonic generator in nonlinear optics.

A guanidine molecule with nine atoms only (CN_3H_5) belongs to the simplest organic chemical compound but plays a crucial role in the features of investigated compounds. The specific planar configuration with sp^2 hybridization of carbon atom makes that investigated cation can be used as potential H-donor in hydrogen bonds network and these “weak” chemical interactions play the most important role in studied compounds.

During the DFT theoretical calculation of equilibrium geometry, vibrational spectra and potential energy distribution (PED) for real guanidinium acetate complex [1] the additional approach was made for two “virtual” complexes: guanidinium trichloroacetate and guanidinium trifluoroacetate. The obtained results (values of calculated enthalpies) suggest strongly that these two compounds should exist in real experiment.

After many attempts the guanidinium trichloroacetate compound was synthesized. The X-ray structure of this new crystal was established by Dhavamurthy [2] and Karuppasamy [3]. On the basis of these results this crystal belongs to tetragonal crystallographic system with $P4_1$ noncentrosymmetric space group.

According to our crystallographic studies we postulated that crystal should belong to space group $P4_12_12$ of the tetragonal system. It is different result that obtained in previous investigation. It should be emphasized that in crystal the huge dynamical disorder on trichloroacetate anion is noticed. Especially, the chlorine atoms are disordered, but surprisingly the dynamical disorder in the case of one carbon atom was found.

Additionally, we performed quite new theoretical calculation for investigated compound, where the cluster with hydrogen bond network was used. These more precise theoretical results are comparable with previous and new crystallographic results.

References

1. M. Drozd, *Spectrochim. Acta A*, 69 (2008) 1223.
2. M. Dhavamurthy, G. Peramaiyan, M. Nizam Mohideen, S. Kalainathan and R. Mohan, *Nonlinear Opt. Phys.*, 24 (2015) 1550045e1.
3. P. Karuppasamy, M. Senthil Pandiana, P. Ramasamy and S. K. Das, *Optik*, 156 (2018) 707.

Hirshfeld Surface Analysis, Spectroscopic Measurements & DFT Calculated Study of Dacarbazine (DTIC)

E. Chelmecka^a, W. E. Śmiszek-Lindert^b, E. Drózd^a, M. Mehlich^a,
M. Kadela-Tomanek^c and D. Wrześniok^d

^a Department of Statistics, School of Pharmacy with the Division of Laboratory Medicine in Sosnowiec, Medical University of Silesia, Katowice, Poland, 30 Ostrogórska Street, 41-200 Sosnowiec, Poland

^b Department of Pharmacognosy and Phytochemistry, SPLMS, SUM, Jagiellońska 4, 41-200 Sosnowiec, Poland

^c Department of Organic Chemistry, SPLMS, SUM, Jagiellońska 4, 41-200 Sosnowiec, Poland

^d Department of Pharmaceutical Chemistry, SPLMS, SUM, Jagiellońska 4, 41-200 Sosnowiec, Poland
echelmecka@sum.edu.pl

Dacarbazine ($C_6H_{10}N_6O$; DTIC), used as antineoplastic in the treatment of the lymph system cancer and malignant melanoma a type of skin cancer. It is the single most active agent for the treatment of malignant melanoma. In DFT calculations two possible isomers and dimer consist from two molecules with two intermolecular hydrogen bonds have been regarded. The experimental 1H , ^{13}C shifts as well as IR and Raman spectra have been compared with calculated spectroscopic characteristic.

Hirshfeld Surfaces (HS) is a way of defining molecules in molecular crystals and have been shown to enhance the description and rationalisation of structural motif [1]. Graphical tools based on HS and two-dimensional (2D) fingerprint plots have been shown to be valuable for visualizing and analyzing intermolecular interactions (H-bonds; $N-H\cdots O=C$; $N-H\cdots N$) in the crystalline DTIC while maintaining a whole-of-molecule approach. This work present that for each point on the surface, two colored distance properties have been defined: d_e and d_i (the distance from the point to the nearest nucleus external and internal to the surface, respectively). In turn, 2D fingerprint plots are derived from the HS by plotting the fraction of points on the surface as a function of the pair: d_i , d_e [2]. The intermolecular interactions in the crystal have been rationalized using the electrostatic potential (EP) mapped on the HS. It should be noted that electrostatic potential surface is valuable in computer-aided drug design because they assist in understanding electrostatic interactions between the macromolecule and the drug. These surfaces can be used to compare different inhibitors with substrates.

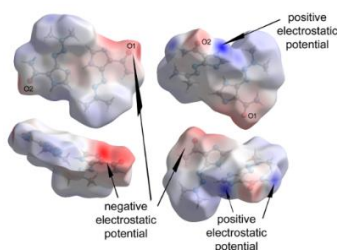


Figure 1 – Electrostatic Potential mapped on the Hirshfeld surface.

References

1. F. P. A. Fabbiani, L. T. Byrne, J. J. McKinnon and M. A. Spackman, *CrystEngComm*, 9 (2007) 728.
2. W. E. Śmiszek-Lindert, E. Chelmecka, S. Góralczyk and M. Kaczmarek, *J. Mol. Struct.*, 1128 (2017) 619.

Acknowledgements: Calculations have been carried out using resources provided by Wrocław Centre for Networking and Supercomputing (<http://wcss.pl>), grant No. 95. This work was founded by the grant KNW-1-053/N/7/Z of the Medical University of Silesia in Katowice.

The Aggregation Behaviour of 2*H*-Imidazole-2-thione Derivatives in the Solid State

Truong Ngoc Hung^{a,b}, Gábor Varga^{a,b}, Zoltán Kónya^{c,d}, Ákos Kukovecz^c, Gábor Kozma^c, Viktor Havasi^c, Pál Sipos^{b,e}, Gregorz Mlostóń^f and István Pálinkó^{a,b}

^a Department of Organic Chemistry, ^b Materials and Solution Structure Research Group, Institute of Chemistry,

^c Department of Applied and Environmental Chemistry, ^d MTA-SZTE Reaction Kinetics and Surface Chemistry Research Group, ^e Department of Inorganic and Analytical Chemistry, University of Szeged, Dóm tér 7-8, Szeged, H-6720 Hungary

^f Department of Organic and Applied Chemistry, University of Łódź, Tamka 12, Łódź, PL-91-402 Poland
palinko@chem.u-szeged.hu

The molecular crystals are kept together by various secondary interactions in the solid state. These forces may be weak individually, but being numerous, they facilitate the formation and existence of stabile aggregates. If these forces are hydrogen bonds, these interactions can be rather strong.

In this contribution, the aggregation behaviour of three 2*H*-imidazole-2-thione derivatives (Figure 1) is described. They are substituted at every possible positions except one of the ring nitrogens. Thus, this ring nitrogen bearing a hydrogen is a potential hydrogen bond donor site, while the thiocarbonyl group may have the role of the hydrogen acceptor. These interactions were investigated by spectroscopic (IR and Raman) methods and *via* molecular modelling.

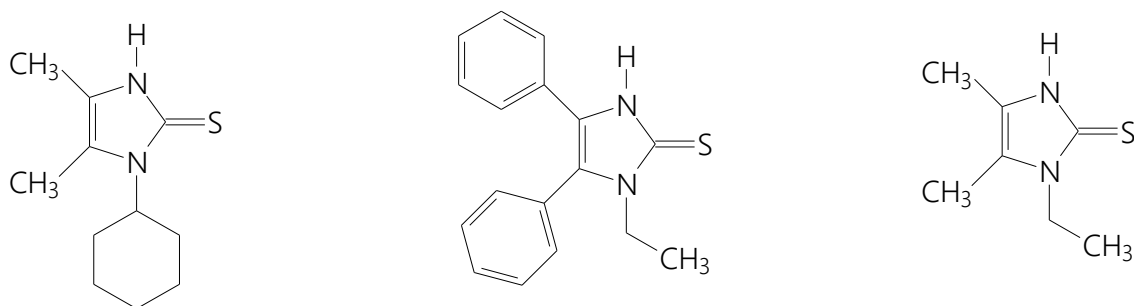


Figure 1 – The compounds of the study.

Dilute (~0.1 M) solutions were prepared first using chloroform as the solvent. The IR as well as the Raman spectra were registered. Then, these spectra were also taken of the solid samples. The spectrum of the solvent was subtracted from the solution spectra, and the resulting curves were compared to those obtained in the solid state. Shifts in the major bands were sought for. It was found that the hydrogen-bearing imidazole nitrogen as well as the sulfur are involved in the hydrogen bonding interaction, indeed. The close contact could be visualized with the help of high-level quantum chemical modelling calculations.

Acknowledgements: This work was supported by the National Science Fund of Hungary through grant OTKA NKFI 106234. The financial help is highly appreciated.

Conformational Equilibrium of Imidazolium-Based Ionic Liquids, Effect of Water, Temperature and Counter Anions

J. Kausteklis, R. Platakytė, E. Zacharovas and V. Aleksa

Institute of Chemical Physics, Vilnius University, Saulėtekio Ave 3, LT- 10257 Vilnius, Lithuania

jonas.kausteklis@ff.vu.lt

Room temperature ionic liquids (RTILs) are well known as molten salts with many attractive physical and chemical properties which are determined by various interactions between anions and cations. In many cases RTILs are called designer solvents and applied as functional materials. Physical and chemical properties of RTILs can be tuned by selecting appropriate combinations of cations and anions. Previous studies reported interesting water structures formed in RTIL and water mixtures. The clusterization process called “water pocket” formation and liquid crystalline (LC) ionogel phase were found in RTILs with different length of cation chain [1-3].

In present study the temperature, counter anions and water effect to conformational equilibrium of eight various ionic liquids was investigated using vibrational spectroscopy. Six different short chain imidazolium based RTILs named 1-butyl-3-methylimidazolium nitrate, chloride, bromide, iodide, trifluoromethanesulfonate, tertafluoroborate ([bmim][NO₃, Cl, Br, I, TfO, BF₄]) and two long chain imidazolium based RTILs 1-decyl-3-methylimidazolium chloride, bromide ([bmim][Cl, Br]) in mixtures with water were analyzed.

Conformational equilibrium of the [bmim]⁺ cation was investigated monitoring the combination of the ring deformation and the CH₂ rocking bands. These two Raman bands in different neat ionic liquids were many times investigated and reported as vibrations of *gauche* at lower frequency (601 cm⁻¹) and *trans* (624 cm⁻¹) conformers.

The discontinuous change of I_{gauche}/I_{trans} ratio was found with addition of water in ionic liquid/water mixtures. These discontinuities in concentration dependences were indicated in water concentration region where water structures formation in different RTIL were reported. Changes of conformational equilibrium could be used to determine the regime when water structures (water pockets and LC phases) were destroyed.

References

1. K. Saihara, Y. Yoshimura and A. Shimizu, *J. Mol. Liq.*, 212 (2015) 1.
2. M. A. Firestone, P. G. Rickert, S. Seifert and M. L. Dietz, *Inorg. Chim. Acta.*, 357 (2004) 3991.
3. H. Abe, T. Takekiyo, M. Aono, H. Kishimura, Y. Yoshimura and N. Hamaya, *J. Mol. Liq.*, 210 (2015) 200.

Mass-Analyzed Threshold Ionization Spectroscopy of *p*-Bromoanisole

Shen-Yuan Tzeng and Wen-Bih Tzeng

*Institute of Atomic and Molecular Science, Academia Sinica, P.O. Box 23-166, 1 Section 4, Roosevelt Road,
Taipei 10617, Taiwan
wbt@sinica.edu.tw (W.B. Tzeng)*

We applied the resonant two-photon ionization (R2PI) and mass-analyzed threshold ionization (MATI) spectroscopic techniques to record the vibronic and cation spectra of *p*-bromoanisole. In particular, a few vibronic states were used as the intermediate levels to record the MATI spectra and to obtain more information about the active cation vibrations. The band origin of the $S_1 \leftarrow S_0$ electronic transition of *p*-bromoanisole was found at $34\,840 \pm 2\text{ cm}^{-1}$ and the adiabatic ionization energy was determined to be $65\,903 \pm 5\text{ cm}^{-1}$. These experimental data suggest that the molecular geometry of *p*-bromoanisole in the cationic ground D_0 state resembles that in the electronically excited neutral S_1 state. Most of the observed distinct MATI bands result from the active vibrations involving in-plane ring deformation and substituent-sensitive bending vibrations of the *p*-bromoanisole cation.

Spectroscopic Studies of Inclusion Complexation between Ortho Derivatives of *p*-Methylaminobenzoate and α - and γ -Cyclodextrins

Karolina Baranowska, Marek Józefowicz

Institute of Experimental Physics, University of Gdańsk, Wita Stwosza 57, 80-952 Gdańsk, Poland

karolina.baranowska@phdstud.ug.edu.pl

Using the steady-state and time-resolved spectroscopic techniques and quantum-chemical calculations, photophysical and photochemical properties of the two ortho derivatives of *p*-methylaminobenzoate (metyl *o*-methoxy *p*-methylaminobenzoate (I) and methyl *o*-hydroxy *p*-methylaminobenzoate (II)) have been studied in binary mixture THF-H₂O and aqueous solutions containing different concentrations of α - and γ -CD. Nonlinear solvatochromic shifts of the absorption and fluorescence bands were observed for both fluorophores in a mixture of polar aprotic (THF) and polar protic (H₂O) solvents. This nonlinearity has been explained in terms of the non-specific (dielectric enrichment of the solvent around the polar solute) and specific (hydrogen bond) solute-solvent interactions. Spectroscopic measurements were used to investigate the role of H-bonding solute-solvent interactions, and the excited-state intramolecular proton transfer process in the formation of inclusion complexes between fluorophore and cyclodextrins. The obtained results were used to calculate, according to Benesi-Hildebrand's plot and nonlinear least-squares regression analysis, equilibrium constants of the fluorophore-cyclodextrin inclusion complexes. Performed analysis indicates also that both 1:1 and 1:2 inclusion complexes were formed between studied compounds and α - and γ -cyclodextrins.

Synthesis, Spectroscopic Characterization of Novel derivatives of 1*H*-Quinoxalin-2-one for the Role of Fluorescent Molecular Probes for Monitoring Very Fast Processes of Photopolymerization

Joanna Ortyl^a, Maciej Pilch^a, Wiktoria Świątek^a, Emila Hola^a and Mariusz Galek^b

^a Cracow University of Technology, Warszawska 24, 31-155 Cracow, Poland

^b PhotoHiTech Ltd., Bobrzyńskiego 14, 30-348 Cracow, Poland

jortyl@chemia.pk.edu.pl

Photoinitiated polymerization is an important industrial process widely used in different applications. Synthesis of polymeric materials carried by these processes is one of the most efficient methods, thanks to a technique is currently very widespread and is still rapidly developing. The photopolymerization offers several advantages compared to traditional methods. The process is solvent-free, energy efficient and generally economical. This type of polymerization can be carried out under a wide range of conditions and at normal temperature too, undergoes a very short exposure time. During photoinitiated polymerization processes, it is crucial to have a method of evaluation of the degree of cure of photocurable materials for optimization of the curing process conditions, and for quality control of cured materials before their release to market. Such method has to be fast to match the high speed of photopolymerization processes, precise in order to see even small differences in degree of cure, and simple to use. Fluorescence probe technology (FPT) is such a method well suited for monitoring of rapid photopolymerization processes in real time. FPT is a new method, which offers the possibility of on-line applications for monitoring of polymerization processes by means of specially designed fluorescent molecular probes that change their fluorescence characteristics upon changes occurring in their environment [1]. During the past few years monitoring of polymerization processes using fluorescent probes has been the most popular and powerful tools that can be used in order to understand the physical and chemical processes that occur at the molecular level. This is possible because their fluorescence is sensitive to the polarity and/or microviscosity of the molecular environment in which the probe molecules are located. Depending on the type of the process and the monitoring parameters, appropriate structure and characteristics of the probe are required. Therefore, there are no completely versatile probes. Search for new probes for monitoring polymerization resulted in the discovery of novel derivatives of 1*H*-quinoxalin-2-one. In this communication new fluorescent probes based on 1*H*-quinoxalin-2-one were characterized and their principal applications are presented. It has been found that the derivatives of 1*H*-quinoxalin-2-one shift their fluorescence spectrum with progress of photopolymerization of the monomer, which enables monitoring of the polymerization progress using the fluorescence intensity ratio measured at two different wavelengths as the progress indicator.

References

1. M. Topa, J. Ortyl, A. Chachaj-Brekiesz, I. Kamińska-Borek, M. Pilch, R. Popielarz, *Spectrochim Acta A Mol Biomol Spectrosc.*, 199 (2018) 430.

Acknowledgements: The authors thank. the Foundation for Polish Science. This work was supported by the Foundation for Polish Science (Warsaw, Poland) within the project POWROTY (Contract No. POWROTY/2016-1/4).

Solvent Effects on Fluorescence and Photochemistry of Flavonols. A Combined Spectroscopic and Computational Study

Alberto Mezzetti^a, Simone Lazzaroni^b, Abdenacer Idrissi^c, Ari Paavo Seitsonen^d,
Daniele Loco^e, Natalia Gelfand^e, Sandro Jurinovich^e, Benedetta Mennucci^e and Stefano Protti^b

^a Laboratoire de Réactivité de Surface UMR 7197, Sorbonne Université, 75005 Paris, France ;

^b Dipartimento di Chimica, University of Pavia, Italy ;

^c Laboratoire de Spectrochimie Infrarouge et Raman UMR 8516, Université de Lille, France ;

^d Département de Chimie, Ecole Normale Supérieure, Paris, France ;

^e Dipartimento di Chimica, Università di Pisa, Italy

alberto.mezzetti@upmc.fr

Flavonols are naturally-occurring molecules with interesting biological properties. They also have a peculiar photochemical behavior: when excited, their fluorescence spectrum is very sensitive to the surrounding environment. This behavior relies mainly on an excited-state intramolecular proton transfer (ESIPT) producing a (usually green) fluorescent tautomeric form of the molecule. Under some conditions, this ESIPT is partially or totally hampered, so that (usually violet) fluorescence from the normal state occur. Other phenomena, like ground-state deprotonation of OH groups, also strongly modify fluorescent properties [1].

Several synthetic flavonols (and 3-hydroxychromone derivatives) have been developed and are currently used as environment-sensitive fluorophors in biomedical research [1]. Similarly, natural flavonols (e.g. quercetin) are used as endogenous fluorophors in biochemistry [1].

We have investigated by electronic (UV-Vis, fluorescence, flash photolysis) and vibrational spectroscopies (Raman, Resonance Raman) the excited-state and ground-state proton transfer of several flavonols, including 3-hydroxyflavone and quercetin [2,3]. Spectroscopic data obtained in several solvents have been interpreted through quantum chemical calculations (TD-DFT) [4], whereas Car-Parrinello molecular dynamics (CPMD) made it possible to visualize processes like hydrogen bond formation and disruption [5]. A peculiar attention has been paid on the effect of the solvent-induced deprotonation of OH groups, not only to rationalize modification of fluorescence and other spectroscopic properties, but also in the chemistry and photochemistry of flavonols (see [6] and refs therein).

For quercetin, deprotonation of OH group(s) was found to be the key parameter in transforming a weakly fluorescent neutral molecule to strongly emitting mono-, di-, tri- anionic species [2]. This aspect is particularly relevant in order to interpret quercetin fluorescence data in biochemical studies [1].

The investigation has been also recently extended to other flavonoids (flavone, luteolin, chrysin, apigenin, 7-hydroxyflavone, 5-hydroxyflavone).

The results will be discussed in the framework of the use of flavonols and 3-hydroxychromone derivatives as fluorophors, as well as of their (photo-)reactivity.

References

1. S. Protti, A. Mezzetti, *Photochemistry*, ed. A. Albini, Royal Society of Chemistry, Cambridge 40 (2012) 295.
2. A. Mezzetti, S. Protti, C. Lapouge, J. P. Cornard, *Phys. Chem. Chem. Phys.* 13 (2011), 6858
3. S. Protti, A. Mezzetti, J. P. Cornard, C. Lapouge, M. Fagnoni. *Chem. Phys. Lett.* 467 (2008), 88
4. D. Loco, N Gelfand, S Jurinovich, S Protti, A Mezzetti, B Mennucci. *J. Phys. Chem. A* 122 (2018) 390
5. A. P. Seitsonen, S. Protti, A. Mezzetti, A. Idrissi, *in preparation*
6. S Protti, A Mezzetti. *J. Mol. Liq.* 205 (2015), 110

Notes

Molecular Structure and Properties [Inorganic Compounds]

Developing New Paramagnetic Copper(II) Complexes Based on 8-Hydroxyquinoline-5-Sulfonate

M. Luísa Ramos, Licínia L. G. Justino, Telma Costa, Artur J. M. Valente
and Hugh D. Burrows

*Chemistry Department and Coimbra Chemistry Centre, University of Coimbra, 3004-535 Coimbra
mlramos@ci.uc.pt*

30 years ago, Tang and VanSlyke [1] showed efficient electroluminescence from a device based on tris(8-hydroxyquinoline)aluminium(III) (Alq3). This takes part in both light emission and charge injection. The area of organic light emitting diodes (OLEDs) based on Alq3 for high resolution displays has developed into a multibillion Euro industry. We have studied complexes formed by the water soluble 8-hydroxyquinoline-5-sulfonate (8-HQS) with various metal ions, using multinuclear NMR, UV/visible absorption, fluorescence spectroscopy, and density functional theory (DFT) [2,3]. It was shown in some cases, that the luminescence of the metal complexes provides a sensitive technique for their detection and quantification, which can give selective metal ion determination through time resolved measurements. We extend those studies to Cu(II) ion, where a full speciation study has been carried out. On binding to Cu²⁺ ion, the weak 8-HQS fluorescence is quenched. In addition there are marked changes in the absorption spectra, which are suggested by DFT studies to be due to a dominant pentacoordinated [Cu(8-QS)₂(H₂O)]²⁻ complex. Additional interest in stable copper(II) complexes stems from their paramagnetic character, which is becoming increasingly useful in applications such as probing metalloprotein active site structure and mechanism, and in the development of contrast agents for magnetic resonance imaging (MRI) [4]. The important properties related with the ¹H fast relaxation of nearby nuclei of the Cu(II) complexes may make them good potential candidates for use as relaxation agents with potential application in magnetic resonance imaging (MRI).

References

1. C. W. Tang and S. A. Van Slyke, *Appl. Phys. Lett.*, 51 (1987) 913.
2. M. L. Ramos, L. L. G. Justino, A. Branco, C. M. G. Duarte, P. E. Abreu, S. M. Fonseca and H. D. Burrows, *Dalton Trans.*, 40 (2011) 11732.
3. M. L. Ramos, L. L. G. Justino, R. Barata, T. Costa, B. A. Nogueira, R. Fausto and H. D. Burrows, *Dalton Trans.*, 46 (2017) 9358.
4. N. N. Murthy, K. D. Karlin, I. Bertini and C. Luchinat, *J. Am. Chem. Soc.*, 119 (1997) 2156.

Acknowledgements: The authors thank the financial support from the Coimbra Chemistry Centre from the FCT (project PEst-OE/QUI/UI0313/2014), Rede Nacional de RMN (REDE/1517/RMN/2005), the Portuguese NMR Network, for the access to the NMR spectroscopy facilities, and the Laboratory for Advanced Computing at University of Coimbra for access to advanced resources that have contributed to this research. LLGJ and TC also acknowledge FCT for the postdoctoral grants SFRH/BPD/97026/2013, SFRH/BPD/47181/2008. TC also thanks the Coimbra Chemistry Centre for the award of a Research grant from the Project 2015/2020 UID/QUI/00313/2013.

Skin Permeation Tracking by Confocal Raman Spectroscopy

Rita Cardoso, Andreia M. Tabanez, Bernardo A. Nogueira and Rui Fausto

CQC, Department of Chemistry, University of Coimbra, 3004-535, Coimbra, Portugal

ritadascardoso@gmail.com

Confocal Raman Spectroscopy is a powerful non-invasive optical technique that allows one to obtain detailed information regarding the chemical composition of molecular compounds, with high specificity. This technique is based on the inelastic light scattering and detects the vibrational modes that are characteristic from each molecule, giving us the “fingerprint” of the studied molecule.

The skin is a special organ with the ability to protect the organism, which main goal is to guaranty the right homeostatic relationship between the body and the external environment. The main barrier that is involved in this function, the stratum corneum (SC), is also the barrier that needs to be overcome by a topically applied drug to get in the body.

The topic application of drugs has been gaining relevance, because strategies have been developed that allow to control the drug release. In this work, we have studied the skin permeability capacity of different compounds involved in the topical administration of a recently developed drug for photodynamic therapy of cancer. The investigations were performed in pig skin model samples, by collecting the Raman spectra of the different Z-points of the studied samples.

It was possible to follow the pattern of penetration of the studied components of the sampled formulation, and conclude that all of them are indeed able to overcome the SC. These results are in favor of the use of the studied formulation as vehicle for topical administration of the drug.

Acknowledgements: The Coimbra Chemistry Centre (CQC) is supported by FCT, through the project UI0313/QUI/2013, also co-funded by FEDER/COMPETE 2020-EU.

Vibrational Spectroscopy of Fe(II) and Zn(II) Complexes With the Phenanthrolinic Ligand Bipyridine-Glicoluril

Norberto S. Gonçalves^a and Jayr H. Marin^b

^a Departamento de Química, Universidade Federal de São Paulo, Campus Diadema, Rua Prof. Artur Riedel, 275, 09972-270, Diadema, SP, Brazil

^b Instituto de Química, Universidade de São Paulo, Av. Prof. Lineu Prestes, 748, 05508-900, Cidade Universitária, São Paulo, SP, Brazil
nsgoncal@gmail.com

The BPG proligand, obtained by condensing 1,10-phenanthroline-5,6-dione with urea, has interesting characteristics because it shows two receptor sites of hydrogen bonds (by oxygen atoms) and four donor sites (N-H groups), which is why their complexes are water soluble and can form highly organized supramolecular structures [1,2].

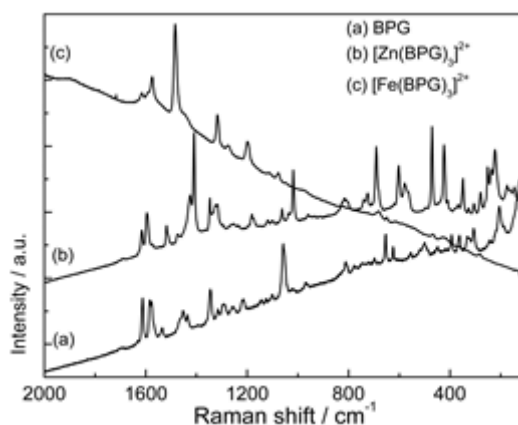


Figure 1 – Raman spectra of BPG and its complexes, excited at 830 nm.

The Raman spectrum of Fe(II) complex presents in the low wavenumber region fewer bands than the Zn(II) complex, probably due to the pre-resonance Raman effect exhibited by the Fe(II) complex (due to the intense CT band in the region of 500 nm), which leads to: (i) greater intensity of the modes in the region between 1000 and 1700 cm⁻¹, making it difficult to see the modes in the region of low wavenumbers (this pattern is usual in Fe(II) complexes with α,α' -diimines); (ii) the bands of the Fe(II) complex in this region show a different intensity pattern of the Zn(II) complex due to the selective intensification of the chromophore modes. The appearance of new bands in the low wavenumber region of Zn(II) complex Raman spectrum is evidence of coordination. The range of 1000 to 1600 cm⁻¹ shows no regular pattern of wavenumber displacement of the free ligand bands and the complexes, indicating the bonding or anti-bonding nature of the molecular orbitals involved in the coordination, which is being investigated by DFT B3LYP/LANL2DZ calculations. Calculated spectra agree well with experimental data.

References

1. D. G. Kurth, K.M. Fromm and J. M. Lehn, *Eur. J. Inorg. Chem.*, (2001) 1523.
2. M. S. Deshpande, A. S. Kumbhar and V. G. Puranik, *Cryst. Growth Des.*, 8 (2008) 1952.

Acknowledgements: The authors thank UNIFESP, USP and FAPESP.

A Theoretical and Experimental Investigation of Vibrational Spectra and Electronic Transitions on Some Aminoethylpyridine Molecules

Özge Bağlayan^a, İlkan Kavlak^b, Mustafa Şenyel^a and Güneş Süheyla Kürkçüoğlu^b

^a Physics Department, Eskişehir Technical University, Eskişehir TR-26470, Turkey

^b Physics Department, Eskişehir Osmangazi University, Eskişehir TR-26480, Turkey
gkurkcuo@ogu.edu.tr

In this study, the structural and spectroscopic investigations of 2-(2-aminoethyl)pyridine, 3-(2-aminoethyl)pyridine and 4-(2-aminoethyl)pyridine molecules were reported. The molecular geometries were optimized from Density Functional Theory-B3LYP and Hartree-Fock methods using 6-31++G(d,p), LANL2DZ, SDD basis sets on the ground state and, the infrared wavenumbers and intensities were predicted by using this geometry. Calculated wavenumbers and intensities were compared with FT-IR spectra of the molecules. Additionally, time depended density functional theory (TD-DFT) method using 6-31++G(d,p), LANL2DZ, SDD basis sets were used to determine the minimum energy structures of 2-(2-aminoethyl)pyridine, 3-(2-aminoethyl)pyridine and 4-(2-aminoethyl)pyridine molecules. The singlet and triplet transitions of these molecules in excited states were investigated. According to the calculated results, the vibrational wavenumbers and excitation energies show an excellent agreement with the experimental data.

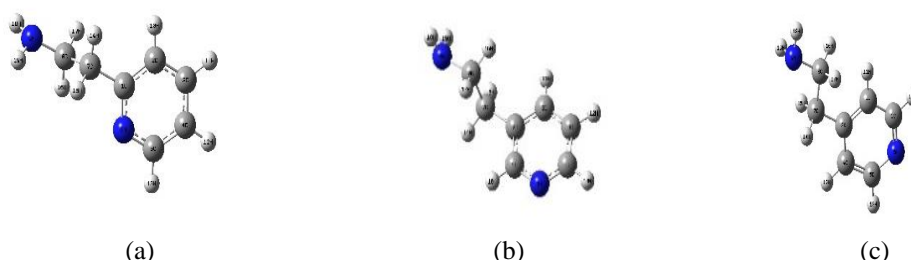


Figure 1 – The molecular structures of 2-(2-aminoethyl)pyridine (a), 3-(2-aminoethyl)pyridine (b) and 4-(2-aminoethyl)pyridine (c).

Acknowledgements: This work was supported by the Research Fund of Anadolu University (Project Number. 1503F103).

Synthesis, Crystal structure and Spectroscopic Properties of Cyanide Complex with 2-Ethylimidazole: $[\text{Cu}(\text{2-etim})_2\text{Ni}(\mu\text{-CN})_4]_n$

Güneş Süheyla Kürkçüoğlu^a, Tuğba Yavuz^a and Onur Şahin^b

^a Physics Department, Eskişehir Osmangazi University, Eskişehir TR-26480, Turkey

^b SUBITAM, Sinop University, Sinop TR-57000, Turkey
gkurkcuo@ogu.edu.tr

In this study, $[\text{Cu}(\text{etim})_2\text{Ni}(\mu\text{-CN})_4]_n$ (1) complex has been synthesized and characterized by vibrational (FT-IR and Raman) spectroscopy, elemental and thermal analyses. The crystal structure of 1 has been determined by single crystal X-ray diffraction technique. The molecular structure of 1, with the atom numbering scheme, is shown in Figure-1. The asymmetric unit of the heterometallic complex consist of one Cu(II) ion, one Ni(II) ion, four cyanide ligands, one etim ligand and one cyanide ligand. The Cu(II) ion is located on inversion center and coordinated by five nitrogen atoms, thus showing a distorted square pyramidal coordination geometry. The Ni(II) ion is coordinated by four carbon atoms from cyanide ligands, thus showing a square planar coordination geometry. The $[\text{Ni}(\text{CN})_4]^{2-}$ complex anions bridged by Cu(II) ions to generate a 1D chain.

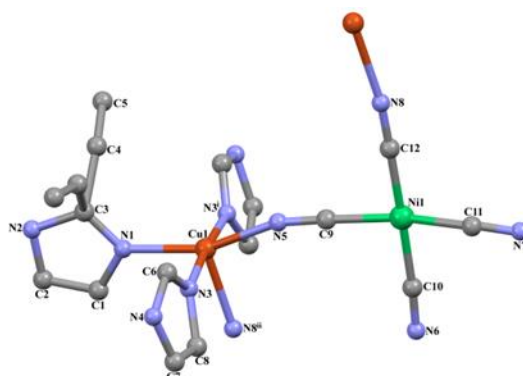


Figure 1 – Crystal structure of 1 showing the atom numbering scheme.

Acknowledgements: This work was supported by the Research Fund of Eskişehir Osmangazi University (Project Number. 2015-830).

Theoretical Study on the Molecular Structure and Vibrational Spectra of Cyanide-Bridged Heteronuclear Polymeric Complex: $[\text{Cd}(\text{mim})_2\text{Ni}(\mu\text{-CN})_4]_n$

Biray Kınık, İlkan Kavlak and Güneş Süheyla Kürkçüoğlu
Physics Department, Eskişehir Osmangazi University, Eskişehir TR-26480, Turkey
gkurkcuo@ogu.edu.tr

The cyanide-bridged complex of 2-methylimidazole (mim) was experimentally investigated by FT-IR, Raman spectroscopy and X-ray single crystal diffraction analysis in our previous study [1]. In this study, the molecular geometry and vibrational frequencies of the $[\text{Cd}(\text{mim})_2\text{Ni}(\mu\text{-CN})_4]_n$ complex in the ground state have been calculated by using DFT-B3LYP and DFT-B3PW91 with LANL2DZ basis set. A good correlation was found via comparison of the experimental and theoretical vibrational frequencies of the complex. The complex of the type: $[\text{Cd}(\text{mim})_2\text{Ni}(\mu\text{-CN})_4]_n$ has been studied in the $4000\text{-}250\text{ cm}^{-1}$ region and assignment of all the observed bands were made. The analysis of the FT-IR and Raman spectra indicates that there are some structure spectra correlations.

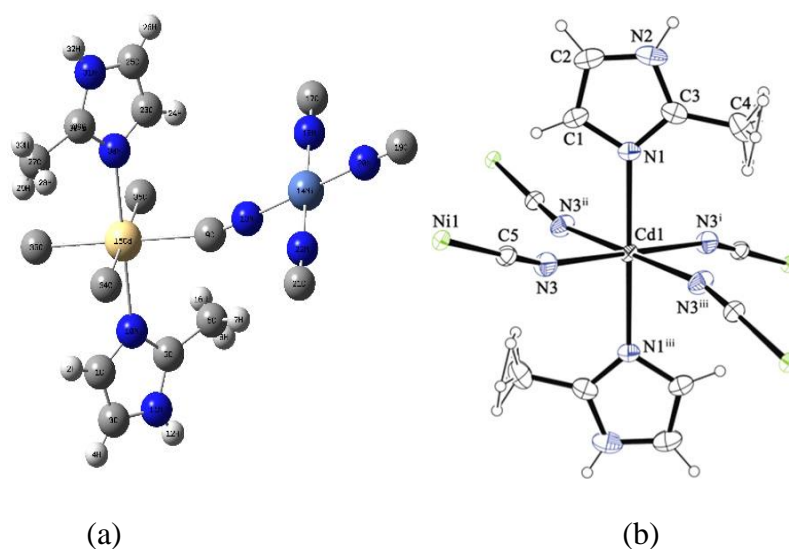


Figure 1 – Molecular model and optimized structure (a), and experimental schema of the complex (b) showing the atom numbering.

References

1. G. S. Kürkçüoğlu, O. Z. Yeşilel, I. Çaylı and O. Büyükgüngör, *J. Inorg. Organomet. Polym.*, 21 (2011) 306.

Acknowledgements: This work was supported by the Research Fund of Eskişehir Osmangazi University (Project Number. 2015-830).

Investigation of Structural Analysis and Thermostatic Properties of Thermal and UV Stabilizer as Organometallic Sn(II), Cu(II) and Cd(II) Barbiturate Complexes

İlkan Kavlak and Güneş Süheyla Kürkcüoğlu

Physics Department, Eskişehir Osmangazi University, Eskişehir TR-26480, Turkey
gkurkcuo@ogu.edu.tr

Previously, zinc(II) barbiturate complex was synthesized by Li and Yao [1]. Li and Yao determined that barbiturate complex act as HCl scavenger molecules during the PVC decomposition. In this study, there new organometallic barbiturate complexes have been synthesized. Their contribution to the thermal and UV stabilization of PVC was investigated by thermostatic analysis via according to ISO 182-2 standard. Additionally, the structural properties of the synthesized complexes were investigated by elemental analysis, single crystal X-ray diffraction (only Cu(II) complex), XRD and vibrational (IR and Raman) spectroscopy. The results are shown that synthesized complexes act as HCl scavengers during the PVC decomposition. The thermal decay of PVC dough which is including in new generation plastic additives are following: Cu(II)>Sn(II)>Cd(II) (Figures 1 and 2).

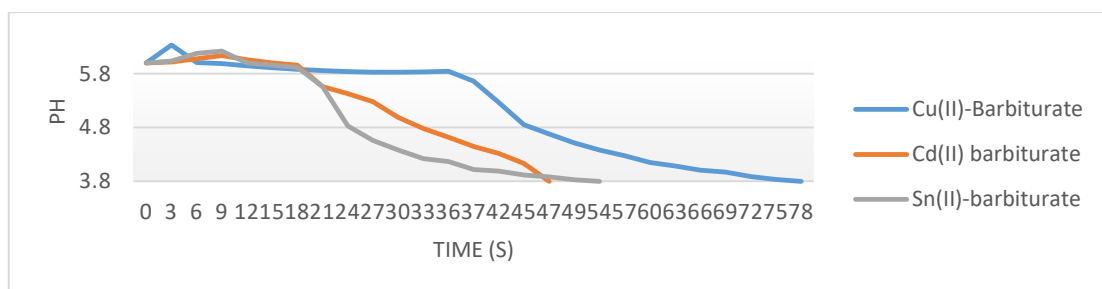


Figure 1 – Thermostatic analysis of barbiturate complexes.

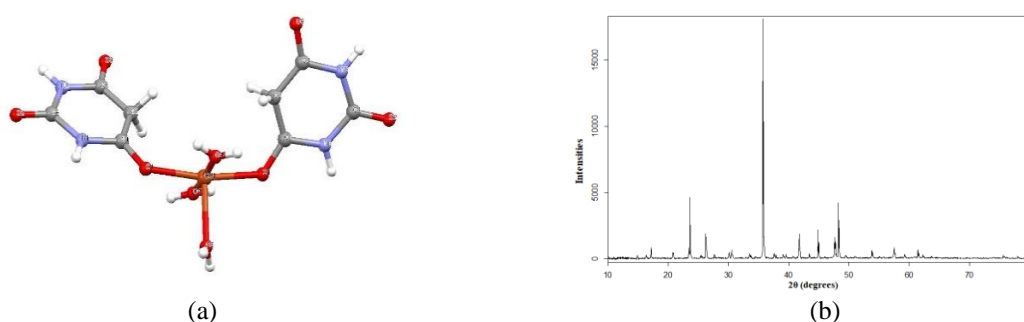


Figure 2 – (a) Molecular structure of $\text{Cu}(\text{C}_4\text{H}_4\text{N}_2\text{O}_3)_2 \cdot 3\text{H}_2\text{O}$, (b) XRD spectra of $\text{Cu}(\text{C}_4\text{H}_4\text{N}_2\text{O}_3)_2 \cdot 3\text{H}_2\text{O}$.

References

1. S. Li, Y. Yao, *Polym. Degrad. Stab.*, 96:4 (2011) 637.

Acknowledgements: This work was supported by the Research Fund of Eskişehir Osmangazi University (Project No. 2017-1588).

Synthesis, Spectral and Thermal Properties of 4-(2-aminoethyl)pyridinium tetracyanometallate(II) Complexes

Güneş Süheyla Kürkcüoğlu^a and Dursun Karaağaç^b

^a Physics Department, Eskişehir Osmangazi University, Eskişehir TR-26480, Turkey

^b Ulubatlı Hasan Anatolian High School, Bursa TR-16320 Turkey

gkurkcuo@ogu.edu.tr

The cyanide complexes of some transition metals with 4-(2-aminoethyl)pyridine (4aepy) of the general formula $(4aepyH)_2[M(CN)_4]$, where M = Ni(II), Pd(II) and Pt(II), were synthesized and were investigated by vibrational (FT-IR and Raman), thermal (TG, DTG and DTA) and elemental analysis techniques. FT-IR and Raman spectra of the complexes were recorded in the 4000-400 cm^{-1} and 4000-150 cm^{-1} regions, respectively, and vibrational assignments were given for all observed groups. The analysis of the FT-IR and Raman spectra of the complexes showed that the M(II) ion has a square plane geometry with four cyanide-carbon atoms and the $[M(CN)_4]^{2-}$ anions act as a counter ion. The 4aepy ligand in the complexes protonated and has acted as a cation. Thermal stability and decomposition products of the complexes were examined in a static air atmosphere at a temperature range of 40-700 °C. The results of the thermal and elemental analysis were found to be compatible with each other.

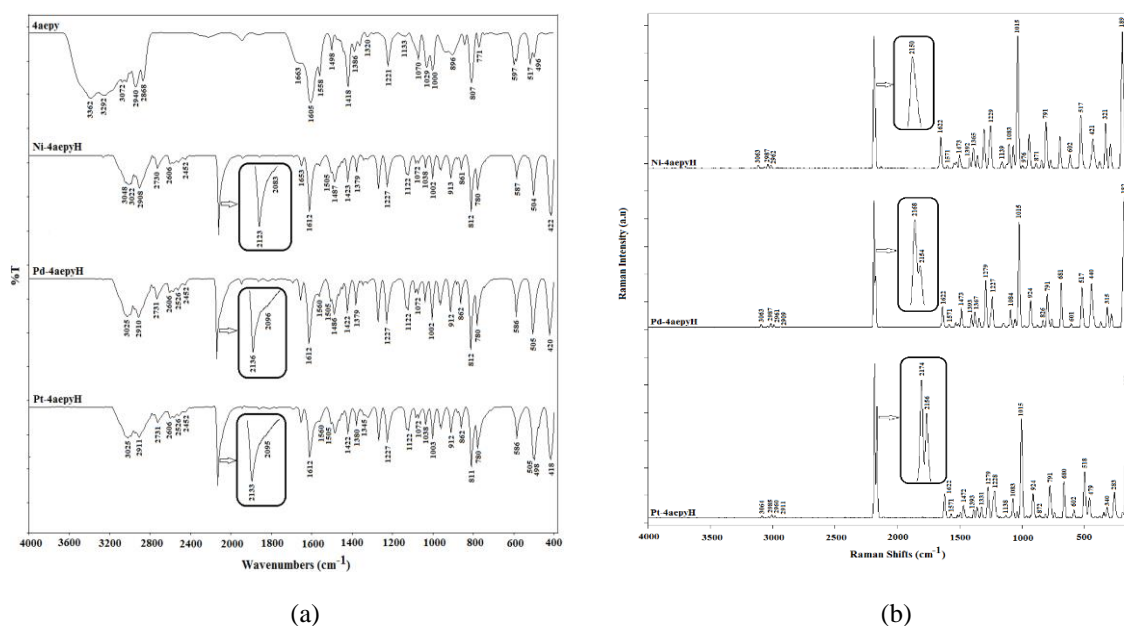


Figure 1 – The FT-IR spectra of the 4aepy and the complexes (a) and Raman spectra of the complexes (b).

Acknowledgements: This work was supported by the Research Fund of Eskişehir Osmangazi University (Project Number. 2015-830).

Spectral, Structural and Thermal Properties of Some Cyanide Complexes Containing Tetracyanonickelate(II) and 2-Aminoethylpyridine

Güneş Süheyla Kürkcüoğlu and Elvan Sayın

Physics Department, Eskişehir Osmangazi University, Eskişehir TR-26480, Turkey
gkurkcuo@ogu.edu.tr

Three new heteronuclear tetracyanonickelate(II) complexes of the type $[M(2aepy)_2Ni(\mu-CN)_2(CN)_2]_n$ ($M(II) = Mn, Fe$ or Ni ; $2aepy = 2\text{-aminoethylpyridine}$, hereafter, abbreviated as $M\text{-Ni-}2aepy$) were prepared in powder form and characterized by FT-IR and Raman spectroscopy, powder X-ray diffraction (PXRD), thermal (TG, DTG and DTA), and elemental analysis techniques. The structures of the complexes were elucidated using vibrational spectra and powder X-ray diffraction patterns with the peak assignment to provide a better understanding of the structures. It is shown that the spectra are consistent with a proposed crystal structure for these compounds derived from powder X-ray diffraction measurements. Vibrational spectra and PXRD patterns of the complexes were presented (Figure 1) and discussed with respect to the internal modes of both the $2aepy$ and the cyanide ligands. The C, H and N analyses were carried out for all the complexes. Thermal behaviors of these complexes were followed using TG, DTG and DTA curves in the temperature range $30\text{-}1000\text{ }^{\circ}\text{C}$ in the static air atmosphere.

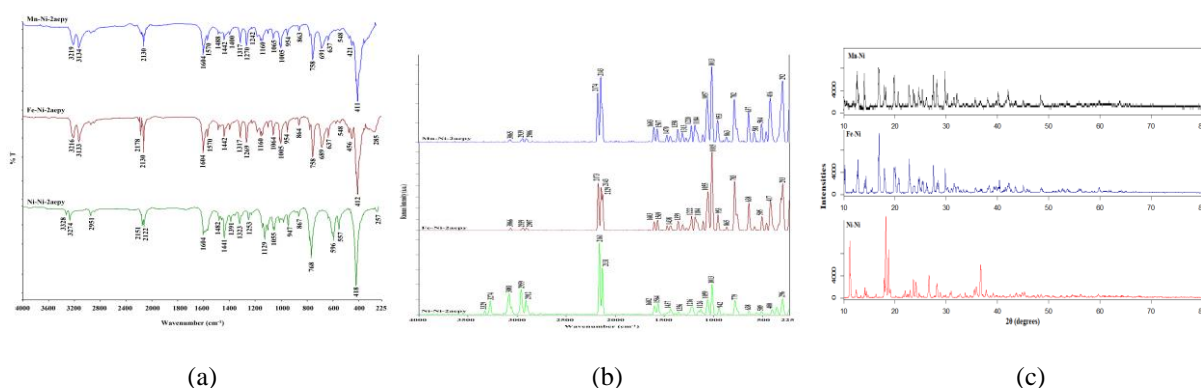


Figure 1 – FT-IR (a) and Raman (b) Spectra and PXRD-patterns (c) of complexes Mn-Ni-2aepy, Fe-Ni-2aepy and Ni-Ni-2aepy.

Acknowledgements: This work was supported by the Research Fund of Eskişehir Osmangazi University (Project Number. 2015-830).

Synthesis, Structural Characterization and C-H...Pd Interactions of the Metal-Cyanide Complex: $[\text{Cd}(\text{mim})_2\text{Pd}(\mu\text{-CN})_4]_n$

Güneş Süheyla Kürkçüoğlu^a, Elvan Sayın^a and Onur Şahin^b

^aPhysics Department, Eskişehir Osmangazi University, Eskişehir TR-26480, Turkey

^bSUBITAM, Sinop University, Sinop TR-57000, Turkey

gkurkcuo@ogu.edu.tr

The metal-cyanide complex with 2-methylimidazole, $[\text{Cd}(\text{mim})_2\text{Pd}(\mu\text{-CN})_4]_n$ (1) (2-methylimidazole abbreviated to mim), has been synthesized and structurally determined by vibrational (FT-IR and Raman) spectra, thermal and elemental analyses and X-ray single crystal diffraction technique. General information was acquired about structural properties of the complex from vibrational spectra by considering changes at characteristic peaks of the cyanide and mim ligands. The coordination environment of Pd(II) ions was coordinated by four carbon atoms from cyanide ligands, thus showing a square planar coordination geometry, whereas Cd(II) ions have identified as distorted octahedral geometry in the complex (Figure-1a). Adjacent 2D layers are further connected by C-H...M interactions resulting in the formation of 3D supramolecular networks. The most remarkable property of the complex is the presence of C-H...M interactions with distance value of 2.79 Å for 1 (Figure-1b). Thermal behaviors of the complex were examined using TG, DTG and DTA curves in the temperature range 30 - 700 °C in the static air atmosphere. The structure of complex 1 is similar to $[\text{Cd}(\text{mim})_2\text{Ni}(\mu\text{-CN})_4]_n$ [1].

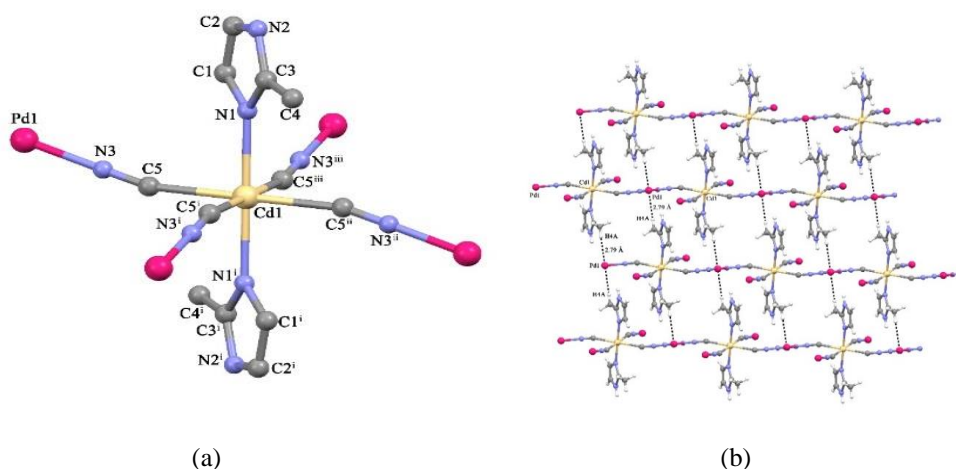


Figure-1 Crystal structure of 1 (a) and C-H...Pd interactions in 1 (b).

References

1. G. S. Kürkçüoğlu, O. Z. Yeşilel, I. Çaylı and O. Büyükgüngör, *J. Inorg. Organomet. Polym. Mater.*, 21 (2011) 306.

Acknowledgements: This work was supported by the Research Fund of Eskişehir Osmangazi University (Project Number. 2015-830).

Structural Characterizations of Cyanide and Fumarate Bridged Cu(II) and Cd(II) Complexes

Güneş Süheyla Kürkcüoğlu^a, Elvan Sayın^a, Okan Zafer Yeşilel^b and Onur Şahin^c

^a Physics Department, Eskişehir Osmangazi University, Eskişehir TR-26480, Turkey

^b Chemistry Department, Eskişehir Osmangazi University, Eskişehir TR-26480 Turkey

^c SUBITAM, Sinop University, Sinop TR-57000, Turkey

gkurkcuo@ogu.edu

The complexes, $[\text{Cu}_2(\mu\text{-fum})(\text{NH}_3)_4\text{Ni}(\mu\text{-CN})_4]_n$ (1) and $[\text{Cd}_2(\mu\text{-fum})(\text{NH}_3)_4\text{Ni}(\mu\text{-CN})_4]$ (2) (H_2fum = Fumaric acid), have been synthesized and characterized by FT-IR and Raman spectroscopies, elemental and thermal analyses. The crystal structure of 1 has been determined by single crystal X-ray diffraction technique. The molecular structure of 1, with the atom numbering scheme, is shown in Figure-1. The asymmetric unit of the heterometallic complex 1 consists of one Cu(II) ion, one Ni(II) ion, one cyanide ligand, half fumaric acid ligand and half ammine molecule. The single crystal x-ray study shows that heterometallic complex 1 has 2D coordination polymer. The $\nu(\text{C}\equiv\text{N})$ stretching vibrations arising from the cyanide groups are very characteristic and exhibit strong sharp absorption bands in the FT-IR and Raman spectra of the complexes (Figure-2). The Ni(II) ions are coordinated by four carbon atoms from cyanide ligands, thus showing a square planar coordination geometry. The $[\text{Ni}(\text{CN})_4]^{2-}$ complex anion bridged four M(II) ($\text{M} = \text{Cu}$ or Cd) ions to generate a 1D chain. The adjacent chains are further linked together by fumarate ligands to form a two-dimensional (2D) network. The 2D layers are connected by strong $\text{N-H}\cdots\text{O}$ hydrogen bonding interactions to form a three-dimensional network.

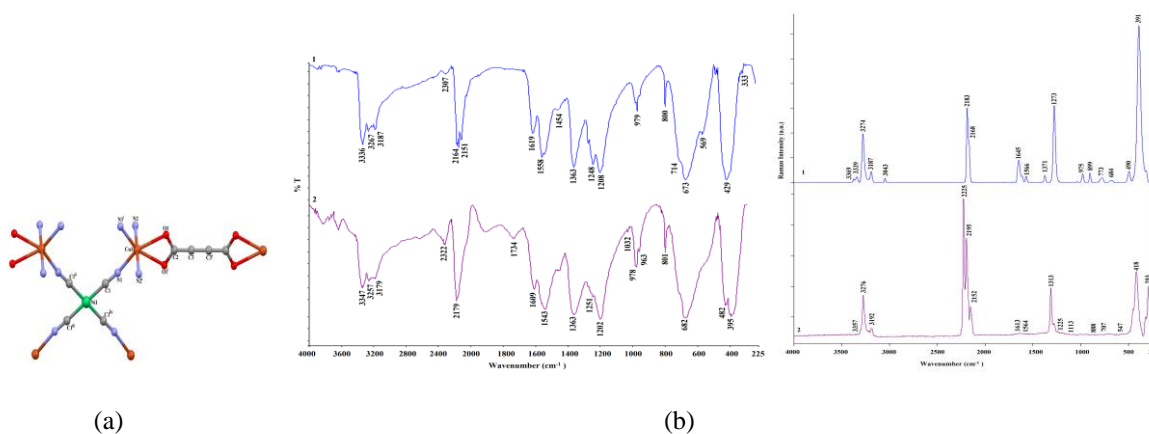


Figure-1 Crystal structure of 1 (a), The FT-IR and Raman spectra of 1 and 2 (b).

Acknowledgements: This work was supported by the Research Fund of Eskişehir Osmangazi University (Project Number. 2015-830).

Structural Analysis of Iron(III) Complexes with Nicotinic Acid Aroylhydrazones by IR Spectroscopy

Snežana Miljanić^a, Vasile Chiș^b, Darko Kontrec^c and Nives Galić^a

^a Division of Analytical Chemistry, Department of Chemistry, Faculty of Science, University of Zagreb, Horvatovac 102a, HR-10000 Zagreb, Croatia

^b Faculty of Physics, Babeș-Bolyai University, Kogălniceanu 1, RO-400084 Cluj-Napoca, Romania

^c Department of Organic Chemistry and Biochemistry, Ruđer Bošković Institute, PO Box 180, HR-10002 Zagreb, Croatia
miljanic@chem.pmf.hr

Among diverse properties of hydrazones resulting in wide range of their applications, particularly interesting are complexing abilities towards various metal ions [1]. Hence three iron(III) complexes, 1, 2 and 3, were synthesized with nicotinic acid aroylhydrazones, which all contained a hydroxyl group at the C2 atom of the phenyl ring, but differed in the position of a methoxy group, being placed at the C3, C4 and C5 atom, respectively. Elemental analysis indicated 1:2 metal to ligand stoichiometry for all the prepared complexes. The proposed structures were based on analysis and assignment of the experimental infrared (IR) spectra of both ligands and complexes, supported by theoretical calculations.

IR spectra implied that aroylhydrazones, consisting of the phenyl ring with the methoxy substituent in *ortho* (1) and *para* (3) position with respect to the hydroxyl group, coordinated Fe(III) in a similar way, but different from that of aroylhydrazone with the methoxy group in *meta* (2) position. Based on distinctive IR bands a coordination of the aroylhydrazone ligand in enolimine form was suggested for 2, binding to the metal cation through enolic oxygen, azomethine nitrogen and very likely hydroxyl group oxygen. Intense carbonyl stretching bands, observed in the IR spectra of the Fe(III) complexes 1 and 3, were associated with the carbonyl group not involved in coordination, implying existence of the ligands in ketoamine form.

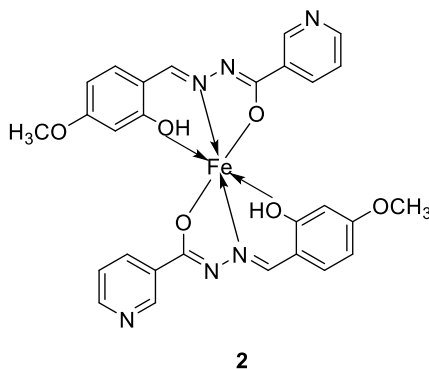


Figure 1 – Proposed structure of Fe(III) complex 2.

References

1. M. M. E. Shakhdoza, M. H. Shtaiwi, N. Morsy and T. M. A. Abdel-Rassel, *MainGroupChem.*, 13 (2014) 187.

Acknowledgements: The authors thank the Croatian science foundation for the support (project IP-2014-09-4841).

Spectroscopic FT-IR, FT-Raman and Ultraviolet-Visible Studies of the Potassium 5-Hydroxypentanoyltrifluoroborate Salt

Silvia A. Brandán^a, Lilian Davies^b and Maximiliano A. Iramain^a

^aCátedra de Química General, Instituto de Química Inorgánica, Facultad de Bioquímica, Química y Farmacia, Universidad Nacional de Tucumán, Ayacucho 471, (4000) San Miguel de Tucumán, Tucumán, Argentina

^bInstituto de Investigaciones para la Industria Química (INQUI, CONICET), Universidad Nacional de Salta, Av. Bolivia 5150, 4400 Salta, Argentina
brandansa@yahoo.com.ar

Different weak intermolecular interactions can be seen in the layered structures of some potassium trifluoroborate salts in the solid phase depending on the mutual arrangement of the potassium cations [1]. Hence, these salts present interesting structural and vibrational properties [2]. In this work, the potassium 5-hydroxypentanoyltrifluoroborate salt was characterized by using FT-IR, FT-Raman and UV-Visible spectroscopies and their structures and properties were studied in gas and aqueous solution phases by using B3LYP/6-31G* and B3LYP/6-311++G** calculations. The anion structure was also studied because it is expected in solution. Both theoretical structures can be seen in Figure 1.

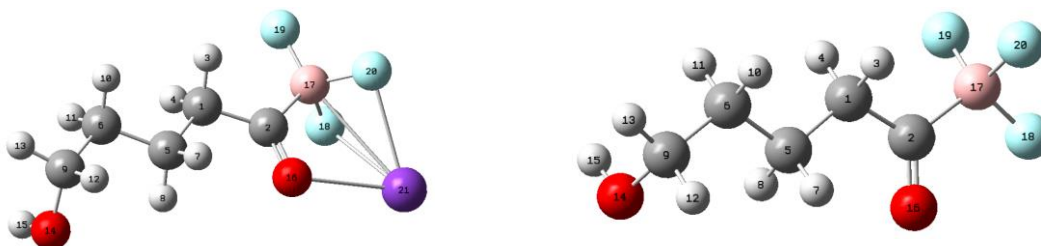


Figure 1 – Theoretical structures of the potassium 5-hydroxypentanoyltrifluoroborate salt and their anionic species.

A dimeric structure was also considered taking into account those layered structures observed for some potassium trifluoroborate salts in the solid phase. The complete vibrational assignments were performed for the salt and their anion combining the experimental FT-IR and FT-Raman spectra of the salt with the scaled quantum mechanical force field (SQMFF) methodology [3], the normal internal coordinates and the Molvib program [4]. The dimer justifies some bands not attributed to the monomer. The force fields and force constants are calculated for the salt and their anion. Here, the force constants are compared with those reported for the potassium 3-furoyltrifluoroborate [2] and 2-isonicotinoyltrifluoroborate salts [5]. Good concordance was observed among the predicted spectra and the experimental ones.

References

1. K. N. Jarzemska, M. Dabrowski, K. Durka, M. Kubsik, J. Serwatowski and K. Wozniak, *Cryst. Growth Des.*, 16 (2016) 1687.
2. M. A. Iramain, L. Davies and S. A. Brandán, *J. Mol. Struct.*, 1158 (2018) 245.
3. G. Rauhut and P. Pulay, *J. Phys. Chem.*, 99 (1995) 3093.
4. T. Sundius, *Vib. Spectrosc.*, 29 (2002) 89.
5. M. A. Iramain, L. Davies and S. A. Brandán, Submitted to *J. Mol. Struct.* (2018).

Acknowledgements: The authors thank to CIUNT, CONICET and Prof. T. Sundius for their permission to use Molvib.

The Electronic Structure of Aqueous Permanganate Ions: Probing Binding Energies and Molecular Bonding Character Using Liquid Jet Photoelectron Spectroscopy

K. Mudryk^{a, b}, R. Seidel^c, M. Pohl^{b, d}, B. Winter^d and I. Wilkinson^a

^a Institut Methoden der Materialentwicklung (EM-IMM), Helmholtz-Zentrum Berlin für Materialien und Energie, Albert-Einstein-Strasse 15, D-12489 Berlin, Germany

^b Fachbereich Physik, Freie Universität Berlin, Arnimallee 14, D-14195 Berlin, Germany

^c Nachwuchsgruppe Operando Grenzflächen-Photochemie (EE-NOGP), Helmholtz-Zentrum Berlin für Materialien und Energie, Albert-Einstein-Strasse 15, D-12489 Berlin, Germany

^d Molekülphysik, Fritz-Haber-Institut der Max-Planck-Gesellschaft, Faradayweg 4-6, D-14195 Berlin, Germany
karen.mudryk@helmholtz-berlin.de

The aqueous permanganate ion (MnO_4^- (aq)) is well-known for its properties as a strong oxidizing agent over a broad range of pH, acting as redox precursor of several manganese species with different oxidation states - namely, MnO_4^{2-} (aq), MnO_4^{3-} (aq), MnO_2 (s), and Mn^{3+} (aq) and Mn^{2+} (aq) complexes. As a result, MnO_4^- (aq) is considered to be a versatile oxidizer suitable for green chemistry [1,2] and alternative energy conversion research [3,4]. In order to investigate the electronic structure of this ion, we performed liquid-micro-jet-based soft X-ray photoelectron spectroscopy (XPS) [5] experiments on MnO_4^- (aq) solutions. Select valence, the Mn 3p, Mn 2p and O 1s binding energies were probed on an absolute energy scale. Additionally, resonantly-enhanced photoelectron spectroscopy (RPES) measurements were performed in the vicinity of the O K-edge and the Mn L_{III}-edge, providing experimental insight into the molecular bonding character of this ion. These measurements are expected to provide a reference for future theoretical calculations and experiments dedicated to the study of manganese complexes in aqueous solution.

References

1. N. Singh and D.G. Lee, *Org. Process Res. Dev.*, 5 (2001) 599.
2. A. Shaabani, P. Mirzaei, S. Naderi and D.G. Lee, *Tetrahedron*, 60 (2004) 11415.
3. A. N. Colli, P. Peljo and H. H. Girault, *Chem. Commun.*, 52 (2016) 14039.
4. T. R. Eliato, T. R., G. Pazuki and N. Majidian, *Energy Sourc. A, Recovery Util. Environ. Effects*, 38 (2016) 644.
5. B. Winter, *Nucl. Instrum. Methods Phys. Res. A*, 601 (2009) 139.

One Dimensional Cyanide Complexes with 4-(2-Aminoethyl)pyridine

Güneş Süheyla Kürkçüoğlu^a, Dursun Karaağaç^b and Tuncer Hökelek^c

^a Physics Department, Eskişehir Osmangazi University, Eskişehir TR-26480, Turkey

^b Ulubatlı Hasan Anatolian High School, Bursa TR-16320 Turkey

^c Physics Department, Hacettepe University, Beytepe TR-06800, Ankara, Turkey

gkurkcuo@ogu.edu.tr

Two new one-dimensional coordination polymers, $[\text{Cu}(\mu\text{-4aepy})_2(\text{H}_2\text{O})_2][\text{Ni}(\text{CN})_4]$ (**1**), and $[\text{Zn}(\mu\text{-4aepy})_2(\text{H}_2\text{O})_2][\text{Pd}(\text{CN})_4]$ (**2**) [4aepy = 4-(2-aminoethyl)pyridine] have been synthesized and characterized by vibrational (FT-IR and Raman) spectroscopy, single crystal X-ray diffraction, thermal and elemental analyses techniques. The FT-IR and Raman spectra are illustrated in Figure-1 (a) and (b), respectively. As can be seen from Figure 1, the presence of bands belonging to the ligands in the spectra of the complexes shows the existence of aqua, 4aepy and cyanide in the complexes. The most significant vibration bands of the aqua ligand are asymmetric and symmetric $\nu(\text{OH})$ stretching vibration bands (at $3550\text{--}3200\text{ cm}^{-1}$) and $\delta(\text{OH}_2)$ deformation vibration band (at $1630\text{--}1600\text{ cm}^{-1}$). The structural analyses revealed that complexes **1** and **2** are isomorphous and isostructural, and have polymeric 1D network. The Ni(II) or Pd(II) atoms exhibit the usual square planar geometry with the cyanide ligands. The coordinations around the Cu(II) or Zn(II) atoms are slightly distorted square-planar arrangements, while the slightly distorted octahedral coordinations are completed by the symmetry related water O atoms in the axial positions. The vibrational spectral data are very much consistent with the structural data presented of the complexes (Figure-1). Thermal stabilities and decomposition products of the complexes were investigated in the temperature range $40\text{--}800\text{ }^\circ\text{C}$ in the static air atmosphere.

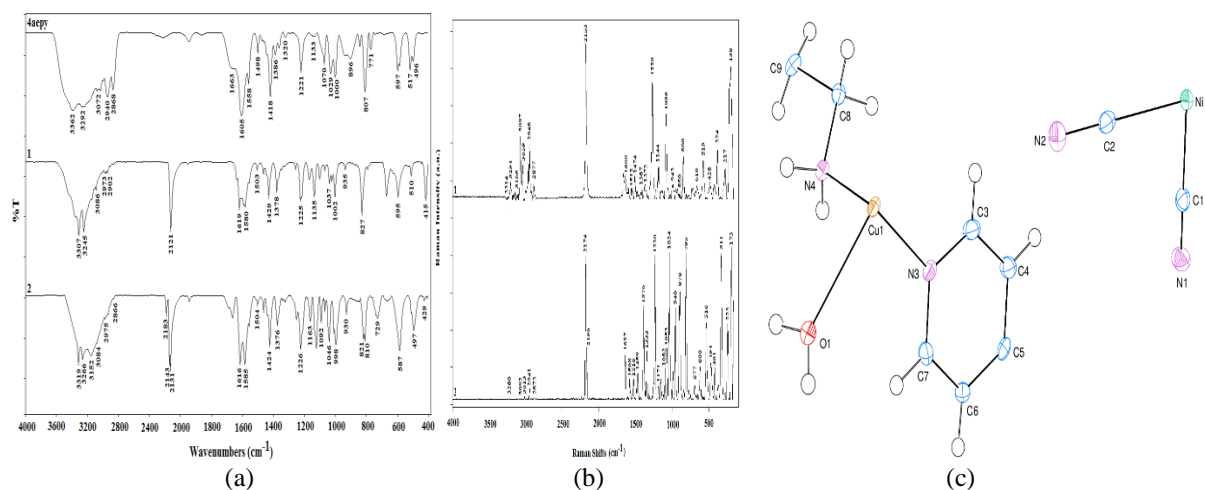


Figure 1 – The FT-IR spectra of the 4aepy and the complexes (a); Raman spectra of the complexes (b) and the asymmetric unit of complex **1** with the atom-numbering scheme.; displacement ellipsoids are drawn at the 50% probability level (c).

Acknowledgements: This work was supported by the Research Fund of Eskişehir Osmangazi University (Project Number. 2015-830).

Vibrationally-Resolved Chiroptical Spectrum Study of Octahedral Cyclometalated Iridium (III)

Qin Yang, Marco Fusè, Franco Egidi, Julien Bloino
Scuola Normale Superiore, Piazza dei Cavalieri 7, 56126 Pisa, Italy
qin.yang@sns.it

Over recent years, cycloiridiated complexes have attracted growing interest, in particular for their application as biomarkers, thanks to their bright phosphorescence [1]. Due to their chirality, the helically shaped Ir(III) complexes can interact very differently with the biological environments. Therefore, chiroptical studies can help investigating their configurations and rationalizing their properties, and in turn support the design of new, more efficient structures. Based on those considerations, electronic circular dichroism (ECD) and circularly polarized phosphorescence (CPP) can be especially valuable. However, an in-depth interpretation of experimental spectra is rarely straightforward since the spectral band-shape is the result of multiple effects, which can be properly studied only with the help of computational spectroscopy. Due to their sensitivity, the mere broadening of the pure electronic transition is often inrarely sufficient for chiroptical spectroscopies and a proper description of the vibrational contribution has to be taken into account [2,3]. To this end, frequency calculations become necessary, which significantly raise the computational cost. Thanks to more efficient algorithms and processors, such an approach can be applied to systems of growing size and complexity. Furthermore, approximated schemes can further reduce the computational cost.

In this contribution, we will present a computational protocol designed for the accurate simulation of vibrationally resolved chiroptical spectra of organometallic complexes. The recently reported chiral cycloiridiated complexes bearing a chiral N-heterocyclic carbene ligand were chosen as test cases. Due to the size of these systems, density functional theory (DFT) and its time-dependent extension (TD-DFT) are the most suitable electronic structure calculation methods. However, exchange-correlation functionals and basis sets can display very diverse performance for a given molecule. Thus, an initial benchmark was carried out using the ECD spectra of those complexes as reference. Next, the issue of the description of the potential energy surfaces (PESs) at the harmonic level with respect to the electronic transitions and its impact on the spectral band-shape will be considered. For CPP, standard electronic structure calculation method cannot be used to evaluate the intensity of the phosphorescence process. Thanks to recent developments to properly account for spin-orbit couplings (SOC) between states of different spin multiplicities, [4] quantitative band-shapes can now be routinely simulated [5]. Finally, we will show how proper graphical representations can greatly help and shade light on the nature of the chiroptical properties and the origin of the band-shape.

References

1. D.-L. Ma, H.-Z. He, K.-H. Leung, D.S.-H. Chan, and C.-H. Leung, *Angew. Chem. Int. Ed.*, 52 (2013) 7666.
2. J. Bloino, A. Baiardi and M. Biczysko, *Int. J. Quantum Chem.*, 116 (2016) 1543.
3. J. Bloino, M. Biczysko, F. Santoro and V. Barone, *J. Chem. Theory Comput.*, 6 (2010) 1256.
4. F. Egidi, S. Sun, J. J. Goings, G. Scalmani, M. J. Frisch and X. Li, *J. Chem. Theory Comput.*, 13 (2017) 2591.
5. F. Egidi, M. Fusè, A. Baiardi, J. Bloino, X. Li and V. Barone, *Chirality*, (2018), DOI:10.1002/chir.22864.

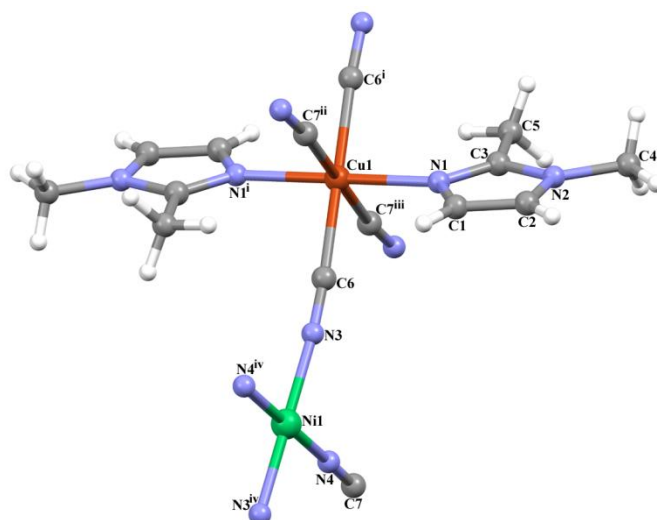
Synthesis, Spectral, Thermal and Crystal Structure of Cyanide Bridged Hetero-Metallic Polymeric Complex: $[\text{Cu}(\text{dmi})_2\text{Ni}(\mu\text{-CN})_4]_n$

Güneş Süheyla Kürkçüoğlu^a and Onur Şahin^b

^a Physics Department, Eskişehir Osmangazi University, Eskişehir TR-26480, Turkey

^b SUBITAM, Sinop University, Sinop TR-57000, Turkey
gkurkcuo@ogu.edu.tr

Cyanide bridged hetero-metallic complex of the formula, $[\text{Cu}(\text{dmi})_2\text{Ni}(\mu\text{-CN})_4]_n$ (dmi = 1,2-dimethylimidazole) have been synthesized and characterized by vibrational (FT-IR and Raman) spectroscopy, single crystal X-ray diffraction, thermal analysis and elemental analysis. The crystallographic analyses reveal that the complex, $[\text{Cu}(\text{dmi})_2\text{Ni}(\mu\text{-CN})_4]$, have polymeric 2D networks. In the complexes, four cyanide groups of $[\text{Ni}(\text{CN})_4]^{2-}$ coordinated to the adjacent Cu(II) ions and distorted octahedral geometries of the complex are completed by two nitrogen atoms of trans dmi ligands. The structure of the complex is similar and linked via intermolecular hydrogen bonding, $\text{C}—\text{H}\cdots\text{Ni}$ interactions to give rise to 3D networks. Vibration assignments are given for all the observed bands and the spectral features also supported to the crystal structure of heteronuclear complex. The FT-IR and Raman spectra of the complex are very much consistent with the structural data presented.



Solvothermal Synthesis of Zinc Oxide: A Combined Experimental and Theoretical Study

Ankica Šarić^a, Ines Despotović^b and Goran Štefanić^a

^a Ruđer Bošković Institute, Centre of Excellence for Advanced Materials and Sensing Devices, Bijenička 54, HR-10002 Zagreb, Croatia

^b Ruđer Bošković Institute, Division of Physical Chemistry, Bijenička 54, HR-10002 Zagreb, Croatia
Ankica.Saric@irb.hr

Zinc oxide is of interest in many applications as an important material with excellent combination of optical, electrical and microstructural properties. In order to optimize the properties of ZnO material for the highly technical or biomedical applications it is necessary to control its structure and morphology. This research is a follow up to our previous investigations [1,2]. In a previous paper [2] we studied and compared the impact of a versatile family of ethanolamines (MEA and TEA) on the microstructural properties of the ZnO particles prepared in ethanol. In the present work zinc oxide particles were synthesized from zinc acetylacetonate in the presence of triethanolamine (TEA) and various alcoholic solvent, ethanol or octanol, at 170 °C. The structural, optical and morphological characteristics of ZnO particles were monitored using X-ray powder diffraction (XRD), UV-Vis spectroscopy and field emission scanning electron microscopy (FE-SEM). The experimental findings are confirmed by means of DFT calculations. On the basis of both microstructural and theoretical studies, the nucleation and growth mechanism of ZnO nanoparticles is proposed. The nucleation and formation mechanism of ZnO nanoparticles was proposed considering the results obtained from a computational study of Gibbs free energies of ZnO–TEA molecular interactions (ΔG^*_{INT}) in various solvent system. The calculations revealed different binding affinities which initiated the nucleation processes of ZnO into nanoparticles in the presence of alcohols of different size and polarity. The high chelating efficiency of TEA towards zinc with tetrahedral geometry is observed.

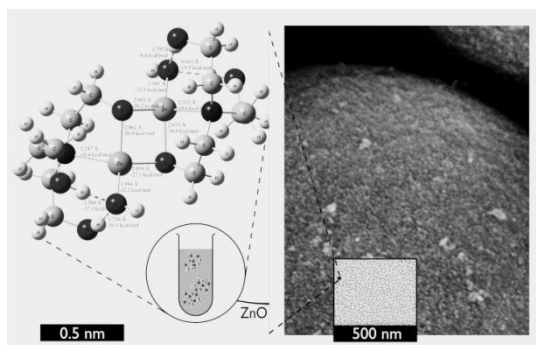


Figure 1 – The most stable structure of ZnO–TEA dimer (left) and FE-SEM image of ZnO (right).

References

1. A. Šarić, G. Štefanić, G. Dražić and M. Gotić, *J. Alloys Comp.* 652 (2015) 91.
2. A. Šarić, I. Despotović, G. Štefanić and G. Dražić, *Chemistry Select* 2 (2017) 10038.

Acknowledgements: This work has been partially supported by SAFU, project KK.01.1.1.01.0001.

The Synthesis and Structural Characterization Co(II)-amino acid–CaAl-Layered Double Hydroxide Composites

Gábor Varga^{a,b}, Zoltán Kónya^{c,d}, Ákos Kukovecz^c, Pál Sipos^{b,e} and István Pálínkó^{a,b}

^a Department of Organic Chemistry, ^b Materials and Solution Structure Research Group, Institute of Chemistry,

^c Department of Applied and Environmental Chemistry, ^d MTA-SZTE Reaction Kinetics and Surface Chemistry

Research Group, ^e Department of Inorganic and Analytical Chemistry, University of Szeged, Dóm tér 7-8,

Szeged, H-6720 Hungary

palinko@chem.u-szeged.hu

Many types of guest materials were incorporated among the layers of layered double hydroxides (LDHs); however, only few studies can be identified in which the intercalation of transition metal complexes are presented, for a recent review [1]. Moreover, the synthesis of composite materials having cobalt-amino acid complexes as guests has not been reported yet.

This study describes the incorporation of Co(II)-amino acid (L-histidine, L-cysteine, L-tyrosine) complexes into CaAl-LDH. The main aim was to form composite materials containing the complexes overwhelmingly among the layers of the LDH. To achieve this goal, the synthesis conditions were varied systematically, and the optimum circumstances were identified.

The stepwise intercalation (introducing the anionic form of the amino acid first, then constructing the Co(II) complex) proved to be unsuccessful, while the direct ion exchange of the anionic form of the separately prepared complex provided with the Co(II) complex intercalated substances. The success of the intercalation was verified by X-ray diffractometry. Due to the optimization efforts, intercalated structure of high crystallinity was obtained without by-product formation.

The resulting composite materials were characterized by a range of instrumental methods like UV–Vis, inductively coupled plasma–optical emission, mid-range as well as far infrared spectroscopies and scanning electron microscopy.

It was found that the amino acid anions acted as bidentate ligands occupying four coordination sites, which were identified as N_{imidasolate}, O_{carboxylate}, N_{amino} and O_{phenolate} and assumed as S_{thiolate}. The remaining two sites were filled by water molecules being abundant in any LDH structure. The possible structural arrangement is visualized with the combination of experimental finding and molecular modelling.

References

1. P. Sipos and I. Pálínkó, *Catal. Today*, 1 (2018) 123.

Acknowledgements: This work was supported by the National Science Fund of Hungary through grant OTKA NKFI 106234. The financial help is highly appreciated.

Demetalation Processes on Clinoptilolite. Kinetic Studies

Kamila Brylewska^{a,b}, Piotr Rożek^a, Magdalena Król^a and Włodzimierz Mozgawa^a

^aAGH University of Science and Technology, A. Mickiewicza Av. 30, 30-059 Krakow, Poland

^bJagiellonian University, Faculty of Chemistry, Gronostajowa 2, 30-387 Krakow, Poland
kamilaaa@agh.edu.pl

Zeolites are crystalline aluminosilicates, built of a three-dimensional framework of alumina [AlO₄] and silica [SiO₄] tetrahedra. It is also known that zeolites are characterized by high ion-exchange capacity and good sorption properties. Because of this, they can be used in environmental protection and catalysis. The first one provides them an ability to sorb harmful molecules or ions, e.g. Ag⁺, Cu²⁺, Ni²⁺, Cd²⁺, Pb²⁺, or Cr³⁺ [1]. Most of them are highly toxic, non-biodegradable and belong to commonly occurring pollutants. An immobilization of heavy metals involves their total deactivation and binding in the zeolite structure [2,3]. Although this process involves adsorption, chemisorption and ion-exchange, it is predominantly the last of these phenomena responsible for high sorption capacity of these materials [4].

In the present study, a natural clinoptilolite (CLI: Si/Al = 4.9) was modified in two ways using two modification agents (MA): (i) desilication with a NaOH solution, and (ii) dealumination with a HNO₃ solution. Cadmium Cd²⁺ immobilization studies were performed in two stages: (i) determination of sorption value on studied samples depending on an initial cation concentration in the solution and (ii) kinetic studies to have a valuable insight into a sorption process mechanism. Additionally, to determine textural and structural properties, XRF, XRD, FT-IR, BET, and SEM studies, were carried out.

Applied modification contributes to a slight disorder of crystalline structure, suggesting that zeolite stability may be disturbed after demetalation processes. The loss of crystallinity is partial and increases with increasing concentration of MA. Demetalation processes contribute to an exposure of unit cell parameters of CLI, with an unnoticeable *c* parameter change, which is parallel to zeolite channels. Consequently, changes in *a* and *b* parameters can be dictated by sorption properties of tested materials. In addition, a slight decrease in cell volume is observed, what can be related to the removal of silicon and aluminum cations from CLI framework (contraction of unit cell). An introduction of foreign extraframework cations by ion-exchange procedure affects the image of oscillation spectra, especially in the range of pseudolattice oscillations (ring vibrations carried out by [AlO₄] and [SiO₂] tetrahedra, forming SBU units). The comparison of IR spectra before and after a sorption of Cd²⁺ cation indicates that there are slight differences in ring oscillation range. A visible growth in the ring bands intensity (4- and 5-MR vibrations coming from 4-4 = 1 units) is observed. The location remains virtually unchanged.

References

1. W. Mozgawa and T. Bajda, *Phys. Chem. Miner.*, 31 (2005) 706.
2. V. J. Inglezakis, M. D. Loizidou and H. P. Grigoropoulou, *J. Colloid Interf. Sci.*, 261 (2003) 49.
3. M. Panayotova and B. Velikov, *J. Environ. Sci. Heal.*, A 37 (2002) 139.
4. J. Fronczyk, *Sci. Rev. Eng. Environ. Sci.* (2006).

Acknowledgements: This work was financially supported by the National Science Centre in Poland as part of grant no. 2016/21/N/ST8/01332.

Hydrothermal Synthesis of Zeolite Aggregate and their Use as a Sorbent of Heavy Metal Cations

Magdalena Król

AGH University of Science and Technology, Faculty of Materials Science and Ceramic, 30 Mickiewicza Av.,
30-059 Krakow, Poland
mkrol@agh.edu.pl

The aim of this study was to obtain suitable absorbent material for environmental applications. The results of synthesis of zeolite granulate from expanded glass aggregate using hydrothermal method under autogenous pressure were presented [1]. The resulting materials were analyzed regarding phase composition. In particular, the structures of materials were examined using FT-IR spectroscopy. This method is particularly useful for following the progress in a crystallization process. The results were compared to the XRD measurements, as well as SEM observations.

The effects of synthesis temperature and time, as well as Si/Al and Na/Si ratios on the obtained products were determined. It has been found that by using suitable chemical composition is possible to efficiently zeolite synthesis at 70°C. The type of resulting zeolite structure was identified based on XRD measurements and confirmed by analysis of the mid infrared spectra. Pseudolattice range, *i.e.* 800–400 cm⁻¹, was detailed analyzed. In this range, there are bands associated with the ring vibrations, which are characteristic for secondary building units (SBU) occurred in zeolite structure [2-4]. Depending on the composition of the reaction system, temperature and time, zeolite X, A, Na-P1 and hydroxysodalite have been identified as synthesis products.

Practical aspects of heavy metal cations sorption onto material synthesized in selected conditions will be presented. The atomic absorption spectroscopy (AAS) has been used as method, from which the concentration of ions in solution before and after sorption process and thus the effective cation exchange capacity (CEC) have been determined [5]. The results were compared with the ones obtained for other zeolite materials. It was found, that zeolitic granules on the basis of expanded glass have very good sorption properties.

References

1. M. Król and A. Mikula, *Microporous Mesoporous Mater.* 243 (2017) 201.
2. M. Król, W. Mozgawa, W. Jastrzębski and K. Barczyk, *Microporous Mesoporous Mater.* 156 (2012) 181.
3. W. Mozgawa, *J. Mol. Struct.* 596 (2001) 129.
4. M. Król, W. Mozgawa, J. Morawska and W. Pichór, *Microporous Mesoporous Mater.* 196 (2014) 216.
5. M. Król, E. Matras and W. Mozgawa, *Int. J. Environ. Sci. Technol.* 13 (2016) 2697.

Acknowledgements: This work was financially supported by the National Science Centre in Poland under grant no. 2016/21/D/ST8/01692.

ATR-FTIR Studies of Zeolite Formation During Alkali-Activation of Metakaolin

Magdalena Król, Piotr Rożek and Włodzimierz Mozgawa

AGH University of Science and Technology, Faculty of Materials Science and Ceramic, 30 Mickiewicza Av.,
30-059 Krakow, Poland
mkrol@agh.edu.pl

Metakaolin is a product of kaoline clay calcination and it is commonly used as an aluminosiliceous raw material in the so-called geopolymerization process [1]. Due to its chemical composition, it is also used in the synthesis of zeolite A [2].

In this work changes in the aluminosilicate structure of the metakaolin during alkali-activation have been analyzed in detail on the basis of ATR/FT-IR spectra [3]. These changes mainly affect both the integral intensity and FWHM of bands in the range of $1200\text{--}950\text{ cm}^{-1}$, however dehydration and carbonation process can be also analyzed based on obtaining results.

Based on the change of ATR-IR spectra over time, the zeolitization/geopolymerization process can be divided into three stages: (1) dissolution of initial aluminosilicate raw material; (2) disappearance of polymeric aluminosilicates in favor of orthosilicate phases with disordered structure; and (3) condensation of tetrahedrons connected with the disappearance of polarized forms.

References

1. M. Król, J. Minkiewicz and W. Mozgawa, *J. Mol. Struct.*, 1126 (2016) 200.
2. S. Chandrasekhar, P. Raghavan, G. Sebastian and A.D. Damodaran, *Appl. Clay Sci.*, 12 (1997) 221.
3. M. Król, P. Rożek, D. Chlebda and W. Mozgawa, *Spectrochim. Acta A*, 198 (2018) 33.

Acknowledgements: This work was financially supported by the National Science Centre in Poland under grant no. 2015/17/B/ST8/01200.

The Influence of Synthetic Conditions on the Structural and Microstructural Properties of $\text{ZrO}_2\text{-Y}_2\text{O}_3$ System

Viktoria Babić, Mile Ivanda and Goran Štefanić

*Center of Excellence for Advanced Materials and Sensing Devices, Ruđer Bošković Institute,
Bijenička c. 54, HR-10002 Zagreb, Croatia
Goran.Stefanic@irb.hr*

Due to their superior mechanical properties (strength and toughness), biocompatibility and aesthetic appearance (white color with natural translucency) bioceramics based on yttria-stabilized tetragonal zirconia polycrystals (Y-TZP) have become prevalent in prosthetic dentistry. However, the main drawback associated with the use of Y-TZP ceramics is the appearance of cracking due to volume expansion during the transition from tetragonal to the thermodynamically stable monoclinic polymorph of zirconia. In the present investigation we examined the influence of synthetic conditions on the structural and microstructural properties of $\text{ZrO}_2\text{-Y}_2\text{O}_3$ system. Amorphous precursors of the $\text{ZrO}_2\text{-Y}_2\text{O}_3$ system with different molar fractions of zirconium and yttrium ions (from 0 to 100 mol %) were obtained by coprecipitation from aqueous solutions of nitrate salts by addition of ammonia up to $\text{pH} = 10.4$. Crystallization of the starting amorphous precursors was carried out using two different synthetic methods: hydrothermal treatment at $150\text{ }^\circ\text{C}$ for 24 h and annealing in the air atmosphere for 2 h at temperatures of $400\text{ }^\circ\text{C}$, $600\text{ }^\circ\text{C}$, $800\text{ }^\circ\text{C}$, $1000\text{ }^\circ\text{C}$ and $1200\text{ }^\circ\text{C}$. Structural analysis of the crystallization product was performed by X-ray powder diffraction (XRPD) and Raman spectroscopy, and the morphology of the crystalline grains was followed by the scanning electron microscope (SEM). The crystallization temperature of amorphous precursors with yttrium content up to 30 mol% was determined by differential scanning calorimetry (DSC). Quantitative analysis of crystalline products was carried out using Rietveld refinements of powder diffraction patterns. Precise determination of the unit-cell parameters in the $\text{ZrO}_2\text{-}$ and $\text{Y}_2\text{O}_3\text{-type}$ solid solutions was carried out by Rietveld refinements of the products with added silicon standard.

The results of DSC analysis show that the incorporation of yttrium ions caused small increase of the crystallization temperature, from $487\text{ }^\circ\text{C}$ (0 mol% of yttrium ions) to $516\text{ }^\circ\text{C}$ (20 mol% of yttrium ions). The unit-cell volume of the tetragonal ZrO_2 solid solutions (up to 20 mol% of yttrium ions) and cubic ZrO_2 solid solutions (above 20 mol% of yttrium ions) increases linearly with the increase in the fraction of the yttrium. This linear dependence continued even after the transition from cubic ZrO_2 solid solution to $\text{Y}_2\text{O}_3\text{-type}$ solid solution in the products with more than 60 mol% of yttrium ions. The results of SEM and diffraction line broadening analysis have shown that the increase in calcination temperature leads to the growth of crystalline grains and the reduction of porosity. On the other hand, the increase in the share of doped cations leads to the decrease in crystallinity.

Acknowledgements: This work has been fully supported by SAFU, project KK.01.1.1.01.0001.

IR Spectroscopy of Small Isolated Cationic Cobalt and Nickel Ethanol Clusters and Implementation of a Desorption Source

M. Becherer, F. Dietrich and M. Gerhards

TU Kaiserslautern, Fachbereich Chemie, 67663 Kaiserslautern, Germany

becherer@chemie.uni-kl.de; gerhards@chemie.uni-kl.de

Clusters containing transition metals and aliphatic ligands provide model systems regarding *e.g.* catalytical properties, magnetism, reactivity and structure. Furthermore, investigation of clusters can reveal potential cooperative effects. Thus, the successive variation of size and ligand number of the metal clusters can give a fundamental insight.

The investigated cationic cobalt, nickel and mixed cobalt/nickel clusters with ethanol contain one, two, three or four metal centers and are produced by applying laser ablation to a rotating metal rod and by attaching the ethanol ligand in a supersonic beam. The ions are detected with a time-of-flight mass spectrometer and the IR spectra are obtained by means of IR-photofragmentation spectroscopy. The frequencies and frequency shifts of CH and OH stretching vibrations with respect to different cluster sizes, spin states and different isomers of one cluster are discussed in comparison with DFT calculations. Both, clusters with intact ethanol aggregated as well as clusters with dissociated ethanol attached are observed depending on the metal core. Especially in the case of clusters containing one Ni atom both intact and dissociated structures are formed. A detailed analysis of the spectroscopic and theoretical results yields insights in the structure and reactivity of the clusters as well as on cooperative effects between the metal centers.

For transition metal containing (neutral) complexes which cannot be formed from in situ in the gas phase experiments, the transfer into a molecular beam is a challenging task since decomposition can occur during the evaporation process. A method of choice is a desorption source, *e.g.* by using a graphite matrix combined with the investigated substance and a pulsed desorption laser with a wavelength at 1064 nm. Here we present our new desorption set-up which is additionally installed in the above mentioned laser ablation apparatus. This allows us to transfer neutral molecules and complexes into the gas phase which are investigated by mass- and isomer selective resonant two-photoionisation (R2PI) or combined IR/R2PI methods.

Novel Platinum(II) Complexes, *cis*-[PtCl₂L₂] with Bioactive Ligands (L): Structures, Vibrational Spectra and Anticancer Properties

Magdalena Malik-Gajewska^a, K. Helios^a, J. Trynda^b, B. M. Kukovec^c, J. Wietrzyk^b
and D. Michalska^a

^a Faculty of Chemistry, Wrocław University of Science and Technology, Smoluchowskiego 23,
50-370 Wrocław, Poland

^b Institute of Immunology and Experimental Therapy of the Polish Academy of Sciences, Weigla 12,
53-114 Wrocław, Poland

^c Department of Chemistry, University of Zagreb, Horvatovac 102a, HR-10000 Zagreb, Croatia
magdalena.malik-gajewska@pwr.edu.pl

Chemotherapy with cisplatin, which is the precursor of platinum drugs, is particularly effective against testicular and ovarian cancers (as well other tumors), but it has a number of toxic side-effects. Therefore, extensive studies are performed on new cisplatin derivatives, where the structural modifications are based on changing the labile ligands (called the leaving groups) and the non-labile ligands (called the carrier ligands). Imidazopyridines can be considered as a new class of the carrier ligands, which replace the ammonia groups in cisplatin. Thus, the platinum complexes with these ligands can make the adducts with DNA of a different structure than that formed by cisplatin with DNA. Imidazopyridines have recently received an increased attention due to their antimicrobial, antiviral, antibacterial, antifungal, antiprotozoal and anticancer activities [1,2].

Recently, we have synthesized novel platinum(II) complexes with substituted imidazopyridines [3,4]. In this work we present the crystal and molecular structures, FT-IR and Raman spectra as well as the DFT calculations on two Pt(II) complexes, of a general formula: *cis*-[PtCl₂L₂] (Fig.1), where L is 3-chloroimidazo[1,2-*a*]pyridine or 6-chloroimidazo[1,2-*a*]pyridine. The in vitro study on anticancer properties have shown that these new agents have a higher activity than cisplatin against the cisplatin-resistant (A2780R) and the sensitive (A2780) human ovarian carcinoma cells. Moreover, they show lower cytotoxicity against the normal cell line (Balb/3T3) as compared to cisplatin.

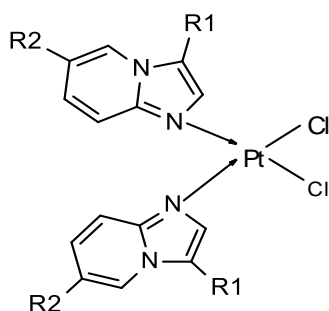


Figure 1. – The general structure of the novel Pt(II) complexes; R1 and R2 can be Cl or H atoms.

References

1. L. Le, Z. Xie and J. Xu, *Molecules*, 17 (2012) 13368.
2. F. Huq, H. Daghir, J.Q. Yu, P. Beale and K. Fisher, *Eur. J. Med. Chem.*, 39 (2004) 691.
3. M. Malik-Gajewska and D. Michalska, *Patent PL Nb 228633* (2018).
4. M. Malik-Gajewska and D. Michalska, *Patent PL Nb 228526* (2018).

Spectroscopic Studies on Non-Heme Iron Nitrosyl Complexes Containing Chelating Phosphine Ligands

Lijuan Li and Omar Becerra

Department of Chemistry and Biochemistry, California State University, Long Beach, 1250 Bellflower Blvd.,
Long Beach, CA 90840, USA
Lijuan.li@csulb.edu

The recent realization that nitric oxide is a biological messenger in many physiological processes has brought about a renewed interest in its chemistry, particularly its iron complexes that are central to the role of nitric oxide in the body. Spectroscopic evidence would appear to implicate species of “Fe(NO)₂⁺” type, so called non-heme iron nitrosyls, or dinitrosyl iron complexes (DNICs), in a variety of processes ranging from polymerization, carcinogenesis, to nitric oxide stores. Our research aims at isolation and spectroscopic studies of non-heme iron nitrosyl complexes that mimic biologically active compounds. We have shown that reactions between Fe(NO)₂(CO)₂ and a series of imidazoles generated new non-heme iron nitrosyls of the form Fe(NO)₂(L)₂ or tetrameric cluster of [Fe(NO)₂(L)]₄, [L = imidazole, 1-methylimidazole, 4-methylimidazole, benzimidazole, 5,6-dimethylbenzimidazole, and L-histidine]. A series of dinitrosyl iron complexes containing N,N'-planar chelating ligands with a general formula of Fe(NO)₂(L), [L = 2,2-bipyridine, 1,10-phenanthroline, and substituted phenanthroline] were also prepared. In this presentation, new chelating dinitrosyl iron complexes containing a series of bis(diphenylphosphine) chelating ligands ranging in sizes and the presence or absence of π -bonds are reported. These chelating products with the general formula of [Fe(NO)₂(CO)]₂(PPh₂-X-PPh₂) and [Fe(NO)₂]₂(PPh₂-X-PPh₂), [where (PPh₂-X-PPh₂) = 1,2-bis(diphenylphosphino)benzene, (DPPBz), 1,3-bis-(diphenylphosphino)propane, (DPPP), cis-1,2-bis(diphenylphosphino)ethylene, (DPPEt), 2,2'-bis(diphenylphosphino)-1,1'-binaphthyl (BINAP), 1,4-bis(diphenylphosphino)butane (DPPBt), and 1,1'-bis(diphenylphosphino)ferrocene (DPPF)] were investigated. A combination of different spectroscopic techniques, such as UV-vis, NMR, IR, EPR, electrochemistry, and X-ray crystallography for study the structures and dynamics of these systems are discussed.

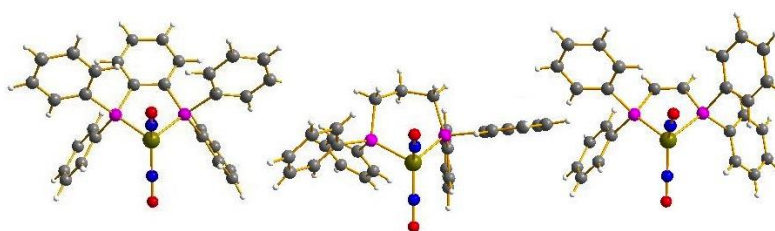


Figure 1

References

1. L. R. Holloway, A. J. Clough, J. Y. Li, E. L. Tao, F. M. Tao and L. Li, *Polyhedron*, 70 (2014) 29.
2. R. Wang, W. Xu, J. Zhang and L. Li, *Inorg. Chem.*, 49 (2010) 4814.
3. R. Wang, M. A. Camacho-Fernandez, W. Xu, J. Zhang and L. Li, *Dalton Trans.*, (2009) 777.

Acknowledgements: The authors thank the National Institute of Health for funding.

Notes

Notes

POSTERS – WEDNESDAY, 22nd AUGUST

Materials

Fluorescent, Colorimetric and FTIR Spectroscopy Studies of a New Textile Material with Sensor Properties

Desislava Staneva

University of Chemical Technology and Metallurgy, Kl. Ohridski Blvd. 8, 1756, Sofia, Bulgaria
grabcheva@mail.bg

Dendrons are new form of organisation of molecular structures with interesting architecture that can be used for production of textile materials with new intelligent properties. The large number of functional groups make them suitable for molecular design to accomplished multifunctionality. In this case, the main challenge is to preserve the valuable properties of dendrons in solution and on the textile matrix, and to achieve durability under conditions of use. In this study we present the synthesis of a new fluorescent dipod, containing 4-butylamine-1,8-naphthalimide units and a reactive primary amino group. Bonding of this compound to cotton fabric has been done via introducing new functional groups into cellulose macromolecules after chemical modification with chloroacetyl chloride (Fig. 1). The reactive chlorine atom reacts with the dendron's amino group to form covalent bonds between the cotton fabric and dendron molecules.

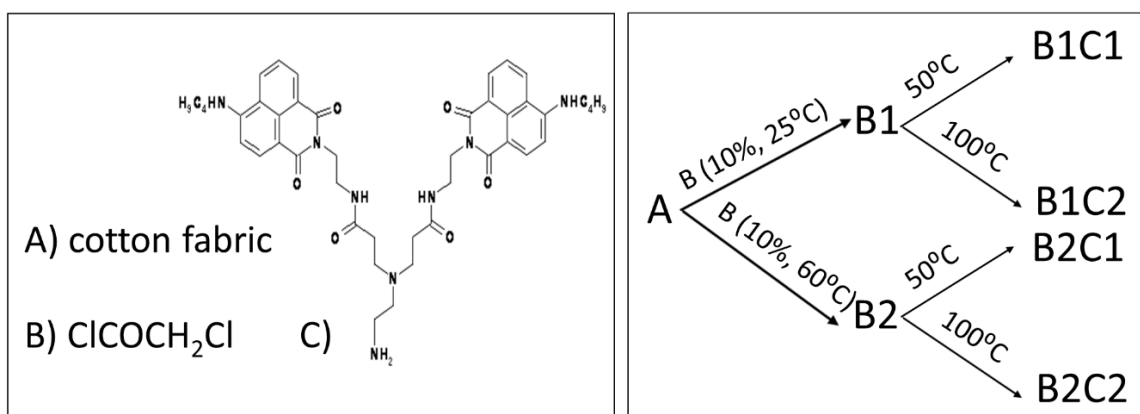


Figure 1 – Cotton fabric modification with new fluorescent dipod.

Different spectroscopic techniques, as Infrared and fluorescent spectroscopy, colour characterization, have been used in each step of cotton modification.

The new materials have been investigated as a heterogeneous pH optical sensor or sensor for detection of sodium benzoate. The results have been shown that the sensor properties of the textile material depend on its degree of modification and dyeing temperature.

Acknowledgements: This study has been funded by the Operational Programme "Science and education for smart growth" 2014-2020 of the European Union cofounded by the European Social Fund through project BG05M2OP001-2.009-0015 "Support for the development of capacity of doctoral students and young researchers in the field of engineering, natural and mathematical sciences."

The Study of Additive Distribution in Polymers Based on the Combination of Raman and Fluorescence Microscopy

Miguel Rubio, Maria Joaquina Caballero and Luis Miguel Méndez
Repsol Technology Centre, c/Agustín de Betancourt s/n, 28935 Móstoles, Madrid, Spain
miguel.rubio@repsol.com

In this contribution we report the combination of two confocal microscopies, Raman and fluorescence, to the study of the distribution of additives in a polymeric matrix. The presence of aromatic rings and disulfide moieties in the additives structure allows the use of both techniques. The fluorescence emission is obtained with a laser of 405 nm and registered in the range of 420-520 nm. In the case of the Raman microscope, the distribution is observed by mapping the intensity of the S-S band at 490 cm^{-1} .

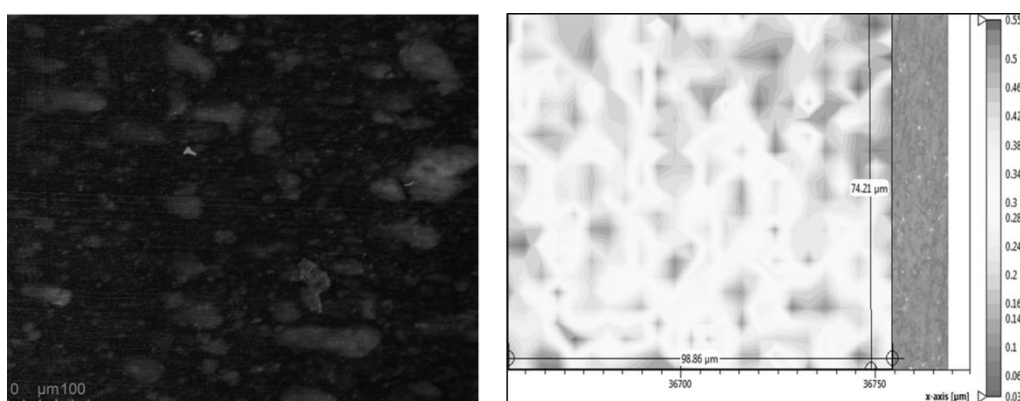


Figure 1 – Additive distribution based on fluorescence (left) and Raman (right) microscopy.

Dielectric Permittivity of Gypsum in Presence of Moisture

K. Kułacz and K. Orzechowski

Faculty of Chemistry, University of Wrocław, F. Joliot Curie 14, 50-383 Wrocław, Poland
karol.kulacz@chem.uni.wroc.pl

Gypsum, $\text{CaSO}_4 \cdot 2\text{H}_2\text{O}$, is widely used in build industry, generally in a form of gypsum boards or plaster mortar. It is the main component of concrete mortars, with increased resistance to environmental. Gypsum was also used to develop intelligent composites containing thermoregulatory microcapsules [1] and even in wastewater treatment [2].

Unfortunately, gypsum exhibits hygroscopic properties, resulting in water adsorption both inside and on the surface of the material, which is favorable condition for the development of mycelium. Additionally, gypsum reduces humidity in living areas, which can be harmful to health [3]. In the project we intend to propose a chemical modification of gypsum directed to the decrease of its ability to adsorb water. In the first step we proved, that the dielectric methods are convenient to investigate influence of humidity on this material. It was already shown, that the dielectric spectroscopy is a sensitive method for detection of even small content of water [4], especially in the case of gypsum [5]. The graph below shows the change in gypsum dielectric permittivity due to the reduction of the amount of water vapor in the atmosphere.

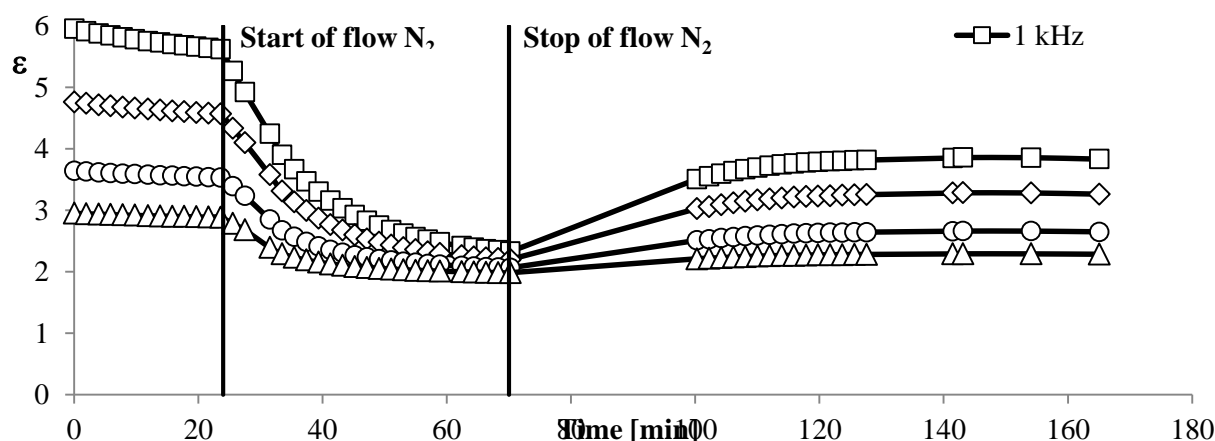


Figure 1 – Results of measure $\text{CaSO}_4 \cdot 2\text{H}_2\text{O}$ without influence of water vapor, HP 4284A (20 Hz - 1 MHz).

References

1. A. M. Borreguero, I. Garrido, J. L. Valverde and J. F. Rodriguez, *Ener. Build.*, 76 (2014) 631.
2. Y. Q. Zhao, *Sep. Sci. Technol.*, 41 (2006) 2785.
3. M. Sato, S. Fukayo and E. Yano, *J. Occup. Health*, 45 (2003) 133.
4. A. E. Charola, J. Pühringer and M. Steiger, *Environ. Geol.*, 52 (2007) 339.
5. P. K. Larsen, *Rest. Build. Monument.*, 6 (2010) 463.

Acknowledgments: The authors are grateful for co-financing of participation in the conference from the KNOW Funds of the Faculty of Chemistry, University of Wrocław.

Density Functional Theory Calculations of the Molecular Structure and Vibrational Properties of Stearic Acid as a Plastic Additive

İlkan Kavlak and Güneş Süheyla Kürkcüoğlu

Physics Department, Eskişehir Osmangazi University, Eskişehir TR-26480, Turkey

gkurkcuo@ogu.edu.tr

Stearic acid is used as thermal protective material in the industry. The most common application of stearic acid as a plastic additive is also known coating on the calside by stearic acid, thus increasing of resistance against thermal degradation during PVC decomposition. Accordingly, molecular structure of the stearic acid was optimized by Density Functional Theory with LANL2DZ basis set in this study (Figure 1). Afterwards, vibrational spectral properties (IR wavenumbers, intensities) were calculated using same quantum chemical methods and basis sets. Fundamental vibrations were assigned on the basis of the potential energy distribution (PED) of the FT-IR and Raman vibration modes of the molecule was determined using both experimental and theoretical methods. Then, the theoretical and experimental wavenumbers were compared each other (Figure 2). In this case, regression equations have been calculated as $y = 0.9929x + 14.132$. According to the results, the good agreement was obtained between theoretical data and experimental ones.

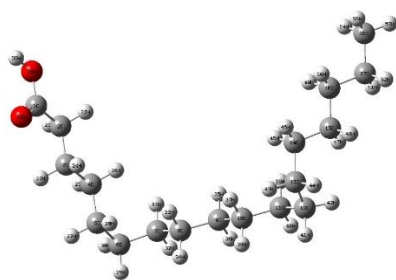


Figure 1 –The optimized geometry of stearic acid.

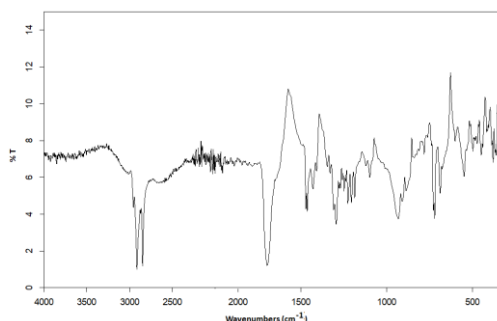


Figure 2 –Observed FT-IR spectra of stearic acid.

Acknowledgements: This work was supported by the Research Fund of Eskişehir Osmangazi University (Project No. 2017-1588).

Structural and Thermostatic Analysis of Organometallic Barbiturate and Tetraborat Complexes as New Generation Plastic Additives

İlkan Kavlak and Güneş Süheyla Kürkçüoğlu

Physics Department, Eskişehir Osmangazi University, Eskişehir TR-26480, Turkey

gkurkcuo@ogu.edu.tr

This study aims to developed new PVC stabilizer and plastic additive materials. During the thermal decomposition of the PVC, HCl gases releases. In order to sweep the released HCl gases, two new organometallic Sn(II) barbiturate complexes were synthesized with nickel(II) and copper(II) tetraborate. It is obtained that synthesized new molecules act as HCl scavenger molecules in the PVC dough. Additionally, these complexes are investigated by elemental analysis, powder XRD difraction and vibrational (FT-IR and Raman) spectroscopic techniques. The molecular formulaes of the synthesized complexes is predicted on the basis of elemental analysis results as $\text{Sn}(\text{C}_4\text{H}_4\text{N}_2\text{O}_3)_2(\text{B}_4\text{O}_7)(\text{H}_2\text{O})\text{Ni}(\text{B}_4\text{O}_7)_4 \cdot 8\text{H}_2\text{O}$ (1) and $\text{Sn}(\text{C}_4\text{H}_4\text{N}_2\text{O}_3)_2\text{Cu}(\text{B}_4\text{O}_7)_4 \cdot 3\text{H}_2\text{O}$ (2). On the other side, powder XRD patterns of the complexes are shown similar to semi-crystalline structures. Dehydrochlorization test results of the complexes are shown that 2 are more stable than 1 according to ISO 182-2 standard.

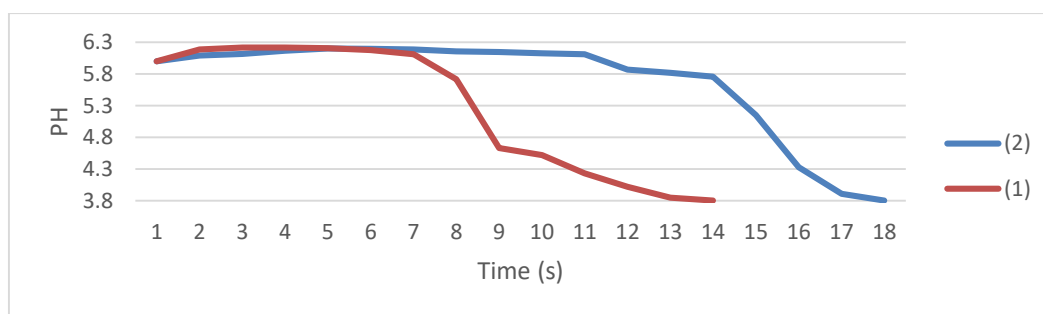


Figure - 1 Thermostatic analysis of barbiturate complexes

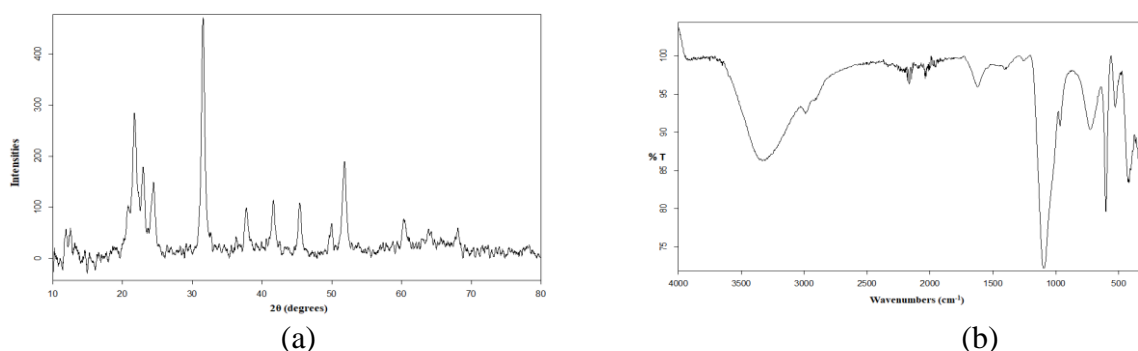


Figure - 2 XRD pattern (a) and FT-IR spectra of complex 1 (b).

Acknowledgements: This work was supported by the Research Fund of Eskişehir Osmangazi University (Project No. 2017-1588).

Structural and Thermostatic Analysis of Imidazole-Based Cu(II) Complex as New Generation Plastic Additive

Güneş Süheyla Kürkcüoğlu and İlkan Kavlak

Physics Department, Eskişehir Osmangazi University, Eskişehir TR-26480, Turkey
gkurkcuo@ogu.edu.tr

In this study, the imidazole-based metal(II) complex was synthesized. The molecular structure of the complex is shown in Figure-1. Afterward, the structural analysis of the complex was performed by single crystal X-Ray diffractometer, PXRD pattern, elemental analysis and vibrational (FT-IR and Raman) spectroscopy. The aim of this study is to investigate the effects imidazole-based metal(II) complex on thermal stabilization during the decomposition of PVC. Consequently, the thermostatic analysis was performed by describing as ISO 182-2 standard (Figure 3). The results are shown that the complex of $\text{Cu}(\text{C}_3\text{H}_4\text{N}_2)_4\cdot\text{CO}_3$ might be suggested as plastic additives due to HCl scavenger properties.

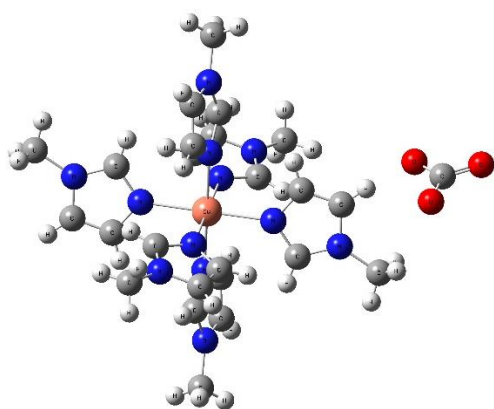


Figure 1 – Molecular structure of the complex.

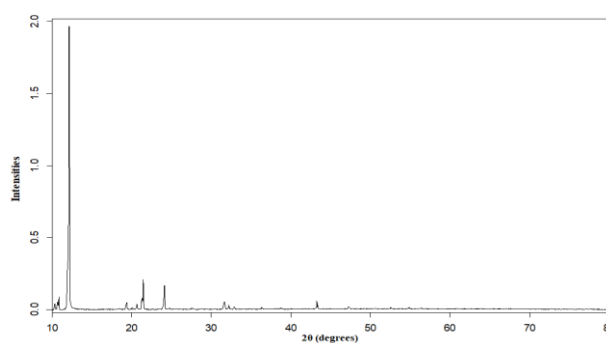


Figure 2 – XRD pattern of the complex.

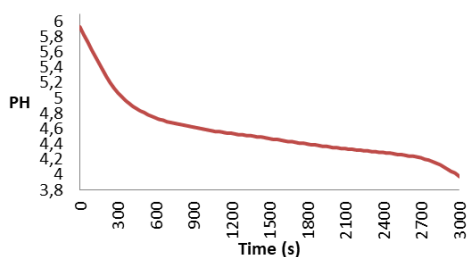


Figure 3 – Thermostatic analysis of $\text{Cu}(\text{C}_3\text{H}_4\text{N}_2)_4\cdot\text{CO}_3$ complex.

Acknowledgements: This work was supported by the Research Fund of Eskişehir Osmangazi University (Project No. 2017-1588).

Crystal Structure and Investigation of Molecular Motions by Dielectric, Vibrational and ^1H NMR Spectroscopies for Organic-Inorganic Hybrid Based on Piperazinium Cation

Marcin Moskwa^a, Grażyna Bator^a, Wojciech Medycki^b and Jan Baran^c

^a Faculty of Chemistry, University of Wrocław, Joliot-Curie 14, 50-383 Wrocław, Poland

^b Institute of Molecular Physics, Polish Academy of Sciences, Smoluchowskiego 17, 60-179 Poznań, Poland

^c Institute of Low Temperatures and Structural Research, Polish Academy of Sciences, Okólna 2, 50-422, Wrocław, Poland

marcin.moskwa@chem.uni.wroc.pl

Well-planned synthesis and design of organic-inorganic hybrid materials based on divalent or trivalent metal halides has attracted scientific attention due not only to the interesting structural topologies of these compounds but also to their unique chemical and physical properties as well as possible novel applications in optoelectronics, data communication, switchable dielectric devices and rewritable optical data storage [1-3].

The family of organic-haloantimonate(III)/halobismuthate(III) hybrids, defined by the general formula $\text{R}_a\text{M}_b\text{X}_{(3b+a)}$ (where: $\text{X} = \text{Cl}, \text{Br}$ or I ; $\text{M} = \text{Sb(III)}$ or Bi(III) and R is an organic cation), has a tendency to constitute bi- or polyoctahedral anions in the crystalline state, where the basic MX_6 octahedra are joined by either corners, edges or faces. In spite of the fact that haloantimonates(III)/bismuthates(III) are characterized by a rich diversity of the anionic networks in the crystal lattices, the ferroelectric properties are limited only to several chemical ratios namely: $\text{R}_5\text{M}_2\text{X}_{11}$, $\text{R}_3\text{M}_2\text{X}_9$, R_2MX_5 and RMX_4 , where the cations are the aliphatic, aromatic and acyclic amines [4]. The majority of the para-ferroelectric phase transitions found in these compounds are characterized by an “order–disorder” mechanism connected with the change in dynamics of the organic cations.

In this poster we present the structure and details of the physicochemical properties (dielectric, IR and ^1H NMR spectroscopy) of a novel organic-inorganic hybrid material based on the piperazinium cation.

References

1. J. F. Scott, *Science*, 315 (2007) 954.
2. S. T. Han, Y. Zhou and V. A. Roy, *Adv. Mater.*, 25 (2013) 5425.
3. J. Li, J. Claude and L. E. Norena-Franco, *Chem. Mater.*, 20 (2008) 6304.
4. L. Sobczyk and R. Jakubas, J. Zaleski, *Pol. J. Chem.*, 71 (1997) 265.

Acknowledgements: This work has been supported by the Polish Ministry of Science and Higher Education Agreement Nr 3580/ZIBJ DUBNA/2016/0 and partially by the International Program ZIBJ Dubna № 04-4-1121-2015/2017.

Organic-Inorganic Hybrid Compound Based on Pyrrolidine $[\text{C}_4\text{H}_{10}\text{N}]_2\text{BiCl}_5$: Structure and Physicochemical Properties

Martyna Wojciechowska, Tadeusz Lis and Ryszard Jakubas

Faculty of Chemistry, University of Wrocław, ul. F. Joliot-Curie 14 50-383 Wrocław, Poland

martyna.wojciechowska@chem.uni.wroc.pl

Organic–inorganic hybrid materials have long been an attractive topic of research due to their interesting physical properties and novel functionalities, where the organic part corresponds to the electrical properties, while the inorganic part determines flexibility, mechanical resistance and thermal stability [1]. Thanks a huge values of dielectric permittivity, possibility of changing of dielectric constant the family of this compounds is successively developed. Over the years, in this group has focused on the search for materials with ferroic properties that give the possibility of their potential application in sensing signal processing, data storage, optoelectronic devices, etc. [2] Among them, haloantimonates(III) and halobismuthates(III) described by the general formula $\text{R}_a\text{M}_b\text{X}_{3b+a}$, where where R denotes organic cations, M stands Sb or Bi and X = Cl, Br, I, have attracted growing attention among scientist around the world, because they combine facile synthesis with sought properties [3].

Ones of the few examples of pyrrolidine-based compounds are isostructural $[\text{C}_4\text{H}_{10}\text{N}]\text{MnCl}_3$ and $[\text{C}_4\text{H}_{10}\text{N}]\text{MnBr}_3$ [4,5]. Both of them exhibit combination of multiferroic (weak ferroelectric and ferromagnetic) with luminescent properties and are the first described materials with such properties. These analogues pass throw one reversible PT of the order-disorder mechanism.

A compound based on the pyrrolidinium cation $[\text{C}_4\text{H}_{10}\text{N}]_2\text{BiCl}_5$ was synthesized and exhibits interesting polymorphism in the solid state. In order to investigate the nature of transformations, methods such as polarization microscopy, dilatometric studies and single-crystal X-ray measurements were used. To explain the mechanism of changes in the dynamic of cations dielectric spectroscopy and ^1H NMR spin-lattice relaxation methods in the solid state were used.

References

1. M. Owczarek, K. A. Hujsak, D. P. Ferris, A. Prokofjevs, I. Majerz, P. Szklarz, H. Zhang, A. A. Sarjeant, C. L. Stern, R. Jakubas, S. Hong, V. P. Dravid and J. F. Stoddart, *Nat. Commun.*, 7 (2016) 13108.
2. C.-Y. Mao, W.-Q. Liao, Z.-X. Wang, Z. Zafar, P.-F. Li, X.-H. Lu and D.-W. Fu, *Inorg. Chem.*, 55 (2016) 7661.
3. L. Sobczyk, R. Jakubas and J. Zaleski, *Pol. J. Chem.*, 71 (1997) 265.
4. Y. Zhang, W.-Q. Liao, D.-W. Fu, H.-Y. Ye, C.-M. Liu, Z.-N. Chen and R.-G. Xiong, *Adv. Mat.*, 27 (2015) 3942.
5. Y. Zhang, W.-Q. Liao, D.-W. Fu, H.-Y. Ye, Z.-N. Chen and R.-G. Xiong, *J. Am. Chem. Soc.*, 137 (2015) 4928.

Acknowledgements: The authors thank Wrocław Centre of Biotechnology, programme: The Leading National Research Centre (KNOW) for years 2014–2018.

Nonlinear Optical Properties of New Phenothiazine Derivatives

É. A. Molnár, E. Gál, B. Brém, L. Găină, C. Cristea and L. Silaghi-Dumitrescu

Faculty of Chemistry and Chemical Engineering, Arany János str. 1, Cluj-Napoca 400028,
"Babeş-Bolyai" University, Romania
gal.emese.81@gmail.com

The ability to design and build molecular architectures in which the energy flow can be controlled constitutes a great (and timely) challenge. The optical, electronic, and photophysical properties of porphyrins have made these molecules desirable targets for incorporation into supramolecular systems and polymers. The porphyrins are reliable precursors in biomimetic chemistry (artificial photosynthesis), multichromophoric assemblies in biology as well as potential application in sensing [1], opto-electronics [2], magnetic, and catalytic materials [3]. The electronic properties of porphyrins can be tuned by appropriate functionalization of their *meso* and β -positions [4,5] with different aromatic or heteroaromatic moieties [6]. The encapsulation of porphyrin core inside of a dendritic structure with various peripheral substituents can modulate the physical properties and also impart the desired chemical characteristics to the macrocycle [7]. The synthesis of symmetric and asymmetric substituted porphyrin was achieved by Adler-Longo method with different aromatic aldehydes. Functionalization of the porphyrins was realised by Suzuki and Ullman coupling reactions using various boronic acid derivatives.

The optical properties of new phenothiazine derivatives (Fig.1) were emphasized in this work.

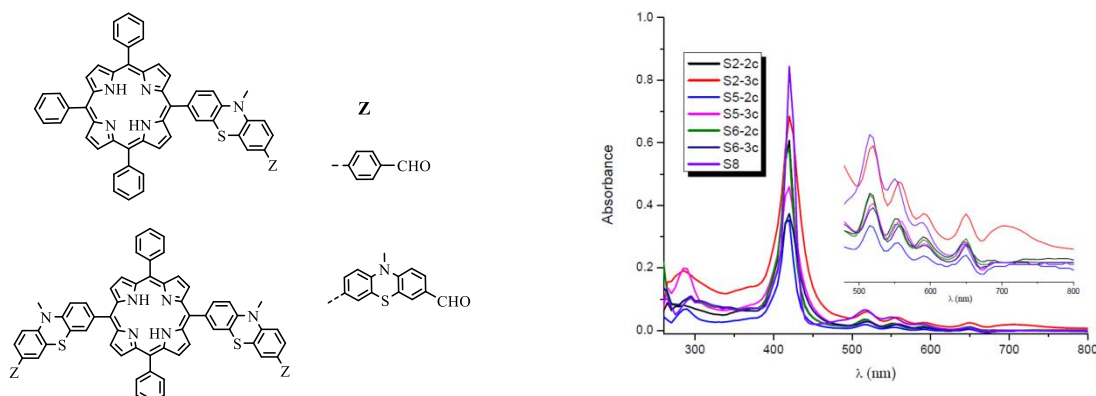


Figure 1 – Aryl-*meso*-phenothiazinyl-porphyrin derivatives and their UV-Vis spectra.

References

1. P. Anzenbacher, Jr., Y. Liu, M. A. Palacios, T. Minami, Z. Wang and R. Nishiyabu, *Chem. Eur. J.*, 19 (2013) 8497.
2. R. J. Mohammad and B. Bahram, *Appl. Phys. A*, 119 (2015).
3. J. C. Barona-Castaño, C. C. Carmona-Vargas, T. J. Brocksom and Kleber T. de Oliveira, *Molecules*, 21 (2016) 310.
4. K. M. Kadish and E. Van Caemelbecke, *J. Solid State Electrochem.*, 7 (2003) 254.
5. F. D'Souza and O. Ito, *Chem. Soc. Rev.*, 41 (2012) 86.
6. B. Brem, E. Gal, L. Gaina, C. Cristea, A. M. Gabudean, S. Astilean and L. Silaghi-Dumitrescu, *Dyes and Pigments*, 123 (2015) 386; E. Gal, B. Brem, I. Pereteanu, L. Gaina, T. Lovasz, M. Perde-Schrepler, L. Silaghi-Dumitrescu, C. Cristea and L. Silaghi-Dumitrescu, *Dyes and Pigments*, 99 (2013) 144.
7. W. R. Dichtel, S. Hecht and J. M. J. Fréchet, *Org. Lett.*, 7 (2005) 4451.

Controlling Molecular Condensation/Diffusion of Copper Phthalocyanine by Local Electric Field Induced with Scanning Tunneling Microscope Tip

Shin Yaginuma^a, Katsumi Nagaoka^b and Tomonobu Nakayama^{b,c}

^a National Institute of Technology, Nagano College, Nagano 381-8550, Japan

^b International Center for Materials Nanoarchitectonics, National Institute for Materials Science, Tsukuba, Ibaraki 305-0044, Japan

^c Graduate School of Pure and Applied Sciences, University of Tsukuba, Tsukuba, Ibaraki 305-0044, Japan
s_yaginuma@nagano-nct.ac.jp

We have discovered the condensation/diffusion phenomena of copper phthalocyanine (CuPc) molecules controlled with a pulsed electric field induced by the scanning tunneling microscope (STM) tip [1]. This behavior is reproducible for CuPc on a Bi(001) substrate (Fig. 1), and is not explained by the conventional induced dipole model. In order to understand the mechanism, we have measured the electronic structure of the molecule by tunneling spectroscopy and also performed theoretical calculations on molecular orbitals (Fig. 2). These data clearly indicate that the molecule is positively charged owing to charge transfer to the substrate, and that hydrogen bonding exists between CuPc molecules, which makes the molecular island stable.

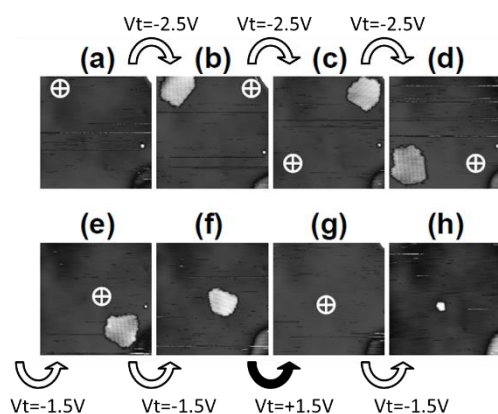


Figure 1 – Sequential STM images of CuPc islands on a Bi(001) surface (90 x 90 nm², $V_s = -1.0$ V, $I = 50$ pA).

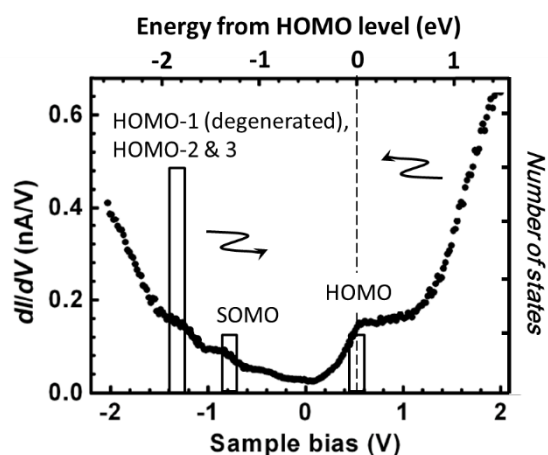


Figure 2 – dI/dV spectrum measured on the CuPc island at 77 K (set-point conditions: $V_s = 2.0$ V, $I = 0.5$ nA), and the calculated number of states for each MO of CuPc molecule.

References

1. K. Nagaoka, S. Yaginuma and T. Nakayama, *Jpn. J. Appl. Phys.*, 57 (2018) 020301.

Acknowledgements: This work was partly supported by JSPS KAKENHI Grant Numbers JP17K05066 and JP16K21573. S.Y. and K.N. contributed equally to this work.

Structural and Spectroscopic Studies of Atropisomerism in Diphenylguanidinium Salts

M. S. C. Henriques^a, S. Et. Ashoor^b, E. M. Brás^{c,d}, R. Fausto^d and J. A. Paixão^a

^aCFisUC, Department of Physics, University of Coimbra, P-3004-516 Coimbra, Portugal

^bCQE, Chemistry Department, Faculty of Sciences, Misurata University, Lybia

^cCenter of Marine Sciences, CCMar, University of Algarve, P-8005-039 Faro, Portugal

^dCQC, Department of Chemistry, University of Coimbra, P-3004-535 Coimbra, Portugal
marta.henriques@uc.pt (Marta Henriques)

Guanidine compounds are known for their biological and therapeutic (neuroleptic and antipsychotic) properties [1]. DPG (1,3-Diphenylguanidine) compounds have also proved interesting for non-linear optical applications, if they crystallise in acentric space-groups [2]. Atropisomerism in DPG was first found in NMR studies of the neutral and cationic species [3], an observation further corroborated by the isolation in the crystal structure of several salts and adducts of the *syn-syn*, *syn-anti* and *anti-anti* conformations of the aryl rings [4-6]. *Ab-initio* and DFT studies of the relative energies of the 3 conformers of DPG⁺ showed that the *syn-syn* conformer is energetically more stable whereas the *anti-anti* is the least stable conformer, ~0.5 kJ/mol higher in energy. The solvent, counter-ion effect and crystal packing, however, can stabilize any of the atropisomers. The extensive capability for hydrogen-bonding provided by the N-H and NH₂ groups, can stabilise the higher energy conformers.

In the search for new NLO compounds, we have synthesised 3 new DPG salts: (1) DPG iodate monohydrate; (2) DPG (4-nitrophenyl) acetate; (3) DPG 2,4-dihydroxybenzoate. The compounds were obtained by reacting DPG with the respective acids in an ethanol/water solution (1)/(2) or ethanol (3) at room temperature.

The 3 compounds were studied by single-crystal XRD and spectroscopy methods. Compounds (1) and (3) crystallise in space groups *P*2₁/*c* and *P*2₁, respectively, and compound (2) in the *P*-1 space group. The two former crystals have only a single ionic pair in the asymmetric unit cell (*Z'*=1), whereas compound (3) features 4 independent ionic pairs (*Z'*=4). Unfortunately, the non-centrosymmetric crystal (3) could only be obtained as a non-merohedral twin. Interestingly, in each of the studied crystals, the DPG⁺ cation exhibits one of the 3 distinct atropisomeric conformations *syn-syn* (1), *syn-anti* (2) and *anti-anti* (3).

References

1. B.L. Largent, H. Wikstrom, A.L. Gundlack, S.H. Snyder, *Mol. Pharmacol.* **32**, 772 (1987).
2. M.S. Kajamuhideen, K. Sethuraman, K. Ramamurthi, P. Ramasamy, *Optics & Laser Technology* **91**, 159 (2017).
3. G. Alagona, C. Ghio, P.I. Nagy, G.J. Durant, *J. Phys. Chem.* **98**, 5422 (1994).
4. J.A. Paixão, P.S. Pereira Silva, A. Matos Beja, M. Ramos Silva, L. Alte da Veiga, *Acta Cryst. C* **54**, 805 (1998).
5. A. Matos Beja, J.A. Paixão, M. Ramos Silva, L. Alte da Veiga, *Z. Kristallogr. NCS.* **213**, 655 (1998).
6. M. Ramos Silva, A. Matos Beja; J.A. Paixão, L. Alte da Veiga, *Z. Kristallogr. NCS.* **216**, 261 (2001).

Acknowledgements: We acknowledge financial support from “Fundação para a Ciência e a Tecnologia” (FCT) and FEDER/COMPETE 2020-EU through projects UID/FIS/04564/2016 (CFisUC) and UI0313/QUI/2013 (CQC). S.Et. Ashoor thanks an Al-Idrisi II scholarship. Access to TAIL-UC facility funded under QREN-Mais Centro project ICT_2009_02_012_1890 is gratefully acknowledged.

Acetate and Benzoate Intercalated CaAl Layered Double Hydroxides – Characterization and Application as Nanoreactor

Z. Timár^a, D. Sztankovics^a, G. Varga^a, P. Sipos^b and I. Pálinkó^a

^a Department of Organic Chemistry, University of Szeged, Dóm tér 8, Szeged, H-6720 Hungary

^b Department of Inorganic and Analytical Chemistry, University of Szeged Dóm tér 7, Szeged, H-6720 Hungary
palinko@chem.u-szeged.hu (I. Pálinkó)

During organic synthesis it is very important to run the reactions without the formation of byproducts and to exclude harmful organic solvents [1,2]. Application of layered materials may be very useful in meeting these requirements.

Layered double hydroxides (LDH) belong to a class of lamellar structured anionic clays consisting of positively charged layers and exchangeable charge-balancing inorganic or organic interlayer anions [3]. These materials function in various areas, they can be useful as drug delivering vehicles [4], adsorbents [5], catalysts [6] and the constrained environment can serve as nanoreactor [7].

In the experimental work leading to this contribution, the main aim was the application of CaAl-LDH as nanoreactor. The first step was the syntheses of the intercalated systems, *i.e.*, the introduction of the acetate or the benzoate ions among the layers. The acetate-intercalated CaAl-LDH was prepared with the co-precipitation method. For the benzoate anions, different type of intercalation method (co-precipitation, delamination, direct anion exchange) were applied. Then, the interlayer reactions were run using benzyl bromide as the alkylation reagent. They were conducted under solventless conditions.

Structural characterization of the intercalated samples was performed by X-ray diffractometry, electron microscopy and infrared spectroscopy. The esterification reaction was followed by attenuated total reflection infrared spectroscopy.

References

1. M. M. Kirchhoff, *Resour. Conserv. Recy.*, 44 (2005) 237.
2. R. A. Sheldon, *Green. Chem.*, 7 (2005) 267.
3. V. Rives, *Layered double hydroxides present and future*, Nova Publishers, Inc., New York, (2001) 10.
4. L. Perioli, T. Posati, M. Nocchetti, F. Bellezza, U. Constantino and A. Cipiciani, *Appl. Clay Sci.*, 53 (2011) 374.
5. J. Das, B. S. Patra, N. Baliarsingh and K. M. Parida, *Appl. Clay. Sci.*, 32 (2006) 252.
6. Z. P. Xu, J. Zhang, M. O. Adebajo, H. Zhang and C. Zhou, *Appl. Clay. Sci.*, 53 (2011) 139.
7. M. Wei, Z. Shi, D. G. Evans and X. Duan, *J. Mater. Chem.*, 16 (2006) 2102.

Exploring the Phase Diagram of a Glass-Forming Ionic Liquid by Raman Spectroscopy under Low Temperature and High Pressure

Mauro C. C. Ribeiro, Thamires A. Lima, Vitor H. Paschoal and Luiz F. O. Faria

Laboratório de Espectroscopia Molecular, Instituto de Química, Universidade de São Paulo,

Av. Prof. Lineu Prestes 748, 05508-000, São Paulo, SP, Brazil

mccribei@iq.usp.br

The study of phase transitions of ionic liquids is on demand from the point of view of technological applications and also from fundamental issues related to the physical-chemistry of these interesting systems. Vibrational spectroscopy has provide a detailed view of phase transitions of ionic liquids as a function of temperature at atmospheric pressure or as a function of pressure at room temperature [1]. However, we are not aware of any previous work exploring the phase diagram of an ionic liquid by simultaneous temperature and pressure variations. In this work, the phase diagram of the ionic liquid 1-butyl-1-methylpyrrolidinium bis(trifluoromethanesulfonyl)imide, [Pyrr_{1,4}][NTf₂], has been unveiled by synchrotron X-ray diffraction and Raman scattering measurements using a diamond anvil cell (DAC) coupled to a cryostat. The pressure dependence of glass transition $T_g(P)$, devitrification (also called cold-crystallization) $T_{cc}(P)$, and melting $T_m(P)$ temperatures have been obtained (see Figure 1).

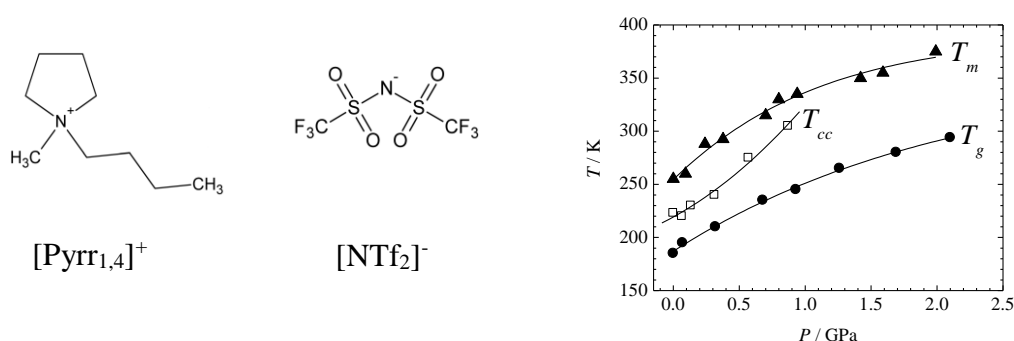


Figure 1 – Temperatures of glass transition (T_g , filled circles), cold-crystallization (T_{cc} , open squares), and melting (T_m , filled triangles) of [Pyrr_{1,4}][NTf₂] as a function of pressure. The full lines are guides to the eyes.

The isochronous $T_g(P)$ curve has been interpreted in terms of thermodynamic scaling using low-temperature and high-pressure extrapolations of empirical equation of states [2]. We show that the well-known empirical Andersson equation for $T_g(P)$ and the Simon equation for $T_m(P)$ fit the [Pyrr_{1,4}][NTf₂] data since both $T_g(P)$ and $T_m(P)$ curves follow essentially the same pressure dependence. The similarity of pressure coefficients, dT_g/dP and dT_m/dP , is discussed on the basis of mechanism of melting (Lindemann's mechanism) and thermodynamics on the assumption that one of the Ehrenfest's equations is appropriated for $T_g(P)$, whereas $T_m(P)$ follows the Clausius-Clapeyron's equation.

References

1. V. H. Paschoal, L. F. O. Faria and M. C. C. Ribeiro, *Chem. Rev.*, 117 (2017) 7053.
2. M. C. C. Ribeiro, A. A. H. Pádua and M. F. C. Gomes, *J. Chem. Phys.*, 140 (2014) 244514.

Acknowledgements: The authors thank FAPESP and CNPq for financial support, and Brazilian Synchrotron Light Laboratory LNLS for synchrotron X-ray diffraction experiments.

The Quasi-Liquid Layer of Ice on Mesoporous Silica Characterized by Confocal Raman and NMR Spectroscopy

Katarzyna Piela, István Furó and Eric C. Tyrode

Department of Chemistry, KTH Royal Institute of Technology, SE-100 44 Stockholm, Sweden
piela@kth.se

The quasi-liquid layer (QLL) or premolten layer (PML), first described by Michael Faraday in 1859, is a thermodynamically stable layer formed on most solids close to their melting points. Molecules in this QLL are more disordered and more mobile than in the crystalline phase, yet less so than in the liquid phase. As surface premelting is prevalent in all classes of solids it is therefore a critical phenomenon in industry, including disciplines such as metallurgy, geology, and meteorology. In ice, premelting shows its effect in frost heave, growth of snowflakes, and movement of glaciers [1]. The structure as well as thickness of the quasi liquid layer has been widely investigated and at times controversially discussed [2-4]. The actual thickness of this layer has been reported to extend from just a few to hundreds of nanometers [2]. The discrepancy is likely connected to the interpretation of the results from different experimental methods, as well as the presence of impurities.

Raman spectroscopy is sensitive to changes between water and ice including hydrogen bonds and is suitable for investigating the presence and properties of QLL. NMR is also a useful technique for distinguishing between solid and liquid phases as well as to determine dynamics in molecules. However, both techniques lack the necessary surface sensitivity to characterize the QLL from a single interface. In this work, we make use of porous silica particles with large surface to volume ratios to go beyond this inherent limitation, and jointly characterize the temperature dependent properties of the QLL between ice and silica. We provide the vibrational spectral signature of the QLL and determine its thickness by NMR spectroscopy.

References

1. A. Michaelides and B. Slater, *PNAS*, 114 (2017) 195.
2. J. Liljeblad, I. Furó and E. C. Tyrode, *Phys. Chem. Chem. Phys.*, 19 (2017) 305.
3. W. J. Smit and H. J. Bakker, *Angew. Chem. Int. Ed.*, 56 (2017) 15540.
4. Y. Li and G.A. Somorjai, *J. Phys. Chem. C.*, 111 (2007) 9631.

An Insight into Electric and Dynamic Properties of Formamidinium Iodide

K. Mencil^a, P. Durlak^a, M. Rok^a, R. Jakubas^a, J. Baran^b, W. Medycki^c
and A. Piecha-Bisiorek^a

^a Faculty of Chemistry, University of Wrocław, Joliot-Curie 14, 50-383 Wrocław, Poland

^b Institute of Low Temperature and Structure Research, PAS, Okólna, PO Box 937, 50-950 Wrocław, Poland

^c Institute of Molecular Physics, PAS, M. Smoluchowskiego 17, 60-179 Poznań, Poland

klaudia.mencil@chem.uni.wroc.pl

The use of the perovskite in solar cells for the first time in history in 2009 by Kojima *et al.* [1] opened the way to the new dynamically developing applications of this material in photovoltaic industry. As for the photoactive layer, organic-inorganic hybrid described by the general formula RMX_3 (where R is an organic cation, M metal, and $\text{X} = \text{Cl}, \text{Br}, \text{I}$) appeared to be promising candidates for application in photovoltaics due to their excellent properties including a direct bandgap or a high absorption factor. Methylammonium lead iodide $(\text{CH}_3\text{NH}_3)\text{PbI}_3$ (MAPbI_3) happened to be the best in this class of compounds. Apart from simplicity with which it can be obtained and low manufacturing costs, this compound's PCE (power conversion efficiency) is almost 20% [2]. In 2014 Koh *et al.* [3] suggested that the cation MA^+ should be replaced by formamidinium one $\text{NH}_2\text{CH}=\text{NH}_2^+$ (FA) in order to improve its efficiency. Research on FAPbI_3 revealed a considerable advantage of this compound over methylammonium analogue resulting mainly from a better thermal stability and smaller bandgap which enabled, among other things, a near infrared absorption.

The discovery of several solar cells based on formamidinium cation, in spite of considerable research on perovskite structures based in turn on FA, physico-chemical properties of the main precursor, formamidinium iodide (FAI) has not been well explored yet. Consequently, the knowledge of FAI's properties and crystal structure can lead to better understanding of the process of crystallization of perovskite-based on FA, and contribute to designing organic-inorganic perovskite materials of specific qualities.

Given the results presented by Petrov *et al.* [4], it appears that FAI undergoes two reversible phase transitions at about 346 K and 387 K, and is described by the monoclinic symmetry (space group $P2_1/c$) in the room temperature phase. PXRD data gathered at different temperatures (along with the thermal analysis) confirm the existence of rhombohedral and cubic phases at 358 K and 400 K, respectively.

In this communication, the structure, thermal and dielectric properties are presented. To throw more light on the molecular mechanism of the high temperature phase transitions the infrared and ^1H NMR studies were carried out in a wide temperature range.

References

1. A. Kojima, K. Teshima, Y. Shirai and T. Miyasaka, *J. Am. Chem. Soc.*, 131 (2009) 6050.
2. H. Zhou, Q. Chen, G. Li, S. Luo, T. B. Song, H. S. Duan, Z. Hong, J. You, Y. Liu and Y. Yang, *Science*, 345 (2015) 542.
3. T. M. Koh, K. Fu, Y. Fang, S. Chen, T. C. Sum, N. Mathews, S. G. Mhaisalkar, P.P. Boix and T. Baikie, *J. Phys. Chem. C*, 118 (2014) 16458.
4. A. A. Petrov, E. A. Goodilin, A. B. Tarasov, V. A. Lazarenko, P. V. Dorovatovskii and V. N. Khrustalev, *Acta Cryst.*, E73 (2017) 569.

Acknowledgements: The authors (K.M. and P.D.) would like to gratefully acknowledge the Wrocław Centre for Networking and Supercomputing (WCSS) for allocation of computer time on the BEM Cluster. This research project was financed by the KNOW grant no 12 (R. Jakubas).

Remineralizing Effect of Bioactive Glass 45S5 on Enamel Surface

E. Klarić Sever^a, B. Štimac^b

^a Department of Endodontics and Restorative Dentistry, School of Dental Medicine,
Gundulićeva 5, Zagreb, Croatia

^b Sixth year student, School of Dental Medicine, Gundulićeva 5, Zagreb, Croatia

Demineralization is the process of removing minerals from hydroxyapatite crystals of dental hard tissues [1]. 45S5 bioglass (BG) is capable of forming hydroxyapatite (HA) and is widely used in hard tissue regeneration [2]. The purpose of this in vitro study was to evaluate the potential remineralizing effect of BG and calcium phosphopeptide-amorphous calcium phosphate [3] Tooth Mousse (TM) on the enamel surface after demineralization. Thirty enamel blocks (n = 10) were prepared and randomly divided into three groups: etched enamel treated with BG, etched enamel treated with TM, etched enamel treated with deionized water. A repeated measures analysis of variance (ANOVA) model was used for statistical analysis. Scanning electron microscopy (SEM) imaging, energy dispersive x-ray spectroscopy (EDS), Raman spectroscopy and Vickers microhardness tests were performed before and after etching for 2 minutes with 37 % orthophosphoric acid, as well as after different treatment procedures. BG treatment showed disorderly packed glass particles, while TM treatment led to crystal formation on enamel surface. EDS analysis showed an increase in calcium, phosphate, sodium and silicon concentrations after BG treatment. A statistically significant drop in the enamel microhardness values was observed after etching ($p < 0.001$). Following a two-week treatment in either bioactive glass or Tooth Mousse, significantly higher microhardness values were recorded ($p < 0.001$ for both treatments), which were on average significantly higher than baseline microhardness measurements for the BG treatment ($p < 0.001$), but not for the TM treatment ($p = 0.331$). Raman spectroscopy was not an effective method for measuring changes after different treatments on enamel surface because of the specimen preparation, so we could not select a single band (for the quantification of HA, it is usually the highest peak at about 960 cm^{-1}) and directly compare its intensity between the different samples. Thus, Micro Raman should be used. Two-week treatment with BG and TM after demineralization can lead to increase in enamel microhardness with accumulation of glass particles and crystal formation reflecting a possible remineralizing effect.

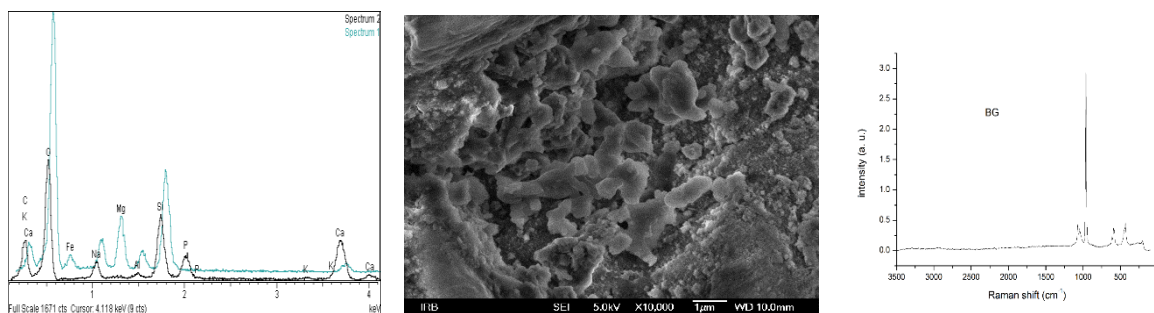


Figure 1 – EDS analysis after BG. **Figure 2** – Disorderly packed BG particles. **Figure 3** – Raman spectroscopy for BG.

References

1. A. B. Mehta, V. Kumari, R. Jose and V. Izadikhah, *J. Conserv. Dent.*, 17 (2014) 3.
2. O. H. Andersson and I. Kangasniemi, *J. Biomed. Mater. Res.*, 25 (1991) 1019.
3. A. A. de Vasconcelos, A. G. Cunha and B. C. Borges, *Acta Odontol. Scand.*, 70 (2012) 337.

UV-Radiation Resistance of Polystyrene-ZnO Nanocomposites

Lahorija Bistričić^a, Petar Tomić^a and Mirela Leskovic^b

^a University of Zagreb, Faculty of Electrical Engineering and Computing, Unska 3, 10000 Zagreb, Croatia

^b University of Zagreb, Faculty of Chemical Engineering and Technology, Marulićev trg 19,
10000 Zagreb, Croatia
lahorija.bistricic@fer.hr

Polystyrene (PS) is a very important polymer with excellent physical properties such as high electrical resistance and good mechanical properties [1]. The exposure to high temperatures and UV radiation may cause the significant degradation of PS [2]. Incorporation of a small amount of inorganic nanoparticles can considerably inhibit the degradation of PS polymer matrix. ZnO is semiconductor with an optical band-gap ($E_g = 3.37$ eV) in the UV region and this makes it an extremely efficient UV absorber. Introduction of ZnO nanofiller into PS can reduce photodegradation of polymeric matrix [3].

In this study amorphous atactic polystyrene ZnO nanocomposites were prepared by using solution mixing process (PS_s) and melt mixing process (PS_m). Nanocomposites were prepared with addition of different volume fractions of ZnO nanoparticles (0, 0.1, 0.3, 0.5, and 1.0 vol. %). Two dimensions of nanoparticles were used, ranging from 10 to 30 nm (ZnO I) and 40 to 100 nm (ZnO II). PS-ZnO nanocomposites were exposed to UV radiation from the mercury lamps wavelength from 350 to 400 nm, and power of 15 W. Samples were exposed to the UV radiation for 7, 14 and 21 days.

The influence of nanoparticles on the structural degradation of irradiated PS-ZnO nanocomposites was investigated using Fourier transform infrared spectroscopy (ATR). The analysis of the vibrational spectra showed that addition of 0.5 vol. % ZnO I, or ZnO II nanoparticles significantly reduces degradation of samples prepared by using solution mixing process (PS_s). The presence of ZnO nanoparticles in nanocomposites prepared from the melt mixing process (PS_m) seemed to have very little impact on resistance to UV radiation.

The thermal behaviour of the PS nanocomposites was studied using differential scanning calorimetry (DSC) and thermogravimetric analysis (TGA). The incorporation of nanofiller into the PS matrix reduce the glass transition temperature (T_g) in samples prepared by solution mixing process. In PS_s -ZnO nanocomposites the polymer chain mobility is increased yielding in a plasticizing effect accompanied with decreased T_g . The UV radiation slightly changed T_g showing that nanofiller affects the flexibility of PS chains in degraded samples. There was no distinctive influence of nanoparticles on the glass transition temperatures of PS_m -ZnO nanocomposites. According to TGA results, the addition of ZnO nanoparticles enhanced thermal stability of unirradiated and irradiated samples.

References

1. E. Yousif and R. Haddad, *Springer Plus*, 2 (2013) 398.
2. B. Jaleha, M. S. Madada, M. F. Tabrizib, S. Habibbia, R. Golbedaghic and M. R. Keymaneshd, *J. Iran. Chem. Soc.*, 8 (2011) S161.
3. Y. Tu, L. Zhou, Y.-Z. Jin, C. Gao, Z. Z. Ye, Y.F. Yanga and Q. L. Wang, *J. Mater. Chem.*, 20 (2010) 1594.

Structural and Optical Properties of Hydrothermally Synthesized Iron/Titanium Oxide Nanoparticles

Ivan Marić^a, Goran Dražić^b, Mile Ivanda^c, Tanja Jurkin^d, Goran Štefanić^c, and Marijan Gotić^c

^a Center of Excellence for Advanced Materials and Sensing Devices, Research Unit New Functional Materials, Bijenička c. 54, 10 000 Zagreb, Croatia

^b National Institute of Chemistry, Hajdrihova 19, SI-1001, Ljubljana, Slovenia

^c Molecular Physics and New Materials Synthesis Laboratory, Ruđer Bošković Institute, Bijenička 54, 10000 Zagreb, Croatia

^d Radiation Chemistry and Dosimetry Laboratory, Ruđer Bošković Institute, Bijenička c. 54, 1 000 Zagreb, Croatia

gotic@irb.hr (Marijan Gotić); Goran.Stefanic@irb.hr (Goran Štefanić)

Iron/titanium oxide nanoparticles with initial molar ratio $[\text{Fe}/(\text{Fe}+\text{Ti})] \leq 0.5$ were hydrothermally synthesized at 180 °C in aqueous ammonia solution (pH = 9). The titanium and iron precursors were TiCl_4 and FeCl_3 , respectively. The amount of doped iron strongly affected microstructural properties as well as the degree of dispersion of iron in Fe-Ti-O system. Anatase was the dominant phase in the iron/titanium oxide samples with $[\text{Fe}/(\text{Fe}+\text{Ti})] \leq 0.25$. The iron/titanium oxide sample with $[\text{Fe}/(\text{Fe}+\text{Ti})] = 0.5$ contained no anatase. The average crystallite size of the anatase phase in iron/titanium oxide samples decreased with the increase of iron doping. The appearance of small diffraction lines of hematite in the product with 10 mol % of iron indicates that the solid solubility limit of Fe^{3+} ions in the TiO_2 lattice has been reached. The results of precise unit-cell parameters measurement, obtained using both Rietveld and Le Bail refinements of the powder diffraction patterns with added silicon indicated that the solid solubility limit of Fe^{3+} ions inside the anatase lattice was ~8 mol %. Iron that could not be incorporated in the TiO_2 lattice separated in the form of hematite ($\alpha\text{-Fe}_2\text{O}_3$) as shown using Mössbauer spectroscopy and XRD. The diffuse reflectance spectra were used for band gap energy calculations. The band gap energy of the undoped TiO_2 sample was 3.1 eV, whereas the band gap energy of Fe-Ti-O samples doped with up to 10 % showed blue shift (3.2 eV). The significant red shift (from 3.2 to 2.4 eV) was observed in the samples with higher iron content (from 10 to 50 mol %).

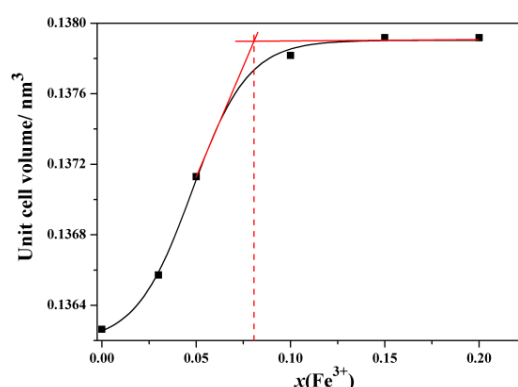


Figure 1 – The influence of the Fe^{3+} ion content on the unit-cell volume of the anatase (TiO_2) solid solutions. The red dashed line indicates the solid solubility limit of Fe^{3+} ions inside the anatase lattice, estimated at ~8 mol %.

Acknowledgements: This work has been fully supported by SAFU, project K.01.1.1.01.0001.

The Impact of Dextran Sulfate on the Radiolytic Synthesis of Magnetic Iron Oxide Nanoparticles

Tanja Jurkin^a, Ivan Marić^a, Goran Štefanić^b and Marijan Gotić^b

^a Radiation Chemistry and Dosimetry Laboratory, Ruđer Bošković Institute, Bijenička 54, 0000 Zagreb, Croatia

^b Center of Excellence for Advanced Materials and Sensing Devices, Research Unit New Functional Materials, Bijenička 54, 10000 Zagreb, Croatia
tjurkin@irb.hr

Recently, the new synthesis route to δ -FeOOH nanodiscs based on the γ -irradiation of a deoxygenated iron(III) chloride alkaline aqueous colloidal solution in the presence of diethylaminoethyl-dextran hydrochloride (DEAE-dextran) has been reported by Jurkin et al. [1]. In that work we supposed that γ -irradiation produced reducing conditions and that δ -FeOOH nanoparticles were formed through oxidation of obtained white suspension characteristic of $\text{Fe}(\text{OH})_2$. In this work, we studied the impact of dextran sulfate polymer (DEX-sulfate) on the radiolytic synthesis of magnetic iron oxide nanoparticles. The syntheses started with γ -irradiation (130 kGy) of deoxygenated iron(III) chloride alkaline aqueous colloidal solution in the presence of 2-propanol and DEX-sulfate. The radiolytically synthesised samples were isolated by conventional process of sample isolation (centrifugation/washing with water or ethanol) or in the presence of glycerol. The XRD results showed that sample isolated in the presence of glycerol contained $\text{Fe}(\text{OH})_2$, hydroxysulfate green rust II (GR SO_4^{2-}) and goethite (α -FeOOH). The Mössbauer results confirmed the presence of $\text{Fe}(\text{OH})_2$ and hydroxysulfate green rust II (GR SO_4^{2-}) in this sample. The radiolytically synthesized samples that were isolated by centrifugation and washing with water or ethanol contained GR SO_4^{2-} and α -Fe₂O₃. Therefore, the DEX-sulfate favoured the formation of α -FeOOH and/or α -Fe₂O₃ through GR-II (SO_4^{2-}) intermediate product.

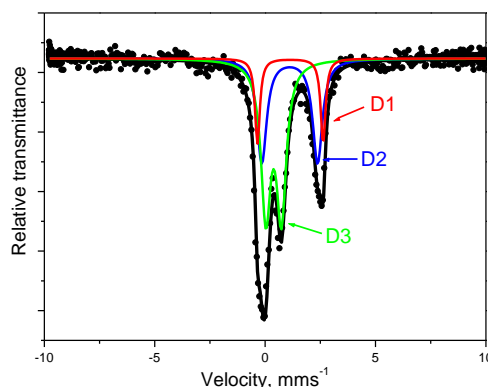


Figure 1 – Mössbauer spectrum of radiolytically synthesised sample that was isolated in the presence of glycerol. D1 and D2 doublets correspond to Fe(II) in $\text{Fe}(\text{OH})_2$ and GR-II (SO_4^{2-}), respectively, whereas D3 corresponds to Fe(III).

References

1. T. Jurkin, G. Štefanić, G. Dražić and M. Gotić, *Mater. Lett.*, 173 (2016) 55.

Acknowledgements: This work has been supported by Croatian Science Foundation under the project UIP-2017-05-7337 (POLRADNANOP).

Nanostructuring Poly[N(1-aza-16-crown-6)carbamido-2,5-thienylene-alt-1,4-phenylene] with Sodium Dodecylsulfate

Hugh D. Burrows^a, T. Costa^a, M. L. Ramos^a, L. L. G. Justino^a, A. J. M. Valente^a,
E. Gomes^a, M. Kraft^b and U. Scherf^b

^a Centro de Química, Department of Chemistry, University of Coimbra, P-3004-535 Coimbra, Portugal

^b Macromolecular Chemistry Group (buwmacro), Bergische Universität Wuppertal, Gauß-Strasse. 20,
42097 Wuppertal, Germany
burrows@ci.uc.pt (Hugh D. Burrows)

Water soluble conjugated polymers are of scientific and technological importance for a wide variety of applications, including sensing, and charge transport layers in various optoelectronic devices. Water-solubility is normally achieved by attaching ionic or hydrophilic side chains to polymer backbone. We show that the conjugated polymer poly[N(1-aza-16-crown-6)carbamido-2,5-thienylene-alt-1,4-phenylene] (BG2, Fig. 1) dissolves in aqueous solutions of the surfactant sodium dodecylsulfate (SDS). Electrical conductivity and ²³Na NMR spectroscopy suggest binding of the sodium cation in the azacrown cavity. Similar behavior has previously been reported for SDS and 18-crown-6 [1]. A marked blue shift in the fluorescence maximum and an increase in the emission quantum yield is observed upon adding SDS to aqueous dispersions of the polymer, leading to values close to that of BG2 in the good solvent CHCl₃. It is suggested that the conjugated polymer backbone adopts a similar conformation in SDS solution to that in chloroform. ¹H and ¹³C NMR spectra are consistent with this.

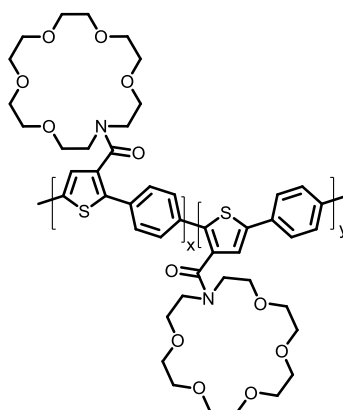


Figure 1 – Structure of BG2.

References

1. T. Mihelj, V. Tomašić, N. Biliškov and F. Liu, *Spectrochim. Acta Part A: Mol. Biomol. Spectrosc.*, 124 (2014) 12.

Acknowledgements: Financial support of the Coimbra Chemistry Centre from the *Fundação para a Ciência e Tecnologia* (FCT) through project UID/QUI/UI0313/2013 and the COMPETE Programme is gratefully acknowledged. Licínia L. G. Justino thanks the FCT for the grant SFRH/BPD/97026/2013.

Synthesis and Spectroscopic Study on the Tautomerization of Substituted 2-Phenyl Imidazoles used for the formation of Metal-Coordinated Assemblies or Suitable Guests for Supramolecular Coordination Nanocapsules

Anife Ahmedova^a, Nikola Burdzhiev^a and Pavletta Shestakova^b

^a Faculty of Chemistry and Pharmacy, Sofia University, 1, J. Bourchier blvd., Sofia 1164, Bulgaria

^b NMR Laboratory, Institute of Organic Chemistry with Centre of Phytochemistry, Bulgarian Academy of Sciences, Acad. G. Bonchev Str. Bl. 9, Sofia 1113, Bulgaria
ahmedova@chem.uni-sofia.bg

As part of an ongoing project of ours, dealing with Pt- and Pd-linked metallocsupramolecular capsules and their cytotoxicity [1,2], we undertook the synthesis of a pyrene functionalized class of Schiff bases that form upon the template effect of a metal ion – Cu(II) or Pd(II) – and are isolated as the corresponding metal complex. The purpose to use pyrene fragment for modification is its high intrinsic fluorescence, and the proved high stability of host-guest complexes between pyrene and the metallocsupramolecular capsules, which also affects their cytotoxicity profile.² Thereby, we aim to obtain pyrene-modified metal complexes of imidazole-based Schiff bases that can either act as suitable guest molecules through their pyrene-propyl fragment or can form cyclic hexameric complexes as described by Matsumoto *et al.* [3].

Herein, we present NMR-spectroscopic and theoretical data on the tautomerization phenomenon of modified imidazole-4(5)-carbaldehyde as an initial step of detailed structural characterization of the aldehyde used for the Schiff base synthesis. Temperature-dependent ¹H-NMR data in solution and the ¹³C-CPMAS NMR complemented each other to describe the dynamics of the imidazole tautomerization. Furthermore, the pyrene-modified imidazole-4(5)-carbaldehyde has been utilized in the synthesis of the Schiff base with 2-(pyridin-2-yl)ethan-1-amine through its complexation with Cu(II) and Pd(II). The formed complexes have been isolated and fully characterized by spectroscopic methods – UV-Vis absorption and fluorescence, IR and NMR. Advanced NMR techniques (including DOSY-NMR) have been used to study the pH-controlled aggregation of the monomeric Pd(II) complex.

By combination of multiple spectroscopic techniques and theoretical data, it was possible to describe the complex structure of the newly synthesized compounds along with the dynamics of the tautomerization and aggregation processes that they take part in. These data are of crucial importance for our future biological studies.

References

1. A. Ahmedova, D. Momekova, M. Yamashina, P. Shestakova, G. Momekov, M. Akita and M. Yoshizawa, *Chem. Asian J.*, 11 (2016) 474.
2. A. Ahmedova, R. Mihaylov, D. Momekova, P. Shestakova, S. Stoykova, J. Zaharieva, M. Yamashina, G. Momekov, M. Akita and M. Yoshizawa, *Dalton Trans.*, 45 (2016) 13214.
3. N. Matsumoto, Y. Motoda, T. Matsuo, T. Nakashima, N. Re, F. Dahan and Jean-Pierre Tuchagues, *Inorg. Chem.*, 38 (1999) 1165.

Acknowledgements: The authors thank the National Science Fund of Bulgaria (DFNI-B02/24) for the financial support.

Interaction of Engineered Nanomaterials with Biomolecules Studied by Spectroscopic Techniques

Karolína M. Šišková

Dept. of Biophysics, Centre of the Region Haná for Biotechnological and Agricultural Research, Faculty of Science, Palacký University, Šlechtitelů 27, Olomouc, CZ-78371, Czech Republic
karolina.siskova@upol.cz

Nanoparticles (NPs) are currently the topic of interest of a bundle of research papers and proposals. There are persistent rumors about NPs toxicity and ecotoxicity, concerns about their increasing release into the environment and attempts to their risk assessment [1-4]. Many researchers often test the impact of different kinds of NPs on cells, tissues, organs, and/or directly on whole organisms. However, in order to understand the possible NPs impacts, it is necessary, in my opinion, at first to evaluate the interaction of NPs with one type of the basic units of all organisms and their cells, i.e. amino acids. Furthermore, it is important to elucidate whether and how can NPs affect the conformation of proteins (their secondary and tertiary structure). Only after gaining such information, the assessment of NPs toxicity and ecotoxicity could be meaningful. In this study, the interaction of synthesized nanoparticles with selected amino acids and a physiologically important transmembrane protein, the sodium/potassium pump (Na^+/K^+ -ATPase) will be investigated by using several spectroscopic techniques. The sodium/potassium pump is an enzyme which is ubiquitous in all animal cells and its malfunctions are related to many diseases such as hypertension, diabetic neuropathies, renal failure, neurological disorders etc. [5-7].

References

1. X. Hu, D. Li, Y. Gao, *et al.*, *Environ. Intl.*, 94 (2016) 8.
2. H. H. Liu and Y. Cohen, *Environ. Sci. Technol.*, 48 (2014) 3281.
3. A. Lopez-Serrano, R. M. Olivas, J. S. Landaluze, *et al.*, *Anal. Methods*, 6 (2014) 38.
4. A. Kaphle, *et al.*, *Environ. Chem. Lett.*, 16 (2018) 43.
5. M. Kubala, *et al.*, *Front. Physiol.*, 7 (2016) 115.
6. B.R. Larsen, *et al.*, *Front. Physiol.*, 7 (2016) 141.
7. T. Friedrich, *et al.*, *Front. Physiol.*, 7 (2016) 239.

Acknowledgements: The author thanks to grant No. LO1204 (Sustainable development of research in the Centre of the Region Haná) from the National Program of Sustainability I, MEYS for financial support. The author also acknowledges to assoc. prof. Peter Mojzeš and Dr. Josef Kapitán for valuable questions and comments during the spectroscopic measurements and data treatment. Dr. Lukáš Nosek is thanked for TEM imaging.

Dielectric Properties of Intercalated Montmorillonite

K. Kułacz and K. Orzechowski

Faculty of Chemistry, University of Wrocław, F. Joliot Curie 14, 50-383 Wrocław, Poland

karol.kulacz@chem.uni.wroc.pl

Montmorillonite belongs to aluminosilicate group (called also phyllosilicates). It is an example of layered clay minerals of prominent sorption properties. Layered minerals form structures consisting of tetragonal and octahedral sheets. They can receive and stabilize between layers polar guest molecules. The process is called intercalation.

Products of intercalation have very promising properties. Previously [1,3] we proved that intercalated kaolinite or hydro – halloysite can effectively absorb electromagnetic wave. It could be used for protection against negative impact of electromagnetic pollution [4].

Montmorillonite has larger sorption ability than the kaolinite or hydro – halloysite, what encourage us to test this material as a wave absorber. In this report we present results obtained by dielectric spectroscopy applied for montmorillonite and intercalated montmorillonite. The measurements of real and imaginary part of dielectric permittivity allow to conclude on a movement of polar guest molecules in the intercalated mineral [4].

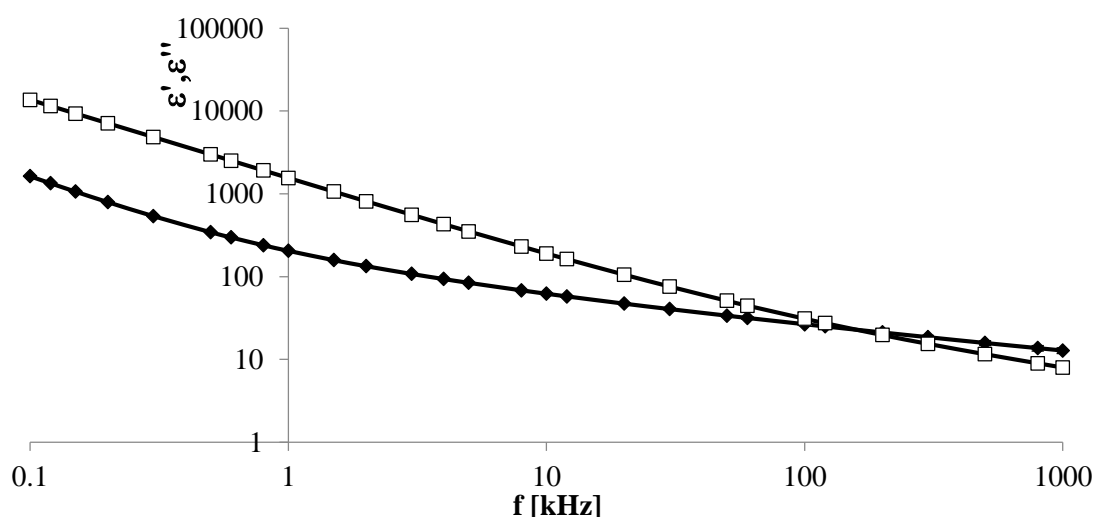


Figure 1 – Real and imaginary dielectric permittivity of hydrated montmorillonite, HP 4284A (20 Hz - 1 MHz).

References

1. K. Orzechowski, T. Słonka and J. Głowinski, *J. Phys. Chem. Solids*, 67 (2006) 915.
2. K. Leluk and K. Orzechowski, *J. Phys. Chem. Solids*, 71 (2010) 827.
3. M. Adamczyk, M. Rok, A. Wolny and K. Orzechowski, *J. Appl. Phys.*, 115 (2014) 024101.
4. M. H. Repacholi, *Bioelectromagnetics*, 19 (1998) 1.

Acknowledgments: The authors are grateful for co-financing of participation in the conference from the KNOW Funds of the Faculty of Chemistry, University of Wrocław.

Modification of the Structure of Metakaolin-Based Geopolymers

Piotr Rożek^a, Kamila Brylewska^{a,b}, Magdalena Król^a and Włodzimierz Mozgawa^a

^a AGH University of Science and Technology, Faculty of Materials Science and Ceramics, Mickiewicza 30, 30-059 Kraków, Poland

^b Jagiellonian University, Faculty of Chemistry, Gronostajowa 2, 30-387 Kraków, Poland
prozek@agh.edu.pl

The term “geopolymers” refers to inorganic, amorphous or partially semi-crystalline, materials which can be obtained in the reaction of aluminosilicates (e.g. fly ash, metakaolin) with alkali-activator [1]. This results in monolithic material with three-dimensional network consisting of [SiO₄] and [AlO₄] tetrahedra bonded together by oxygen atoms. Geopolymers are used as e.g. sustainable equivalents of cementitious materials, or heavy metal sorbents. Also, first attempts to exploit them in catalysis were made [2]. The aim of this work was to modify the metakaolin-based geopolymers by desilication and dealumination treatments in order to obtain hierarchical mesoporosity.

The parent geopolymer was obtained by alkali-activation of metakaolin with sodium hydroxide solution at 80 °C. It was then ion-exchanged with NH₄NO₃ and this form was subjected to desilication (NaOH), dealumination (Na₂H₂EDTA), and the combination of both processes. The textural and structural characterization of the obtained materials was carried out. For this purpose, X-ray diffraction (XRD), nitrogen adsorption-desorption experiment, scanning electron microscopy (SEM), infrared spectroscopy (MIR) and Raman spectroscopy were used. The presence of zeolite A and hydroxysodalite in parent geopolymer was confirmed. The raised background in XRD pattern indicated the formation of amorphous phase, i.e. sodium-alumino-silicate-hydrate gel (N-A-S-H). The applied modification processes resulted in the degradation of zeolite A structure, which was observed as the decrease in the intensity of a band at 560 cm⁻¹ in MIR spectra as well as its characteristic peaks in XRD patterns. The sequential dealumination and desilication treatment caused the significant increase in mesopores volume. Also, it seems to be more effective than a not-combined treatment. Therefore, such a modification can be applied to enhance geopolymer properties for catalysis and environmental protection.

References

1. J. Davidovits, *J. Therm. Anal.*, 37 (1991) 1633.
2. P. Sazama, O. Bortnovsky, J. Dědeček, Z. Tvarůžková and Z. Sobalík, *Catal. Today*, 164 (2011) 92.

Acknowledgements: This work was supported by AGH University of Science and Technology, Faculty of Materials Science and Ceramics grant 15.11.160.210.

Spectroscopic Study of Titanium Slag Obtained from Ilmenite Smelting

Avishek Kumar Gupta, Matti Aula and Timo Fabritius

Process Metallurgy Group, Faculty of Technology, University of Oulu, Finland
avishek.gupta@oulu.fi

Growing demand of TiO_2 pigment and superior mechanical properties of titanium has attracted considerable attraction of TiO_2 slag production by ilmenite smelting. The slag must contain around 90% titanium to be used as a feedstock for the TiO_2 pigment production. The composition and the cooling rate can have a significant effect on the oxides formed in the slag. For example, tetravalent titanium (TiO_2) is more favorable in the slag than trivalent titanium (Ti_2O_3). To have a better understanding of the slag properties and the phase formations, various spectroscopic techniques were used to analyze the slag samples. The characterization of the slag is done by XRD, FESEM, optical microscopy and FTIR measurements. FTIR measurements will be used to estimate the relative amounts of separate phases. The various phase formed and the effect of cooling rates on these phase formations is studied. The results from these tests will be used to develop a system for on-line analysis of the slag surface composition. The system will help to measure composition of the slag in metallurgical processes, which can be used to control processes more accurately.

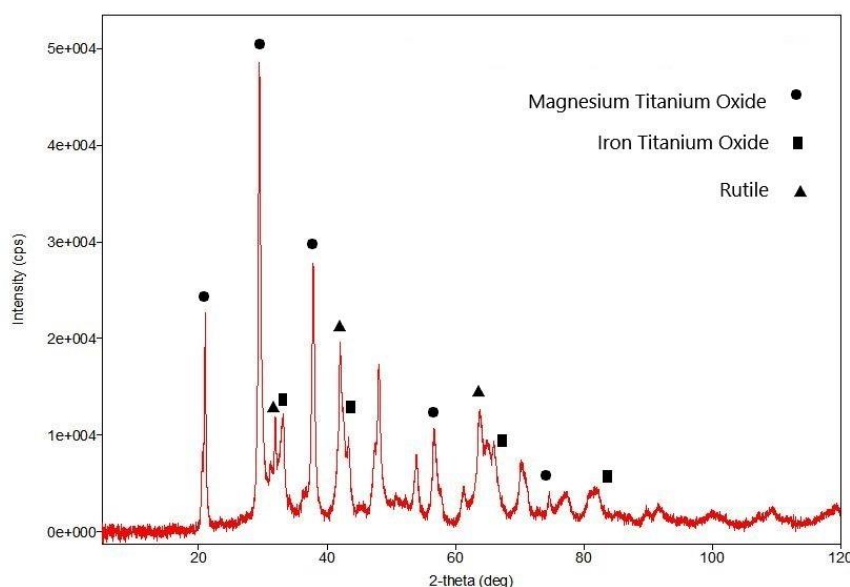


Figure 1 – XRD diagram of the re-melted titanium slag obtained from Outotec Oy.

References

1. T. Bezrodnay, T. Gavrilko, G. Puchkovskaya, V. Shimanovskaya, J. Baran and M. Marchewka, *J. Mol. Struct.*, 614 (2002) 315.
2. S. Samala, B.K. Mohapatra, P.S. Mukherjee and S.K. Chatterjee, *J. Alloys Compd.*, 474 (2009) 484.

Acknowledgements: The author acknowledges I4Future, funded by University of Oulu and European Union's Horizon 2020 under the Marie Skłodowska-Curie grant for the financial funding.

Surfaces Interfaces

Use of Vibrational Spectroscopic Techniques for the Understanding of Evaporation Induced Pattern Formation of Decanol Droplets

Vadym Prokopec^a, Lucia Becherová^a and Jitka Čejková^b

^a Department of Analytical Chemistry, Faculty of chemical engineering, University of chemistry and technology in Prague, Technická 5, 166 28, Prague, Czech Republic

^b Department of Chemical Engineering, Faculty of chemical engineering, University of chemistry and technology in Prague, Technická 5, 166 28, Prague, Czech Republic
prokopec@vscht.cz

Pattern formation in far from equilibrium systems is observed in several disciplines including biology and reaction diffusion chemistry, comprising both living and non-living systems. In nature we can observe pattern formation on various spatial and temporal scales; various patterns like spots, stripes, waves, spirals or dendrites could appear in both the inanimate world and in biological systems [1]. The spontaneous formation of spatial or spatio-temporal patterns under homogeneous external conditions is a characteristic feature of systems far from equilibrium. Such spontaneous pattern formation is of interest in scientific areas such as hydrodynamics, reaction-diffusion systems, oceanography, meteorology, geophysical and biological morphogenesis, semi-conductors etc. Recently we have found a novel type of pattern formation that, to our best knowledge, had not been described before [2].

We aim to study such non-equilibrium dynamics of a novel system based on a 1-decanol droplet placed in a solution of alkaline decanoate. Recently, we have found that when the system is open to the environment and the evaporation of water from decanoate solution occurs we observe dramatic morphological changes of the decanol droplet. Such reproducible morphological changes in simple droplets open a path for exploration of shape-based effects in larger scale pattern formation studies.

This work is aimed at monitoring and characterization of visual and spectral changes occurred during the evaporating process in the systems containing droplets of sodium decanoate solution without or with addition of decanol. The study used vibration spectroscopic methods, namely normal (non-enhanced) Raman spectroscopy with different excitation wavelengths and surface-enhanced Raman scattering spectroscopy (SERS) on large-scaled gold coated SERS-active substrates. All experiments were carried out using both optical and confocal Raman microscope in order to monitor the process of pattern formation in the studied system.

References

1. H. Haken, Pattern Formation by Dynamic Systems and Pattern Recognition: Proceedings of the International Symposium on Synergetics at Schloß Elmau, Bavaria, April 30 – May 5, 1979; Springer Berlin Heidelberg 2012.
2. J. Čejková, F. Štěpánek and M. M. Hanczyc, *Langmuir* 32 (2016) 4800.

Acknowledgements: Financial support from Grant agency of Czech Republic (Project No. 17-21696Y) is gratefully acknowledged.

SERS Active Filter Membranes for Extraction and Detection of Pesticides in Aqueous Solutions

S. Fateixa, M. Raposo, H. I. S. Nogueira and T. Trindade

Department of Chemistry – CICECO, University of Aveiro, 3810-193 Aveiro, Portugal
sarafateixa@ua.pt

Chemical pesticides have been used for crop protection and are essential to guarantee food supplies for a growing world population. On the other hand, their exhaustive use in the agriculture has raised serious concerns due to contamination of soils and water sources [1]. The fate of these contaminants are very often the aquatic eco-systems, namely those located in remote areas of the globe. Thus, sensitive/simple and easy to handle methods for the detection of these pesticides are needed. Spectroscopic methods based on surface-enhanced Raman scattering (SERS) are among the analytical tools that have been exploited in recent years for detecting the presence of water pollutants. These methods are foreseen with great utility namely when associated to the use of analytical kits and portable equipment [2,3].

Conventional substrates based on rigid solid substrates or metal hydrosols are not suitable for sample extraction, limiting their application in water quality monitoring [4]. The fabrication of SERS platforms that allows the rapid collection and analysis of vestigial analytes is quite challenging but desirable. This communication describes the development of SERS active substrates (LCP/Ag) based on liquid-crystal polymer (LCP) textile fibers decorated with Ag nanoparticles (NPs) for the extraction and detection of thiram in water samples spiked with this pesticide [5]. Firstly, we will demonstrate that the SERS effect together with confocal Raman microscopy can be explored as a tool to map the local distribution of chemisorbed thiram molecules over the Ag/LCP substrates. Then, thiram spiked water samples, such as Aveiro Estuary water and fruit juices, have been analysed using the SERS substrates with the best performance. In addition, SERS active membranes were also prepared by using the above mentioned Ag/LCP composites supported on polyamide (PA) filters. It will be demonstrated that these composites can be used for the extraction of thiram dissolved in aqueous solutions and subsequent SERS detection, thus providing new active filter membranes for water analysis.

References

1. N. Verma and A. Bhardwaj, *Appl. Biochem. Biotechnol.*, 175 (2015) 3093.
2. J. Zheng, S. Pang, T. P. Labuza and L. He, *Talanta*, 129 (2014) 79.
3. J. Chen, Y. Huang, P. Kannan, L. Zhang, Z. Lin, J. Zhang, T. Chen and L. Guo, *Anal. Chem.*, 88 (2016) 2149.
4. S. Fateixa, H. I. S. Nogueira and T. Trindade, *Phys. Chem. Chem. Phys.*, 17 (2015) 21046.
5. S. Fateixa, M. Raposo, H. I. S. Nogueira and T. Trindade, *Talanta*, 182 (2018) 558.

Acknowledgements: This work was developed within the scope of the project CICECO- Aveiro Institute of Materials, POCI-01-0145-FEDER-007679 (FCT Ref. UID /CTM /50011/2013), financed by national funds through the FCT/ MEC and when appropriate co-financed by Fundo Europeu de Desenvolvimento Regional (FEDER) under the PT2020 Partnership Agreement. S. Fateixa thanks Fundação para a Ciência e Tecnologia (FCT) for the Grant SFRH/BPD/ 93547/2013.

Spectroscopic and Imaging Studies of Sporopollenin Metal Complexes

Fatmah M. Alkhatib, Nigel A. Young and Stephen J. Archibald

*School of Mathematics and Physical Sciences (Chemistry), University of Hull, Cottingham Road,
Hull HU6 7RX, UK*

F.Alkhatib@2009.hull.ac.uk

The main objective of this work has been the determination of the nature of the interactions between metal complexes and salts and the surface of sporopollen exines capsules (SECs) and other naturally occurring spore exines. SECs are natural materials derived from plant pollen and spores [1] and SEC-metal complexes are ideal materials for investigation as they can be used in a wide variety of applications including catalysis, imaging and biological delivery. SEC – metal complexes between the first row transition metals iron, copper, nickel, and zinc had metal loadings of 5 – 15 mg g⁻¹. A selection of spectroscopic techniques (IR, Raman, ICP-OES, UV-Vis, NMR, EPR, Mössbauer and X-ray absorption spectroscopy) have been used to characterise the interaction between the metal and the SEC surface. IR spectroscopy revealed the presence of aliphatic chains and hydroxyls, aliphatic carbons, carbonyls, unsaturation and ether groups in the SEC [2], and for the complexes derived from acetate salts there was evidence indicating the presence of bound acetate, which was also observed in the UV-vis data of the copper complexes. X-ray absorption spectroscopy has identified octahedral mononuclear coordination environments for the nickel and zinc complexes, a Jahn-Teller distortion for the mononuclear copper complexes (supported by EPR data) and the presence of small iron oxyhydroxide clusters. In addition, XRF imaging data using synchrotron radiation has shown that the metal distribution is very closely associated with the underlying physical structure of the SEC.

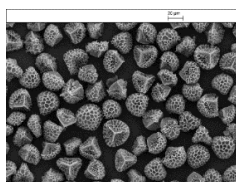


Figure 1 – The image of the physical structure of exine.

References

1. S. Barrier, A. Lobbert, A. J. Boasman, A. N. Boa, M. Lorch, S. L. Atkin and G. Mackenzie, *Green. Chem.*, 12 (2010) 234.
2. A. Diego-Taboada, S. T. Beckett, S. L. Atkin and G. Mackenzie, *Pharmaceutics*, 6 (2014) 80.

Acknowledgements: I would like to thank Dr. N. A. Young, Prof. S. J. Archibald and Dr. G. Mackenzie for their support and advice. Special thanks are due to Umm Al- Qura University for their financial support and the Ministry of Higher Education in Saudi Arabia.

Formation of Metal Nanoparticle Films for Trace Analysis of OCT Drugs in Biological Fluids by Means of SERS Spectroscopy

Martynas Velicka, Sonata Adomaviciute and Valdas Sablinskas

Vilnius University, Institute of Chemical Physics, Sauletekio av. 3, Vilnius, LT-10257, Lithuania

martynas.velicka@ff.vu.lt

Self-medication – the use of over the counter (OCT) drugs as a self-regulated remedy - has grown in numbers over the recent years. Unfortunately, the use of medicine without the supervision of a certified health expert can lead to overdosing and serious health issues followed by hospitalisation or even death [1]. This is especially common amongst elders [2]. The chronic overdose of OCT drugs such as aspirin is frequent and determines different pharmacokinetics with increased half-life of the drug due to saturated excretion channels. This means that the abused OCT drug must be monitored over a period of time to ensure the well-being of the patient. Consumption of drugs can be detected by trace analysis performed on biological fluids such as blood, saliva and etc. However, most of the detection methods like the commonly used chromatography either are time consuming or lack the sensitivity to identify molecules of trace concentrations thus no resolution could be made.

Fast and precise analysis of complicated biological mixtures such as blood can be performed using vibrational spectroscopy due to uniqueness of the spectra of different molecules. Meanwhile, the needed sensitivity for detection of molecules at concentrations as low as nanomolar can be achieved using colloidal surface enhanced Raman scattering (SERS) spectroscopy. Nonetheless the application of the SERS method is not trivial. It is not always easy to find an optimal conditions for enhancement or Raman signal and can take a lot of efforts. Furthermore, the reproducibility of active SERS films is an issue that must be taken into account.

In this work we present a study on various colloidal SERS approaches for a fast detection of OCT drugs in biological fluids using silver and gold nanoparticle films deposited on glass or aluminium substrates. Various colloidal AgNP and AuNP colloidal solutions were synthesised and tested through the work. The usability of the formed active metal surfaces was tested using easily available and the commonly used OCT drugs like acetylsalicylic acid and its derivative salicylic acid in biological fluids such as blood, tears and saliva. Results showed that it is indeed possible to obtain a nanoparticle film with sufficient sensitivity and reproducibility to be used as a fast and reliable alternative for a laboratory tests conducted nowadays in the formentioned OCT drug problem. The SERS approach enables to detect acetylsalicylic acid and its derivative salicylic acid in the biological fluids at concentrations down to 0.5 mM.

References

1. D. D. Gummin, J. B. Mowry, D. A. Spyker, D. E. Brooks, M. O. Fraser and W. Banner, *Clin. Toxicol. (Phila)*, 55 (2017) 1072.
2. S. Schmiedl, M. Rottenkolber, J. Hasford, D. Rottenkolber, K. Farker, B. Drewelow, M. Hippus, K. Salje and P. Thurmman, *Drug Safety*, 37 (2014) 225.

Influence of TiO₂ Nanoparticles and UV Radiation on Raman Spectra

V. Skoupá^a, A. Jenišťová^b and V. Setnička^a

^a Department of Analytical Chemistry, Faculty of Chemical Engineering, University of Chemistry and Technology Prague, Technická 5, Praha 6 - Dejvice, 166 28, Czech Republic

^b Department of Physical Chemistry, Faculty of Chemical Engineering, University of Chemistry and Technology Prague, Technická 5, Praha 6 - Dejvice, 166 28, Czech Republic
Skoupave@vscht.cz

Surface enhanced Raman spectroscopy (SERS) is non-invasive and non-destructive method with low detection limit suitable for analysing drugs and controlled substances. For analytic and forensic purposes it is necessary to detect very low concentrations of analytes. Detection of adulterants usually contaminating the samples is also required.

The self-cleaning effects of the Au-TiO₂ composite nanoparticles by UV radiation are known [1-3]. These effects were investigated on large-area SERS substrates immersed into the TiO₂ suspense of nanoparticles in demineralized water. Samples of cocaine were measured on electrolytically plated platinum targets. The intensity of the SERS spectra of pure cocaine did not change after immersion into a suspense of TiO₂ under UV irradiation. But for some real cocaine samples, the intensity of SERS spectra was even higher after using TiO₂ and UV radiation. This signal amplification was found to be due to the content of levamisole. Levamisole is used as a medical drug and it is one of the frequently used adulterants of cocaine. We tested the sole effect of TiO₂ on intensity of the levamisole spectrum. Also, we separately tested the effect of UV radiation. Final test of TiO₂ and UV radiation combined together was conducted.

References

1. X. Jiang, X. Sun, D. Yin, X. Li, M. Yang, X. Han, L. Yang and B. Zhao, *Phys. Chem. Chem. Phys.*, 19 (2017) 11206.
2. A. Mikolajczyk, A. Malankowska, G. Nowaczyk, A. Gajewicz, S. Hirano, S. Jurga, A. Zaleska-Medynska and T. Puzyn, *Environ. Sci.: Nano*, 3 (2016) 1425.
3. D. Han, H. Huang, D. Du, X. L. K. Long, Q. Hao and T. Qiu, *Mater. Chem. Phys.*, 153 (2015) 88.

Acknowledgements: Financial support from specific university research (MSMT No 21-SVV/2018) and grant VI20172020056 Ministry of Interior of the Czech Republic.

SERS Activity of Ag-Polypyrrole Nanocomposites

Tomasz Czaja, Kamil Wójcik, Maria Grzeszczuk and Roman Szostak

Department of Chemistry, University of Wrocław, 14 F. Joliot-Curie, 50-383 Wrocław, Poland

tomasz.czaja@chem.uni.wroc.pl

Hybrid materials composed of organic and inorganic chemical components have been shown to demonstrate new properties of foremost importance in energy conversion, catalysis, chemical analysis and other applications. Conducting polymer nanocomposites composed of inorganic nanoparticles residing in the polymer matrix can provide particle stability, mechanical strength and easy control of processing.

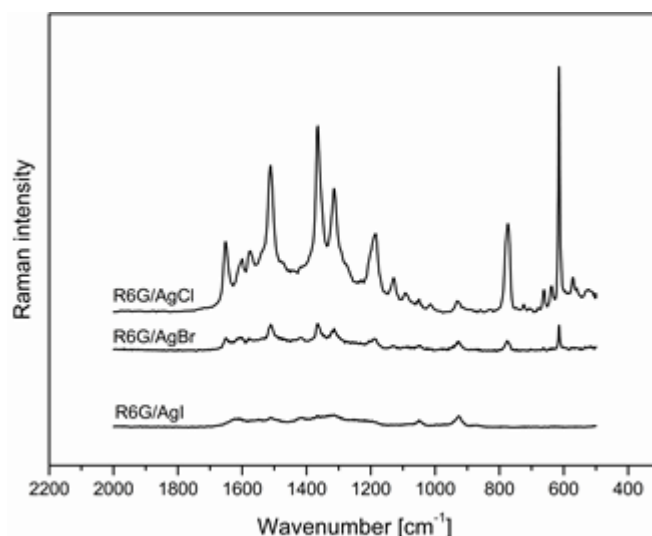


Figure 1 – Spectra of aqueous 50 μM rhodamine 6G solution for the studied composites.

Silver(I) halide particles embodied in a polypyrrole (PPy) matrix are synthesized and further processed electrochemically to obtain nanoparticles of silver with significant activity in the surface-enhanced Raman spectroscopy (SERS). The application of PPy/Ag/AgX (X= Cl, Br, I) nanocomposites as a SERS platform was investigated by applying rhodamine 6G (R6G) as a probe. Raman spectra of R6G solutions in water (50 μM) registered using obtained substrates in the presence of KX salts (X= Cl, Br, I) exhibited an intensity pattern different from that of an off-resonance Raman spectrum of R6G. This means that despite an almost 3500 cm^{-1} difference between the absorption maximum of an R6G molecule at 528 nm and the 647.1 nm excitation line, pre-resonance effects are observed. The average enhancement factor is higher for the PPy/AgCl/KCl than for the PPy/AgBr/KBr system, 1.5×10^4 and 2.5×10^3 , respectively. For the PPy/AgI/KI substrate, the amplification of the R6G Raman signal is not observed at all.

Gold Nanoclusters Shining on Gold Nanostars

B. Casteleiro, T. Ribeiro, J. M. G. Martinho, J. P. S. Farinha
CQE and IN, Instituto Superior Técnico, Universidade de Lisboa, Lisbon, Portugal
barbara.casteleiro@tecnico.ulisboa.pt

Gold Nanoclusters (AuNCs) are unique gold nanostructures with dimensions below 2nm, size dependent luminescence, very high photostability, catalytic activity, low toxicity and biocompatibility [1,2]. Across different fields from medicine and biology to chemistry and physics, their applications have been widely explored, like catalysis, sensing, imaging and theranostic.

We are mainly interested in the application of AuNCs as labels for advanced optical imaging. With the aim of increasing the luminescence emission of AuNCs in the near infrared tissue penetration window, we conjugate AuNCs with Gold Nanostars [3] (AuNStars – Figure 1), to take advantage of the emission enhanced at the hotspots on the star tips. We observe an increase in the luminescence emission intensity when compared with the AuNCs without AuNStars.

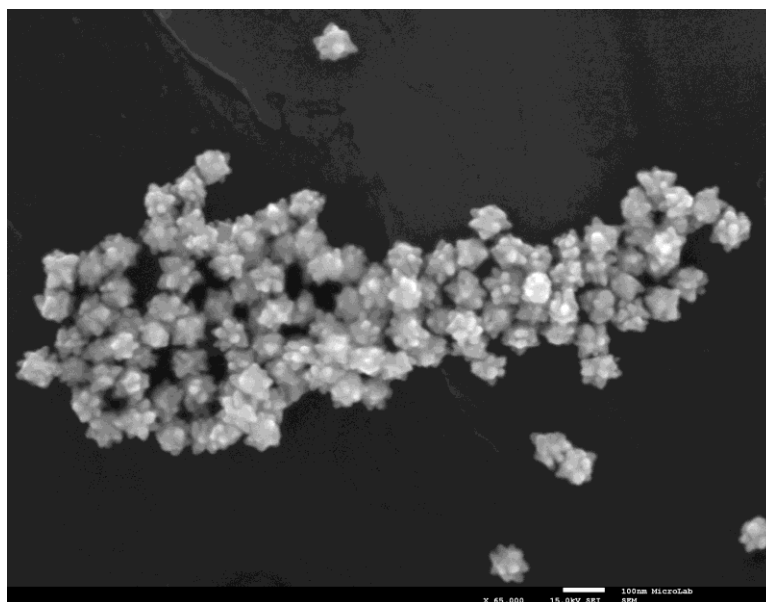


Figura 1 – SEM image of AuNStar

References

1. R. Jin, *Nanoscale* 2, 343 (2010).
2. Y. Zheng et al, *Advances in Colloid and Interface Science* 242, 1(2017).
3. Carrasco, S. et al, *Chem. Mater.* 28, 7947-7954 (2016)

Acknowledgements: This work was partially supported by Fundação para a Ciência e a Tecnologia (FCT-Portugal) and COMPETE (FEDER), projects UID/NAN/50024/2013 and PTDC/CTM-POL/3698/2014. B.C. thanks FCT for PhD grant PD/BD/137511/2018 from the program ChemMat.

Structure-Forming Properties of 2*H*-Imidazole-2-thione Derivatives over Polycrystalline Gold Surfaces

Truong Ngoc Hung^{a,b}, Gábor Varga^{a,b}, Zoltán Kónya^{c,d}, Ákos Kukovecz^c, Gábor Kozma^c, Viktor Havasi^c, Pál Sipos^{b,e}, Gregorz Mlostóń^f and István Pálinkó^{a,b}

^a Department of Organic Chemistry, ^b Materials and Solution Structure Research Group, Institute of Chemistry,

^c Department of Applied and Environmental Chemistry, ^d MTA-SZTE Reaction Kinetics and Surface Chemistry Research Group, ^e Department of Inorganic and Analytical Chemistry, University of Szeged, Dóm tér 7-8, Szeged, H-6720 Hungary

^f Department of Organic and Applied Chemistry, University of Łódź, Tamka 12, Łódź, PL-91-402 Poland
palinko@chem.u-szeged.hu

After learning about the aggregation behaviour of three 2*H*-imidazole-2-thione derivatives (Figure 1), another dimension has been added, *i.e.*, the structure-forming properties over polycrystalline gold surface was investigated. Since it is known that sulfur is aurophilic, it was expected that a stable layer will be formed over the gold surface, and perhaps, the adsorbed molecules will interact with each other *via* hydrogen bonding. The results obtained are communicated in this contribution.

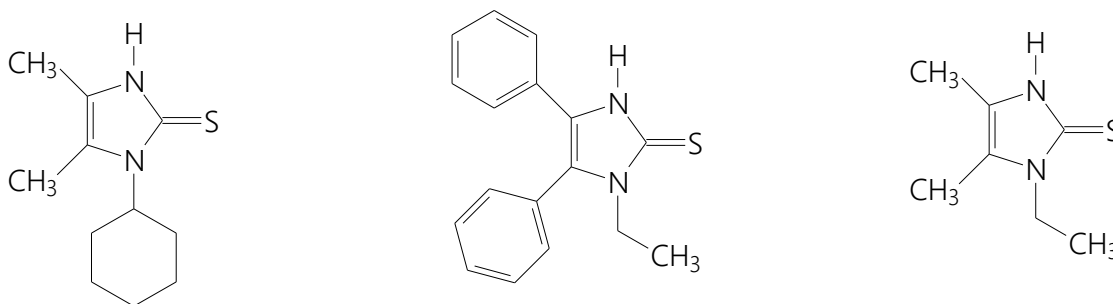


Figure 1 – The compounds of the study.

The polycrystalline gold surfaces were made using the gold-coating facility of a SEM-EDX (energy dispersive X-ray analyzer coupled to the scanning electron microscope) instrument on quartz slides. The organic matter containing overlayers were prepared by the dip-coating technique. The clean as well as the treated surfaces were studied by SEM measurements, infrared and atomic force microscopies.

It was found that stable overlayers could be formed. The first layer was attached to the surface *via* the sulfur atom, while the others are kept together with hydrogen bonding. AFM images revealed important information from the topology of the layers.

Acknowledgements: This work was supported by the National Science Fund of Hungary through grant OTKA NKFI 106234. The financial help is highly appreciated.

Development of Composite Plasmonic Nanostructured Substrates Focused on Reusability for Surface Enhanced Spectroscopy

M. Plicka and P. Matějka

*Department of Physical Chemistry, Technická 5 Praha, University of Chemistry and Technology Prague,
Czech Republic
plickami@vscht.cz*

Surface-Enhanced Raman Scattering (SERS) represents an analytical method with low detection limits up to theoretical possibility of detection single molecule. Enhancement of the measured signal is closely linked to the substrate surface, which is generally composed of noble metals, such as: Au, Ag, and Cu in form of colloidal solution or large-scaled substrate. Such substrate should fulfil several criteria's such as: stability, high reproducibility of preparation method and defined surface morphology in order of nanometres. Current development in the area is partly focusing on preparation SERS-active substrates using environmentally friendly reduction methods/agents (saccharides, flavonoids, etc.).

The aim of this work is preparation of nanostructured composite large-scaled substrate by immobilization of Ag on TiO₂ thin film prepared by dip coating [1], using combination of physical and chemical routes (saccharide reduction) of reduction Ag⁺ ions. Such prepared substrates are being tested in term of SERS-activity using model analyte: 3,6-dichloropyridine-2-carboxylic acid, which is widely used herbicide for broadleaf weeds. Such modified substrates are afterwards treated with UV irradiation in purpose of clean the surface of substrate (using photocatalytic properties of TiO₂ film), allowing it's recyclability. SERS spectra were measured using dispersive Raman spectrometer with excitation wavelength at 532 nm. Characterization of substrate surface pre and post UV irradiation has been performed using following techniques: Scanning Electron Microscopy (SEM) and Atomic Force Microscopy (AFM). Last but not least has been measured UV-VIS (Ultraviolet-Visible Spectroscopy) spectra to determine plasmon resonance maximum of prepared substrate and monitoring it's shift after the UV decomposition process.

References

1. J. Krysa, M. Baudys, M. Zlámál, H. Krýsová, M. Morozová and P. Kluson, *Catal. Today*, 230 (2014) 2.

Acknowledgements: Financial support for specific university research (MSMT No 20-SVV/2018) is gratefully acknowledged.

Hybrid Polymer Templates Synthesized *via* RAFT and Loaded with AgNPs as Tool for SERS

Julita Muszyńska^a, Yaoming Zhang^b, Paulina Filipczak^a, Gokhan Demirci^b, Onur Centikaya^b, Marcin Kozanecki^a, Joanna Pietrasik^b and Krzysztof Matyjaszewski^{a,c}

^a Department of Molecular Physics, Lodz University of Technology, Żeromskiego 116, 90-924 Lodz, Poland

^b Institute of Polymer and Dye Technology, Lodz University of Technology, Stefanowskiego 12/16, Lodz, Poland

^c Department of Chemistry, Department of Chemistry, 4400 Fifth Avenue, Pittsburgh, PA 15213, USA

julita.muszynska@edu.p.lodz.pl

Surface Enhanced Raman Scattering is a powerful tool for examination of various molecules. It occurs in immediate vicinity of noble metal nanoparticles and targeting molecules. This method allows to detect even trace amount of a substance (even as small quantities as 10^{-11} M) what is extremely important in terms of biological species. SERS requires certain conditions like, among others: applicable substrate, homogenous thin layer of analyte, type and morphology of metal nanoparticles, kind of targeting molecule and appearance of hot spot regions. The interest of producing efficient SERS substrates has grown in recent years. It is a huge challenge to produce very homogenous monolayer of examining solution on substrates which can allows to create region with very high enhancement of signal – hot spots regions. Hot spots are caused probably by local surface plasmon resonance (LSPR) [1,2] leading to intensification of local field enhancement and can be created by uniformly distributed well-defined noble metal nanoparticles. The aim of this study was synthesizing size-controlled silver nanoparticles using hybrid polymer structures as highly efficient templates. Polymer templates were synthesized via polymerization induced self-assembly (PISA) method consist of the synthesis of a block copolymer with blocks differing on solubility in a given solvent. Self-assembly exploits the increasing insolubility of growing second block. Obtained poly(acrylic acid)-*block*-polystyrene (PAA-*b*-PS) spheres with PS core and PAA shell were decorated with nanoparticles through AgNO₃ reduction and stabilised by electrostatic interactions with carboxylic groups from PAA [3]. Nanohybrids with several molar ratios of Ag⁺ to COOH groups and different length of PAA were studied. Obtained PISA objects with diameter in the range 60-80 nm were examined by Raman spectroscopy using as targeting molecules adenine and crystal violet. All samples containing adenine and crystal violet with various concentration were deposited by drop casting, zone casting and spin coating methods onto chromed metallic plates, silicon wafers, glass slides and chromed glass slides and measured after evaporation. The most uniform and thin layers were obtained from zone casting and spin coating methods, layers formed by drop casting were irregular and much thicker. The most prominent SERS effect was recorded for samples with Ag⁺/COO⁻ ratio: 1:1 and 1:3. The samples were also characterized by AFM, UV-Vis and IR spectroscopy.

References

1. H.-Y. Chen, M.-H. Lin, C.-Y. Wang, Y.-M. Chang and S. Gwo, *J. Am. Chem. Soc.*, 137 (2015) 13698.
2. R. C. Mahler, *SERS Hot Spots* in Challa S. S. R. Kumar (ed.), *Raman Spectroscopy for Nanomaterials Characterization*, Springer-Verlag Berlin Heidelberg 10 (2012) 215.
3. Y. Zhang, P. Filipczak, G. He, G. Nowaczyk, L. Witczak, W. Raj, M. Kozanecki, K. Matyjaszewski and J. Pietrasik, *Polymer*, 129 (2017) 144.

Acknowledgements: Investigations were financially supported by NCN MAESTRO project: UMO-2014/14/A/ST5/00204.

Raman Spectroscopy as a Tool to Probe Surfaces of Graphene Oxide Decorated with ZnS Nanophases

Joana L. Lopes, Sara Fateixa, Ana C. Estrada and Tito Trindade

Department of Chemistry-CICECO, University of Aveiro, 3810-193 Aveiro, Portugal

jllopes@ua.pt

The growth of inorganic phases on carbon nanostructures has been an important route to produce materials for optoelectronic devices and photocatalysts [1]. We have been particularly interested in developing carbon nanostructures (*e.g.* graphene oxide: GO) decorated with semiconductor nanophases as photocatalysts for water treatment technologies [2,3]. Because surface chemistry plays an important role in these applications, there is an obvious interest to explore new methods for nanoscale characterization of such photoactive surfaces. This communication reports our preliminary work in using both Raman spectroscopy and confocal Raman microcopy for the characterization of photocatalytic GO@ZnS substrates (Fig. 1). A new strategy has been implemented that uses 4-mercaptopyridine (4-Mpy) as a Raman reporter to probe the ZnS nanophases over the GO substrates. Our studies demonstrate the potential of confocal Raman microcopy for obtaining nanoscale maps of these hybrid surfaces. An important consequence of this approach is the potential to correlate the distribution of the ZnS nanophases with regions enriched in structural defects present in the sp^2 -carbon 2D nanosheets, such as oxygen moieties that result from the fabrication of the GO substrates.

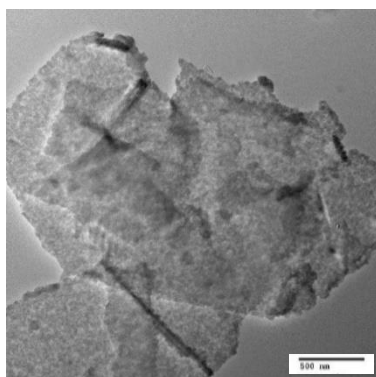


Figure 1 – TEM image of GO@ZnS hybrid nanostructures.

References

1. V. Georgakilas, J. N. Tiwari, K. C. Kemp, J. A. Perman, A. B. Bourlinos, K. S. Kim and R. Zboril, *Chem Rev.*, 116 (2016) 5464.
2. J. L. Lopes, A. C. Estrada, S. Fateixa, M. Ferro and T. Trindade, *Nanomaterials*, 7 (2017) 245.
3. A. C. Estrada, E. Mendoza and T. Trindade, *Eur. J. Inorg. Chem.*, 2014 (2014) 3184.

Acknowledgements: This research was financed in the scope of the FCT Project UTAP-ICDT/CTMNAN/0025/2014 and through the project CICECO-Aveiro Institute of Materials, POCI-01-0145-FEDER-007679 (FCT Ref. UID /CTM /50011/2013), financed by national funds through the FCT/MEC and when appropriate co-financed by FEDER under the PT2020 Partnership Agreement. Sara Fateixa (SFRH/BPD/93547/2013), Ana C. Estrada (SFRH/BPD/86780/2012) and Joana L. Lopes (SFRH/BD/126241/2016) also thank FCT for post-doctoral and PhD grants.

The Elucidation of the Structure of Zinc and Silver 2,2':6',2''-Terpyridine Surface Complexes Formed on Ag Nanoparticles

Ivana Šloufová^a, Blanka Vlčková^a, Peter Mojzeš^b, Irena Matulková^a, Ivana Císařová^a,
Miroslav Šlouf^c, Robert Gyepes^a and Jiří Vohlídal^a

^a Charles University, Faculty of Science, Hlavova 2030, 128 40 Prague 2, Czech Republic

^b Charles University, Faculty of Mathematics and Physics, Ke Karlovu 5, 121 16 Prague 2, Czech Republic

^c Institute of Macromolecular Chemistry, CAS v.v.i., Heyrovského náměstí 2, 162 00 Prague 6, Czech Republic
matulkov@natur.cuni.cz

The surface-enhanced Raman scattering (SERS) [1] spectroscopy enables us to investigate molecules (adsorbates) localized in the close vicinity of the plasmonic metal surfaces. Interaction of the adsorbate with the metal surface can result in formation of surface plasmonic metal-adsorbate complex² or, if the adsorbate is a metal complex, its structure can be preserved³ or distorted [4]. The investigation of surface metal complexes [2,3] is almost impossible by traditional techniques (NMR, X-Ray diffraction, electron diffraction etc.).

In this study [4] we demonstrate how the SERS spectral measurement of $[\text{Zn}(\text{tpy})_2]^{2+}$ complex (tpy = terpyridine) can be seriously hampered by the ligand-exchange surface reaction between chloride anions and one tpy ligand, which resulted in formation of the $[\text{Zn}(\text{tpy})\text{Cl}_2]$ and the $[\text{Ag}^+(\text{tpy})]_n$ surface species. The structure of the surface species was elucidated by combination of several methods: (i) The time-dependent SERS spectral measurements of tpy and its metal (Zn^{2+} and Ag^+) complexes and followed by factor analysis (FA) aiming to receiving the SERS spectra of pure components; (ii) The measurement of Raman spectra of their synthetic analogues, which were characterized by the single crystal X-ray diffraction; and (iii) The DFT calculations of Raman spectra of various model complexes.

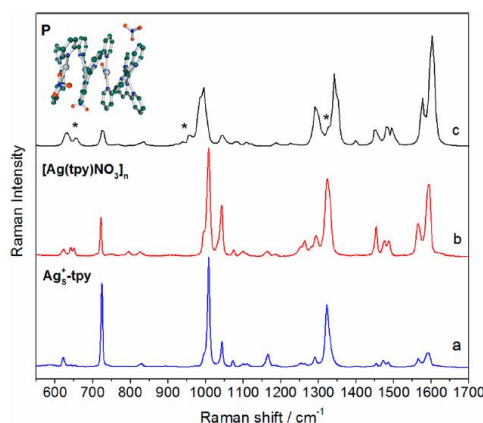


Figure 1 – Comparison of the SERS spectrum of the surface complex (a) with the Raman spectrum of the syntetically prepared polymeric Ag-complex (b) and the calculated Raman spectrum of the polymeric Ag-complex (c).

References

1. R. Aroca, Surface-Enhanced Vibrational Spectroscopy, John Wiley and Sons, Ltd., Chichester, UK, 2006.
2. I. Šloufová, M. Procházka and B. Vlčková, *J. Raman Spectrosc.*, 46 (2015) 39.
3. I. Šloufová, B. Vlčková, M. Procházka, J. Svoboda and J. Vohlídal, *J. Raman Spectrosc.*, 45 (2014) 338.
4. I. Šloufová, B. Vlčková, P. Mojzeš, I. Matulková, I. Císařová, M. Procházka and J. Vohlídal, *J. Phys. Chem. C*, DOI: 10.1021/acs.jpcc.7b12157.

Acknowledgements: This work was supported by the Czech Science Foundation (17-05007S).

Identifying Binding Sequences of Intact Protein Molecules on Gold Nanoparticles with Surface-Enhanced Raman Scattering

Gergo Peter Szekeres^{a,b} and Janina Kneipp^{a,b}

^a Humboldt-Universität zu Berlin, Department of Chemistry, Brook-Taylor-Str. 2, 12489, Berlin, Germany

^b School of Analytical Sciences Adlershof (SALSA), Albert-Einstein-Str. 5-9, 12489, Berlin, Germany
janina.kneipp@chemie.hu-berlin.de

In the biomedical application of nanocarriers, such as targeted therapy and diagnostics, the protein corona formed on the surface of nanostructures plays a determining role in the efficiency of the application. Furthermore, it can have short- and long-term health effects of the accumulated nanoparticles inside an organism [1]. Surface-enhanced Raman scattering (SERS) is an excellent tool for the investigation of the protein corona since it provides qualitative information of the molecular environment and the protein-nanoparticle interactions at the same time [2,3]. Over the last decades, many studies have provided methodologies for the SERS data acquisition of protein solutions with high average enhancement, which mostly rely on the chemical functionalization of nanoparticles (including their fixing on a flat surface) or optical tweezing [4-6].

Here, we present a refined sample preparation method for the SERS investigation of dilute protein solutions. This approach is based on the aggregation of protein-nanoparticle conjugates without additional chemicals or optical tweezing, and it requires accumulation times of only 1 s. Therefore, the acquired spectra do not include contributions of other molecules, and the tertiary structure of the protein molecules is not damaged by photodecomposition. The high enhancement of protein vibrational bands allows us to gain information of the composition of the protein corona and the protein-nanoparticle surface interactions. We show that experiments at protein concentrations lower than 150 pM still result in acquisition of high signal-to-noise spectra. As a second system, we present results obtained with a DNA solution, extracted from 3T3 fibroblast cells. These results also demonstrate that this sample preparation method is a very useful approach for the investigation of biomolecule solutions, *e.g.*, of enzymes, blood sera and cell lysates. Exploiting the selectivity of SERS, we can distinguish between two very similar proteins, bovine serum albumin and human serum albumin, and draw conclusions on nanoparticle binding sites in human serum albumin.

References

1. S. Zanganeh, R. Spitler, M. Erhanzadeh, A. M. Alkilany and M. Mahmoudi, *Int. J. Biochem. Cell Biol.*, 75 (2016) 143.
2. D. Drescher, P. Guttman, T. Büchner, S. Werner, G. Laube, A. Hornemann, B. Tarek, G. Schneider and J. Kneipp, *Nanoscale*, 5 (2013) 9193.
3. J. Kneipp, *ACS Nano*, 11 (2017) 1136.
4. V. P. Drachev, M. D. Thoreson, V. Nashine, E. N. Khaliullin, D. Ben-Amotz, V. J. Davisson and V. M. Shalaev, *J. Raman Spectrosc.*, 36 (2005) 648.
5. Y. Ozaki, B. Zhao, G. G. Huang and X. X. Han, *Anal. Chem.*, 81 (2009) 3329.
6. Y. Yuan, Y. Lin, B. Gu, N. Panwar, S. C. Tjin, J. Song, J. Qu and K. Yong, *Coord. Chem. Rev.*, 339 (2017) 138.

Acknowledgements: Funding by DFG GSC 1013 School of Analytical Sciences Adlershof (SALSA) and ERC grant 259432 to J.K. is gratefully acknowledged.

Investigating Interfacial Biomolecules using 100-kHz Repetition-Rate Broadband Vibrational Sum-Frequency Generation Spectroscopy

Freeda Yesudas^{a,b}, Mark Mero^c, Janina Kneipp^{a,b} and Zsuzsanna Heiner^{a,b}

^a School of Analytical Sciences Adlershof, Humboldt Universität zu Berlin, Albert-Einstein-Str.5-11, 12489 Berlin, Germany

^b Department of Chemistry, Humboldt Universität zu Berlin, Brook-Taylor-Str.2, 12489 Berlin, Germany

^c Max Born Institute for Nonlinear Optics and Short Pulse Spectroscopy, Max-Born-Str. 2a, 12489 Berlin, Germany

heinerzs@hu-berlin.de (Zsuzsanna Heiner)

Broadband vibrational sum-frequency generation spectroscopy (BB-VSFG) is a promising label-free, nonlinear spectroscopic technique which provides information about composition, orientation, interaction, and dynamics of the molecules at surfaces and interfaces. In order to study interfacial molecules, surface-specificity and sub-monolayer sensitivity is needed, both provided by BB-VSFG. The selectivity arises from the fact that the centro-symmetry is broken at interfaces, hence BB-VSFG spectroscopy allows us to study different interfaces including solid/solid, solid/liquid, and solid/gas boundaries. State-of-the-art BB-VSFG spectroscopy has reached monolayer sensitivity, but higher signal-to-noise (SNR) ratios are needed in a wide range of applications. Various routes to improving the SNR ratio are possible, such as employing higher laser intensities, repetition rates, and increasing the intensity and pointing stability of the laser beams at the sample. Recently, we developed the first high-repetition-rate BB-VSFG spectrometer [1], promising a boost in SNR ratio at reduced acquisition times [2]. However, the high repetition rate implies high average power at constant laser pulse energies, and possible laser induced thermal artifacts in the BB-VSFG spectra need to be explored. To demonstrate the capability and sensitivity of our BB-VSFG spectrometer, vibrational spectra of different phospholipids at a solid/air interface will be demonstrated at repetition rates up to 100 kHz with improved spectral resolution. In order to study possible thermal effects, CaF₂ as solid substrate was chosen, because it is transparent both in the mid-IR and visible wavelength range, and potential thermal effects can be expected only from the mid-IR laser pulses absorbed in the phospholipids. The laser induced orientational changes and disorder in the phospholipid layers were monitored by checking the stability of BB-VSFG spectral parameters such as the amplitude and width of vibrational bands. No heat induced spectral distortions were found, indicating that high repetition rate, high-resolution BB-VSFG spectrometers are promising for future investigations of interfacial biomolecular sub-/monolayers. The obtained results can bring new insight in laser-matter interaction in biomolecules with lasers operating at high repetition rates up to 100 kHz.

References

1. Z. Heiner, V. Petrov and M. Mero, *APL Photonics*, 2 (2017) 066102.
2. F. Yesudas, M. Mero, J. Kneipp and Z. Heiner, *J. Chem. Phys.*, 148 (2018) 104702.

Acknowledgements: Funding by the Deutsche Forschungsgemeinschaft (DFG GSC 1013 SALSA) to F.Y. and Z.H., by Leibniz- Gemeinschaft Grant No. SAW-2012-MBI-2 to M.M., and by ERC grant No. 259432 to J.K. are gratefully acknowledged.

**Analytical
New Methods
Instrumentation**

^{13}C O and C^{17}O Molecules as References for NMR Absolute Shielding Scales

Włodzimierz Makulski

*Laboratory of NMR Spectroscopy, Faculty of Chemistry, University of Warsaw, Pasteura 1,
02-093 Warszawa, Poland
wmakul@chem.uw.edu.pl*

Thanks to its simplicity - CO molecule - was chosen as the reference standard of absolute shielding scale in ^{13}C and ^{17}O NMR research [1]. The absolute shielding values in ^{13}C O and C^{17}O molecules were examined against helium-3 nuclear magnetic shielding in $^3\text{He}/^{13}\text{C}$ O and $^3\text{He}/\text{C}^{17}\text{O}$ in different buffer gases like Xe, SF_6 . The simple relationships between ^3He , ^{13}C and ^{17}O radio frequencies and nuclear magnetic moments lead to new absolute shielding constants in isolated carbon monoxide molecules: $\sigma_0(^{13}\text{C}\text{O}) = 0.80(90)$ and $\sigma_0(\text{C}^{17}\text{O}) = -59.20(10)$ ppm. The ^{13}C NMR reference value is in line with previously established theoretical and experimental results. Several ^{13}C shielding constants for benchmarking molecules were collected from gas phase extrapolation to the zero-pressure limit. On the other hand, the new ^{17}O NMR shielding value is in the excellent agreement with a new theoretical calculation performed in the relativistic approximation. This value differs substantially by ~ 2 ppm from result received recently on the basis of H_2^{17}O molecule limiting the precision of oxygen shielding scale [2]. The short discussion of new results was done in the light of available studies [3,4].

References

1. C. J. Jameson, in *Encyclopedia of NMR*, Eds. R. K. Harris & R. E. Wasylishen, Vol.1, 2012, 493.
2. W. Makulski, M. Wilczek and K. Jackowski, *Phys. Chem. Chem. Phys.*, (2018) sent to publish.
3. S. Komorovsky, M. Repisky, E. Malkin, K. Ruud and J. Gauss, *J. Chem. Phys.*, 112 (2015) 091102.
4. C. Puzzarini, G. Cazzoli, M. E. Harding, J. Vázquez and J. Gauss, *J. Chem. Phys.*, 112 (2015) 124308.

Acknowledgements: This work was financed by the National Science Centre (Poland) as the OPUS grant No 2015/19/B/ST4/03757.

Heat Induced Preparation of Silver Nanoparticles Coated Magnetic Composites for Sensitive Detection of Uric Acid

Melisew Tadele Alula^a and Peter Lemmens^b

^aBotswana International University of Science and Technology, Private bag 16, Palapye, Botswana

^bBraunschweig University of Technology, Institute for condensed matter physics, Mendelssohnsstr. 3, 38106 Braunschweig, Germany
alulam@biust.ac.bw

In this study, silver nanostructures decorated magnetic nanoparticles for surface-enhanced Raman scattering (SERS) measurements were prepared via heat induced catalytic activity of ZnO nanostructure. The ZnO/Fe₃O₄ composite was first prepared by dispersing pre-formed magnetic nanoparticles into alkaline zinc nitrate solutions. After annealing of the precipitates, the formed ZnO/Fe₃O₄ composites were successfully decorated with silver nanostructures by soaking the composites into silver nitrate/ethylene glycol solution at 95 °C in water bath. To find the optimal condition when preparing Ag@ZnO/Fe₃O₄ composites for SERS measurements, factors such as reaction time and concentration of silver nitrate were studied. Results indicated that the formation of AgNPs on ZnO/Fe₃O₄ was significantly improved with the assistance of ZnO. The concentration of silver nitrate and reaction time affected the morphologies of the formed composites and optimal condition in preparation of the composites for SERS measurement was found using 100 mM of silver nitrate with reaction time of 20 min. Under the optimized condition, the obtained SERS intensities were highly reproducible. Quantitative analyses showed that a linear range up to 15 µM of uric acid in aqueous solution could be obtained. Successful application of these prepared composites to determine uric acid in urine sample was obtained.

References

1. L. Yang, P. Li, H. Liu, X. Tang, J. Liu, *Chem. Soc. Rev.*, 44 (2015) 2837.
2. M. Tadele Alula, J. Yang, *Anal. Chim. Acta*, 812 (2014) 114.

Acknowledgements: The authors thank TWAS-DFG for sponsoring this study.

Development of Composite SEVS-Active Substrates with Low Detection Limit, Used for Trace Analysis

Zuzana Němečková^a and Marcela Dendisová^b

^a Department of Analytical Chemistry, Technická 5 Praha, University of Chemistry and Technology Prague, Czech Republic

^b Department of Physical Chemistry, Technická 5 Praha, University of Chemistry and Technology Prague, Czech Republic

nemeckoz@vscht.cz

Surface Enhanced Vibrational Spectroscopy (SEVS) are sensitive non-invasive detection methods. The most widely used techniques of SEVS are Surface-Enhanced Raman Scattering (SERS) and Surface-Enhanced Infrared Absorption (SEIRA). By contrast to classic methods Surface enhanced methods allows detection of trace amount of analyte due to the signal amplification on the interface metal (substrate)-analyte. The key element of measurement of trace amount of substances by SEVS techniques is suitable nanostructured surface, which allows adsorption of analyte molecules. This study is focused on preparation of large-scaled metal composite substrates with appropriate roughness of the surface. As convenient material for formation of metal layers are used platinum targets. Enhancing substrate is prepared by electrochemical coating from electrophoretic bath containing gold and zinc or titanium dioxide complex. Therefore, it is always utilized of chloride solution containing Au⁺ another metal. Development of optimal coating sequences of Au chloride bath, was part of work in recent years. Such substrate has good enhancement properties and it proved itself also as a base for sensor. The objective in case of composite substrates is reduction of detection limits and achieving of better results in SEIRA measurements, where is the usability of gold substrate limited. For characterization of surface morphology and chemical composition of surface the following methods have been applied: Scanning Electron Microscope (SEM) in combination with Energy-dispersive X-ray Spectroscopy (EDS). Enhancement potential of substrates was examined by adsorption of model analyte on the substrate surface and measurement of SERS and SEIRA spectra. 16-MHDA (16-mercaptohexadecanoic acid) was used as model analyte, which has good affinity to the surface, due to the thiol group.

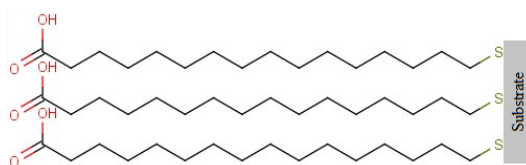


Figure 1 – 16-MHDA (16-mercaptohexadecanoic acid) adsorbed on enhancing substrate.

References

1. G. Broncová, P. Matějka, Z. Němečková, V. Vrkoslav and T. V. Shishkanova, T. V., *Electroanal.*, 1 (2017).

Acknowledgement: Financial support for specific university research (MSMT No 20-SVV/2018) is gratefully acknowledged.

Phenylboronic Acid Based Carbon Dots for Glucose Sensing

Eliana F. C. Simões^a, João M. M. Leitão^a and Joaquim C. G. Esteves da Silva^b

^a Chemistry Research Unit (CIQUP), Faculdade de Farmácia da Universidade de Coimbra,
3000-548 Coimbra, Portugal

^b Chemistry Research Unit (CIQUP), Faculty of Sciences of University of Porto, R. Campo Alegre 697,
4169-007 Porto, Portugal
jcsilva@fc.up.pt

Glucose is the major energy source in cellular metabolism and has a vital role in the natural growth of cells. Its quantification is of high importance in controlling several biochemical processes, and in the diagnoses of several metabolic disorders, like diabetes. The nanoparticles, as the carbon dots, became one of the most object of research for the glucose fluorescence sensing. Carbon Dots (CDs) are carbon based nanoparticles with interesting optical and analytical properties with a great potential for the glucose fluorescence sensing [1]. Generally the fluorescence sensing of glucose by CDs, as for other nanoparticles, it's done directly after the doping or functionalization of the CDs or indirectly through the hydrogen peroxide detection by the CDs. The boronic acids due to their linked array of hydroxyl groups are ideal for binding the glucose and for its recognition. So, diol modified CDs probes with boronic acids could be synthesized for the fluorescence sensing of glucose [2]. Some boronic acids functionalized CDs have already been used for the direct fluorescence sensing of glucose [3-6]. Phenylboronic acid functionalized CDs were synthesized by a hydrothermal method [3] and aminophenylboronic acid functionalized CDs were obtained by a microwave synthesis method [4]. The CDs fluorescence quenching was observed for both functionalized CDs by addition of glucose. Also an analytical methodology was developed for the fluorescence sensing of glucose based on the CDs fluorescence quenching by the 4-cyanophenylboronic acid and posterior fluorescence recovery by the addition of glucose [5]. Finally, a glucose sensor was developed by the hydrothermal synthesis of CDs from collagen, through the covalent attaching of the 3-aminophenylboronic to CDs [6].

In this communication, are presented the results found in the fluorescence glucose sensing by microwave synthesized CDs functionalized with selected boronic acids. The evaluated boronic acids were the phenylboronic acid, 3 and 4-hydroxyphenylboronic acid (3-HPBA, 4-HPBA) and 3 and 4-aminophenylboronic acid (3-APBA). Different response fluorescent profiles were observed for the CDs prepared from the different phenylboronic acid precursors in the presence of glucose.

References

1. J. Zhou, *et al.*, *Microchim. Acta*, 184 (2017) 343.
2. S. K. Basiruddin and S. K. Swain, *Mater. Sci. Eng.: C*, 58 (2016) 103.
3. P. Shen and Y. Xia, *Anal. Chem.*, 86 (2014) 5323.
4. S. Kiran and R. D. Misra, *J. Biomed. Mater. Res. A*, 103 (2015) 2888.
5. A. S. Krishna, *et al.*, *Mater. Res. Express*, 3 (2016) 055001.
6. J. Guohua, *et al.*, *Mater. Res. Express*, 1 (2014) 025708.

Acknowledgements: The authors thank to project PTDC/QEQ-QAN/5955/ 2014 cofunded by FCT/MEC (PIDDAC) and by FEDER through “COMPETE– Programa Operacional Fatores de Competitividade” (COMPETE-POFC).

Acid-Base and Calcium Complexing Properties of Lactate in Neutral to Alkaline Medium

Csilla Dudás^{a,c}, Bence Kutus^{a,c}, Éva Böszörményi^{a,c}, István Pálinkó^{b,c}, Pál Sipos^{a,c}

^a Department of Inorganic and Analytical Chemistry, University of Szeged, Dóm tér 7, H-6720 Szeged, Hungary

^b Department of Organic Chemistry, University of Szeged, Dóm tér 7, H-6720 Szeged, Hungary

^c Material and Solution Structure Research Group, University of Szeged

sipos@chem.u-szeged.hu (Pál Sipos)

It has been shown previously that in highly alkaline medium calcium ions are able to form stable complexes with polyhydroxy carboxylate type ligands such as D-gluconate [1] (Gluc^-), α -D-isosaccharinate [2] (Isa^-), D-heptagluconate [3] (Hpgl^-), etc. Lactate ion (2-hydroxypropanoate, Lac^-) is a small molecular mass hydroxy carboxylate containing structural elements similar to those found in the ligands mentioned above (Figure 1). In neutral medium Lac^- was previously shown to form CaLac^+ and CaLac_2^0 complexes at $I = 0.5 \text{ M}$ (NaCl), with formation constants of $\log K_{1,1} = 0.92$ and $\log \beta_{1,2} = 1.62$, respectively [4].

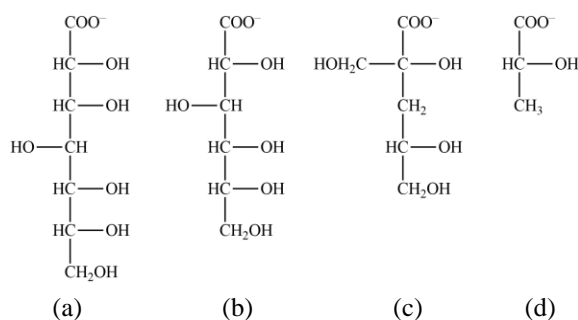


Figure 1 – Structure of Hpgl^- (a), Gluc^- (b), Isa^- (c) and Lac^- (d)

In the present study the complex formation between calcium and Lac^- was studied at $I = 4 \text{ M}$ (NaCl) in neutral medium by Ca-ISE potentiometry, solubility and ^{13}C NMR spectroscopy. The formation constants of the CaLac^+ and CaLac_2^0 complexes were found to be $\log K_{1,1} = 0.89 \pm 0.02$ and $\log \beta_{1,2} = 1.34 \pm 0.02$, respectively. The structure of the complexes was calculated with the aid of molecular modelling calculations. The alkaline deprotonation constant of Lac^- was found to be $\text{p}K = 15.6 \pm 0.2$ from ^{13}C NMR spectroscopy. This value is considerably higher than those found for Hpgl^- , Gluc^- and Isa^- ($\text{p}K = 13.4\text{--}14.5$). From solubility measurements, in strongly alkaline solutions the formation of the CaLacH_{-1}^0 complex was inferred.

References

1. A. Pallagi, É. G. Bajnóczi, S. E. Canton, T. Bolin, G. Peintler, B. Kutus, Z. Kele, I. Pálinkó and P. Sipos, *Environ. Sci. Technol.*, 48 (2014) 6604.
2. C. Dudás, B. Kutus, É. Böszörményi, G. Peintler, Z. Kele, I. Pálinkó and P. Sipos, *Dalton Trans.*, 46 (2017) 13888.
3. A. Pallagi, Z. Csendes, B. Kutus, E. Czeglédi, G. Peintler, P. Forgó, I. Pálinkó and P. Sipos, *Dalton Trans.*, 42 (2013) 8460.
4. M. Masone and M. Vicedomini, *Ann. Chim. (Rome)*, 71 (1981) 517.

Acknowledgements: The authors thank the financial support of NKFIH (grant No. K 124 265) and the UNKP-17-2 New National Excellence Program of the Ministry of Human Capacities.

Lipid/Protein Ratio Contents of Soybean Mutants: A Raman Spectroscopic and Chemometrics Investigation

Gulce Ogruc Ildiz^{a,d}, Ozge Celik^b, Cimen Atak^b, Ayberk Yilmaz^c, Hayr nnisa Nur Kabuk^a, Ersin Kaygisiz^c, Alp Ayan^b, Sinan Meri ^b and Rui Fausto^d

^aDepartment of Physics, Science and Letters Faculty, Istanbul Kultur University, Atakoy Campus, Bakirkoy 34156, Istanbul, Turkey; ^bDepartment of Molecular Biology and Genetics, Science and Letters Faculty, Istanbul Kultur University, Atakoy Campus, Bakirkoy 34156, Istanbul, Turkey; ^c Department of Physics, Faculty of Sciences, Istanbul University, Vezneciler-Fatih, 34134 Istanbul, Turkey; ^dCQC, Department of Chemistry, University of Coimbra, P-3004-535 Coimbra, Portugal
g.ogruc@iku.edu.tr

The relative lipid/protein contents of Ataem-7 variety and S04-05 breeding line salt-tolerant soybean seeds belonging to fourth generation mutants, together with the corresponding controls, were investigated by means of Raman spectroscopy and compared with the data obtained by the GC-FID detection method [1]. Both techniques showed that γ -irradiation caused a noticeable increase in the lipid to protein ratio of the studied Ataem-7 variety mutant, while it caused a decrease of this ratio in the investigated S04-05 breeding line mutants. The Raman data also indicated and increase in the characteristic bands of phenylalanine of S-mutants, compared to the control, which indicates an increase in the relative amount of this nutritionally relevant amino acid contents in the genetically modified plants' seeds. Dendrograms for both studied soybean species, obtained by Ward's cluster analysis, showed a clear discrimination between mutants and controls. The grouping scheme is also in good general agreement with the compositional information extracted from the analysis of the lipid/protein contents of the different samples. Similar results were obtained through principal component analysis, with the obtained PCA scores associated with the major principal component axes allowing a good discrimination between mutants and controls, and grouping the different mutants in a way that is in consonance with the results obtained from the cluster analysis and also with the compositional information extracted from the Raman data and GC-FID measurements.

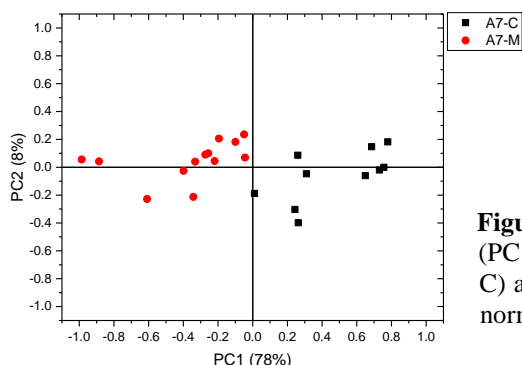


Figure 1 – PCA scores plot of the first two principal components (PC1 vs. PC2) obtained from PCA of Raman spectra of control (A7-C) and mutant (A7-M) A Ataem-7 soybean seeds (left). Axes were normalized to unity.

References

1.  . Atak,  .  elik, A. Ayan, S. Meri  and M. Erdo mu , “Development of Salinity and Drought Tolerant Soybean Plants by Mutation Breeding” (Unpublished Data).

Acknowledgements: This study has been funded by the Scientific and Technological Research Council of Turkey-TUBITAK 1001 (Project No.: 116Z294). The CQC is supported by FCT, through the project UI0313/QUI/2013, also co-funded by FEDER/COMPETE 2020-EU. Acknowledgement is also due to the Portugal 2020 Grant MATIS #06.

Identification of Forced Degradation Products of Tofacitinib Citrate by HPLC-DAD and MALDI-TOF/MS Techniques

Hülya Yilmaz Ortak^a, Hale Seçilmiş Canbay^b, Güleren Alsancak^a, Ebru Çubuk Demiralay^a

^aDepartment of Analytical Chemistry, Suleyman Demirel University, Isparta, 32260 Turkey

^bDepartment of Bioengineering, Mehmet Akif Ersoy University, Burdur, Turkey
hulya.yilmaz0006@gmail.com

Tofacitinib citrate (3-((3R,4R)-4-methyl-3-[methyl-(7H-pyrrolo[2,3-d] pyrimidin-4-yl)-amino]-piperidin-1-yl)-3-oxopropionitrile citrate, TOFT) is a novel oral Janus Kinase (JAK) inhibitor developed by Pfizer for the treatment of rheumatoid arthritis (RA) [1]. It blocks by targeting the Janus kinase/signal transducer and activator of transcription (JAK/STAT) interferon-dependent signaling pathway and inhibits the production of inflammatory mediators in joint tissue [2-4].

In this study, it was aimed to develop a HPLC method to identify the degradation products of tofacitinib formed under ICH recommended stress conditions of hydrolysis, photolysis, oxidation, temperature with the aid of LC-DAD and MALDI-TOF MS techniques TOFT was exposed to acidic (0.1 M HCl), alkaline (0.1 M NaOH), hydrolytic and oxidative conditions (3% (v/v) H₂O₂) at room temperature. In addition, photolytic and thermal stability of the drug was evaluated by exposing to 254 nm UV light, and the temperatures at 30°C, 40°C, and 50°C. A high-performance liquid chromatography system equipped with a diode array detection (HPLC-DAD) was used for separation and identification of degradation products. The separation was achieved on a Kinetex EVO C18 column (150 mm × 4.6 mm, 5 µm) by isocratic condition of mobile phase comprising acetonitrile-water binary mixture (30:70, % v/v) at pH 6 at a flow rate of 1 mL/minute at 25 °C temperature. Moreover, a complete mass fragmentation pathway of the drug was established with the help of Matriks assisted laser desorption ionization time of flight mass spectrometry (MALDI-TOF MS) in the mass range of 100-2000 m/z.

In conclusion, the results of the study provide clues about the degradation pathways and products of the drug in the tissue.

References

1. J. S. Smolen, D. Aletaha, J.W. J. Bijlsma *et al.*, *Ann. Rheum. Dis.* 69 (2010) 631.
2. K. Ghoreschi, M. I. Jesson, X. Li, J. L. Lee, S. Ghosh *et al.*, *J. Immunol.* 186 (2011) 4234.
3. J. M. Kremer, S. Cohen, B. E. Wilkinson, C. A. Connell *et al.*, *Arthritis Rheum.* 64 (2012) 970.
4. D. M. Meyer, M. I. Jesson, X. Li, M. M. Elrick, C. L. Funckes-Shippy *et al.*, *J. Inflamm.* 7 (2010) 41.

Acknowledgement: The Project was supported by SDU-BAP (4580-D2-16).

Spectroscopic Methods in the Study of Bio-Inhibitor Influence on the Corrosion Process of the Iron

Dominika Świąch^a, Czesława Paluszkiewicz^b, Natalia Piergies^b, Ewa Pięta^b and Wojciech M. Kwiatek^b

^a Faculty of Foundry Engineering, AGH University of Science and Technology, 30-059 Krakow, Poland

^b Institute of Nuclear Physics, Polish Academy of Science, 31-342 Krakow, Poland

dswiech@agh.edu.pl

Complementary spectroscopic methods such as Raman spectroscopy (RS) and Fourier transform infrared absorption spectroscopy (FTIR) has been used to study the mechanism of corrosion inhibition of iron by bio-inhibitor (amino acid – Thr). These methods enabled detailed analysis of the molecular structure of Thr adsorbed on the iron corroded surfaces. Compounds that contain functional groups such as the carbonyl group, the hydroxyl group are effective metal corrosion inhibitors in many corrosive environments, e.g. in chloride solution [1,2]. The effectiveness of the discussed inhibition strongly depends on the adsorption process on the metallic surface [1,3].

Despite the range of corrosion investigation, there is very little known about structural changes of inhibitors immobilized onto metal surface. The RS and FTIR data indicated that distribution of bio-inhibitor adsorbed on the iron surface is homogeneous. Figure 1 presents representative RS spectra for the investigated samples.

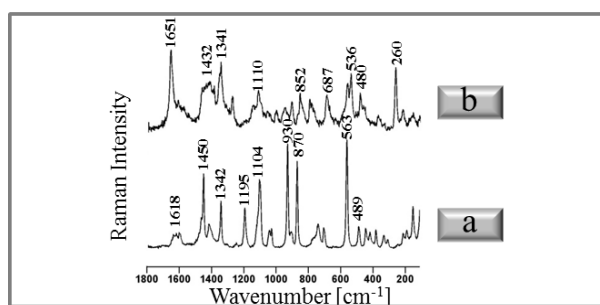


Figure 1 – RS spectra of a -Thr (solid state) and b- mixture of Thr (0.25M) and NaCl (1M) adsorbed onto the iron surface.

Significant changes in the adsorption geometry of the Thr molecules adsorbed onto iron surface are observed what is indicated by bands at 1651 cm⁻¹, 1432 cm⁻¹, 1110 cm⁻¹, 852 cm⁻¹, 536 cm⁻¹. The results indicate that spectroscopic methods such as RS and FTIR are excellent tools for study and analysis of the mechanism of corrosion inhibition.

References

1. D. Kesavan, M. Gopiraman and N. Sulochana, *Chem. Sci. Rev. Lett.*, 1 (2012) 1.
2. D. Q. Zhang, Q. R. Cai, L. X. Gao and K. Y. Lee, *Corros. Sci.*, 50 (2008) 3615.
3. E. E. Oguzie, Y. Li and F. H. Wang, *J. Colloid. Interface Sci.*, 310 (2007) 90.

Acknowledgements: The research was carried out using equipment purchased in the frame of the project co-funded by the Małopolska Regional Operational Program Measure 5.1. Krakow Metropolitan Area as an important hub of the European Research Area for 2007-2013, project No. MRPO.05.01.00-12-013/15.

Impact of the Evaporation Rate of Water on Siloxane Structures

Vesna Volovšek, Iva Movre Šapić, Zrinka Buhin Šturlić and Krešimir Furić
Faculty of Chemical Engineering and Technology, University of Zagreb, Marulićev trg 19,
10000 Zagreb, Croatia
volovsek@fkit.hr

As a part of our study of polymerization process of aminopropylsilanetriol (APST) we investigated the behavior of APST in water solution (original concentration 25%) and after the pumping under low pressure (at nearly 5 mbar) by Raman spectroscopy. It has been already noticed that the polymerized structure of APST depends significantly on the temperature at which the condensation takes place. At the same time the rate of evaporation of water could also play important role in forming different polymer structures. In order to resolve between these two effects, the glass tubes with solution were pumped on the vacuum line exposing samples to the low pressure of ~ 5 mbar for one to three hours. The samples with different starting concentrations of water were then left to polymerize under atmospheric conditions. Raman spectra of solutions and of condensed samples were recorded. The spectra of solutions show the change in distribution of water clusters present in different solutions [1]. Concentration of higher H_2O agglomerates (tetramers, pentamers, hexamers) is increasing with decreased water content. The same circumstances favor formation of *gauche* conformation of propyl chain in APST molecules [2].

We have also examined mechanism of the solidification by precise weighting of the original solution (25%), which was left to evaporate at different temperatures in the grey-light for 66 days. The experimental points can be nicely fitted to the two exponential functions. One of them describes the evaporation of water, while the other describes the creation of water molecules during the process of hydrolysis and consequently the formation of siloxane bridges. DSC measurements were also performed in order to characterize the state of water in the samples.

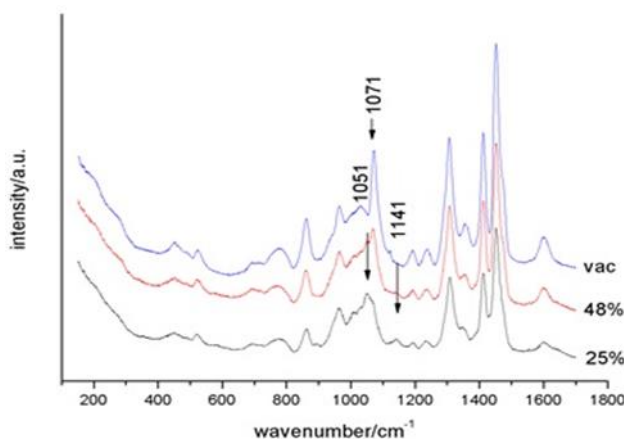


Figure 1 – Raman spectra of APST samples.

References

1. M. Starzak and M. Mathlouthi, *Food Chemistry*, 82 (2003) 3.
2. V. Volovšek, V. Dananić, L. Bistričić, I. Movre Šapić and K. Furić, *Spectrochim. Acta*, 117 (2014) 478.

Dragline Silk of *Araneus Quadratus*: Effect of Altitude on the Silk Structure

Sevgi Haman Bayarı^a, Tuncay Türkeş^b, Damla Kararslan^a and Semra İde^a

^aHacettepe University, Department of Physics Engineering, 06800 Ankara, Turkey.

^bÖmer Halisdemir University, Department of Biology, 51240 Niğde, Turkey.

bayari@hacettepe.edu.tr

In this study, we combined Small Angle X-ray Scattering (SAXS) and Attenuated Total Reflection Infrared Spectroscopy (ATR-FTIR) techniques to investigate nano and molecular structure of the dragline silk from the spider species *Araneus quadratus* which is known as Four-spot Orb-weaver, belongs to the genus *Araneus*, in the family *Araneidae*. The specimens were collected from the Eastern Blacksea Region (Rize-Çamlıhemsin, 1837 m and 2100 m above sea level) and the Çorum-Samsun speedway, Kavak, 621 m above sea level) in Turkey, in July and August 2017. Dragline silk produced by the spider under controlled conditions in laborator were investigated. Spider major ampullate (dragline) silk is an extracellular fibrous protein with unique characteristics of strength and elasticity. Analysis of the Amide I region ($1700\text{--}1600\text{ cm}^{-1}$) of the infrared spectra revealed that silk protein contains a high amount of beta-sheets. The relative content of amino acids such as polyalanine (PAla) and polyalanine glycine (PGly) present in draglines were determined using the $1100\text{--}900\text{ cm}^{-1}$ infrared spectral region. Even though the molecular contents are not very different, the nano structural changes are noteworthy as seen in Figure 1.

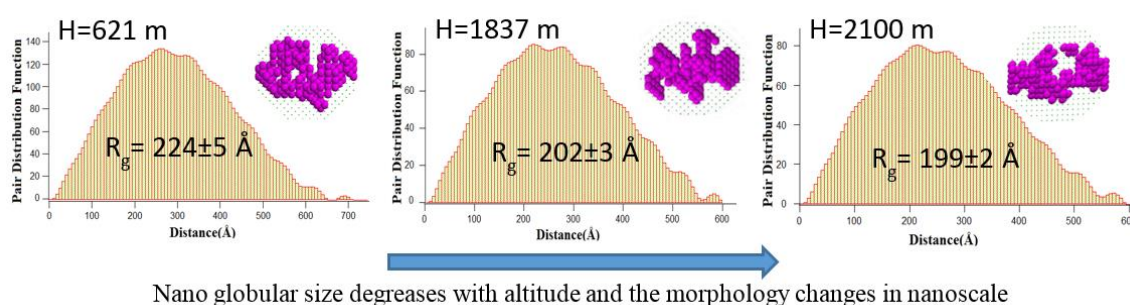


Figure 1 – The structural information [size (R_g), shape1 and distance distributions (histograms) of the nanoglobules] obtained by SAXS analyses. H: Altitude.

References

1. D. I. Svergun, *Biophys. J.*, 76 (1999) 2879.

Acknowledgements: This study is currently being supported by the Scientific and Technological Research Council of Turkey (TUBITAK) under the project number KBAG 214Z049.

Investigations of FTIR Spectra for Analysis of Irradiated Sheep Wool

Liga Avotina^a, Vanda Voikiva^a, Valentina Kinerte^a, Karlis Shvirksts^b,
Mara Grube^b and Gunta Kizane^a

^a University of Latvia, Institute of Chemical Physics, Jelgavas str.1, Riga LV-1004, Latvia

^b University of Latvia, Institute of Microbiology and Biotechnology, Jelgavas str.1, Riga LV-1004, Latvia
Liga.avotina@lu.lv

Modification of natural fibres, such as sheep wool, is a perspective way for increasing their variety of applications, such as metal ion absorption from the wastewaters [1], removing metal ions from industrial solutions and/or recover metal ions [2]. As well as sheep wool is an excellent material with good characteristics for thermal insulation, moisture management and sound absorption [3]. To estimate the initial chemical composition and understand the changes caused by electron irradiation of the sheep wool, infrared spectra of wool samples were recorded and analysed.

The analysis was performed by using a Fourier transform infrared (FTIR) spectrometer Vertex 70v (Bruker Optics, Germany) with attenuated total reflection module and a special holder for wool sample analysis. FTIR spectra were recorded in vacuum 2.95 hPa, in the frequency range 4000-400 cm⁻¹, with the spectral resolution of 2 cm⁻¹ and 20 scans, 3 parallel measurements for each wool sample. Modification of wool was performed by irradiating the wool with accelerated electrons (ELU-4, maximal electron energy 5 MeV, absorbed dose up to 100 kGy).

Analysis of FTIR spectra showed, that spectra of the non-irradiated sheep wool contain the signals at 720 and 1390 cm⁻¹. These signals could correspond to the rocking of CH₂ and bending of CH₃ functional groups respectively [4]. A signal at 875 cm⁻¹ could be attributed to the epoxide groups, 1075 cm⁻¹ to the C-O bonds. Group of signals at 1240-1650 cm⁻¹ are due to amide groups [5,6] and 1740 cm⁻¹ shows presence of aliphatic esters [4].

Signals corresponding to the valence vibrations of hydrocarbon groups [7] occur at 2850 and 2920 cm⁻¹. Deformations of OH groups [8] are in the range of 3100-3500 cm⁻¹.

The obtained results show some changes caused by irradiation, main occurring in amide I-II region with decrease of amide I at 1625 and increase of amide II at 1565 cm⁻¹. FTIR spectra can be used for the quality analysis of the sheep wool.

References

1. Z. Hanzlikova, J. Branisa, K. Jomová, M. Fulop, P. Hyber and M. Porubská, *Sep. Purif. Technol.*, 193 (2018) 345.
2. G. Wen, R. Naik, P.G. Cookson, S. V. Smith, X. Liu and X. G. Wang, *Adv. Powder Technol.*, 197 (2010) 235.
3. R. del Rey, *et al.*, *Materials*, 10 (2017) 1277, 1.
4. Z. Hanzlikova, P. Hybler, M. Fulop, J. Ondruska, K. Jomonova, M. Porubská and M. Valko, *Radiat. Phys. Chem.*, 113 (2015) 41.
5. J. Broda, S. Przybylo, K. Kobiela-Mendrek, D. Binias, M. Rom, J. Grzybowska-Pietras and R. Laszczak, *Int. Biodeterior. Biodegradation*, 115 (2016) 31.
6. E. Wojciechowska, M. Rom, A. Wlochowicz, M. Wysocki and A. Weselucha-Birczynska, *J. Mol. Struct.*, 704 (2004) 315.
7. M. Porubská, Z. Hanzlikova, J. Branisa, A. Kleinova, P. Hybler, M. Fulop, J. Ondruska and K. Jomova, *Polym. Degr. Stab.*, 111 (2015) 151.
8. A. Salama and M. El-Sakhawy, *Int. J. Biol. Macromol.*, 92 (2016) 920.

Acknowledgements: The authors thank to University of Latvia financed project No. Y9-B044-ZF-N-300, “Nano, Quantum Technologies, and Innovative Materials for Economics”.

Identification of Microplastics within Beach Sediment Samples Based on a Robust Chemometric Approach for Infrared Spectroscopy Library Searching

Gerrit Renner, Torsten C. Schmidt and Jürgen Schram

*Environmental and Instrumental Analytics, Niederrhein University of Applied Sciences, Frankenring 20,
D-47798 Krefeld, Germany
schram@hsnr.de*

Even after almost 15 years of research on microplastics within environmental samples, it is still a challenge to evaluate measured infrared (IR) spectra in order to identify microplastics [1]. In this context, one main problem is the huge differences of real environmental microplastics, which degrade highly variable and can be contaminated with diverse (in)organic and/or biological matter, *e.g.* sand, wood or algae. Therefore, a suitable identification algorithm has to be very robust, and to handle the huge sample throughput, the procedure has to be fully automated and fast. The main concept of the presented chemometric approach is based on focussing on relevant vibrational bands for the respected microplastics [2] instead of using complete IR spectra, which is the most common practise. To follow this concept, a fully automated detection routine for vibrational bands was developed. In a next step, each vibrational band was fitted by applying a theoretical Voigt function, and each area was then calculated using the fit parameters. These area values combined with their corresponding positions within the IR spectrum were used to create highly characteristic and robust fingerprints by calculating all permutable unique area ratios. In a last step, these fingerprints were compared to already stored fingerprints from a homemade microplastics IR spectra library, which contains the most common polymers and matrix components for the presented analytical task. The whole algorithm is based on Python and will be available for free as a standalone application. To examine the developed identification tool, diverse beach sediments including positive (polypropylene and polyvinyl chloride microplastics) and negative control samples were investigated. All samples were filled in 500 ml vessels, and microplastics as well as other microparticles were separated by manipulating floating conditions using a stirrer and an impinger. The vessels were continuously overfilled, and the floating particles were transferred onto a stainless steel sieve with a mesh size of 28 μm , while the filtrate was pumped back into the main vessels. The particle residues on the metal sieve were analysed with Shimadzu IRTracer-100 spectrometer combined with Shimadzu AIM-9000 IR microscope. In addition, microparticles were mixed with potassium bromide for integral KBr pellet measurements using Shimadzu IRTracer-100 only. All spectra were evaluated using the new developed identification tool in parallel to manual spectra inspection.

In summary, the new chemometric approach seems to be very suitable for microplastics identification within beach sediments as it is much more robust than conventional library searching in this concern and it is much faster and more objective than manual spectra inspection.

References

1. T. Rocha-Santos and A. C. Duarte, *Trends Anal. Chem.*, 65 (2015) 47.
2. G. Renner, T. C. Schmidt and J. Schram, *Anal. Chem. (Washington, DC, U. S.)*, 89.22 (2017) 12045.

Acknowledgements: We thank Shimadzu Europe GmbH for their support and technical advice.

Comparison of the Oxidative Desulphurization of Petroleum Product and Waste Tires Pyrolysis Oil by Spectral Methods

Vesislava Toteva, Daniela Angelova and Anton Georgiev

University of Chemical Technology and Metallurgy, 1756, 8 "Kl. Ohridsky" boul, Sofia, Bulgaria.

vesislava@uctm.edu

The oxidative desulphurization (ODS) is developed as an alternative/addition to the present day hydrodesulphurization (HDS) processes. The oxidation of sulfur compounds in petroleum fuels to sulfones with hydrogen peroxide allows for production of diesel fuels with sulfur content of 10 ppm or lower at atmospheric pressure and room temperature [1].

The comparison of oxidative desulphurization (ODS) of petroleum diesel fuels and of pyrolysis fractions obtained from waste tires is the aim of this study.

Elemental analysis, FT-IR, NMR and GC-MS advanced analytical techniques are used for identification and quantification possible compounds in the fuels and pyrolytic fluids obtained from different types of organic waste [2]. In this study spectral methods for observing of desulphurized fuels are used: FTIR analysis allows estimating degree of the oxidation of sulphur compounds and sulphur reduction; monitoring of the sulfur components was accomplished by GC-FID, and the degree of dearomatization was assessed using NMR spectroscopy.

The results show that oxidative desulphurization with hydrogen peroxide and formic acid results in a higher degree of desulfurization for petroleum diesel (70%), while pyrolysis diesel fractions have a potential for sulfur decrease of 40% and a reduction of its specific acute smell. Spectral studies have shown that oxidative desulphurization of pyrolysis fractions from waste tires processing is effective in removing the highly refractive by hydrodesulphurization dimethyldibenzothiophene derivatives.

References

1. Z. Ismagilov, S. Yashnik, M. Kerzhentsev, V. Parmon, A. Bourane, F. M. Al-Shahrani, A. A. Hajji and O. R. Koseoglu, *Catal. Rev. Sci. Eng.*, 53 (2011) 199.
2. M. R. Islam, H. Haniu and M. R. A. Beg, *Fuel*, 87 (2008) 3112.

Acknowledgements: This study has been financially supported by the Operational Programme "Science and education for smart growth" 2014-2020 of the European Union cofounded by the European Social Fund through the project BG05M2OP001-2.009-0015 "Support for the development of capacity of doctoral students and young researchers in the field of engineering, natural and mathematical sciences".

Identification of Components of the Ceramics and Color Layers Used in Ceramic Artworks by Non-Invasive and Non-Destructive Methods

Radka Šefců^a, Martina Kmoníčková^a, Hana Bilavčíková^a and Alexandra Kloužková^b

^a National Gallery in Prague, Staroměstské nám. 12, 110 15 Prague, Czech Republic,

^b University of Chemistry and Technology, Technická 5, 166 28 Prague, Czech Republic
radka.sefcu@ngprague.cz

This paper presents an investigation of ceramic sculptures and glazed reliefs from the collection of the National Gallery in Prague. A multi-analytical approach was used to study the glaze and color layers. To achieve appropriate results, when investigating materials of the artworks, the use of the non-invasive or non-destructive technique is often necessary. Ceramic glazes are complex mixtures of silica, fluxes and metallic oxides, prepared at high temperature. The elemental composition of the glaze and color layers depends on raw materials and specific workshop practice and recipes. The precise determination of all components, minor and trace elements and their structure can be important to differentiate and possibly to establish the provenance of the artefact and the origin of the pigment. The time evolution of the use of materials and techniques can also be observed.

The chemical characterisation of the pigments and the structure was performed combining complementary techniques. The initial investigation of materials was realized in-situ by means of portable X-ray fluorescence analyzer and mobile Raman spectroscopy. The samples have been taken subsequently and analyzed using optical microscopy, scanning electron microscopy coupled with energy dispersive x-ray spectroscopy and micro-Raman spectroscopy. The use of Raman spectroscopy was crucial for the analysis of some pigments in the non-destructive way. The measurements were performed on the individual pigment grains or on the cross-sections using the mapping mode for better observation of individual components present in colour glazed layers and polychromy.

The use of the combination of Raman spectroscopy and mobile X-ray fluorescence analysis was crucial to identify blue, white and yellow pigments. Thanks to the analytical methodology carried out, it was possible to determine the presence of pigments in different layers of the cross-sections. The evaluation of the results of Raman technique compared to those obtained by optical microscopy and SEM-EDS highlights that Raman spectroscopy shows a great potential in the analysis of ceramics and glazed materials. The results obtained from application of complementary analytical techniques allowed qualitative evaluation of the applied ceramic and glazes materials and significantly broadened the knowledge of the production processes and of the historical methods used.

References

1. P. Ferrer, S. Ruiz-Moreno, A. López-Gil, M.C. Chillón and C. Sandalinas, *J. Raman Spectrosc.*, 43 (2012) 1805.
2. A. Zucchiatti, A. Bouquillon, I. Katona and A. D'Alessandro, *Archaeometry*, 48 (2006) 131.
3. G. Pappalardo, E. Costa, C. Marchetta, L. Pappalardo, F. P. Romano, A. Zucchiatti, P. Prati, P. A. Mandò, A. Migliori, L. Palombo, M. G. Vaccari, *et al.*, *J. Cult. Her.* 5 (2004) 183.

Acknowledgements: This work has been financially supported by the project of the Ministry of Culture Czech Republic: Technology of Treatment and Identification of Degradation Processes of Ceramic Finds from Hradčany Palaces - Methods of Restoration and Conservation of Porous and Dense Ceramics and Porcelain (DG18P02OVV028).

Josefa de Óbidos Workshop: From Panel to Canvas. Materials and Technical Evolution of the Most Significant Portuguese Painting Workshop of the 17th Century

Vanessa Antunes^{a,b}, Sara Valadas^c, Vitor Serrão^a, Maria L. Carvalho^b, António Candeias^c, José Mirão^c, Ana Cardoso^c, Alexandra Lauw^d, Sofia Pessanha^b and Marta Manso^{b,e}

^a ARTIS-Instituto História da Arte, Faculdade de Letras, Universidade de Lisboa (ARTIS-FLUL),
Alameda da Universidade, 1600-214 Lisboa, Portugal

^b LIBPhys-UNL, Laboratório de Instrumentação, Engenharia Biomédica e Física da Radiação, Departamento de Física, Faculdade de Ciências e Tecnologia, Universidade Nova de Lisboa, 2829-516, Caparica, Portugal

^c Laboratório HERCULES, Escola de Ciências e Tecnologia, Universidade de Évora,
Largo Marquês de Marialva 8, 7000-676 Évora, Portugal

^d Centro de Estudos Florestais, Instituto Superior de Agronomia, Universidade de Lisboa,
Tapada da Ajuda, 1349-017 Lisboa, Portugal

^e Faculdade de Belas-Artes, Universidade de Lisboa, Largo da Academia Nacional de Belas-Artes,
1249-058 Lisboa, Portugal
luisa.carvalho@fct.unl.pt

Josefa de Óbidos (1630-1684) and her father Baltazar Gomes Figueira (1604-1674) were the most important pair of painters of the 17th century in Portugal. The materiality and painting techniques used in these painters' workshop is practically unknown. This work intends to study a group of paintings assigned to both painters and their workshop in order to define the materials used and the particular techniques employed, from ground to priming and painting layers. The scope of the paintings under study covers since the earliest paintings, made in panel support, to the paintings in canvas support, of the middle and final period of Óbidos workshop practices. The range of the analytical procedures employed to characterize the materials and painting techniques involve molecular spectroscopy with μ -Confocal Raman (μ -Raman) and Fourier Transform Infrared Spectrometry (μ -FTIR) in combination with other complementary methods such as X-ray Fluorescence Spectrometry (XRF), μ -X-ray diffraction (μ -XRD) Scanning Electron Microscopy with Energy Dispersive spectroscopy (SEM-EDS) and dendrochronology. The results are compared with the instructions of the most significant coeval technical painting treatises: the 1615 "Arte da Pintura" [1], of the Portuguese Filipe Nunes, and the namesake treatise "Arte de la pintura" [2], finished in 1641 by the Spanish painter Francisco Pacheco that influenced directly Óbidos workshop. The conclusions of this study bring the first insight on the materials used, technical procedures and evolution from panel to canvas of Óbidos painting workshop, particularly highlighting the work of Josefa de Óbidos, the greatest female Portuguese painter of all times.

References

1. P. Nunes, *Arte da Pintura, Symmetria e Perspectiva, fac-simile da edição de 1615 com um estudo introdutório de Leontina Ventura*, L. Ventura, Editor. 1982, Editorial Paisagem: Porto.
2. F. Pacheco, *Arte de la pintura*, B. Bassegoda i Hugas, Editor. 2009, Cátedra: Madrid.

Acknowledgements: The authors thank to the research center grant no. UID/FIS/04559/2013 to LIBPhys-UNL, from the FCT/MCTES/PIDDAC and research center grant no. UID/Multi/04449/2013 to Hercules Laboratory. The authors also acknowledge Fundação para a Ciência e Tecnologia for financial support, Post-doc grant SFRH/BPD/103315/2014 through program QREN-POPH-typology 4.1., co-participated by the Social European Fund (FSE) and MCTES National Fund; Also wish to acknowledge to Bombarral city council, to Father Sérgio Bruno at Columbeira chapel, Bombarral, to Father Ricardo Franco at Santo António church, Lourinhã, to Holy House of Mercy of Lourinhã and to Évora Museum for allowing this study.

Quantification of Active Ingredients in *Potentilla tormentilla* by Infrared and Raman Spectroscopy

M. Węglińska^a, S. Mazurek^a, R. Szostak^a and I. Fecka^b

^a Faculty of Chemistry, University of Wrocław F. Joliot Curie 14, 50-383 Wrocław, Poland

^b Wrocław Medical University, Department of Pharmacognosy, Borowska 211, 50-556 Wrocław, Poland
magdalena.weglinska@chem.uni.wroc.pl

The most important active compounds present in *Potentilla tormentilla* rhizomes were quantitatively determined on the basis of Raman, attenuated total reflection and diffuse reflectance mid- and near- infrared spectra collected for the untreated plant material. Partial least-squares models were constructed utilizing vibrational spectra and the results of high-performance liquid chromatography reference analyses. Applying Raman spectroscopy, total polyphenols, tannins, ellagitannins, agrimoniin, racemic catechins and galloylquinic acid were simultaneously quantified in tormentil rhizomes, with the relative standard errors of prediction in the 2.1 – 4.9 % range for both calibration and validation sets. These error ranges were found to be slightly higher for infrared techniques and amounted to 3.2 – 6.8 %.

Simultaneous Determination of Oleic and Elaidic Acids in their Mixed Solutions by Raman Spectroscopy

Yasushi Numata, Hayato Kobayashi, Norihiko Oonami, Yuki Kasai and Hiroyuki Tanaka

Department of Chemical Biology and Applied Chemistry, College of Engineering, Nihon University,
963-8642 Koriyama, Japan
numata.yasushi@nihon-u.ac.jp

Since spectroscopy provides information regarding the energy levels of molecules, it is used in analytical chemistry. Vibrational spectroscopy such as Infrared (IR) and Raman spectroscopy is used for qualitative analyses or structural studies. Although IR spectroscopy is also used for quantitative analyses, Raman spectroscopy is not applied as much because of the scattering technique. We developed a method of quantitative analysis using Raman spectroscopy [1]. In the present study, simultaneous quantification of oleic (*cis*) and elaidic (*trans*) acids in their mixed solutions was carried out by Raman spectroscopy.

The Raman spectrum was measured by a Renishaw inVia Raman microscope. The 532 nm semiconductor laser was used as an excitation light source. The laser was focused by a 15L objective lens. The scattered light passed into a monochromator after removing the Rayleigh scattering by an edge filter and detected using a CCD detector. The acquisition time was 1 s, and the spectra represent the sum of 50 scans.

Figure 1 shows the Raman spectra of oleic (a) and elaidic acids (b). The Raman spectrum of oleic acid is very similar to that of elaidic acid except for the band around the 1660 cm^{-1} region that is assigned to the C = C double bond stretching vibration mode.

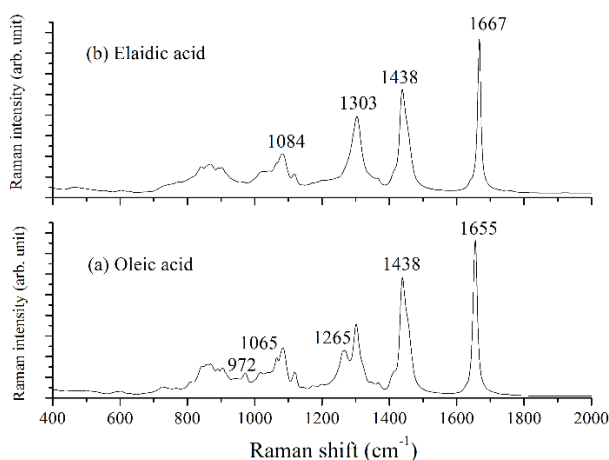


Figure 1 - Raman spectra of oleic (a) and elaidic acids.

To make the PLS model, the Raman spectra of the mixed solutions with known concentrations were measured. The concentration of each fatty acid was investigated using the PLS model. The concentrations predicted by the PLS model were in good agreement with the actual concentrations. Thus, Raman spectroscopy with multivariate analysis can be used for the determination of *cis-trans* fatty acids simultaneously.

References

1. Y. Numata, M. Otsuka, K. Yamagishi and H. Tanaka, *Anal. Lett.*, 50 (2017) 651.

High Pressure Induced Changes in Pork Macromolecular Structure

S. Sazonova^a, K. Shvirksts^b, M. Grube^b, R. Galoburda^a and I. Gramatina^a

^a Faculty of Food Technology, Latvia University of Life Sciences and Technologies, Rīgas str. 22, Jelgava LV3004, Latvia

^b Institute of Microbiology and Biotechnology, University of Latvia, 1 Jelgavas str., Rīga LV1004, Latvia
kshvirksts@gmail.com

High pressure processing is applied for microorganism and enzyme inactivation in foods, however simultaneous changes in texture and colour are observed [1]. In this study FTIR spectroscopy was used to establish the high pressure-induced structural changes of substantial macromolecules of pork meat.

Pork meat slices from *musculus longissimus lumborum* were vacuum packaged and treated in a high pressure processor ISO-Lab S-FL-100-250-09-W at 300 and 600 MPa for 1 and 15 min at each pressure. Untreated vacuum packaged sample was used as a control. The juice released from meat samples in the packages was collected for further analysis. FTIR spectra of control and high pressure treated pork – muscle and juice, were registered using HTS-XT microplate reader coupled with Vertex 70 (Bruker), and recorded in the frequency range of 4000–600 cm⁻¹, with the spectral resolution of 4 cm⁻¹ and 64 scans. For spectral data analyses were used the average of 5-12 spectra of three experimental replications.

In spectra of initial meat juice and muscle, the protein – Amide I and Amide II, bands were the most intensive. Strong bands at 2957 cm⁻¹, 2925 cm⁻¹ and 1745 cm⁻¹ indicated relatively high amounts of lipids in muscle compared to that in juice. In spectra of muscle the increase of pressure from 300 to 600 MPa and exposure for 1-15 minutes resulted in the intensity decrease of the band at 1745 cm⁻¹, assigned to lipids, due to oxidation [2]. Spectra also showed changes of the protein bands Amide I (C=O stretching, C–N stretching and in-plane N–H bending vibrations of α -helices, β -sheets, turns, nonordered or irregular structures) and Amide II (mixed vibration involving N–H in-plane bending and the C–N stretching). Changes of the band intensities and shape can be assigned to the protein structure changes. The spectra of meat juice treated at high pressure changed remarkably compared to that of control. The content of total lipids (being significantly lower than in muscle) decreased. While spectra of control samples and treated with 300 MPa for 1 minute were similar, showing separate Amide bands, these bands were strongly overlapped in the samples treated at higher pressure for longer time. These data show that high pressure affects the protein structures. Juice spectra showed a peak at 1454 cm⁻¹ of collagen type I and its content increased with increasing pressure and dwell time. These FTIR spectroscopy data correlate with pork texture and colour.

References

1. S. Sazonova, R. Galoburda and I. Grāmatiņa, 63rd Int. congress of meat science and technology “Nurturing locally, growing globally”, Cork, Ireland, 13–18th August 2017. – Wageningen, (2017) 610.
2. C. Guyon, A. Meynier and M. de Lamballerie, *Trends Food Sci. Technol.*, 50 (2016) 131.

Acknowledgements: The authors thank funding of the programme “Strengthening Research Capacity in the LLU” project Z13.

Macronutrients Quantification in Dairy Products by FT-Raman Spectroscopy

Tomasz Czaja^a, Maria Baranowska^b, Sylwester Mazurek^a and Roman Szostak^a

^a Department of Chemistry, University of Wrocław, 14 F. Joliot-Curie, 50-383 Wrocław, Poland

^b Chair of Dairy Science and Quality Management, University of Warmia and Mazury, 7 Oczapowskiego, 10-719 Olsztyn, Poland

tomasz.czaja@chem.uni.wroc.pl

Dairy is an important food group consumed by the world's population. Foods such as milk and yoghurt contain nearly all the nutrients necessary to sustain life. Being complex, natural fluids in which water is a major constituent, they contain varying quantities of lipids, proteins and carbohydrates as well as smaller amounts of minerals, vitamins and other components. Analysis of dairy products can be performed using different methods. Some of them are time-consuming and allow quantification of only one ingredient in the system. Increasing food production requires versatile, reliable, rapid and low-cost analytical methods. These criteria fulfil various vibrational spectroscopy methods. Infrared and near infrared spectroscopy is a well-established method for the quantitative analysis of milk and dairy products. However, Raman spectroscopy, another vibrational spectroscopy technique, is rarely used for this purpose.

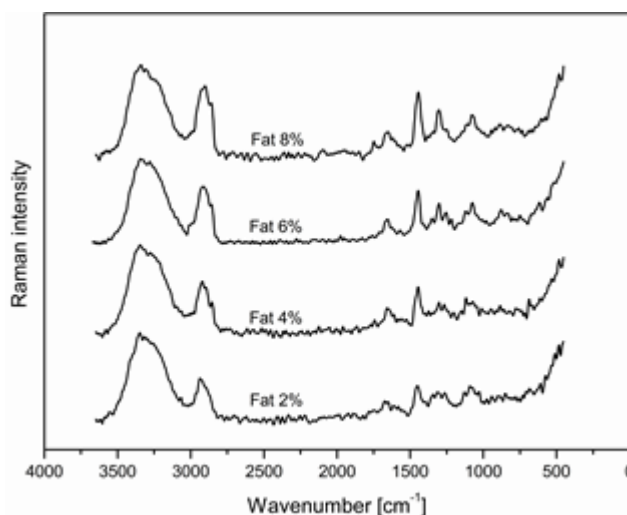


Figure 1 – Representative Raman spectra of commercial yoghurts containing various fat levels.

We performed FT-Raman quantitative analysis of nutritional parameters of milk and yoghurt with the help of partial least squares models. The relative standard errors of prediction for fat, lactose and protein determination in the quantified commercial samples were in the range of 2.8%-4.6% and 3.2%-3.9% for milk and yoghurt, respectively. Simultaneously, we constructed PLS models based on attenuated total reflectance spectra of the liquid milk and yoghurt samples collected with the single reflection diamond accessory. It follows from our results that despite a relatively low signal-to-noise ratio in the obtained spectra, Raman spectroscopy combined with chemometrics constitutes a powerful tool for macronutrients quantification in dairy products.

On the Acquisition of Non-Saturated Hyperspectral Images

Dragos Trinca and Pedro Melo-Pinto

*Centre for the Research and Technology of Agro-Environmental and Biological Sciences,
Universidade de Trás-os-Montes e Alto Douro, 5000-801 Vila Real, Portugal
dragost@utad.pt*

In this work we propose an algorithm for acquiring non-saturated hyperspectral images, in the context of studying the optimal harvest time of grapes using hyperspectral imaging. The proposed algorithm starts from an initial solution that depends on the current sunlight exposure and then progressively finds a non-saturated hyperspectral image.

Recently there has been much work in using hyperspectral imaging for estimating the optimal harvest time of fruits, and particularly of grapes (in [1], neural networks are used to predict the optimal harvest time of wine grapes). A hyperspectral image (which we will call simply “image”) has to be non-saturated (*i.e.* with a maximum value of 254) in order for the reflectances to be correctly calculated out of it; thus finding the right exposure time (which determines whether the image is saturated or not) is of great practical importance [2] (although the methods already existing are only approximations that try to correct saturated images instead of trying to acquire non-saturated images). After a number of experiments, we have observed that the automatic exposure time (the exposure time set by camera automatically at the moment of experiment to acquire a bright enough image) always provides a saturated image, and that the automatic exposure time is proportional to the optimal exposure time (the largest exposure time available at the camera that provides, at the moment of the experiment, a non-saturated image). In 3 experiments we have done in constant (*i.e.* without clouds covering Sun intermittently) sunny weather the automatic exposure times were 28.2 ms (at 10:30am), 22.0 ms (at 13:30 pm), and 32.8 ms (at 17:00 pm); the respective optimal exposure times were 10.3 ms, 8.2 ms, and 11.5 ms. Based on this, the following algorithm can be used to find an optimal non-saturated image (*i.e.* image obtained at the optimal exposure time):

Step 1: acquire an image at the automatic exposure time; let aet be the respective automatic exposure time; then see what number corresponds to aet on the graph given by (at least) the numbers 2.67 ($= 22.0 / 8.22$), 2.73 ($= 28.2 / 10.3$), 2.85 ($= 32.8 / 11.5$); for example, if aet is in the interval $[28.2, 32.8]$ then its corresponding number would be somewhere between 2.73 and 2.85; let x be that number, obtained for example by interpolation;

Step 2: execute a number of iterations until the optimal exposure time is found; at each iteration an image is acquired at the currently set exposure time and: if it is saturated then in the next iteration a smaller exposure time is considered, otherwise in the next iteration a larger exposure time is considered, chosen proportionally with the maximum value of the image acquired in the current iteration; in the first iteration, the exposure time set is $et1 = (aet / x)$.

We have observed that the algorithm finds the optimal exposure time usually in 2-3 iterations; it has to be studied further in different weather conditions and possibly improved if necessary.

References

1. R. Silva, V. Gomes, A. Mendes-Faia and P. Melo-Pinto, *Remote Sensing*, 10(2), 312 (2018).
2. S. W. Hasinoff, *Computer Vision, A Reference Guide 2014*: 699-701, editors: Katsushi Ikeuchi, Springer.

Acknowledgements: This work was supported by Projeto de I&D Symbiotic technology for societal efficiency gains: Deus ex Machina (DEM), n.º da operação NORTE-01-0145-FEDER-000026, co-financiado pelo Fundo Europeu de Desenvolvimento Regional (FEDER) através do NORTE 2020

Application of Low-temperature FTIR Spectroscopy of Adsorbed CO for Characterization of Copper species in Mordenites

O. Pestsov^a, R. Belykh^a, R. Novikov^a, A. Tsyganenko^a, M. Shelyapina^a, V. Petranovski^b

^a Saint Petersburg State University, 7/9 Universitetskaya nab., St. Petersburg, Russia 199034

^b Centro de Nanociencias y Nanotecnologia, Universidad Nacional Autonoma de Mexico, Ensenada 22860
atsyg@yandex.ru (A. Tsyganenko)

Low-temperature infrared (IR) spectroscopy of adsorbed molecules is widely used to identify surface species. Copper-exchanged zeolites are highly promising catalysts for removal of nitrogen oxides (de-NO_x) and other processes. To improve their properties it is necessary to understand the state of copper sites. The content and specific forms of copper species are highly affected by preparation method. Recently it has been shown that microwave assisted copper ion-exchange treatment of sodium mordenite leads to diversification of copper species stabilized inside the mordenitepores [1]. By means of ESR [1] and FTIR spectroscopy [2,3] one can detect Cu²⁺, Cu⁺ and [Cu–O–Cu]²⁺ species.

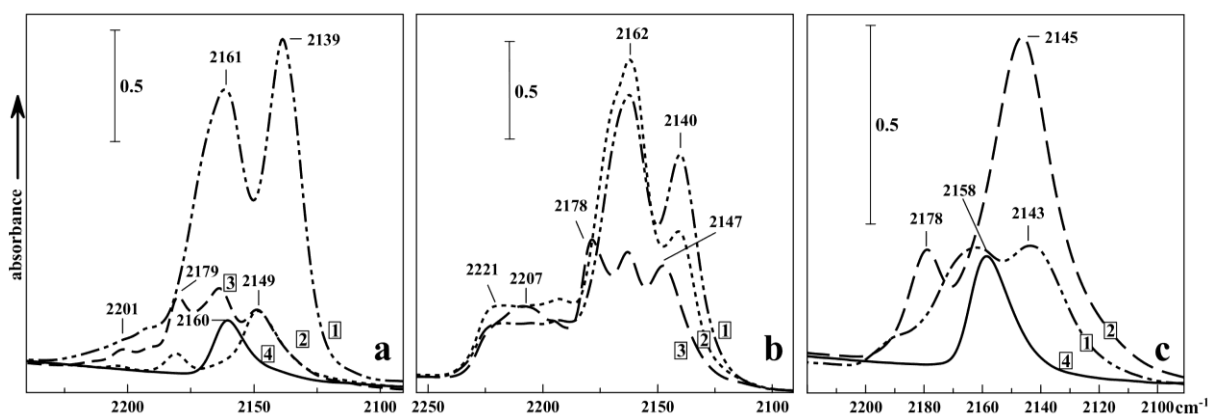


Figure 1 – FTIR spectra of CO adsorbed on Cu-mordenites at progressively decreasing coverages (1-4)

Figure 1 shows the spectra of CO adsorbed on a sample of Cu mordenite prepared by microwave treatment and evacuated at 450°C at different conditions. Spectrum of an oxidized sample heated and cooled in oxygen (Fig. 1a) in the presence of CO at 77K exhibits a pair of bands near 2160 and 2140 cm⁻¹, accompanied with perturbation of OH groups at 3624 cm⁻¹. The perturbation disappears after removal of gaseous CO, leaving the bands of CO at 2180 and 2148 cm⁻¹. After further lowering of CO coverage the only band at 2160 cm⁻¹ remains. Subsequent heating the sample in vacuum (Fig. 1b) results in new bands of adsorbed CO between 2220 and 2200 cm⁻¹, which do not arise if a fresh sample is evacuated in the absence of oxygen (Fig. 1c). The method of isotopic dilution with ¹²CO-¹³CO mixtures enables us to distinguish bands of single adsorbed molecules from those of binary CO species at the same surface Cu sites.

References

1. M.G. Shelyapina et al., *J Therm Anal Calorim*, (2018).
2. K. Hadjiivanov, H. Knözinger, *J. Catalysis*, 191 (2000) 480.
3. C.Lamberti et al., *J. Chem. Soc., Faraday Trans.*, 94 (1998) 1519.

Acknowledgement: The work was supported by the RFBR, grant 17-03-01372

Obtaining Extinction Spectra from the Reflection Spectra of Low-Temperature Molecular Liquids

T. S. Kataeva, O. S. Golubkova, D. N. Shchepkin and R. E. Asfin
 Department of Physics, Saint Petersburg State University, 7/9 Universitetskaya Nab.,
 199034 Saint Petersburg, Russian Federation
 st016902@student.spbu.ru

The main goal of our work is to develop a sophisticated method of obtaining extinction (dimensionless absorption coefficient) and refractive index spectra from the reflection spectra of the low-temperature condensed phases in the strong in absorption band region. In this investigation the reflection spectra of several low-temperature molecular liquid have been recorded and analyzed. The reflection spectra of C_2F_6 , CF_4 and CO_2 liquids have been obtained from thick layers. It was made in order to obtain contours of the strong fundamental bands ($A > 100$ km/mole). The extinction and refractive index spectra of the studied bands were obtained by a special program based on Kramers-Kronig ratios [1]. The integral absorption coefficients of these bands were calculated and compared with literature data.

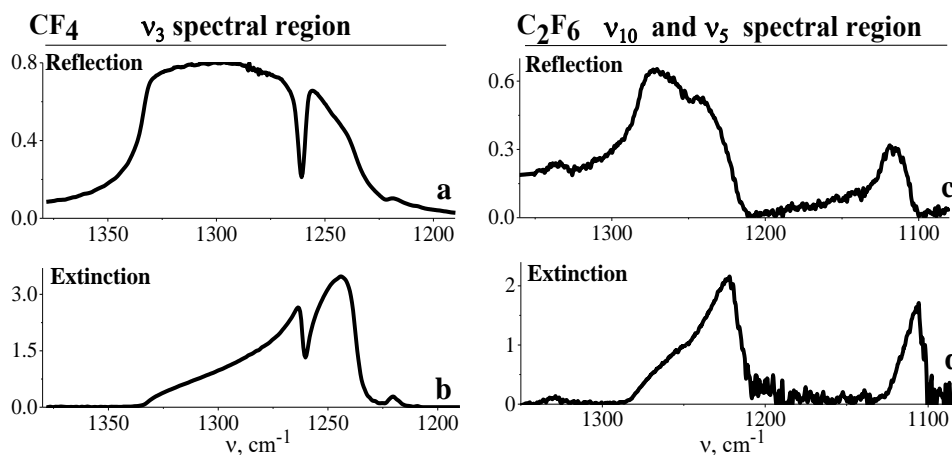


Figure 1 – reflection (a) and extinction (b) spectra of liquid CF_4 in the region of ν_3 band ($T=90$ K) (left); reflection (c) and extinction (d) spectra of liquid C_2F_6 ($T=198$ K) in the region of ν_5 and ν_{10} fundamental bands (right)

In the C_2F_6 extinction spectra it was found that a strong high-frequency ν_{10} band affects a weaker low-frequency ν_5 band, which is manifested by an increase in its integral absorption coefficient. In addition, the method of normalizing experimental reflection spectrum by the high-frequency wing of the reflection band was developed.

References

1. Pavel K. Sergeev, Dmitriy N. Shchepkin, Tatiana D. Kolomiitsova, Vladimir V. Bertsev, Ruslan E. Asfin, *Appl. Spectr.*, 69 (2015) 509-512.

Acknowledgements: The authors thank T. D. Kolomiitsova for valuable remarks. This work was supported by the Russian Foundation for Basic Research, project no 18-03-00520 A. The experiment was performed at the center for Geo-Environment Research and Modeling (GEOMODEL) of Research park of St. Petersburg State University.

Notes

Biospectroscopy Biomedical Applications

Discrimination Analysis of Blood Plasma Associated with Schizophrenia Disease Using FTIR Spectroscopy

Gülce Ogruc Ildiz^a and Sevgi Haman Bayari^b

^a Department of Physics, Science and Letters Faculty, Istanbul Kultur University, Atakoy Campus, Bakirkoy 34156, Istanbul, Turkey

^b Department of Physics Engineering, Hacettepe University, Beytepe, 06800, Ankara, Turkey
g.ogruc@iku.edu.tr

Schizophrenia is a severe mental disorder in which people interpret reality abnormally. It will impact the individual's feelings and their ability to communicate, to focus, to complete tasks, to sleep, and to relate to others. The Attenuated Total Reflection Fourier Transform Infrared (ATR-FTIR) spectroscopy is highly favored and sensitive analytical tool widely used to detect the changes in the functional groups and molecular conformations of biochemical composition, such as nucleic acids, proteins, and lipids of normal and disease states. In this study, ATR-FTIR spectroscopy coupled with hierarchical cluster analysis methods were used to determine the biochemical variations in the blood plasma of schizophrenic patients compared with those of healthy control group. The variations in the area under the spectral bands give information about concentration of the functional groups belonging to the relevant molecules. In order to investigate possible disease-induced variations, the ratio of the area of the bands assigned to lipids, proteins, and nucleic acids were calculated. The first, most striking difference occurs in the bands associated with lipids. The lipid to protein ratio was lower in schizophrenic patients than controls, suggesting a decrease in total lipid content, in accordance with other studies.¹ The band at around 1080 cm⁻¹ is due to symmetric stretching vibrations of phosphodiester groups (PO₂⁻) in nucleic acids. The area ratios of the 1080 to 1550 cm⁻¹ (amide II; protein) bands could be used to probe nucleic acids. We also found a significant decrease in the phosphodiester content for the schizophrenic group compared to the control. The use of hierarchical clustering analysis (HC) enabled us to explore in an efficient way the spectra of healthy and diseases groups. The best results were achieved in the C-H (3100- 2800 cm⁻¹) and 1300-900 cm⁻¹ spectral regions.

References

1. J. Matsumoto *et. al.*, *Scientific Reports*, 7 (2017) 45050.

Acknowledgements: This study has been funded by the Scientific and Technological Research Council of Turkey-TUBITAK 1001 Project (Project No.: 116Z294).

Investigation of Light-Vibration Coupling Coefficient of Glassy Glucose by Terahertz Time-Domain Spectroscopy and Low-Temperature Specific Heat

Wakana Terao^a, Mikitoshi Kabeya^a, Tatsuya Mori^a, Suguru Kitani^b, Yasuhiro Fujii^c,
Akitoshi Koreeda^c, Hitoshi Kawaji^b and Seiji Kojima^a

^a Division of Materials Science, University of Tsukuba, 1-1-1 Tennodai, Tsukuba, Ibaraki 305-8573, Japan

^b Materials and Structures Laboratory, Tokyo Institute of Technology, 4259 Nagatsuta-cho, Midori-ku, Yokohama 226-8503, Japan

^c Department of Physical Sciences, Ritsumeikan University, 1-1-1 Noji-higashi, Kusatsu, Shiga 525-8577, Japan
mori@ims.tsukuba.ac.jp

The boson peak is a low energy excitation universally observed in the terahertz region of the glassy materials [1]. As we have pointed out recently [2,3], the boson peak of infrared spectra appears in the spectra of $\alpha(\nu)/\nu^2$ [$\alpha(\nu)$ is the absorption coefficient].

In this study, we performed terahertz time-domain spectroscopy on glassy glucose to investigate the boson peak dynamics. Moreover, we determined infrared light-vibration coupling coefficient $C_{\text{IR}}(\nu)$ using the $\alpha(\nu)$ and vibrational density of states $g(\nu)$ obtained from the low-temperature specific heat measurement. The charge fluctuations of the densified silica glasses were quantitatively evaluated using Taraskin's model [4].

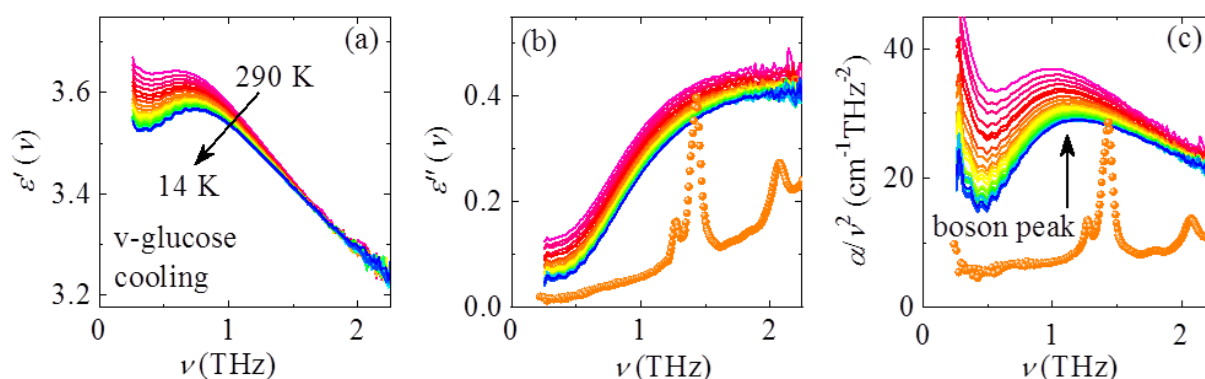


Figure 1 – Temperature dependence of (a) real and (b) imaginary parts of the complex dielectric constants and (c) BP spectra, of glassy glucose during the cooling process. The spectra of crystalline glucose are also plotted as orange dot.

References

1. T. Nakayama, *Rep. Prog. Phys.*, 65 (2002) 1195.
2. M. Kabeya, T. Mori, Y. Fujii, A. Koreeda, B. W. Lee, J. H. Ko and S. Kojima, *Phys. Rev. B*, 94 (2016) 224204.
3. W. Terao, T. Mori, Y. Fujii, A. Koreeda, M. Kabeya and S. Kojima, *Spectrochim. Acta A*, 192 (2018) 446.
4. S. N. Taraskin, S. I. Simdyankin, S. R. Elliott and J. R. Neilson, T. Lo, *Phys. Rev. Lett.*, 97 (2006) 055504.

Acknowledgements: This work was partially supported by JSPS KAKENHI Grants No. 17K14318, the Nippon Sheet Glass Foundation for Materials Science and Engineering, and the Asahi Glass Foundation.

Molecular Modelling and NMR Studies of Cyclodextrin Inclusion Complexes with New Oxazolidinone Antibiotics

Wojciech Bocian, Elżbieta Bednarek, Katarzyna Michalska
National Medicines Institute, Chelmska 30/34, 00-725 Warsaw, Poland
w.bocian@nil.gov.pl

The oxazolidinones are a novel class of synthetic antimicrobial agents, unrelated to any other class, showing a comprehensive spectrum of activity against the major and nosocomial Gram-positive pathogens. The first oxazolidinone introduced into treatment was linezolid in 2000, the next agent – tedizolid – was approved in 2014 and radezolid is in clinical development. Cyclodextrins forming host-guest inclusion complexes *via* noncovalent interactions with a variety of hydrophobic molecules can significantly change their water solubility, bioavailability and stability.

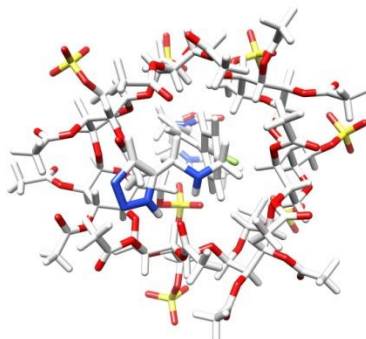


Figure 1 - The average geometry from 1 ms molecular dynamic calculation in explicit water solvent for radezolid/HDAS- β -CD complex.

The aim of molecular modelling and NMR studies were to increase knowledge on the formation of the inclusion complex between oxazolidinones and HDAS- β -CD.

The molecular modeling calculations were performed utilizing Amber software and graphical processor units (GPUs) hardware. We have used ten microsecond time scale molecular dynamics simulations, with explicit solvent consisting water and all ions to compute binding enthalpies.

In order to experimentally evaluate the binding affinities we have performed the NMR PGSE experiments. The parallel interpretation of chemical shift changes and dipolar contacts allows the mode of binding to be established.

Molecular modelling and NMR studies revealed that oxazolidinones interacts mainly with the inside region of the CDs cavity.

References

1. K. Michalska, E. Gruba, J. Cielecka-Piontek and E. Bednarek, *J. Pharm. Biomed. Anal.* 120 (2016) 402.
2. E. Bednarek, W. Bocian, K. Michalska, *J. Chromatogr. A*, 1193 (2008) 164.

Acknowledgements: This study was supported by SONATA grant from the National Science Centre Poland-UMO-2013/11/D/NZ7/01230.

Estimation of the Cancer Cell Metabolic Response to the Growth Environment by FTIR Spectroscopy

Z. Kalnina^a, K. Shvirksts^b, E. Rubena^a, R. Kovaldins^c and M. Grube^b

^a Latvian Biomedical Research and Study Centre, 1 Ratsupites str., Riga LV1067, Latvia

^b Institute of Microbiology and Biotechnology, University of Latvia, 1 Jelgavas str., Riga LV1004, Latvia

^c Nuclear Medicine Clinic Ltd, 25 Patversmes str., Riga LV100, Latvia

grube@lu.lv

FTIR spectroscopy techniques, methods and data analyses have become widely available, easier to use, and more convenient for studies of various bio-samples and cell metabolic response to the growth environment. In our previous studies, FTIR spectroscopy quantitative analysis was used to evaluate the breast cancer cell response to gold nanoclusters [1] and hypoxia induced effects in human colorectal cancer cell lines. The aim of this study was to estimate the lung and prostate cancer cell response to hypoxia and molecularly targeted Ga68 radionuclides used in radio-oncology. Lung cancer cell lines NCI-H69, COR-L23, prostate cancer cell line PC3, and primary prostate cancer culture NFI-56 were seeded in serum-free medium in density 1×10^6 cells per well in triplicates in 6-well plates and incubated as 3D cell cultures for 48 h under normoxic or hypoxic (5% CO₂, 1% O₂ and 94% N₂) conditions. Ga68-PSMA and Ga68-DOTA-TATE radionuclides were synthesized in TEMA isolators class A zone (Scintomics Ltd); added at the activity of 3 MBq to 1×10^6 cells and incubated for 48 h at 37°C in normoxic conditions. FTIR spectra of $\sim 200'000$ cells were recorded with HTS-XT microplate reader (Bruker, Germany) in the frequency range of 4000–600 cm⁻¹, with the spectral resolution of 4 cm⁻¹ and 64 scans. Quantitative analysis of cell macromolecular composition was carried out as in [2]. As characteristic absorption bands were used 1080 cm⁻¹ for carbohydrates, 1250 cm⁻¹ for nucleic acids, 1550 cm⁻¹ for proteins and 2930 cm⁻¹ for lipids.

The results of FTIR spectroscopy quantitative analyses showed initial differences in the biochemical composition of both prostate cancer cell lines as well as among both lung cancer cell lines incubated either under normoxic or hypoxic conditions. Particularly the lipid content lung cancer cell line NCI-H69 grown under normoxic environment was lower than in cells grown under hypoxic environment (10.85 and 13.29% of dry weight (dw) correspondingly). The lipid content in prostate cancer cell line PC3 and NFI-56 was higher than in lung cancer cells incubated under normoxic or hypoxic conditions – 15-17% dw and 11-13% dw correspondingly. Data on metabolic responses of lung and prostate cancer cells to Ga68 radionuclides will be presented. These *in vitro* studies of cancer cells revealed FTIR spectroscopy as a valuable method to elucidate the cell metabolic answers to external factors.

References

1. M. Grube, K. Shvirksts, D. Dapkute, M. Matulionyte, E. Zandberga, A. Line and R. Rotomskis, *J. Biotech.*, 231S (2016) S93.
2. M. Grube, M. Bekers, D. Upite and E. Kaminska, *Vibr. Spectrosc.*, 28 (2002) 277.

Acknowledgments: This study was financed by the project "Sustainable use of nature resources in the context of climate changes" (Nr. ZD2016/AZ03) and the University of Latvia Foundation and "MIKROTĪKLS" Ltd. donation project "Development and introduction of innovative methods in clinical practice for the diagnosis and treatment of malignant tumors using molecularly targeted radionuclides produced in Latvia."

Probing Lysozyme Aggregation at Lipid Monolayers with Vibrational Sum-Frequency Generation Spectroscopy

Simona Strazdaite, Edvinas Navakauskas and Gediminas Niaura

Center for Physical Sciences and Technology (FTMC), Saulėtekio al. 3, LT-10257 Vilnius, Lithuania

simona.strazdaite@ftmc.lt

Aggregation of proteins is a pathological hallmark of many neurodegenerative disorders. Most recent research suggests that cell membrane can be one of the main triggers for protein aggregation [1]. Here, we use vibrational sum-frequency generation (VSFG) to investigate the interaction of hen egg white lysozyme (HEWL) and its aggregates with the lipid monolayer formed on the water surface. Aggregation of HEWL in the bulk of water is a well-studied process [2]. To induce aggregation of HEWL, destabilization of the native structure is needed, which can be achieved at an elevated temperature and acidic conditions (62 °C, pH = 2). Structure of HEWL aggregates formed in the bulk was checked using Fourier transform infrared (FTIR) spectroscopy. Small oligomers with anti-parallel β -sheet structure are formed after ~10 – 60 h of incubation time at elevated temperature, whereas stable fibrils with parallel β -sheet structure are formed after longer than ~60 h incubation times.

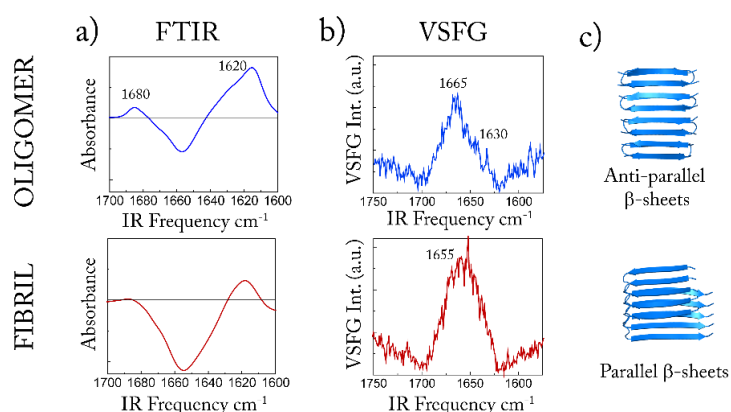


Figure 1 – FTIR difference spectra of HEWL oligomeric and fibril aggregates (a), corresponding VSFG spectra (ssp polarization combination) (b), and predicted secondary structures of the aggregates (c).

For the VSFG measurements, we took aliquots of HEWL incubation solution at different time points and injected it into the water phase beneath DOPG lipid monolayer. An intense amide I peak signal was observed for all the cases and much less intense chiral amide I and NH stretching signals were also visible. From the positions of those peaks, secondary structures of oligomeric and fibril aggregates were determined, which matched secondary structures determined from FTIR (Fig. 1). We will continue the investigation of lysozyme aggregation by changing various parameters such as pH, protein concentration, salt concentration, and others.

References

1. S. A. Kotler, P. Walsh, J. R. Brender and A. Ramamoorthy, *Chem. Soc. Rev.*, 43 (2014) 6692.
2. Y. Zou, Y. Li, W. Hao, X. Hu and G. Ma, *J. Phys. Chem. B*, 117 (2013) 4003.

Acknowledgements: S. Strazdaite gratefully acknowledges European Commission for funding this research through a Marie-Skłodowska Curie individual fellowship.

ATR-IR Real-Time Monitoring of Biofilm Formation During Bacterial Growth

Pavla Štenclová^a, Simon Freisinger^b, Alexander Kromka^a and Boris Mizaikoff^b

^a Institute of Physics of the Czech Academy of Sciences, Cukrovarnická 10, 162 00 Prague 6, Czech Republic

^b Institute of Analytical and Bioanalytical Chemistry, University of Ulm, Albert Einstein-Allee 11, 89081 Ulm, Germany
stenclova@fzu.cz

Contrary to a planktonic form of bacteria, its biofilm form represents severe complications in human medicine or food industry due to its high resistance to harsh conditions or treatment. Therefore, an understanding of early-stage biofilm formation is a crucial factor in preventing bacterial contamination and its understanding attracted scientific and industrial community. Here, Attenuated Total Reflection Fourier-Transform Infrared (ATR-FTIR) spectroscopy provides an excellent analytic tool for studying the biofilm formation in the real-time. The ATR-FTIR spectroscopy is a non-destructive and non-invasive method in which the evanescent wave formed on the optical crystal/sample interface penetrates into the first layers of the biofilm and thus, provides information about the initial attachment of the bacteria and subsequent formation of extracellular matrix.

In this contribution, we report on the biofilm formation using ZnSe ATR crystal capable to probe the biofilm height up to approx. 2 μm at 1000 cm^{-1} . Our realized measurement setup with continuous media flow allows us to examine the biofilm dynamics up to several days.

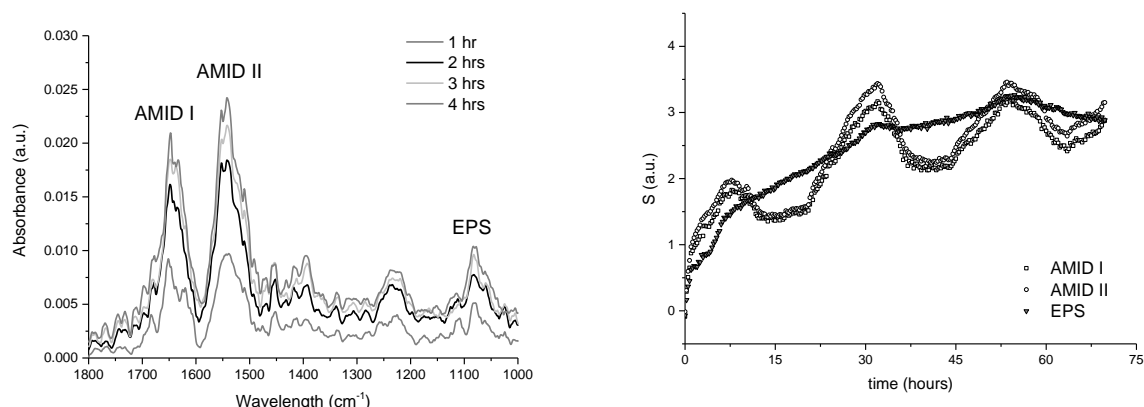


Figure 1 - ATR-IR spectra of *E. coli* biofilm formation on a bare ZnSe crystal for first 4 hours (left) and time evolution of selected absorption bands areas (S) for long-term experiments up to 76 hours (ca. 3 days) (right).

In the *E. coli* biofilm spectra (Figure 1, left) we can distinguish AMID I (1700–1590 cm^{-1}) and AMID II (1580–1490 cm^{-1}) bands related to the proteins in bacterial membranes and EPS band (1141–1006 cm^{-1}), which is considered as the indicator of biofilm formation related to extracellular polymeric saccharides. During the long-term experiments up to 3 days (Figure 1, right) we have found out oscillations in the AMID bands, while the EPS band steadily increased. Possible explanations of AMID bands fluctuations, dynamic of the biofilm and advantages and drawback of the presented method will be discussed.

Acknowledgements: The work was conducted at the University of Ulm within the project “IR imaging of biological systems using structural and functional optical elements” of the Czech Academy of Science (project no. MSM100101703).

Vibrational Microspectroscopy of Sodium Valproate-Treated DNA

Maria Luiza S. Mello and Benedicto de Campos Vidal

University of Campinas (Unicamp), Institute of Biology, 13083-862 Campinas, SP, Brazil
mlsmello@unicamp.br

Valproic acid (VPA), a drug classically prescribed as an anticonvulsant, inhibits histone deacetylases and concomitantly induces histone acetylation. It also affects the methylation status of DNA and histones through complex mechanisms not yet fully understood [1]. In addition, a direct effect of VPA on histone H1 and less strongly on DNA molecules has currently been proposed [2,3]. Considering that the crystallization of DNA molecules was shown to be affected by sodium valproate [3], we investigated whether the FT-IR spectral signatures of DNA was also affected by this drug. Acquisition of FT-IR spectra was obtained for thymus DNA, sodium valproate and DNA-valproate dried samples prepared as simultaneously informed in this Congress [3]. The samples were examined using an Illuminat IR II™ microspectroscope (Smiths Detection, Danbury, USA) equipped with a liquid nitrogen-cooled mercury-cadmium-telluride detector and GRAMS/AI™ 8.0 spectroscopy software (Thermo-Electron Co., Waltham, USA); a BMX 51 microscope (Olympus) with an ATR objective (36 x) was part of the equipment. Absorbances for samples and background were estimated using 64 scans for each individual spectral profile in the 3500-650 cm⁻¹ wavenumber spectral range and assuming a resolution of 4 cm⁻¹ as informed by the equipment supplier. The band peaks assigned to $\nu_{\text{as}} \text{PO}_2^-$ groups (1222-1220 cm⁻¹), $\nu_{\text{s}} \text{PO}_2^-$ groups (1081-1080 cm⁻¹) and O-P-O bending (961-960 cm⁻¹) in the DNA FT-IR spectrum [4] were also frequently present in the spectral curves of the valproate-DNA mixtures. However, the absorbances at these peaks as well as the $\nu_{\text{as}} \text{PO}_2^- / \nu_{\text{s}} \text{PO}_2^-$ ratio decreased significantly ($p < 0.05$) in the valproate-DNA mixtures. This finding suggests DNA conformational changes in presence of the valproate and agrees with data showing valproate-induced changes in the DNA supramolecular texture obtained using polarization microscopy ([3] – this Congress). Spectral curves obtained in valproate-DNA regions where valproate crystals were evident, resembled the curves for valproate crystal forms B+C and D [5], with the exception of similarities with the DNA spectrum in the 3500-3000 cm⁻¹ spectral window, which may have resulted from some valproate crystal assemblies.

References

1. S. Chateauvieux, F. Morceau, M. Dicato and M. Diederich, *J. Biomed. Biotechnol.*, 2010 (2010) 1.
2. J. Sargolzaei, A. Rabbani-Chadegani, H. Mollaei and A. Deezagi, *Int. J. Biol. Macromol.*, 99 (2017) 427.
3. B. C. Vidal and M. L. S. Mello, *EUCMOS* (2018).
4. M. L. S. Mello and B. C. Vidal, *PLoS ONE*, 7 (2012) e43169.
5. G. Petrushevski, P. Naumov, G. Jovanovski, G. Bogoeva-Gaceva and S. W. Ng, *ChemMedChem*, 3 (2008) 1377.

Acknowledgments: FAPESP (grant No. 2015/10356-2); CNPq (grant no. 304668/2014-1).

Structural Modifications of PLL by Chalcone Molecules

Katarzyna Cieřlik-Boczula

Faculty of Chemistry, University of Wrocław, F. Joliot-Curie 14, 50-383 Wrocław, Poland

katarzyna.cieslik@chem.uni.wroc.pl

The effect of chalcone molecules (*trans*-chalcone, chloro-chalcone and fluoro-chalkone) on the temperature-induced α -helix to β -sheet transition in long-chain poly-L-lysine (PLL), accompanied by the formation of β -sheet as well as α -helix fibrillar aggregates of PLL has been studied using Fourier-transform infrared (FT-IR) and vibrational circular dichroism (VCD) spectroscopy, and transmission electron microscopy (TEM). Poly-L-lysine (PLL) is an excellent candidate system for modeling properties of protein structures because PLL can easily adopt all of the most important secondary structures of proteins after a relatively simple manipulation [1,2]. Additionally, the long-chain PLL is a good candidate to choose as a model for both β -sheet and α -helical fibrillar proteins [1,2]. In one peptide, different structures of fibrils are formed by simply changing only the temperature. Bioactive molecules, such as chalcones, present in plants are key components in therapeutic studies against infectious diseases, cancer, and metabolic disorders [3]. It was stated that chalcone molecules differently influenced the temperature of α -helix to β -sheet transition in PLL, depending on their structure. These molecules modulated fibrillogenesis in PLL by changing the secondary structure of PLL. The effect of chalcones on the morphology of β -sheet-rich and α -helix-rich fibrils of PLL was determined using TEM method.

References

1. K. Cieřlik-Boczula, *Biochim.*, 137 (2017) 106.
2. K. Cieřlik-Boczula, *Biophys. Chem.*, 227 (2017) 14.
3. N. Mateeva, S. V. K. Eyunni, K. K. Redda, U. Ononuju, T. D. Hansberry, C. Aikens and A. Nag, *Bioorgan. Medicinc. Chem. Lett.*, 27 (2017) 2350.

Acknowledgements: The author acknowledges the financial support provided by the National Science Centre, Poland, with decision numbers of OPUS projects: 2015/17/B/ST4/03717.

Absorption Spectra Simulations of Green Fluorescence Protein Chromophore Models

Ivelina Georgieva^a, Adelia J. A. Aquino^{b,c,d}, Natasha Trendafilova^a and Hans Lischka^{b,c,d}

^a*Institute of General and Inorganic Chemistry, Bulgarian Academy of Sciences,
11 Acad. G. Bonchev Str., 1113 Sofia, Bulgaria*

^b*Institute for Theoretical Chemistry, University of Vienna, A-1090 Vienna, Austria*

^c*Department of Chemistry and Biochemistry, Texas Tech University, Lubbock 79409, Texas, USA*

^d*School of Pharmaceutical Sciences and Technology, Tianjin University, Tianjin 300072, China
ivelina@svr.igic.bas.bg*

Semi-classical *ab initio* simulations of the absorption spectra of neutral and anionic *p*-hydroxybenzylidene-2,3-dimethylimidazolinone (*p*-HBDI) (a model chromophore of Green Fluorescent Protein (GFP)) and of a positively charged neutral (N⁺)-HBDI chromophore model were performed in gas phase at the resolution-of-identity coupled cluster to second-order (RI-ADC(2)) level. The calculated absorption spectra are composed of one band centered at 3.51 eV (HBDI), 2.50 eV (HBDI[−]) and 3.02 eV ((N⁺)-HBDI) owing to the absorption of the first ¹ $\pi\pi^*$ transition. Band maxima are red-shifted by 0.1 eV with respect to the corresponding vertical energies. The calculated band maxima in gas phase are consistent with the experimental ones at 3.51 eV (HBDI), 2.58 eV (HBDI[−]) and 2.99 eV (N⁺)-HBDI. The COSMO-RI-ADC(2) calculations of the first vertical excitation energy of HBDI, HBDI[−] and (N⁺)-HBDI forms in polar solution including microsolvation simulate the observed solvent red-shift for neutral HBDI and the solvent blue-shift of the HBDI[−] and (N⁺)-HBDI forms. As compared to the A (3.05-3.12 eV) and B (2.59-2.63 eV) bands observed for GFP, the ADC(2) computed range of excitation energies for HBDI[−] (2.52 eV, in gas phase and 2.59 eV in water) agree well with the experimental B band of GFP. In case of the A band, which is expected to originate from the neutral chromophore, the estimated band maximum at ADC(2) level in water (3.07 eV) fits very well.

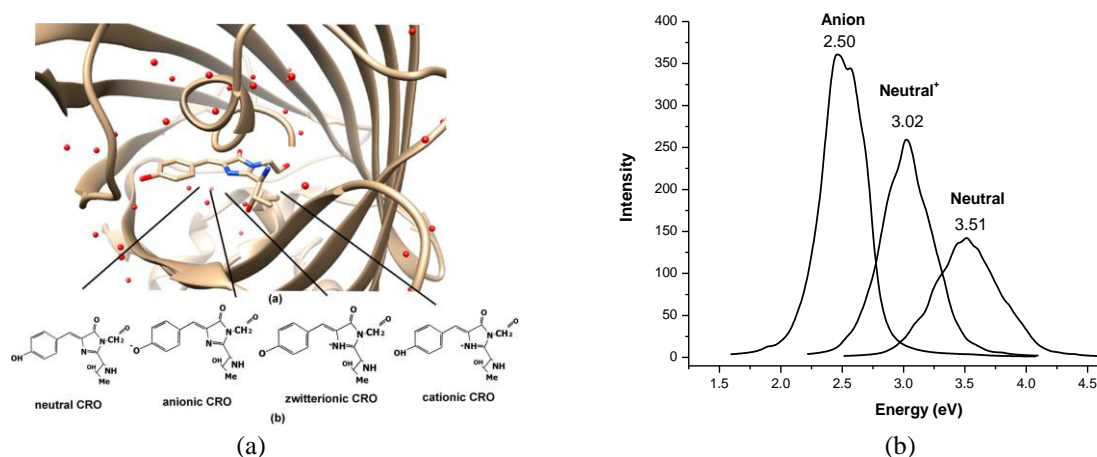


Figure 1 – (a) The chromophore (CRO), *p*-HBI located in the center of the β -can of wild-GFP and sketch of CRO structures representing different protonated forms; (b) Simulated absorption spectra via vibrational broadening of neutral, anionic and (N⁺)-HBDI at ADC(2) method.

Acknowledgements: I.G. and N.T. thank the National Science Fund of the Bulgarian Ministry of Education and Science for the financial support under Grant DH09/9/2016. Computer time at the Vienna Scientific Cluster (VSC), project 70376, is gratefully acknowledged.

Peculiarities of Interaction of Non-Histone Nuclear Proteins HMGB1 and HMGB2 with DNA Damaged by Cisplatin

Elena Chikhirzhina^a, Ekaterina Tymchenko^b, Anastasia Soldatova^b, Tatiana Starkova^a,
Elena Kostyleva^a, Alexey Tomilin^{a,b} and Alexander Polyanichko^{a,b}

^a *Institute of Cytology, Russian Science Academy, 4 Tikhoretsky ave., Saint-Petersburg 194064,
Russian Federation*

^b *Saint-Petersburg State University, 7/9 Universitetskaya nab., Saint-Petersburg 199034, Russian Federation
chikhir@gmail.com*

DNA of eukaryotic cells forms nucleoprotein complex with different histones and non-histone proteins. Non-histone proteins HMGB1 and HMGB2 are the members of a large family of High Mobility Group proteins and provide additional levels of structural and functional unity of chromatin. These proteins are involved in formation of DNA–protein complexes responsible for activation of gene transcription. The interest to these proteins is also explained by the fact that structural motifs similar to its DNA-binding domains (known as HMGB domains) were found in many regulatory proteins. Although HMGB1 and HMGB2 proteins are very similar (more than 80% homology) both proteins are present in the cell. The exact difference in the functioning of these two proteins is not clear yet. One of the characteristic features of these proteins is to recognize and preferentially bind to cisplatin. Cisplatin (cis-DDP) is a chemotherapeutic agent widely used to treat some types of human malignancies. Biological activity of cisplatin based on the ability to form stable adducts on DNA. The binding of HMGB1 and HMGB2 proteins to the platinum adduct can block the repair of this damage. We assume that the antitumor activity of cis-DDP can be directly related to the stability and structure of the complexes that HMGB1 and HMGB2 form on the platinum adducts. We have studied the interaction of DNA with proteins HMGB1 and HMGB2 in presence of cisplatin using Circular Dichroism, and UV absorption spectroscopy. It was shown in case of HMGB1 the features of the DNA structure are determined primarily by the interaction of DNA with cis-DDP, HMGB1 binds to the adduct without altering the structure of the DNA itself. Both DNA-binding domains are involved in the interaction of HMGB2 with DNA. The presence of cisplatin in the system prevents the formation of supramolecular structures, which is manifested in a sharp decrease in the CD DNA band. Thus, the differences in the structure of complexes DNA with HMGB1 and 2 show that despite these two proteins are almost identical in their structure, the mechanisms of their interactions with DNA might be different which can lead to the different function of these proteins in living cell.

Acknowledgements: The work was supported by RSF 17-14-01407 and RFBR 18-08-01500. Part of the work was performed using the equipment of the Research park of St. Petersburg State University: “Center for Optical and Laser Research”, “Centre for Diagnostics of Functional Materials for Medicine, Pharmacology and Nanoelectronics”, “Centre for Molecular and Cell Technologies”.

Sodium Valproate-Induced Changes in Chiral Supramolecular Texture Formed During DNA Crystallization

Benedicto de Campos Vidal and Maria Luiza S. Mello

University of Campinas, Institute of Biology, 13083-862 Campinas, SP, Brazil

camposvi@unicamp.br

Valproic acid (VPA), a widely prescribed drug for treatment of seizure disorders, inhibits class I histone deacetylases and affects DNA methylation and several histone epigenetic marks [1]. Apart from affecting epigenetic marks, VPA has been recently proposed as having a high affinity for histone H1 and a low affinity for DNA, based on thermal denaturation, fluorescence spectroscopy and circular dichroism analyses [2]. However, no effects of VPA on the DNA chiral properties, like those revealed during crystallization of DNA standards [3], as well as on DNA FT-IR spectral signatures [4] have so far been described. In the present work, we studied the effects of sodium valproate on DNA crystallization patterns using high-performance polarization microscopy, including DIC optics, and preceding an analysis using FT-IR microspectroscopy [5]. Drying of 10- μ L drops from calf thymus DNA (Sigma[®]) prepared as previously described [3], and from 40 mM aqueous sodium valproate (Sigma[®]) was monitored microscopically under ambient relative humidity less than 75% at 27°C. Next, drops of valproate and DNA (5- μ L each) were mixed and dripped on slides. The drops were allowed to dry and examined 24 h and 14 days later. The drug control revealed formation of various birefringent crystal forms, the most frequent of which was represented by previously described B+C and D types [6]. When mixed to DNA, the sodium valproate induced disturbance in the textural patterns formed during DNA crystallization, promoting a discontinuous distribution of DNA birefringent crystals at the outer edge of the hemispheric structure formed during the drying of the drops. Changes in the patterned texture of the DNA intertwined crystal columns were also promoted by the valproate. The results suggest that besides affecting chromatin epigenetic marks, sodium valproate may affect the chiral supramolecular texture of the DNA.

References

1. S. Chateauvieux, F. Morceau, M. Dicato and M. Diederich, *J. Biomed. Biotechnol.*, 2010 (2010) 1.
2. J. Sargolzaei, A. Rabbani-Chadegani, H. Mollaei and A. Deezagi, *Int. J. Biol. Macromol.*, 99 (2017) 427.
3. B. C. Vidal and M. L. S. Mello, *Micron*, 102 (2017) 44.
4. M. L. S. Mello and B. C. Vidal, *PLoS ONE*, 7 (2012) e43169.
5. M. L. S. Mello and B. C. Vidal, *EUCMOS* (2018).
6. G. Petrusevski, P. Naumov, G. Jovanovski, G. Bogoeva-Gaceva and S. W. Ng, *ChemMedChem*, 3 (2008) 1377.

Acknowledgements: Financial support from FAPESP (grant no. 2015/10356-2); CNPq (grant no. 304668/2014-1).

**Structural, Spectroscopic and Microbiological Characterization of
Chalcone 2*E*-1-(2'-Hydroxy-3',4',6'-trimethoxyphenyl)-3-(phenyl)-prop-2-
en-1-one Derivative of the Natural Product
2-Hydroxy-3,4,6-trimethoxyacetophenone**

A. M. R. Teixeira^a, V. N. Lima^a, H. S. Santos^b, P. N. Bandeira^b, P. T. C. Freire^c, B. G. Cruz^a,
D. M. Sena Junior^a, H. D. M. Coutinho^a and M. S. S. Julião^b

^a Department of Biological Chemistry, Regional University of Cariri, Crato, CE, 63105-000, Brazil

^b Course of Chemistry, State University Vale do Acaraú, Sobral, CE, 62040-370, Brazil

^c Department of Physics, Federal University of Ceará, Fortaleza, CE, 60455-760, Brazil
amrteixeira@gmail.com

Chalcones and its derivatives are substances of great chemical and pharmacological interest and have received great attention due mainly to their relatively simple structure and exhibit a broad spectrum of biological properties, including antinociceptive, anti-inflammatory, antitumor, antibacterial, antifungal and antioxidant activity. It is worth mentioning that the synthesis of analogues and derivatives of natural products may enable the discovery of new active substances. This assertion corroborates with other reports in the literature that combine natural products with antibiotics against bacteria to decrease microbial resistance. Previous studies on antimicrobial and modulatory activities of the compound 2-hydroxy-3,4,6-trimethoxyacetophenone (C₁₁O₅H₁₄) isolated of the stem bark of *Croton anisodontus* [1] have shown that this natural acetophenone when associated with amikacin antibiotic showed synergism against *Pseudomonas aeruginosa* 03 and *Staphylococcus aureus* 358. In this work, we have synthesized a new chalcone 2*E*-1-(2'-Hydroxy-3',4',6'-trimethoxyphenyl)-3-(phenyl)-prop-2-en-1-one (C₁₈O₅H₁₈, hereafter named HYTPHENYL) by Claisen-Schmidt condensation between 2-hydroxy-3,4,6-trimethoxyacetophenone and benzaldehyde. Its structure was determined by Nuclear Magnetic Resonance and structurally characterized through Fourier transform Raman (FT-Raman) and Fourier transform infrared (FTIR) spectroscopy at room temperature in the regions 400 cm⁻¹ to 4000 cm⁻¹ and 25 cm⁻¹ to 4000 cm⁻¹, respectively. Vibrational wavenumber and wavevector have been predicted using the Density Functional Theory (DFT) calculations with the hybrid functional B3LYP and the basis set 6-31 G(d,p). The vibrational assignments of the HYTPHENYL chalcone were supported with the PED and discussed on basis of literature survey. Furthermore, we draw a comparison between the quantum chemical parameters of HYTPHENYL with other chalcones. Additionally, analysis of the antimicrobial activity and antibiotic resistance modulation was carried out to evaluate the antibacterial potential of the HYTPHENYL compound. Modulatory activities of the tested antibiotics were observed to HYTPHENYL compound against strains of *Escherichia coli* 27 and *Staphylococcus aureus* 358. Therefore, our results demonstrate that HYTPHENYL compound presents potential antimicrobial and may contribute to the control of bacterial resistance.

References

1. M. T. A. Oliveira, A. M. R. Teixeira, H. D. M. Coutinho, I. R. A. Menezes, D. M. Sena, Jr., H. S. Santos, B. M. de Mesquita, M. R. J. R. Albuquerque, P. N. Bandeira and R. Braz Filho. *Nat. Prod. Commun.*, 9 (2014) 665.

Acknowledgements: The authors thank the CENAPAD-SP for the use of the *Gaussian09* software package for computational facilities made available through the project “proj373” and the financial support from CNPq (Grant#: 303963/2015-8) and FUNCAP (Grant#: BP2-0107-00026.01.00/15).

Biochemistry of Hepatocytes in Non-Alcoholic Fatty Liver Disease studied by means of Raman Imaging

Adrianna Wislocka^a, Ewelina Szafraniec^b, Ewa Sierka^b, Edyta Kus^a, Stefan Chlopicki^c and Malgorzata Baranska^{a,b}

^a Jagiellonian Centre for Experimental Therapeutics (JCET), Bobrzynskiego 14, 30-348 Krakow, Poland

^b Jagiellonian University, Faculty of Chemistry, Gronostajowa 2, 30-397 Krakow, Poland

^c Jagiellonian University Medical College, Chair of Pharmacology, Grzegorzeczka 16, 31-531 Krakow, Poland
baranska@chemia.uj.edu.pl

Non-alcoholic fatty liver disease (NAFLD) is one of the most common, chronic medical conditions that people in well-developed countries are struggling with as a result of obesity and sedentary lifestyle. Despite its high prevalence, the knowledge on the pathogenesis of NAFLD is still incomplete. The mechanism underlying the developments and progression of NAFLD is complex, and various theories have been formulated. According to the ‘two hits theory’ dietary and environmental factors, lead to raised serum levels of free fatty acids (FFAs), cholesterol and development of insulin resistance. Hepatic FFAs flux leads to synthesis accumulation of triglycerides, what could represent a defensive mechanism to balance FFAs excess. However, the ‘toxic’ levels of fatty acids, free cholesterol and other lipid metabolites cause the mitochondrial dysfunction, endoplasmic reticulum stress, production of ROS, all leading to hepatic inflammation [1,2]. In order to understand better the mechanisms of NAFLD development various animal and *in vitro* models have been used [3].

Raman spectroscopy provides a specific chemical information and therefore allows fast identification of sample components. Combination of Raman spectroscopy with digital imaging enables precise identification of the molecular changes in the sample and also the determination of its location. Here we present a spectroscopic evaluation of changes in primary hepatocytes’ biochemistry induced by high fat diet in mouse dietary model. Raman imaging provides an insight into hepatic lipids accumulation achieved by the possibility to analyze hepatocytes’ lipid droplets composition, size and distribution. We were able to determine an increase in the degree of unsaturation of lipids forming lipid droplets due to the development of NAFLD. Considering the fact that our model is based on high fat diet containing in the majority saturated fat, we hypothesize that the increase in the content of unsaturated lipids originates from *de novo* lipogenesis and reflects the increased expression of stearoylCoA desaturase-1 (SCD-1) [4].

References

1. E. Buzetti, M. Pinzani and E. A. Tsochatzis, *Metabol.*, 65 (2016) 1038.
2. B. A. Neuschwander-Tetri, *Hepatology.*, 52 (2010) 774.
3. G. Kanuri and I. Bergheim, *Int. J. Mol. Sci.*, 14 (2013) 11963.
4. K. Kochan, E. Kus, E. Szafraniec, A. Wislocka, S. Chlopicki and M. Baranska, *Analyst.*, 142 (2017) 3948.

Acknowledgements: The authors thank the National Science Centre (NCN) for financial support in the framework of grant no. UMO-2015/16/W/NZ4/00070.

Label-Free Characterization of Acute Ischemic Stroke-Retrieved Clot Composition with Vibrational Spectroscopy

Aneta Blat^{a,b}, Jakub Dybas^{a,b}, Karolina Chrabaszcz^{a,b,c}, Katarzyna Bulat^a, Agnieszka Jasztal^a,
Tadeusz Popiela^d, Agnieszka Słowik^d, Stefan Chłopicki^{a,e}, Kamilla Malek^{a,b},
Mateusz G. Adamski^a and Katarzyna M. Marzec^{a,c}

^a Jagiellonian Center for Experimental Therapeutics, Jagiellonian University 14 Bobrzyńskiego St.,
30-348 Krakow, Poland

^b Faculty of Chemistry, Jagiellonian University, 3 Ingardena St., 30-060 Krakow, Poland

^c Center for Medical Genomics (OMICRON), Jagiellonian University Medical College, 7c Kopernika St.,
31-034 Krakow, Poland

^d Department of Neurology, Jagiellonian University Medical College, Kraków, Poland

^e Chair of Pharmacology, Jagiellonian University Medical College, Krakow, Poland
katarzyna.marzec@jcet.eu

The knowledge about the clot composition may provide information about stroke etiology what is crucial in the selection of the proper clinical treatment strategy [1,2]. The studies on the correlation between lysisability of the thrombus in acute ischemic stroke and its density¹ as well as histological, clinical and neurointerventional studies [2], were previously reported. Factors such as the location of the clot, its origin and size have an additional impact on the success of intravenous thrombolysis [3]. Previous clot studies with the application of CT and MRI suggested that those techniques have limited clinical diagnostic value [4,5]. Therefore there is a worldwide need for the innovative technology which could provide additional information regarding clot composition in non-invasive, label-free and objective manner.

Here we present the application of the vibrational spectroscopy (FT-IR and Raman spectroscopies) supported with the atomic force microscopy (AFM) and reference technique of the histological staining as a potential set of tools for the clot evaluation. We have previously reported the use of such set of techniques to the atherosclerotic plaque characterization [6]. Vibrational spectroscopy allowed for detection, visualization and differentiation of the various lipid content as well as areas of the fibrin and red blood cells (RBCs) accumulation. We have analyzed the erythrocyte rich clots as well as fibrin-predominant thrombi, and proofed the potential of vibrational spectroscopy in detection of potential prognostic biomarkers of clot origin.

References

8. P. Moftakhar, J. D. English, D. L. Cooke, W. T. Kim, C. Stout, W. S. Smith, C. F. Dowd, R. T. Higashida, V. V. Halbach and S. W. Hetts, *Stroke*, 44 (2013) 243.
9. T. Boeckh-Behrens, M. Schubert, A. Förchler, S. Prothmann, K. Kreiser, C. Zimmer, J. Riegger, J. Bauer, F. Neff, V. Kehl, J. Pelisek, L. Schirmer, M. Mehr and H. Poppert, *Clin. Neuroradiol.*, 26 (2016) 189.
10. I. K. Jang, H. K. Gold, A. A. Ziskind, J. T. Fallon, R. E. Holt, R. C. Leinbach, J. W. May and D. Collen, *Circulation*, 79 (1989) 920.
11. D. S. Liebeskind, N. Sanossian, W. H. Yong, S. Starkman, M. P. Tsang, A. L. Moya, D. D. Zheng, *et al.*, *Stroke*, 42 (2011) 1237.
12. K. H. Cho, J. S. Kim, S. U. Kwon, A. H. Cho and D. W. Kang, *Stroke*, 36 (2005) 2379.
13. K. M. Marzec, T. P. Wrobel, A. Rygula, E. Maslak, A. Jasztal, A. Fedorowicz, S. Chłopicki and M. Baranska, *J. Biophotonics*, 7 (2014) 744.

Acknowledgements: Financial support of the Polish National Science Centre (UMO-2016/23/B/ST4/00795) is greatly acknowledged.

Oxidative Damage of the Murine RBC Membrane in Advanced Atherosclerosis studied by Vibrational Spectroscopy and AFM Microscopy

Jakub Dybas^{a,b}, Aneta Blat^{a,b}, Katarzyna Bulat^a, Mateusz Mardyla^{a,c}, Małgorzata Baranska^{a,b},
Stafan Chlopicki^{a,d} and Katarzyna M. Marzec^{a,e}

^a Jagiellonian Centre for Experimental Therapeutics (JCET), Jagiellonian University, 30-348, Kraków, Poland

^b Faculty of Chemistry, Jagiellonian University, Gronostajowa 2, Krakow, Poland

^c Faculty of Motor Rehabilitation, University School of Physical Education, Jana Pawla 78,
31-571 Krakow, Poland

^d Chair of Pharmacology, Jagiellonian University Medical College, Krakow, Poland

^e Center for Medical Genomics (OMICRON), Jagiellonian University, Kopernika 7C, 31-034 Krakow, Poland
katarzyna.marzec@jcet.eu

The red blood cell (RBC) membrane is consisted of three basic components, including a lipid bilayer, transmembrane proteins and a cytoskeletal network [1]. Oxidative damage caused by various pathogenesis and environmental agents can lead to changes in any of these components, affecting RBCs deformability and shape leading in consequence to their decreased survivability [2]. Both, haemoglobin (Hb) enclosed within RBCs and RBC membrane are vulnerable to atherosclerotic lesions, including Hb oxidation and changes in lipid deposition, respectively [3]. Studies on RBC membrane are often conducted after fixation of RBCs with glutaraldehyde solution, whereas neither of it checked influence of such preparation on the molecular structure and the RBCs stiffness. In our work we studied the molecular structure of healthy and pathogenetic RBC membrane with the use of vibrational spectroscopy techniques (Raman and IR spectroscopies) whereas their stiffness with AFM microscopy.

The murine RBCs were obtained from whole blood of healthy (C57BL/6J) and atherosclerotic (ApoE/LDLR^{-/-}) mice models. The isolation of RBCs was assessed by gentle spinning in order not to damage RBCs membranes. After the isolation, RBCs were suspended in saline solution in hematocrit established to 10%. Part of RBCs were measured with and without fixation with application of IR, RS and AFM and some were kept frozen overnight (-20°C) to cause the hemolysis by growing saline crystals. To isolate RBCs membranes another centrifugation was performed. RBCs membranes were flushed, resuspended in saline solution and measured (with and without fixation) with the application of IR and RS. RBCs as well as isolated membranes were measured with the application of Raman spectroscopy with a use of 532 and 1064 nm laser wavelength. The FTIR measurements were performed in transmission mode as well as using attenuated total reflection Fourier transform infrared (ATR-FTIR) technique. AFM measurements were carried out on the monolayer of the RBCs prepared on CaF₂ windows and measured with the application of the DPFM and AC modes. Combination of vibrational spectroscopy with AFM microscopy allowed us to assess detailed information about changes of both biomechanical and mechanical alterations of atherosclerotic RBC membrane compering to the healthy control.

References

1. K. Kaushansky, M. Lichtman, J. Prchal, M. M. Levi, O. Press, L. Burns and M. Caligiuri, Eds., *Hematology*, McGraw-Hill Education, New York, 9th edn., 2016.
2. J. Kim, H. Lee and S. Shin, *J. Cell. Biotechnol.*, 1 (2015) 63.
3. V. Jeney, G. Balla and J. Balla, *Front. Physiol.*, 5 (2014) 379.

Acknowledgements: This work was supported by the Polish National Science Centre (UMO-2016/23/B/ST4/00795).

Dental Materials based on Stabilized Zirconia Ceramics

Marius Rada^b, An Pengfei^c, Mioara Zagrai^{a,b}, Simona Rada^{a,b},
Jing Zhang^c and Eugen Culea^a

^a Department of Physics & Chemistry, Technical University, Cluj-Napoca 400020, Romania

^b National Institute for Research & Development of Isotopic and Molecular Technologies,
Cluj-Napoca 400293, Romania

^c Beijing Synchrotron Radiation Facilities of Beijing Electron Positron Collider National Laboratory,
Beijing 100049, China
radasimona@yahoo.com

In the zirconia-based ceramics, the tetragonal and cubic ZrO₂ phases have generated considerable interest in the dental community due to their suitable and extraordinary properties (mechanical, electrical, catalytic and optical properties). The two polymorph forms of ZrO₂ are high-temperature modifications but they can be stable at room temperature after sintering by the addition of divalent and trivalent metal oxides.

The pure zirconia ceramics can move from the tetragonal to the monoclinic phase through a spontaneous stress-induced martensitic transformation when cooling from a high temperature to room temperature. This process is accompanied by an important variation in volume.

Zirconia, ZrO₂ exists as the monoclinic ZrO₂ phase for temperatures below 1170 °C and for room temperature. Tetragonal ZrO₂ crystalline phase is stabilized for temperatures ranging between 1170 and 2370 °C. The cubic ZrO₂ phase exists at temperatures greater than 2370 °C.

This paper presents the stabilization of the high temperature zirconia phases in the presence of Y₂O₃, SiO₂, Fe₂O₃ and MgO contents at room temperature after sintering. The aim is to determine correlations between changes in microstructure and the effect of the MgO contents. The investigation of the prepared ceramics was performed by using X-ray diffraction (XRD), X-ray Absorption Fine Structure (XAFS) studies, Fourier Transform Infrared (FTIR) and Electron Paramagnetic Resonance (EPR) spectroscopy.

Acknowledgements: This research was supported by the Bridge Program Projects 2016 (BG77/2016).

Stabilized Zirconia Ceramics with Additions of Y_2O_3 , SiO_2 , Fe_2O_3 and Na_2O Contents for Dental Applications

Simona Rada^{a,b}, Mioara Zagrai^{a,b}, Marius Rada^b, An Pengfei^c, Jing Zhang^c,
Adrian Bot^b and Eugen Culea^a

^a *Department of Physics and Chemistry, Technical University, Cluj-Napoca 400020, Romania*

^b *National Institute for Research & Development of Isotopic and Molecular Technologies,
Cluj-Napoca 400293, Romania*

^c *Beijing Synchrotron Radiation Facilities of Beijing Electron Positron Collider National Laboratory,
Beijing 100049, China
radasimona@yahoo.com*

The recent use of zirconia-based ceramics as restorative dental materials is highly desirable due to their excellent mechanical and thermal properties, including improved biocompatibility, wear resistance, high chemical durability and good transparency and color.

Zirconia, ZrO_2 is a polycrystalline ceramic without a glassy form and exists in three allotropic forms, namely the monoclinic, tetragonal and cubic phases, depending on the temperature. It exists in a monoclinic crystalline phase at room temperature and through sintering changes to tetragonal and cubic crystalline phases. Among these polymorph ZrO_2 phases, the tetragonal and cubic phases received considerable attention due to their wide applications including dental restorations. The main problem of the high temperature ZrO_2 phases consists in the reversion to a monoclinic state after sintering process by the cooling of either crystalline phase. The most common method of stabilizing the tetragonal and cubic crystalline phases at room temperature after sintering is by the adding of different dopants such as: Y_2O_3 , MgO , CaO , Al_2O_3 , SrO .

In this paper will be used two main methods to stabilize high temperature ZrO_2 crystalline phases, namely: *i.* the reduction of the crystallite size and *ii.* the use of different dopants. The aim of the present study is to investigate the influence of Y_2O_3 , SiO_2 , Fe_2O_3 and Na_2O in the stabilization of the high temperature zirconia ceramics. The investigation was performed by using X-ray diffraction (XRD), Fourier Transform Infrared (FTIR) and Electron Paramagnetic Resonance (EPR) spectroscopy. Also, the influence of iron ions and oxygen deficiency on the local structure of the prepared zirconia ceramics was examined by X-ray absorption fine structure (XAFS) studies.

Acknowledgements: This research was supported by the Bridge Program Projects 2016 (BG77/2016) and Mobility Projects 2017 (MC1008/2017).

Raman Laser Heating – the Effect in Dental Composite Materials

Matej Par^a, Nika Spanovic^b, Ruza Bjelovucic^b, Ozren Gamulin^c,
Eva Klaric Sever^a and Zrinka Tarle^a

^a University of Zagreb, School of Dental Medicine, Gunduliceva 5, 10000 Zagreb, Croatia

² Private Dental Practice, 10000 Zagreb, Croatia

^b University of Zagreb, School of Medicine, Salata 3b, 10000 Zagreb, Croatia
mpar@inet.hr

Raman spectroscopy is commonly used for evaluating the degree of conversion (DC) of C=C bonds in dental composites which generally comprise bifunctional methacrylate resins filled with glass particles [1]. DC is conveniently calculated from the change in the intensity of the C=C band at 1640 cm⁻¹ during composite polymerization, according to the equation: $DC = 1 - R_{cured}/R_{uncured}$, where $R = (\text{intensity at } 1640 \text{ cm}^{-1}) / (\text{intensity at } 1610 \text{ cm}^{-1})$. If DC is investigated immediately after light-curing while the post-cure polymerization is still occurring, the laser-induced heating may improve the mobility of reactive species in vitrified polymer, thereby increasing the measured DC. The effect of laser-induced heating in Raman spectroscopy has not been reported for dental composites, although it is recognized in various other compounds [2,3]. This study aimed to explore if varying the laser energy between 300 and 1000 mW would measurably affect DC assessed immediately after light-curing two dental composites: an established commercial composite (Tetric EvoCeram) and an experimental composite containing methacrylate resin and silanized barium glass. Raman spectra were collected using a FT-Raman spectrometer with an NdYAG laser excitation (1064 nm) using 40 scans, resolution of 4 cm⁻¹, exposed surface $\theta = 0.5$ mm, and $n = 10$ per experimental group. Mean DC values were compared among different levels of laser power using Welch ANOVA with Games-Howell post-hoc test. Increasing laser power improved the signal/noise ratio (Figure 1a) which was reflected as a decrease in data variability for Tetric EvoCeram but not for the experimental composite (Figure 1b-c). In both composites, a statistically significant increase in DC was measured with higher excitation power. The effect of laser heating should be taken into account in evaluations of the “immediate” DC in dental composites by Raman spectroscopy, as increasing the laser power in order to improve data quality may have an effect on obtained DC values.

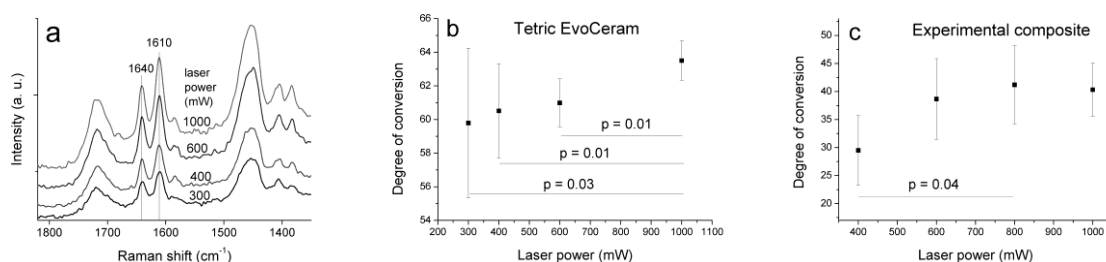


Figure 1 – Raman spectra (a) and mean (\pm s.d.) degree of conversion values (b-c) obtained by using laser power in the range of 300 – 1000 Mw.

References

1. V. Miletic and A. Santini, *J. Dent.*, 40 (2012) 106.
2. N. A. Marigheto, E. K. Kemsley, J. Potter, P. S. Belton and R. H. Wilson, *Spectrochim. Acta A: Mol. Biomol. Spectrosc.*, 52 (1996) 1571.
3. N. J. Everall, J. Lumsdon and D. J. Christopher, *Carbon*, 29 (1991) 133.

Effects of Bleaching Products Containing Fluoride on Tooth Enamel: Application of Polarized Raman Spectroscopy

S. Silva^{a,b}, J. M. Silveira^{a,c}, M. Fonseca^{b,d}, A. Amaral^{a,c}, H. Silva^{a,b}, A. Jesus^{a,b}, A. Mata^{a,c},
M. L. Carvalho^{a,b} and S. Pessanha^{a,b}

^a LIBPHYS – Laboratory of Instrumentation, Biomedical Engineering and Radiation Physics, Faculdade de Ciências e Tecnologia, Universidade Nova de Lisboa, 2829-516l Caparica, Portugal

^b Faculdade de Ciências e Tecnologia, Universidade Nova de Lisboa, 2829-516 Caparica, Portugal

^c Faculdade de Medicina Dentária, Universidade de Lisboa, 1649-003 Lisboa, Portugal

^d Universidade Europeia, Laureate International Universities, 1500-210 Lisboa, Portugal

sl.silva@campus.fct.unl.pt

In this study, polarized Raman spectroscopy was used to study the effects of whitening agents in human enamel. Tooth whitening products can change enamel mineral content, leading to demineralization [1]. In order to minimize this effect, new products incorporating fluoride (F) have appeared in the market. The fluoride is responsible for decreasing hydroxyapatite (HAp) solubility, promoting fluorapatite formation in enamel and dental erosion resistance [2]. Polarized Raman spectroscopy is sensitive to orientational and structural changes on enamel rods: for sound enamel, the Raman peak arising from the symmetric ν_1 vibration of PO_4^{3-} at 959 cm^{-1} is strongly polarized, while the spectra of demineralized enamel displays weaker polarization dependence. These variations can be quantified through the ratio of the integrated peak intensities of the 959 cm^{-1} peak detected with the analyzer oriented perpendicular to and parallel to the polarization direction of the linearly polarized laser light – depolarization ratio (ρ) [3].

This study aims to quantify the depolarization ratio of enamel samples before and after bleaching in the presence and absence of F to complement the analysis of the mechanical properties and elemental composition obtained by other non-destructive techniques (Vickers microhardness, gamma-induced gamma emission and X-ray fluorescence) and thus evaluate the protective potential of the element in the context of tooth whitening. Forty samples of human enamel were divided into groups and subject to bleaching products with carbamide peroxide (CP) or hydrogen peroxide (HP) as active agentes, fluoridated and non-fluoridated, and kept in human saliva between applications. For each sample, ρ was evaluated with a confocal Raman spectroscopy equipment on 20 different spots along its length and averaged.

This method has shown great sensitivity, pointing to its effectiveness in the quantification of enamel demineralization after bleaching. The combination of the results obtained by all techniques will likely clarify the degree of dental erosion and the role of F in dental whitening.

References

1. M. Alqahtani, *Saudi Dent. J.*, 26 (2014) 33.
2. J. M. Cate, *Acta Odontol. Scand.*, 57 (1999) 325.
3. Alex C.-T. Ko, L.-P. Choo-Smith, M. Hewko, M.G. Sowa, C.C.S. Dong and B. Cleghorn, *Opt. Express*, 14 (2006) 203.

The Biochemical and Spectroscopic Characteristic of Isolated and Cultured Eosinophils

Anna Ryguła^a, Marek Grosicki^{b,c}, Bożena Kukla^a, Patrycja Leszczenko^a, Dominika Augustynska^b, Kamilla Małek^a, Stefan Chłopicki^{b,d} and Małgorzata Baranska^{a,b}

^a Faculty of Chemistry, Jagiellonian University, Gronostajowa 2, 30-387, Kraków, Poland

^b Jagiellonian Centre for Experimental Therapeutics, Jagiellonian University, 30-348, Kraków, Poland

^c Department of Technology and Biotechnology of Drugs, Faculty of Pharmacy, Jagiellonian University Medical College, Medyczna 9, 30-688, Kraków, Poland

^d Chair of Pharmacology, Jagiellonian University Medical College, Grzegórska 16, 33-332, Kraków, Poland
baranska@chemia.uj.edu.pl

Eosinophils are acidophilic granulocytes developed in the bone marrow. Although their population contributes to approx. 2-6% of all white blood cells only, they possess a wide range of specific functions. These leucocytes play a key role in inflammation-regulating processes, including antiparasitic activity, bacterial and viral removal, antigen presentation, tumor immunity, the cross-talk between mast cells, dendritic cells and granulocytes, etc. In severe eosinophilia the amount of eosinophils is increased even above 5000 eosinophils per microliter of peripheral blood. Their characteristic feature is the presence of granules containing, among others, the eosinophils peroxidase (EPO), a highly cytotoxic cationic protein. Released EPO triggers a cascade of events promoting oxidative stress, leading finally to cell death through apoptosis or necrosis. The chromophore in EPO (protoporphyrin IX) makes it clearly detected using Raman spectroscopy. Another cell structures associated with inflammation are lipid bodies, the lipid-rich cytoplasmic inclusions, also well recognized and imaged in high resolution using Raman confocal spectroscopy.

In this work we compare eosinophils isolated from blood of human donors (Eos) and cultured cells, the established human eosinophilic leukemia cell line ('Eol-1'), being a well-known laboratory model of eosinophils. The main difference between Eos and Eol-1 cells is related to EPO. The Eos cells contain large amount of EPO, which is observed in the whole volume of cytoplasm, while Eol-1 cells do not show the presence of EPO. The influence of cell activation with PMA (phorbol 12-myristate 13-acetate) on creating of lipid bodies was also investigated. We present the spectroscopic and biochemical characteristics for eosinophils, both from the culture and isolated from blood, as well as a comparison between them.

Acknowledgements: The authors thank the National Science Centre (Poland) for financial support in the framework of grant and UMO-2016/22/M/ST4/00150.

Spectroscopic and Optical Properties of Silicone Hydrogel Contact Lenses

Sevgi Haman Bayarı^a, Akın Bacıoğlu^a, Tuğba Gocen^b and Ali Özenç Çavuş^a

^a Hacettepe University, Department of Physics Engineering, 06800 Ankara, Turkey.

^b Ahmet Erdogan Vocational School of Health Services 67100 Zonguldak, Turkey.

bayari@hacettepe.edu.tr

Contact lens, thin artificial lens worn on corneal surface of the eye to correct defects of vision. Silicone hydrogel contact lenses are advanced type of commercial soft contact lenses that allow more oxygen to pass through the lens to the cornea. Silicone hydrogels materials are usually prepared by the copolymerization of hydrophobic silicone containing monomers with hydrophilic monomers. This study was performed on new, unworn commercially available silicone-hydrogel contact lenses. Attenuated Total Reflectance Fourier Transform Infrared (ATR-FTIR) and Raman spectroscopy were used to obtain structural information of four different silicone hydrogel lens materials. The spectral transmittance properties of contact lenses are particularly important for visual performance level. The spectral transmittance and UV blocking properties of silicone-hydrogel contact lenses were measured by using a monochromator operating with the spectral range from 350 to 800 nm. Refractive index (RI) were calculated based on the analysis of transmittance (T) and/ reflectance (R) data of a samples.

Acknowledgements: This study is currently being supported by Research Fund of the Hacettepe University. Project Number 17084.

Raman Imaging Studies on Primary Cardiac Microvascular Endothelial Cells (CMECs)

Szymon Tott^a, Beata Klimas^a, Marek Grosicki^{b,c}, Dominika Augustyńska^c, Stefan Chłopicki^{c,d} and Małgorzata Barańska^{a,c}

^a Faculty of Chemistry, Jagiellonian University, Gronostajowa 2, 30-387, Kraków, Poland

^b Department of Technology and Biotechnology of Drugs, Faculty of Pharmacy, Jagiellonian University Medical College, Medyczna 9, 30-688, Kraków, Poland

^c Jagiellonian Centre for Experimental Therapeutics (JCET), Jagiellonian University, Bobrzyńskiego 14, Kraków, 30-348, Poland

^d Chair of Pharmacology, Jagiellonian University Medical College, Grzegórzecka 16, 33-332, Kraków, Poland
baranska@chemia.uj.edu.pl

Endothelium, the tissue forming the inner layer of all blood vessels in living organisms plays a variety of critical roles in the circulatory system. One of them is the regulatory activity of vascular endothelial cells. Cross-talk between cardiomyocytes and cardiac microvascular endothelial cells (CMECs) is crucial for maintaining cardiac homeostasis and autoregulation. Such communication, with the use of cardio-active factors like nitric oxide (NO), endothelin-1 (ET-1), prostaglandin (PGI-2) and growth factors, affects many myocardium functions [1]. There are many factors including oxidative, inflammatory and hemodynamic stress, infections, or diabetes which can affect this communication and finally lead to development of different cardiovascular disorders resulting in the appearance of cardiac pathologies such as heart failure. The crucial is the relation between endothelial dysfunction and development of diseases, which is still under investigation [2].

We present results of Raman imaging of CMECs, performed on primary isolated CMECs from murine hearts and transformed endothelial cell line from heart (H5V). Both primary CMECs and cell line has been stimulated with inflammatory cytokine, i.e. tumor necrosis factor alpha (TNF- α). The aim of our work was to compare primary cells, primary non-endothelial cells from heart and endothelial cell line in the context of their chemical composition. Primary CMECs are characterized by none or a few lipid droplets, in contrast to the cell line, which showed an ability to develop low-unsaturated lipid droplets. In turn, non-endothelial cells were characterized by high- unsaturated lipid droplets. Due to this feature it was possible to differentiate CMECs in the mixture of all cells isolated from the heart. Using Raman imaging we observed the markers of inflammation (*i.e.*, a formation of lipid droplets) and apoptosis (the changes in amounts of DNA/RNA). Stimulation of CMECs with TNF- α resulted in the emergence of inflammation and different stages of apoptosis.

References:

1. A. M. Shah, A. M. Shah, R. M. Grocott-Mason, C. B. Pepper, A. Mebazaa, A. H. Henderson, M. J. Lewis and W. J. Paulus, *Prog. Cardiovasc. Dis.*, 39 (1996) 263.
2. D. L. Brutsaert, *Physiol. Rev.*, 83 (2003) 59.

Acknowledgements: This work was supported by National Science Centre (Poland), on the basis of the decision No. DEC2015/16/W/NZ4/00070.

Thermal Effects in Skin Components Studied by ATR-IR Spectroscopy

S. Olsztyńska-Janus^a, A. Pietruszka^a, Z. Kielbowicz^b and M. A. Czarnecki^c

^a Department of Biomedical Engineering, Wrocław University of Science and Technology,
pl. Grunwaldzki 13, 50-370 Wrocław, Poland

^b Department of Surgery, Faculty of Veterinary Medicine, Wrocław University of Environmental
and Life Sciences, pl. Grunwaldzki 51, 50-366 Wrocław, Poland

^c Faculty of Chemistry, University of Wrocław, F. Joliot-Curie 14, 50-383 Wrocław, Poland
sylwia.olsztynska-janus@pwr.edu.pl

Temperature has an important effect on human body. Its variation leads to modifications in tissue components such as water, proteins and lipids. This work provides new results on temperature-induced changes in skin components. The changes were examined by ATR-IR spectroscopy since this technique provides detailed structural information at a molecular level. ATR-IR spectroscopy is a powerful tool in studying of vibrational bands of both highly polar groups (amide, OH) and hydrophobic groups of lipids (CH). Due to small depth of penetration (0.6–5.6 μm), ATR-IR spectroscopy probes only the outermost layer of the skin, *i.e.* the *stratum corneum* (SC).

Healthy skin used for this study is of porcine origin (Polish Landrace breed). Skin was provided by Department of Surgery, Faculty of Veterinary Medicine, Wrocław University of Environmental and Life Sciences, Wrocław, Poland. Removal of skin from Polish Landrace breed was approved by the *Local Ethical Committee for the Affairs of Experiments on Animals* of Wrocław University of Environmental and Life Sciences, Poland.

Heating of the skin samples from 20 to 90 °C induced two phase transitions in lipids. These transitions were observed in ATR-IR spectra as characteristic temperature dependencies of intensities and positions for $\nu_{\text{as}}(\text{CH}_2)$ and $\nu_{\text{s}}(\text{CH}_2)$ bands. The transition temperatures were determined by using two different methods. The first method was based on the first derivative of Boltzmann function and the second one employed the tangent lines of sigmoidal function. The phase transitions in lipids were correlated with modifications in the structure of water and proteins. Examination of the thermal effects on tissues is an important step towards better understanding of the molecular processes taking place during thermotherapy. The preliminary results on temperature effects on skin components have been published recently [1].

References

1. S. Olsztyńska-Janus, A. Pietruszka, Z. Kielbowicz and M.A. Czarnecki, *Spectrochim. Acta A*, 188 (2018) 37.

Acknowledgements: This work was supported by statutory funds of Department of Biomedical Engineering, Faculty of Fundamental Problems of Technology, Wrocław University of Science and Technology, Poland. Measurements were taken with ATR Accessory with Heated Diamond Top-plate compatible with NICOLET 6700 spectrometer (Thermo Scientific, USA) purchased under a grant for Scientific Research of Ministry of Education No 6180/IA/119/2012.

The Application of mREV Method in the Targeted Delivery of Cancer Therapeutics

D. Pentak, A. Ploch, A. Szkudlarek and M. Maciążek-Jurczyk

*Department of Physical Pharmacy, School of Pharmacy with the Division of Laboratory Medicine in Sosnowiec, Medical University of Silesia, Jagiellońska 4, 41-200 Sosnowiec, Poland
dpentak@sum.edu.pl*

Chemotherapy is the basic method of anti-cancer therapy. Due to the action of cytostatics causes numerous complications and organ damage. The variety of anticancer drugs mechanisms of action allows the use of multidrug therapies more effective than monotherapy. Unfortunately, the multidrug therapy in addition to high efficacy carries the risk of pharmaceuticals side effects. The use of nanostructures in the treatment of tumors is of great practical importance as it eliminates unwanted side effects at the stage of supply, absorption, transport and metabolism up to their excretion [1]. There are many techniques for obtaining nanostructures that allow the transport of medicinal substances. However, only a few of them are the methods allowing to obtain carriers with size up to 100 nm. The transport of medicinal substances in liposomes increases their stability and pharmacokinetic effect by lowering the elimination of the drug from the system and prolonging the half-life of the drug. The reversed – phase evaporation method (mREV) allows obtaining single-layer structures with size up to 100 nm [2]. The monolayeriness of obtained structures and their small size is of great practical importance as it facilitates the penetration of nanocarriers to the diseased site and drug rapid elimination.

The aim of the study was to use the mREV method in obtaining the liposomal form of doxorubicin (DOX) and cytarabine (AraC). Cytarabine and doxorubicin are the most common regimens used to treat non-Hodgkin's lymphoma. Spectrophotometry UV-Vis, differential scanning calorimetry (DSC) and NTA (Nanoparticle Tracking Analysis) were used in the research.

References

1. R. Sinha, G. J. Kim, S. Nie and D. M. Shin, *Mol. Cancer Ther.*, 5 (2006) 1909.
2. D. Pentak, *J. Nanopart. Res.*, 18 (2016) 1.

Acknowledgements: This work was supported by Grant KNW-1-034/K/8/O from the Medical University of Silesia, Poland.

Comparison of the Degree of Binding of Derivatives of 5-Alkyl-12 (H)-quin [3,4-b] [1,4] Benzothiazine Salts with Human Serum Albumin

A. Ploch^a, M. Maciążek-Jurczyk^a, D. Pentak^a, A. Szkudlarek^a and A. Zięba^b

^a*Department of Physical Pharmacy, School of Pharmacy with the Division of Laboratory Medicine in Sosnowiec, Medical University of Silesia, Jagiellońska 4, 41-200 Sosnowiec, Poland*

^b*Department of Organic Chemistry, School of Pharmacy with the Division of Laboratory Medicine in Sosnowiec, Medical University of Silesia, Jagiellońska 4, 41-200 Sosnowiec, Poland*

dpentak@sum.edu.pl

According to the latest statistics published by the World Health Organization, neoplastic diseases are the second most common cause of death in the world. It is estimated that in 2015 about 8.8 million people died of cancer, which is 17% of all deaths in the world. Nowadays, anticancer substances are one of the main subjects of research of many scientific teams. One of the compounds that have been tested for antitumor activity are derivatives of 5-alkyl-12(H)-quinoline[3,4-b][1,4]benzothiazine salts. These compounds were obtained by the reaction of thiochine aveninium salts with the corresponding arylamines. The antiproliferative activity of both preparaters was tested in vitro against the HCT 116 and LLC cancer cell lines. The aim of the study was to analyze the interaction of unmodified human serum albumin with derivatives of 5-alkyl-12(H)-quin[3,4-b][1,4]benzothiazine salts with potential anticancer properties. Human serum albumin (HSA) is a human plasma protein found with the highest concentration compared to its other components. It consists of 585 amino acid residues that make up 9 loops and 3 domains. HSA plays a key role in maintaining homeostasis. It demonstrates the ability to bind many endo- and exogenous ligands, including drugs, drug substances and their metabolites, fatty acids and vitamins, which affects their pharmacological effect. Using the fluorescence spectroscopy technique, the emission spectra of HSA fluorescence with a concentration of $5 \cdot 10^{-6}$ mol / dm³ were recorded without and in the presence of 5-methyl-12(H)chino[3,4-b]-1,4-benzothiazine chloride and a 9-fluoro-5-methyl-12(H)-chino[3,4-b]-1,4-benzothiazine with increasing concentration ($1 \cdot 10^{-5} \div 1 \cdot 10^{-4}$ mol/dm³). The fluorescence of the system was excited by the wavelengths at λ_{ex} 275 nm and λ_{ex} 295 nm. Based on the obtained results, it was found that both compounds form a complex with human serum albumin, however, 9-fluoro-5-methyl-12(H)-chino[3,4-b]-1,4-benzothiazine chloride more strongly quenches fluorescence protein, which has a greater therapeutic effect.

References

1. F. Yang, Y. Zhang and H. Liang, *Int. J. Mol. Sci.*, 15 (2014) 3580.
2. A. Zięba, A. Sochanik, A. Szurkoc, M. Rams, A. Mrozek and P. Cmoch, *Eur. J. Med. Chem.*, 45 (2010) 4733.

Acknowledgements: This work was supported by Grant KNW-1-034/K/8/O from the Medical University of Silesia, Poland.

Tailoring the Architecture of Charged Molecules to Enhance the Two-photon Brightness in Bioimaging

Inês F. A. Mariz, José M. G. Martinho and Ermelinda M. S. Maçôas

Centro de Química-Física Molecular and IN-Institute of Nanoscience and Nanotechnology, Instituto Superior Técnico, Universidade de Lisboa, Av. Rovisco Pais, 1049-001 Lisboa, Portugal
ines.mariz@tecnico.ulisboa.pt

Two-photon fluorescence microscopy is a common 3D-bioimaging method based on nonlinear excitation of fluorophores. The quadratic dependence of the TPA probability on the light intensity can confine absorption to a highly localized focal volume simultaneously allowing for a greater depth of penetration of light due to the use of longer wavelengths when compared to linear excitation [1]. Nevertheless, the development of better fluorophores is needed to reduce the excitation power and the associated photodamage

In our previous work, a charged molecule based on the quinolizinium cation was used as a single dye to stain all the compartments of living cells by means of fluorescence lifetime imaging microscopy (FLIM) [2]. In the present study, new fluorescent markers based on the quinolizinium and benzimidazolium cation have been designed aiming to increase the two-photon brightness and tuning the excitation and emission window for applications in bioimaging. One of these compounds have the unique properties of large Stokes shift (avoiding reabsorb of emitted photons which leads to undesired back-ground interferences), emission close to the near infrared range where the penetration of light in the tissues is greater (due to the low absorption of biological molecules in this region) and localized two-photon excitation avoiding photodamage of the tissues allowing further applications for in vivo imaging.

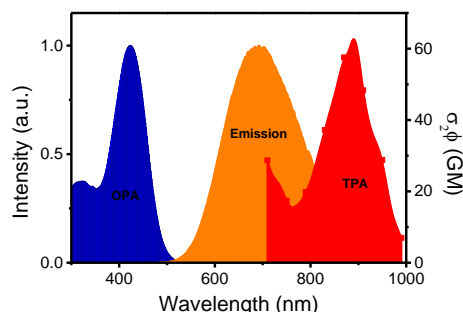


Figure1. Plot of one- (OPA) and two-photon absorption (TPA) and emission of one of the studied dyes.

References

1. G. S. He, L-S. Tan, Q. Zheng, P. N. Prasad, *Chem Rev.*, 108, 2008, 1245.
2. G. Marcelo, S. Pinto, T. Cañeque, I. F. A. Mariz, A. M. Cuadro, J. J. Vaquero, J. M. G. Martinho and E. M. S. Maçôas, *J. Phys. Chem. A* 119, 11, 2351.

Acknowledgements: This work was partially supported by Fundação para a Ciência e a Tecnologia (FCT-Portugal) (IF/00759/2013 and post-doc grant SFRH/BPD/75782/2011) and COMPETE (FEDER), project UID/NAN/50024/2013.

NIR and EPR Studies of the Effect of Inhaled Anesthetics on the Structure and Order of Model Lipid Bilayers

Marta Kuć, Agnieszka Lewińska, Katarzyna Cieřlik-Boczula and Maria Rospenk
Faculty of Chemistry, University of Wrocław F. Joliot Curie 14, 50-383 Wrocław, Poland
marta.kuc@chem.uni.wroc.pl

The NIR (Near-infrared Spectroscopy) and EPR (Electron Paramagnetic Resonance Spectroscopy) techniques were applied to study the structure and dynamic of DPPC (dipalmitoylphosphatidylcholine) bilayers incorporated by one of four inhalation anesthetics: enflurane, isoflurane, sevoflurane or halothane.

NIR spectra were obtained to analyzed changes occurring in hydrophobic part of lipid bilayers. The PCA analysis was applied to regions of NIR spectra associated with the first overtones of the symmetric and antisymmetric stretching vibrations of CH₂ groups of lipid aliphatic chains measured as a function of increasing anesthetic concentration in 25 degrees Celsius [1,2].

The 5-DSA (2-(3-carboxypropyl)-2-tridecyl-4,4-dimethyl-3-oxazolidinyloxy), 5-DSE (2-(4-Methoxy-4-oxobutyl)-4,4-dimethyl-2-tridecyl-3-oxazolidinyloxy) and 16-DSA (2-(14-Carboxytetradecyl)-2-ethyl-4,4-dimethyl-3-oxazolidinyloxy) were used as a spin probes for detection of modifications in both areas of lipid membranes: hydrophilic (5-DSA and 5-DSE) and hydrophobic (16-DSA) parts [3].

The EPR spectra revealed a differential broadening of three nitrogen hyperfine lines of nitroxyl spin probe indicating incorporation anesthetics drug into the interface layer.

Different locations of spin probes enabled an opportunity to deepen their insights into the local microenvironment of the bilayer study and determined parameters: τ_R – correlation time; I_1/I_0 – fluidity parameter; H – polarity index; S – ordering index [3-5].

For the 5-DSA and 5-DSE spin probes the decrease in correlation time and fluidity parameter and increase in ordering index were received. It was observed that halothane is the strongest modifier of hydrophilic region of model lipid membranes. Sevoflurane is the least effectively penetrated into the polar part of bilayers, while enflurane and isoflurane have indirect influence on structure of this area of DPPC membranes [6].

For the 16-DSA spin probe the parameters change were similar but much lower than in the case of 5-DSA and 5-DSE which allows us to conclude that studied anesthetics have stronger influence at the polar region of biomembranes rather than on their hydrophobic part [1,2,6].

References

1. M. Kuć, K. Cieřlik-Boczula and M. Rospenk, *Vibr. Spectrosc.*, 85 (2016) 55.
2. M. Kuć, K. Cieřlik-Boczula and M. Rospenk, *Spectrochim. Acta A: Mol. Biomol. Spectrosc.*, 186 (2017) 37.
3. A. Lewińska, M. Witwicki, R. Frąckowiak, A. Jezierski and K.A. Wilk, *J. Phys. Chem. B*, 116 (2012) 14324.
4. T. Koklic, *Chem. Phys. Lipids*, 183 (2014) 50.
5. I. Voszka, Z. Szabó, G. Csík, P. Maillard and P. Gróf, *J. Photochem. Photobiol. B: Biol.*, 79 (2005) 83.
6. B. W. Urban, M. Bleckwenn, M. Barann, *Pharmacol. Therapeut.*, 111 (2006) 729.

Acknowledgements: This work was supported by Ministry of Science and Higher Education, Poland, with a decision number of 0420/2647/17. The Authors also thank for funding this work from KNOW subsidy.

LIST OF PLENARY LECTURES

PL1 - Mischa Bonn (<i>Mainz, Germany</i>)	
Novel Molecular Terahertz Spectroscopies.....	31
PL2 - Wybren Jan Buma (<i>Amsterdam, The Netherlands</i>)	
Tailoring Photoactive Materials: Light on the Dark Side of the Force.....	39
PL3 - Robert J. McMahon (<i>Madison USA</i>) – and co-workers	
Rotational Spectroscopy, Molecular Structure Determination, and Radioastronomy.....	51
PL4 - Luca Evangelisti (<i>Bologna, Italy</i>)	
Investigation of Non-Covalent Interactions by Microwave Spectroscopy.....	71
PL5 - Harold Linnartz (<i>Leiden, The Netherlands</i>)	
Solid State Spectroscopy in Support of Interstellar Chemistry.....	81
PL6 - Eberhard Riedle (<i>Munich, Germany</i>)	
From Lasers to High Power LEDs, from Photochemistry to Photocatalysis.....	101
PL7 - Janina Diekmann (<i>Munich, Germany</i>) – and co-workers	
Photo-Addition of Psoralen to DNA Traced by Time Resolved Spectroscopy.....	111
PL8 – Klaus Gerwert (<i>Bochum, Germany</i>)	
Label-Free Tissue Classification by QCL based IR-Imaging.....	121

LIST OF KEYNOTE LECTURES

KL1 - André Peremans (<i>Namur, Belgium</i>) – and co-workers NLO at Interfaces: Sensitive Probing of Biomolecular Recognition by Sum Frequency Generation and the Quest of Super Resolution IR Microscopy of Biological Tissues.....	32
KL2 - Tito Trindade (<i>Aveiro, Portugal</i>) Developing the Surface Chemistry of Hybrid Nanomaterials for SERS.....	33
KL3 - José M. G. Martinho (<i>Lisbon, Portugal</i>) – and co-workers Biphotonic Materials for Bioimaging.....	43
KL4 - Martin A. Suhm (<i>Göttingen, Germany</i>) Vibrational Spectroscopy at the Service of Quantum Chemistry.....	52
KL5 - Nigel A. Young (<i>Hull, UK</i>) – and co-workers Matrix Isolation Studies of Transition Metal and Main Group Fluorides.....	53
KL6 - Igor Reva (<i>Coimbra, Portugal</i>) Calculations of Spectra and Kinetics in the Context of Matrix Isolation.....	54
KL7 - Nikolay Kotov (<i>Prague, Czech Republic</i>) – and co-workers Investigation of Phase-Behavior of an Ionic Liquid at Sub-Zero Temperatures in the Presence of Additives.....	55
KL8 - Mike N. R. Ashfold (<i>Bristol, UK</i>) Exploring Photoinduced Bond Fissions in the Gas and Solution Phase.....	59
KL9 - Cláudio M. Nunes (<i>Coimbra, Portugal</i>) – and co-workers Spectroscopic Observation of Quantum Tunneling: Discoveries on the Potential Energy Surfaces of Phenylnitrenes.....	60
KL10 - Anna Gudmundsdottir (<i>Cincinnati, USA</i>) Using Transient Spectroscopy to Understand Photosensitive Behavior of Vinyl Azides Crystals.....	61
KL11 - Jan Lundell (<i>Jyväskylä, Finland</i>) Vibrational Excitation Induced Chemistry.....	65
KL12 - Elangannan Arunan (<i>Bangalore, India</i>) – and co-workers Microwave Spectroscopic Investigations on Large Amplitude Motions: Intermolecular Bonding in Ar-(H ₂ O) ₂ , (H ₂ S) ₂ and CH ₃ CN-CO ₂	66
KL13 - José Luis Alonso (<i>Valladolid, Spain</i>) – and co-workers Laboratory Millimeter and Submillimeter Wave Studies of Interstellar Molecules.....	67
KL14 - Otto Dopfer (<i>Berlin, Germany</i>) Geometric and Electronic Structure of Flavins.....	72

KL15 - Leonardo Álvarez-Valtierra (<i>León, Mexico</i>) – and co-workers Towards High Resolution Phosphorescence Spectroscopy.....	73
KL16 - Michael Schmitt (<i>Düsseldorf, Germany</i>) Excited State Dipole Moments from High Resolution Spectroscopy.....	75
KL17 - Elena R. Alonso (<i>Valladolid, Spain</i>) – and co-workers The Gas Phase Study of Artificial Sweeteners: Structure-Sweetness Connection.....	76
KL18 - Andrzej L. Sobolewski (<i>Warsaw, Poland</i>) Burning Water with Sunlight: insights from Computational Chemistry.....	82
KL19 - Michael I. Oshtrakh (<i>Ekaterinburg, Russian Federation</i>) – and co-workers Ordinary Chondrites: What Can We Learn Using Mössbauer Spectroscopy?.....	83
KL20 - Frédéric Merkt (<i>Zurich, Switzerland</i>) – and co-workers Precision Spectroscopy in Cold Samples of Few-Electron Molecules.....	89
KL21 - Anders Engdahl (<i>Lund, Sweden</i>) – and co-workers Pre-Plaque Conformational Changes in Alzheimer’s Disease-Linked A β and APP.....	95
KL22 - Mustafa Çulha (<i>Istanbul, Turkey</i>) – and co-workers Surface-Enhanced Raman Scattering: A Potential Technique to Study Living Single Cells.....	102
KL23 - Marco van de Weert (<i>Copenhagen, Denmark</i>) The Trials and Tribulations of Becoming a Spectroscopy Specialist.....	112
KL24 - Markus Arndt (<i>Wien, Austria</i>) New Avenues for Matter-Wave Assisted Spectroscopy.....	113
KL25 - Nancy Pleshko (<i>Philadelphia, USA</i>) Non-Destructive Applications of Infrared Spectroscopy for Assessment of Tissue Pathology and Regeneration.....	122
KL26 - Hugh J. Byrne (<i>Dublin, Ireland</i>) – and co-workers Advancing Raman Microspectroscopy for Cellular and Subcellular Analysis: Towards In vitro High Content Spectralomic Analysis.....	123
KL27 - Herbert Michael Heise (<i>Iserlohn, Germany</i>) Infrared Spectroscopy for Clinical Chemistry and Medical Diagnostics - Techniques and Chemometrics for a Successful Marriage of Two Fields.....	124
KL28 - Luís G. Arnaut (<i>Coimbra, Portugal</i>) Spectroscopic Determinants in Photodynamic Therapy.....	125
KL29 - Henry Horst Mantsch (<i>Ottawa, Canada</i>) Spectroscopy in the 21 st Century: The Future of Molecular Spectroscopy.....	126

LIST OF ORAL COMMUNICATIONS

OC1 - Andrzej Kudelski (<i>Warsaw, Poland</i>) Plasmonic Nanoparticles with Many Sharp Apexes and Edges as Efficient Nanoresonators for Shell-Isolated Nanoparticle-Enhanced Raman Spectroscopy.....	34
OC2 - Veronika Sutrová (<i>Prague, Czech Republic</i>) – and co-workers Ag Nanosponge Aggregate with Incorporated Hydrophobic Adsorbates as a Sample for Effective SER(R)S Spectral Detection.....	35
OC3 - Daria Ruth Galimberti (<i>Paris, France</i>) – and co-workers Molecular Organization at Charged Solid-Water Interfaces: vSFG $\chi(2)(\omega)$ signal, $\chi(3)(\omega)$ Contribution and How to Use Them for Revealing Interfacial Structures.....	36
OC4 - Paula C. Pinheiro (<i>Aveiro, Portugal</i>) – and co-workers Magneto-Plasmonic Nanoparticles for Separation and SERS Detection of Antibiotics.....	37
OC5 - Petr Praus (<i>Prague, Czech Republic</i>) – and co-workers Metal-Enhanced Fluorescence of Riboflavin Deposited on Spacer-Modified Ag Substrate: Spectral Intensity and Lifetime Study.....	38
OC6 - Monika Plass (<i>Horgen, Switzerland</i>) – and co-workers Thermal Degradation Behaviour of Elastomers.....	40
OC7 - Sven P. K. Koehler (<i>Manchester, UK</i>) – and co-workers Characterisation, Coverage, and Orientation of Functionalised Graphene using Sum-Frequency Generation Spectroscopy.....	41
OC8 - Terao Wakana (<i>Tsukuba, Japan</i>) – and co-workers Detection of Boson Peak and Fracton of Sodium Carboxymethyl Starch by Terahertz Time-Domain Spectroscopy.....	42
OC9 - Sylvia Turrell (<i>Villeneuve d'Ascq, France</i>) – and co-workers The What, How and Where in Art and Archaeology: Use of Raman Spectroscopy for the Study of Ceramics, Glasses and Porcelains.....	44
OC10 - Yasmine Schulenburg (<i>Krefeld, Germany</i>) – and co-workers Analysis of the Historical Collection of Dyes at the Hochschule Niederrhein Using Infrared Spectroscopy.....	45
OC11 - Dhanya Puthenmadom (<i>Seneffe, Belgium</i>) – and co-workers Fourier Transform-Infrared Microscopic Investigation of Cysteic Acid in Virgin and Damaged Hair.....	46
OC12 - Lucia Bonoldi (<i>S. Donato Milanese, Italy</i>) – and co-workers Thermal Maturity of Organic Matter from Fossil Fuel Fields by Raman Spectroscopy: Spectral Parameters and Chemometric Data Treatment.....	47

OC13 - Joanna Hetmańczyk (<i>Krakow, Poland</i>) – and co-workers Phase Transition, Structure and Reorientational Dynamics of H ₂ O Ligands and ReO ₄ ⁻ Anions in [Ba(H ₂ O) ₄](ReO ₄) ₂	56
OC14 - Ivan S. Giba (<i>St. Petersburg, Russian Federation</i>) – and co-workers Spectral Diagnostics of Hydrogen Bonds by ³¹ P NMR Chemical Shifts.....	57
OC15 - Eva Scholtzová (<i>Bratislava, Slovakia</i>) – and co-workers Beidellite Intercalates and their Characterization by Means of DFT Method.....	58
OC16 - Julien Guthmuller (<i>Gdąnsk, Poland</i>) Theoretical Investigation of Herzberg-Teller Effects in Resonance Raman Spectra.....	62
OC17 - Kess M. Marks (<i>Stockholm, Sweeden</i>) – and co-workers Sum Frequency Generation Spectroscopy Studies of Temperature Dependent Naphthalene Dehydrogenation on Nickel (111).....	63
OC18 - Lucia Kiyomi Noda (<i>Diadema, Brazil</i>) – and co-workers Assignment of the Electronic Transition of Phenothiazine Radical Cation in the Visible Region – A Resonance Raman Spectroscopy and Theoretical Calculation Investigation.....	64
OC19 - Sérgio R. Domingos (<i>Hamburg, Germany</i>) – and co-workers Sensing Chirality with Rotational Spectroscopy: from Enantiomer Differentiation to Molecular Recognition.....	68
OC20 - Thomas E. Wall (<i>London, UK</i>) – and co-workers Mid-IR Detection and Spectroscopy of Polyatomic Molecules inside a Cryogenic Buffer Gas Cell.....	69
OC21 - György Tarczay (<i>Budapest, Hungary</i>) The Role of Matrix Isolation Spectroscopy in Conformational Studies of Small and Medium Sized Biomolecules.....	70
OC22 - Mirko Lindic (<i>Düsseldorf, Germany</i>) – and co-workers Dipole Moments of Anisole in Ground and Excited State via Condensed Phase Thermochromic Spectroscopy and Gas Phase HRLIF Spectroscopy.....	74
OC23 - América Torres-Boy (<i>León, Mexico</i>) – and co-workers Analysis of the Rotationally Resolved Electronic spectra of 3CI and its Water Cluster through Genetic Algorithms.....	77
OC24 - Irina Alenkina (<i>Ekaterinburg, Russian Federation</i>) - and co-workers Characterization of the Iron Core in Ferrifol [®] , a Pharmaceutical Analogue of Ferritin, Using Mössbauer Spectroscopy and Magnetization Measurement.....	84
OC25 - Jorge Costa Pereira (<i>Coimbra, Portugal</i>) – and co-workers Excitation-Emission Fluorescence Analysis: Resolving Relevant Underlying Contributions.....	85

OC26 - Bence Kutus (<i>Szeged, Hungary</i>) – and co-workers The Hydrolysis of Mg^{2+} Ions in the Presence of Gluconate.....	86
OC27 - Seoncheol Cha (<i>Mainz, Germany</i>) – and co-workers Correlation of Hydrogen-Bonding and Catalytic Activity for Diol-based Asymmetric Organocatalysts.....	87
OC28 - Svetlana S. Khokhlova (<i>Volgograd, Russian Federation</i>) – and co-workers Fluorescence Quenching of Xanthone and Xanthione Derivatives in Protic and Aprotic Solvents.....	88
OC29 - Franco Egidi (<i>Pisa, Italy</i>) – and co-workers New Avenues for Computational Chiral Spectroscopy.....	90
OC30 - Bernardo de Souza (<i>Florianópolis, Brazil</i>) – and co-workers Predicting Excited State Dynamics from Scratch – a Path Integral Approach Implemented on ORCA.....	91
OC31 - Malgorzata Biczysko (<i>Shanghai, China</i>) – and co-workers Simulation of Fully Anharmonic Vibrational Spectra of Biomolecular Building Blocks.....	92
OC32 - Elena Yu. Tupikina (<i>St. Petersburg, Russian Federation</i>) – and co-workers 3D Outer Electronic Shell Visualizaton by Laplacian of a Helium Chemical Shift.....	93
OC33 - Marco Mendolicchio (<i>Pisa, Italy</i>) – and co-workers The MSR Route to Accurate Equilibrium Molecular Structures through the Semi-Experimental Approach.....	94
OC34 - Katarzyna M. Marzec (<i>Krakow, Poland</i>) – and co-workers Raman, FT-IR, AFM and Complementary Techniques in Studies of the Biochemical, Mechanical and Functional Alterations in Red Blood Cells.....	96
OC35 - Martynas Velicka (<i>Vilnius, Lithuania</i>) – and co-workers ATR-FTIR Spectroscopy: Towards In vivo Detection of Cancerous Tissue Areas.....	97
OC36 - Czesława Paluszkiewicz (<i>Krakow, Poland</i>) – and co-workers Vibrational Studies of Salivary Glands Tissues.....	98
OC37 - Maciej Roman (<i>Krakow, Poland</i>) – and co-workers Raman Spectroscopy of Urine Extracellular Vesicles in Diabetic Patients.....	99
OC38 - Ewelina Szafraniec (<i>Krakow, Poland</i>) – and co-workers Raman Imaging Study of Lipid Droplets in Liver Sinusoidal Endothelial Cells upon Non-Alcoholic Fatty Liver Disease Progression.....	100

OC39 - Mirosław A. Czarnecki (<i>Wrocław, Poland</i>) – and co-workers Microheterogeneity in Binary Mixtures: Spectroscopic and Chemometric Studies.....	103
OC40 - Omar A. El Seoud (<i>São Paulo, Brazil</i>) Perichromism: A Successful Approach for Probing Molecular Interactions in Different Media.....	104
OC41 - Helena Nogueira (<i>Aveiro, Portugal</i>) – and co-workers Raman Imaging in SERS Studies of Silver Loaded Textiles.....	105
OC42 - Ivan Němec (<i>Prague, Czech Republic</i>) – and co-workers Vibrational Spectroscopic Study of NLO Molecular Crystals Based on Aminopyrimidinium Salts.....	106
OC43 - Simona Rada (<i>Cluj-Napoca, Romania</i>) – and co-workers The Optimization of the Recycled Lead with Manganese Dioxide Contents for Applications in Automobile Batteries.....	107
OC44 - Alberto Mezzetti (<i>Paris, France</i>) – and co-authors Photoprotective Mechanisms in Photosynthesis Studied by Time-Resolved FTIR Difference Spectroscopy.....	114
OC45 - Valery Andrushchenko (<i>Prague, Czech Republic</i>) VCD Spectroscopy of Nucleic Acid Supramolecular Structures.....	115
OC46 - Tatsuya Mori (<i>Tsukuba, Japan</i>) – and co-workers Detection of Fractal Dynamics of Protein by Terahertz Spectroscopy.....	116
OC47 - Jakub Kaminsky (<i>Prague, Czech Republic</i>) – and co-workers Structure and Interactions of Saccharides Studied by Vibrational Optical Activity Methods.....	117
OC48 – Maria de Lurdes Cristiano (<i>Faro, Portugal; Coimbra, Portugal</i>) – and co-workers Saccharinate-based Ligands: Structure, Reactivity and Properties.....	118

LIST OF POSTERS

P1.1 - Natasha Trendafilova (<i>Sofia, Bulgaria</i>) – and co-workers Excited State Energy Mechanism and Luminescent Properties of Eu(III) Complex with Phenanthroline - Theoretical and Experimental Study.....	131
P1.2 - Anton Georgiev (<i>Sofia, Bulgaria</i>) – and co-workers Synthesis, Photophysical Properties and DFT Quantum Chemical Calculations of Novel Azo Diketopyrrolopyrrole Dyes.....	132
P1.3 - Sandra M. V. Pinto (<i>Pisa, Italy</i>) – and co-workers Quantum Chemical Characterization of the IR Spectra of <i>E</i> - and <i>Z</i> -Ethanamine and its Isotopes	133
P1.4 - Anton Gatial (<i>Bratislava, Slovakia</i>) – and co-workers Conformational Studies of 3-Cyclopropylaminomethylene-pentane-2,4-dione Using Vibrational and NMR Spectra, and Ab initio Calculations.....	134
P1.5 - Güneş Süheyla Kürkçüoğlu (<i>Eskişehir, Turkey</i>) – and co-workers Density Functional Theory Approaching on Structural Analysis of New Tetramer Barbiturate Molecule.....	135
P1.6 - Alice Balbi (<i>Pisa, Italy</i>) – and co-workers Structural, Spectroscopic and Energetic Properties of Creatinine Conformers by Quantum-chemical Calculations.....	136
P1.7 - Magdalena Staniszewska (<i>Gdansk, Poland</i>) – and co-workers Theoretical Investigation of the Electron Transfer Dynamics in a Hydrogen-Evolving Ru-Pd Molecular Photocatalyst.....	137
P1.8 - Dovilė Lengvinaitė (<i>Vilnius, Lithuania</i>) – and co-workers Structure and NMR Properties of Acetic Acid/Cyclohexane Binary Solutions Studied Using Molecular Dynamics/Quantum Mechanics Approaches.....	138
P1.9 - Güneş Süheyla Kürkçüoğlu (<i>Eskişehir, Turkey</i>) – and co-workers A Theoretical Study on Molecular Structures and Vibrational Spectra of Cyanide Complexes with 1,2-Dimethylimidazole: $[M(dmi)_2Ni(\mu-CN)_4]_n$ ($M = Cu, Zn$ or Cd).....	139
P1.10 - Güneş Süheyla Kürkçüoğlu (<i>Eskişehir, Turkey</i>) – and co-workers A Theoretical Study on the Molecular Structure and Vibrational Spectra of Homonuclear Cyanide Complex of $[Ni(etim)_4Ni(\mu-CN)_2(CN)_2]_n$	140
P1.11 - Potlaki F. Tseki (<i>Mthata, South Africa</i>) Coordinative Bonding Perturbation of some First Series Transition Metal Ions by the Glycine Ligand.....	141
P1.12 - Ines Despotović (<i>Zagreb, Croatia</i>) Computational Insight into the PNP-Lariat Ether Complexes with Some Alkali and Alkaline Earth Metal Cations.....	142

P2.1 - Susy Lopes (<i>Coimbra, Portugal</i>) – and co-workers Formic Acid Dimers in a Nitrogen Matrix.....	147
P2.2 - Jussi Ahokas (<i>Jyvaskyla, Finland</i>) – and co-workers Raman Spectroscopy of Matrix Isolated Complex between Glycolic Acid and Nitrogen: High Overtone Induced Isomerization	148
P2.3 - Rasa Platakyte (<i>Vilnius, Lithuania</i>) – and co-workers Study of Acetylsalicylic Acid by the Means of Matrix Isolation.....	149
P2.4 - Magdalena Pagacz-Kostrzewa (<i>Wroclaw, Poland</i>) – and co-workers Photochemistry of Matrix-Isolated 3-(Tetrazol-5-yl)aniline.....	150
P2.5 - Magdalena Sałdyka (<i>Wroclaw, Poland</i>) Photochemistry of Acetohydroxamic Acid in Solid Argon. FTIR and Theoretical Studies.....	151
P2.6 - Sandra M. V. Pinto (<i>Pisa, Italy/ Coimbra, Portugal</i>) – and co-workers UV-Induced Conformational Isomerization Study of Matrix-Isolated 2-Amino-5-Chlorobenzoic Acid	152
P2.7 - Justyna Krupa (<i>Wroclaw, Poland</i>) – and co-workers Structural and Spectroscopic Properties of Weak Complexes of Atmospheric Relevance.....	153
P2.8 - Iwona Kosendiak (<i>Wroclaw, Poland</i>) – and co-workers FTIR, DFT and MP2 Studies on Glycolic Acid Nitrogen Complexes.....	154
P2.9 - Julia A. Davies (<i>Leicester, UK</i>) – and co-workers IR Spectroscopy of Acetic Acid Dimers in Helium Nanodroplets.....	155
P2.10 - Sándor Góbi (<i>Coimbra, Portugal</i>) – and co-workers Chemistry Triggered by Infrared Vibrational Excitation – A Case Study of Thiourea.....	156
P2.11 - György Tarczay (<i>Budapest, Hungary</i>) – and co-workers Jet-Cooled Laser Induced Fluorescence and Dispersed Fluorescence of $\text{CH}_x\text{F}_3-x\text{CH}_2\text{O}$ ($x=1, 2, 3$) Radicals.....	157
P2.12 - Ahmed K. Sakr (<i>Hull, UK</i>) – and co-workers Matrix Isolation Studies of Nickel Fluorides.....	158
P2.13 - José Arturo Ruiz-Santoyo (<i>León, Mexico</i>) – and co-workers Rotationally Resolved Electronic Spectrum of N-MethylCarbazole in the Gas Phase: A Study of Methyl Group Internal Rotation.....	159
P2.14 - Michael Schneider (<i>Düsseldorf, Germany</i>) – and co-workers Rotationally Resolved Electronic Stark Spectroscopy of 3-Cyanoindole and the 3-Cyanoindole- Water Complex.....	160

P2.15 - Marie-Luise Hebestreit (<i>Düsseldorf, Germany</i>) – and co-workers Observation of 1,2-, 1,3- and 1,4-Dimethoxybenzenes via High Resolution Laser Induced Fluorescence Stark Spectroscopy.....	161
P2.16 - Christian Henrichs (<i>Düsseldorf, Germany</i>) – and co-workers Electronic Spectra of 1,2 Dimethoxybenzene.....	162
P2.17 - Rômulo A. Ando (<i>São Paulo, Brazil</i>) – and co-workers Photophysics of 2-[4-(Dimethylamino)benzylidene]malononitrile in Ionic Liquids Probed by Time Resolved Infrared Spectroscopy.....	163
P2.18 - Hartmut Borchert (<i>Saint Louis, France</i>) – and co-workers Time Resolved Spectroscopic Temperature Measurement Techniques During CW-Laser Matter Interaction of Glass-Fiber-Reinforced-Polymers (GFRP).....	164
P2.19 - Anuradha Das (<i>Bern, Switzerland</i>) – and co-workers Ultrafast Transient Absorption Spectroscopy: Probing the Excited State Dynamics of Charge Transfer Reactions in Ionic Deep Eutectic Solvents.....	165
P2.20 - Nataliia Kuzkova (<i>Berlin, Germany</i>) – and co-workers Photoinduced Relaxation Dynamics of Ferricyanide Ion Dissolved in Ionic Liquid Studied by Ultrafast XUV Photoelectron Spectroscopy.....	166
P2.21 - Julia Stachowiak (<i>Göttingen, Germany</i>) – and co-workers Intermolecular Energy Balances based on Acetophenone.....	167
P2.22 - Caroline Stelbrink (<i>Göttingen, Germany</i>) – and co-workers Contest of Molecular Noses: Chirality Recognition between α -Pinene and Alcohols.....	168
P2.23 - Elisa M. Brás (<i>Faro/Coimbra, Portugal</i>) – and co-workers Photochemistry of a Matrix Isolated Dispiro-1,2,4- Trioxolane: Criagee Intermediate Formation and Ring Expansion.....	169
P2.24 - Timur Nikitin (<i>Coimbra, Portugal</i>) – and co-workers Matrix Isolation Study of Fumaric and Maleic Acids in Solid Nitrogen.....	170
P2.25 - António J. Lopes Jesus (<i>Coimbra, Portugal</i>) – and co-workers Conformational Control of an Aldehyde Fragment by Selective Vibrational Excitation of Interchangeable Remote Antennas.....	171
P2.26 - Tania Kataeva (<i>Saint Petersburg, Russian Federation</i>) – and co-workers Regularities in the Manifestation of Resonance Dipole-Dipole Interaction in the Spectra of Low-Temperature Condensed Molecular Systems.....	172
P3.1 - Elzbieta Chelmecka (<i>Katowice, Poland</i>) – and co-workers Theoretical and Experimental Studies on Sulindac.....	177

P3.2 – Matthias Zajonz (<i>Düsseldorf, Germany</i>) – and co-workers Determination of Dipole Moments in the Electronically Excited State of Quinoxaline <i>via</i> Thermochromic Methods.....	178
P3.3 - Seda G. Sagdinc (<i>Kocaeli, Turkey</i>) – and co-workers The Study of Vibrational Spectroscopies for 5-Bromo-2-oxindole (5Br2O) Dimer.....	179
P3.4 - Seda G. Sagdinc (<i>Kocaeli, Turkey</i>) – and co-workers Spectroscopic (FT–IR, FT–Raman, UV–Vis) Analysis on Monomeric and Dimeric Structures of 4–Pyridazinecarboxylic Acid by HF and DFT Methods.....	180
P3.5 - Silvia A. Brandán (<i>Tucumán, Argentina</i>) – and co-workers Structural and Vibrational Investigation on Alkaloid Scopolamine Hydrobromine by Using their FTIR and FT-Raman Spectra.....	181
P3.6 - Güneş Süheyla Kürkçüoğlu (<i>Eskişehir, Turkey</i>) – and co-workers A Theoretical and Experimental Investigation of Vibrational Spectra and Electronic Transitions on 2-Pyridineethanol and 2-Pyridinemethanol.....	182
P3.7 - Ana E. Ledesma (<i>Santiago del Estero, Argentina</i>) – and co-workers Thermal <i>Trans-Cis</i> Isomerization of Cloro-Azobenzene System.....	183
P3.8 - Sergio A. Romero-Servín (<i>León, Mexico</i>) – and co-workers Photoreduction Study of Benzophenone in Condensed Phase.....	184
P3.9 - Barbara Golec (<i>Warsaw, Poland</i>) – and co-workers Combined Effect of Hydrogen Bonding Interactions and Freezing of Rotameric Equilibrium on the Enhancement of Photostability.....	185
P3.10 - Yukihiro Shimoi (<i>Tsukuba, Japan</i>) – and co-workers Photorelaxation Processes in Dipyriddypolyenes.....	186
P3.11 - Juana Bellanato (<i>Madrid, Spain</i>) – and co-workers Synthesis and Conformational Study of Alcohols Derived from 3-Methyl-3-aza-bicyclo[3.3.1]nonane.....	187
P3.12 - Elżbieta Bednarek (<i>Warsaw, Poland</i>) – and co-workers Identification and Structural Characterization of Novel Synthetic Cathinones.....	188
P3.13 - Marek Drozd (<i>Wroclaw, Poland</i>) – and co-workers Molecular Complex of Guanidinium Trichloracetate. Resumption X-ray and Theoretical DFT Studies.....	189
P3.14 - Elzbieta Chelmecka (<i>Katowice, Poland</i>) – and co-workers Hisrhfeld Surface Analysis, Spectroscopic Measurements & DFT Calculated Study of Dacarbazine (DTIC).....	190

P3.15 - István Pálkó (<i>Szeged, Hungary</i>) – and co-workers The Aggregation Behaviour of 2 <i>H</i> -Imidazole-2-thione Derivatives in the Solid State.....	191
P3.16 - Rasa Platakytė (<i>Vilnius, Lithuania</i>) – and co-workers Conformational Equilibrium of Imidazolium-Based Ionic Liquids, Effect of Water, Temperature and Counter Anions.....	192
P3.17 - Shen-Yuan Tzeng (<i>Taipei, Taiwan</i>) – and co-workers Mass-Analyzed Threshold Ionization Spectroscopy of <i>p</i> -Bromoanisole.....	193
P3.18 - Karolina Baranowska (<i>Gdańsk, Poland</i>) – and co-workers Spectroscopic Studies of Inclusion Complexation between Ortho Derivatives of <i>p</i> -Methylaminobenzoate and α - and γ -Cyclodextrins.....	194
P3.19 – Joanna Ortyl (<i>Krakow, Poland</i>) – and co-workers Synthesis, Spectroscopic Characterization of Novel derivatives of 1 <i>H</i> -Quinoxalin-2-one for the Role of Fluorescent Molecular Probes for Monitoring Very Fast Processes of Photopolymerization.....	195
P3.20 - Alberto Mezzetti (<i>Paris, France</i>) – and co-workers Solvent Effects on Fluorescence and Photochemistry of Flavonols. A Combined Spectroscopic and Computational Study.....	196
P4.1 - Maria Luísa Ramos (<i>Coimbra, Portugal</i>) – and co-workers Developing New Paramagnetic Copper(II) Complexes Based on 8-Hydroxyquinoline-5-Sulfonate.....	201
P4.2 – Rita Cardoso, Andreia M. Tabanez and Bernardo A. Nogueira (<i>Coimbra, Portugal</i>) – and co-workers Skin Permeation Tracking by Confocal Raman Spectroscopy.....	202
P4.3 - Norberto S. Gonçalves (<i>São Paulo, Brazil</i>) – and co-workers Vibrational Spectroscopy of Fe(II) and Zn(II) Complexes with the Phenanthroline Ligand Bipyridine-Glicoluril.....	203
P4.4 - Güneş Süheyla Kürkçüoğlu (<i>Eskişehir, Turkey</i>) – and co-workers A Theoretical and Experimental Investigation of Vibrational Spectra and Electronic Transitions on Some Aminoethylpyridine Molecules.....	204
P4.5 - Güneş Süheyla Kürkçüoğlu (<i>Eskişehir, Turkey</i>) – and co-workers Synthesis, Crystal structure and Spectroscopic Properties of Cyanide Complex with 2-Ethylimidazole: $[\text{Cu}(\text{2-etim})_2\text{Ni}(\mu\text{-CN})_4]_n$	205
P4.6 - Güneş Süheyla Kürkçüoğlu (<i>Eskişehir, Turkey</i>) – and co-workers Theoretical Study on the Molecular Structure and Vibrational Spectra of Cyanide-Bridged Heteronuclear Polymeric Complex: $[\text{Cd}(\text{mim})_2\text{Ni}(\mu\text{-CN})_4]_n$	206

P4.7 - Güneş Süheyla Kürkçüoğlu (Eskişehir, Turkey) – and co-workers Investigation of Structural Analysis and Thermostatic Properties of Thermal and UV Stabilizer as Organometallic Sn(II), Cu(II) and Cd(II) Barbiturate Complexes.....	207
P4.8 - Güneş Süheyla Kürkçüoğlu (Eskişehir, Turkey) – and co-workers Synthesis, Spectral and Thermal Properties of 4-(2-aminoethyl)pyridinium tetracyano-metallate(II) Complexes.....	208
P4.9 - Güneş Süheyla Kürkçüoğlu (Eskişehir, Turkey) – and co-workers Spectral, Structural and Thermal Properties of Some Cyanide Complexes Containing Tetracyanonickelate(II) and 2-Aminoethylpyridine.....	209
P4.10 - Güneş Süheyla Kürkçüoğlu (Eskişehir, Turkey) – and co-workers Synthesis, Structural Characterization and C-H...Pd Interactions of the Metal-Cyanide Complex: $[\text{Cd}(\text{mim})_2\text{Pd}(\mu\text{-CN})_4]_n$	210
P4.11 - Güneş Süheyla Kürkçüoğlu (Eskişehir, Turkey) – and co-workers Structural Characterizations of Cyanide and Fumarate Bridged Cu(II) and Cd(II) Complexes.....	211
P4.12 - Snežana Miljanić (Zagreb, Croatia) – and co-workers Structural Analysis of Iron(III) Complexes with Nicotinic Acid Aroylhydrazones by IR Spectroscopy.....	212
P4.13 - Silvia A. Brandán (Tucomán, Argentina) – and co-workers Spectroscopic FT-IR, FT-Raman and Ultraviolet-Visible Studies of the Potassium 5-Hydroxypentanoyltrifluoroborate Salt.....	213
P4.14 - Karen Mudryk (Berlin, Germany) – and co-workers The Electronic Structure of Aqueous Permanganate Ions: Probing Binding Energies and Molecular Bonding Character Using Liquid Jet Photoelectron Spectroscopy.....	214
P4.15 - Güneş Süheyla Kürkçüoğlu (Eskişehir, Turkey) – and co-workers One Dimensional Cyanide Complexes with 4-(2-Aminoethyl)pyridine.....	215
P4.16 - Qin Yang (Pisa, Italy) – and co-workers Vibrationally-Resolved Chiroptical Spectrum Study of Octahedral Cyclometalated Iridium (III).....	216
P4.17 - Güneş Süheyla Kürkçüoğlu (Eskişehir, Turkey) – and co-workers Synthesis, Spectral, Thermal and Crystal Structure of Cyanide Bridged Hetero-Metallic Polymeric Complex: $[\text{Cu}(\text{dmi})_2\text{Ni}(\mu\text{-CN})_4]_n$	217
P4.18 - Ankica Šarić (Zagreb, Croatia) – and co-workers Solvothermal Synthesis of Zinc Oxide: A Combined Experimental and Theoretical Study.....	218

P4.19 - István Pálincó (<i>Szeged, Hungary</i>) – and co-workers The Synthesis and Structural Characterization Co(II)-amino acid–CaAl-Layered Double Hydroxide Composites.....	219
P4.20 - Kamila Brylewska (<i>Krakow, Poland</i>) – and co-workers Demetalation Processes on Clinoptilolite. Kinetic Studies.....	220
P4.21 - Magdalena Król (<i>Krakow, Poland</i>) Hydrothermal Synthesis of Zeolite Aggregate and their Use as a Sorbent of Heavy Metal Cations.....	221
P4.22 - Magdalena Król (<i>Krakow, Poland</i>) – and co-workers ATR-FTIR Studies of Zeolite Formation During Alkali-Activation of Metakaolin.....	222
P4.23 - Goran Štefanić (<i>Zagreb, Croatia</i>) – and co-workers The Influence of Synthetic Conditions on the Structural and Microstructural Properties of ZrO ₂ -Y ₂ O ₃ System.....	223
P4.24 - Markus Becherer (<i>Kaiserslautern, Germany</i>) – and co-workers IR Spectroscopy of Small Isolated Cationic Cobalt and Nickel Ethanol Clusters and Implementation of a Desorption Sources.....	224
P4.25 - Magdalena Malik-Gajewska (<i>Wroclaw, Poland</i>) – and co-workers Novel Platinum(II) Complexes, <i>cis</i> -[PtCl ₂ L ₂] with Bioactive Ligands (L): Structures, Vibrational Spectra and Anticancer Properties.....	225
P4.26 - Lijuan Li (<i>Long Beach, USA</i>) – and co-workers Spectroscopic Studies on Non-Heme Iron Nitrosyl Complexes Containing Chelating Phosphine Ligands.....	226
P5.1 - Desislava Staneva (<i>Sofia, Bulgaria</i>) Fluorescent, Colorimetric and FTIR Spectroscopy Studies of a New Textile Material with Sensor Properties.....	235
P5.2 - Miguel Rubio (<i>Madrid, Spain</i>) – and co-workers The Study of Additive Distribution in Polymers Based on the Combination of Raman and Fluorescence Microscopy.....	236
P5.3 - Karol Kułacz (<i>Wroclaw, Poland</i>) – and co-workers Dielectric Permittivity of Gypsum in Presence of Moisture.....	237
P5.4 - Güneş Süheyla Kürkçüoğlu (<i>Eskişehir, Turkey</i>) – and co-workers Density Functional Theory Calculations of the Molecular Structure and Vibrational Properties of Stearic Acid as a Plastic Additive.....	238
P5.5 - Güneş Süheyla Kürkçüoğlu (<i>Eskişehir, Turkey</i>) – and co-workers Structural and Thermoanalytical Analysis of Organometallic Barbiturate and Tetraborat Complexes as New Generation Plastic Additives.....	239

P5.6 - Güneş Süheyla Kürkçüoğlu (<i>Eskişehir, Turkey</i>) – and co-workers Structural and Thermostatic Analysis of Imidazole-Based Cu(II) Complex as New Generation Plastic Additive.....	240
P5.7 - Marcin Moskwa (<i>Wrocław, Poland</i>) – and co-workers Crystal Structure and Investigation of Molecular Motions by Dielectric, Vibrational and ¹ H NMR Spectroscopies for Organic-Inorganic Hybrid Based on Piperazinium Cation.....	241
P5.8 - Martyna Wojciechowska (<i>Wrocław, Poland</i>) – and co-workers Organic-Inorganic Hybrid Compound Based on Pyrrolidine [C ₄ H ₁₀ N]2BiCl ₅ : Structure and Physicochemical Properties.....	242
P5.9 - Emese Gál (<i>Cluj-Napoca, Romania</i>) – and co-workers Nonlinear Optical Properties of New Phenothiazine Derivatives.....	243
P5.10 - Shin Yaginuma (<i>Nagano, Japan</i>) – and co-workers Controlling Molecular Condensation/Diffusion of Copper Phthalocyanine by Local Electric Field Induced with Scanning Tunneling Microscope Tip.....	244
P5.11 - José António Paixão (<i>Coimbra, Portugal</i>) – and co-workers Structural and Spectroscopic Studies of Atropisomerism in Diphenylguanidinium Salts.....	245
P5.12 - Zita Timár (<i>Szeged, Hungary</i>) – and co-workers Acetate and Benzoate Intercalated CaAl Layered Double Hydroxides – Characterization and Application as Nanoreactor.....	246
P5.13 - Mauro C. C. Ribeiro (<i>São Paulo, Brazil</i>) – and co-workers Exploring the Phase Diagram of a Glass-Forming Ionic Liquid by Raman Spectroscopy under Low Temperature and High Pressure.....	247
P5.14 - Katarzyna Piela (<i>Stockholm, Sweden</i>) – and co-workers The Quasi-Liquid Layer of Ice on Mesoporous Silica Characterized by Confocal Raman and NMR Spectroscopy.....	248
P5.15 - Klaudia Mencil (<i>Wrocław, Poland</i>) – and co-workers An Insight into Electric and Dynamic Properties of Formamidinium Iodide.....	249
P5.16 - B. Štimac (<i>Zagreb, Croatia</i>) – and co-workers Remineralizing Effect of Bioactive Glass 45S5 on Enamel Surface.....	250
P5.17 - Lahorija Bistričić (<i>Zagreb, Croatia</i>) – and co-workers UV-Radiation Resistance of Polystyrene-ZnO Nanocomposites.....	251
P5.18 - Ivan Marić and Marijan Gotić (<i>Zagreb, Croatia</i>) – and co-workers Structural and Optical Properties of Hydrothermally Synthesized Iron/Titanium Oxide Nanoparticles.....	252

P5.19 - Tanja Jurkin (<i>Zagreb, Croatia</i>) – and co-workers The Impact of Dextran Sulfate on the Radiolytic Synthesis of Magnetic Iron Oxide Nanoparticles.....	253
P5.20 - Hugh D. Burrows (<i>Coimbra, Portugal</i>) – and co-workers Nanostructuring Poly[N(1-aza-16-crown-6)carbamido-2,5-thienylene- <i>alt</i> -1,4-phenylene]] with Sodium Dodecylsulfate.....	254
P5.21 - Anife Ahmedova (<i>Sofia, Bulgaria</i>) – and co-workers Synthesis and Spectroscopic Study on the Tautomerization of Substituted 2-Phenyl Imidazoles used for the formation of Metal-Coordinated Assemblies or Suitable Guests for Supramolecular Coordination Nanocapsules.....	255
P5.22 - Karolína M. Šišková (<i>Olomouc, Czech Republic</i>) Interaction of Engineered Nanomaterials with Biomolecules Studied by Spectroscopic Techniques.....	256
P5.23 - Karol Kułacz (<i>Wroclaw, Poland</i>) – and co-workers Dielectric Properties of Intercalated Montmorillonite.....	257
P5.24 - Piotr Rożek (<i>Krakow, Poland</i>) – and co-workers Modification of the Structure of Metakaolin-Based Geopolymers.....	258
P5.25 - Avishek Kumar Gupta (<i>Oulu, Finland</i>) – and co-workers Spectroscopic Study of Titanium Slag Obtained from Ilmenite Smelting.....	258
P6.1 - Vadym Prokopec (<i>Prague, Czech Republic</i>) – and co-workers Use of Vibrational Spectroscopic Techniques for the Understanding of Evaporation Induced Pattern Formation of Decanol Droplets.....	263
P6.2 - Sara Fateixa (<i>Aveiro, Portugal</i>) – and co-workers SERS Active Filter Membranes for Extraction and Detection of Pesticides in Aqueous Solutions.....	264
P6.3 - Fatmah M. Alkhatib (<i>Hull, UK</i>) – and co-workers Spectroscopic and Imaging Studies of Sporopollenin Metal Complexes.....	265
P6.4 - Martynas Velicka (<i>Vilnius, Lithuania</i>) – and co-workers Formation of Metal Nanoparticle Films for Trace Analysis of OCT Drugs in Biological Fluids by Means of SERS Spectroscopy.....	266
P6.5 - Veronika Skoupá (<i>Prague, Czech Republic</i>) – and co-workers Influence of TiO ₂ Nanoparticles and UV Radiation on Raman Spectra.....	267
P6.6 - Tomasz Czaja (<i>Wroclaw, Poland</i>) – and co-workers SERS Activity of Ag-Polypyrrole Nanocomposites.....	268

P6.7 - Barbara Casteleiro (<i>Lisbon, Portugal</i>) – and co-workers Gold Nanoclusters Shining on Gold Nanostars.....	269
P6.8 - István Pálkó (<i>Szeged, Hungary</i>) – and co-workers Structure-Forming Properties of 2 <i>H</i> -Imidazole-2-thione Derivatives over Polycrystalline Gold Surfaces.....	270
P6.9 - Milan Plicka (<i>Prague, Czech Republic</i>) – and co-workers Development of Composite Plasmonic Nanostructured Substrates Focused on Reusability for Surface Enhanced Spectroscopy.....	271
P6.10 - Julita Muszyńska (<i>Lodz, Poland</i>) – and co-workers Hybrid Polymer Templates Synthesized via RAFT and Loaded with AgNPs as Tool for SERS.....	272
P6.11 - Joana L. Lopes (<i>Aveiro, Portugal</i>) – and co-workers Raman Spectroscopy as a Tool to Probe Surfaces of Graphene Oxide Decorated with ZnS Nanophases.....	273
P6.12 - Irena Matulková (<i>Czech Republic</i>) – and co-workers The Elucidation of the Structure of Zinc and Silver 2,2':6',2''-Terpyridine Surface Complexes Formed on Ag Nanoparticles.....	274
P6.13 - Gergo Peter Szekeres (<i>Berlin, Germany</i>) – and co-workers Identifying Binding Sequences of Intact Protein Molecules on Gold Nanoparticles with Surface-Enhanced Raman Scattering.....	275
P6.14 - Freeda Yesudas (<i>Berlin, Germany</i>) – and co-workers Investigating Interfacial Biomolecules using 100-kHz Repetition-Rate Broadband Vibrational Sum-Frequency Generation Spectroscopy.....	276
P7.1 - Włodzimierz Makulski (<i>Warsaw, Poland</i>) ¹³ CO and C ¹⁷ O Molecules as References for NMR Absolute Shielding Scales.....	279
P7.2 - Melisew Tadele Alula (<i>Palapye, Botswana</i>) – and co-workers Heat Induced Preparation of Silver Nanoparticles Coated Magnetic Composites for Sensitive Detection of Uric Acid.....	280
P7.3 - Zuzana Němečková (<i>Prague, Czech Republic</i>) – and co-workers Development of Composite SEVS-Active Substrates with Low Detection Limit, Used for Trace Analysis.....	281
P7.4 - Eliana F. C. Simões (<i>Coimbra, Portugal</i>) – and co-workers Phenylboronic Acid Based Carbon Dots for Glucose Sensing.....	282
P7.5 – Bence Kutus (<i>Szeged, Hungary</i>) – and co-workers Acid-Base and Calcium Complexing Properties of Lactate in Neutral to Alkaline Medium.....	283

P7.6 - Gulce Ogruc-Ildiz (<i>Istanbul, Turkey</i>) – and co-workers Lipid/Protein Ratio Contents of Soybean Mutants: A Raman Spectroscopic and Chemometrics Investigation.....	284
P7.7 - Hülia Y. Ortak (<i>Isparta, Turkey</i>) – and co-workers Identification of Forced Degradation Products of Tofacitinib Citrate by HPLC-DAD and MALDI-TOF/MS Techniques.....	285
P7.8 - Czesława Paluszkiewicz (<i>Krakow, Poland</i>) – and co-workers Spectroscopic Methods in the Study of Bio-Inhibitor Influence on the Corrosion Process of the Iron.....	286
P7.9 - Vesna Volovšek (<i>Zagreb, Croatia</i>) – and co-workers Impact of the Evaporation Rate of Water on Siloxane Structures.....	287
P7.10 - Sevgi Haman Bayarı (<i>Ankara, Turkey</i>) – and co-workers Dragline Silk of Araneus Quadratus: Effect of Altitude on the Silk Structure.....	288
P7.11 - Liga Avotina (<i>Riga, Latvia</i>) – and co-workers Investigations of FTIR Spectra for Analysis of Irradiated Sheep Wool.....	289
P7.12 - Gerrit Renner (<i>Krefeld, Germany</i>) – and co-workers Identification of Microplastics within Beach Sediment Samples Based on a Robust Chemometric Approach for Infrared Spectroscopy Library Searching.....	290
P7.13 - Vesislava Toteva (<i>Sofia, Bulgaria</i>) – and co-workers Comparison of the Oxidative Desulphurization of Petroleum Product and Waste Tires Pyrolysis Oil by Spectral Methods.....	291
P7.14 - María F. Mellano (<i>Santiago de Estero, Argentina</i>) – and co-workers Stabilization of Soils with Vinasse, Analysis by X-Ray Diffraction and Scanning Electron Microscopy (SEM) to Evaluate Application in Roads Embankments.....	292
P7.15 - Radka Šefců (<i>Prague, Czech Reopublic</i>) – and co-workers Identification of Components of the Ceramics and Color Layers Used in Ceramic Artworks by Non-Invasive and Non-Destructive Methods.....	293
P7.16 – Maria Luísa Carvalho (<i>Lisbon, Portugal</i>) – and co-workers Josefa de Óbidos Workshop: From Panel to Canvas. Materials and Technical Evolution of the Most Significant Portuguese Painting Workshop of the 17 th Century.....	294
P7.17 – Magdalena Węglińska (<i>Wroclaw, Poland</i>) – and co-workers Quantification of Active Ingredients in Potentilla tormentilla by Infrared and Raman Spectroscopy.....	295

P7.18 - Yasushi Numata (<i>Koriyama, Japan</i>) – and co-workers Simultaneous Determination of Oleic and Elaidic Acids in their Mixed Solutions by Raman Spectroscopy.....	296
P7.19 - Karlis Shvirksts (<i>Riga, Latvia</i>) – and co-workers High Pressure Induced Changes in Pork Macromolecular Structure.....	297
P7.20 - Tomasz Czaja (<i>Wroclaw, Poland</i>) – and co-workers Macronutrients Quantification in Dairy Products by FT-Raman Spectroscopy.....	298
P7.21 - Dragos Trinca (<i>Vila Real, Portugal</i>) – and co-workers On the Acquisition of Non-Saturated Hyperspectral Images.....	299
P7.22 - Oleg Pestsov (<i>Saint Petersburg, Russian Federation</i>) – and co-workers Application of Low-temperature FTIR Spectroscopy of Adsorbed CO for Characterization of Copper species in Mordenites.....	300
P7.23 - Tania Kataeva (<i>Saint Petersburg, Russian Federation</i>) – and co-workers Obtaining Extinction Spectra from the Reflection Spectra of Low-Temperature Molecular Liquids.....	301
P8.1 – Gülce Ogruc Ildiz (<i>Istanbul, Turkey</i>) – and co-workers Discrimination Analysis of Blood Plasma Associated with Schizophrenia Disease Using FTIR Spectroscopy.....	307
P8.2 - Tatsuya Mori (<i>Tsukuba, Japan</i>) – and co-workers Investigation of Light-Vibration Coupling Coefficient of Glassy Glucose by Terahertz Time-Domain Spectroscopy and Low-Temperature Specific Heat.....	308
P8.3 - Wojciech Bocian (<i>Warsaw, Poland</i>) – and co-workers Molecular Modelling and NMR Studies of Cyclodextrin Inclusion Complexes with New Oxazolidinone Antibiotics.....	309
P8.4 - Mara Grube (<i>Riga, Latvia</i>) – and co-workers Estimation of the Cancer Cell Metabolic Response to the Growth Environment by FTIR Spectroscopy.....	310
P8.5 - Simona Strazdaite (<i>Vilnius, Lithuania</i>) – and co-workers Probing Lysozyme Aggregation at Lipid Monolayers with Vibrational Sum-Frequency Generation Spectroscopy.....	311
P8.6 - Pavla Štenclová (<i>Prague, Czech Republic</i>) – and co-workers ATR-IR Real-Time Monitoring of Biofilm Formation During Bacterial Growth.....	312
P8.7 - Maria Luiza S. Mello (<i>Campinas, Brazil</i>) – and co-workers Vibrational Microspectroscopy of Sodium Valproate-Treated DNA.....	313

P8.8 - Katarzyna Cieřlik-Boczula (<i>Wroclaw, Poland</i>) Structural Modifications of PLL by Chalcone Molecules.....	314
P8.9 - Ivelina Georgieva (<i>Sofia, Bulgaria</i>) – and co-workers Absorption Spectra Simulations of Green Fluorescence Protein Chromophore Models.....	315
P8.10 - Elena Chikhirzhina (<i>Saint Petersburg, Russian Federation</i>) – and co-workers Peculiarities of Interaction of Non-Histone Nuclear Proteins HMGB1 and HMGB2 with DNA Damaged by Cisplatin.....	316
P8.11 - Benedicto de Campos Vidal (<i>Campinas, Brazil</i>) – and co-workers Sodium Valproate-Induced Changes in Chiral Supramolecular Texture Formed During DNA Crystallization.....	317
P8.12 - Alexandre M. R. Teixeira (<i>Crato, Brazil</i>) – and co-workers Structural, Spectroscopic and Microbiological Characterization of Chalcone 2E-1-(2'-Hydroxy-3',4',6'-trimethoxyphenyl)-3-(phenyl)-prop-2-en-1-one Derivative of the Natural Product 2-Hydroxy-3,4,6-trimethoxyacetophenone.....	318
P8.13 - Adrianna Wislocka (<i>Krakow, Poland</i>) – and co-workers Biochemistry of Hepatocytes in Non-Alcoholic Fatty Liver Disease studied by means of Raman Imaging.....	319
P8.14 - Katarzyna M. Marzec (<i>Krakow, Poland</i>) – and co-workers Label-Free Characterization of Acute Ischemic Stroke-Retrieved Clot Composition with Vibrational Spectroscopy.....	320
P8.15 - Katarzyna M. Marzec (<i>Krakow, Poland</i>) – and co-workers Oxidative Damage of the Murine RBC Membrane in Advanced Atherosclerosis studied by Vibrational Spectroscopy and AFM Microscopy.....	321
P8.16 - Marius Rada (<i>Cluj-Napoca, Romania</i>) – and co-workers Dental Materials based on Stabilized Zirconia Ceramics.....	322
P8.17 - Simona Rada (<i>Cluj-Napoca, Romania</i>) – and co-workers Stabilized Zirconia Ceramics with Additions of Y ₂ O ₃ , SiO ₂ , Fe ₂ O ₃ and Na ₂ O Contents for Dental Applications.....	323
P8.18 - Eva Klaric Sever (<i>Zagreb, Croatia</i>) – and co-workers Raman Laser Heating – the Effect in Dental Composite Materials.....	324
P8.19 - Sara Silva (<i>Lisbon, Portugal</i>) – and co-workers Effects of Bleaching Products Containing Fluoride on Tooth Enamel: Application of Polarized Raman Spectroscopy.....	325

P8.20 - Dominika Augustynska (<i>Krakow, Poland</i>) – and co-workers The Biochemical and Spectroscopic Characteristic of Isolated and Cultured Eosinophils.....	326
P8.21 - Sevgi Haman Bayarı (<i>Ankara, Turkey</i>) – and co-workers Spectroscopic and Optical Properties of Silicone Hydrogel Contact Lenses.....	327
P8.22 - Dominika Augustyńska (<i>Krakow, Poland</i>) – and co-workers Raman Imaging Studies on Primary Cardiac Microvascular Endothelial Cells (CMECs).....	328
P8.23 - S. Olsztyńska-Janus and Mirosław A. Czarnecki (<i>Wroclaw, Poland</i>) – and co-workers Thermal Effects in Skin Components Studied by ATR-IR Spectroscopy.....	329
P8.24 - Danuta Pentak (<i>Sosnowiec, Poland</i>) – and co-workers The Application of mREV Method in the Targeted Delivery of Cancer Therapeutics.....	330
P8.25 - Danuta Pentak (<i>Sosnowiec, Poland</i>) – and co-workers Comparison of the Degree of Binding of Derivatives of 5-Alkyl-12 (H)-quin [3,4-b] [1,4] Benzothiazine Salts with Human Serum Albumin.....	331
P8.26 - Inês Mariz (<i>Lisbon, Portugal</i>) – and co-workers Tailoring the Architecture of Charged Molecules to Enhance the Two-photon Brightness in Bioimaging.....	332
P8.27 - Marta Kuć (<i>Wroclaw, Poland</i>) – and co-workers NIR and EPR Studies of the Effect of Inhaled Anesthetics on the Structure and Order of Model Lipid Bilayers.....	313

LIST OF AUTHORS

Adamski, M. G.	P8.14	320	Babić, V.	P4.23	223
Adomaviciute, S.	P6.4	266	Bacıoglu, A.	P8.21	327
Ahmedova, A.	P5.21	255	Bağlayan, Ö	P3.6	182
Ahokas, J.	P2.2	148		P4.4	204
	P2.8	154	Balbi, A.	P1.6	136
Aidas, K.	P1.8	138	Bandeira, P. N.	P8.12	318
Aleksa, V.	P3.16	192	Bandzeviciute, R.	OC35	97
Alenkina, I. V.	OC24	84	Baran, J.	P5.7	241
Alexandre, M.	OC44	114		P5.15	249
Alieva, R.	OC49	118	Baranowska, K.	P3.18	194
Alkhatib, F. M.	P6.3	265	Baranowska, M.	P7.20	298
Allheily, V.	P2.18	164	Baranska, M.	OC34	96
Alonso, E. R.	KL13	67		OC38	100
	KL17	76		P8.13	319
Alonso, J. L.	KL13	67		P8.15	321
	KL17	76		P8.20	326
AlSalem, H.	OC7	41		P8.22	328
Alsancak, G.	P7.7	285	Barbieri, D.	OC12	47
Altunbek, M.	KL22	102	Barone, V.	OC29	90
Álvarez-Valtierra, L.	KL15	73		OC33	94
	OC23	77		P1.3	133
	P3.8	184		P1.6	136
Amaral, A.	P8.19	325	Basualdo, P.J.	P7.14	292
Amberger, B. K.	PL3	51	Bator, G.	P5.7	241
Ando, R. A.	P2.17	163	Bayarı, S. H.	P7.10	288
Andrushchenko, V.	OC45	115		P8.1	307
Angelova, D.	P7.13	291		P8.21	327
Antunes, V.	P7.16	294	Bazsó, G.	P2.11	157
Aquino, A. J. A.	P8.9	315	Becerra, O.	P4.26	226
Archibald, S. J.	P6.3	265	Becherer, M.	P4.24	224
Arnaut, L. G.	KL28	125	Becherová, L.	P6.1	263
Arndt, M.	KL24	113	Bednarek, E.	P3.12	188
Arunan, E.	KL12	66		P8.3	309
Asfin, R. E.	P7.23	301	Bellanato, J.	P3.11	187
Ashfold, M. N. R.	KL8	59	Belykh, R.	P7.22	300
Ashoor, S. Et.	P5.11	245	Besley, N. A.	P2.9	155
Astilean, S.	P8.1	307	Beyer, M.	KL20	89
Atak, C.	P7.6	284	Biczysko, M.	OC31	92
Augustynska, D.	P8.20	326	Bieniewska, J. M.	OC20	69
	P8.22	328	Bilavčíková, H.	P7.15	293
Aula, M.	P5.25	259	Bistričić, L.	P5.17	251
Avotina, L.	P7.11	289	Bjelovucic, R.	P8.18	324
Ayan, A.	P7.6	284	Blat, A.	OC34	96
Azevedo, J. C. R.	OC25	85		P8.14	320

Blat, A.	P8.15	321	Castro-Beltrán, R.	P3.8	184
Błażewicz, A.	P3.12	188	Catalán, C. A. N.	P3.5	181
Bloino, J.	OC29	90	Çavuş, A. Ö.	P8.21	327
	P4.16	216	Čejková, J.	P6.1	263
Bocian, W.	P8.3	309	Celik, O.	P7.6	284
Bondarev, S. L.	OC28	88	Centikaya, O.	P6.10	272
Bonn, M.	PL1	31	Ceponkus, J.	OC35	97
Bonnier, F	KL26	123		P2.3	149
Bonoldi, L.	OC12	47	Cha, S.	OC27	87
Borchert, H.	P2.18	164	Checa, M. A.	P3.5	181
Böszörményi, E.	P7.5	283	Chelmecka, E.	P3.1	177
Bot, A.	P8.17	323		P3.4	190
Bouchened, C.	KL1	32	Chikhirzhina, E.	P8.10	316
Brandán, S. A.	P3.5	181	Chiş, V.	P4.12	212
	P4.13	213	Chlopicki, S.	OC34	96
Brás, E. M.	P2.23	169		OC38	100
	P5.11	245		P8.13	319
Brém, B.	P5.9	243		P8.14	320
Brylewska, K.	P4.20	220		P8.15	321
	P5.24	258		P8.20	326
Buchel, C.	OC44	114		P8.22	328
Buckó, Á.	OC26	86	Chrabaszc, K.	P8.14	320
Buganov, O. V.	OC28	88	Cieślik-Boczula, K.	P8.8	314
Bulat, K.	OC34	96		P8.27	333
	P8.14	320	Císařová, I.	OC42	106
	P8.15	321		P6.12	274
Buma, W. J.	PL2	39	Cladera, J.	KL21	95
Burdzhiev, N.	P5.21	255	Costa Pereira, J.	OC25	85
Burrows, H. D.	OC25	85	Costa, T.	P4.1	201
	P4.1	201		P5.20	254
	P5.20	254	Coutinho, H. D. M.	P8.12	318
Byrne, H. J.	KL26	123	Craciun, A.-M.	P8.1	307
Caballero, M. J.	P5.2	236	Cristea, C.	P5.9	243
Cabral, L. I. L.	P2.23	169	Cristiano, M. L. S.	P2.23	169
Caliskan, H.	P3.3	179		OC48	118
Campos-Amador, J. J.	P3.8	184	Cruz, B. G.	P8.12	318
Canbay, H. S.	P7.7	285	Cuevas, R.	P7.14	292
Candeias, A.	P7.16	294	Cuibus, D.	OC43	107
Cardoso, A.	P7.16	294	Culea, E.	OC43	107
Cardoso, R.	P4.2	202		P8.16	322
Carvalho, M. L.	P7.16	294		P8.17	323
Carvalho, M. L.	P8.19	325	Çulha, M.	KL22	102
Casey, A.	KL26	123	Czaja, T.	P6.6	268
Casteleiro, B.	P6.7	269		P7.20	298

Czarnecki, M. A.	OC39	103	Esselman, B. J.	PL3	51
	P8.23	329	Esteves da Silva, J. C. G.	P7.4	282
Danchova, N.	P1.1	131	Estrada, A. C.	P6.11	273
Darquié, B.	OC20	69	Evangelisti, L.	PL4	71
Das, A.	KL12	66	Fabritius, T.	P5.25	259
	P2.19	165	Farhane, Z.	KL26	123
Daszkiewicz, M.	P3.13	189	Faria, L. F. O.	P5.13	247
Davies, J. A.	P2.9	155	Farinha, J. P. S.	P6.7	269
Davies, L.	P4.13	213	Fateixa, S.	OC4	37
de Souza, B.	OC30	91		OC41	105
Demiralay, E. Ç.	P7.7	285		P6.2	264
Demirci, G.	P6.10	272		P6.11	273
Dendisová, M.	P7.3	281	Fausto, R.	KL9	60
Denisov, G. S.	OC32	93		P2.1	147
Despotović, I.	P1.12	142		P2.6	152
	P4.18	218		P2.10	156
Di Paolo, L.	OC12	47		P2.23	169
Didier, A.	OC9	44		P2.24	170
Diekmann, J.	PL7	111		P2.25	171
Dietrich, F.	P4.24	224		P4.2	202
Dimov, D.	P1.2	132		P5.11	245
Domingos, S. R.	OC19	68		P7.6	284
Dopfer, O.	KL14	72	Fecka, I.	P7.17	295
Dražić, G.	P5.18	252	Fedunov, R. G.	OC28	88
Drozd, M.	P3.13	189	Felner, I.	OC24	84
Drózdź, E.	P3.14	190	Feurer, T.	P2.19	165
Dudás, C.	OC26	86	Filipczak, P.	P6.10	272
	P7.5	283	Fonseca, M.	P8.19	325
Durán, F.	P7.14	292	Fournier, C.	OC11	46
Durlak, P.	P5.15	249	Freire, P. T. C.	P8.2	318
Dybal, J.	KL7	55	Freisinger, S.	P8.6	312
Dybas, J.	OC34	96	Frigerio, F.	OC12	47
	P8.14	320	Fujii, Y.	OC8	42
	P8.15	321		OC46	116
Efeoglu, E.	KL26	123		P8.2	308
Egidi, F.	OC29	90	Furić, K.	P7.9	287
	P4.16	216	Furó, I.	P5.14	248
El Seoud, O. A.	OC40	104	Fusè, M.	OC29	90
Ellis, A. M.	P2.9	155	Fusè, M.	P4.16	216
Engdahl, A.	KL21	95	Gaigeot, M.-P.	OC3	36
Engvall, K.	OC17	63	Găină, L.	P5.9	243
Escalada, F. C. A.	P3.7	183	Gál, E.	P5.9	243
Eşme, A.	P3.3	179	Galek, M.	P3.29	195
	P3.4	180	Galić, N.	P4.12	212

Galimberti, D. R.	OC3	36	Gupta, A. K.	P5.25	259
Galinovskii, N. A.	OC28	88	Gustafson, T. L.	P2.17	163
Galoburda, R.	P7.19	297	Guthmuller, J.	OC16	62
Gamulin, O.	P8.18	324		P1.7	137
Gąssowska, K.	OC13	56	Gutmann, J. S.	OC10	45
Gatjal, A.	P1.4	134	Gutzov, S.	P1.1	131
Gecen, T.	P8.23	329	Gyepes, R.	OC42	106
Gelfand, N.	P3.20	196		P6.12	274
Georgiev, A.	P1.2	132	Holsch, N.	KL20	89
	P7.13	291	Hanson-Heine, M. W. D.	P2.9	155
Georgieva, I.	P1.1	131	Hansson, T.	OC17	63
	P8.9	315	Hasnain, A.	OC6	40
Gerhards, M.	P4.24	224	Havasi, V.	P3.15	191
Gerwert, K.	PL8	121		P6.8	270
Giba, I. S.	OC14	57	Hebestreit, M.-L.	OC22	74
Gilch, P.	PL7	111		OC23	77
Gipta, A. K.	P5.26	260		P2.14	160
Gnanasekar, S. P.	KL12	66		P2.15	161
Góbi, S.	P2.10	156		P2.16	162
Gocen, T.	P8.21	327		P3.2	178
Golec, B.	P3.9	185	Hedaoui, N.	KL1	32
Golubkova, O. S.	P2.26	172	Hegedús, K.	P2.11	157
	P7.23	301	Heim, Z. N.	PL3	51
Gomes, E.	P5.20	254	Heiner, Z.	P6.14	276
Gonçalves, N. S.	OC18	64	Heise, H. M.	KL27	124
	P4.3	203	Helios, K.	P4.25	225
Gontcharov, J.	PL7	111	Henrichs, C.	P2.14	160
Gorski, A.	P3.9	185		P2.15	161
Göthelid, M.	OC17	63		P2.16	162
Gotić, M.	P5.18	252	Henriques, M. S. C.	P5.11	245
	P5.19	253	Herbich, J.	P3.9	185
Gottschalk, H. C.	P2.21	167	Herich, P.	P1.4	134
Gouras, G. K.	KL21	95	Hetmańczyk, J.	OC13	56
Grabowska, B.	OC8	42	Hetmańczyk, L.	OC13	56
Gramatina, I.	P7.19	297	Hökelek, T.	P4.15	215
Grigo, D.	OC12	47	Hola, E.	P3.19	195
Grosicki, A.	P8.20	326	Holroyd, C.	OC7	41
	P8.22	328	Hung, T. N.	P3.15	191
Grube, M.	P7.11	289		P6.8	270
Grube, M.	P7.19	297	Hunger, J.	OC27	87
	P8.4	310	Ide, S.	P7.10	288
Grzeszczuk, M.	P6.6	268	Idrissi, A.	P3.20	196
Gudmundsdottir, A.	KL10	61	Iramain, M. A.	P4.13	213
Guidi, M. C.	OC36	98	Iriepa, I.	P3.11	187

Israelsson, B.	KL21	95	Kavlak, I.	P5.5	239
Iszak, R.	OC30	91		P5.6	240
Ivanda, M.	P4.23	223	Kawaji, H.	P8.2	308
	P5.18	252	Kaygisiz, E.	P7.6	284
Ivanov, A. I.	OC28	88	Khokholova, S. S.	OC28	88
Jakubas, R.	P5.8	242	Khriachtchev, L.	P2.1	147
	P5.15	249	Kiełbowicz, Z.	P8.23	329
Jankevivius, F.	OC35	97	Kinerte, V.	P7.11	289
Jankovič, L.	OC15	58	Kinik, B.	P1.9	139
Jansen, P.	KL20	89		P4.6	206
Jasztal, A.	P8.14	320	Kirilovsky, D.	OC45	114
Jeništová, A.	P6.5	267	Kisiel, Z.	PL3	51
Jesus, A.	P8.19	325	Kitani, S.	OC44	116
Jiang, Z.	OC31	92		P8.2	308
Jiefer, J.	OC43	107	Kiyan, I. Yu.	P2.20	166
Józefowicz, M.	P3.18	194	Kizane, G.	P7.11	289
Julião, M. S. S.	P8.12	318	Klementieva, O.	KL21	95
Jurinovich, S.	P3.20	196	Klimas, B.	P8.22	328
Jurkin, T.	P5.18	252	Kloda, M.	OC42	106
	P5.19	253	Kloužková, A.	P7.15	293
Justino, L. L. G.	P4.1	201	Kmoníčková, M.	P7.15	293
	P5.20	254	Knapik, H. G.	OC25	85
Kabeya, M.	P8.2	308	Kneipp, J.	P6.13	275
Kaczmarska, K.	OC8	42		P6.14	276
Kadela-Tomanek, M.	P3.1	177	Ko, J.-H	OC8	42
	P3.14	190	Kobayashi, H.	P7.18	296
Kalnina, Z.	P8.4	310	Kočišová, E.	OC5	38
Kaminska, A.	OC37	99	Koehler, S. P. K.	OC7	41
Kaminsky, J.	OC47	117	Kojima, S.	OC8	42
Karaağaç, D.	P4.8	208		OC46	116
	P4.15	215		P8.2	308
Kararslan, D.	P7.10	288	Kokot, J.	P2.18	164
Kasai, Y.	P7.18	296	Kolesnikova, L.	KL13	67
Kataeva, T.	P2.26	172		KL17	76
	P7.23	301	Kolomiitsova, T. D.	P2.26	172
Kausteklis, J.	P3.16	192	Koncz, B.	P2.11	157
Kavlak, I.	P1.5	135	Kontrec, D.	P4.12	212
	P1.9	139	Kónya, Z.	P3.5	193
	P1.10	140		P4.19	220
	P3.6	182		P6.8	270
	P4.4	204	Kopecky, V.	OC47	117
	P4.6	206	Koreeda, A.	OC8	42
	P4.7	207		OC46	116
	P5.4	238		P8.2	308

Kosendiak, I.	P2.2	148	Kürkçüoğlu, G. S.	P4.15	215
	P2.8	154		P4.17	217
Kostyleva, E.	P8.10	318		P5.4	238
Kotarba, A.	OC17	63		P5.5	239
Kotov, N.	KL7	55		P5.6	240
Kovaldins, R.	P8.4	310	Kus, E.	OC38	100
Kozanecki, M.	P6.10	272		P8.13	319
Kozerski, L.	P3.12	190	Kuş, N.	P2.6	152
Kozma, G.	P3.15	193	Kutus, B.	OC26	86
	P6.8	270		P7.5	283
Kraft, M.	P5.20	255	Kuzkova, N.	P2.20	166
Krajčovič, J.	P1.2	132	Kuzmann, E.	OC24	84
Król, M.	P4.20	221	Kuzminova, A.	OC5	38
	P4.21	222	Kwiatek, W. M.	OC36	98
	P4.22	223		P7.8	286
	P5.24	259	Kylián, O.	OC5	38
Kromka, A.	P8.6	312	Lauw, A.	P7.16	294
Krupa, J.	P2.2	148	Lazzaroni, S.	P3.20	196
	P2.7	153	Ledesma, A. E.	P3.7	183
	P2.8	154	Leitão, J. M. M.	P7.4	282
Kuč, M.	P8.27	314	Lemmens, P.	P7.2	280
Kudelski, A.	OC1	34	Lengvinaitė, D.	P1.8	138
Kudryasheva, N.	OC49	118	Leon, I.	KL13	67
Kukla, B.	P8.20	328		KL17	76
Kukovec, B. N.	P4.25	228	Leskovac, M.	P5.17	251
Kukovecz, Á.	P3.5	193	Leszczenko, P.	P8.20	326
	P4.19	220	Lewińska, A.	P8.27	333
	P6.8	270	Li, L.	P4.26	226
Kuku, G.	KL22	102	Licarete, E.	P8.1	307
Kułac, K.	P5.3	237	Licari, D.	OC33	94
	P5.23	258	Lima, T. A.	P5.13	247
Kupfer, S.	P1.8	137	Lima, V. N.	P8.12	318
Kürkçüoğlu, G. S.	P1.6	135	Lindic, M.	OC22	74
	P1.11	139	Lindic, M.	P3.2	178
	P1.12	140	Linnartz, H.	PL5	81
	P3.6	182	Lis, T.	P5.8	242
	P4.4	204	Lischka, H.	P8.9	315
	P4.5	205	Loco, D.	P3.20	196
	P4.6	206	Lopes de Jesus, A. J.	P2.25	171
	P4.7	207	Lopes, J. L.	P6.11	273
	P4.8	208	Lopes, S.	P2.1	147
	P4.9	209		P2.24	170
	P4.10	210	Lundell, J.	KL11	65
	P4.11	211		P2.2	148

Lundell, J.	P2.8	154	Mellano, M. F.	P7.14	292
Maciążek-Jurczyk. M.	P8.24	330	Mello, M. L. S.	P8.7	313
	P8.25	331		P8.11	317
Maçôas, E. M. S.	KL3	43	Mencel, K.	P5.15	249
	P8.26	332	Méndez, L. M.	P5.2	236
Maher, M.	KL26	123	Mendolicchio, M.	OC33	94
Maksimova, A. A.	KL19	83	Mennucci, B.	P3.20	196
Makulski, W.	P7.1	279	Meriç, S.	P7.6	284
Malek, K.	P8.14	320	Merkt, F.	KL20	89
	P8.20	326	Merlat, L.	P2.18	164
Malik-Gajewska. M.	P4.25	225	Mero, M.	P6.14	276
Manso, M.	P7.16	294	Merschjann, C.	P2.20	166
Mantsch, H. H.	KL29	126	Mezzetti, A.	OC44	114
Mardyla, M.	OC34	96		P3.21	196
	P8.15	321	Michalska, D.	P4.25	225
Marić, I.	P5.18	252	Michalska, K.	P8.3	309
Marin, J. H.	P4.3	203	Miklata, V.	P1.4	134
Mariz, I. F. A.	KL3	43	Miliński, M.	P3.1	177
	P8.26	334	Miljanić, S.	P4.12	212
Marks, K. M.	OC17	63	Mirão, J.	P7.16	294
Martinho, J. M. G.	KL3	43	Mizaikoff, B.	P8.6	312
	P6.7	269	Mlostoń, G.	P3.5	191
	P8.26	332		P6.8	270
Martinsson, I.	KL21	95	Mojzeš, P.	P6.12	274
Marzec, K. M.	OC34	96	Molnár, É. A.	P5.9	243
	P8.14	320	Moreaus, M.	OC9	44
	P8.15	321	Mori, T.	OC8	42
Mata, A.	P8.19	325		OC46	116
Mata, S.	KL13	67		P8.2	308
	KL17	76	Moskwa, M.	P5.7	241
Matějka, P.	P6.9	271	Motoji, L.	OC46	116
Matulková, i.	OC42	106	Moud, P. H.	OC17	63
Matulková, i.	P6.12	274	Mozgawa, W.	P4.20	220
Matyjaszewski, K.	P6.10	272		P4.22	222
Mazurek, S.	OC39	103		P5.24	258
	P7.17	295	Mudryk, K.	P4.14	214
	P7.20	298	Mulloyarova, V. V.	OC14	57
McIntyre, J.	KL26	123	Muszyńska, J.	P6.10	272
McMahon, R. J.	PL3	51	Nagaoka, K.	P5.10	244
	KL9	60	Nakayama, T.	P5.10	244
Medel, R.	P2.22	168	Namdeiram P. N.	P8.14	320
Medycki, W.	P5.7	241	Navakauskas, E.	P8.5	311
	P5.15	249	Nawara, K.	P3.9	185
Mehlich, M.	P3.14	190	Neese, F.	OC30	91

Němec, I.	OC42	106	Peintler, G.	OC26	86
Němečková, Z.	P7.3	281	Pengfei, A.	P8.16	322
Nguyen, L. N. Q.	P2.17	163		P8.17	323
Niaura, G.	P8.5	311	Pentak, D.	P8.24	330
Nikitin, T.	P2.24	170		P8.25	331
Noda, L. K.	OC18	64	Peremans A.	KL1	32
Nogueira, B. A.	P4.2	202	Pérez, C.	OC19	68
Nogueira, H. I. S.	OC41	105	Pessanha, S.	P7.16	294
	P6.2	264		P8.19	325
Novikov, R.	P7.22	302	Pestsov, O.	P7.22	300
Numata, Y.	P7.18	296	Petranovski, V.	P7.22	300
Nunes, C. M.	KL9	60	Petrova, A.	OC49	118
	P2.10	156	Pezzotti, S.	OC3	36
	P2.25	171	Piecha-Bisiorek, A.	P5.15	249
Nur Kabuk, H.	P7.6	284	Piela, K.	P5.14	248
Ogruc-Ildiz, G.	P7.6	284	Piergies, N.	P7.8	286
	P8.1	307	Pięta, E.	P7.8	286
Ol'khobiv, V. K.	OC28	88	Pietrasik, J.	P6.10	272
Olsztyńska-Janus, S.	P8.23	329	Pietruszka, A.	P8.23	329
Oonami, N.	P7.18	296	Pilch. M.	P3.19	195
Orbán, E.	OC26	86	Pinheiro, P. C.	OC4	37
Ortak, H. Y.	P7.7	285	Pinto, P. M.	P7.21	299
Ortyl, J.	P3.19	195	Pinto, S. M. V.	P1.3	133
Orzechowski, K.	P5.3	237		P2.6	152
	P5.23	257	Piskorz, W.	OC17	63
Oshtrakh, M. I.	KL19	83	Plamitzer, L.	OC47	117
	OC24	84	Plass, M.	OC6	40
Öström, H.	OC17	63	Platakyte, R.	P2.3	149
Oztas, D. Y.	KL22	102		P3.16	192
Pagacz-Kostrzewa, M.	P2.4	150	Pleshko, N.	KL25	122
Pais, A. A. C. C.	OC25	85	Plicka, M.	P6.9	271
Paixão, J. A.	P5.11	245	Ploch, A.	P8.24	330
	OC26	86		P8.25	331
Pálinkó, I.	P3.15	191	Pohl, M.	P4.14	214
	P4.19	219	Pohl, R.	OC47	117
	P5.12	246	Polyanichko, A.	P8.10	316
	P6.8	270	Popiela, T.	P8.14	320
	P7.5	283	Praus, P.	OC5	38
Paluszkiewicz, C.	OC36	98	Procházka, M.	OC5	38
	OC37	99	Prokopec, V.	P6.1	263
	P7.8	286	Protti, S.	P3.20	196
Par, M.	P8.18	325	Pucetaite, M.	OC35	97
Paschoal, V. H.	P5.13	247	Puthenmadom, D.	OC11	46
Pavlova, E.	OC2	35	Puzzarini, C.	P1.6	136

Rada, M.	OC43	107	Şahin, O.	P4.11	211
	P8.16	322		P4.17	217
	P8.17	323	Sakr, A. K.	KL5	53
Rada, S.	OC43	107		P2.12	158
	P8.16	322	Saldyka, M.	P2.4	150
	P8.17	323		P2.5	151
Raichenok, T. F.	OC28	88	Santos, H. S.	P8.12	318
Ramos, M. L.	P4.1	201	Šapić, I. M.	P7.9	287
	P5.20	254	Šarić, A.	P4.18	218
Raposo, M.	P6.2	264	Saricam, M.	KL22	102
Rathke, B.	OC43	107	Sauer, B. E.	OC20	69
Raus, V.	KL7	55	Savoini, A.	OC12	47
Renner, G.	P7.12	290	Sayin, E.	P4.9	209
Reva, I.	KL6	54		P4.10	210
	KL9	60		P4.11	211
	P2.10	156	Sazonova, S.	P7.19	297
	P2.25	171	Scherf, U.	P5.20	254
Rey, V.	P3.7	183	Schlopicki, S.	P8.15	321
Ribeiro, M. C. C.	P5.13	247	Schmidt, T. C.	P7.12	290
Ribeiro, T.	P6.7	269	Schmitt, M.	KL15	73
Richard, B.	OC9	44		OC22	74
Riedle, E.	PL6	101		KL16	75
Robbe-Cristini, O.	OC9	44		P2.14	160
Robert, B.	OC44	114		P2.15	161
Rohwer, E. J.	P2.19	165		P2.16	162
Rok, M.	P5.15	249		P3.2	178
Romero-Servín, S. A.	P2.13	159	Schmitt, R.	P2.18	164
	P3.8	184	Schneider, M.	OC22	74
Rospenk, M.	P8.27	333		OC23	77
Rozek, P.	P4.20	220		P2.14	160
	P4.22	222		P2.15	161
Rozek, P.	P5.24	258	Schneider, M.	P2.16	162
Rubena, E.	P8.4	310	Schnell, M.	OC19	68
Rubio, M.	P5.2	236	Scholtzová, E.	OC15	58
Rudyk, R. A.	P3.5	181	Schram, J.	OC10	45
Ruiz-Santoyo, J. A.	P2.13	159		P7.12	290
Rullich, C. C.	OC43	107	Schulenburg, Y.	OC10	45
Ryguła, A.	P8.20	326	Sears, T. J.	OC20	69
Sablinkas, V.	OC35	97	Šefců, R.	P7.15	293
	P6.4	266	Seidel, R.	P4.14	214
Sagdinc, S. G.	P3.3	179	Seitsonen, A. P.	P3.20	196
	P3.4	180	Semeria, L.	KL20	89
Şahin, O.	P4.5	205	Sena Junior, D. M.	P8.12	318
	P4.10	210	Şenyel, M.	P3.6	182

Şenyel, M.	P4.4	204	Spanovic, N.	P8.18	324
Serrão, V.	P7.16	294	Stachwiak, J.	P2.21	167
Setnička, V.	P6.5	267	Staneva, D.	P5.1	235
Sever, E. K.	P5.16	250	Staniszewska, M.	P1.7	137
	P8.18	324	Stanton, J. F.	PL3	51
Shchepkin, D. N.	P2.26	172	Starkova, T.	P8.10	316
	P7.23	301	Štefanić, G.	P4.18	218
Shelyapina, M.	P7.22	300		P4.23	223
Shestakova, P.	P5.21	255		P5.18	252
Shimoi, Y.	P3.10	186		P5.19	253
Shiraki, K.	OC46	116	Steiner, G.	OC35	97
Shutter, J. D.	PL3	51	Stelbrink, C.	P2.22	168
Shvirksts, K.	P7.11	289	Štenclová, P	P8.6	312
	P7.19	297	Štěpánek, J.	OC5	38
	P8.4	310	Stepien, E.	OC37	99
Sierka, E.	P8.13	319	Štimac, B.	P5.16	250
Silaghi-Dumistrescu, L.	P5.9	243	Stoilova, A.	P1.2	132
Silva, H.	P8.19	325	Storniolo, Á. R.	P7.14	292
Silva, S.	P8.19	325	Strazdaite, S.	P8.5	311
Silveira, J. M.	P8.19	325	Stuckenholtz, M.	OC43	107
Simões, E. F. C.	P7.4	282	Štuncová, A.	KL7	55
Sipos, P.	OC26	86	Šturlić, Z. B.	P7.9	287
	P3.15	191	Suarasn, S.	P8.1	307
	P4.19	219	Šubr, M.	OC5	38
	P5.12	246	Suhm, M. A.	KL4	52
	P6.8	270		P2.21	167
	P7.5	283		P2.22	168
Šišková, K. M.	P5.22	256	Sureau, F.	OC5	38
Sitkowski, J.	P3.12	188	Sutrová, V.	OC2	35
Škorňa, P.	OC15	58	Świątek, W.	P3.19	195
Skoupá, V.	P6.5	267	Święch, D.	P7.8	286
Šlouf, M.	P6.12	274	Szafraniec, E.	OC38	100
Šloufová, I.	OC2	35		P8.13	319
	P6.12	274		P6.13	275
Słowik, A.	P8.14	320	Szekeres, G. P.	P8.24	330
Śmiszek-Lindert, W. E.	P3.1	177	Szkudlarek, A.	P8.25	331
	P3.14	190		OC39	103
Snelling, H. V.	KL5	53	Szostak, R.	P6.6	268
	P2.12	158		P7.17	295
Sobolewski, A. L.	KL18	82		P7.20	298
Soldatova, A.	P8.10	316	Sztankovics, D.	P5.12	246
Sonoda, Y.	P3.10	186	Tabanez, A. M.	P4.2	202
Šoral, M.	P1.4	134	Tadele Alula, M.	P7.2	280
Spada, L.	P1.6	136	Tanaka, H.	P7.18	296

Tarbutt, M. R.	OC20	69	Valadas, S.	P7.16	294
Tarczay, G.	OC21	70	Valente, A. J. M.	P4.1	201
	P2.11	157		P5.20	254
Tarle, Z.	P8.18	324	van de Weert, M.	KL23	112
Tasinato, N.	OC33	94	Varga, G.	P3.15	191
	P1.3	133		P4.19	219
	P1.6	136		P5.12	246
Teixeira, A. M. R.	P8.12	318		P6.8	270
Terao, W	OC46	116	Velicka, M.	OC35	97
	P8.2	308		P6.4	266
Thakur, V.	OC6	40	Vermesan, H.	OC43	107
Thummel, R. P.	P3.9	185	Vidal, B. C.	P8.7	313
Tikhomirov, S. A.	OC28	88		P8.11	317
Timár, Z.	P5.12	246	Vlčková, B.	OC2	35
Tolstoy, P. M.	OC14	57		P6.12	274
	OC32	93	Vohlídal, J.	P6.12	274
Toman, M.	OC37	99	Voikiva, V.	P7.11	289
Tomić, P	P5.17	251	Volovšek, V.	P7.9	287
Tomilin, A.	P8.10	316	Wagner, M.	OC27	87
Tomza, P.	OC39	103	Wakana, T.	OC8	42
Torres-Boy, A.	OC23	77	Wall, T. E.	OC20	69
Toteva, V.	P7.13	291	Waluk, J.	P3.9	185
Tott, S.	P8.22	328	Węglińska, M.	P7.17	295
Trendafilova, N.	P1.1	131	Weiter, M.	P1.2	132
	P8.9	315	Wierzejewska, M.	P2.2	148
Trinca, D.	P7.21	299		P2.4	150
Trindade, T.	KL2	33		P2.7	153
	OC4	37		P2.8	154
	OC41	105	Wietrzyk, J.	P4.25	225
	P6.2	264	Wilkinson, I.	P4.14	214
	P6.11	273	Willen, K.	KL21	95
Trynda, J.	P4.25	225	Winter, B.	P4.14	214
Tseki, P. F.	P1.11	141	Wislocka, A.	P8.13	319
Tsyganenko, A.	P7.22	300	Wojciechowska, M.	P5.8	242
Tunega, D.	OC15	58	Wójcik, M.	P6.6	268
Tupikina, E. Yu.	OC32	93	Woods, R. C.	PL3	51
Türkeş, T.	P7.10	288	Wrześniok, D.	P3.14	190
Turrel, S.	OC9	44	Wrzeszcz, W.	OC39	103
Tymchenko, E.	P8.10	316	Yaginuma, S.	P5.10	244
Tyrode, E. C.	P5.14	248	Yamamoto, Y.	OC46	116
Tzeng, S.-Y.	P3.17	193	Yang, Q.	P4.16	216
Tzeng, W.-B.	P3.17	193	Yang, S.	P2.9	155
Urboniene, V.	OC35	97	Yavuz, T.	P4.5	205
Uvdal, P.	KL21	95	Yazdi, M. G.	OC17	63

Yeşilel, O. Z.	P4.11	211	Zajonz, M.	P3.2	178
Yesudas, F.	P6.14	276	Zdanovskaia, M. A.	PL3	51
Yi, J. T.	P2.13	159	Zhang, H.	OC31	92
Yilmaz, A.	P7.6	284	Zhang, J.	P8.16	322
Young, N. A.	KL5	53		P8.17	323
	P2.12	158	Zhang, Y.	P6.10	272
	P6.3	265	Zhigunov, A.	KL7	55
Yue, J.	OC46	116	Zhivkov, I.	P1.2	132
Zacharovas, E.	P3.16	192	Zięba, A.	P8.25	331
Zagrai, M.	P8.16	322	Ziegenbein, C. T.	PL7	111
	P8.17	323	Zimmermann, C.	P2.21	167
Zahariev, T.	P1.1	131	Zinth, W.	PL7	111



